INVESTIGATION OF WINTER AEROSOL DISPERSION USING THE MM5/WRF-CAMX4 NUMERICAL MODELLING SYSTEM: APPLICATION TO THE AEROSOL ABATEMENT STRATEGY FOR THE CITY OF CHRISTCHURCH

A thesis
submitted in fulfilment
of the requirements for the Degree
of
Doctor of Philosophy in Environmental Science
at the University of Canterbury

by
Mikhail Titov
Department of Geography

University of Canterbury
2008

Contents

Thanks and acknowledgements

First of all my sincerest thanks to Professor Andy Sturman (principal supervisor) and Dr Peyman Zawar-Reza (associate supervisor), who supervised my work and provided all assistance to guide me, not only during my 3-year PhD research, but also in my everyday working life in the Department of Geography at the University of Canterbury. I am very grateful to them for their support, which provided me with the opportunity to make full use of the Department's and the University's computer and other resources, as well as for commenting on the final drafts of the thesis. Their experience and advice are greatly appreciated. I also especially want to express my gratitude to Professor Andy Sturman for his strong support of my successful application for a PhD Scholarship.

I am grateful to the Department of Geography and Environment Canterbury (ECan), and first of all Teresa Aberkane, for providing meteorological and air pollution data (for CAPS2000, winter 2005 and 2006), both from fixed observation sites and vertical atmospheric balloon soundings that had been used in this research as the ultimate 'tuning fork' in the process of utilization, assimilation and fine tuning of the MM5 (WRF)–CAMx4 numerical system.

Many thanks are due to the technical staff of the Geography Department for their support of my everyday work, especially to John Thyne (for his vital help in the creation of landuse files), to computing administrator Steven Sykes, and to software analyst Graham Furniss. Separately, I want to acknowledge the work of my former colleague researcher James Sturman for the very big and complex job of creating CAMx4 input gridded aerosol and gaseous concentration files. In reviewing drafts of this thesis, the guidance of Professor Andy Sturman and Dr Peyman Zawar-Reza was greatly appreciated. Other people around me also continued to provide their friendship and support. In particular, I would like to thank especially my mother Olga Titova, and her partner Henry Wrassky for their inspiration.

Abstract

Air circulation and air pollution dispersion models are used by a range of stakeholders involved in managing air quality in New Zealand following the recent establishment and implementation of the National Environmental (Air Quality) Standards by the Ministry for the Environment. MM5-CAMx4 and WRF-CAMx4 numerical modelling systems were utilized to air circulation over the complex terrain of the Christchurch area for investigation applied to winter aerosol pollution, following the recent establishment and implementation of the National Environmental Standards.

A new method using several different chemical scenarios is developed to calculate optimal chemical composition of the input gridded aerosol emissions. This method improves the accuracy of predicted PM concentrations. The MM5-CAMx4.2 numerical system is evaluated to predict aerosol concentrations over a 48-72 hour time period for Christchurch for winter 2005. The aerosol concentrations are obtained for four different chemical compositions of the input aerosol emissions. The fine-total PM regression error between observed and modelled aerosol is used to find the minimum difference between modelled and ambient aerosol. Combination of the chemical scenarios with the minimum error between modelled and ambient data is employed to create a new complex chemical scenario.

A reduction of the systematic error in the scenario method is achieved by applying the MM5/WRF - CAMx4.2 numerical system and observations for winter 2006, aerosol data from 2 observation sites. Assessment of the efficiency of PM abatement strategies for the period 2005-2013 is undertaken using winter 2005 meteorology and application of a linear reduction in emissions according to Environment Canterbury proposed plan for aerosol reduction. A new numerical approach to selection of PM monitoring sites optimal localisation is also developed and could be applied to any air pollutant to find the optimal positions for installing new observation sites.

LIST of FIGURES

LIST of TABLES

List of acronyms and abbreviations

EC- **E**lemental **C**arbon
BC – **B**lack **C**arbon
Ca – Calcium
CAMx – **C**omprehensive **A**ir quality **M**odel with e**x**tensions
CCRS – **C**oarse **C**R**u**S**t**al elements
CG – **C**ondensable **G**ases
CO – Carbon monoxide
CLiP – **C**urved **Li**ne **P**aths
CO_2 – Carbon dioxide
CPRM – **C**oarse **PR**i**M**ary elements
CPRM – **C**oarse **CR**u**S**tal elements
FCRS – **F**ine **CR**u**S**tal elements
FPRM – **F**ine **PR**i**M**ary elements
K – Potassium
MfE – **M**inistry **f**or **E**nvironment
MM5 – **M**esoscale **M**odel version **5**
Na – Sodium
NH_3 - Ammonia
NH_4^+ - Ammonium
$(NH_4)_2SO_4$, NH_4NO_3 – sulphate and nitrate ammonium
NO_2 – Nitrogen dioxide
NO_x – Nitrogen oxides
OC – **O**rganic **C**arbon
OM – **O**rganic **M**atter
PM – **P**articulate **M**atter
$PM_{2.5}$ – **P**articulate **M**atter less than **2.5** microns in aerodynamic diameter
PM_{10} - **P**articulate **M**atter less than **10** microns in aerodynamic diameter
$PM_{10-2.5}$ – **P**articulate **M**atter between **2.5** and **10** microns in aerodynamic diameter
POC – **P**rimary **O**rganic **C**arbon
POA – **P**rimary **O**rganic **A**erosol
PSO_4, PNO_3, PNH_4, PCl – particulate soluble inorganic ions (salts): **SO_4^{-2}, NO_3^{-1}, NH_4^{+1}, Cl^-**
PSVM - **P**articulate **S**emi-**V**olatile **M**aterial
RH – **R**elative **H**umidity
SLiP – **S**traight **Li**ne **P**aths
SO_2 – Sulphur dioxide
SOC – **S**econdary **O**rganic **C**arbon
SOA – **S**econdary **O**rganic **A**erosol
TC = EC+OC – **T**otal **C**arbon
TEOM – **T**apered-**E**lement **O**scillating **M**icrobalance
TOC = POC+SOC – **T**otal **O**rganic **C**arbon
WHO – **W**orld **H**ealth **O**rganization
WSOM - **W**ater-**S**oluble **O**rganic **M**atter
WISOM - **W**ater-**Ins**oluble **O**rganic **M**atter
WRF – **W**eather **R**esearch and **F**orecasting system

Chapter 1: Introduction

Local and regional meteorological models have been developed to simulate the atmospheric processes that control air pollution dispersion (Dudhia and Bresh, 2000; Klausmann *et al.,* 2001; Kotroni *et al*., 1999; Dailey and Keller, 2002; Low-Nam and Davis, 2002). The potential of the limited area models that include ideal and real simulation of atmospheric circulations ranging in scale from an entire hemisphere down to eddy flux simulations of the planetary boundary layer is elucidated in the works of Arya (1988) and Sorteberg *et al*. (2001). The ability of regional limited area models to simulate atmospheric phenomena at the mesoscale level (horizontal scales from 2000 km to 2 km) for applications from operational weather forecasting to air quality dispersion, and in fundamental research, are described by Otte and Loscer (2001). Limited area models are also successfully used at much higher resolutions to simulate boundary layer processes (boundary layer eddies with 10–100 m grid spacing), air flow over individual building or direct wind tunnel simulations (Kotroni *et al*., 2003; Pietrowicz, 2002). Such limited area models as MM5 and WRF were developed to undertake research in modelling physiographically-driven weather systems and simulation of convective clouds, mesoscale systems, cirrus clouds, precipitation weather systems in general and extreme precipitation events (Someshwar *et al.,* 2002). Limited area modelling is also a basic numerical tool in teleconnection research (Krichak *et al*., 2002), in back- and forward trajectory numerical methods (Sturman and Zawar-Reza, 2002), and in investigation of many other atmospheric phenomena.

Three-dimensional prognostic photochemistry models have been developed alongside the growth of three-dimensional prognostic, mesoscale meteorological models (Russel, 1997). Limited area meteorological models are now commonly used to provide meteorological fields with the aim of estimating urban air pollution, especially over complex terrain dominated by local air circulations (Souto *et al.,* 1998). They have a lot of advantages, especially from the point of view of representing important pollution prediction factors, such as very complex terrain air flow, and the complex distribution and redistribution of spatial and point emission sources in space and time. Meteorological mesoscale models, firstly predict the meteorological fields and then the predicted wind, temperature and humidity fields are used to drive three-dimensional air pollution models to estimate the dispersion of air pollutants from different kinds of source (Hernandez, *et al.,* 1997). Cox *et al*. (1998) developed a modelling scheme for use in providing short-term (1–4 hour) predictions for accidental release of hazardous materials. This approach required good real-time weather data at a high resolution from regional meteorological models to produce useful results.

New studies have applied 3-dimensional pollution models to much longer-range pollutant transport than city-scale pollution dispersion (Jaeckervoirol *et al.,* 1998).

The air circulation (e.g. MM5/WRF) and air pollution photochemical (e. g. CAMx4) models (and their numerical interface) are excellent tools to apply to a range of air pollution research tasks aimed at managing air quality in New Zealand (Ministry for Environment, 2004). There is also a great need to adapt such complex and sophisticated regional meteorological models (like MM5 and WRF) to air circulation of different parts of New Zealand for use in decision making by regional councils and environmental consultants, following the recent establishment and implementation of the National Environmental (Air Quality) Standards (Ministry for Environment, 2003). It is important to stress that the configuration of the modelling system could differ according to emissions source type (vehicles, industry, domestic, and commercial) and region. The numerical dispersion modelling system previously developed by Mikhail Titov (MM5-CAMx4) has been upgraded with new versions of MM5 and CAMx (MM5 v3.7.3 and CAMx4.2-4.4). MM5-CAMx numerical system and the new one (WRF-CAMx), are used initially for gaining deeper understanding of observed spatial and temporal variations in air quality (by comparing model output with ambient air quality observations). The modelling systems are used as the basic tools to assess air quality in locations without observations under a range of different chemical and environmental scenarios. The environmental scenarios depend on the local/regional situation and may vary from 'business-as-usual' to a range of pollution abatement strategies. Extensive use of numerical modelling systems such as MM5-CAMx4 and WRF-CAMx4 helps to validate progress in achieving the new air quality standards.

The developed mesoscale modelling techniques are applied to specific urban air quality problems, relating to both the re-distribution (dispersion) of air pollutants and PM chemical reactions over similar time intervals in Christchurch (New Zealand). They also identify the pathways of possible local range transport of air pollution using trajectory analysis (forward and backward) module of the meteorological models postprocessing software. Special modelling methods have been developed to determine more precisely (from different scenarios) the chemical content of aerosol pollution for different PM emission sources in the Christchurch region for winter time smog episodes.

The application of above-mentioned comprehensive integrated numerical modelling systems for assessment and management of urban air quality in the Christchurch area of New Zealand has

provided a number of distinct benefits, including optimal location of air pollution monitoring sites and assessment of the accuracy of air pollution emissions inventories. Through development of such advanced atmospheric modelling techniques, this research has benefited other applied research programmes undertaken by the University of Canterbury's atmospheric research group, such as wind energy resource mapping, short-term forecasting and numerical investigation of dust storms in Afghanistan and Iran.

Broad aims and rationale

Atmospheric numerical models are major tools used in both improving knowledge of atmospheric processes and the application of this improved knowledge to human activity. They can be used to reduce the impacts of the atmosphere on humans (e.g. day-to-day weather forecasting and longer term climate prediction), as well as to allow humans to make the most of their climate environment (e.g. in agriculture and wind energy generation). The most useful atmospheric numerical models are those based on the physical equations that are used to describe fundamental atmospheric processes (Smagorinsky, 1983; Manabe, 1985**)**. Such models have evolved and developed rapidly over the last two decades due to advances in computer technology. The modern models are very sophisticated huge pieces of computer code, which allow multi-scale interaction through grid nesting, as well as coupling with complex atmospheric chemistry models (Sturman, 2000; McGruffie and Henderson-Sellers, 2001**)**. Coupling with complex chemistry models opens tremendous possibilities of improving knowledge of the influence of human activity on the environment at different spatial and time scales from long-range transport of air pollution and dust at spatial scales of several hundred kilometres over several days to air pollution concentration and circulation in a street canyon over several minutes (Byun and Ching, 1999; Michelson *et al*., 2002**)**.

The fundamental aim of this research is to use limited-area atmospheric modelling tools to improve understanding of local and regional atmospheric circulations and their application to air pollution dispersion. This includes implementation of the most appropriate coupled atmospheric and air pollution models driven by existing and proposed scenarios of chemical composition of air pollutants, to improve understanding of present-day and future accumulation and dispersal of air pollution, especially in regions of complex terrain.

The main practical aim of the project is to apply the numerical modelling system to extend knowledge of issues in air pollution, including improved understanding of meteorological controls

on spatial and temporal variations in air pollution in complex terrain, knowledge of spatial variability in human exposure to air pollution, improvements in predicting the impact of proposed new sources of pollution, assessment of the effectiveness of air quality management strategies, optimal location of air pollution monitoring sites, and the use of statistical techniques to assess the accuracy of emissions inventories.

Air circulation and air pollution dispersion models are used by a range of stakeholders involved in managing air quality in New Zealand (Ministry for Environment, 2004). There is currently an urgent need to adapt the more complex and sophisticated models to use in decision-making by regional councils and environmental consultants, following the recent establishment and implementation of the National Environmental (Air Quality) Standards by the Ministry for the Environment (Ministry for Environment, 2003 – see also **http://gpacts.knowledge-basket.co.nz/regs/regs/text/2004/2004309.txt)**. Advanced numerical models have an advantage over earlier simplistic models (such as the box model) as they use a system of basic primitive equations that can better describe the physical and dynamical processes operating in the atmosphere.

Objectives

Main objective: to adjust and to apply coupled atmospheric/air pollution modelling tools that are driven by chemical scenarios of aerosol emissions, and to improve understanding of the accumulation and dispersal of air pollution in the Christchurch region of complex terrain and for future proposed PM abatement strategies.

Secondary objective: to apply the coupled numerical modelling systems to extend knowledge of a number of contemporary issues in air pollution science, including:

- Improved understanding of meteorological controls of spatial and temporal variations in air pollution in complex terrain;
- Improved knowledge of spatial variability in human exposure to air pollution;
- Improvements in predicting the impact of proposed new sources of pollution on ambient air pollution concentrations;
- Improved assessment of the effectiveness of air quality management strategies;
- Optimal location of air pollution monitoring sites in relation to the main sources of pollution: domestic heating, industrial and transport;

- The use of modelling and statistical techniques to assess the accuracy of emissions inventories, especially the 1999 inventory for the Christchurch area used as the basic for several applications of air pollution modelling.

Overview

The study focuses basically on research into spatial and temporal variation of winter fine and total PM for Christchurch pollution episodes using the numerical modelling system:

- Improved understanding of meteorological controls of spatial and temporal variations of PM pollution in the complex terrain of the Christchurch region;
- Improved knowledge about component content of fine and total PM air pollution for different pollution origins ;
- Improvements in predicting the impact of proposed new sources of pollution on ambient air pollution concentrations and assessment of the effectiveness of air quality management strategies;
- Improvement in the evaluation of a new observation site in assessment of the aerosol air pollution in the Christchurch area.

The study describes the main numerical modelling systems utilized for winter PM pollution research for the city of Christchurch, and identifies optimal chemical composition of fine and total PM on the basis of numerical experiments for winter 2005 and winter 2006. Assessment of human exposure and efficiency of the PM management strategies are described in application of the optimal chemical scenario method to PM emissions in "Domestic", "Transport", "Industry" and "Total" groups. The study is organised into the following fourteen chapters.

Chapter 1: Introduces the issues addressed by the study, outlines the objectives of the research and provides a study overview.

Chapter 2: Provides background information regarding particulate matter. In particular, it describes the physical properties of PM, the principal chemical components; methods of PM shape assessment, and briefly describe the most important impacts of fine ($PM_{2.5}$) and total (PM_{10}) PM on health and microclimate.

Chapter 3: Describes methods of numerical evaluation of particulate matter that include application of meteorological, air quality and coupled modelling systems. Main emission data assimilation systems used for input data are considered. It provides a short description of the Eulerian, Lagrangian and puff models adopted for applications by EPA (USA) and WHO (EU). The final section briefly describes the basic principle of aerosol primary and secondary chemistry used in the state-of-science 3-D Eulerian models for more accurate reproduction of PM chemistry in time and space.

Chapter 4: Reviews the main methods of airborne PM evaluation in the Christchurch area, including observational, statistical and numerical methods of investigating spatial and temporal variation of aerosol assessment during winter time. Basic features of the study area and observation methods are described, including the Christchurch Air Pollution Study 2000 (CAPS 2000). Special focus is given to conceptual modelling as an alternative to numerical modelling of aerosol data.

Chapter 5: This chapter introductive chapter introduces the methodology adopted for the research and describes two limited area meteorological models (MM5 and WRF) used for reproduction of the Christchurch area circulation at different stages of the study. TAPM applications are also outlined. The last part is dedicated to a discussion of possible operational use of MM5 and WRF on multi-parallel processing (MPP) computers.

Chapter 6: Describes the main advantages of the 3-D Eulerian chemical model CAMx4 and its recent extensions including the main mechanisms of PM assimilation, chemical solving, dispersion (advection) and scavenging. Special attention is devoted to chemical and numerical stability of CAMx4 during integration over time, and influence of particulate water parameterization on PM output concentrations.

Chapter 7: The last chapter of the methodology evaluates coupled (meteorological – chemical) numerical systems used for reproducing PM spatial-temporal dispersion over the city of Christchurch, starting with TAPM and finishing with the newest WRF-CAMx4 system. The application of the numerical modelling systems MM5-CAMx4 and WRF-CAMx4 are described separately.

Chapter 8: Is the first of three chapters presenting modelling results. This chapter describes the ability of limited area model (LAM) MM5 to capture near-surface air circulation for the complex terrain of the South Island (in coarse resolution) and of the city of Christchurch (in fine resolution) for winter 2005. Special focus is given to the modelled process of night-time near-surface inversion development, stabilization and break down. A separate section is dedicated to synoptic scale air circulation and influence of complex terrain.

Chapter 9: Outlines the principle ideas behind a method of several different chemical scenarios, developed on the basis of local research and international studies of the chemical content of winter aerosol. Description of all proposed scenarios, the method of comparison of predicted and observed fine and total PM concentrations for co-located PM measurements and a procedure for building an optimal chemical scenario are also described in Chapter 9.

Chapter 10: Assesses the validity of the method of several chemical scenarios and evaluates winter 2006 pollution episodes for the optimal chemical scenario found for winter 2005 compared to initial chemical scenarios. In chapter are described the methods of the optimal chemical scenario seasonal, numerical and observational error (bias) reduction. A possibility of spatial variability of the optimal chemical scenario is also investigated.

Chapter 11: This chapter is the first of 3 elucidating main applications of the method of several chemical outlined and described earlier. It describes two (linear and non-linear) methods of assessment of the 1999 inventory, and the legitimacy of the linear approach to validation of the 1999 inventory for the “Domestic”, “Transport” and “Industry” PM exposure groups. Modelled results of the proposed direct (aerosol in groups) and indirect (via gaseous precursors) reduction of airborne PM are also considered.

Chapter 12: Assesses the efficiency of proposed fine and total PM reduction strategies based on the ECan 2002 inventory and aerosol reductions in the emission groups for the 2005–2013 time period. It outlines numerical non-linear PM concentration decrease on linear PM reduction emissions in groups “Domestic, “Transport” and “Industry” using proposed future PM emission scenarios, and describes possible future re-distribution of PM basic species up to year 2013.

Chapter 13: Describes a new numerical method of monitoring sites optimal localization to obtain the maximum information relating to spatial and temporal PM concentration distribution. It

delineates a method based on a site efficiency to capture smog peak event, and describes the basic experience of winter 2005 (single site approach), winter 2006 (2 sites approach) and winter 2000 (multi-site approach).

Chapter 14: Provides a summary of the study findings and outlines implications of the research for proposed future strategies of PM reduction for the 2005–2013 time period.

PART A: BACKGROUND

Chapter 2: Particulate matter (PM) and methods of observation-analysis

Particulate matter (*abbreviation* as PM) can be defined as:

"Material suspended in the air in the form of minute solid particles or liquid droplets, especially when considered as an atmospheric pollutant." (American interpretation dictionary, 2006).

An airborne particle can be defined as:
"A single continuous unit of solid or liquid containing many molecules held together by intermolecular forces and primarily larger than molecular dimensions (>0.001 m). A particle may also be considered to consist of two or more such unit structures held together by inter-particle adhesive forces such that it behaves as a single unit in suspension or upon deposit."
(Seinfeld and Pandis, 1998)

Particles suspended in a gas may be referred to as aerosols or particulate matter (PM), have natural or anthropogenic origin and exist in a variety of shapes and sizes. WHO determine PM from a health aspect as:
"*Particulate air pollution is a mixture of solid, liquid or solid and liquid particles suspended in the air. Airborne particulate matter represents a complex mixture of organic and inorganic substances*." (WHO Working Group, 2003).

Regardless of whether an aerosol's primary origin is natural or anthropogenic, PM evolves in the atmosphere as a consequence of the multiple physico-chemical processes that can affect PM from its release point as a primary aerosol, or via gas-to-particle conversion processes, that give rise to a secondary aerosol. Figure 2.1 presents an electronic microscope image where different particle shapes are evident, from angular, salt crystals (A) and elongated, branched hydrocarbon chains (B), to sticky agglomerations (C). PM sometimes may be chemically uniform (crustal particulate matter), but mostly consists of a variety of chemical compounds (Baron and Willeke, 2001). Particles are either discharged directly from a source (primary particles) or formed through a complex of chemical reactions under certain atmospheric conditions (secondary-tertiary particles).

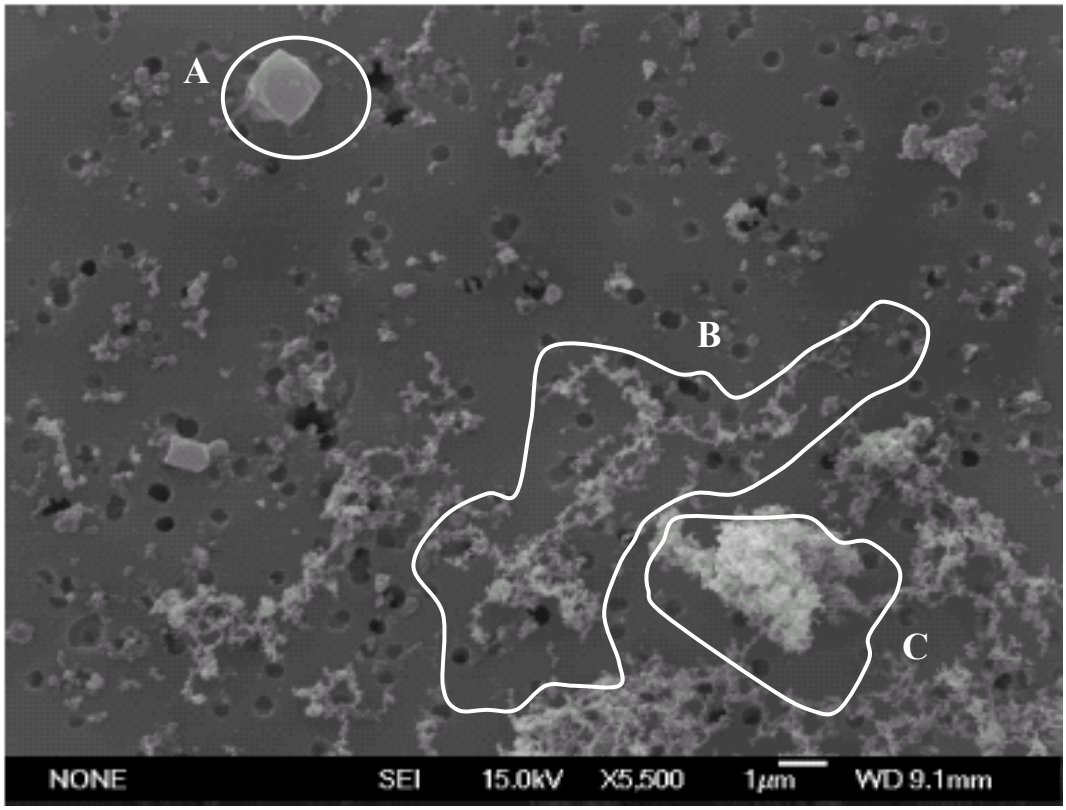

Figure 2.1 Scanning electron microscope (SEM) photograph of fine particles measured in Christchurch on a polycarbonate filter (after Davy et al., 2002).

This chapter provides background information regarding airborne particulate matter (PM). In particular, it describes the physical properties of PM (size and formation) and main chemical components. The basic methods of PM shape assessment and analysis are detailed and the most important impacts of fine ($PM_{2.5}$) and total (PM_{10}) PM on health and microclimate are described.

2.1 PM size and formation

The size of PM in urban environments is divided into two principal groups: coarse fraction ($PM_{10-2.5}$) and fine fraction ($PM_{2.5}$). The sum of fine and coarse particles is defined as total PM_{10}. The separation between these two PM fractions usually lies between 1 μm and 2.5 μm (WHO Working Group, 2003) depending on the chemical transformation processes involved. However, for measurement purposes only it is usually fixed by convention at 2.1 - 2.5 μm aerodynamic diameter ($PM_{2.5}$).

PM or suspended particulate matter varies in size, composition and origin. It is convenient to classify PM by its aerodynamic properties because: (a) these properties govern the transport and removal of particles from the air; (b) they also govern deposition efficiency within the respiratory system and (c) they are associated with the chemical composition and sources of particles. These

properties are conveniently summarized by the aerodynamic diameter, which is the size of a sphere with the same aerodynamic characteristics (Figure 2.2). Particles are sampled and described on the basis of their aerodynamic diameter, usually called simply the particle size. Aerodynamic diameter is defined by Baron and Willeke (2001) as the diameter of a standard-density sphere (1000 kg m^{-3} or 1 g cm^{-3}) with the same gravitational settling velocity as the particle being measured. Size determines particle behaviour and residence time in the atmosphere, and provides an indication of the mechanisms that created the particle (Claes et al, 1998; Seinfeld and Pandis, 1998).

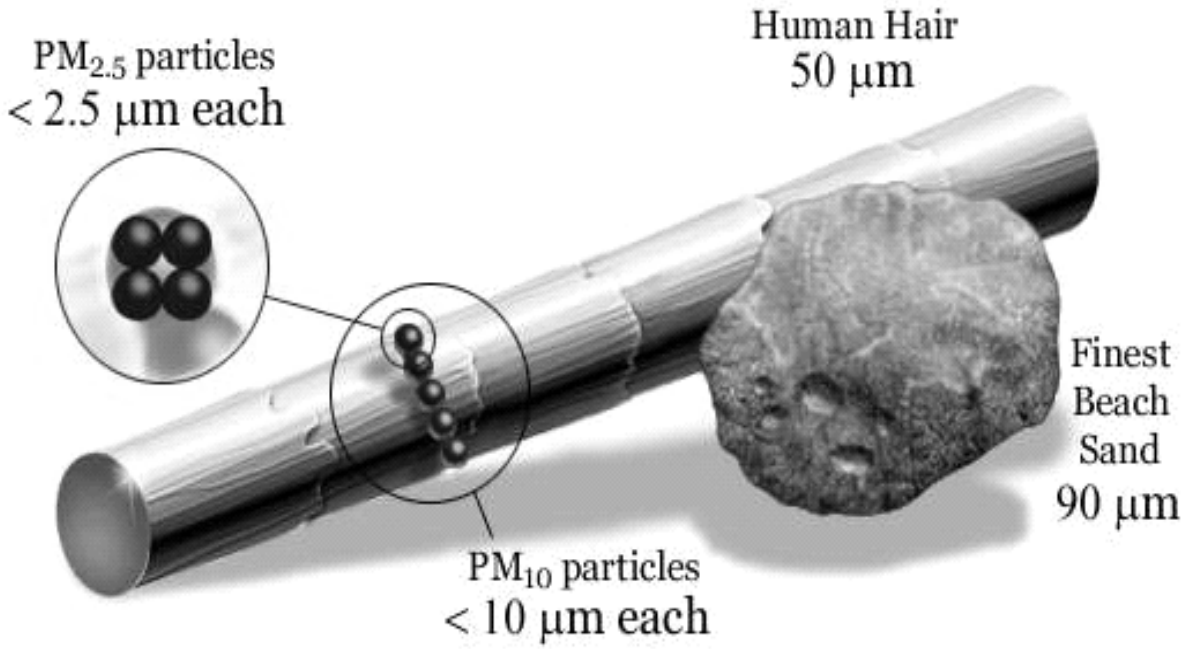

Figure 2.2 Schematic illustration of particle size in relation to human hair and beach sand (courtesy of Environment Canterbury, Scott, 2005).

Fine particulate matter ($PM_{2.5}$)

Particles are between 0.001 to 100 μm in diameter and grouped into size ranges or modes for measurement purposes. These are generally described as the fine (<2.5 μm) and coarse particle (>2.5 μm) modes (Figure 2.3).

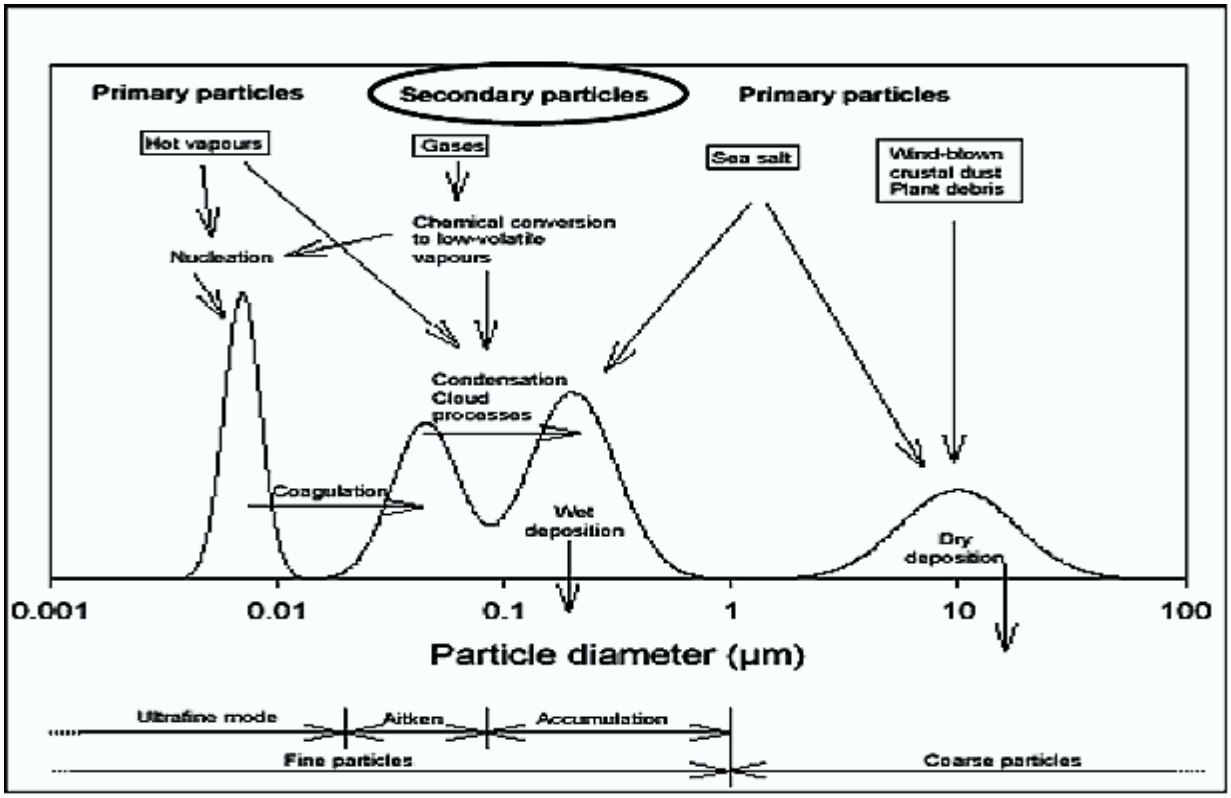

Figure 2.3 Simplified schematic illustrations of atmospheric aerosol (PM), including sources, transformation and sinks. The different size ranges (modes) are also shown (after Temime B. 2005).

The smallest particles (nucleation or ultra-fines including nano-particles) of PM are emitted directly from combustion or formed through photochemical gas-to-particle conversion. The highest numbers of particles are in the nucleation mode, although they are usually present in the atmosphere for limited periods of time. These particles readily coagulate with existing particles or become nuclei for droplets (Chow and Watson, 1998; John, 2001). Individual particles are usually slightly positively or negatively charged and, as a result, differently charged particles are attracted to each other, resulting in coagulation. The particles are held together, or separated, by forces that depend on particle size and surface parameters (including shape, roughness and chemistry), the properties of the surrounding air (temperature and humidity) and the mechanics of the particles (relative particle velocity and contact time (Baron and Willeke, 2001)). These particles are most numerous in close proximity to emission sources in urban environments (Hobbs, 2000; Chow and Watson, 1998).

Particles in the accumulation mode (approximately 0.1-1.1 µm) of $PM_{2.5}$ contain most of the fine particle mass, including fine sea salt (sea spray) and dust particles, and particles formed from the coagulation of nuclei mode particles and gas condensation processes. Aged aerosol is likely to be

present if $PM_{2.5}$ is dominated by particles in the accumulation mode (Hobbs, 2000). These fine particles, as a whole, remain in the atmosphere for longer periods of time than coarse particles, and are eventually removed through dry deposition (settling) or wet deposition (wash-out) mechanisms. The length of time a particle remains suspended in the atmosphere (residence time) is a direct function of particle size and altitude.

Combustion processes including the anthropogenic combustion of fossil fuels and biomass burning are the primary sources of particles in the $PM_{2.5}$ size fraction. Fossil fuels include solid fuel (coal and wood), liquid (diesel oil) and gas are used in many cities as fuel for motor vehicles and industry, and as a heating source for private dwellings. However, incomplete combustion depends on the burning load level (Fung et al., 2002) and leads to the emission of a mixture of gases and particles. Primary particles from combustion sources are usually less than 0.2 μm in diameter (like elemental carbon – EC) and are subject to chemical and physical processes, leading to the formation of secondary particulate.

Coarse particulate matter ($PM_{10-2.5}$)

Coarse particles (>2.5 μm) are mainly produced through mechanical processes. These processes include surface abrasion, crushing, and grinding, and generate coarse particles such as marine aerosol and wind-blown dust (Figure 2.3). While some marine aerosol is produced through agitation of the sea surface by the wind, the majority of the aerosol is released by gas bubbles from the water surface. Bursting bubbles release large and smaller droplets of water containing surface-active organic material. The large droplets fall back into the water, while the smaller ones become airborne and are transported long distances by the wind. Typically, 95% of marine aerosol mass comprises particles >0.6 μm (Seinfeld and Pandis, 1998). Dust particle formation, conversely, occurs through wind movement along the ground surface and depends on soil type and humidity. Wind speeds of only 0.2 m s^{-1} are capable of ejecting soil particles into the air. These large-sized particles are generally deposited, but collision with the ground surface results in further fragmentation and re-entrainment. Bioaerosols or plant debris (such as pollen, spores, leaf-litter decay and viruses) may also be found in the coarse particle mode, with some, such as viruses and bacteria, present in the fine particle fraction (<2.5 μm). Coarse particles do not remain in the atmosphere for long periods as high sedimentation rates lead to quick removal (Seinfeld and Pandis, 1998).

Size distribution of PM in relation to number, surface area and volume shows that the peak of the distribution varies with the parameter considered (Figure 2.4). PM number has the largest peak in the ultrafine mode, but the accumulation mode absolutely dominates in the relation to surface area, while for volume two peaks are detected in accumulation and coarse modes (with maximum mass in the coarse mode).

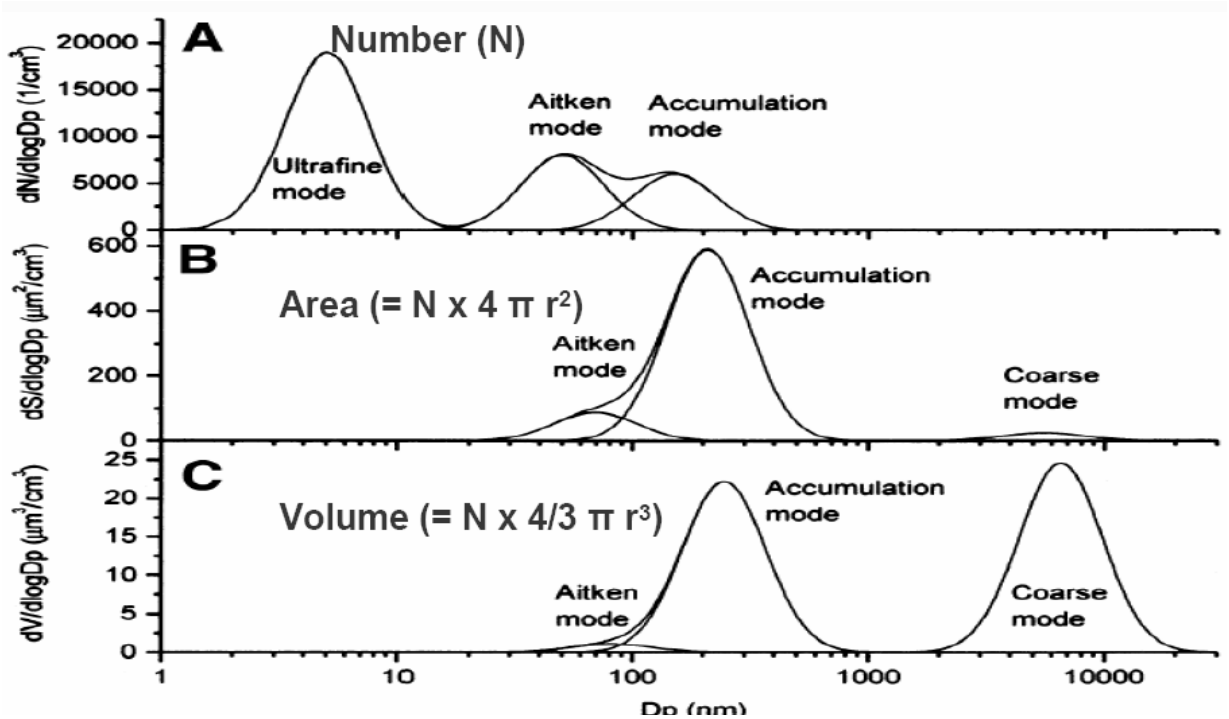

Figure 2.4 PM size distribution in relation to number (cm^{-3}), surface area (μm^2 cm^{-3}) and volume (μm^3 cm^{-3}), where r is the average radius of a particle and $\pi = 3.1415$ (after Temime, 2005).

2.2 Chemical composition of PM

Airborne particles are comprised of numerous chemical compounds and may have anthropogenic or natural source origins, or both. The chemical constituents of fine particles ($PM_{2.5}$) include carbon compounds, water-soluble inorganic salts, and some metallic elements. The chemical composition of coarse particles ($PM_{10-2.5}$) includes mostly crustal elements (including Ca, Fe, Ti and Al), marine aerosol particles (Na, K, Cl) and plants debris (Brimblecombe, 1996). These chemical species can provide an initial indication of particle origin (Figure 2.5).

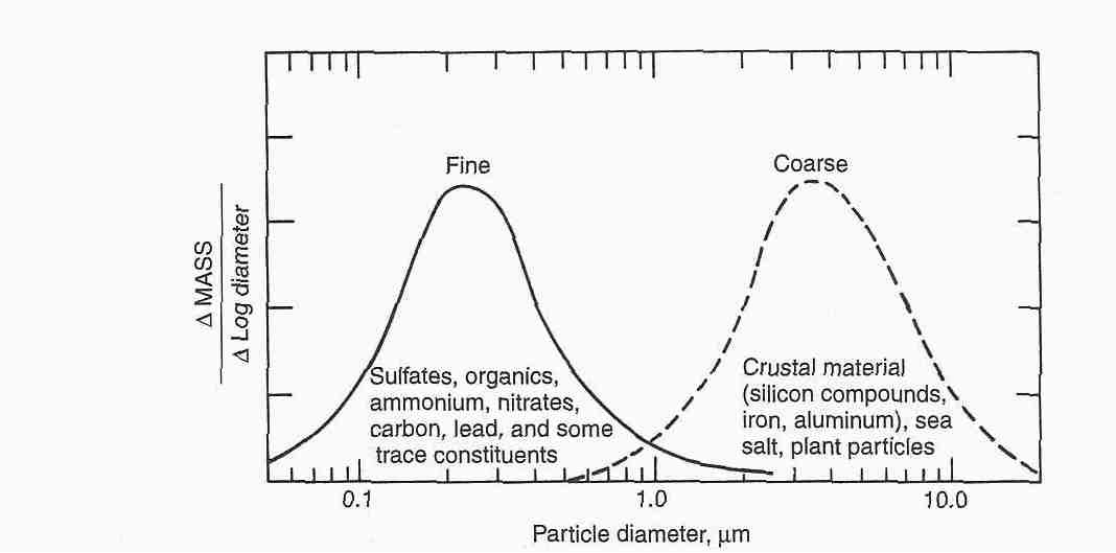

Figure 2.5 Typical urban fine and coarse aerosol distribution by particle size fraction and chemical composition (axis Y is dimensionless, John, 2001).

$PM_{2.5}$ basic chemical content

Elemental carbon (EC) and primary organic carbon (POC) are the essential species of any anthropogenic fine PM. Elemental carbon/black carbon (EC/BC) is discharged directly into the atmosphere during fossil fuel combustion, as a product of low efficient combustion process. Other carbon compounds included in this category are high molecular weight, non-volatile organic species (Chow and Watson, 1998). EC can be produced by a variety of sources (including residential heating, industry) but mostly by diesel-petrol vehicles. Identifying sources contributing to emissions of this substance is difficult, due to its non-uniqueness. The proportion of OC to EC in emissions is considered indicative of source origin (Aria, 1999). Ratios vary depending on combustion technology and fuel composition, and should not be used independently of other supportable information to identify emission sources.

OC compounds are defined by Chow and Watson (1998) as those with more than 20 carbon atoms. These particles may be discharged directly into the atmosphere or formed by the condensation of organic gases. Hydroxyl (OH) and nitrate (NO_3) radicals oxidise these gases and the oxidation products accumulate. The low-volatile products of these reactions condense on the available particles to achieve equilibrium between the gas (condensable gas – CG) and particle phase (Seinfeld and Pandis, 1998). However, accurate measurement of these substances is problematic, due to the tendency for organics to continuously transfer between the gas and particle phase and depends on the ambient air temperature and humidity. OC is derived from the same sources as EC, that is, mainly residential heating, industry and motor vehicles. The relative proportion of these

two species in emissions can indicate particle origin. OC is more abundant than EC in emissions from low temperature combustion processes such as biomass burning (home heating).

Inorganic ions including nitrates, sulphates and ammonium are all secondary particulate species formed by chemical reactions in the atmosphere. Particulate sulphates (PSO_4) are water-soluble inorganic ions that usually exist in the fine particle fraction. The precursors of sulphates (sulphur gases) are generated by natural and (mainly) anthropogenic processes (Brimblecombe, 1996; Arya, 1999). Gaseous acid reacts with gaseous ammonia (NH_3) and produces the main atmospheric forms of sulphate, ammonium sulphate ($(NH_4)_2SO_4$) and ammonium bisulphate (NH_4HSO_4). At night, the nitrate radical (NO_3) becomes the most important oxidising agent and reacts with a number of other atmospheric species creating particulate nitrate (PNO_3). PNO_3 is formed when NO_2 and O_3 are present in the same air mass (Seinfeld and Pandis, 1998). Particulate ammonium is usually present as $(NH_4)_2SO_4$, NH_4HSO_4 and NH_4NO_3. As indicated previously, these compounds are formed in the atmosphere by reactions with NH_3, nitrogen oxides (NO_x) and SO_2 gases. NH_3 is released from animal urine and microbiological activity in soils (Hobbs, 2000).

$PM_{10-2.5}$ basic chemical content

The coarse fraction of PM_{10} includes first of all geological material (crustal elements, primary dust), secondary (re-suspended) dust, soot, salt, biological origin particles (plants debris), and also big secondary particulate complexes consisting mostly of NH_4NO_3 with particulate water (Chow et al., 2002). Dust plays important roles in the Earth's climate system and the biogeochemical cycle. Asian dust rising from the arid and semi-arid regions in China and Mongolia, an important source of mineral dust worldwide, is easily delivered into the free troposphere and transported over thousands of kilometres during spring by the westerlies. It is estimated that 800 Mt of dust aerosols emitted annually into the atmosphere from East Asia almost accounts for 1/3 of the global yearly dust emissions (Chen et al., 2006). Dust storms from Sahara play an important role in coarse PM loading in many European countries like Spain, Italy and Portugal (Salvador et al., 2007; Gobbi et al., 2007) decreasing pH of secondary aerosol in atmosphere and increasing micro flora during spring time. Some complains about the influence of Asian dust storms on increase of total PM (including fine PM) can be traced from research done in south-west states of the USA (Gebhart et al. 2005), but these results can not be accepted as reliable speaking about serious increase of PM, as the output from the dust trace methods are mostly lower than background values of local aerosol. At rural and the near-city sites crustal elements like Al, Mg, Ca, and Fe are predominant in the $PM_{10-2.5}$ fraction, while typical anthropogenic elements like As, Cd, Tl, and Pb are mainly

associated with $PM_{2.5}$, and elements like Cu, Mn, Mo, Na, and Sb are roughly evenly distributed between $PM_{2.5}$ and $PM_{10-2.5}$ (Hueglin et al., 2005).

Re-suspended dust and mechanically generated particles from road traffic (road, tires and brakes abrasion) are most pronounced for kerb-sides and play minimal role at urban and rural background sites. Re-suspended dust has a peak during working days and is lowest at week-ends, when heavy traffic is lowest on the roads. The life cycle of re-suspended dust and mechanically generated particles in air depends of transport activity and meteorological conditions (especially wind speed), but usually doesn't exceed 2-3 hours (Hueglin et al., 2005).

Marine aerosol particles, produced through agitation of the sea surface by the wind and released by gas bubbles from the water surface, consist of inorganic ions (K, Cl, S) and their mixture with water and can be a dominate portion of $PM_{10-2.5}$ in coastal regions leading to fog, smog and precipitation (Mihajlidi-Zelic et al., 2006).

Secondary particulate matter, consisting mostly of ammonium nitrate NH_4NO_3 complexes and particulate water, has two size peaks (0.6 μm and 4.1 μm) sometimes equally distributed (Chow et al., 2002). Depending on the chemical composition, water can be an important constituent of the coarse fraction of ambient PM (Pilinis et al., 1989). Especially inorganic salts like ammonium nitrate can absorb water. Inorganic salts are solid until the ambient relative humidity (RH) reaches the deliquescence point (about 67%). At the deliquescence points of the individual inorganic salts, water is absorbed until a saturated aqueous solution of that salt is formed (Mihajlidi-Zelic et al., 2006).

Agricultural biomass burning and open wildfires are important global sources of coarse aerosol particles (soot) for the atmosphere (Lee et al., 2005). Biological originating particles (plant debris) like pollen, lichen and other origin spores (grains) are very active contribution to coarse PM fraction and usually have a clearly good pronounced seasonal trend. The contribution of biological particles as aggressive allergic provokers has been actively researched (Pasken and Pietrowicz, 2005).

2.3 Methods of PM shape assessment

The size of PM in the atmosphere varies over four orders of magnitude, from a few nanometres to tens of micrometers. The coarse fraction ($PM_{10-2.5}$) is mechanically produced by the break-up of larger solid particles. This size fraction can include wind-blown dust from agricultural processes, uncovered soil, unpaved roads or mining operations. Traffic produces road dust and air turbulence that can stir up road dust. Near coasts, evaporation of sea spray can produce large particles. Pollen grains, mould spores, and plant and insect parts all contribute to this larger size range. The amount of energy required to break these particles into smaller sizes increases as the size decreases, which effectively establishes a lower limit for the production of these coarse particles of approximately 1.1 μm (WHO, 2003).

PM may be present in a variety of shapes ranging from simple spheres and rods to more complex forms. Particle shape can be indicative of particle origin and history (Baron and Willeke, 2001). Fume particles formed from vapours discharged into the atmosphere, for example, condense into spherules, which diffuse rapidly and coagulate into branched chains. The chains increase in size, intercept one another and form large agglomerates over time. Therefore, recently formed combustion particles usually comprise relatively simple elongated chains, whereas aged combustion particles are denser and may be coated with organic compounds (Cachier, 1998). This is illustrated schematically in Figure 2.6, and is also demonstrated in Figure 2.1 where B is a fresh combustion particle and C is an aged aerosol.

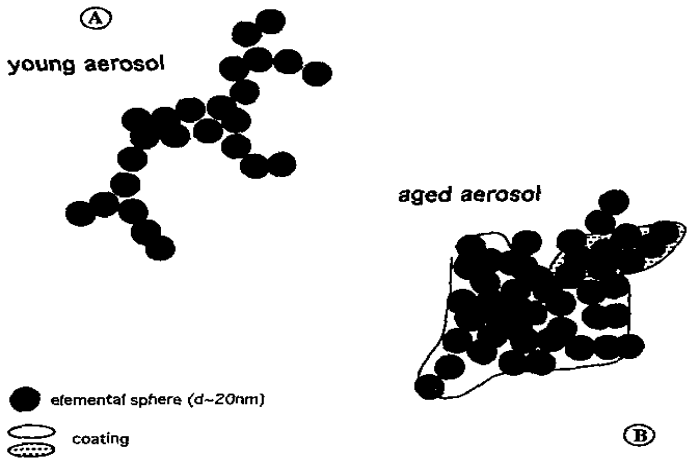

Figure 2.6 Schematic illustration of young and aged black carbon aerosols (after Cachier, 1998).

The molecular structure and origin of a particle also influence its shape, as the surface and shape of a particle influences on the particle nucleation-accumulation activity. For example, carbon

compounds discharged during combustion tend to form convoluted, fractal-like structures (complex branched chains), whereas fly ash and pollens are present as distinct spheres. Chemicals such as potassium and chloride, often evident as inorganic salts, are present as angular, crystal-like structures. Ionic activity of the secondary formed PM fraction also influences the shape of fine PM. Coarse crustal particles usually have a regular or crystal shape, while complex particles tend to be some kind of compact or chain agglomerates (Lee and Chou, 1994).

Numerical representation of fine and coarse PM shape is very important for description of particle origin and activity (like in photochemical models). Accurate reproduction of aerosol shape variation is therefore important for retrieval of aerosol scattering information from satellite measurements. More realistic numerical representation of PM shape is also of prime importance for absorption-scattering (micro-climate function) aerosol numerical modelling. Chen et al. (2001) in their research of PM in Taipei City, Taiwan selected 15 typical particles and stipulated calculated fractional dimensions for the particle boundary (D_{b2}), projected area (D_p), and surface texture (D_r). The calculated fractional dimensions are further identified in the coordinate system illustrated in Figure 2.7. A high fractional dimension value based on the particle boundary implies a kinky periphery, while a more compact particle exhibits a value close to 2 in fractional dimension based on projected area. The third fractional dimension, based on particle surface structure, deviates more from 2 as the particle shape differs further from a smooth surface. Based on the calculated fractional dimension, particles 1 to 9 of the selected 15 typical particles (Chen et al., 2001) all attribute a less kinky periphery, a compact structure, and a rugged surface. Meanwhile, beginning from number 10, particle boundaries tend to be kinkier and have a boundary value much higher than 1. The fractional dimension based on projection area is similar for most particles; although particle 13 is less compact, resulting in a value of 1.64 (Chen et al., 2001).

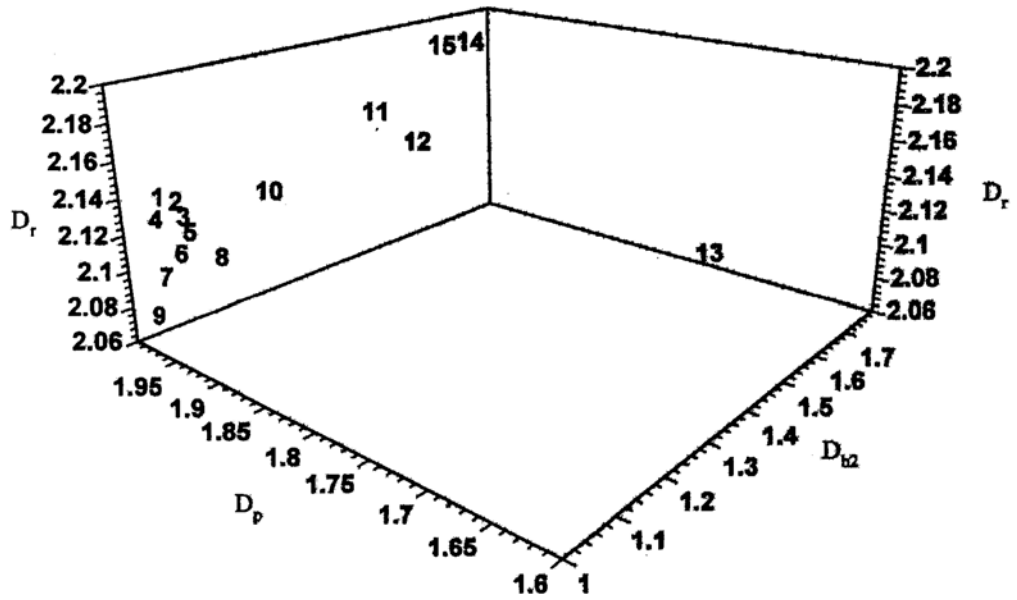

Figure 2.7 Aerosol fractal dimensions from particle boundary (D_{b2}), projected area (D_p), and surface texture (D_r) distributed in a coordinate system (after Chen et al., 2001).

The system applied by Chen et al. (2001) may be developed in future work through application of greater diversity of PM particles of different origins, and as a result of more diverse 3-D or maybe 4-D space (including mass concentration). Such 3-D particles description can be used for PM shapes numerical visualisation and for visual research.

2.4 Impact of PM

Coarse and fine particles, present in outdoor (and in indoor) ambient air adversely affect both human and animal health, cause vegetation damage, soil degradation, corrode cars and buildings, and degrade visibility. PM also influences on microclimate, first of all through the acceleration of coagulation and formation of droplets under conditions of high concentration of PM in accumulation mode. Activation of precipitation by high values of fine PM leads to change of local precipitation run-off and bio-diversity. Degradation of visibility due to increased atmosphere optical thickness (AOT) directly correlates with re-distribution of net radiation flux density.

Efforts to understand and mitigate the effects of air pollution on human health and welfare have a rich and interesting history. By the 1970s and 1980s, attributed largely to earlier well-documented increases in morbidity and mortality from extreme air pollution episodes, the link between cardiopulmonary disease and very high concentrations of particulate matter air pollution was generally accepted (U.K. Ministry of Health, 1954). There remained, however, disagreement about

what levels of PM exposure and what type of PM affected human health. Several prominent scientists concluded that there was obvious evidence of substantive health effects at low-to-moderate particulate pollution levels (Holland et al., 1979). Others disagreed and argued that particulate air pollution may adversely affect human health even at relatively low concentrations (Shy, 1979).

In 1996, the last US air quality criteria document on particulate matter was published and in the same year review of the literature for the revised version of the WHO air quality guidelines for Europe were finished, although the document was published only recently (WHO, 2000). At the same time, WHO decided not to propose an Air Quality Guide (AQG) for PM as it was not possible to identify maximum long-term and/or short-term average concentrations protecting public health. Exposure-response relationships are based on the notion that a threshold below which no effect on health is expected tends to zero. Since then a large number of new epidemiological studies on nearly all aspects of exposure and health effects of PM have been completed. These have added greatly to the available knowledge, and therefore reconsideration of the current WHO AQG (WHO, 2000) is justified. The United States Environment Protection Agency has compiled recent literature in a new Criteria Document that is currently still being reviewed and finalized (USA EPA, 2002). In Christchurch, the potential for substantial human health and amenity effects is considerable as a consequence of high $PM_{2.5}$ concentrations for winter time (Scott, 2005).

Fine particulate matter ($PM_{2.5}$) health effect

Public health policy, in terms of establishing guidelines or standards for acceptable levels of ambient PM pollution (WHO, 2005) has focused primarily on indicators of fine particles ($PM_{2.5}$), inhalable or thoracic particles (PM_{10}), and thoracic coarse particles ($PM_{10-2.5}$). With regard to $PM_{2.5}$, various toxicological and physiological considerations suggest that fine particles may play the largest role in effecting human health. For example, $PM_{2.5}$ components may be more toxic because they include sulphates, nitrates, acids, metals, and particles with various chemicals adsorbed onto their surfaces. Furthermore, relative to larger particles, $PM_{2.5}$ can be breathed more deeply into the lungs, remain suspended for longer periods of time, penetrate more readily into indoor environments, and are transported over much longer distances.

Particle properties, such as size, shape, density and reactivity, determine how particles are transported; react in the human respiratory tract and impact on health. PM_{10} is generally exhaled

but (like the fine aerosol particles) can penetrate deeply into the lung. Individuals most at risk include those with chronic lung disease, asthmatics, infants and the elderly. Health effects range from minor irritation of the eyes and nose, to exacerbation of existing respiratory and cardiac illnesses among young children and the elderly. It seems unlikely that relatively small elevations in exposure to particulate air pollution over short periods of only 1 or a few days could be responsible for very large increases in death. In fact, studies of mortality and short-term daily changes in $PM_{2.5}$ have observed small effects. For example, short-term elevation of $PM_{2.5}$ of 10 $\mu g\ m^{-3}$ is said to result in 1% increase in mortality (Pope and Dockery, 2006). Based on the average death rate for the United States in 2000 (8.54 deaths/1000 per year), a 50 $\mu g\ m^{-3}$ short-term increase in $PM_{2.5}$ would result in an average of only 1.2 deaths per day in a population of 1 million (compared with an expected rate of 23.5/day).

By 1997, two cohort-based mortality studies reported evidence of mortality effects of chronic exposure to fine particulate air pollution. The first study referred to as the Harvard Six Cities Study (Dockery et al., 1993) reported on a 14- to 16-yr prospective follow-up of 8000 adults living in six U.S. cities, representing a wide range of pollution exposure. The second study, referred to as the ACS study, linked individual risk factor data from the Cancer Prevention Study II with national ambient air pollution data (Pope et al., 1997). The analysis included data from 500,000 adults who lived in 151 metropolitan areas and were followed prospectively from 1982 through 1989. Both the Harvard Six Cities and the ACS cohort studies used Cox proportional hazard regression modelling to analyze survival times and to control for individual differences in age, sex, cigarette smoking, education levels, body mass index, and other individual risk factors. In both studies, cardiopulmonary mortality was significantly and most strongly associated with sulphate and $PM_{2.5}$ concentrations. In both the Harvard Six Cities and the ACS prospective cohort studies, the estimated effects for all-cause and cardiopulmonary mortality were relatively stable across different analyses (Pope and Dockery, 2006).

Neither short-term studies nor long-term studies were designed to evaluate alternative time scales of exposure. These studies were designed primarily to exploit observable sources of exposure variability. Short-term temporal variability is examined in daily time series studies. In most of these studies, various approaches are used to focus only on short-term variability while taking out or controlling for longer-term temporal variability, such as seasonality and time trends. Thus, by design, opportunities to evaluate effects of intermediate or long-term exposure are largely eliminated. The major prospective cohort studies have been designed primarily to exploit this

much longer-term spatial variability. Efforts to estimate the dynamic exposure-response relationship between $PM_{2.5}$ exposure and human response must integrate evidence from long-term, intermediate, and short-term time scales (Roosli et al., 2005). The European Community Respiratory Health Survey II (ECRHS II, WHO, 2005) is a cohort study addressing long-term associations of air pollution with respiratory health among adults. Twenty-one European communities took part in this study, which assessed the association of ambient air quality with both respiratory mobility and lung function. The main aim was to assess the health effects of those pollutants for which exposure can be sufficiently well characterized by a single monitor, in particular $PM_{2.5}$ (Gotchi et al., 2005).

Health studies held in Christchurch confirm that effects documented overseas also occur in New Zealand (Scott, 2005). It is estimated that for every 10 $\mu g\ m^{-3}$ increase of PM_{10} gives 1% increase in "all-cause" mortality and a 4% increase in respiratory morbidity occurs (Hales *et al.*, 1999; Wilson and Zawar-Reza, 2006). Based on these studies, it was estimated that 40-70 deaths per year may be associated with high PM_{10} concentrations in Christchurch (Wilton, 1999).

Health effects of $PM_{2.5}$ (Pope and Dockery, 2006) include: (1) long-term exposure results in acute exposure and exacerbates existing pulmonary disease; (2) pulmonary and systemic oxidative stress, inflammation, atherosclerosis, and related cardiovascular disease; (3) adverse changes in cardiac autonomic function; (4) vasculature alterations, including vascular tone and endothelial function; (5) systemic translocation of PM and prothrombotic effects; (6) modulated host defences and immunity; and (7) PM-induced lung damage, declines in lung function, respiratory distress, and hypoxemia. Incomplete but intriguing evidence provides several hypothetical and interdependent mechanistic pathways that could plausibly link $PM_{2.5}$ exposure with cardiopulmonary morbidity and mortality.

Coarse particulate matter ($PM_{10-2.5}$) health effect

The extension of the ACS study (described in the previous section) has found statistically significant increases of relative risks for $PM_{2.5}$ for all causes, cardiopulmonary and lung cancer deaths. But total suspended particles (TSP) and coarse fraction of aerosol ($PM_{10-2.5}$) were not significantly associated with mortality (Pope et al., 2002). Since routine monitoring methods for the coarse fraction of PM number concentration are not yet established to compare with total and fine PM measurements, it is important to maintain established PM_{10} monitoring programmes for a

number of years. While estimates of $PM_{10-2.5}$ from the algebraic difference of PM_{10} and $PM_{2.5}$ measurements have a high degree of imprecision, especially when $PM_{2.5}$ is a major fraction of the PM_{10} concentration (like in Christchurch), the resulting estimates of $PM_{10-2.5}$ can still be informative about the mass concentration of coarse PM. They can also be useful for refinement of new methods that can provide future monitoring data simultaneously on fine, coarse and total PM for verification and calibration of the measuring equipment.

Quite a few studies suggest that fine PM is more biologically active than coarse PM (McDonnell et al., 2000), but other studies have also found that coarse PM is associated with adverse health effects (Ostro et al., 1999; Lippmann et al., 2000). The relative importance of fine and coarse PM may depend on specific sources present in some areas but not others.

Possibly relevant chemical characteristics include transition metals, crustal material, secondary components such as sulphates and nitrates, polycyclic aromatic hydrocarbons and carbonaceous material, reflecting the various sources that contribute to PM in the atmosphere. In general, fine PM consists to a large extent of primary and secondary combustion. Coarse PM usually contains more crustal material such as silicates. So far, no single component has been identified that could explain most of the PM effects. Studies from Utah Valley have suggested that close to steel mills, transition of metals could be important (Soukup et al., 2000; Barnett et al., 2000).

On a mass basis, small particles generally induce more inflammation than larger particles, due to a relatively larger surface area. The coarse fraction of ambient PM may, however, be more potent to induce inflammation than smaller particles due to differences in chemical composition (Soukup and Becker, 2001). The bacterial endotoxins (lipopolysaccharides), known to exert inflammatory effects, are virtually ubiquitous and have been shown to be present in both indoor and outdoor PM, but mainly in the coarse ($PM_{10-2.5}$) fraction (WHO, 2005). The endotoxins may contribute to the health effects of urban air particulates, although this has not been shown at lower concentrations. As mentioned before, recent evidence has implicated endotoxin especially in the biological activity of coarse PM (Becker et al., 2002).

Visibility effect

Coarse and fine aerosol (natural and anthropogenic PM) viewed at a distance can degrade visibility and reduce amenity, even at low concentrations. Visual impacts occur as a consequence of visibility reduction or degradation, which is defined by the USEPA (1999) as:

Visibility: The ability to see an object or scene as affected by distance and atmospheric conditions; to perceive form, colour and texture. Visibility Reduction: The impairment or degradation of atmospheric clarity. It becomes significant when the colour and contrast values of a scene to the horizon are altered or distorted by airborne impurities.

The ability of an observer to view an object is determined by the optical properties of the atmosphere (optical thickness first of all), the amount and distribution of light, characteristics of the object being viewed and properties of the human eye (Seinfeld and Pandis, 1998). Visibility is impacted by PM when light is scattered and absorbed by fine and coarse particles (liquid and solid), and gases that lead to haze formation.

Visibility degradation has become a problem of public concern in most metropolitan areas in recent years. Visibility degradation is not just an amenity problem, but also a visual indicator of air quality. It is often considered to be a primary and general index of ambient air quality in an urban area (Watson, 2002). Atmospheric visibility impairment is attributed mainly to the scattering and absorption of visible light by gaseous pollutants (such as NO_2), as well as by suspended fine particles in the ambient atmosphere; and among them, PM light scattering has often been found to be the dominant cause of light extinction in urban areas (Chan et al., 1999). Diverse studies revealed that the size, chemical composition, and concentration of airborne particulate matter substantially affect visibility (Malm and Pitchford, 1997). Fine particulate matter is believed to be responsible for the degradation of visibility by aerosols (Sloane et al., 1991). Although the extinction of light from gas species can also impair visibility, such species have been shown to have a much weaker influence. Meanwhile, meteorological factors, especially humidity, also contribute to degrade visibility (Tsai and Cheng, 1999).

After rapid population growth and increasing industrialization over the past three decades, poor ambient air quality has become one of the major environmental concerns of the general public in many urban and metropolitan areas, industrial cities like Kaohsiung City (Lee et al., 2006), residential cities like Christchurch (Wilson and Spronken-Smith, 2002), and megalopolises like Mexico city (Chow et al., 2002). Visibility reduction is considered to be a significant issue in areas

such as the United States (US) where legislation has been introduced to protect visibility in areas of great scenic importance (such as national parks and reserves). An amenity review of the issues in New Zealand found that degraded visibility, in the form of brown or white haze, is evident over cities such as Christchurch and Auckland (Environet Ltd, 2003). Accordingly, it was suggested that it may be appropriate for a national visibility or guideline standard to eventually be introduced.

A new visibility study was conducted in Christchurch during 2000/2001 to investigate the origin of haze in the city (Wilton, 2003). This haze was evident in the winter months, and frequently obscured views to the Port Hills and Southern Alps. Fine particles were the greatest contributors to reduced visibility, and visibility was worse on days when $PM_{2.5}$ was elevated (Wilton, 2003). Haze was also present on days when $PM_{2.5}$ concentrations were low, and did not cause a significant health effect. This suggests that amenity in Christchurch may be affected at very low concentrations, given a background of clean air and very good visibility. The study also concluded that motor vehicles and secondary particles could be the most significant contributors to daybreak urban haze, especially when near-surface temperature inversions occur. The visibility study raised some important issues that may need to be addressed in future management strategies. Knowledge of the spatial and temporal $PM_{2.5}$ and PM_{10} distribution is essential for visibility reduction analysis. Also, it is very important for the evaluation of possible future scenarios using the numerical modelling technique, which can help better in investigation of the tendency in atmospheric visibility in relation to PM pollution abatement management strategies.

Microclimate effect

Airborne PM is known to influence microclimate through acceleration of coagulation and droplet formation (aggravating precipitation) in PM accumulation mode (Figure 2.3), affecting atmosphere optical thickness, which directly correlates with re-distribution of the net radiation balance and degradation of visibility. Also, ultrafine particles/aerosol penetrates into the stratosphere. The length of time an ultrafine particle remains suspended in the atmosphere (residence time) is a direct function of particle size and altitude. The Intergovernmental Panel on Climate Change (IPCC, 2001) estimated the direct and indirect impacts of aerosols on the global radiative forcing at the top of the atmosphere to be similar orders of magnitude, almost compensating the effect of CO_2. This is illustrated in Figure 2.8 that shows that fine particles can have a residence time of several years.

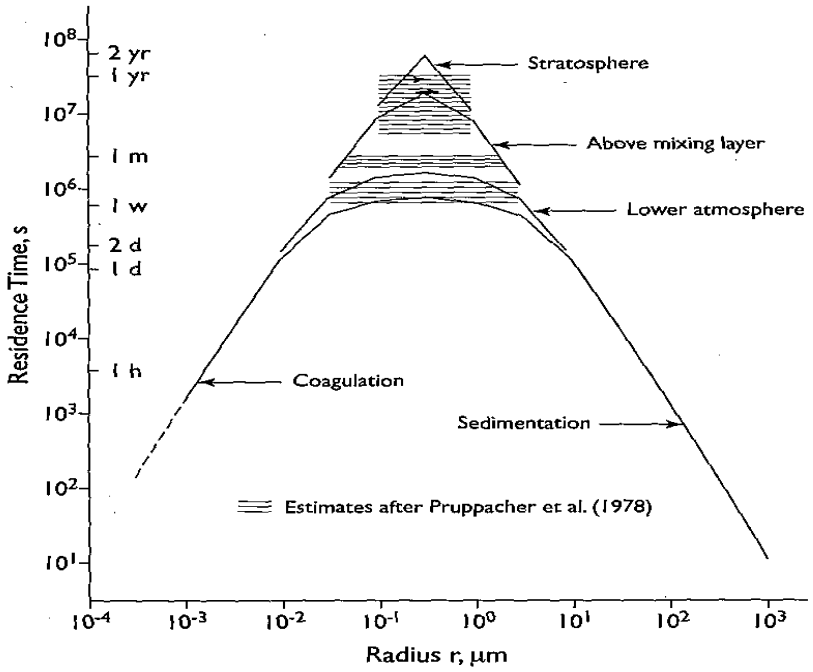

Figure 2.8 Residence time in relation to particle size and altitude (Koutrakis and Sioutas, 1996).

The problem of the greenhouse effect is not a microclimate problem but the global pollution is the integration of local and micro-scale pollution routine events associated with industry, urbanisation and agriculture (Ford-Robenson et al., 1999; Beniston and Stephenson, 2004).

The effect of aerosol pollution (especially the fine fraction – $PM_{2.5}$) on re-distribution of precipitation in the wake zone of urban regions is well-known and is investigated mostly for urban-industrialized zones situated not too far from complex topography with mountains. Induced activation of accumulation-droplet phase by aerosol in the atmosphere leads to an artificial increase of precipitation on the windward side of a mountain, and produces a deficit of precipitation on leeward side. Such situations are well described for winter time in the Rocky Mountains and Snowdonia (Jirak and Cotton, 2006; Dore et al., 2006), and also in summer-time for low mountains over southwest Germany (Kunz and Kottmeier, 2006a, 2006b). Acceleration of the coagulation-droplet process creates prematurely excessive rain and insufficient snow in the mountains in the aerosol wake zone. Applications of 2-D modelling to cases of heavy precipitation reproduction over low mountains (Kunz and Kottmeier, 2006b) show that artificial redistribution of rain leads to up to 50% deficit of rain water on the leeward side of a mountain, which dramatically influence the local microclimate.

PM increase influences the net radiation balance in urbanized areas leading to increase of average temperatures and mitigation of temperature peaks during night time and to intensification of so-called heat islands (Arya, 1999; Sarrat et al., 2006). Under certain circumstances aerosol created additional heating can lead to acceleration of locally induced circulations or breezes, as in Houston area (Nielsen-Gammon, 2003), producing heat pump responding of re-circulation of anthropogenic pollution over several days.

2.5 Methods of observed PM analysis

As mentioned in former paragraphs fine ($PM_{2.5}$), coarse ($PM_{10-2.5}$) and total PM_{10} values are comprised of numerous chemical compounds and often a synthetic secondary product of anthropogenic and natural sources. Basic methods of PM analysis include first of all chemical analysis (described in Section 2.2) and source identification. Complex statistical analysis (as a result of compiling observations) is very important for investigating any spatial and temporal trends of PM emissions. Any temporal and spatial trend should be founded on emission inventories for an emission group, including emission group PM precursors (Kawamoto et al., 2004). Emission inventories should be consistent for all PM groups in time.

Chemical composition of the outdoor total (PM_{10}), fine ($PM_{2.5}$) and coarse ($PM_{10-2.5}$) fractions of the aerosol obtained using complex and expensive equipment is an essential part of contemporary studies of aerosol chemistry in different geographical areas (Ho et al., 2003; Dan et al., 2004; Chow et al., 2005; Duan et al., 2006). Improved understanding of the origin and chemical composition of ambient levels of particulate material (PM) in the air has been gained by large air pollution projects and experiments (Spronken-Smith et al., 2001; Kossman and Sturman, 2002; Minvielle et al., 2004; Baertch-Ritter et al., 2003; Arnold et al., 2004), and local aerosol pollution studies (Putaud et al., 2004; Senaratne et al., 2005; Glasius et al., 2006), they often involve detailed investigation of the chemical composition of PM (Senaratne 2003; Scott and Gunatilaka 2004; Sun et al., 2004; Senaratne et al., 2005; Borrego et al., 2005; Wu et al., 2006). Such experiments, involving measurement and subsequent analysis of the chemical composition of PM, require highly technical field sampling and laboratory analysis, which time-consuming and expensive (Fung et al., 2002; Chow et al., 2005).

Once the chemical composition of PM has been obtained it is usually used to identify the most important sources of natural and anthropogenic PM (Senaratne et al., 2005; Scott 2005; Ho et al.,

2006). There are two key methods used to identify sources and quantify their contributions to fine particle emissions or concentrations. These are emission inventories and receptor models. The most appropriate method used internationally for a diversity of analytical and numerical purposes, is to identify pollutant sources and estimate relative contributions to PM using an emission inventory (Scott and Gunatilaka, 2004). Emission inventories allow identification and quantification of PM sources so that emission control strategies can be established (Scott, 2005). Inventories identify the main sources contributing to ambient aerosol emissions and provide a breakdown of the sub-sources within each category. This information allows air quality managers to identify problem sources and introduce measures to reduce PM emissions from those sources. Inventories can also assist with identifying previously unknown sources of PM. Emission trends may be established over time (when consistent inventory methodologies are used between years), thus enabling the effect of air quality strategies on emissions to be evaluated (Mobley et al., 2003; Hogrefe et al., 2003; Scott and Gunatilaka, 2004).

Source apportionment methods, that directly relate source emissions to quantitative impacts on measured PM concentrations, have been developed for many years. Most widespread between them, receptor modelling is a cost-effective diagnostic technique (Colvile et al., 2003; Lewis et al., 2003; Senaratne et al., 2005). It takes speciated concentrations measured at a receptor (or point of impact) and works in reverse to determine the contributions of sources to measured concentrations. The relationship between measured concentrations and emission sources is inferred, without the need for simulating dispersion processes, as the model works directly with concentrations rather than emissions. The information required to conduct receptor modelling is simply knowledge of the chemical composition of particulate concentrations at the source and receptor. Additional information such as meteorology, topography, location and magnitude of sources, while useful for interpretative purposes, is not vital (Seinfeld and Pandis, 1998). One of the weakest aspects of receptor modelling is an impossibility to analyse sources of secondary aerosol (Lewis et al., 2003). Also, the source appointment technology is 1-D, without allowing a choice of accurate spatial representation of the PM emission sources (Hwang and Hopke, 2007).

2.6 Summary

Particulate matter (PM) exists in many different shapes and sizes, which explicitly can provide an indication of source origin, formative mechanisms, life time and impact. The most common characteristic used to classify particles is equivalent aerodynamic diameter or size. Particles are usually found in the fine $PM_{2.5}$ fraction (PM < 2.5 μm) or coarse $PM_{10\text{-}2.5}$ fraction (10 μm >PM>2.5 μm) modes. Fine particles are generally of combustion origin and include both primary and secondary (formed through chemical reactions in the atmosphere) particles. Coarse particles are produced by mechanical processes and only remain in the atmosphere for short periods of time or are reduced to a fine fraction by processes of fracture (e.g. abrasion). Chemical composition of PM dominantly consists of organic and elemental carbon, nitrate, sulphate, ammonium, potassium, sodium, chlorine, iron, aluminium, silicon, sulphur, biological spores, fungus and debris. Fine particles are of greatest concern in contemporary research, due to their extended atmospheric retention time, ability to actively penetrate into the human blood and lungs (resulting in significant health effects), capacity to scatter light contributing to visibility degradation (amenity effects), and because of their ability to cause climate change over a range of cases. Management of fine and total PM is necessary to protect community health, especially in areas with a high long-term PM load. Scientific research into PM emissions and concentrations and their spatial and temporal variation includes (except numerical methods) different scales of observation programmes and networks. Development and active improvement of statistical (emission inventory) and source appointment methods of airborne aerosol appraisal is very important for an understanding of the sources contributing to outdoor PM concentrations.

Chapter 3: Numerical evaluation and modelling methods

Several different modelling approaches and techniques are being explored today to investigate spatial and temporal variations of PM. They include different model types that consist of empirical, statistical, neural network, Gaussian, Lagrangian, physical/numerical/chemical and Geographic Information System (GIS) components (Beyea and Hatch, 1999**)**. However, all improvements in research and development in computer technology have moved aerosol air pollution modelling towards more complex 3-dimensional numerical models, often based around limited area airflow models (LAM), coupled with atmospheric dispersion modules with a range of chemical processes.

3.1 Applications of numerical modelling

Numerical models are major tools used in both improving knowledge of atmospheric processes and the application of this improved knowledge to human activity such as in air pollution studies. Numerical models can be used to reduce the impacts of the atmosphere on humans (e.g. day-to-day weather forecasting and longer term climate prediction), as well as making the most of the micro-climate environment for rural and urban landscapes. The most advanced atmospheric numerical models are those based on the physical equations that are used to describe fundamental atmospheric processes (Smagorinsky, 1983; Manabe, 1985**)**. These have evolved and developed rapidly over the last three decades due to advances in computer technology, and allow down-scale interaction in time, and coupling with complex atmospheric chemistry models (Sturman, 2000; McGruffie and Henderson-Sellers, 2001**)**. Complex chemistry 3-D Eulerian photochemical modelling has significant potential to improve our knowledge about human activity and its impact on the environment at different spatial and time scales: from long-range transport of air pollution and dust at spatial scales about several hundred kilometres over several days to airborne PM emissions and concentration in a district or a street canyon (Byun and Ching, 1999; Michelson *et al*., 2002**)**.

3.1.1 Prognostic modelling systems

In the second part of the 20th century only the meteorological organizations in a few countries (e.g. the United States, the Soviet Union, Japan, Great Britain, France, Sweden, Australia and Canada) had the ability to create their own global atmospheric models (GAM). However, various problems limited the extent of development of global numerical atmospheric models for researching

different kinds of meteorological–environmental phenomena. These problems were mostly technical and associated with restricted access to powerful computers, restricted computer speed, and the absence of reliable gridded input data (Smagorinsky, 1983). Also, it was nearly impossible to investigate meso- and local scale atmospheric circulations using global numerical models.

Theoretical formulation and numerical realization of limited area models using nested grids has provided a great tool for researchers all over the world, who can now take a regional modelling approach, evaluated using local observations, for modelling a range of local climate situations (Sturman, 2000). Reviews of regional meteorological and chemical modelling have been provided by many authors from different countries (Arya, 1988; Russel, 1997; Arya, 1999; Sturman, 2000; McGruffie and Henderson-Sellers, 2001). Local and regional meteorological models have been developed to simulate the atmospheric processes that control air pollution dispersion conditions (Dudhia and Bresh, 2000; Klausmann *et al.,* 2001; Kotroni *et al*., 1999; Dailey and Keller, 2002; Low-Nam and Davis, 2002). Three-dimensional prognostic pollution chemistry models have been developed with the growth of three-dimensional prognostic, mesoscale meteorological models (Russel, 1997). Limited area meteorological models are now commonly used to provide meteorological fields with the purpose of estimating urban air pollution, especially over complex terrain dominated by local air circulations (Souto *et al.,* 1998).

Meteorological models

Global Atmospheric Models (GAM) started to develop in the late 1960s based on the system of primitive hydrodynamic equations transformed to finite-difference form using time schemes with different levels of precision (Pedlosky, 1979; Manabe, Hahn, 1981)**.** Nowadays, global models are run on super computers with speeds of about several teraflops (n x 10^{14}), because of the enormous number of grid nodes (due to increased spatial and temporal resolution), which allow global models to be applied over a wide range of scales.

Many problems have limited the extent to which research groups could develop global atmospheric models for modelling meteorological-environmental problems:

1. Complex numerical global models with a spatial resolution better than 110 km (about 1^{o} of longitude at 45° latitude) require huge computer resources, although the situation is improving because of technological developments

2. The development of global models requires a global network of meteorological data that has to cover the whole Earth using a grid that is regular in space and time. This situation has been improved by using meteorological satellite data, but has not been properly resolved
3. The resolution of global models did not allow them to represent accurately regional and local scale meteorological and pollution situations that included the effects of complex terrain (Krishnamurti *et al*., 1984).

All these problems led to the appearance of limited area models (LAM); firstly, as part of a global model (as a nested grid) and then as completely independent numerical models with a theoretically unlimited number of nested grids (Pielke, 1984; Pielke *et al.,* 1992). The theory and practice of using nested grids in mesoscale models to investigate more accurately the different scales of phenomena in meteorology, climatology and environment pollution started to develop very rapidly in the middle of the 1980s (Dudhia, 1993). The possibility to research small-scale features using limited area models in different geographical areas all over the world has been an outstanding step in the development of regional numerical modelling. Local models with regional initial data have been used for a lot of special meteorological purposes (Dudhia and Bresh, 2000; Klausmann *et al.,* 2001; Dailey and Keller, 2002; Low-Nam and Davis, 2002; Miranda and Borrego, 1996; Smallcomb, 2002; Someshwar *et al.,* 2002; Spronken-Smith *et al.,* 2004). Global and regional modelling are now two essential parts of one main aim, to investigate atmosphere circulation across the whole range of scales.

The practice of using nested grids in mesoscale models to investigate more accurately the different scales of phenomena in meteorology, climatology and environment pollution started to develop very rapidly in the middle of the 1980s (Dudhia, 1993). The global meteorological community now has the possibility to install and adjust regional numerical models. MM 5 and WRF can be downloaded free from the big national and international meteorological research centres. These centres have started to accumulate the results of research undertaken by local scientific groups, to use these results for additional improvement and development of regional models and for the improvement of global numerical atmospheric models for better weather prediction. Numerical regional modelling is now possible in every atmospheric research department that has basic computational resources. For example, in New Zealand five scientific centres use various versions of mesoscale model - MM5 (McKendry, 1989; McGill, 1987), and more than 10 institutes use some other kind of regional weather prediction model (WPM), such as TAPM (The Air Pollution Model) or RAMS (Regional Atmospheric Modeling System) (Spronken-Smith *et al.,* 2004). MM5

and WRF are considered to be the most widespread limited area models among the international modelling community. RAMS has been actively used in New Zealand (NIWA) but had not become so widespread as it was not a free domain for a long time and became a free distributed only in 2006 (RAMS was installed on Sun station "Tornado" by M.Titov in September 2007).

Air quality models

Photochemical numerical models started to develop approximately at the same time as the meteorological limited area models (Arya, 1999) as they use meteorological information from these models (especially in the planetary boundary layer-PBL - Arya, 1988; Oke, 1978) as an input for analysis of different kinds of case study. Examples include the influence of pollen on asthma increase (Pietrowicz, 2002), as well as such global problems as ozone layer migration and of its depletion in the middle stratosphere (Goldfrey, Clackson, 1998), regional tropospheric ozone concentration research (Stein *et al*., 2000), scenarios of nuclear winter resulting from nuclear war, and the effects of reactor accidents such as the Chernobyl catastrophe (Ackermann *et al.,* 1998). Limited area and Eulerian dispersion models play a dominant part in chemical-air pollution models (Russel, 1997). Some pollution models can be applied to the entire hemisphere (e.g. Modal Aerosol Dynamic model for Europe – MADE and the variable grid Urban Airshed Model system – UAM-V) and include a well-developed plotting, visualization and decision support system (CAMx can be used with Environment Decision Supporting System – EDSS that includes Plotting, Analysis and Visualization of the Environmental data program – PAVE).

There is also a large variety of air pollution models tuned to specific conditions to investigate a limited range of problems. The Denver Air Quality Model Version 2 (DAQM-V2) and Advanced Texas Air Quality Model (ATAQM) are good examples of such pollution models. However, most air pollution–air quality models are developed for application to study a variety of problems anywhere in the world: CAMx, MAQSIP (Multiscale Air Quality Simulation Platform), CMAQ (Community Multiscale Air Quality system), EURAD (European Air Pollution Dispersion model system) (Byun, Ching, 1999; Coats, Tryanov *et al.,* 1999; Ebel, *et al.,* 1997). All of the above-mentioned models include calculations of PM_{10} and $PM_{2.5}$ as an essential part of their chemistry mechanism compiler (CMC).

Usually, air pollution models receive meteorological information from limited area models (MM5 or WRF) or from global models (ETA, ECMWF, UKMO, NOGAPS – Navy Operational Global Analysis and Prediction System) (Davis *et al*., 1998). Some chemical models have their own

meteorological module and well-developed graphic user interface (GUI) but are not the 'open-code' models, for example TAPM vX (The Air Pollution Model Version X) described in the technical report of Hurley (2002). Also it is worth mentioning that some systems have a combination of meteorological limited (global) area models with an additional chemistry module: MM5- chemistry block, WRF-chemistry block.

Coupled models

Coupling of two or more numerical models has become a normal feature of the air 'circulation–pollution' modelling systems. Classical examples are nested grids in limited area models. In these cases, so-called direct coupling between two numerical models describing different levels of the circulation can be run in parallel, exchanging results and creating multi-scale two-way interaction during a numerical experiment.

Indirect coupling means use of output results from one numerical model for use by a second numerical model (as basic input data, additional input data, correction data and correction coefficients). In such situations, we deal with so-called one-way interaction with postponed backward response. Postponed backward response means representing the indirect influence of the results of the second numerical model on a process in the first model, with the aim of achieving more finely tuned experimental results. There is no direct interaction between the two models, except through experimental repetition using corrected model parameters. The link created in most coupled meteorological and air pollution models is an illustration of indirect coupling. One-way interaction is also widespread in LAM meteorological models.

There are many examples of coupled limited area models in environmental research, such as MM5–UAM, MM5–CMAQ, MM5–CAMx, WRF–CAMx, WRF-CMAQ, MM5–DAQM (Byun and Ching, 1999; Kotroni, *et al.,* 1999; Michelson *et al*., 2002) and so on (Peters-Lidard *et al*., 2002). Depending on the aims of a particular study, the coupling methods can differ. The most consistent component of the air circulation–air pollution numerical modelling system is the use of particular limited area meteorological models. In most cases, research groups now work with MM5 or WRF. Also the WRF-chem model presents a new generation of direct coupling that includes the state-of-the-science WRF LAM and a special block of gaseous chemistry (Tie et al., 2007).

3.1.2 Emission data assimilation

Preparation of accurate emission fields for air quality models is one of the most important (if not the most important) stages of numerical modelling, in order to generate real and reliable predicted PM concentrations (Loibl and Orthofer, 2005; Levin, 2006; Miller et al., 2006; Parrish, 2006). Input gridded emission fields vitally depend on the quality of emission inventories such as that for the Christchurch area winter time pollution (Canterbury Regional Council, 1998; Titov, 2004; Zawar-Reza et al., 2006). Active treatment of the inventory data assimilation platform nowadays is quite a wide-spread practice to obtain gridded emissions. PM emissions obtained with the application of emission data assimilation platforms for different geographical locations, emission sources and seasons are actively employed (Hogrefe et al., 2003; Kawamoto et al., 2004; Barna et al., 2006a; Barna et al., 2006b).

Sparse Matrix Operator Kernel Emissions Modeling System (SMOKE) developed by the Center for Environmental Modelling for Policy Development (CEMPD) at the University of North Carolina (under protection of US EPA) is most widespread (especially in North America) emission data assimilation platform. SMOKE is an active open-source development project supported and distributed by the CEMPD through the Community Modelling and Analysis System Center (Hogrefe et al., 2003). SMOKE continues to develop and improve at the University of North Carolina, and is considered to be the fastest emissions proceeding tool available to download on-line (http://www.smoke-model.org/index.cfm). The Sparse Matrix Operator Kernel Emissions (SMOKE) Modeling System was created to allow emissions data processing methods to integrate high-performance-computing (HPC) sparse-matrix algorithms. The SMOKE system is a significant addition to the available resources for decision-making about emissions control for both urban and regional applications. It provides a mechanism for preparing specialized inputs for air quality modeling research, and is very actively used with the CMAQ numerical model (Arnold et al., 2003; Otte et al., 2005; Mao et al., 2006; Smith et al., 2006).

The SMOKE prototype, available since 1996, was an effective tool for emissions processing in a number of regional air quality modelling applications. In 1998 and 1999, SMOKE was redesigned and improved with the support of the U.S. Environmental Protection Agency (EPA), for use with EPA's Models-3 (CMAQ) Air Quality Modeling System. The primary purposes of the first SMOKE re-design were support of (1) emissions processing with user-selected chemical

mechanisms; and (2) emissions processing for reactivity assessment. In 2002, SMOKE was enhanced to develop vehicle emissions through a transport model used to create on-road mobile emission factors and to support on-road and non-road mobile toxics inventories. The latest version of SMOKE (version 2.3) features enhance processing of fire data, more streamlined processing for the CMAQ, CAMx, REMSAD, and UAM models (Hogrefe et al., 2003). SMOKE can process criteria gaseous pollutants such as carbon monoxide (CO), nitrogen oxides (NO_x), volatile organic compounds (VOC), ammonia (NH_3), sulfur dioxide (SO_2); and particulate matter (PM) pollutants such as $PM_{2.5}$ and PM_{10}. The principal purpose of SMOKE is to convert the resolution of the emission inventory data to the resolution needed by an air quality model. Emission inventories are typically available with an annual-total emissions value for each emissions source, or perhaps with an average-day emissions value (Hogrefe et al., 2003). Consequently, emissions processing involves transforming an emission inventory through temporal allocation, chemical speciation, and spatial allocation, to achieve the input requirements approved by EPA or WHO Air Quality Model (AQM). Currently, SMOKE supports area-, mobile-, and point-source emissions processing and also includes biogenic emissions (http://www.smoke-model.org/version2.3/html/ch01.html).

A principally new method of input emission field creation for aerosol and gaseous pollutants for big geographical areas with no observation network (like China or Russia) is associated with NASA TRACE-P emission project (Street et al., 2003; Street et al., 2006). Emissions taken from the NASA TRACE-P emission inventory were updated for the city of Beijing to take account of detailed local information on source strengths and locations. Control calculations of fine PM concentrations for the city of Beijing with application of CMAQ have provided realistic results and identified the potential to obtain emissions to estimate various future PM scenarios (for the Olympic Games 2008 in summer time) including the influence of local and regional aerosol pollution (Street et al., 2007).

3.2 Lagrangian particle-puff modelling

Lagrangian particle or puff models are widely used to simulate dispersion for various air quality and emergency response applications. Usually the dispersion of a pollutant is calculated by assuming either puff or particle dispersion. In the puff model, puffs expand until they exceed the size of the meteorological grid cell (either horizontally or vertically) and then split into several new puffs, each with its share of the pollutant mass. In the particle model, a fixed number of initial particles are advected about the model domain by the mean wind field and a turbulent component. The model's default configuration assumes a puff distribution in the horizontal and particle dispersion in the vertical direction. In this way, the greater accuracy of the vertical dispersion parameterization of the particle model is combined with the advantage of having an ever expanding number of particles represent the pollutant distribution (Draxler and Hess, 1998). Basic numerical principles of Lagrangian particle and puff models were founded by Austrian meteorologists who developed the atmospheric trajectory model FLEXTRA and particle dispersion model FLEXPART respectively (Stohl and Wotawa, 1994; Stohl and Wotawa, 1995; Wotawa et al., 1998).

Basic dispersion models adopted by WHO and EPA will be described in the next section, although two specific models are described here: Lagrangian random particle (LAP) dispersion model (Koracin et al., 1998, 1999) driven by meteorological input from MM5, and on-line HYbrid Single-Particle Lagrangian Integrated Trajectory (HYSPLIT) model using meteorological input from any meteorological model or NCAR/NCEP database (Draxler and Hess, 1997).

HYSPLIT 4.8 is the latest version of the complete HYSPLIT system for computing simple air parcel trajectories to complex dispersion and deposition simulations and is the result of a joint effort between NOAA and Australia's Bureau of Meteorology. Without the additional dispersion modules, HYSPLIT computes the advection (trajectory) of single pollutant particles, or of an ensemble of particles (Figure 3.1).

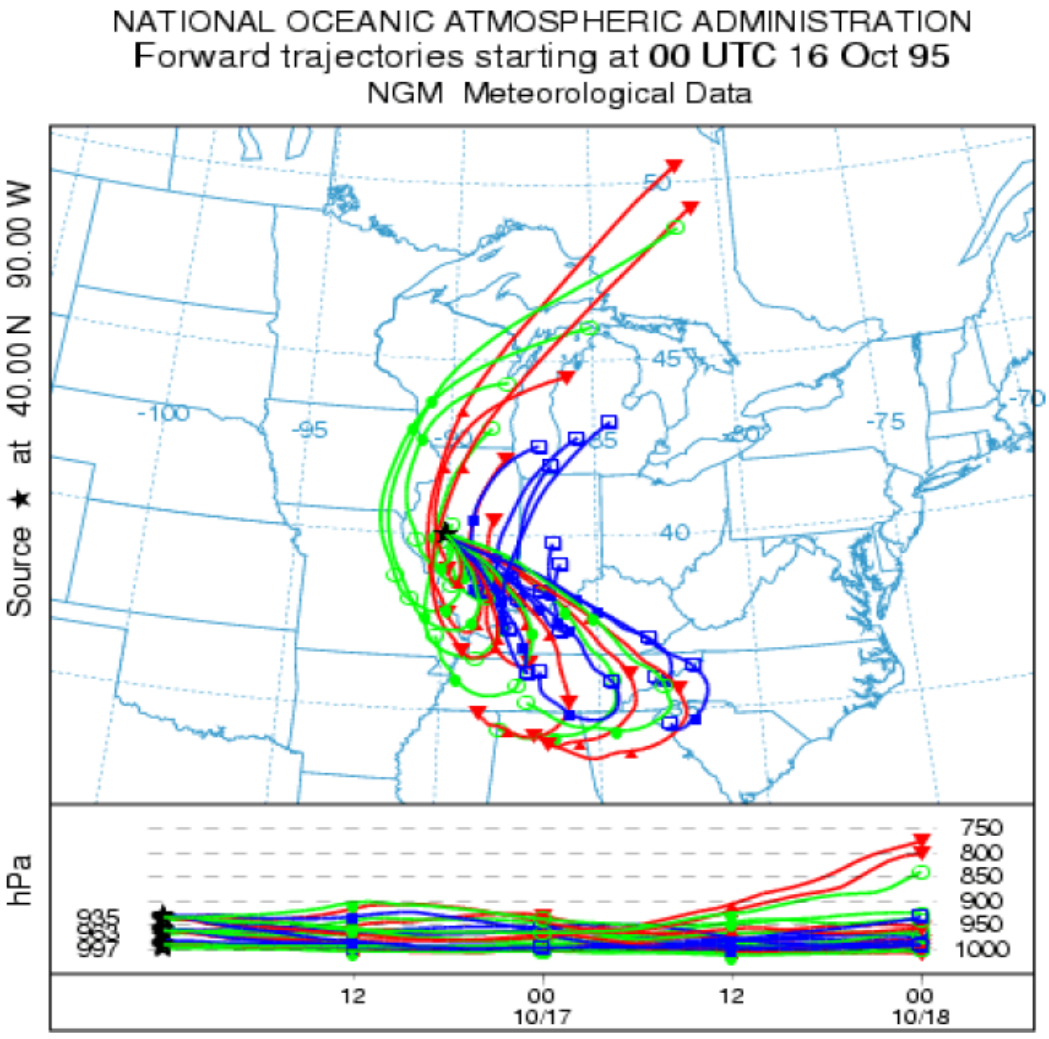

Figure 3.1 An example of the ensemble trajectory using the NGM meteorological data (the default vertical offset is about 250 m).

In case of puff dispersion the model's default configuration assumes a puff distribution in the horizontal and particle dispersion in the vertical direction (Figure 3.2).

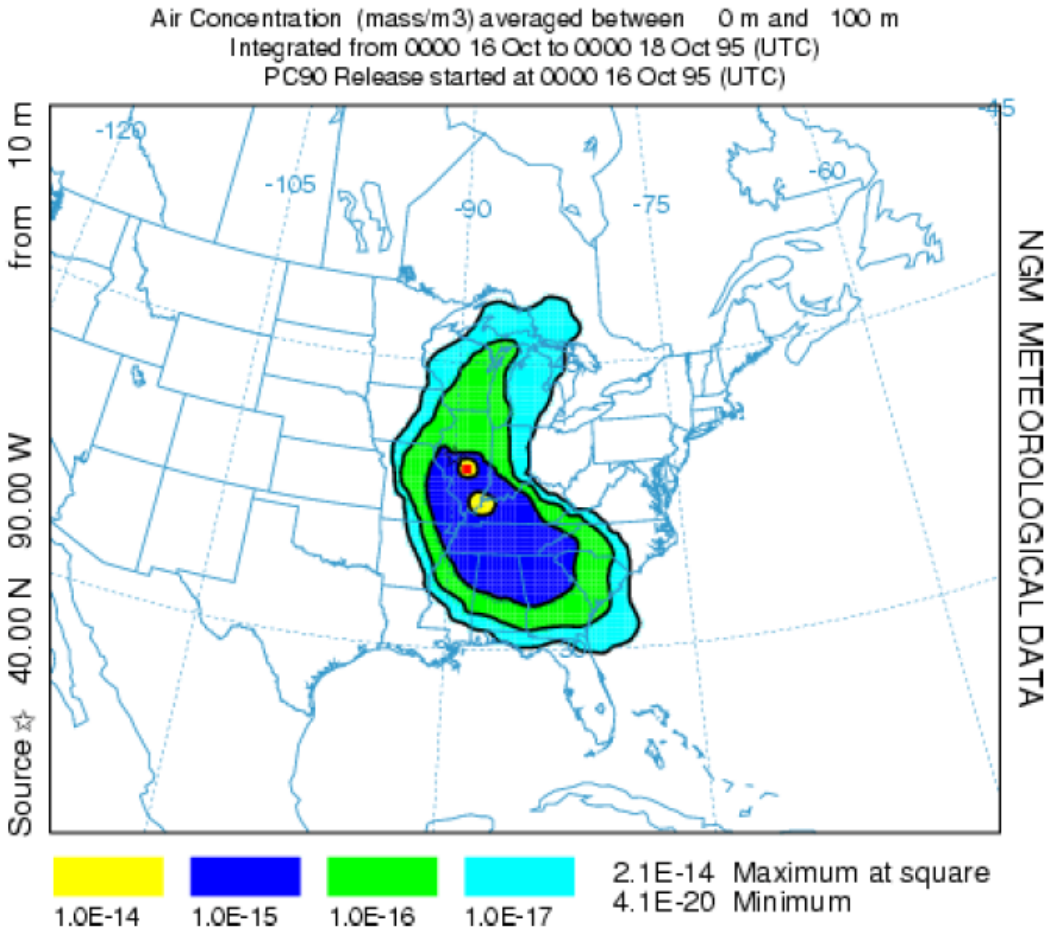

Figure 3.2 An example of the puff dispersion of HYSPLIT run using the NGM meteorological data.

The model can be run forward and backward for the trajectory version. HYSPLIT can be run interactively on the Web. The Web version has been configured with some limitations to avoid computational saturation of the web server. Big number of recent studies was done with application of HYSPLIT 4 as a basic tool to exude geographical and synoptic regional scale patterns for ozone and aerosol air pollution (Abdalmogith and Harrison, 2005; Gangoiti et al., 2006; Marenco et al., 006; Hwang and Hopke, 2007; Salvador et al., 2007).

One of the most modern applications of HYSPLIT is associated with Potential Source Contribution Function (PSCF). The PSCF is the conditional probability that a parcel with a certain level of pollutant concentrations arrives at a receptor site after having passed through a specific upwind source area (Hsu et al., 2003). In order to identify the potential locations of the regional sources of pollution, PSCF has been used in a number of studies (Liu et al., 2003a, b; Zhou et al., 2004). The PSCF values are calculated using the source contributions and backward trajectories produced by the hybrid single particle Lagrangian integrated trajectory (HYSPLIT-4) model. $PSCF_{ij}$, is defined

as $PCSF_{ij} = m_{ij}/n_{ij}$, where n_{ij} is the total number of end points that fall in the ij-th cell and m_{ij} is the number of end points in the same cell that are associated with samples that exceeded the threshold criterion. Usually the average contribution of each source is used for the threshold criterion. If a trajectory is connected to a sample which has contribution higher than a selected criterion, all sequence end points of this trajectory are considered to be high. Therefore, a high PSCF value in a cell indicates a potential source area. Cells containing sources are identified with conditional probabilities approaching 1 if trajectories that have crossed the cells effectively transport the emitted pollutant to the receptor site (Liu et al., 2003 a, b). Hwang and Hopke (2007) in order to identify the potential locations of the regional sources of pollution calculated PSCF using the mass contribution of each source and backward trajectories data. Three-day backward trajectories were calculated every 6 h four times a day at 08, 14, 20, and 02 UTC (coordinated universal time) at height of 500m above the ground level using the National Centres for Environmental Prediction/National Center for Atmospheric Research (NCEP/NCAR) re-analysis (NNRP) meteorological data. The total number of the end point was 143,664 and the geophysical region covered by the trajectories was divided into 74,880 grid cells of 0.51^0-0.51^0 latitude and longitude. An example of PSCF plot calculated for wood/fire burning factor (factor 1) is introduced in Figure 3.3 (Hwang and Hopke, 2007).

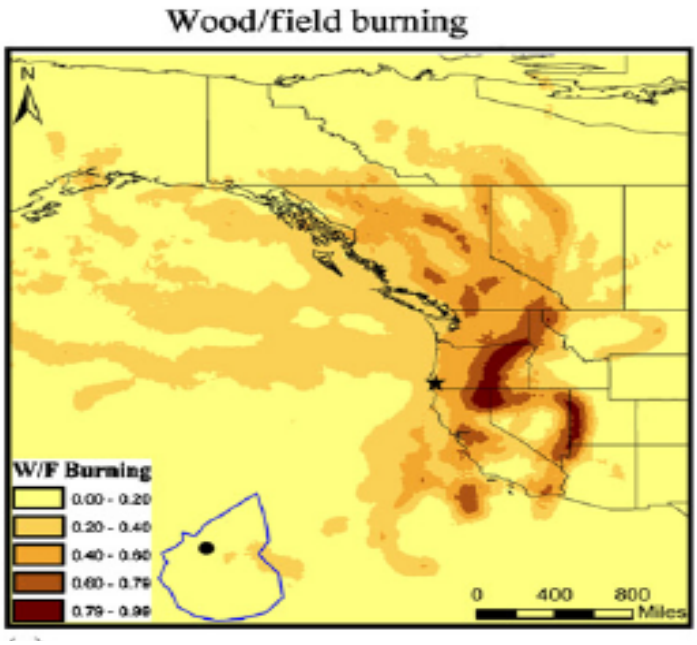

Figure 3.3 Potential source contribution function (PSCF) plot for wood/field burning source resolved by PMF in Kalmiopsis IMPROVE site (after Hwang and Hopke, 2007).

Lagrangian random particle (LAP) dispersion model (Koracin et al., 1998, 1999) is evaluated with meteorological inputs from MM5 (Grell et al., 1994). The LAP model was developed following

basic concepts of the model structure and applications described by Pielke (1984) and developed by Koracin et al. (1998, 1999). Model parameterization includes an option of spatially and temporarily variable or constant time scales, a drift correction term, a plume rise algorithm, and several optional turbulence parameterizations. Meteorological input to the LAP model includes 3D fields of U, V, and W wind components, and potential temperature simulated by MM5 (Koracin et al. 2000). Choosing different turbulence parameterizations allows estimating uncertainty due to LAP physics, and is an essential part of the model capabilities. Figure 3.4 (an example of particles release) shows the model domain including the complexity of the terrain and a top view of the simulated particle distribution for the model runs with all three turbulence parameterization options.

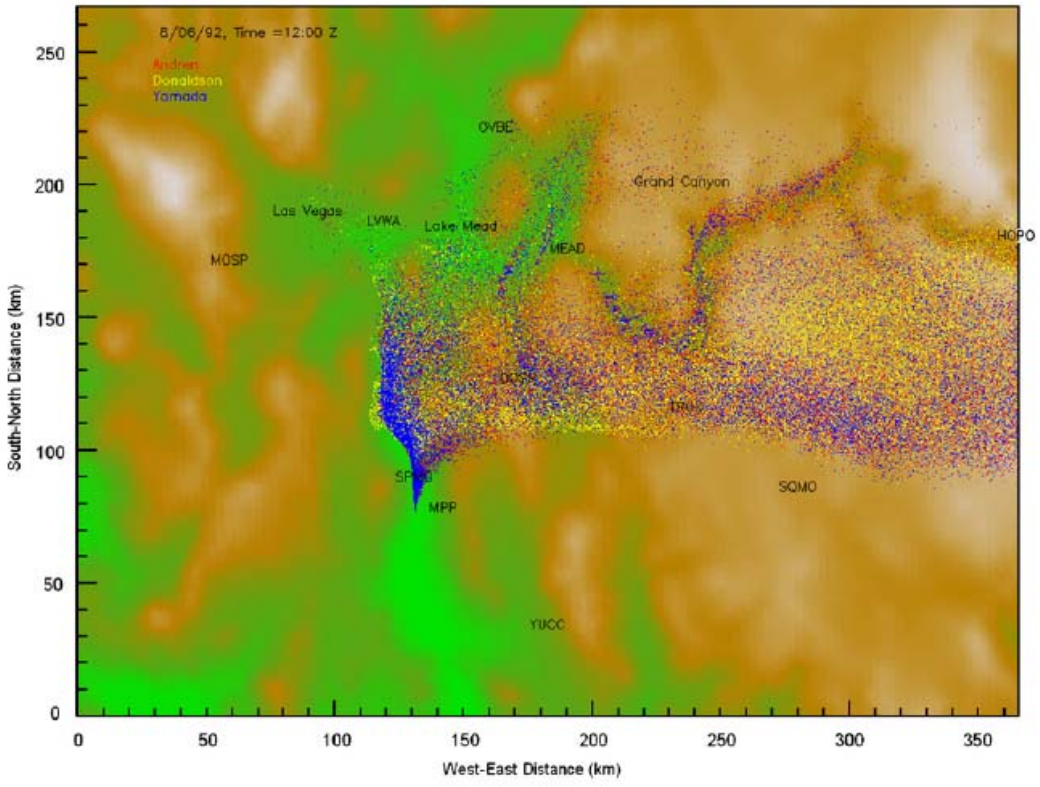

Figure 3.4 Top view of simulated particle distribution using three optional turbulence parameterizations (1-red, 2-yellow, 3-blue dots) on 6 August 1992 at 1200 UTC.

Figure 3.4 also illustrates differences in particle distribution due to the treatment of turbulence transfer with respect to channelling and particle entrapment. Therefore Lagrangian models, used to simulate dispersion (without chemistry and sedimentation) for various air quality and emergency response applications, are an essential part of PM transport-distribution research and management with application of different complexity dynamical schemes and different types of the input data for different scale (local, regional, hemispheric) processes.

3.3 Main aerosol models approved by EPA and EEA

There are atmospheric dispersion models of many different types - all sorts of simple models as well as complex models. The principal demand of the European Environmental Agency (EEA), US EPA and WHO is that a model should be fit for the purpose it is applied to. Numerous ways to classify models can be applied. The models, for instance, can be classified according to the policy issue they address: industrial pollution, urban air quality, nuclear emergencies, chemical emergencies, climate change, etc. Another option is to classify models according to model concept, like: Gaussian models, Eulerian models, Lagrangian models, receptor models, etc. There are several other schemes for the classification of dispersion models. In this section the most popular approved models are divided into 2 categories, classified based on the model's level of reproduction of real processes: state-of-science models (with full chemistry) and dispersion-transport models (with limited chemistry).

State-of-the-science models

The principal "the models should be fit for the purpose it is applied to" doesn't work in the real world, especially in the USA, where the EPA prefers to standardize and control the techniques of numerical assessment and evaluation of PM for the sake of compatibility. CMAQ is the most popular and officially adopted state-of-the-science photochemical dispersion model recommended by EPA. Models-3/CMAQ (the latest version of the Community Multi-scale Air Quality model) model has state-of-the-science capabilities for conducting urban to regional scale simulations of multiple air quality issues, including tropospheric ozone, fine particles, toxics, acid deposition, and visibility degradation (Otte et al. 2005; Smith et al., 2006). CAMx (the Comprehensive Air quality Model with extensions) being the second official model is applied to simulations of air quality over many geographic scales (Titov et al., 2007). It handles a variety of inert and chemically active pollutants, including ozone, particulate matter, inorganic and organic $PM_{2.5}/PM_{10}$, and mercury and other toxics (Hogrefe et al., 2003; Tesche et al., 2006). REMSAD (the Regional Modeling System for Aerosols and Deposition) is used to calculate concentrations of both inert and chemically reactive pollutants by simulating the atmospheric processes that affect pollutant concentrations over regional scales. It includes processes relevant to regional haze, particulate matter and other airborne pollutants, including soluble acidic components and mercury (Oanh and Zhang, 2003). UAM-V (the Urban Airshed Model with Variable grid) was a pioneering effort in photochemical

air quality modelling in the early 1970s, was used as a template for creation of CAMx, and has been used widely for air quality studies focusing on ozone (Sista et al., 2002).

The most important European photochemical dispersion models don't coincide with American ones except for CAMx that was run for the CAFÉ research programme CityDelta (Cuvelier et al., 2007). The main photochemical models chosen by the European Environmental Agency (EEA) for the project CAFÉ (Clean Air For Europe 2010) are considered to be recommended by EEA and described below (Thunis et al., 2007): REM-CALGRID (Stern et al., 2003), CHIMERE (Bessagnet et al., 2004), LOTOS (Schaap et al., 2004), OFIS (Moussiopoulos and Douros, 2005), CAMx (ENVIRON, 2004), and EMEP (Simpson et al., 2003). Each model uses its own meteorological pre-processor and boundary conditions. Some (REM, CHIMERE and LOTOS) obtain meteorology from regional-scale simulations, while others (OFIS) use values calculated with the Unified EMEP Eulerian model. All these models are photochemical models and differ in the treatment of initial-boundary meteorological conditions, in dynamical solving of aerosol (and gases) chemistry, re-distribution and scavenging, and by the total number of primary-secondary chemical reactions (Thunis et al., 2007).

Dispersion-transport models

Preferred dispersion models include, first of all AERMOD (AERosol MODelling steady-state plume model) that incorporates air pollution dispersion based on planetary boundary layer turbulence structure and scaling concepts, including treatment of both surface and elevated sources, and both for simple and complex terrain. Preferred dispersion models also include CALPUFF (CALifornia non-steady-state PUFF dispersion model) that simulates the effects of time- and space-varying meteorological conditions on pollution transport, transformation, and removal. CALPUFF can be applied for long-range transport and for complex terrain. To this description can be added so-called "alternative models", like ADAM, SCIPUFF and so on.

Screening models are models that are often used before applying a refined air quality model to determine if refined modelling is needed. AERSCREEN is the screening version of AERMOD. It produces estimates of concentrations, without the need for meteorological data that are equal to or greater than the estimates produced by AERMOD with a full set of meteorological data. TSCREEN (Toxics Screening Model) is a Gaussian model for screening toxic air pollutant emissions release and subsequent dispersion over different sites. It contains 3 modules: SCREEN3, PUFF, and RVD (Relief Valve Discharge). VALLEY is a screening, complex terrain, Gaussian

dispersion model for estimating 24-hour or annual concentrations resulting from up to 50 point and area emission sources. COMPLEX1 is a multiple point source screening model with terrain adjustment that uses the plume impaction algorithm of the VALLEY model. RTDM3.2 (Rough Terrain Diffusion Model) is a Gaussian model for estimating ground-level concentrations of one or more co-located point sources in rough (or flat) terrain. Full description of these models and all information about them (including program code for downloading can be found on-line at: http://atmosphericdispersion.wikia.com/wiki/Compilation_of_U.S._EPA_Models) and in the main journals of the EPA and A&WMA (Air & Waste Management Association), such as "Journal of the A&WMA" and "Environmental Manager".

Among dispersion models developed outside of the USA should be mentioned Atmospheric Dispersion Modeling System (ADMS-3) that is an advanced dispersion model developed in England for calculating concentrations of pollutants emitted both continuously from point, line, volume and area sources, and discretely from point sources (Hanna et al., 2003). Also there are two more different versions of ADMS: ADMS-URBAN is a version for simulating dispersion on scales ranging from a street scale to city-wide or county-wide scale, handling most relevant emission sources such as traffic, industrial, commercial, and domestic sources; and ADMS-Roads is a version for simulating dispersion of vehicular pollutant emissions from small road networks in combination with emissions from industrial plants. It handles multiple road sources as well as multiple point, line or area emission sources and the model operation is similar to the other ADMS models.

Many of PM studies in New Zealand (Zawar-Reza et al., 2006) and Australia (Hurley et al., 2003) are associated with 2 models created by Australia's Commonwealth Scientific and Industrial Research Organization (CSIRO). First of all, TAPM is an advanced dispersion model integrated with a pre-processor for providing meteorological data inputs. TAPM can handle multiple pollutants, and point, line, area and volume sources on a local, city or regional scale (Hurley, 2002). The model capabilities include building effects, plume depletion by deposition, and a photochemistry module. The second one is a Local Advanced Dispersion Model LADM also developed by CSIRO for simulating the dispersion of buoyant pollution plumes and predicting the photochemical formation of smog over complex terrain on a local to regional scale. Both ADMS and CSIRO models are not open domain programs, which definitely slows their development and removes the possibility of these models being further developed by the global scientific

community. Politics of CSIRO regarding to these models development is close to the one of the USA APEA

3.4 Numerical parameterisation of PM chemistry

Three-dimensional prognostic pollution chemistry models have been developed with the growth of three-dimensional prognostic, mesoscale meteorological models. It was suggested (de Haan and Rotach, 1998) that the integration of a Gaussian emission-based (gridded or source emission) 3-dimensional photochemical prognostic meteorologically based model with a stochastic Lagrangian particle module provides a good compromise in reproducing more closely the observed aerosol and gaseous air pollution patterns. A large amount of research has been conducted in the USA and Europe to improve urban-scale air pollution dispersion models that included such models as Urban Air-shed Model with Variable grid–UAM-V, EURopean Air pollution Dispersion model system–EURAD, and Modal Aerosol Dynamic model for Europe–MADE (Arya, 1999; ENVIRON, 2005).

It should be stressed that modern 3-dimensional air pollution models with different kinds of chemistry mechanisms (CM), different version of carbon bond (CB 3, 4, 5) and chemistry mechanism compilers (CMC) are becoming increasingly complex, often consisting of several modular components simulating emission sources, atmospheric boundary layer processes, upper troposphere–lower stratosphere processes, and a complex representation of different kinds of primary and secondary chemical reactions. For example, the 3-dimensional Eulerian Comprehensive Air quality Model with extensions–CAMx version 4.2 (ENVIRON, 2005), designed for the urban environment and PM studies by the Environmental Protection Agency (USA), includes up to 74 chemical species and 211 primary reactions for carbon bond mechanism 4 (CB 4), and up to 305 primary reactions for CB 5. As emitted pollutants undergo a range of chemical reactions resulting in the production of secondary volatile organic components (SVOC) and secondary PM, a significant amount of research work has been devoted to incorporating important chemical processes into air pollution dispersion models (Russell, 1997). Bergin *et al.* (1998) have illustrated the importance of getting correct parameterisations of chemical reactions into applied dispersion models and stressed the significant variation in sensitivity of the predictions from chemical models to different chemical processes. PM chemical composition and particle size distribution have become important factors during consideration of interactions between aerosol and gas phases. Ackermann *et al.* (1998) successfully coupled an aerosol model with an atmospheric dispersion model and applied it to Western Europe. Although the general patterns

were realistic, insufficient input field data seriously reduced the quality of the final research results. In this study, primary and secondary aerosol chemistry is represented by aerosol parameterization in CAMx4.2 (Titov et al., 2007).

Carbon bond aerosol chemistry

The chemical mechanisms supported in photochemical dispersion models are usually based on version 4 of the carbon bond mechanism (CB4, Gery *et al.,* 1989), and/or the SAPRC99 mechanism (Carter, 2000). CB4 (Gery et al., 1989) basic mechanism 1 is formulated as gas-phase chemistry with revised radical-radical termination reactions that are necessary for regional modelling: 91 reactions and 36 species (24 state gases and 12 radicals). The CB 4 aerosol mechanism is mechanism 3 (ENVIRON, 2005) expanded to include aerosol and mercury chemistry: secondary organic aerosol formation from condensable gases, aqueous PM chemistry, inorganic PM thermodynamics, aerosol size evolution, and several additional inorganic reactions appropriate for regional modelling: 117 reactions and up to 67 species (37 state gases, up to 18 state particulates, and 12 radicals).

CAMx includes special model structures to treat aerosol chemistry. Aerosol processes are currently linked to the CB4 gas-phase chemical mechanism and are selected by choosing mechanism 4 with up to 18 state particulates that include 13 PM species (including particulate water) and 5 condensable gas (CG) species for the nucleation of secondary organic aerosol (SOA). Mechanism 4 provides two options for treating aerosol size distributions: the CF (coarse-fine) scheme and CMU (coarse, middle, ultra) scheme. The CF scheme divides the size distribution into two static modes. Primary species are modelled as fine and/or coarse particles, while all secondary species are modelled as fine particles. The CMU scheme employs a sectional approach that dynamically models the size evolution of each aerosol constituent among a number of fixed size spatial sections. Aerosol water is explicitly treated in both CF and CMU options; it affects aerosol size and density.

CAMx tracks thirteen chemical components of aerosols as shown in Table 3.1. These components account for all of the major primary and secondary aerosol constituents. Each component is represented in every size section. The number of size sections and their size ranges can be defined by the user for each CAMx simulation. The size distribution developed for the Los Angeles test case contains 10 sections defined according to a lognormal distribution and with cut-points at both

2.5 μm and 10 μm. The mass of $PM_{2.5}$ can be calculated by summing over the first six sections, and the mass of PM_{10} can be calculated by summing over the eight-thirteen sections. Thirteen components in ten size sections lead to a total of 130 aerosol species in total PM (Morris et al., 2003).

Table 3.1 Aerosol constituents in CAMx 4.2 total PM (after Morris et al., 2003).

PMCAMx Name	Description	Primary	Secondary	Molecular Weight*
SOA1	Secondary organic aerosol 1		X	n/a
SOA2	Secondary organic aerosol 2		X	n/a
SOA3	Secondary organic aerosol 3		X	n/a
SOA4	Secondary organic aerosol 4		X	n/a
POC	Primary organic carbon (matter)	X		n/a
PEC	Primary elemental carbon	X		n/a
CRST	Crustal material (dust)	X		n/a
PH2O	Water in aerosol phase		X	18
PCL	Chloride ion	X		36.5
NA	Sodium ion	X		23
PNH4	Ammonium ion		X	18
PNO3	Nitrate ion		X	62
PSO4	Sulfate ion	X	X	96

The CAMx gas-phase chemistry was modified to simulate the formation of secondary aerosol precursors. The changes include first of all tracking production of four condensable gasses (CG1 – CG4) formed in the oxidation of VOCs that are secondary organic aerosol (SOA) precursors, and also tracking ammonia as a precursor to ammonium aerosols, tracking SO_2 and gaseous sulphuric acid as precursors to sulphate aerosols, and tracking HCl as a precursor to and vaporization product of sea salt (sodium chloride) aerosols.

Secondary particulate matter chemical formation

The partitioning of the condensable organic gases between the gas and aerosol phases is simulated using the methods developed by Strader et al. (1999). The secondary organic aerosol (SOA) module was designed to accommodate varying levels of chemical detail in the condensable organic components. In aerosol chemistry of CAMx the SOA module is implemented with four classes of semi-volatile organics that have different volatility properties defined by saturation concentration and heat of vaporization. The four condensable gases are called CG1–CG4 and the corresponding secondary organic aerosols are called SOA1–SOA4 shown in Table 3.1. The SOA module calculates the equilibrium distribution between the gas and aerosol phase for each CG/SOA pair (i.e., the amount of the gas and aerosol phases). Secondary organic material may condense to the

aerosol phase or evaporate to the gas phase depending upon the CG/SOA equilibrium distribution. Evaporation and condensation change the aerosol size distribution, which is accounted for using the same algorithms as for the inorganic aerosol described in the next section.

The chemical composition of the inorganic aerosol phase is calculated using the ISORROPIA model (Nenes et al., 1998). ISORROPIA was selected over alternative algorithms because it provides good performance for accuracy, speed and stability. Solid, liquid and gas phase chemistry is modelled for the sulphate, nitrate, ammonium, chloride aerosol system using the internally mixed assumption (Morris et al., 2003). The chemical species that are possible in each phase are listed in Table 3.2.

Table 3.2 Species considered by ISORROPIA for gas, liquid and solid phases (after Morris et al., 2003).

Phase	Possible Species
Gas	NH_3, HNO_3, HCl, H_2O
Liquid	H^+, NH_4^+, Na^+, NO_3^-, Cl^-, SO_4^{2-}, HSO_4^-, H_2O
Solid	NH_4HSO_4, NH_4NO_3, $(NH_4)_2SO_4$, NaCl, NH_4Cl, $NaNO_3$, $NaHSO_4$, Na_2SO_4, $(NH_4)_3H(SO_4)_2$

The ISSOROPIA model can solve the composition of the aerosol system in either partitioning mode or equilibrium concentration mode.

PM dynamical and chemical solving schemes

The dynamic behaviour of a spatially homogeneous aerosol is described by the so-called aerosol general dynamic equation (Pilinis and Seinfeld, 1987):

$$\frac{dn(m,t)}{dt} = -\frac{\partial}{\partial m}[I(m,t)\cdot n(m,t)] + \frac{1}{2}\int_0^m K(m,m-m')\cdot n(m',t)\cdot n(m-m',t)dm' - n(m,t)\int_0^\infty K(m,m')\cdot n(m',t)dm' + E(m,t) + N(m,t) - D(m,t)$$

Where m is the particle mass, $n(m,t)$ is the size distribution function at time t, such that $n(m,t)dm$ is the number concentration of particles having masses in the range $[m,m+dm]$, $K(m,m')$ is the **coagulation** coefficient for particles with mass m and m', $I(m,t)$ is the rate of change of particle mass resulting from condensation and evaporation, $E(m,t)$ is the **emission** rate of particles, $N(m,t)$

is the rate of **production** by homogeneous nucleation[8], and *D(m,t)* is the rate of **removal** due to dry deposition. The composition of particles of the same mass *m* can vary from particle to particle due to external mixing. Due to our lack of understanding of these variations and for mathematical simplicity, all particles are assumed to be of the same size and have the same chemical composition (internal mixture assumption). Basic PM transformations are marked bold and described in this section.

Basic principles behind secondary inorganic particulate matter chemical formations are described in the previous section. Gas-phase formation of the organic secondary PM precursors includes tracking production of four condensable gasses (CG1–CG4) formed by the oxidation of VOCs that are secondary organic aerosol (SOA) precursors. The selection and properties of these four SOA precursors is described in more detail in ENVIRON (2003). Olefin species, called OLE2, added to the CB4 mechanism, represent biogenic olefins so that high SOA-yield biogenic olefins can be distinguished from low SOA-yield anthropogenic olefins. All these changes were implemented in the CB4 mechanism 3, which already includes updated isoprene chemistry and radical-radical termination reactions.

The size distribution of aerosols is solved using the algorithms described by Pilinis and Seinfeld (1987). The aerosol size distribution can be modified by the following physical processes: condensation/evaporation of inorganic and organic aerosol constituents; coagulation; nucleation of sulphuric acid; aqueous-phase chemistry; deposition. Coagulation is modelled assuming Brownian diffusion. To improve the accuracy of the coagulation calculation, the PM size distribution is over-resolved to finer distribution, coagulation is modelled, and the modified size distribution is placed back onto the PM size divisions. Nucleation is modelled based on the parameterization of Russell and co-workers (1994) and the work of Jaecker-Voirol and Mirabel (1989). The nucleation rate depends on the gaseous sulphuric acid concentration, which is from the gas-phase OH + SO_2 reaction. This approach is appropriate for estimating the effect of nucleation on the particle mass distribution, but not the number distribution. The inclusion of a nucleation process ensures some particle population in the finest size sections to provide a surface area onto which condensation can occur (Yarwood et al., 2003).

Aqueous-phase chemistry is important for modelling the production of sulphate from the oxidation of sulphur dioxide in cloud and/or fog water droplets. The rate of sulphate production is a nonlinear function of aqueous concentrations, cloud water pH and the size of the water droplets.

For simplicity and efficiency, many aqueous-phase chemistry algorithms assume that all the cloud droplets are the same size, which may be called a “bulk approximation”, because it leads to the simplifying assumption that the concentrations in all cloud droplets can be represented by bulk average values. The aqueous-phase chemistry in secondary inorganic PM treatment uses either bulk or size-resolved droplet models depending upon ambient conditions.

Removal of particles by dry deposition processes are modelled as a lower boundary condition in the solution of the vertical diffusion process. This means that the removal of pollutants from each column of grid cells is governed both by the deposition velocity at the surface layer and the diffusive coupling of layers moving up the column from the surface. Dry deposition is modelled based on an improved version of the Wesley resistance model (ENVIRON, 2005). Wet deposition is an important removal process for PM. Aerosol particles act as cloud condensation nuclei, the cloud droplets grow and collect into sufficiently large sizes to fall as precipitation. A fraction of particles that are subsequently entrained into the cloud, and that exists within sub-cloud layers, are scavenged by liquid precipitation via impaction. The rates of nucleation and impaction depend upon cloud type, relative humidity, and rainfall rate and particle size distribution. Wet deposition is treated using a simple scavenging coefficient approach. Emission rate of particles directly depends on initial-nudging gridded (source) emissions of PM that would be discussed for all PM chemical components later.

3.5 Summary

Methods of numerical research into PM include a great diversity of meteorological numerical limited area models and a whole range of photochemical and dispersion-puff models of varying complexity. Aerosol models have been appraised with input meteorological data obtained from meteorological datasets, global or limited area models. Air pollution models can also include meteorological block as a part of the whole dispersion model (but without chemistry).

The main numerical air pollution models approved by the US EPA and EEA include several State-of-Science models and a large variety of dispersion-puff models for local, urban and regional scale applications. Sometimes the choice of the officially supported model is just a result of the official standing of the model developing group, especially in the USA. Numerical simulation of PM chemistry is a very complicated process and results from replication of the observed spatial and temporal variations of gaseous-aerosol chemistry. Reproduction of temporal variation of aerosol

chemistry is possible only by using dynamical and chemical solving schemes that include processes of nucleation, accumulation, evaporation and scavenging.

Chapter 4: Investigation of airborne PM in Christchurch

Air quality has been a major issue in Christchurch for many years. Several factors that include topography, meteorology, and number and type of emission sources combine to create an unhealthy wintertime living environment. Concerns regarding health impacts associated with elevated PM levels in Christchurch have led to substantial study of degraded air quality and its spatial and temporal distribution. Christchurch has a significant wintertime air pollution problem that is dominated by smoke generated by domestic fires burning coal and wood on cold nights (Spronken-Smith et al., 2001). The emissions consist mostly of fine particulate matter ($PM_{2.5}$). After sunset, under anticyclonic weather conditions, a strong surface-based temperature inversion due to long-wave radiative cooling increases the pollution potential, resulting in high air pollution concentrations. The winter season can be characterized by the frequent occurrence of severe nocturnal smog events, when the health guidelines are exceeded on about 30 days each winter (Sturman et al., 2001; Aberkane et al., 2004). This Chapter places the study area in context by briefly describing the Christchurch study area, methods of routine PM observation, principal aerosol chemical components and principal sources. The main PM investigation methods in Christchurch are also described.

4.1 Study area

The city of Christchurch is situated on the coastal edge of the Canterbury Plains in the South Island of New Zealand (Figure 4.1). The plains slope gently from the Southern Alps to the eastern coast. Banks Peninsula is an eroded volcanic crater that lies on the southern border of the city and reaches a maximum height of 906 m. The Christchurch urban area covers more than 20,000 hectares of land with an immediate rural fringe of 30,000 hectares. Ninety-seven percent of the population lives in the urban area and the total population is estimated at more than 410,000. Topographically induced local wind systems over Canterbury play an important role in the mesoscale climate of Christchurch (Kossmann and Sturman 2004). These wind systems include regional scale airflow resulting from the dynamic blocking effect of the New Zealand Southern Alps, as well as thermally generated sea breezes and nocturnal cold air drainage (McKendry et al., 1986). Temperature inversions occur frequently during the wintertime, trapping emissions at the surface, resulting in elevated contaminant concentrations.

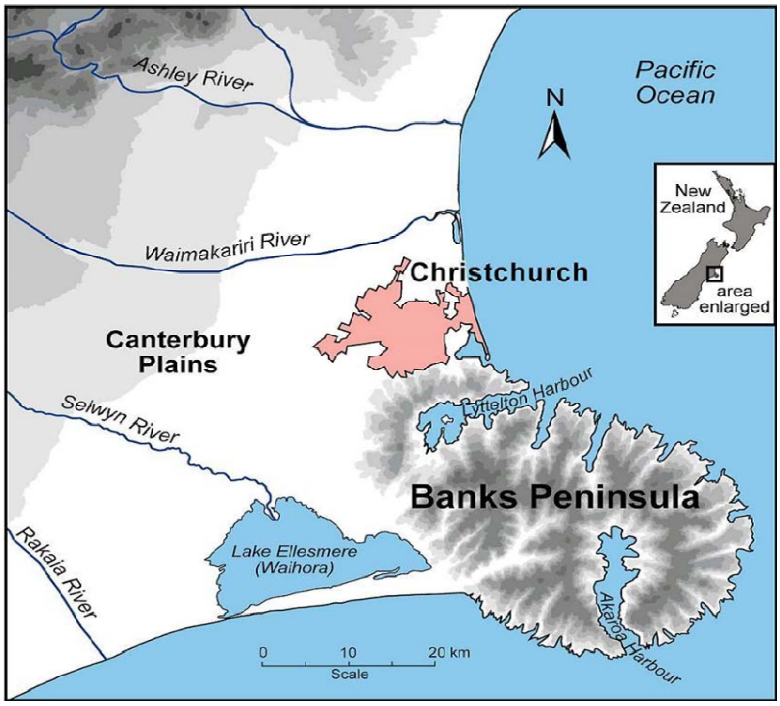

Figure 4.1 Christchurch and its surroundings.

4.2 Observational methods

Air quality monitoring in Christchurch was initiated by the Department of Health in the 1960s. Monitoring was conducted sporadically until 1988 when a permanent, continuous monitoring site was established at Packe Street in St Albans district. Ten years later, re-development of the site resulted in the establishment of a new Christchurch residential monitoring site at Coles Place, St Albans. Environment Canterbury (ECan) managed the new site from its inception in 1998. Subsequently, monitoring has been conducted in numerous locations around Christchurch and in other regional centres (especially during the Christchurch Air Pollution Study – CAPS2000). Comprehensive assessments of air quality measurements obtained from these areas are provided in Environment Canterbury's annual air quality monitoring reports (Wilton, 2003; Aberkane et al., 2004).

Routine PM monitoring at Coles Place, St Albans

Air quality measurements collected at the Christchurch fixed site, are used to establish long-term trends in air quality. Airborne contaminations are measured routinely at the permanent residential monitoring site at Coles Place, St.Albans and include PM_{10}, $PM_{2.5}$ (1999, 2000 and 2005 winters only), CO, SO_2 and NO_x. The site is in an area of medium–high density residential dwellings, with the majority of air pollutants sourced from domestic space heating. All measurements of PM are

made with a TEOM Series 1400a ambient particulate monitor (Rupprecht and Patashnick Co. Inc., 1993). The TEOM Series 1400a is one of the few continuous monitors established as an EPA equivalent method for PM monitoring. The instrument is able to continuously measure the mass of PM accumulating on a filter mounted upon an oscillating balance. Changes in the frequency of oscillations, related to the mass of material accumulating on the filter are detected in quasi-real-time and converted by a microprocessor into an equivalent PM mass concentration every few seconds, with a 10 minute running average. A debatable feature of the instrument is the heating of the air stream to prevent the condensation of water vapour on the samples collected. In standard operation the TEOM maintains a constant air stream temperature of 50^0 C. A number of studies have argued that operation at this temperature (as at temperatures 30^0 or 40^0 C) causes volatilization of the particulate semi-volatile material (PSVM) component of PM, leading to a systematic under-measurement of the true PM mass in the sampled air (Cyrys et al., 2001; Price et al., 2003). The mass on volatile material lost is associated with the type of volatiles within the sampled aerosol, which are site-specific and may vary from day-to-day (Kingham et al., 2006). As a result, standardized correction coefficients (ranging within 1.3-1.7 depending of the season, site location, and chemical composition of fine PM) have been developed for use with TEOM (Meyer et al., 2000; Price et al., 2003). The obtained aerosol and gaseous precursor data obtained are averaged to receive hourly values. Application of the TEOM standardized correction coefficients is not mentioned in any description of the Christchurch site measurements.

The measurements are evaluated against ambient air quality guidelines and the National Environmental Standard (NES), as established by the Ministry for Environment (MfE, 2003), to assess whether air quality is an issue in the Christchurch area. Key guidelines and NES values are outlined in Table 4.1. The NES allow for a number of exceedences of each standard value per year. For example, one annual exceedence of the 24-hour average standard for PM_{10} is permitted.

Table 4.1 Ambient air quality guidelines and National Environmental Standards (MfE, 2003; 2004).

Contaminant	Status	Concentration	Averaging period	Permitted exceedences
PM_{10}	**NES**	**50 µg m^{-3}**	**24-hour**	**1 annually**
	Guideline	**20 µg m^{-3}**	**Annual**	**N/A**
NO_2	NES	200 µg m^{-3}	1-hour	9 hours annually
	Guideline	100 µg m^{-3}	24-hour	N/A
SO_2	NES	350 µg m^{-3}	1-hour	9 hours annually
	NES	570 µg m^{-3}	1-hour	0
	Guideline	120 µg m^{-3}	24-hour	N/A

The MfE for 24-hour averaged PM_{10} (Table 4.1) usually is exceeded more than 30 times only during winter time in the Christchurch area, as is obvious from Figure 4.2 for winter 2005.

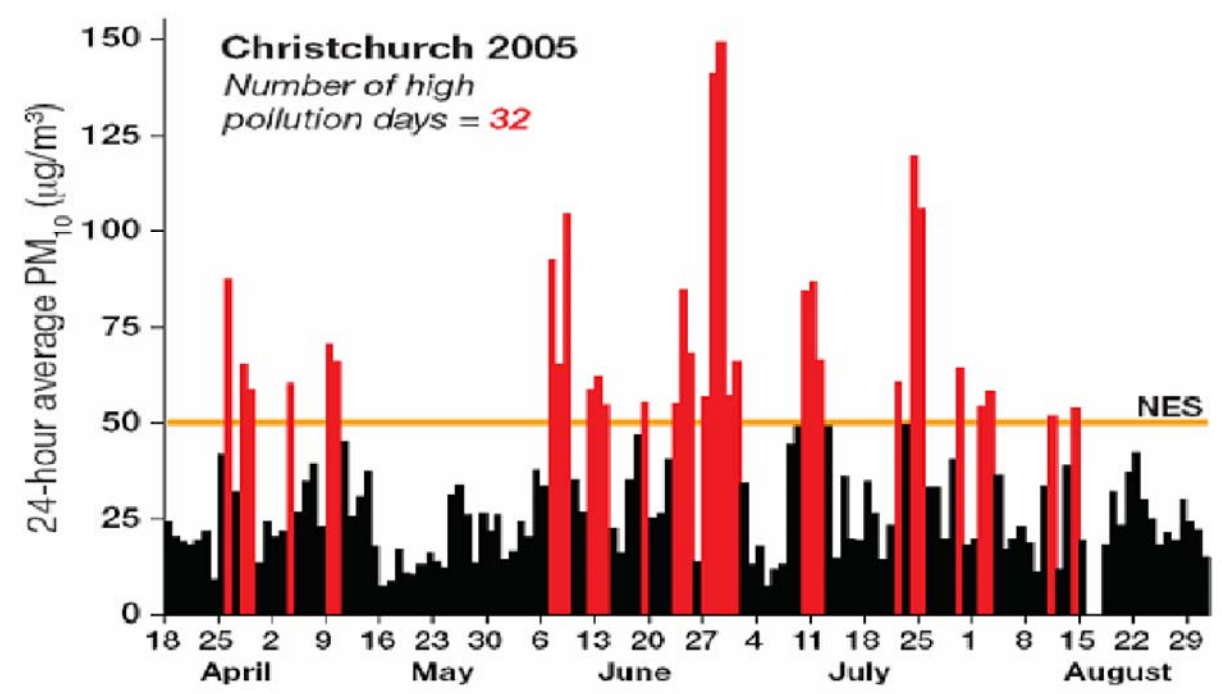

Figure 4.2 24-hour average PM_{10} concentrations (µg m^{-3}) for April–August 2005, Coles Place, St. Albans (from ECan).

From Figure 4.2, it is evident that the WHO and MfE standard was exceeded 32 times for the Coles Place observation site. The annual number of PM_{10} exceedences varies from year to year. The greatest number of exceedences was in 2001 with 11% of daily PM_{10} exceeding the NES.

This is higher than that indicated for most years, when the proportion of exceedences was around 8 to 9% (Scott, 2005).

CAPS2000

The Christchurch Air Pollution Study 2000 (CAPS2000) was a major field campaign in Christchurch, undertaken during winter 2000 to provide measurements of both meteorology and air pollution. The main aim of the study was to improve the fundamental theoretical and practical knowledge of air pollution dispersion over Christchurch and surrounding small towns, and to use data collected in air quality numerical modelling and management programmes (Spronken-Smith *et al.,* 2002).

As discussed in Titov (2004), local circulations are superimposed on weak synoptic scale winds, producing diurnal variations associated with easterly sea breezes, and night-time decoupling of the offshore drainage winds and land-see breezes (Sturman and Tyson, 1981). Such features are typical of the mesoscale air circulation frequently associated with severe nocturnal smog events during cold and calm nights in Christchurch and other towns during the winter season. Before the CAPS2000 study, the wintertime wind field studies in Canterbury were mainly based on data composited from different years and did not focus on near-surface meteorological conditions during night-time smog events (McKendry *et al.,* 1987), or they were limited to only parts of coastal Canterbury (McGowan and Sturman, 1993). The CAPS2000 field campaign was undertaken during winter, when meteorological data were collected by a network of 15 weather stations within the city, as well as two instrumented towers with two levels each measuring net radiation, temperature, relative humidity, and wind speed and wind direction. In addition, surface energy exchanges were measured over a suburban neighbourhood at one of the towers, and continuous vertical profiles of wind and atmospheric stability were obtained from a SODAR at another site. The observation programme ran from June to August 2000 with an intensive period during July, when several special observation periods were undertaken. These involved measurements of vertical profiles of the atmosphere using radiosondes and tethered balloons. A full list of place names and coordinates, with a list of meteorological and pollution measurements and time intervals, is provided by Titov (2004).

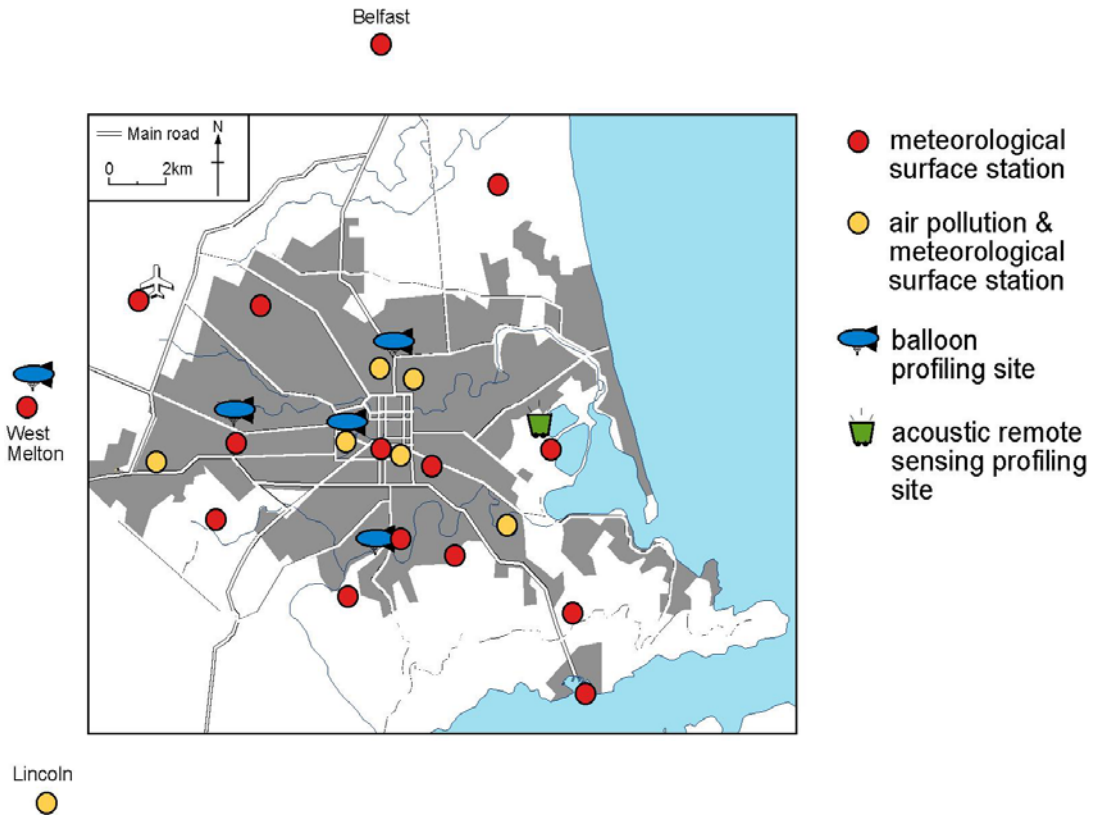

Figure 4.3 Network of observation sites in Christchurch during the winter period of CAPS2000 (after Sturman *et al.,* 2001).

July 2000 was the warmest on record with a mean temperature of 8.4^0C – two degrees higher than the long-term average (Sturman et al*.,* 2001). Warmer than usual nights resulted in a reduced incidence of frost, with only two air frosts recorded. Rainfall for the month was only 25% of normal and sunshine was 92% of normal. As a result of the warm winter Christchurch experienced an unusually low number of smog nights. During winter 2000 there were only 21 days in Christchurch when the 24-hour mean concentration guideline of 50 μg m^{-3} for PM_{10} was exceeded. This is in contrast to the average numbers of 30-40 exceedence days for Christchurch. During the active winter period of CAPS2000, PM_{10} and gaseous pollutants were measured at six locations throughout the city operated by ECan and NIWA, with a time frequency of either 10 minute or 1-hour. Three of these sites (Coles Place, the Polytechnic and Packe Street) were operated permanently during the observation period from 1st of June till 31st of August 2000. The three other sites hold fragmentary information about near-surface PM_{10}, CO and NO_2 air pollution concentrations, which can be used only occasionally for very specific short-term studies.

The winter was warm and pollutant concentrations were much lower than the long term average, although the daily cycle of PM_{10} concentrations still showed the typical pattern of low values

during late afternoon and a rapid increase after sunset due to both an increase in emissions from traffic (evening rush hour) and as domestic fires were lit in the evening. The reduced capacity for dispersion in the atmospheric boundary layer was also evident, with radiative cooling creating a dramatic reduction of mixing depth as nocturnal surface inversions developed in association with minimal vertical energy fluxes (due to strong stability and negative buoyancy), resulting in accumulation of aerosol and gaseous air pollution during night time (Figure 4.4).

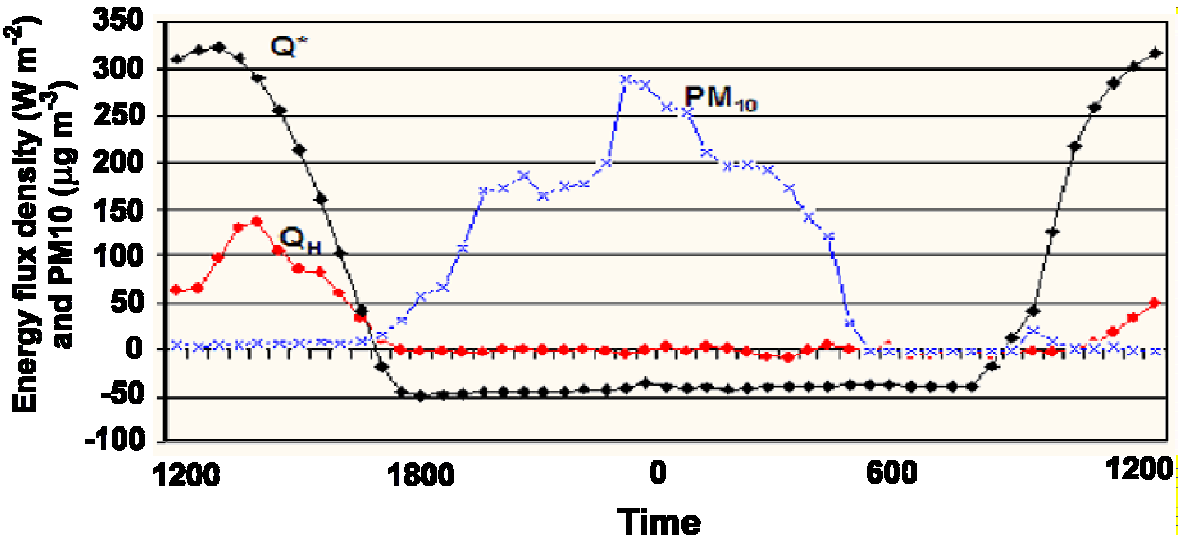

Figure 4.4 Vertical energy fluxes and PM_{10} for July 29-30, 2000, Coles Place (after Spronken-Smith et al. 2004).

From observations, the concentrations of PM_{10} increased through the evening and typically peaked in the one to two hours before midnight, after which they started to decline as emission from domestic fires decreased (Figure 4.4) and the cold drainage wind dispersion developed. This example of an observed PM_{10} time trend from CAPS2000 stresses the complexity of the relationship between different meteorological and human factors in controlling the accumulation and redistribution of near-surface pollutants. Measurements of the fine PM fraction ($PM_{2.5}$) were provided for the Polytechnic site only (roof location – about 20 m above ground) and mostly during the active phase of CAPS2000 – the month of July 2000.

Fine particulate matter ($PM_{2.5}$) measurements

A guideline for $PM_{2.5}$ has not yet been established by the MfE as there is no real health affect threshold for fine aerosol (WHO Working Group, 2003). It was originally intended that a guideline would be introduced by 2004, after conducting an investigation of $PM_{2.5}$ in New Zealand. However, this process has been substituted by the development of national standards for

key contaminants. In the interim, $PM_{2.5}$ data may be assessed against a 24-hour average monitoring value of 25 μg m^{-3} (MfE, 2002).

PM monitoring in Christchurch, has until relatively recently, focused on the measurement of total PM. Although several air quality studies included measurement of $PM_{2.5}$ (e.g. Wilton, 2003; Mikael, 1999; Fisher *et al.* 1998; Scott, 2005), routine measurement of 24-hour $PM_{2.5}$ concentrations did not commence until May 2001. Since 2001, $PM_{2.5}$ has been measured at Coles Place using a TEOM, fitted with a $PM_{2.5}$ sampling head (Aberkane, 2004). But for this research, only winter 2005 May-July fine aerosol routine measurements were obtained. Also, $PM_{2.5}$ measurements were stopped in August 2005 because of faulty results received from the TEOM while $PM_{2.5}$ concentrations regularly were higher than PM_{10} concentrations during evening-morning peaks of aerosol pollution.

Several of the studies noted above also provided speciated measurements for $PM_{2.5}$. These studies did not focus specifically on 24-hour concentrations or supply sufficient data to provide adequate elemental representation of $PM_{2.5}$ in Christchurch. Mikael (1999) measured fine and coarse PM on 23 winter nights during the hours of 4 pm to 9 am; Gunatilaka (2000) provided 28 weekly samples of fine and coarse particles from April to October 1999; and Fisher, *et al.* (1998) collected 21 $PM_{2.5}$ samples for 4-hour time periods. Wilton (2003), conversely, provided some 24-hour measurements of $PM_{2.5}$ and its key chemical constituents. The study was specifically targeted at addressing visibility and the measurements were conducted at an elevated location (on the top floor of a six-story building) at the Christchurch Polytechnic during CAPS 2000. Wang et al. (2005) made a short-term studying of PM_{10} for July 2004 (10-day study, Coles Place) to reproduce chemical composition of the winter total PM.

The data, with $PM_{2.5}$ measurements collected by TEOM, indicated that like PM_{10}, $PM_{2.5}$ concentrations were seasonally distributed, with low concentrations in the summer and substantially higher concentrations in the winter. The concentrations were frequently elevated during the winter months with 30-40 exceedences of the MfE monitoring value of 25 μg m^{-3} (24-hour average). The maximum value of 143 μg m^3 occurred on 12 June 2001.

Major PM chemical studies

The major winter PM chemical received for the Christchurch area includes studies of Scott (2002, 2005), Scott and Gunatilaka (2004), Senaratne (2003, 2005), Wang and Shooter (2002, 2005). Scott (2002) indicated that the major chemical species present in wintertime $PM_{2.5}$ during winter time were organic (OC) and elemental (EC) carbon as a product of fossil fuel burning. OC concentrations were generally higher than EC (ranging from 1.9 to 42.5 $\mu g\ m^{-3}$). The ratio between organic and elemental carbon varied between 1.5 and 4, with maximum EC concentration attaining 28 $\mu g\ m^{-3}$. The peak concentrations of EC and OC were found to occur on the same days, suggesting that these species were derived from similar sources or occur under the same meteorological conditions. Inorganic ion species were also abundant in $PM_{2.5}$. Species measured included ammonium, nitrate and sulphate. Peak concentrations of these species fell on different days, with maxima of 3.3 $\mu g\ m^{-3}$ for sulphate, 2.3 $\mu g\ m^{-3}$ for nitrate, and 2.1 $\mu g\ m^{-3}$ for ammonium (Scott, 2002). Other elemental species included chlorine, sulphur, potassium and sodium but with maximum concentrations less than 1.5 $\mu g\ m^{-3}$ for each of them. The peak potassium concentration occurred on the same day as maximum OC and EC. Potassium is a marker of wood smoke and its association with the carbon species suggests that residential heating was a major source of $PM_{2.5}$ on that day. Maximum concentrations of sodium and chlorine also occurred concurrently and therefore proved that marine aerosol was a contributor to fine particles at that time. As total PM (PM_{10}) was considered to consist of about 90% of fine PM fraction the additional chemical species of PM_{10} were associated with crustal primary elements (natural origin) and re-suspended road dust (anthropogenic origin). The major chemical species of PM obtained by Scott were reflected in the Christchurch emission inventory 2002 (Scott and Gunatilaka, 2004).

An alternative view was developed in the work of Senaratne and authors, which suggested that there was a more balanced contribution from home heating and transport emission sources (40-50% - domestic, 20-30% - transport) at times of peak and average aerosol concentrations during winter episodes in the Christchurch area (Senaratne 2003; Senaratne et al., 2005). The factors' closure scheme demonstrated decreased contribution of total organic carbon (TOC) and increased contribution of the secondary inorganic soluble ions (especially nitrate ammonia) and elemental carbon to $PM_{2.5}$ compared with ECan studies (Scott, 2002; 2005).

In the study of Wang et al. (2005), daily PM_{10} samples were collected during 2 weeks of July 2004 in Christchurch (St.Albans observation site) for the characterisation of carbonaceous materials, where wood and coal burning was a dominant energy source for home heating. On average, in the

Christchurch winter water-soluble organic matter (WSOM) makes the greatest contribution to PM_{10} mass (mean: 34%, range: 21–49%), followed by water-insoluble organic matter WIOM (mean: 19%, range: 5–37%). In total, carbonaceous materials (WSOM+WIOM+EC) constitute 67% (range: 33–91%) of PM_{10} mass. A chemical mass closure approach demonstrates that PM_{10} mass in the Christchurch winter, was heavily influenced by solid fuel burning with approximately 70% being contributed by carbonaceous materials (Wang et al., 2005). The results of Wang and authors (2005) are close to the chemical closure scheme of Senaratne but both studies didn't supply sufficient data.

Principal PM sources: inventories 1999 and 2002

The major aerosol and precursor emission sources in Christchurch have been identified by emission inventory techniques. Emission inventories identify the main PM sources and quantify the relative contributions of local-regional sources to emissions. In Christchurch, emission inventories were prepared for 1996 (NIWA, 1998), 1999 (Wilton, 2001a) and 2002 (Scott and Gunatilaka, 2004). Emissions were calculated for a cold ordinary winter day, and airborne contaminants utilized PM_{10}, $PM_{2.5}$, carbon monoxide (CO), carbon dioxide (CO_2,) nitrite oxides (NO_x), and sulphur oxides (SO_x). In 2002, emissions from the metropolitan Christchurch area (Christchurch City Council territorial boundary) were quantified and divided into three sub-areas: Inner Christchurch, Suburban Christchurch, and Outer Christchurch (Figure 4.5). The 2002 Christchurch emission inventory of airborne aerosol shows that in the Christchurch winter smog, 80% of PM_{10} (90% of $PM_{2.5}$) was generated from domestic home heating with vehicular emissions and industrial/commercial activities each contributing about 10%. Of the PM_{10} emissions from domestic home heating, residential wood combustion was accounted for nearly 90%, with the remaining 10% from residential coal burning (Scott and Gunatilaka, 2004). The 2002 inventory pointed out that in metropolitan Christchurch 82% of PM_{10} was derived from residential heating, 9% from industrial and commercial activities and 9% from motor vehicles (see Figure 4.5).

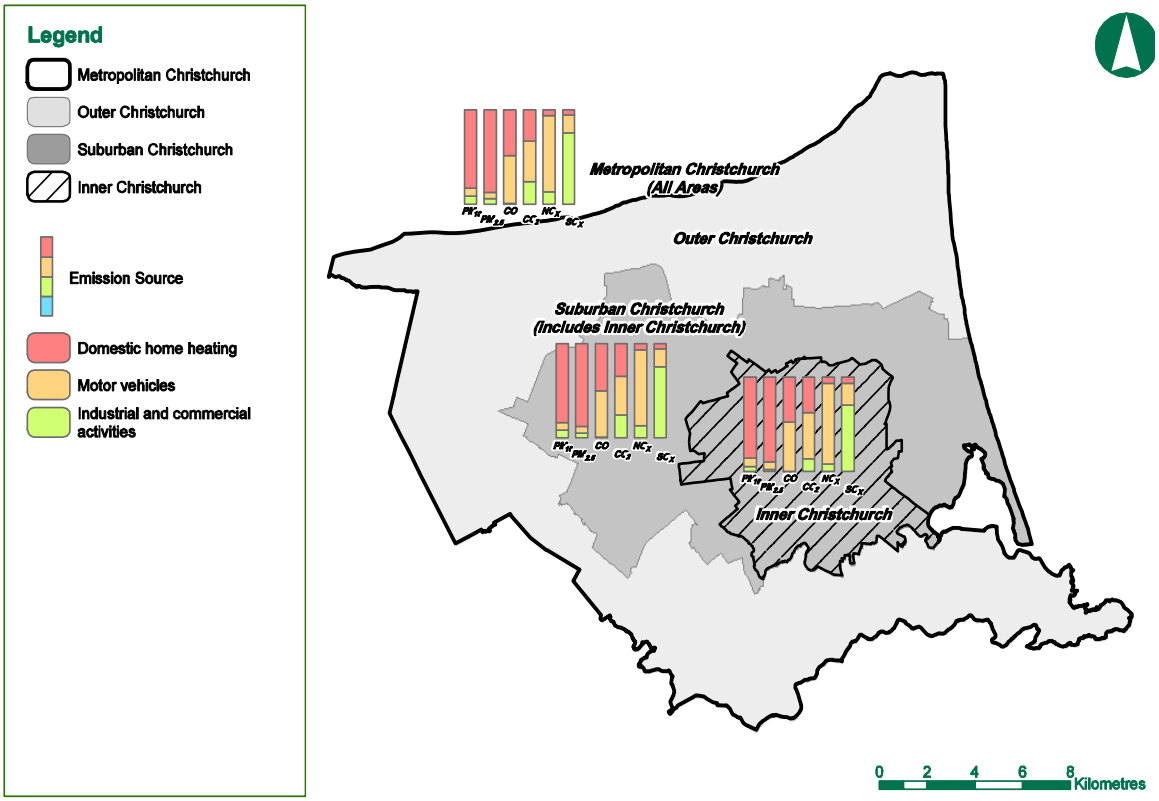

Figure 4.5 Relative source contributions to contaminant emissions in Christchurch, 2002 (from Scott and Gunatilaka, 2004)

For the 1999 emission inventory (Wilton, 2001a), a high proportion of $PM_{2.5}$ emissions were discharged from residential heating sources, with a contribution of 83%. Motor vehicle emissions contributed to 10% of $PM_{2.5}$, with 7% derived from industrial and commercial activities. Peak emissions occurred in the evening period between the hours of 4 pm and 10 pm. Wood burners contributed about 65% of residential heating $PM_{2.5}$ emissions and were considered to be the major source in residential category.

Three inventories have been prepared for Christchurch, allowing trends in emissions over time (1996 to 2002) to be determined. Scott and Gunatilaka (2004) found that PM_{10} emissions in Metropolitan Christchurch decreased from 16 t in 1999 to 14 t in 2002 (-13%). Reductions were mainly from residential heating (-15%) and motor vehicle sectors (-15%). The decline in PM_{10} emissions was attributed to the tightening of wood burner emission standards and increased publicity associated with the proposed new aerosol health guideline for PM. Relative reduction in motor vehicle emissions was the same and reckoned to be a result of improved engine technology of new generation of motor vehicles. Industrial emissions, conversely, appeared to be enhanced. Unfortunately fine aerosol ($PM_{2.5}$) emissions were not quantified in the 1996 inventory, so that

trends in emissions could not be established. However as emissions in the Christchurch area are dominated by combustion sources, where a strong relationship between $PM_{2.5}$ and PM_{10} is evident, it is high likelihood that $PM_{2.5}$ emissions are also declining, following the total PM trend.

It should be stressed that emission inventories provide basic spatial and temporal information with regard to the relative contribution of main sources (domestic, vehicular, industry) to total emission fields. However emission inventories themselves cannot reveal proportional contributions of different emission groups to actual measured concentrations, and for these purposes numerical dispersion or photochemical modelling are used.

4.3 Methods of investigation

Spatial and temporal analysis of PM includes different methods starting from visual analysis of visibility degradation, and finishing with application of sophisticated methods of the numerical modelling using the state-of-the-science modelling tools. In this section, a number of statistical methods are considered that are basic tools for any data evaluation. Other analysis techniques described include numerical methods as dynamical tools to expand our knowledge of air pollution in time and space, and conceptual modelling as a way to combine the observed and modelled information.

PM_{10} statistics for Christchurch

Observations are generally subjected to statistical analysis, and in the Christchurch area most research into winter PM pollution has involved with application of statistics. The first statistics of aerosol air pollution in Christchurch appeared after June 1954, while systematic monitoring of sulphur dioxide (SO_2) began in central Christchurch and monitoring was extended in 1956 to include deposited particulate matter and smoke in three additional suburbs. Wilkinson (1959) was the first to show that the air pollution problem in Christchurch was clearly seasonal with a winter maximum, when pollutant concentrations reached levels warranting serious consideration of their significance. Wilkinson's report initiated further research by the Christchurch Regional Planning Authority (1966), leading to a comprehensive city study of air pollution and associated fuel use from 1960–1964. Moody (1983) discussed the findings of a three-year survey and noticed that a decline in solid fuel use for domestic heating had been matched by a decrease in the aerosol part of smoke concentrations. In 1988, a continuous air quality monitoring site was established in the residential suburb of St. Albans to measure basic boundary layer meteorology and gas and aerosol

(PM_{10}, and from 2001 – $PM_{2.5}$) pollutants. While monitoring in the St. Albans area continues to provide the main measurements of air pollution for Christchurch, three more sites in Beckenham, Hornby and Opawa were established in 1995 to identify spatial variability across the city. Since recordings began in St. Albans in 1988, the 24-hour average PM_{10} concentrations statistically have exceeded the local guideline (50 μg m^{-3}) on average more than 30 times each year.

The Christchurch City Council (CCC) recently adopted a new motto for the city – 'Fresh Each Day', which is rather ironic given the continuing air pollution problem in winter. Although the maximum 24-hour concentrations of PM_{10} have decreased dramatically (from as high as 800–1300 μg m^{-3} total suspended particulates in the late 1950s to 280–320 μg m^{-3} PM_{10} in 2002–2003) they are still too high compared to World Health Organization standards, especially for the size of the city. Furthermore, the statistical 24-hour averages obscure extremely high hourly and 10-minute values that occur overnight that can be more than 400–500 μg m^{-3} and influence dramatically health conditions of vulnerable parts of the Christchurch community. The methods of home heating were also assessed to determine which method contributed the most to particulate matter levels. ECan indicates that the main emitters of PM are open fires and older woodburners. Given that urban Christchurch has an estimated 52,000 households using solid fuel burners the potential for significant air pollution from particulate matter is high. Figure 4.6 indicates that the main emitters of PM are open fires and older woodburners.

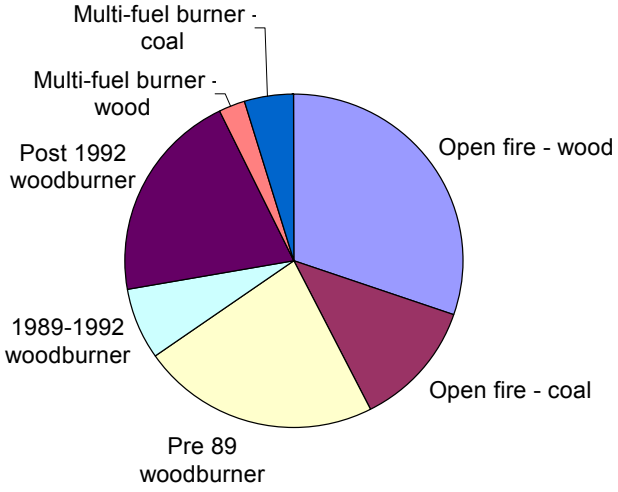

Figure 4.6 Contribution of different methods of home heating to total domestic emissions of PM_{10} (after Ecan annual report, 2000).

Statistical methods of PM evaluation are actively being developed by ECan, especially since the new policies of MfE (2003). The Clean Heat Project actively promoted by ECan includes numerous visual statistics provided by Environment Canterbury, but only the basic statistical diagrams are presented here. Figures 4.7 shows PM_{10} concentrations measured at St Albans from 1995 to 2002 grouped into the MfE management action (MfE, 2003) categories (data were provided by Aberkane et al., 2004). The proportion of PM concentrations within different management categories for a given year is presented and shows low % gap between 'Acceptable' and 'Action' categories that potentially provokes a passive management.

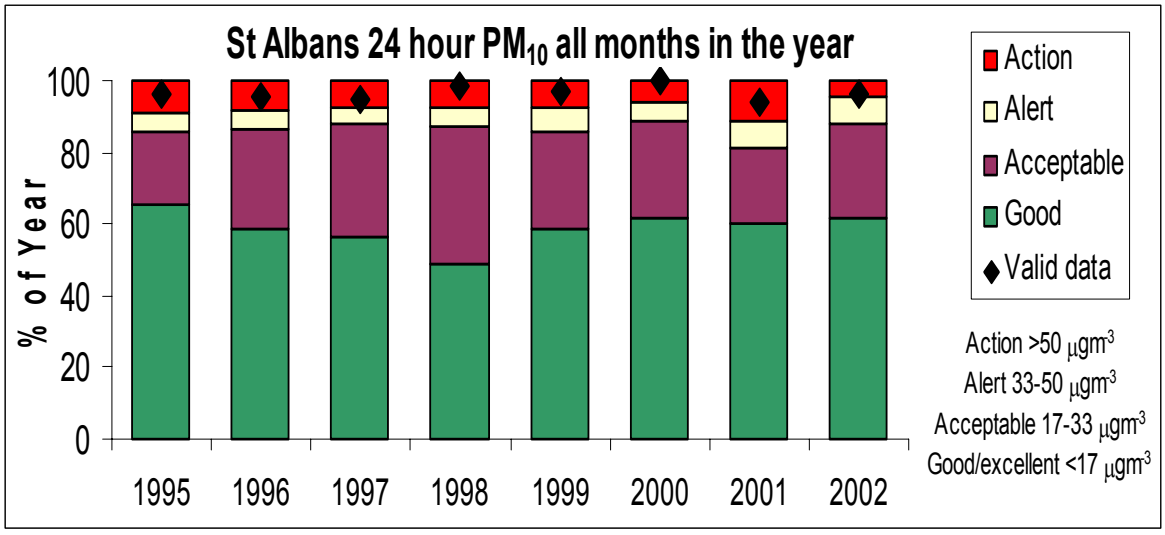

Figure 4.7 Comparison of 24-hour PM_{10} concentrations at St Albans by MfE management categories. 'Valid data' indicates the proportion of the year for which valid data were available. Source: Environment Canterbury (after Scott, 2005).

Considering 24-hour average trends of PM_{10} and CO (precursor of the carbonaceous component of aerosol) the most important conclusion is that PM_{10} are highest between sunset and midnight (Figure 4.8).

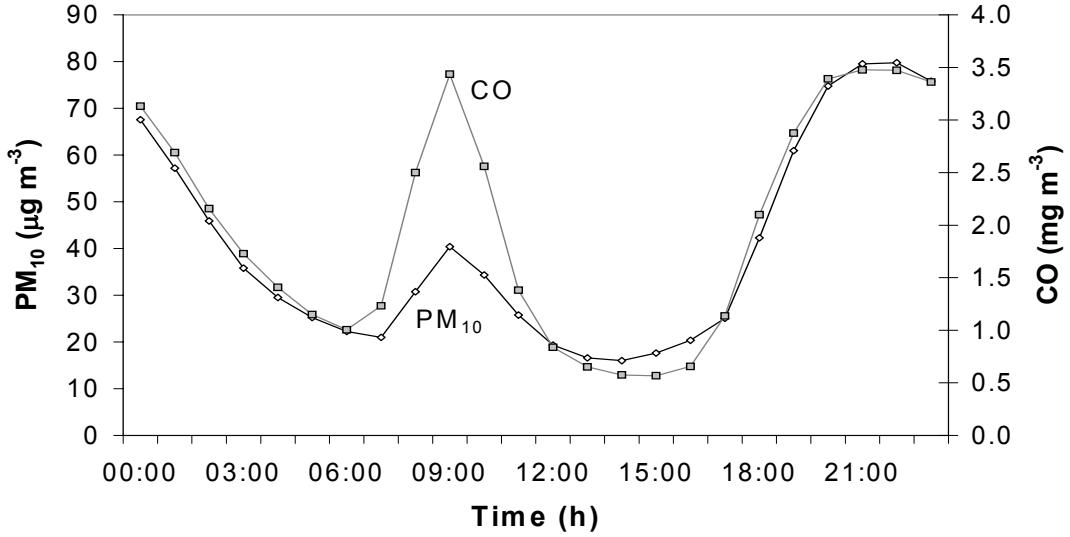

Figure 4.8 Diurnal cycle of hourly average concentrations of particulate material < 10 µm in diameter (PM_{10}) and carbon monoxide (CO) during winter (June–August), averaged for the years 1988–1999 (data supplied by Environment Canterbury).

Emissions of total and fine PM are considered to be the highest ones from home heating (especially during the first half of the night), whereas during daytime aerosol emissions originate partly from traffic and industry, and partly from domestic heating (Figure 4.9).

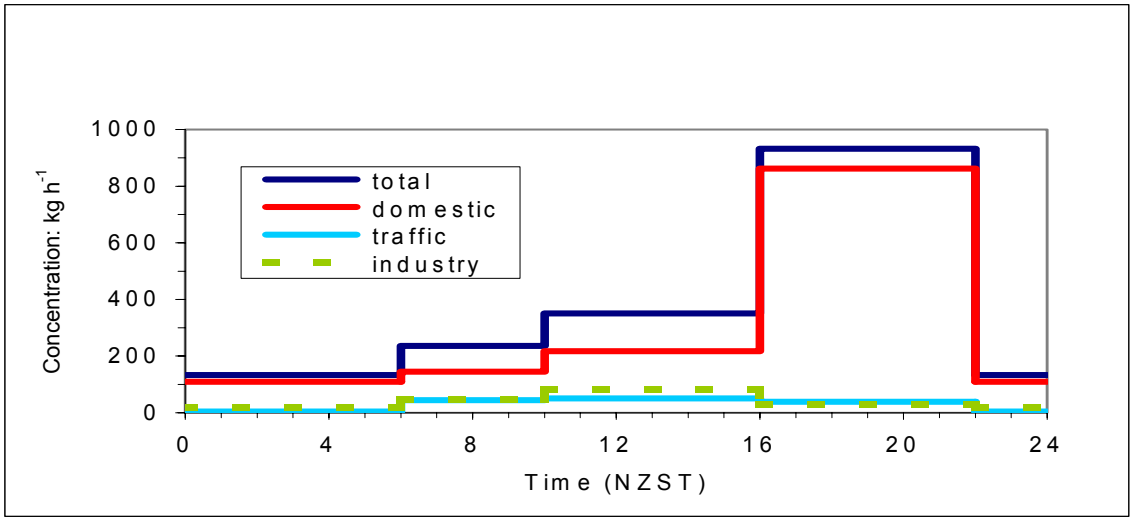

Figure 4.9 Contribution of domestic heating, traffic and industry to emissions of PM_{10} during winter 1999, Christchurch 25 suburbs area – 177.6 km^2 (after Spronken-Smith *et al.,* 2001).

To the basic statistics very useful for PM evaluation should be reckoned 24-hour average PM_{10} concentrations for winter time at Coles Place (St. Albans) prepared by ECan for every winter

(Figure 4.2 – winter 2005), and weekly-monthly 24-hour average PM_{10} concentrations for last week or month (Figure 4.10 – summer 2007) for St.Albans (and Woolston).

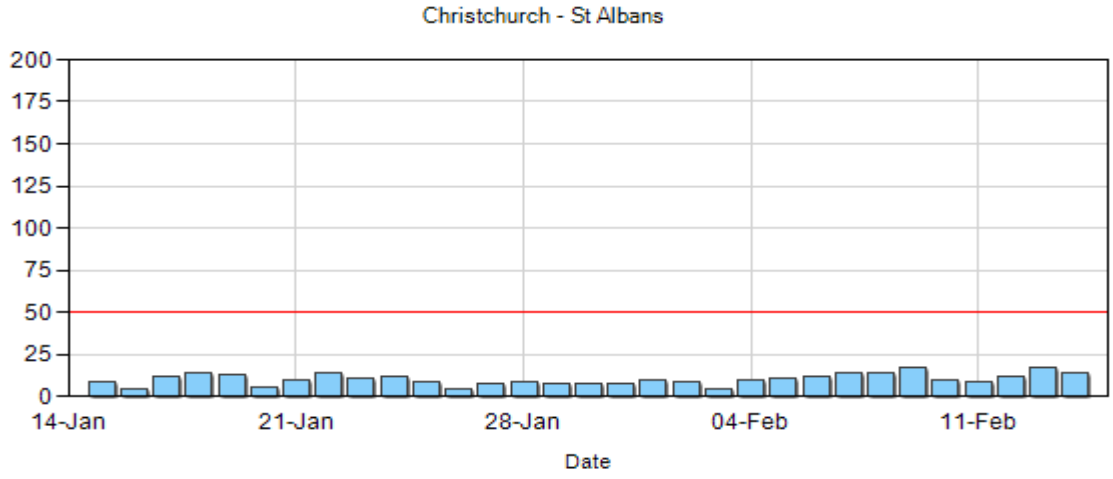

Figure 4.10 24-hour average PM_{10} concentrations (µg m^{-3}) for January-February 2007, Coles Place, St. Albans (from ECan web site).

Numerical methods

Numerical modelling of winter PM spatial and temporal variation over the Christchurch area was actively developed over the last 10 years and started from quite simple 2-dimensional chemical box modelling with a reliability a little more than 50%. A chemical box model was modified and applied to the Christchurch situation by Gimson (1998), and Gimson and Fisher (1997). The model simulated the influence of the near-surface meteorology (especially wind speed and wind direction, air temperature and height of the mixing layer) on dispersion of PM emissions, thus allowing prediction of concentrations. Foster (1998b) applied the box model to 1996 inventory data and found that night-time emissions had a greater impact on the 24-hour concentration than day-time emissions. The relative contributions from the different sources changed accordingly, about 85% for residential heating, 8% for transport and 7% for industry, as estimated by the 1996 inventory and box model, respectively (Foster, 1998a).

Complex air pollution dispersion modelling at an urban scale is commonly achieved using two approaches. The first one is based on Gaussian diffusion theory, which is applied to dispersion in the atmosphere (Arya, 1999). The aim of the second approach is to simulate the motion and turbulence characteristics of the atmosphere by solving the detailed system of mathematical hydrodynamic equations describing fluid flow (the system of the primitive equations). Models based on these equations can simulate a spectrum of meteorological phenomena and are used in air

pollution climatology to simulate atmospheric conditions associated with dispersion of PM concentrations in PBL mixing layer. Usually the modelled output meteorology directly or via interpolation is used in pollution dispersion modelling. But before 1999, models with detailed chemistry had not been applied in New Zealand. McKendry *et al*., (1986) provided the first attempt to simulate the complex north-easterly winds over Christchurch, and later van den Assem (1997) used Regional Atmospheric Modelling system (RAMS) to study two wintertime haze episodes. Van den Assem simulations with high resolution captured the effect of cold air downslope drainage winds around Christchurch and showed their role in contributing to the spatial redistribution of PM_{10} concentrations. Verification of the simulated winds showed that the model was able to predict the main airflow characteristics of significance for air pollution dispersion (Zawar-Reza et al., 2005a).

Simulated meteorology from RAMS has also been used by Barna and Gimson (2002) to drive the CALMET/CALPUFF (Scire *et al*., 1999) modelling system for a polluted night in Christchurch (where CALMET is a diagnostic meteorological model, and CALPUFF is its associated air quality dispersion model). In this case, a hybrid approach is applied since the simulated meteorology from the prognostic model RAMS is used to drive the diagnostic model CALMET (Godfrey, 2002). CALMET/CALPUFF numerical system was number one model for dispersion modelling in the USA (EPA) for many years until it was substituted by AEROMOD.

RAMS was used by Sturman and Zawar-Reza (2002) to perform high-resolution simulations for the three most common Christchurch near-surface wind regimes that lead to high PM_{10} concentrations (i.e. north-easterly, weak southerly and weak north-westerly). Modelled wind fields were used to construct back-trajectories in order to determine the distance air travelled during a typical air pollution episode. The back-trajectories were then used as a subjective guideline to determine a clean air zone boundary around the city (Zawar-Reza, et al., 2005a). Much work was done to construct PM_{10} exposure maps for Christchurch by performing long-term runs with TAPM. Methodological details of the model equations, parameterisation and numerical methods are described in a technical paper by Hurley (2002). However, the poor spatial and temporal resolution of the available emissions inventory (2002 Inventory – Scott, Gunatilaka, 2004) in Christchurch decreased the quality of these cohort studies (Zawar-Reza, *et al*., 2006). Evaluation of the MM5-CAMx4 modelling system output for particulate matter (PM_{10} and $PM_{2.5}$) against observations for winter 2000 and 2003, and an inter-comparison of MM5-CAMx4 output with the output of The Air Pollution Model (TAPM) were undertaken by Titov (2004). Model

intercomparison studies between TAPM and MM5/CAMx4 have shown that the more sophisticated MM5/CAMx4 system performs better in the case of Christchurch, but the convenient computational requirements and GUI for TAPM still make it a very attractive tool (Zawar-Reza, *et al*., 2005b).

Conceptual modelling

Conceptual modelling is one of the unique possibilities for developing comprehensive knowledge of the physical processes of complex pollution event combining observed and modelled information with application of the prior knowledge and experience. In the case of winter night-time aerosol smog over Christchurch conceptual model development has extended over 2 decades, becoming more detailed with acquiring of new information. A significant jump in the understanding of nigh-time smog has been achieved since the CAPS2000 experiment (Spronken-Smith, et al., 2002).

As was mentioned before, the topographically induced local wind regime over Canterbury and the Christchurch region play an important role in the microclimate of Christchurch. While New Zealand is located in the mid-latitudes of the Southern Hemisphere and its' wind climate is largely controlled by eastward travelling pressure systems (Sturman and Tapper, 2002). In the Canterbury region, located on the eastern side of the South Island of New Zealand (Figure 4.11), the synoptic-scale wind is strongly modified by dynamic and thermotopographic effects caused by the land-sea discontinuity, the Southern Alps and Banks Peninsula (McKendry, 1983).

'Synoptic-scale westerly winds are known to cause flow over and around New Zealand's South Island, resulting in frequent foehn winds and onshore northeasterly winds over the Canterbury Plains' (Kossmann and Sturman, 2002, page 452). The onshore northeasterlies appear to be due to localized pressure gradients resulting from the development of lee troughs over the Canterbury region, as described by McKendry, *et al.* (1986). In the initial stages of a westerly wind event (caused by a trough approaching from the west), the convergence zone between the northwesterly foehn winds and the northeasterly onshore flow occurs at some distance inland, whereas during the prefrontal final stage the convergence zone often moves out to sea. As a result of cold front passage the Christchurch area experiences a period of cold southwesterly airflow and the development of a short-lived high-pressure system (Kossmann and Sturman, 2002).

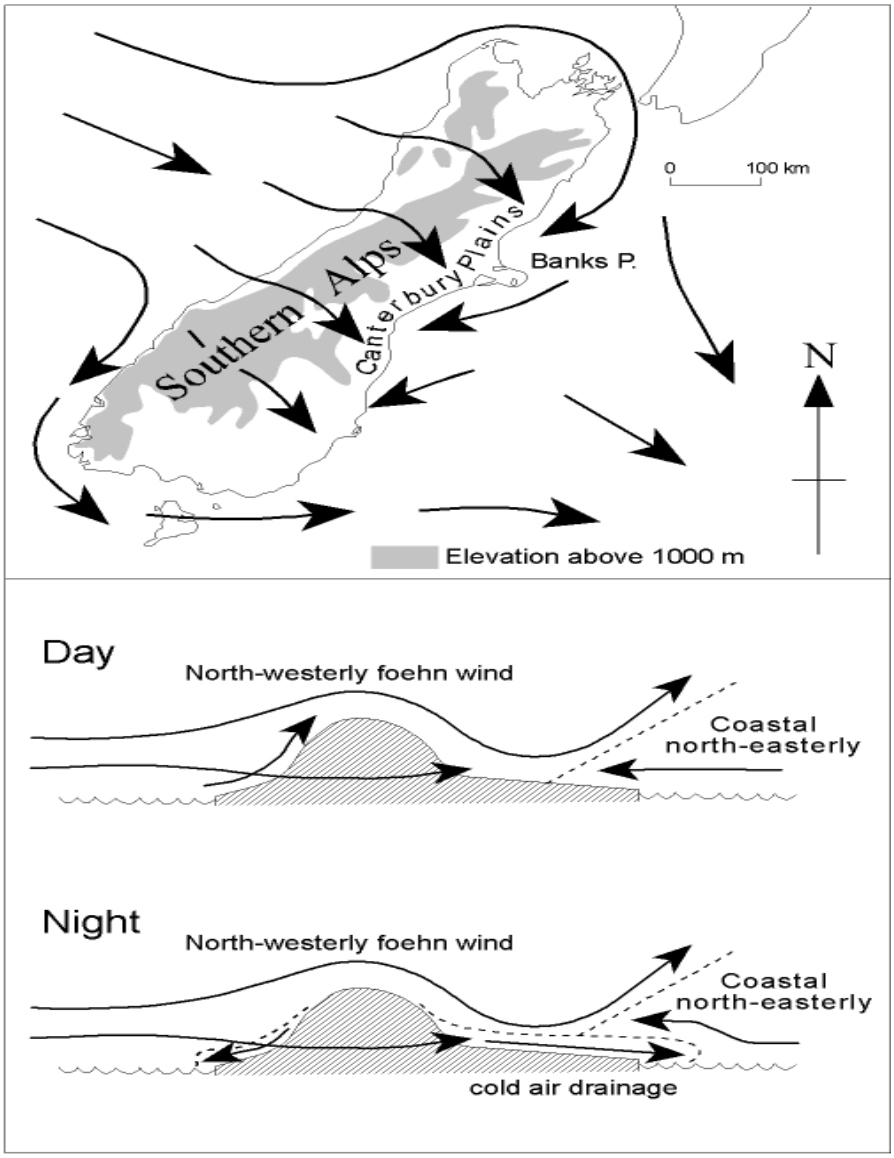

Figure 4.11 Effects of the Southern Alps on regional airflow over New Zealand's South Island during synoptic-scale northwest winds (after McKendry *et al.,* 1987)

Kossmann and Sturman (2004), relying on data obtained during CAP2000 field experiment, described the cycle of airflow patterns over Christchurch during a typical aerosol smog night. Superimposed on the synoptic-scale airflow, diurnal wind variations caused by the development of the easterly day-time sea breeze (Sturman and Tyson, 1981) and night-time stratification air layer with cold air drainage creates specific local circulation inside the near-surface layer. This near-surface wind cycle is particularly well-expressed when synoptic pressure gradients are weak (Kossmann and Sturman, 2002). Figure 4.12 provides a schematic illustration of the typical drainage flow patterns over the Canterbury Plains and Christchurch during smog nights for 2100–2400 NZST, when pollutant concentrations tend to be particularly high.

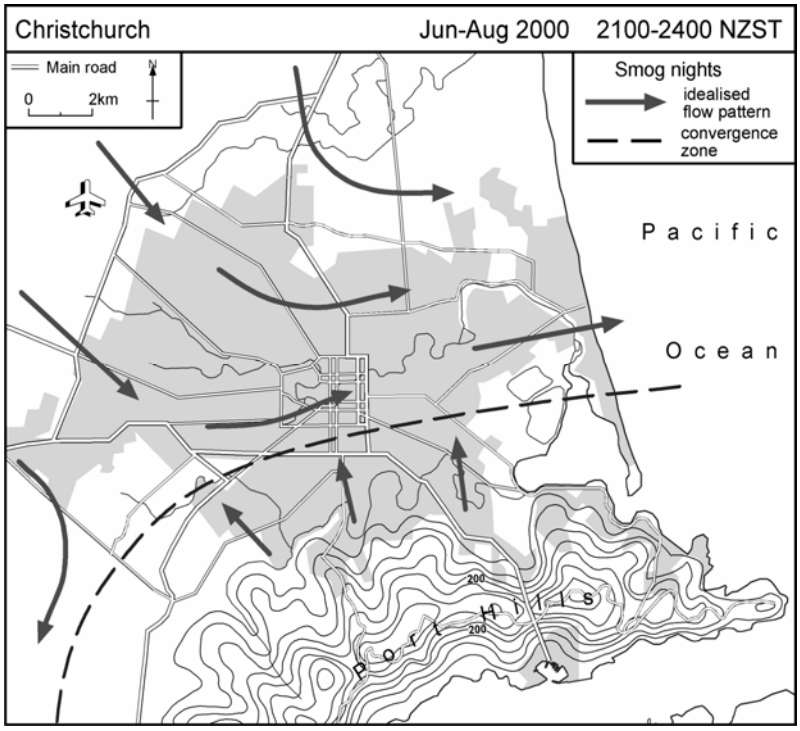

Figure 4.12 Night-time decoupling of observed downslope and offshore drainage winds and land breezes and the migrating convergence zone in the near-surface air layer (after Kossmann and Sturman, 2004).

Radiative cooling of hill slopes on calm nights with clear skies and subsequent cooling of the air in contact with them by conduction and convection, results in cold air drainage, which follows the terrain of the Christchurch area, where it becomes nearly stagnant over the city. The airshed for many cities is intricate because of the complex topography of the surrounding area (Sortberg *et al.,* 2001) as for Christchurch, where the airshed can be delimited clearly to the south of the city by the ridgeline of the Port Hills, but to the west and north, it is much more difficult to demarcate because of the configuration of the plains in front of the Southern Alps (Sturman and Zawar-Reza, 2002). This situation makes the catchment for cold air drainage extremely large. Such processes may lead to high levels of aerosol pollution that are often visible over Christchurch till the late morning (Kossmann and Sturman, 2004).

4.4 Summary

The geographical location, meteorological pattern and origin of source emissions in Christchurch are favourable for significant PM build-up on cold winter days (and especially nights). PM_{10} and $PM_{2.5}$ measurements for the last several years are undertaken routinely for the ECan observation site in St.Albans and occasionally at several additional sites. PM measurements currently exceed the recently established by MfE guideline on a regular basis during the winter months. The major chemical constituents of particles during winter time are carbonaceous species and inorganic soluble ions, which make up the fine PM fraction. These chemical species are derived from different kinds of anthropogenic combustion processes. In determination of the principal source inventories of 1996, 1999 and 2002 have identified residential heating as the major source of the particulate matter. Substantial reductions in PM emissions also include a reduction of transport exhaust.

PM analysis methods are very diverse and vary from simple statistical analysis to very sophisticated simulation of PM spatial and temporal trends using numerical modelling. Conceptual modelling built on the analysis of the unique meteorological and pollution data gained during the CAPS2000 field study reproduces very accurately the near-surface dynamics of PM patterns over the Christchurch airshed. It is also considered to be an excellent comparative tool for numerically modelled results.

PART B: METHODOLOGY

The most important part of the methodology includes 2 meteorological LAMs (MM5 and WRF) and a photochemical model (CAMx4) utilized for the Christchurch area (Canterbury, New Zealand). Numerical modelling systems that include MM5-CAMx and WRF-CAMx as powerful tools for winter PM investigation are also discussed.

Chapter 5: Meteorological limited area model

A three-dimensional, prognostic, meteorological limited area model (LAM) has a lot of advantages over the other modelling methods in reproducing the important factors influencing PM, such as the complicated distribution of near-surface airflow in space and time for very complex terrain (Souto *et al.,* 1998). Main application of limited area atmospheric models in the research is associated not only with simulation of meteorological fields for chemical modelling, but also with analysis of the local atmospheric circulation and model verification.

While applied to air pollution research, limited area meteorological models are excellent tools for predict near-surface meteorological fields, which are used to drive air pollution photochemical or dispersion modelling. Limited area models can be used for ideal and real simulation of atmospheric circulations ranging in scale from an entire hemisphere down to eddy flux simulations of the planetary boundary layer. Most frequently, limited area modelling is used to simulate atmospheric phenomena at the mesoscale level (horizontal scales from 2000 km to 1 km (Otte and Loscer, 2001) for applications from operational weather forecasting to air pollution dispersion. Limited area models are also successfully used at much higher resolutions to simulate boundary layer near-surface fine scale processes (boundary layer eddies with 10–100 m grid spacing) or individual building simulations (1 m grid spacing), that is very beneficial for LAM future applications. Basically, the resolution of limited area modelling depends on the scale of the phenomena being studied, the scale at which observations are available (for realistic simulations), the availability of computer resources, and the skills of the research group involved.

5.1 MM5 version 3

Understanding mesoscale and miscroscale controls on local airflow and atmospheric boundary layer structure is a principal step in studying a particular air pollution problem. Mesoscale Model (MM) generation 5 (MM5) was developed by Pennsylvania State University (PSU) and the

National Centre for Atmospheric Research (NCAR) Mesoscale and Microscale Meteorology division (MMM) from 1978 and by the University Corporation for Atmospheric Research (UCAR) since 1986 (Grell *et al*., 1994). It is developed on a multi-platform principle (it can be run on such platforms as Compaq, IBM, Hewlett-Packard, Sun, and PC Linux) and has the option of multi-nesting (stationary, moving and overlapping) as an essential feature of the model. MM5 is also available as a multi-parallel version on Compaq, IBM and Linux cluster computers.

Two final versions of MM5 (MM5 v3.7.3 and v3.7.4) were released in February 2006 and May 2006. MM5 is supported and actively explored by the world community, but is no longer an official model of NCAR (MM5 was substituted by WRF). MM5 is a prognostic model with sufficient spatial resolution to undertake research into the development of Microscale eddy fluxes up to studies of hemispherical energy redistribution from the tropics toward the poles. It is mostly used for multi-purpose prognostic or basic research simulations from mesoscale up to hemispherical applications. A special numerical system Antarctic Mesoscale Prediction System (AMPS) is based on MM5 and four dimensional data assimilation to undertake research on the influence of the Antarctic continent on the weather and climate of the Southern Hemisphere. A more detailed description of the latest versions of MM5 will be given later in this chapter (Dudhia, 2000b; 2005).

Application to the complex terrain

In terms of terrain following coordinates (x, y, σ) the basic primitive equations for the MM5 basic variables (excluding moisture) are the pressure and momentum prognostic equations, and the diagnostic equation of thermodynamics (Holton, 1992; Dudhia, *et al.,* 2000). The modelling system usually gets and analyses its data on pressure surfaces, but they have to be interpolated to the model's vertical coordinates before being input into MM5. The vertical terrain following coordinate system means that the lower grid levels follow the terrain, while the upper level is flat. Intermediate levels are progressively flattened as the pressure decreases toward the fixed (chosen) top pressure level. A dimensionless quantity σ is used to define MM5 levels, where:

$$\sigma = \quad (p - p_t) / (p_s - p_t), \tag{5.1}$$

where p is the pressure, p_t is a specified constant top pressure and p_s is the surface pressure.

The model vertical resolution is therefore defined by a list of values between zero and one that do not necessarily have to be evenly spaced. In cases of complex terrain and research into near-surface local processes the resolution in the boundary layer is much finer than above. The number

of levels may vary unlimitedly, but in most case studies lies in the range of 20–45 full σ levels (Figure 5.1) including 10-20 in the lowest 1500-2000 metres depending on the orography complexity and the vertical scale of interest. In the case of complex terrain (like the Christchurch area) it is also important to have a high top layer (not lower than 26-32 km) to reproduce accurately vertically propagating orographic baroclinic waves (Sorteberg et al., 2001).

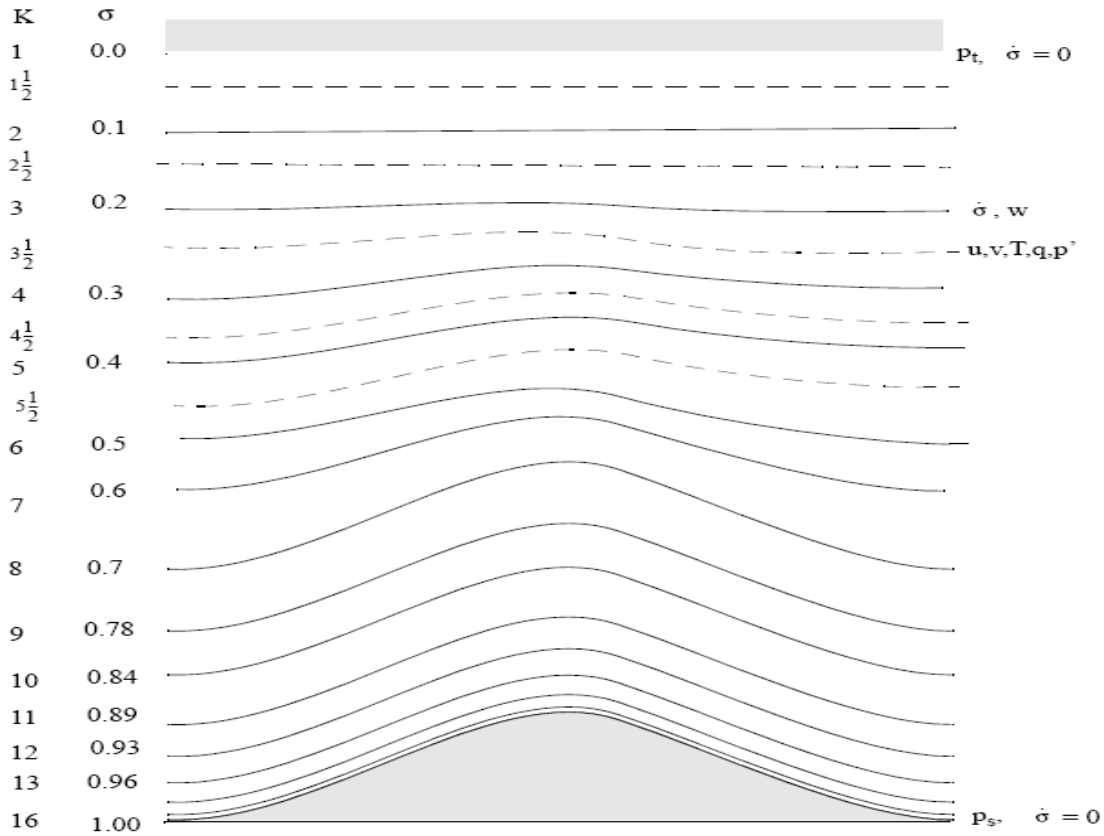

Figure 5.1 Schematic representation of the vertical structure of MM5. The example is for 15 vertical layers. Dashed lines denote half-sigma levels and solid lines denote full-sigma levels (after MM5 user's guide, http://www.mmm.ucar.edu/mm5/).

MM5 contains the capability of multiple nesting with up to 9 domains at the same time, which are completely interacting (Figure 5.2). The nesting ratio is always 1:3 for two-way interaction, which means that the input of information to the grid nests from the coarse grid comes via its boundaries, while the feedback to the coarser grid occurs over the daughter nest interior 3-dimensional space. However, the ratio 1:3 is not required for one-way interacting mother–daughter grids **(**Dudhia *et al.,* 1993**).** Number of daughter domains can be up to 6 for MM5 v3.7.3 and nested grids are allowed on one given level (multi-nesting).

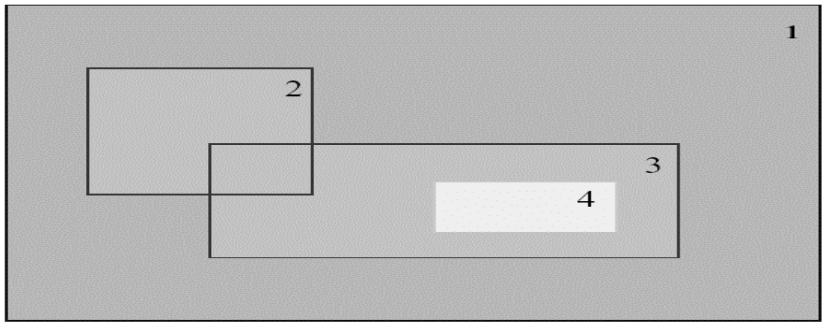

Figure 5.2 Example of different levels of nesting configuration for the mother (coarse) grid (grid1) (after MM5 user's guide, http://www.mmm.ucar.edu/mm5/).

Physical options in MM5 include choice of an appropriate cumulus parameterisation scheme, explicit moisture scheme, and type of land-surface model (LSM) parameterisation. The choice of schemes for physical processes in MM5 following the process of the model tuning and includes a selection of the number of vertical levels and depth of the modelled atmosphere, spatial resolution, time step and number of nested grids. The chosen parameterisation schemes strictly depend on application of MM5 to the particular local meteorological and topographic situation. In this study Grell parameterisation was used based on the rate of destabilization or the quasi-equilibrium simple single-cloud scheme (Grell *et al.,* 1994), as well as a simple ice scheme with ice phase processes in addition to the warm rain scheme (Grell *et al*., 1994), and Dudhia's short wave parameterisation. Two different kinds of PBL schemes were exploited: high resolution PBL (Blackadar, 1979) and the Pleim–Chang urban PBL scheme, which was developed to work with special LSM parameterisation (Chang *et. al*., 1987).

Only the MM5 non-hydrostatic version was evaluated over the Christchurch area and its complex terrain. The additional term in non-hydrostatic dynamics is the vertical acceleration that contributes to the vertical pressure gradient, so that hydrostatic balance is no longer valid. The reference state in the non-hydrostatic MM5 is an idealized temperature profile in hydrostatic equilibrium. It is specified by the equation

$$T_0 = T_{s0} + A\log_e(p_0/(p_{00})) \qquad (5.2)$$

T_0 (p_0) is specified by 3 constants: p_{00} is sea-level pressure (taken to be 1013 hPa), T_{s0} is the reference temperature at p_{00}, and A is a measure of the lapse rate. Application of this scheme effectively raises the model top height (Dudhia *et al.,* 1993).

Four grids were chosen for accurate air circulation modelling over the South Island and the Christchurch area (3 nested grids) with spatial resolutions of 27 km, 9 km, 3 km and 1 km. As can be seen in Figure 5.3, the coarse (mother) grid covers nearly all of New Zealand and grid 4 (the finest one) covers inner (metropolitan) Christchurch, its suburbs and the western section of Bank Peninsula (Titov, 2004).

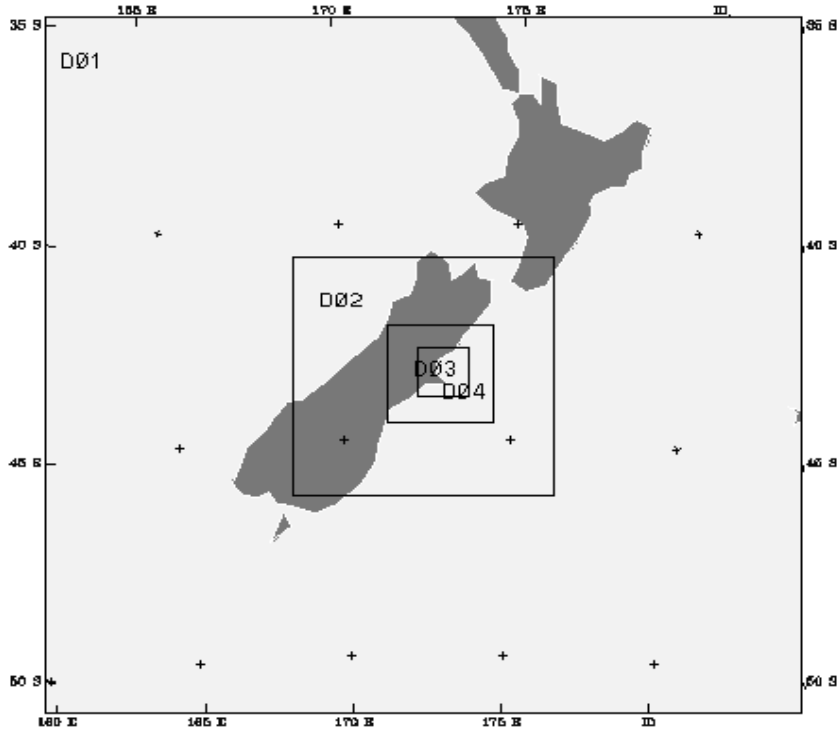

Figure 5.3 Coarse (outer or mother) grid and 3 nested (daughter) MM5 grids.

The centre of all 4 grids was pinpointed on the University of Canterbury in Christchurch, with latitude φ = - 43°.3183 and longitude λ = 172°.345. The total number of spatial nodes for every grid remained constant throughout all runs. The horizontal dimensions of each grid are as follows: grid 1 (27 km resolution) – 65x65 numerical nodes, grid 2 (9 km resolution) – 67x67 nodes, grid 3 (3 km resolution) – 82x82 nodes and grid 4 (1 km resolution) – 121x121 nodes. Number of vertical

levels was also constant and equal to 44 levels (with 20 levels in the PBL). All 4 grids started together with one-way interaction between mother-daughter grids and 12-hourly nudging.

Advantages of modelling the Christchurch air circulation

Several advantages of the use of MM5 version 3.x for simulating the Christchurch winter air circulation simulation will be mentioned in this section. One of the most important advantages is associated with well-developed pre- and post-processing of MM5 that allow manipulation of input files, including entering of local topography instead of the US Geological Survey data that have maximum resolution of only 30 seconds (900 m). As MM5 was developed for 30 years by the global research community the amount of additional software written for MM5 is very large and includes a wide range of MM5 applications, and MM5 input-output data communication with other models (meteorological, photochemical, dispersion and etc.). Substitution of USGS orography by local topography for the fine grid (grid 4 – 1 km spatial resolution) is illustrated in Figure 5.4 showing USGS 30-second global topography (Figure 5.4a) and local (GIS produced) topography (Figure 5b) for Okura area in the North Island of New Zealand.

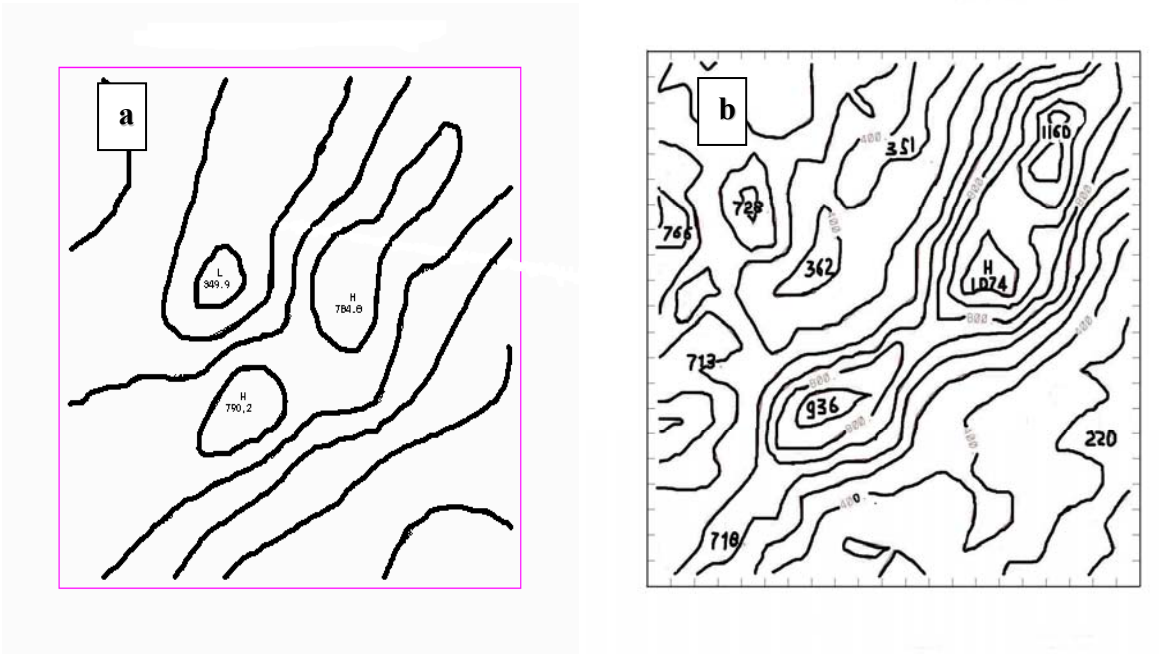

Figure 5.4 Grid 4 (1 km spatial resolution) topography (in metres) obtained from the USGS 30-second global dataset (a) and from local GIS-based height information with a resolution of 100m (b).

From Figure 5.4 it is evident that the decrease in height for the smoothed USGS topography particularly affects peaks and reaches up to 400 metres (760 m against 1075 m for locally reproduced topography). The contours are much more even (Figure 5.4a), which removes

important features of real topography that are important for local scale air circulation (Figure 5.4b). However USGS topography is generally more realistic in localization of peaks. This suggests that additional work should be done to fix differences in projection between USGS (Lambert confrontal) and GIS (UTM projection) topography.

Recent versions of MM5 have the selections of cumulus and boundary layer parameterization schemes. MM5 cumulus parameterisation includes 8 schemes, including the scheme of Anthes-Kuo based on moisture convergence (Kuo, 1974; Grell *et al.,* 1994); Grell parameterisation based on the rate of destabilization or the quasi-equilibrium simple single-cloud scheme (Grell *et al.,* 1994); the Arakawa-Shubert multi-cloud scheme (Arakawa, Schubert, 1974); the Fritsch-Chappell scheme based on relaxation to a profile due to updraft, downdraft and subsidence region properties; the Kain-Fritsch scheme that uses a sophisticated cloud-mixing scheme to determine entrainment/detrainment and also removes all available buoyant energy during the relaxation time (Kain, Fritsch, 1993); the Betts-Miller scheme based on relaxation adjustment to a reference post-convective thermodynamic profile; and the Kain–Fritsch2 new cumulus scheme that includes also shallow convection with a spatial scale between 15–10 km (Dudhia*,* 2002).

MM5 also has seven options of explicit moisture parameterisation that include:

1. Stable precipitation scheme that is nonconvective;
2. Warm rain scheme including cloud and rain water grids;
3. Dudhia's simple ice scheme with ice phase processes in addition to the warm rain scheme;
4. Mixed-phase (Reisner *et al.,* 1998) scheme, which adds a super-cooled water phase to the above 2 schemes;
5. Goddard microphysics scheme, including an equation of graupel prediction (Tao, Simpson, 1993);
6. Reisner graupel scheme (Reisner 2), suitable for cloud-resolving ;
7. Schultz microphysics scheme, which is a highly efficient and simplified scheme and is designed for fast running, containing ice and graupel/hail processes.

MM5 has 7 options of different kinds of PBL schemes to run, including:

1. Bulk PBL scheme, suitable for coarse vertical resolution in the boundary layer;
2. High-resolution Blackadar scheme, suitable for high resolution PBL (Blackadar, 1979);
3. Bulk-Thompson PBL scheme, based on Mellor–Yamada formula;
4. ETA global model PBL, based on the Mellor–Yamada scheme but with long time steps for stability;

5. MRF or Hong–Pan PBL, suitable for high-resolution PBL;
6. Gayano-Seaman PBL scheme, which is close to the MRF scheme, but using split time steps instead of surface temperature from the LSM (Land Surface Model);
7. Pleim–Chang PBL scheme, which was developed to use with LSM parameterisation type 3 (Chang *et. al*., 1987).

The diverse range of studies underlined using MM5 improves the ability to apply the model to a range of problems without repeating earlier mistakes. This has made this LAM a really universal tool. For example MM5 just only as a prognostic model is used to research and predict severe events such as tropical cyclones (MM5 includes a special option of moving nested grids) (Low-Nam, Davis, 2002), heavy monsoon rain based on prediction of ITCZ (InterTropical Convergence Zone) movement (Someshwar *et al*., 2002), gusting winds as a result of drainage of cold air masses (Dailey, Keller, 2002), severe cold frontogenesis as a result of local conditions (Brown, Locatelli, *et al.*, 1999), and simulation of ozone episodes (Boucouvala *et al.,* 2003). It is useful to mention that MM5 was successfully applied during the 2002 winter Olympic Games (Steenburg *et al.,* 2001) and was also used as a basic prognostic model during the summer Olympic Games 2004 in Athens (Kotroni *et al.*, 1999; Kotroni and Lagouvardos, 2002). MM5 numerical code is very compact (compared with WRF), and optimization of hard disk space and CPU time allows use of MM5 in research departments with restricted computational possibilities. Flexibility of the MM5 executable file definition (mm5.deck) while developing an experiment should also be mentioned.

Problematic issues – 5 years of experience

MM5 is a State-of-the-Science model, and demands a certain level of knowledge and experience in numerical modelling to operate fluently with the model's open code interface. Many pre-processing, processing and post-processing problems are related to the level of the user's skills only. Local experience acquired during 5 years of using MM5 in New Zealand and especially for the city of Christchurch.

MM5 pre-processing problems are mostly associated with the absence of GUI. From extended experience of working with the MM5 pre-processing interface it is clear that the GUI for most MM5 computer platforms is not an advantage, but a problem that involves installation and support of a range of additional visualisation software. Also, use of a GUI leads to restriction in MM5 code manipulation and correction. It should be mentioned that the last version of WRF (WRF v2.2)

issued in late December 2006 appeared without GUI as a principal pre-processing interface, unlike earlier WRF versions (like WRF v2.1.2).

Use of the US Geological Survey 30-second resolution database is definitely a big problem for New Zealand for reproducing soil type distribution, land-water mask and especially for topography. The USGS 30-second spatial resolution dataset was created for the 1993-1994 time period, and has not been re-calculated since that time (at last for New Zealand). Underestimation of the terrain heights can be extreme and the level of precision is so low (especially after terrain smoothing procedure) that it's difficult to recognize the place of simulation for MM5 fine domains (Figure 5.4 a-b). The worst problem that sometimes the 30-second USGS database loses local terrain as can be seen in Figure 5.5 with an example from Matira (near Auckland). Terrain for grid 4 (1 km spatial resolution) was obtained from the 30-second USGS dataset (Figure 5.5a) and from the 2-minute USGS dataset.

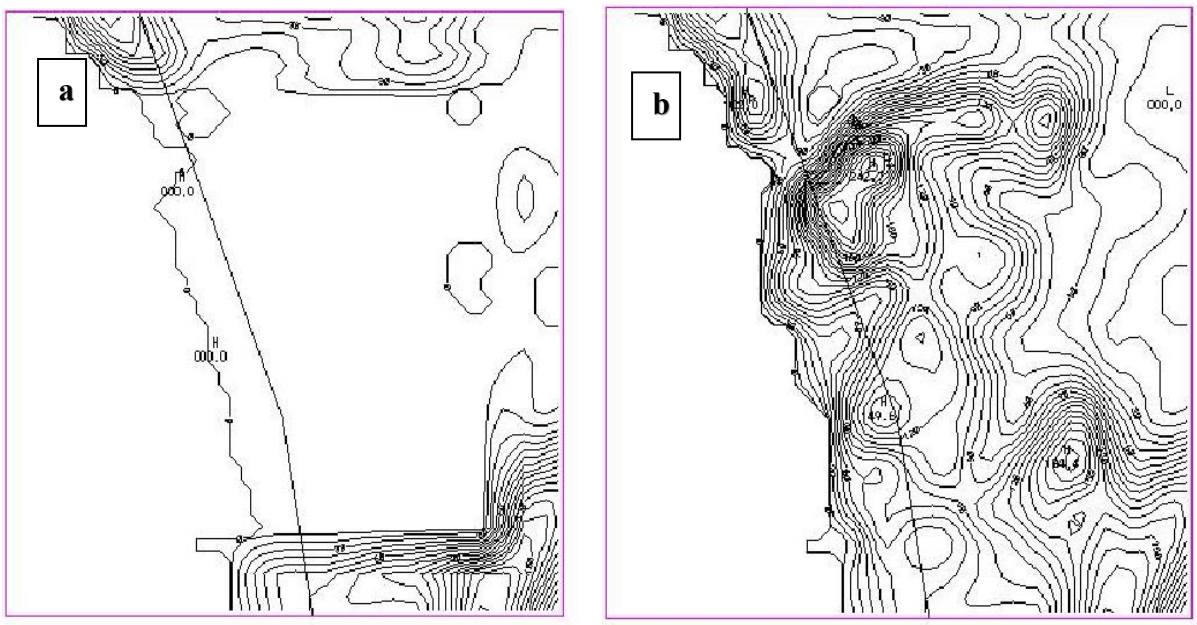

Figure 5.5 Grid 4 (1 km spatial resolution) topography (in metres) obtained from a) the USGS 30-second dataset, and b) the USGS 2-minute dataset (Matira, North Island).

An interesting problem is found in the program 'pregrid' that extracts input information files from GRId Binary (GRIB1) format zipped input data. The fault situation means that 'pregrid' doesn't read input information if the number of data files (nudging time points) is more than 240, as is the case for climatic runs. A correction of the FORTRAN code and re-compilation could help in such situations. For the MM5 model itself, an absence of 4-D variation well-developed software and ensemble forecasting with inclusion of randomly processed error is a big disadvantage compared

with a modern LAM such as WRF. Also arbitrary choice of the numerical 4-dimensional data assimilation stipulated in the 'mm5.deck' executable program demands abundance of sensitivity studies to use this option, or not to use this option at all. To MM5 problems points can be reckoned a case of split MM5 output file on several parts that always leads to creation of the first output file with initial time point only.

A significant problem (for IBM computers only) is considered to be a situation when MM5 (serial and parallel versions) is running but keeping inside some kind of faulty output information (not a number – NaN) that can be shown with application of MM5toGrADS program from MM5 post-processing tools during MM5 run. Just NaN inside output instead of variables after some time point is a systematic breakdown situation for MM5 running on IBM for certain cumulus parameterization schemes (Grell cumulus scheme for instance). This problem seems to disappear with application of the more complicated cumulus parameterisation schemes like Kain-Fitch or Kain-Fitch 2. The only explanation is that precision of MM5 stability controlling procedures in the old physical schemes is not enough for a 64-bit IBM word. As Kain-Fitch and Kain-Fitch 2 cumulus parameterisation schemes were developed for the last 5th generation of MM and includes more accurate stability tests (with IBM precision 16 digits after a decimal point) that allow to terminate MM5 before it begins to accumulate faulty data in an output file.

In case of the Christchurch area winter time simulations it is constructive to mention about systematic over-prediction of the near-surface wind speed by MM5, especially with USGS topography. But the over-prediction of near-surface local scale wind speed is a common problem for all numerical air circulation models, being a result of poor analytical-numerical parameterisation of the PBL and Land-Surface Model (LSM) physical processes.

Multi Parallel Processing (MPP) prognostic potential

Installation of MM5 MPP v3.7.3 on an IBM P575 computer provided a great opportunity to use MM5 in operational (real-time) regime. The operational regime includes the total cycle from initial and nudging data assimilation to transform of 1-3 day predicted fields' to ASCII code for the output data applications. One operational cycle takes about 2-3 hours for MM5 MPP on IBM P575 and higher.

The prognostic potential of the MM5 MPP core was tested on the IBM P575 using 32 virtual CPU in a single physical node to minimize calculation time due to exchange of information between

different nodes. It is calculated that an MM5 MPP run with 3 nested grids (finest resolution was equal to 1.0 km) takes about 2.5 minutes for 4-grid run with one grid 4, and 4.0 minutes for 4-grid run with 2 one-level nested grids 4. These benchmark calculations provide the possibility of MM5 MPP working in operational regime for a nested multi-grid configuration with a maximum number of spatial points not more than 60x60 and maximum number of vertical levels about 32-35.

MM5 MPP version 3.7.3 was successfully employed as an operational model during winter Olympic Games in Salt Lake city (Steenburg et al., 2001), the summer Olympic Games 2004 in Athens (Kotroni and Lagouvardos, 2003), and is already being used for the summer Olympic Games 2008 in Beijing (Chen et al., 2007), demonstrating the very high reliability and potential of MM5. However preparation of MPP as the operational version of MM5 demands special attention to physical parameterisation, as instabilities associated with some atmospheric physics parameterizations could lead to destruction of the whole operational process on IBM type computers.

5.2 TAPM

The Air Pollution Model (TAPM) is created and supported by the Commonwealth Scientific and Industrial Research Organisation (CSIRO, Australia) and described by Hurley (2002). TAPM includes the ability to simulate air pollution episodes with meteorology calculated by TAPM itself. TAPM is a PC-based, prognostic meteorological and/or air pollution model driven by GUI. Being fast and operationally easy to use and having integrated aerosol chemistry, TAPM provides wide-ranging scientific possibilities. TAPM includes a nested approach for meteorological and air pollution parts, which allows a user to zoom-in the simulation to any scale of interest. The meteorology of the model contains synoptic-scale analysis input fields that drive the model at the boundaries of the mother-daughter grid. TAPM includes integrated plume rise, Lagrangian particle, building wake, Eulerian grid, and condensed chemistry modules. The distinguishing feature of TAPM is that it allows urban area emissions to be modelled at fine resolution for long simulation times (up to a year). For air pollution applications emission information (point, line, area, or gridded emissions) should be provided for the whole integration period (Zawar-Reza et al., 2005a).

TAPM has been extensively evaluated against a wide range of observed meteorological and air pollution situations. Significant work was undertaken to construct PM_{10} exposure maps for

Christchurch by performing long-term runs using TAPM. However, low spatial and temporal resolution of the 2002 emission inventory for the Christchurch area has decreased the value of the undertaken research (Zawar-Reza *et al*., 2006). Model intercomparison studies between TAPM and MM5/CAMx4 have shown that the more detailed MM5/CAMx4 system performs better in the case of Christchurch (Zawar-Reza *et al*., 2005b), but the simple computational requirements for TAPM make it a very attractive tool in winter air pollution studies (Wilson and Zawar-Reza, 2006).

5.3 ARW WRF

The Advanced Research WRF (ARW) modelling system has been in development for the past few years as a new generation limited area model to replace MM5. The current release is Version 2.2, but WRF Version 2.1.2 was used in the study described here. A latest version of WRF (Version 2.2) was issued on 29 of December 2006, and has a number changes in pre-processing and processing structure.

The ARW is designed to be a flexible, state-of-the-art atmospheric simulation system that is portable and efficient, especially on parallel processing computing platforms. The ARW is suitable for use in a broad range of applications across scales ranging from meters to thousands of kilometres. It can be used for idealized simulations, parameterization research, data assimilation research, forecast, real-time NWP, and coupled-model applications like WRF – chemistry model (WRF ARW guide, 2006). The Mesoscale and Microscale Meteorology Division of NCAR is currently maintaining and supporting a subset of the overall WRF code that includes:

- WRF Software Framework (WSF);
- Advanced Research WRF (ARW) dynamic solver, including one-way and two-way nesting and moving nest;
- Standard Initialization package (SI) or WRF Pre-processing System (WPS);
- WRF Variation Data Assimilation system which currently supports 3DVAR capability;
- Numerous physics packages contributed by WRF partners and the research community;
- Several graphics programs and conversion programs for other graphics tools.

The WRF system software is in the public domain and is freely available for community use. The following figure shows the flowchart for the WRF Modelling System Version 2.1.2.

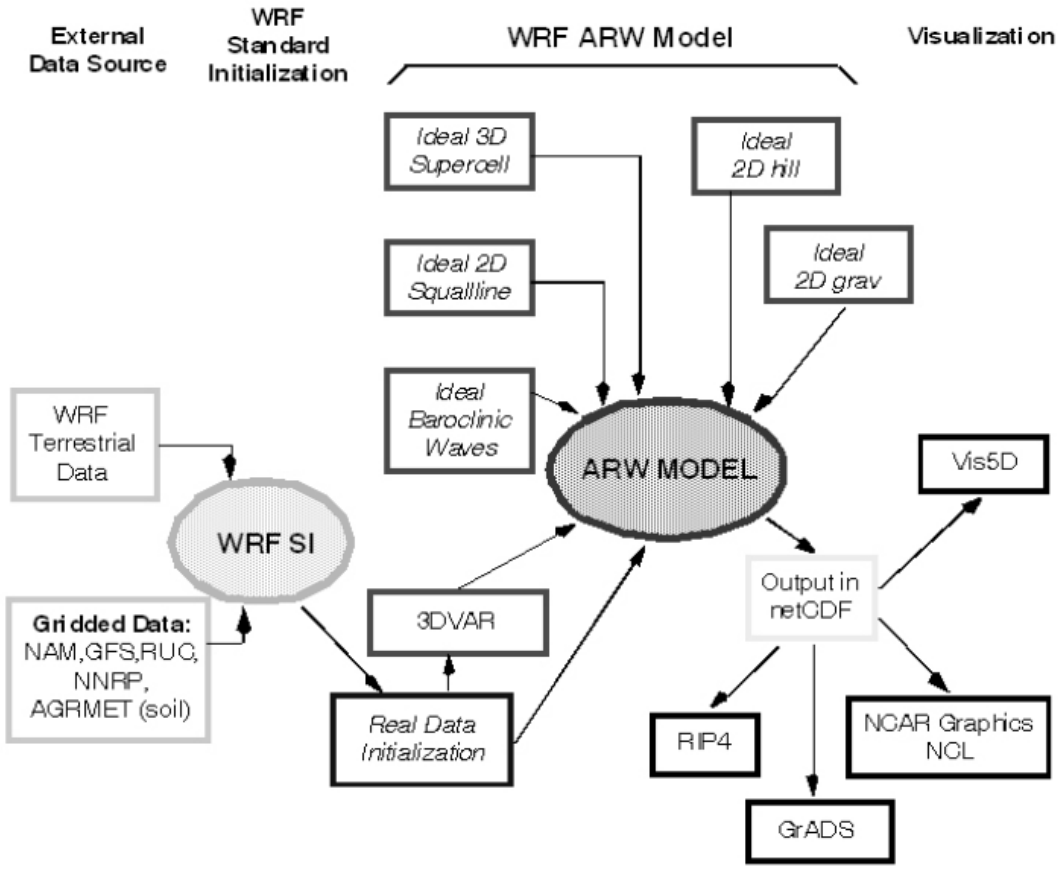

Figure 5.6 ARW WRF modelling system version 2.1.2 flow chart (from WRF ARW guide, 2006).

As shown in the diagram, the WRF Modelling System consists of the major programs: WRF Standard Initialization (WRFSI), WRF 3DVAR, ARW solver, post-processing graphics tools, and ARW Tutorial (beta-version).

WRFSI program is used primarily for real-data simulations only. Its functions include: 1) definition of simulation domains; 2) interpolation of terrestrial data (such as terrain, landuse, and soil types) to the simulation domain; and 3) extraction and interpolation meteorological data from another model or observations to a simulation domain and to the model vertical coordinate. WRF 3-dimensional variation (WRF 3DVAR) is optional, but can be used to ingest observations into the interpolated analyses created by WRFSI. It can also be used to update the WRF model's initial condition when the WRF model is run in cycling mode. ARW solver is the key component of the modelling system, which is composed of several initialization programs for idealized and real-data simulations, and the numerical integration program. The key feature of the WRF model includes:

• Fully compressible nonhydrostatic equations with a hydrostatic option;

• Complete Coriolis and curvature terms;

• One and two-way nesting with multiple nests, nest levels, and moving nests;
• Mass-based terrain following coordinate and vertical grid-spacing that vary with height;
• Map-scale factor for 3 projections: polar stereographic, Lambert-conformal and Mercator;
• Arakawa C-grid staggering and Runge-Kutta 2^{nd} and 3^{rd} order time step options;
• Scalar-conserving flux form for prognostic variables plus 2^{nd} to 6^{th} order advection options;
• Time-split small step for acoustic and gravity-wave modes, including an external-mode filtering option;
• Lateral boundary conditions for idealized and real cases, specified with a relaxation zone;
• Full physics options for land-surface, PBL, radiation, microphysics and cumulus parameterization.

Graphics tools contain several programs, including RIP4 (based on NCAR Graphics), NCAR Graphics Command Language (NCL), and conversion programs for other readily available graphics packages: GrADS and Vis5D (WRF ARW guide, 2006).

Application to the Christchurch area

ARW WRF v2.1.2 was configured on an IBM P575 Cluster 1600 High Performance Computer (HPC) - a Unix-based machine (AIX UNIX) with Power Series hardware and vendor compiler. The WRF code is run on a distributed cluster (physical node, consisting of 16 physical or 32 virtual processors) utilizing both Open MP and MPI.

The WRF Standard Initialisation (WRFSI) program uses a definition of 4 domains (3 nested grids), together with various terrestrial datasets for terrain, landuse, soil type, annual deep soil temperature, monthly vegetation fraction, maximum snow albedo, monthly albedo, slope data, and meteorological data to create a mesoscale domain, and interpolate the above data to this domain. The output from WRFSI is in network Common Data Form (netCDF) format and it conforms to WRF Input/Output interface. The WRFSI was successfully installed and debugged using both PGI and Intel compiler. The WRFSI code runs on single processor machines only. It is memory efficient and a flow chat of the WRF standard initialisation is presented in Figure 5.7. The module consists of 3 parts: domain generation and input data assimilation (independent of each other), and horizontal and vertical interpolation of the input data for created domains. Nudging conditions are constructed for a mother grid only.

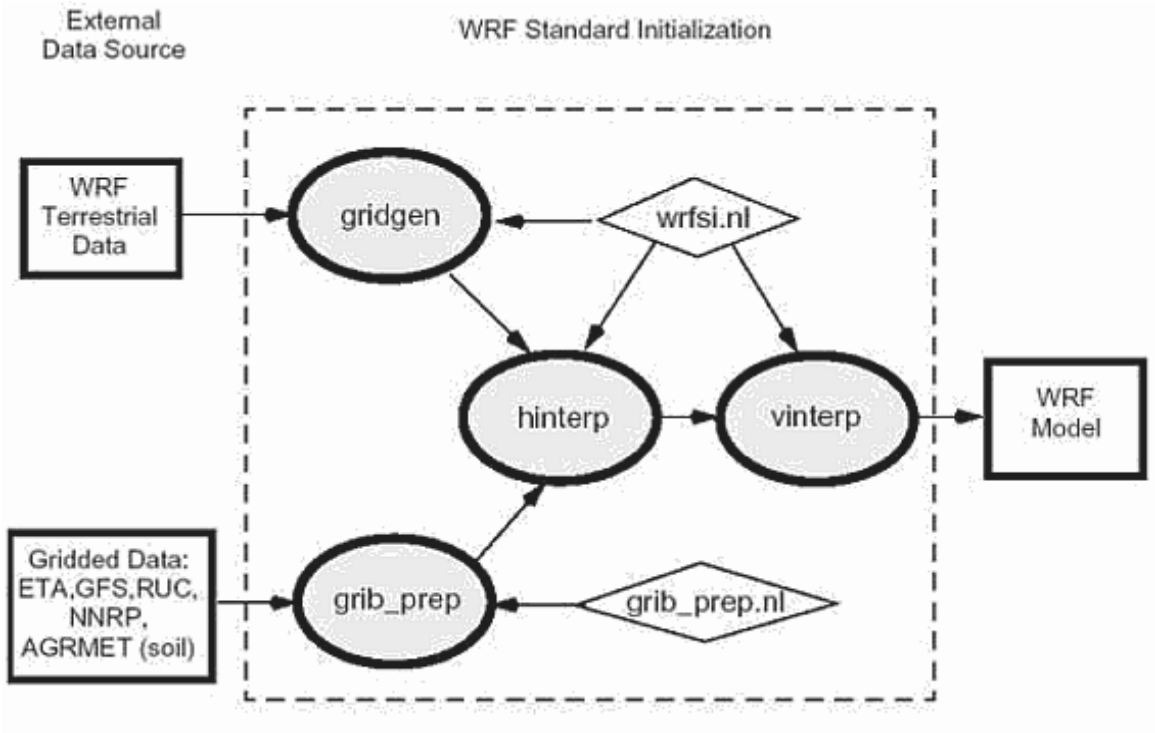

Figure 5.7 WRF Standard Initialisation (version 2.1.2) flow chart (WRF ARW guide, 2006).

The GUI was also installed (Perl 5.04 visual programming language), but assessment of the GUI revealed instability and faultiness of the graphical interface that led to the decision not to use it.
The WRF model code contains several initialization programs (ideal.exe and real.exe), a numerical integration program (wrf.exe), and a program to prepare one-way nesting (ndown.exe) experiments, a described for MM5 in Titov (2004). As mentioned before WRF supports a variety of capabilities, that include real-data and idealized simulations, various lateral boundary condition options for both real-data and idealized simulations, full physics options, non-hydrostatic and hydrostatic runtime options, one-way and two-way nesting and moving nests. Running of WRF ideal and real cases consists of two steps. Initialization (step one) prepares input files for the ideal (ideal.exe) or real (real.exe) model experiment, which consist of wrfinput and wrfbdy files (boundary file is calculated for a mother domain only). The second step is the numerical integration of WRF itself started by using executable command "wrf.exe –procs N" with different value of N depending of the number of active processors.

The flow chart of ARW WRF core execution is shown in Figure 5.8 for real case and for a case of one-way nesting (ndown.exe. The output WRF files with name always starting "wrf_out" are used with postprocessing software for visualisation and actual data extraction. Most part of the post-

processing software (programs RIP4 and WRF2GrADS–GrADS) were inherited from the MM5 interface that made the process of their installation much easier.

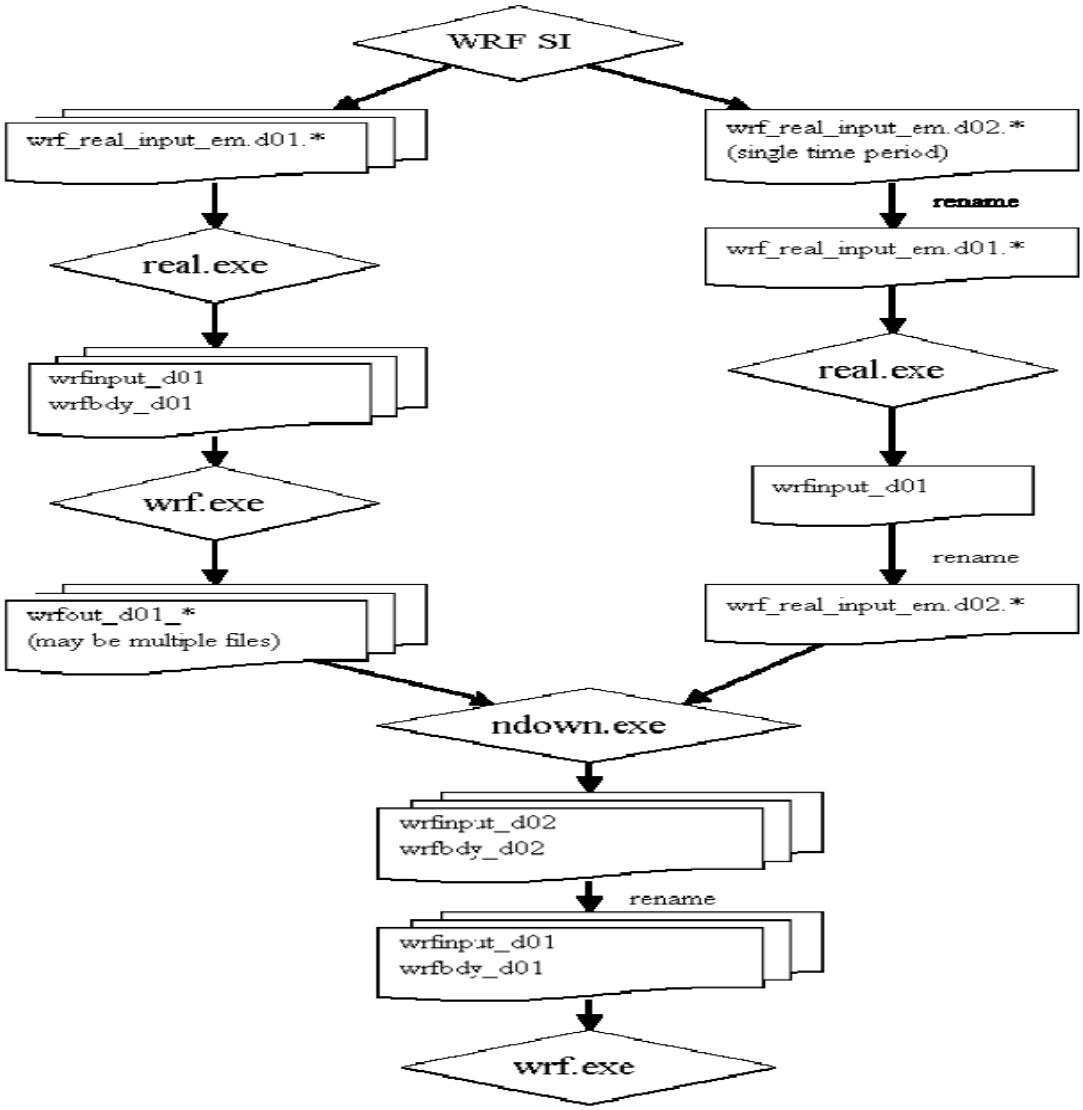

Figure 5.8 WRF (version 2.1.2) flow chart for ideal and real cases (WRF ARW guide, 2006).

WRF utilisation for the Christchurch area included not only WRF pre-processing and numerical time integration, but also extraction of near-surface meteorological data from WRF output files (for grid 4 – 1 km spatial resolution) used in CAMx input.

Advantages and difficulties

Being a new generation limited area numerical models, WRF offers more possibilities, but creates obstacles and problems as a new model (with many bugs especially in pre- and post-processing software. Advantages of the model include new more accurate dynamical and physical parameterisation of atmospherical processes that could potentially lead to better reproduction of the atmospheric phenomena, to better understanding of the actual processes and to an improvement of a forecast. Physical options used for the Christchurch area parameterisation and provided by WRF are considered in this section because of duality in the WRF core physical module behaviour.

In WRF application to the city of Christchurch, the Single-Moment 3-class scheme was used: a simple efficient scheme with ice and snow processes suitable for mesoscale grid sizes (WRF has 9 options). Long-wave radiation was parameterized using the Rapid Radiative Transfer Model (RRTM), which is known to be an accurate scheme using look-up tables for efficiency and accounting for multiple bands and trace gases (WRF has 2 options). The short-wave radiation scheme was the Dudhia scheme: simple downward integration allowing efficiently for clouds and clear-sky absorption and scattering (WRF has 3 options). Surface layer parameterization used the MM5 similarity model based on Monin-Obukhov with a Carslon-Boland viscous sub-layer and standard similarity functions from look-up tables (WRF offers 2 options). Land Surface Model (LSM) was a 5-layer thermal diffusion The LSM including soil temperature only for five layers (WRF offers 3 options). Planetary Boundary Layer was simulated using the non-local-K scheme with an explicit entrainment layer and parabolic K profile in the unstable mixed layer (WRF has 3 options). The very important cumulus parameterization was the well-known MM5 Kain-Fitch scheme: a deep and shallow sub-grid scheme using a mass flux approach with downdrafts and a specially defined removal time step (WRF has 3 options). The diffusion in WRF is categorized under two parameters, the diffusion option and the K option. The diffusion option selects how the derivatives used in diffusion are calculated, and the K option selects how the K coefficients are calculated. Diffusion option was a simple diffusion when gradients are simply taken along coordinate surfaces (WRF has 2 options). The K option with a PBL scheme was a 2d deformation scheme: K for horizontal diffusion was diagnosed from horizontal deformation (WRF offers 4 options). Upper layer damping involved a Rayleigh relaxation added near the model top to control reflection from the upper boundary.

So the number of options provided by developers in dynamical and physical blocks in WRF is stunning but very confusing. It is really tricky to find an appropriate parameterization without a large number of sensitivity studies, and only MM5 experience helps in finding something appropriate for stable time integration. Use of default parameterization options with some cosmetic changes works, but anyone should be very careful when choosing them. WRF crashes very quickly if any incompatibility is inside this very complex mechanism. On-line tutorials don't help much as they consider only a small fraction of potential possibilities. Very few sensitivity studies have been published (except for WRF Workshops in Boulder, Colorado, USA). The price of running WRF run on modern multi-parallel processing computers just adds problems when studying WRF physical-dynamical parameterization options. An evident problem with distribution of vertical layers should be added to what has been said – WRF is not very flexible to changes in the vertical structure.

Advantages of WRF as a future generation model are countered by the complexity of the model numerical interface. In addition to this it should be noticed that post-processing software, inherited mostly from MM5, does not always works with the WRF structure and new bugs in the output data extraction-assimilation procedures are numerous. This situation suggests that maybe it is better to wait until WRF is more communicable and friendly (the new Version 2.2 is the first step in this direction), and to use MM5 for regular work now, only applying WRF for comparison purposes. However progress in the assimilation of new numerical methods is usually very quick and underrated. One of the most advantages features of WRF is a possibility to generate a randomized input numerical error to decrease systematic error in calculations, and the possibility of an ensemble forecast as an essential tool of future weather forecasting (Hamill, 2003; Buizza et al., 2005; Nenrkorn and Hoffman, 2006).

Assessment of MM5 and WRF: research and operational status – 2007

This assessment of MM5 and WRF research status is for the beginning of 2007 and includes the latest version of MM5 (v3.7.3) and the latest version of ARW WRF (v2.2). From the point of view of pre-processing software and possibilities, the MM5 interface is considered to be still better, but it should be stressed that the last version of WRF Standard Initialisation (WRF Pre-processing System - WPS) shows more flexibility in assimilation of local data. The local data could include any variable starting from local topography or surface cover distribution, and finishing by ingesting single observation using a 3-D variation assimilation method. These input data assimilation feature were excellently developed for MM5 by the global community but were

lacking in the previous versions of WRF SI (Standard Initialisation). The possibility of WPS to assimilate local datasets by creating users' own Vtables is one more step for WRF SI to occupy a leading position ahead of MM5. Some aspects of nested grid parameterisation and mother-daughter grid ratio for WRF SI are more promising than the MM5 pre-processing options (ARW User Guide, 2007). However the possibilities for checking WRF WPS output at different steps are more restricted than for MM5 SI, and include only a new version of RIP4 (read-interpolate-plot software) for visualisation.

Comparison of WRF with MM5 definitely supports the supremacy of MM5 from the point of view of the research status of two LAM. The diversity of MM5's physical and dynamical parameterization makes it more flexible and easier to use for different research projects, including more accurate and realistic output results. As mentioned before, the number of WRF validation studies is small and researchers have to rely on MM5 experience, to avoid a big number of sensitive studies, or apply default WRF options. This status of WRF will change over the next few years, but at last now there are no serious pilot studies (except the ones presented at the WRF workshop in Boulder, Colorado, USA) in the literature that compare different physical-dynamical parameterization schemes of MM5 and WRF.

The flexibility of post-processing software is a very difficult question and its usefulness depends on the needs of the user. However MM5 post-processing software is currently considered to be more flexible compared with WRF for a wide range of tasks. One of the "inbuilt bugs" of the ARF WRF post-processing software results from the initial priority of WRF to be an operational model. This leads to difficulties to obtain time series from WRF long runs, which could be decided by changes to the WRF FORTRAN code re-compilation. Also, WRF output files are several times bigger than MM5 because of use of the netCDF format for WRF input-output.

Comparison of the operational status of WRF versus MM5 indicates the more preferable position of MM5 with regards to several very important aspects of operational forecasting: MM5 is much faster, less space consuming model (for the same computing system) with more accurate reproduction of the real synoptic situation. The operational status of WRF depends on the available computing facilities, and usually WRF should be run on the new generation of high-performance computers (HPC). Advantages of running WRF on HPC are evident for big domains (like North America) only. WRF application for small domains (like New Zealand) using more than 1 physical

node leads to decrease of calculation speed, and there is no reason to run ARF WRF operationally on more than 1 node.

5.4 Summary

Meteorological limited area models used for the Christchurch area and described in Chapter 4 include MM5 and ARW WRF. The MM5 limited-area meteorological model was considered the preferred LAM in the USA for many years, but is now gradually being substituted by a new generation limited area model WRF (WRF User Guide, 2007). The process of MM5 replacing by a new model officially supported by NCAR will take some time. At this stage MM5 is the preferable model and is actively used for research applications such as the Christchurch winter PM studies. The future of WRF seriously depends on NCAR developers undertaking pilot sensitivity studies for ARW WRF in comparison to MM5.

Chapter 6: 3-D Eulerian modelling of Particulate Matter

It is apparent that study of the air pollution problems is an active topic in applied numerical modelling. Several special reviews of air pollution research have been published, and the majority of the works are dedicated to air pollution modelling (Sturman, 2000) or descriptive analysis of the air quality degradation problem in a range of different environments. This research illustrates the complex interactions between the atmosphere, topography and resulting quality of air for defined regions.

The technique of 3-D Eulerian modelling in regional meteorology can be applied to the problem of PM dispersion. Understanding mesoscale and miscroscale controls of local airflow and atmospheric boundary layer structure is a principal step in studying atmospheric aerosol pollution problems. For instance, the problem of near-surface air pollution dispersion during synoptic stagnant situations and the dominance of local circulations over areas of complex terrain are now well known, and is applied in a number of numerical chemical studies using 3-dimensional dispersion models. Air quality prediction models can generally reproduce these processes accurately and have a tendency to provide more realistic forecasts of the air pollution in the nearest future (Arya, 1999).

Improvements in knowledge and rapid developments of computer technology have created a trend in air pollution research towards more complex hybrid numerical models including 3-D Eulerian type models and applications in different forms (Lagrangian and Puff modules). Complex photochemical hybrid models, often based around mesoscale limited area meteorological models, include composite atmospheric dispersion modules and incorporate a large number of input chemical species and a large range of primary and secondary chemical reactions of gases and pollutants.

6.1 CAMx version 4

The Comprehensive Air quality Model with extensions (CAMx) is Eulerian photochemical dispersion model that allows for an integrated ‘one-atmosphere’ assessment of gaseous and particulate air pollution over many scales, ranging from urban to ‘super-regional’. It is designed to unify all of the technical features required of ‘State-of-the-Science’ air quality models into a single efficient system, which is publicly available. The input/output formats are based on the Urban Airshed Model (UAM-IV) and are compatible with many existing formats.

CAMx4 simulates the emission, chemical reactions during dispersion, and removal of pollutants in the lower troposphere by solving the pollutant continuity equation for each chemical species (l) on a system of nested three-dimensional grids. The Eulerian continuity equation describes the time dependency of the averaged species concentration ($c_l(t)$) within each grid cell volume as a sum of all of the physical and chemical processes operating in that volume (ENVIRON Int. Corp., 2003; 2005):

$$\partial c_l/\partial t = -\nabla_H \bullet \boldsymbol{V}_H c_l + [\,\partial(c_l\eta)/(\partial z) - c_l\,\partial/\partial z(\partial h/\partial t)\,] + \nabla \bullet \rho\, K\nabla(\,c_l/\rho) + \partial c_l/\partial t\,|_{Chemistry} + \partial c_l/\partial t\,|_{Emission} + \partial c_l/\partial t\,|_{Removal} \qquad (6.1)$$

where $\boldsymbol{V}_H$ is the horizontal wind vector, η is the net vertical 'entrainment rate', h is the layer interface height, ρ is atmospheric density, K is the turbulence exchange (diffusion) coefficient (CAMx receives all these characteristics from the meteorological numerical model – MM5 or WRF).

The physical representation and numerical methods used in CAMx4 for each of the terms of the pollutant continuity equation (6.1) include 6 modules (ENVIRON Int. Corp., 2003): horizontal advection/diffusion, vertical transport/diffusion, chemistry module with Carbon Bond IV (CB IV) mechanism, dry deposition module, wet deposition, and plume in grid (PiG) with inorganic chemistry (ENVIRON Int. Corp., 2005).

CAMx4 allocates concentrations to the centre of each grid cell, representing the average concentration over the entire cell. CAMx4 internally carries meteorological fields in an arrangement of the 'Arakawa C' grid configuration: temperature, pressure, water vapour and cloud water are located at the cell centre together with concentrations; wind components and diffusion coefficients are carried at cell interfaces to describe the transfer of mass in and out of each cell. In the vertical, most variables are loaded at each layer midpoint except those variables that describe the rate of mass transport across the layer interface, which include the vertical diffusion coefficient K_v and the vertical entrainment rate η. These variables are carried in the centre of each cell horizontally, but are located at the top of the layer (i.e. interface) vertically.

CAMx4 can perform simulations on the three types of Cartesian map projections: Universal Transverse Mercator, Rotated Polar Stereographic and Lambert Conic Conformal. CAMx also offers the option of operating on a curvi-linear geodetic latitude/longitude grid system. The vertical grid structure is defined externally, so that layer interface heights may be specified as any arbitrary function of space and time.

CAMx incorporates two-way grid nesting, which means that pollutant concentration information propagates into and out of all grid nests. Any number of grid nests can be specified in a single run, while grid spacing and vertical layer structures can vary from one grid nest to another. Nesting in the vertical is allowed, but only by sub-dividing parent grid layers into a series of finer layers. To maximize flexibility in the vertical structure, each parent grid layer may be individually split into a unique set of fine layers, or not split at all. The flexi-nest option in CAMx allows users to redefine the nested grid configuration at any point in a simulation. Nested grids can be introduced or removed only at the time of a model restart, when users can redefine the nested grids structure in the CAMx input general configuration information file. Flexi-nesting provides flexibility to both meteorological and emission input files to a nested grid and allows CAMx4 to interpolate data from the parent grid.

The approach to pollutant transport solving in CAMx4 provides both mass conservation and mass consistency. To be mass conservative, CAMx4 carries concentrations of each species internally as a density and solves the advection equations in flux form. Mass consistency refers to CAMx4's ability to transport pollutant mass exactly equivalent to the input atmospheric momentum field. Sources of mass inconsistency in CAMx4 can be from: input meteorology that is inherently inconsistent from an interpolated objective analysis with meteorological fields numerically developed; spatial interpolating or averaging MM5 three-dimensional wind vector fields to a different size grid of CAMx4; and employing differently parameterized numerical and physical techniques in CAMx4 and MM5. It is therefore best if translation of meteorological data to CAMx4 is achieved with as few additional manipulations as possible. Horizontal advection is performed using the area preserving flux-form advection solver from Bott (Bott, 1989) or the Piecewise Parabolic Method (PPM) of Colella and Woodward (Colella and Woodward, 1984), as implemented by Odman (Odman *et al.,* 1996).

Profile development for PM investigation

In the research PM numerical evaluation is developed on a basis of CAMx version 4.01 (issued in 2003 with implemented PM module), CAMx version 4.1 (with aerosol chemistry improvements and establishment of the Particulate Source Appointment Technology - PSAT), and CAMx version 4.2 (with implementation of first features of the CB05 chemistry mechanism). Full CB05 will be available in the release of CAMx v4.50 year 2008.

CAMx4 code was developed during the late 1990s using modern modular coding practices. This has made the model an ideal platform for addressing a variety of air quality issues including particulate matter (PM), visibility, and acid deposition. ENVIRON corporation, together with Sonoma Technology, Inc. (STI) and Carnegie Mellon University (CMU), added an algorithm for aerosol modeling to CAMx4 to create a new particulate matter model called PMCAMx inside CAMx (starting from CAMx version 4.01). The extension to handle PM involved the addition of science modules to represent important physical processes for aerosols:

- Size distribution is represented using the Multi-component Aerosol Dynamics Model (MADM), which uses a sectional approach to represent the aerosol particle size distribution (Pilinis et al., 1989). MADM treats the effects of condensation/evaporation, coagulation and nucleation upon the particle size distribution.
- Inorganic aerosol thermodynamics are represented using ISORROPIA model (Nennes et al., 1998) within MADM.
- Secondary organic aerosol thermodynamics are represented using the semi-volatile scheme of Strader and co-workers (1999).
- Aqueous-phase chemical reactions are modelled using the Variable Size-Resolution Model (VRSM), which automatically determines whether water droplets can be represented by a single 'bulk' droplet-size mode or whether it is necessary to use fine and coarse droplet-size modes to account for the different pH effects on sulphate formation.
- The CAMx deposition algorithms were improved for particle deposition.

The dynamic behaviour of a spatially homogeneous PM species or PM's thirteen chemical components of aerosol in 3-10 weight groups (Yarwood et al., 2003) were described in Table 3.1 (sections 3.4). The example of 130 aerosol species is introduced in Table 6.1 for the Los Angeles region.

Table 6.1 Aerosol size groups for PMCAMx application to the Los Angeles region (after Yarwood et al., 2003).

Section	Lower Cut-point (µm)	Upper Cut-point (µm)
1	0.039063	0.078125
2	0.078125	0.15625
3	0.15625	0.3125
4	0.3125	0.625
5	0.625	1.25
6	1.25	2.5
7	2.5	5
8	5	10
9	10	20
10	20	40

The PMCAMx gas-phase chemistry was modified to simulate more accurately the formation of secondary aerosol precursors, including:

- Track production of four condensable gasses (CG1–CG4) formed in the oxidation of 14 VOCs that are secondary organic aerosol (SOA) precursors (Yarwood et al., 2003).
- Add a new olefin species, called OLE2, to the CB4 mechanism to represent biogenic olefins so that high SOA-yield biogenic olefins can be distinguished from low SOA-yield anthropogenic olefins.
- Track ammonia as a precursor to ammonium aerosols.
- Track SO_2 and gaseous sulphuric acid as precursors to sulphate aerosols.
- Track HCl as a precursor to and vaporization product of sea salt (sodium chloride) aerosols.

The partitioning of the condensable organic gases between the gas and aerosol phases is simulated using the methods developed by Strader et al. (1999). In PMCAMx, the SOA module is implemented with four classes of semi-volatile organics that have different volatility properties (defined by saturation concentration and heat of vaporization as shown in Table 6.2). The four condensable gasses are called CG1–CG4 and the corresponding secondary organic aerosols are called SOA1–SOA4, as shown in Tables 3.1 and 6.2. The SOA module calculates the equilibrium distribution between the gas and aerosol phase for each CG/SOA pair. Secondary organic material may condense to the aerosol phase or evaporate to the gas phase depending upon the CG/SOA equilibrium distribution. The volatility properties of the condensable gases (CG1–CG4) are shown in Table 6.2 along with the aerosol yields (µg m^{-3} of aerosol precursor per ppm of gas reacted)

from different VOC precursors. The CG species are the only gas species in CAMx that are not defined in ppm (particles per million) units but in µg m^{-3} because the aerosol yields are conventionally defined this way.

Table 6.2 Properties of condensable gas precursors (CG1-CG4) to the secondary organic aerosols (after Yarwood et al., 2003).

CB4 VOC precursor	condensable gas species	aerosol Yield (µg m^{-3} ppm^{-1})	saturation concentration (µg m^{-3} at 281.5 K)	heat of vaporization ΔH_{vap}	molecular Weight
PAR	CG3	53.6	0.007	0	150
OLE	CG3	14.6	0.007	0	150
TOL	CG1	430	0.023	156,250	150
TOL	CG2	836	0.674	156,250	150
XYL	CG1	268	0.023	156,250	150
XYL	CG3	1178	0.007	0	150
CRES	CG1	221	0.023	156,250	150
OLE2	CG4	999	0.008	0	180

The chemical composition of the inorganic aerosol phase is calculated using the ISORROPIA model, which was selected over alternative algorithms because it provides good performance with regards to accuracy, speed and stability (Ansari and Pandis, 1999). Solid, liquid and gas phase chemistry is modelled for the sulphate, nitrate, ammonium, chloride aerosol system, as described earlier in Section 3.4 (Table 3.2).

The size distribution of aerosols is solved using the algorithms described by Pilinis et al. (2000) for the Multi-component Aerosol Dynamics Model (MADM). The aerosol size distribution can be modified by the following physical processes that are represented in PMCAMx:

- Condensation/evaporation of inorganic and organic aerosol constituents.
- Coagulation.
- Nucleation of sulphuric acid.
- Aqueous-phase chemistry.
- Deposition.

In PMCAMx the coagulation size distribution is three times finer than the PMCAMx size distribution. The degree of over-resolution is determined by a model parameter that may need to be

changed if PMCAMx is used with different size groups in the future. Nucleation is modelled based on the parameterization of Russell et al. (1994). The nucleation rate depends upon the gaseous sulphuric acid concentration, which in PMCAMx is from the gas-phase OH + SO_2 reaction. MADM simulates the complete atmospheric aerosol size/composition distribution by solving the condensation-evaporation equation. MADM includes three methods for solving the particle size distribution called the equilibrium, hybrid and dynamic methods. The equilibrium algorithm is the fastest and most stable approach, but may introduce errors or instability under certain condition (next section). PMCAMx always uses the equilibrium assumption within MADM to solve the particle size distribution.

Aqueous-phase chemistry is important for modeling the production of sulphate from the oxidation of sulphur dioxide in cloud and/or fog water droplets. The rate of sulphate production is a nonlinear function of aqueous concentrations, cloud water pH and the size of the water droplets. In these cases, improved accuracy can be obtained by using a more computationally demanding size-resolved algorithm that explicitly represents cloud droplets of several different sizes. The aqueous phase chemistry in PMCAMx uses either bulk or size-resolved droplet models depending upon ambient conditions.

Aqueous-phase chemistry is simulated using the method described using the Variable Size-Resolution Model (VSRM). The VSRM allows both bulk and size-resolved (two sections) aqueous-phase chemistry. Selection of either the bulk algorithm or the two-section algorithm is made automatically using heuristic rules (Fahey and Pandis, 2001) every time the aqueous-phase chemistry module is called (i.e., for each grid cell at each time step). Both algorithms simulate the dissolution of gaseous and aerosol material into cloud water droplets, partitioning of species between the aqueous and gas phases, and chemical reactions within the aqueous phase.

Differences between bulk and size-resolved model predictions can be linked to the pH differences across the droplet size spectrum and the pH-dependent reactions forming aqueous-phase sulphate. A set of heuristic rules can determine whether the bulk or size-resolved calculations are used. The "decisions" are based on six input conditions: liquid water content, aerosol alkalinity, dust content and the initial gas-phase concentrations of SO_2, H_2O_2, NH_3 and HNO_3.

The removal of pollutants from each column of grid cells is governed by the deposition velocity in the surface layer and the diffusive coupling of layers moving up the column from the surface. Dry deposition of gases is modelled based on an improved version of the Wesley (1989) resistance model. Deposition velocities are derived from models that account for the reactivity, solubility, and diffusivity of gases, local meteorological conditions and surface characteristics. Wet deposition is treated in PMCAMx using a simple scavenging coefficient approach. An improved wet deposition algorithm has been developed for gases and particles that are suitable for aerosol modelling.

The Particulate Matter Source Apportioning Technology (PSAT) has been developed for CAMx4 (since version 4.1) to provide geographic region and source category specific PM source apportionment. Source apportionment for primary PM is relatively simple to obtain from any air pollution model because source-receptor relationships are essentially linear for primary pollutants. Gaussian 3D models and Lagrangian puff models have been used extensively to model primary PM pollution from specific sources. The Gaussian and Lagrangian approaches work for primary PM because the models can assume that emissions from separate sources do not interact. This assumption breaks down for secondary PM pollutants (e.g., sulphate, nitrate, ammonium, secondary organic aerosol) and so puff models may dramatically simplify the chemistry (to eliminate interactions between sources) so that they can be applied to secondary PM. Eulerian photochemical grid models are better suited to modelling secondary pollutants because they account for chemical interactions between sources. PSAT in CAMx4 was developed to retain the advantage of using a grid model to describe the secondary PM chemistry and provide source apportionment. PSAT is designed to source apportion the following PM species modelled in CAMx4: sulphate, particulate nitrate, ammonium, particulate mercury, secondary organic aerosol (SOA), and six categories of primary PM.

The PSAT “reactive tracers” that are added for each source category/region (i) are described below. In general, a single tracer can track primary PM species whereas secondary PM species require several tracers to track the relationship between gaseous precursors and the resulting PM. Nitrate and secondary organic PM are the most complex aerosol species to apportion because the emitted gases (NO, VOCs) are several steps removed from the resulting PM (nitrate, SOA). The reactive tracers used by PSAT include a total of 32 tracers for each source group if source apportionment is applied to all types of PM. Since source apportionment may not always be needed for all species, the PSAT implementation is flexible and allows source apportionment of

selected chemical classes in each CAMx4 simulation. For example, source apportionment for sulphate/nitrate/ammonium requires just 9 tracers per source group (Yarwood et al., 2004).

The PSAT approach to source apportionment is quite simple and robust. When considering two model species A and B that are apportioned by reactive tracers a_i and b_i, respectively, reactive tracers must be included for all sources of A and B including emissions, initial conditions and boundary conditions so that complete source apportionment is obtained, i.e., $A = \Sigma a_i$ and $B = \Sigma b_i$. The general approach to modelling change over a model time step Δt is illustrated for a chemical reaction:

$A \rightarrow B$

The general equation for species destruction is:

$a_i(t+\Delta t) = a_i(t) + \Delta A\ [a_i / \Sigma a_i\ ]$

Here the relative apportionment of A is preserved as the total amount changes. This equation applies to chemical removal of A and also physical removal by processes such as deposition. The general equation for species chemical production is:

$b_i(t+\Delta t) = b_i(t) + \Delta B\ [a_i / \Sigma a_i\ ]$

Here the product B inherits the apportionment of the precursor A. In some cases, source category specific weighting factors (w_i) must be added to the equation for species destruction:

$a_i(t+\Delta t) = a_i(t) + \Delta A\ [w_i a_i / \Sigma w_i a_i\ ]$

An example is chemical decay of the aromatic VOC tracers (ARO), which must be weighted by the average OH rate constant of each ARO_i as ARO tracers for different source groups have different average VOC reactivity (Yarwood et al., 2004).

In 2005, an updated version of the Carbon Bond mechanism were developed by ENVIRON corporation for use in EPA atmospheric modelling studies. Updates in CB05 compared to the earlier CB4 mechanisms are (Yarwood and Rao, 2005):

- Updated rate constants based on recent (2003–2005) IUPAC and NASA evaluations.
- An extended inorganic reaction set for urban to remote tropospheric conditions.
- NO_x recycling reactions to represent the fate of NO_x over multiple days.
- Explicit organic chemistry for methane and ethane.
- Lumped higher organic peroxides, organic acids and peracids.
- Higher aldehyde species ALDX making ALD2 explicitly acetaldehyde.
- Higher peroxyacetyl nitrate species from ALDX called PANX.
- Optional mechanism extension for reactive chlorine chemistry.

• Optional extended mechanism with explicit reactions for air-toxics.

The core CB05 mechanism has 51 species and 156 reactions. The CB05 was evaluated against smog chamber data from the Universities of North Carolina and California at Riverside. The addition of higher aldehyde (ALDX) and internal olefin (IOLE) species to CB05 improve mechanism performance for simulating these species groups. The addition of organic peroxide species improves the simulation of oxidants that are involved in PM sulphate formation. Two CB05 mechanism extensions were developed. The reactive chlorine chemistry mechanism can be used in conjunction with the CB05 core mechanism to model the impact of CL2 and/or HOCl emissions on oxidant formation and VOC decay rates. The explicit species extension can be used in conjunction with the CB05 (or another) core mechanism to model the following toxic species: primary formaldehyde, primary acetaldehyde, 1,3-butadiene, primary and secondary acrolein. These include the main precursors to secondary organic aerosol (SOA) and could be used as the basis for a refined modelling approach for SOA that is independent of the core chemical mechanism selected (Yarwood and Rao, 2005).

Numerical investigation of a $PM_{2.5}$ night smog episode using 3 versions of CAMx4 is presented in Figure 6.1 (8-10 of May 2005) compared with observations obtained from the Coles Place observation site. The two-day (48 hours) aerosol pollution episode is considered to be a non-standard one with observed $PM_{2.5}$ maximum after midnight (9 of May 2005), and MM5-CAMx4 failed to reproduce this episode (CAMx version 4.31 is an extensive version of CAMx version 4.2).

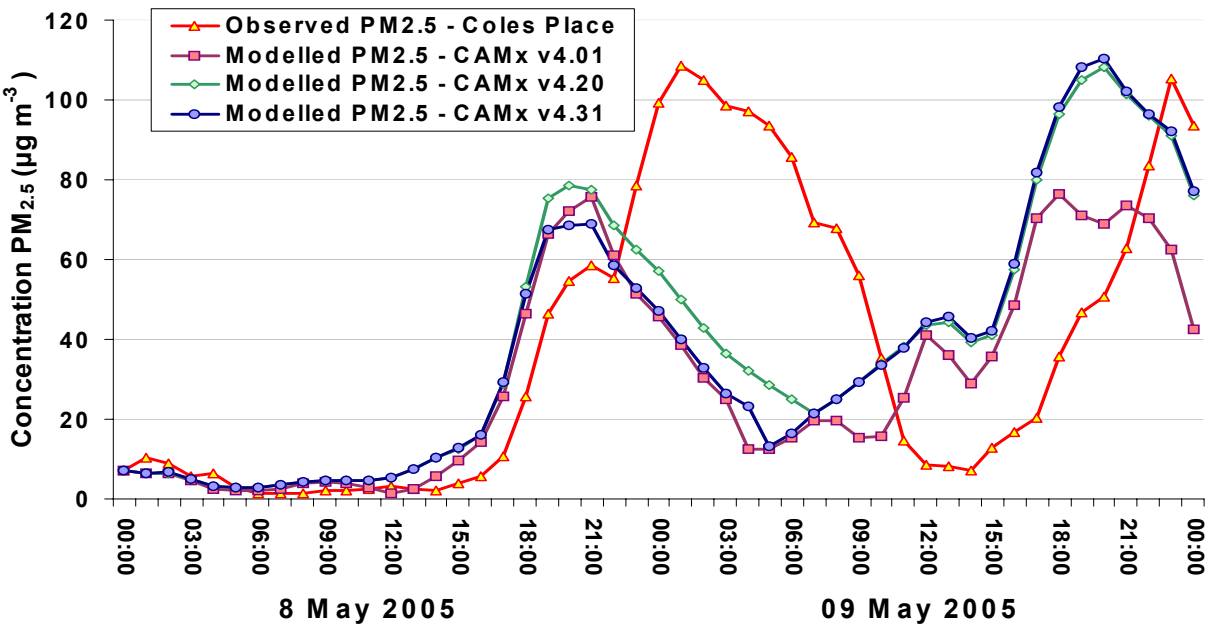

Figure 6.1 Observed and predicted $PM_{2.5}$ concentrations (µg m^{-3}) for 8-9 May 2005, Coles Place, St.Albans.

The quality of reproduction of the second night (9 May 2005) $PM_{2.5}$ maximum concentrations is much better (still being low quality) for CAMx version 4.2 (green line) and version 4.31 (blue line), than for version 4.01 (violet line) compared with observations (red line). Input near-surface meteorology was the same for all 3 CAMx4 runs. This example indicates some improvement of more recent CAMx4 versions to reproduce the time trend real aerosol concentrations, especially after 24 hours of modelling. CAMx4 failed to reproduce the first night's PM peak, but succeeded in replicating the second night's aerosol peak magnitude (but not the phase). This fact proves the improved chemical solver in time for the secondary organic (SOA) and inorganic (soluble ions) PM species in the more recent CAMx4 versions. The phase error between observed and modelled PM peaks is the same for all three CAMx4 versions and speaks about origin of this mistake inside input modelled meteorology. The amplitude and phase errors in reproducing real PM spatial-temporal distribution lead to the CAMx4 numerical instability (modelling uncertainty).

Chemical and numerical flexibility and instability

Numerical flexibility of CAMx4 is expressed in the model's ability to assimilate a large diversity of the additional applications. The flexible CAMx4 framework has also made it a convenient and robust host model for the implementation of "probing tool" techniques such as Process Analysis, the Decoupled Direct Method (DDM), the Ozone Source Apportionment Technology (OSAT), and the Particulate Source Appointment Technology (PSAT). However amplitude and phase errors in

reproduction of real PM as a result of CAMx modelling uncertainties (unrealistic description of particulate and gaseous chemistry processes, uncertainties of formation and scavenging mechanisms, and so on) lead to CAMx4 numerical instability. There is an extensive literature that discusses sources of modelling uncertainty (numerical instability) and methods for its evaluation. For example, Fine et al. (2003) reviewed the issues associated with evaluation of model numerical instability in photochemical models. The authors explored the range of sensitivity, diagnostic and other constructive studies used in performing modelling uncertainty analyses. Numerical instability, in general, consists of contributions from all sources in varying degrees, associated with deterministic or stochastic causes (Lohman et al., 2000). The sources of numerical instability include model inputs such as emissions, meteorology, land-use, initial and boundary conditions, and deficiency in model formulations (parameterizations) of the physical and chemical processes.

Stochastic variability is due to turbulence and other random processes not simulated by deterministic models. This type of photochemical model numerical instability arises from the grid scale dependency of models. A fundamental attribute of deterministically modelled air-pollutant concentrations is that they are grid size-dependent (Odman and Russell, 1991). Thus, quantitative comparisons of modelled aerosol concentrations with observations will change due to different choice grid cell size. When numerical instability of sub-grid processes is significant, the comparison of grid model outputs with measurements is often not very encouraging (see Figure 6.1). Moreover, any observation reflects an event out of a population, while a model prediction represents an average of the population.

Regarding chemical flexibility, the mechanisms supported in CAMx4 (versions issued before v4.5, 2008) are based on version 4 of the Carbon Bond mechanism (CB4, Gery *et al.,* 1989) and the SAPRC99 mechanism (Carter, 2000). CAMx4 included five chemistry mechanisms: two versions of the ‘standard’ CB4 mechanism, chlorine chemistry mechanism, the mechanism of aerosol modelling and the fixed parameter version of the SAPRC99 mechanism. CB4 (mechanism 3) with reactive chlorine chemistry contains: 110 primary reactions and 48 species (34 state gases and 14 radicals). For mechanism 3 with particulate matter extension CAMx includes (for aerosol modelling): 100 primary reactions and 62 species (35 state gases, 14 radicals and 13 aerosols).

Part implementation of a new CB05 (Carbon Bond 05) was founded in CAMx version 4.2 (and extensions 4.4 and 4.4.2), but will be fully available only from CAMx v4.5 (2008). New Carbon Bond mechanism will extend CB4 adopted by US EPA in the mid 1990 (ENVIRON, 2005). The

new version of the Carbon Bond mechanism was called CB05 because it was developed in 2005. The CB05 is a condensed mechanism of atmospheric oxidant chemistry that provides the basis for computer modeling studies of ozone, particulate matter (PM), visibility, and acid deposition and air toxics issues (Yarwood and Rao, 2005). The CB05 mechanism updates developed for the study were as follows:

1. Incorporating current kinetic and photolysis data in the core mechanism;
2. Extending the chemical mechanism to better support PM modelling needs, such as formation of secondary organic aerosols (SOA);
3. Adding extra species and reactions to treat a number of volatile organic compounds (VOCs) explicitly for modelling air toxics;
4. Accounting for the role of reactive chlorine emissions in VOC oxidant chemistry.

Initial gridded concentrations of gases and particulate matter are used by the mother grid of CAMx4 when gridded emissions of pollutants are to be modelled. Gridded emissions of gases and aerosols are supplied at specific time intervals during CAMx4 runs (the time interval can range from 1.5 minutes to a few hours depending on the process to be investigated and computer resources), but only for the lowest (boundary) layer of the model.

The removal of PM and gases from the modelling cycle during CAMx4 integration includes 2 ways of scavenging. Trace gases and small particles are removed from the atmosphere via deposition: dry deposition refers to the direct sedimentation and/or diffusion of material to various terrestrial surfaces and uptake into biota, wet deposition refers to the uptake of material via chemical absorption (gases) or nucleation/impaction (particles) into cloud water, and the subsequent transfer to the Earth surface by precipitation. Wet deposition is an important removal process for particles, as they act as cloud condensation nuclei. The cloud droplets grow and collect into sufficiently large sizes to fall as precipitation. A fraction of particles that are subsequently entrained into the cloud are scavenged by liquid precipitation via impaction. The rates of nucleation and impaction depend upon cloud type, rainfall rate and particle size distribution. Wet deposition occurs through the following series of steps: mixing of trace gas and condensed water in common air space, absorption of gas molecules by water droplets, possible reactions of the pollutant within water droplets, precipitation of droplets and diffusion of ambient gases into falling precipitation.

Numerically solving the time evolution of the gas and particle phase chemistry is typically the most 'expensive' part of a photochemical grid model simulation, especially for the aerosol phase. Two chemistry solver options are available in CAMx4, the Implicit-Explicit Hybrid (IEH) solver (Sun *et al.,* 2000) and the Chemistry Mechanism Compiler (CMC) fast solver. CMC solver is nearly three times faster than IEH, and solution of both solvers is very similar for daytime conditions, but differs at night. The accuracy of the CMC fast solver is an improvement over many commonly used solvers and the availability of the IEH solver option provides a way to evaluate the CMC solver performance and provides an alternative for CAMx users who choose to accept longer run-times (more than 24-48 hours).

As was described in the previous section, the size distribution of aerosols is solved using special algorithms (Pilinis et al. 2000) for the Multi-component Aerosol Dynamics Model (MADM). MADM simulates the complete atmospheric aerosol size/composition distribution by solving the condensation-evaporation equation, and includes three methods for solving the particle size distribution called the equilibrium, hybrid and dynamic methods. The equilibrium algorithm is the fastest and most stable approach but may introduce errors under certain conditions (Wexler and Seinfeld, 1990). Meng and Seinfeld (1996) suggested that while the sub-micron aerosol may reach equilibrium in a few minutes, it may take hours or days for the coarse particles to attain this state as the time integration scale is larger. Laboratory measurements of Dassios and Pandis (1999) showed that the mass transport of ammonium nitrate is significantly faster than the above theoretical studies had assumed, and that the time scale for equilibration of the accumulation mode is probably less than 20 minutes. But laboratory studies use to operate with continuous fields (with unlimited number of the freedom degrees).

Evidence of the instability of the MADM equilibrium mechanism over the period 0000 NZST on 7 June 2005 to 0000 NZNT 9 June 2005 (Coles Place) is shown in Figure 6.2.

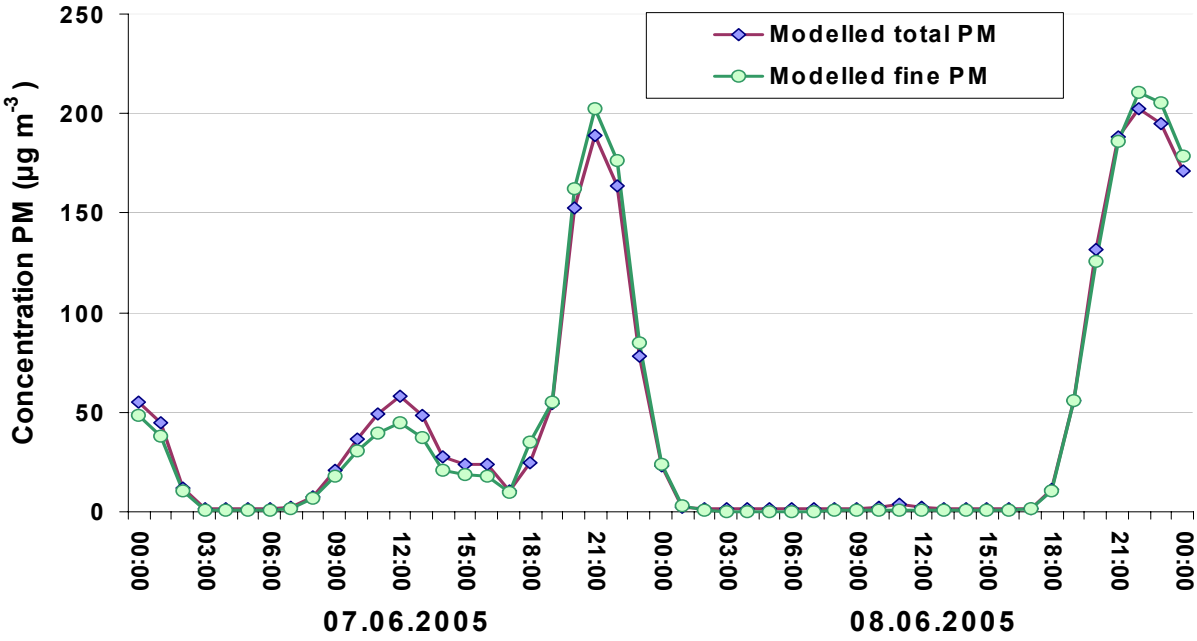

Figure 6.2 Predicted $PM_{2.5}$ (green line) and PM_{10} (blue line) concentrations (µg m^{-3}) for 7-9 June 2005 modelled episode (Coles Place).

Hourly averaged concentrations of fine PM (green line) exceed total PM (blue line) over several hours of the night-time aerosol peaks. The modelling results support suggestion of CAMx4 numerical chemical instability for the coarse PM mode described in Meng and Seinfeld (1996). Overestimation of fine PM (or underestimation of coarse PM) leads to obscure statistical results for predicted PM, when coarse PM_{10} fraction becomes equal to zero while $PM_{2.5}$ concentrations are positive (chemical instability will be traced in the modelling results). Number of fine and coarse PM fractions defined in CAMx4 can also invest in the numerical chemical instability.

Particulate water parameterization via TEOM observations

One more class of CAMx4 chemical instability is associated with the aerosol water (PH_2O) that is considered in CAMx particulate matter specie with a positive correlation with atmosphere relative humidity and negative correlation with ambient air temperature.

As described in Chapter 4, airborne aerosol is measured routinely at the permanent residential monitoring site at Coles Place and all measurements are conducted using a TEOM Series 1400a Ambient Particulate Monitor (Rupprecht and Patashnick Co. Inc., 1993). The instrument is able to continuously measure the mass of PM accumulating on a filter mounted on an oscillating balance. But the essential feature of the instrument is the heating of the air stream to prevent the condensation of water vapour on the samples collected. In typical operation regime TEOM

maintains a constant air stream temperature of 40^0 C (Kingham et al., 2005), but operation at this temperature in any way cause volatilization of the particulate semi-volatile material (PSVM) component of PM, leading to a systematic under-estimation of the true PM mass in ambient data. As a result, TEOM gives so-called "dry PM" concentrations, and a correction coefficient (1.4-1.8) is recommended to balance the loss of PSVM (Charron et al., 2004; Kingham et al., 2005).

In CAMx4 aerosol parameterization (starting from version 4.2) aerosol water is explicitly treated in coarse-fine groups or in several groups of PM chemistry that affects secondary aerosol size and density (ENVIRON, 2005). Aerosol water is treated as independent specie of PM chemical content that is evident from Table 6.3, which lists the PM species included in CAMx4 mechanism 4. Also aerosol water (PH_2O) is included in the enumeration of the mandatory inorganic species of PM jointly with particulate sulphate (PSO_4), particulate nitrate (PNO_3), particulate ammonia (PNH_4) and 5 groups of secondary organic aerosols (SOA1-5).

Table 6.3 List of PM species included in CAMx4 mechanism 4 (after ENVIRON, 2005).

Internal Label	Name	Mandatory Species
PSO4	Sulfate	X
PNO3	Particulate Nitrate	X
PNH4	Particulate Ammonium	X
PH2O	Aerosol Water Content	X
SOA1-5	Five Secondary Organic Aerosols	X
NA	Sodium	
PCL	Particulate Chloride	
POA	Primary Organic Aerosol	
PEC	Primary Elemental Carbon	
FPRM	Fine Other Primary (<2.5 µm)	
FCRS	Fine Crustal (<2.5 µm)	
CPRM	Coarse Other Primary	
CCRS	Coarse Crustal	

The results of PM water active treatment in the latest versions of CAMx4 under conditions of low temperature and consequent very high relative humidity lead to enormous overestimation of predicted PM compared with ambient observations. Meteorological conditions leading to such CAMx4 chemical instability (huge increases of aerosol water contribution to PM) are ultimately favourable for the Christchurch area during winter night-time heavy pollution episodes (described in Chapter 4). Figure 6.3 presents predicted concentration of PM_{10} calculated for the dry PM case (blue line) and for PM including aerosol water (green line) for 4–5 May 2005 smog episode.

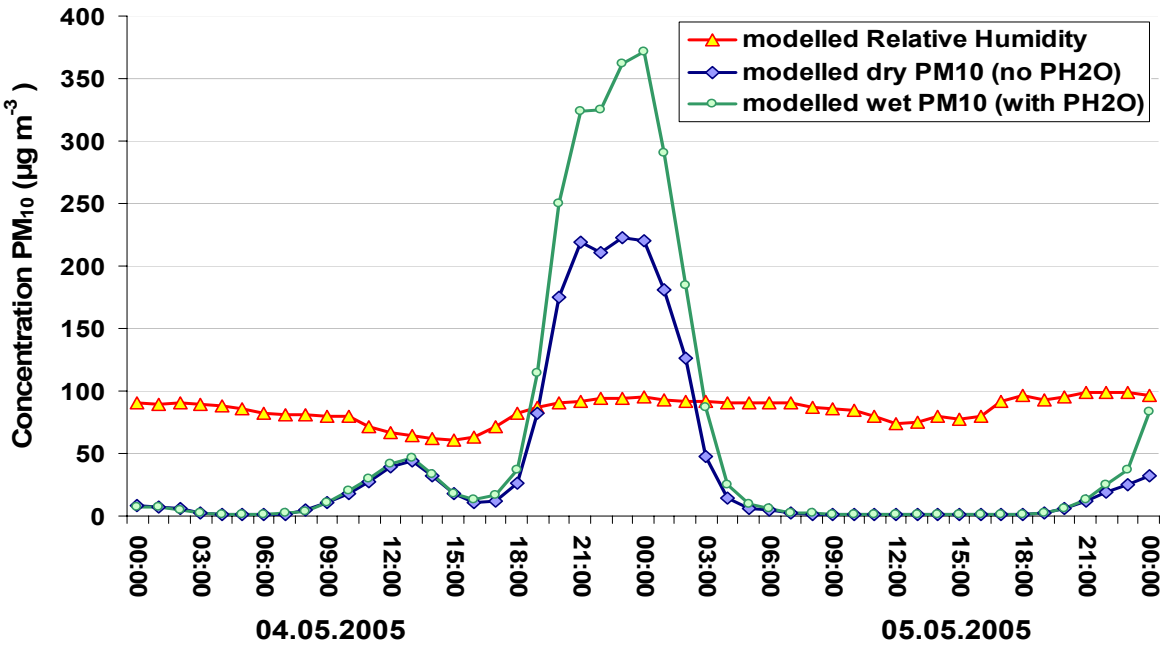

Figure 6.3 Predicted concentrations (µg m^{-3}) of dry PM_{10} (blue) and PM_{10} including aerosol water, 00:04.05–00:06.05.2005 modelled episode (Coles Place location point). Red line – predicted relative humidity (%).

Increase of total PM concentration because of aerosol water during night time and this chemical process gives unrealistic values of aerosol peak concentrations incompatible with dry calculated PM_{10} and observed values (observed PM_{10} was 220 µg m^{-3} at midnight). CAMx4 chemical instability triggered by aerosol water parameterisation gives an excessive growth of PM mass concentration. This process correlates with relative humidity (R = 0.89) and, in a smaller degree, negatively correlates with near-surface temperature (R = -0.58). Discussion of this problem with scientists from ENVIRON (including Chris Emery) brought no positive results.

6.2 CAMx input gridded emissions (1999 inventory)

Input gridded emissions of gases and particulate matter are the central part of CAMx4 input data used to predict the numerical PM concentrations that are comparable with observed ambient data. For single grid runs (like in this study) gridded emissions are prepared for every point of a single coarse grid, while for experiments with nested grids gridded emissions are interpolated from the mother grid to the points of the nested grids. Gridded emissions of gases and aerosols are supplied at specific time intervals during CAMx runs (the time interval can range from 1.5 minutes to a few hours depending on the process to be investigated and computer resources), but only for the lowest (boundary) layer of the model. Gridded input emission fields of PM and gases supplied at 1-hour

interval were used to investigate temporal variation of spatial patterns of aerosols and gases in the lowest 50–100 metres of the atmospheric boundary layer in the Christchurch area.

Spatial fields of gridded concentrations of PM_{10}, $PM_{2.5}$, CO_x, NO_x, SO_x and VOC (Volatile Organic Compounds), based on emissions inventory data from Environment Canterbury (1999 inventory – Wilton 2001), were utilized in GIS form as initial and nudging data for creating CAMx4 input gridded emission files. The gridded emission files of particulate matter and gases have a 1 km spatial resolution (coinciding with the resolution of the finest MM5 grid), covering the inner part of Christchurch with 34 x 39 horizontal points (with units of kg m^{-3} hr^{-1}). A special procedure was applied to transform input emission files with 34 x 39 regular grid points into an MM5 121 x 121 regular grid, with an additional check procedure to ensure that central points coincide.

The initial emission fields are considered to be averages for the whole wintertime (late May to early September) for the Christchurch area, and split into four groups according to the origin of the pollutant emission. This produced a 'domestic' group representing home use of open fires and log burners with different qualities of fuel; an 'industry' group representing wood/coal combustion for industrial purposes; a 'vehicle' group representing transport during rush-hours, and a 'total' group that includes all three former groups. The 'domestic', 'vehicular' and 'industry' groups are the main contributors to the aerosol (PM) air pollution with up to 95–98 % of pollutants derived from these groups and up to 90–92 % from the 'domestic' group alone (Wilton, 2003; Scott, 2005). They are dominated by processes of solid fuel combustion.

The level of aerosol and gases in the input gridded emission files varies not only in space but also in time throughout the day over the city of Christchurch. As a result, for all 4 emission groups, the day was split into four time intervals with differing levels of pollution emission depending on the 'pollution production' activity of each time period (Scott, 2005).

1. Night time: 10pm–6am next day (mostly reduced activity);
2. Morning time: 6am–10am (morning secondary 'vehicle–industrial' peak);
3. Midday time: 10am–4 pm (industrial subpeaks);
4. Evening time: 4pm–10 pm (the maximum peak of pollution–'domestic' factor).

The mean and grid-point values of aerosol and gaseous emissions in the gridded fields differ significantly between one time period and another, so that a 5 time-point smoothing filter (TPF)

was applied to all initial fields to smooth the difference of values between different time periods for all 4 groups. So, if moving from one time interval to another a TPF factor for the current time group will be:

1. TPF = 0.00 ($t = t_b - 2$);
2. TPF = 0.75 ($t = t_b - 1$);
3. TPF = 0.50 ($t = t_b$);
4. TPF = 0.25 ($t = t_b + 1$);
5. TPF = 0.00 ($t = t_b + 2$).

Where t_b is the border time between two time groups (6am, 10am, 4pm or 10pm) and t is the current time in the current time group (in hours).

The next step in assimilation of initial gridded emissions fields for CAMx4 involved splitting of the aerosol ($PM_{2.5}$ and PM_{10}) and gaseous (CO, NO_x, SO_x and VOC) components based on the species in the input gridded emission file for CAMx4 chemistry mechanism 4 (CB4). A description of 4 different ways of splitting input fine PM emissions based on chemical components will be presented in Chapter 9.

For gases, the procedure of input data preparation was easier for CO, NO_x and SO_x, as it demanded only knowledge of the molecular weight of a species to apply an equation to convert the input (kg m^{-3} hr^{-1}) units to ppm (parts per million) units, as all gaseous species are represented in ppm in CAMx4. However, for organic gases the process is different, as emissions of organic gases are typically reported in emission inventories only as aggregate organics, either as VOC or as Reactive Organic Gases (ROG). The specification profiles used to split aggregate organic gas estimates into individual compounds are initially based on those outlined for total organic gases in Ryan (2002). The lumping molecular approach in the CB4 mechanism, where individual compounds with similar reactivity characteristics or carbon bond structures are grouped into a single mechanism species, involves three steps for the specification of VOC: assignment of a speciation profile, conversion of VOC to TOG (Total Organic Gases), and multiplication of the assigned profile's split factors by the TOG estimate to create emissions estimates for the species used in the model.
The final step in specification of VOC emissions consists of generation of input species in either molar (ppm) or mass form using the specification profiles from the CB4 profiles file (Titov, 2004). After the above pre-processing of initial aerosol and gas spatial fields, the emission input file contained from 18 to 25 (with 6 to 13 PM species) gridded input species representing the complex PM compounds in the atmosphere over the Christchurch area. A special procedure is applied to

compile all the input species together and to create the single input and nudging emissions binary file containing aerosol and gaseous emissions for the CAMx4 experiments.

6.3 Summary

Analysis of CAMx chemical parameterisation and the PM treatment mechanism is presented in this chapter. Different versions of CAMx4 provide improvement in numerical reproduction of fine and total primary and secondary aerosol in more recent versions of the photochemical model. However the advantages of the flexibility and diversity of the CAMx4 chemical solver are also associated with weak points in numerical and chemical instability of the PM prediction. The combination of 'model uncertainty' with 'instability' creates a problem of deterministic error accumulation. The construction of more accurate input initial and nudging gridded aerosol and gaseous emissions prove to be most important for reducing CAMx4 chemical and numerical instability.

Chapter 7: Coupled numerical modelling systems

The most popular type of coupled meteorology–chemistry model includes global or regional (limited area) numerical atmospheric models as a first step, and some prototype chemical/numerical (mostly Eulerian) model, which is dependent on the meteorological model output fields. Examples of such coupled systems include MM5 (WRF) –Comprehensive Air quality Model version x (CAMx), MM5–Modal Aerosol Dynamical model for Europe (MADE), MM5 (WRF)–Community Multi-scale Air Quality model (CMAQ), MM5–Variable grid Urban Airshed Model with extensions (V-UAM), MM5–Advanced Texas Air Quality Model (ATAQM), MM5–TOPOMODEL-based Land Atmosphere Transfer Scheme (TOPLATS) (Peters-Lidard *et al.,* 2002), MM5–EURopean Air pollution Dispersion model (EURAD), MM5–Multiscale Air Quality Simulation Platform (MAQSIP). To this group can be added such meteorological model amalgamations as MM5 – chemistry block (MM5–chem) and Weather Research and Forecasting system (WRF) – chemistry block (WRF–chem).

There are also so-called integrated meteorological–air quality modelling systems, which include such models as The Air Pollution Model (TAPM) of the Commonwealth Scientific and Industrial Research Organisation (CSIRO, Australia) described by Hurley (2002), and CALPUFF (created initially by CALifornia Air Resources Board–CARB) described by Allwine *et al.* (1998). The first includes a numerical–graphical user interface (GUI) for simulating air pollution episodes using meteorology calculated in another part of the same model. CALPUFF is an advanced non-steady-state meteorological and air quality modelling system that consists of three main components with a GUI and a set of meteorological conditions. These comprise CALMET (a diagnostic 3-dimensional meteorological model), CALPUFF (an air quality dispersion model) and CALPOST (a postprocessing statistical–plotting package). These types of diagnostic models also were used for global scale tracing of long term dispersion of airborne particular materials.

The level of precision of coupled limited area atmospheric–air pollution models is very difficult to assess and, first of all is much more difficult to obtain, as the quality level of research/forecast results is created not only inside one model, but also between different models of one modelling system. The numerical instability (deterministic error) of the dispersion models was discussed earlier. With many improvements in modelling systems it is now possible not only to develop a very complex numerical system, but to predict concentrations of atmospheric pollutants every day within a sufficient time range and with quite high forecast reliability (in the range of 70–85 %

consistency) depending on the input data, spatial resolution of the grid, and complexity of the region. It is very important to have good quality input gridded emissions for gaseous and particulate matter compounds of the main air pollutants to be able to maintain a relatively good agreement between observed and predicted ambient data (up to 90%). The level of reliability also depends on the type of species predicted. The level of reliability is higher for total PM forecasts than for fine PM forecast, and for inert gases it is higher than for active and unstable gases (like O_3). The mean level of accuracy of research applications is higher than the one of forecast applications of numerical air pollution systems, but there is a tendency toward equalizing the levels of reliability of the two modelling time regimes (Peters-Lidard *et al*., 2002; Stein *et al*., 2000).

7.1 TAPM as a tool in cohort studies

The Air Pollution Model (TAPM: CSIRO, Australia) basically described by Hurley (2002) includes the ability to simulate air pollution episodes with meteorology calculated by TAPM itself for long time periods. TAPM (as was described before) includes nesting for meteorological and air pollution parts. The meteorology of the model contains synoptic-scale input meteorological fields that drive the model at the boundaries of the coarse-nested grid. TAPM includes Eulerian grid and condensed chemistry modules, but not aerosol chemistry. The distinguishing feature of TAPM is that it allows urban area aerosol concentrations to be modelled at fine spatial resolution over long time periods. TAPM is a good numerical tool for cohort studies over the Christchurch area because of low computer-time requirements resulting from some simplifications in the model used for long-term runs.

TAPM is a fast, directly coupled, PC-based, air pollution dispersion model with a Graphical User Interface (GUI) allowing configuration of inputs and the analysis of outputs. High-resolution simulation of meteorology and dispersion is achieved by progressive nesting from large geographical domains to finer spatial domains (1 km and less). TAPM requires two basic types of input data: meteorology and emissions. Synoptic meteorology is ingested by the model using data from the Limited Area Prediction System (LAPS) analysis from the Australian Bureau of Meteorology (Puri et al., 1998). Sea surface temperatures and surface properties can be configured and corrected manually through the GUI that decreases a complexity of the model for local specific simulations. In addition, the TAPM GUI allows corrections for the input of various emission species in gridded, area, and line source configurations. To improve the simulated meteorological fields, a data assimilation option is also incorporated in TAPM, and the model is

nudged towards actual measured wind data that are crucial for forecasting PM near-surface concentrations (Wilson and Zawar-Reza, 2006).

Cohort studies with TAPM configured using three telescoping grids centred at the Coles Place observation site were done for grids spatial resolution 13.5, 3.5 and 1.5 km. The high-resolution domain was set to cover Christchurch and most of the Canterbury Plains, for more accurate simulation of the local wind systems. As the emission grid data were only available for the metropolitan area of Christchurch, the gridded emissions were smaller in area than the high-resolution meteorological grid of TAPM. To simulate the dispersion of total PM the air pollution module of TAPM was utilised with no chemistry and was based on three emission sources: domestic emissions, transport emissions, and industrial emissions (Scott and Ganatilaka, 2004).

Daily predicted PM_{10} concentrations were compared with the airborne data for eleven monitoring sites over 2 months in July 2003 and June 2004. Mean IOA was 0.60, with a minimum of 0.40 and a maximum of 0.70. IOA for wind speed, wind direction, and temperature at Coles Place observation site were 0.63, 0.75, and 0.87, respectively, indicating that the model sufficiently defines the meteorology over the urban area and its complex orography (Wilson and Zawar-Reza, 2006). Figure 7.1 shows that from a spatial perspective, there is more agreement closer to the central Christchurch districts than for the outskirts, which is expected as the gridded emissions had a more accurate representation of the inner city only.

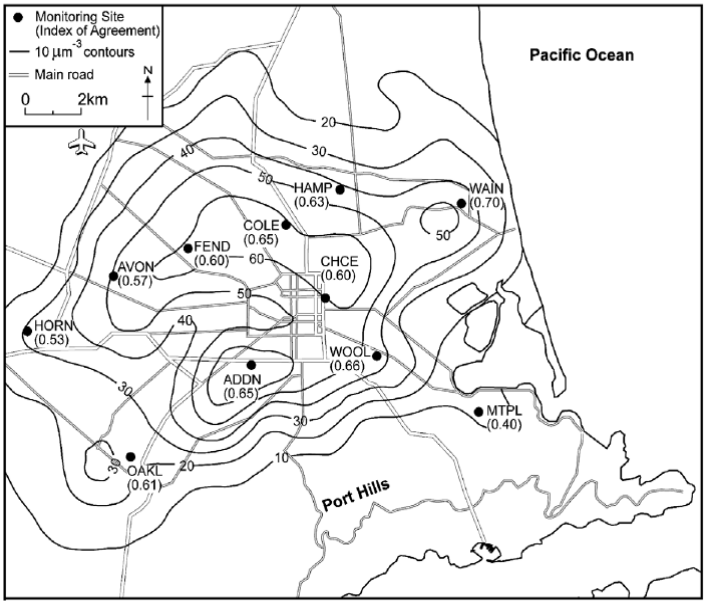

Figure 7.1 Contours (10 μg m^{-3} intervals) of winter average modelled PM_{10} concentrations and Index of Agreement (IOA) at monitoring station locations. An IOA > 0.50 indicates good agreement (after Wilson and Zawar-Reza, 2006).

Possible causes of the lower IOA for the southern and western areas of the city are the nocturnal complex wind and lower resolution emission inventories. It is important to stress that the daily statistical index between observed and modelled PM_{10} give lower values of agreement than 2-monthly averaged ones, which opens possibilities to make the model more universal.

7.2 MM5-CAMx numerical system

The photochemical model CAMx4 uses MM5 output fields of wind, temperature, water vapour, coefficient of vertical turbulence, and information about clouds and cloud water content as input meteorological information. Input meteorology is used on levels determined in the CAMx4 input file and the distribution of vertical levels coincides with near-surface distribution in MM5 (or WRF). CAMx4 uses MM5 basic meteorology for initialisation and for boundary conditions, as well as for nudging data at certain time intervals. It was possible to evaluate the most successful MM5 experiments against CAPS2000 observation data to find the optimal MM5 physical parameterization to obtain the most realistic meteorological input for fine tuning the dispersion model (Titov, 2004). All the experiments using the coupled MM5–CAMx4 numerical system had the spatial resolution of the MM5 fourth grid (1 km mesh), and meteorological fields were obtained for use in the photochemical model with the same 1 km spatial resolution. This procedure

is stipulated initially to minimise loss of meteorological information during the processes of conversion of MM5 output information into the CAMx4 input format.

CAPS2000 and winter seasons 2005-2006

Initial analysis of the near-surface air circulation on smog nights has relied on observations from the Christchurch sites established during CAPS2000 (Kossmann and Sturman, 2004), and was useful for more detailed understanding of the total PM spatial and temporal variations. The analysis of CAPS2000 results was used to tune CAMx4 using MM5 input meteorology to more accurately reproduce ambient observations. In Figure 7.2 wind roses for smog nights are displayed (data were collected and analysed for winter months of the CAPS2000 field experiment) for evening (Figure 7.2a) and early morning (Figure 7.2b) to illustrate the influence of the wind field on redistribution of PM_{10} concentrations over the Christchurch urban zone (shaded).

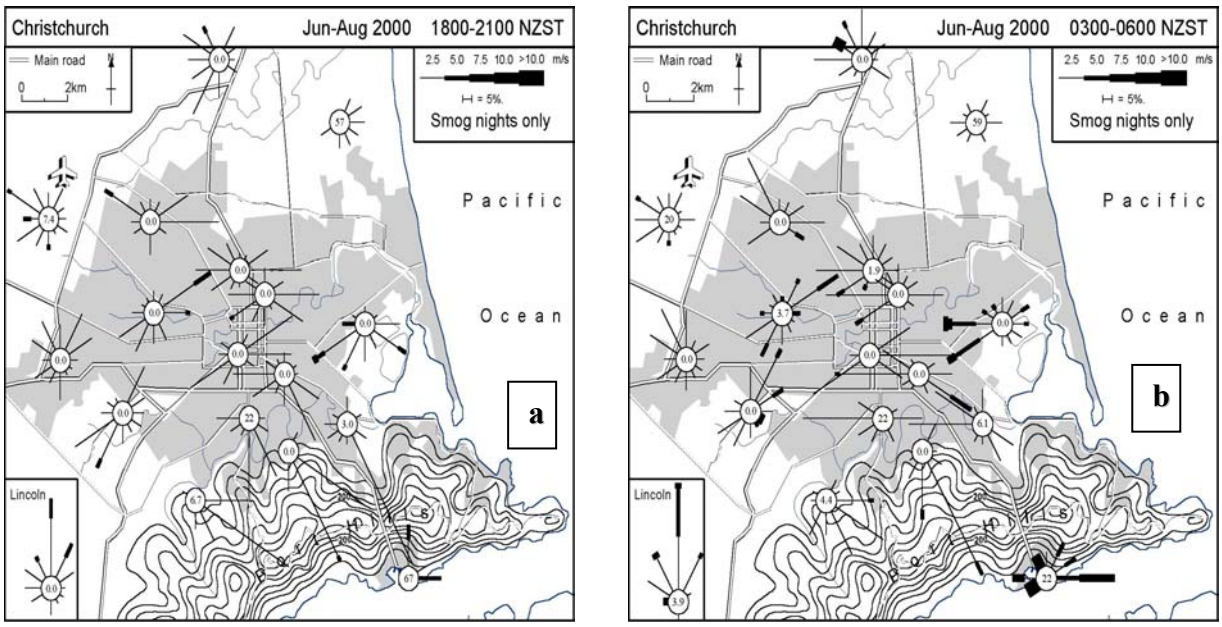

Figure 7.2 Observed near-surface wind speed and direction distribution for 16 observation sites in the Christchurch area during CAPS2000, averaged for June–August, smog nights only: a) 6pm–9pm, b) 3am–6am (after Kossmann and Sturman, 2004).

From Figure 7.2, it is apparent that the drainage winds from the Canterbury Plains and Port Hills create a convergence zone (or some kind of localised frontal zone) of cold dense air in the evening under stagnant synoptic situations, with advection of total aerosol toward the central part of Christchurch (Figure 7.2a) during evening, and movement of high PM_{10} concentration values towards coastal areas and the ocean (Figure 7.2b) during early morning. In Figure 7.3, time

variability of the near-surface temperature and vertical temperature gradient (indicative of vertical atmosphere stability) is shown for smog nights (sm.) averaged for Jade Stadium tower (J), Christchurch Airport (A), and Greers Road tower (G). The difference between sites as a result of the effect of the urban area was well shown using the CAPS2000 database.

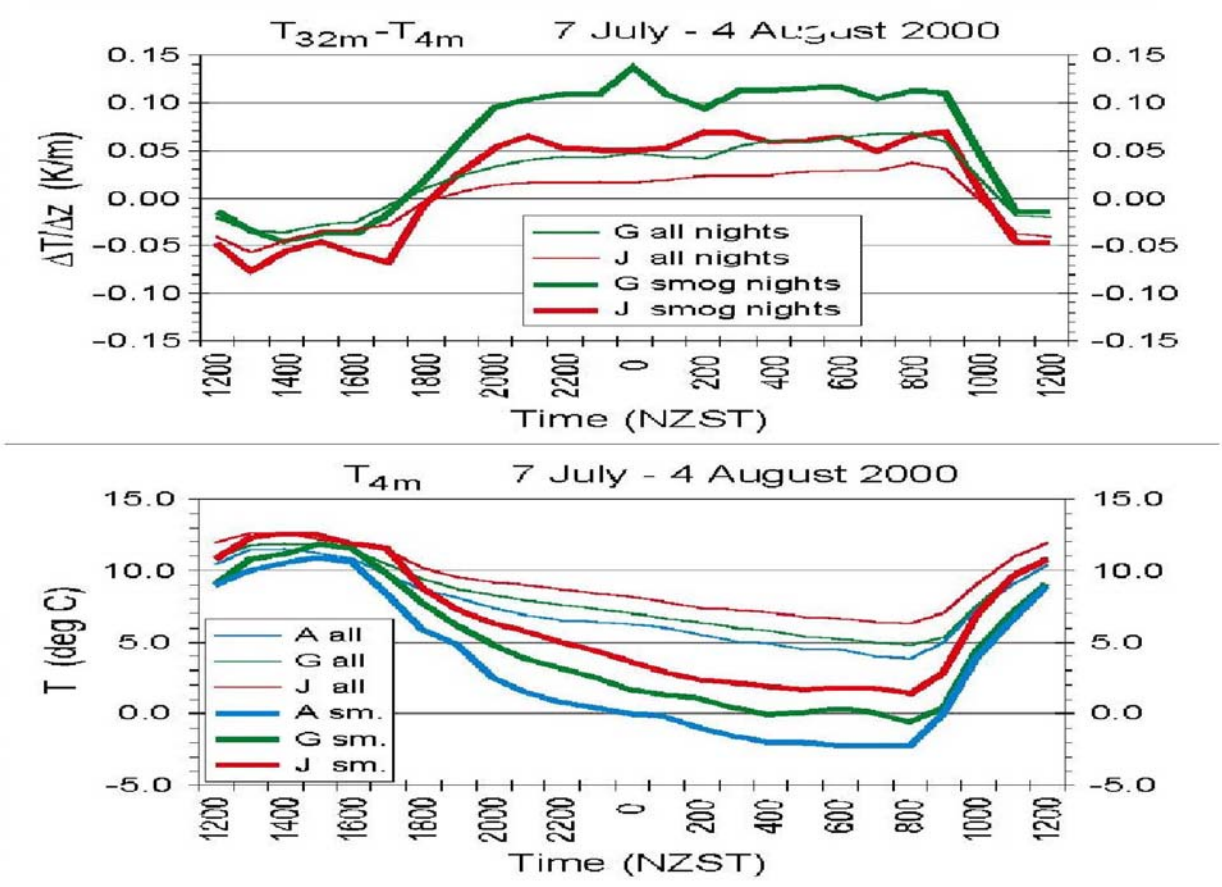

Figure 7.3 Time variability of the average vertical temperature gradient (top) and near-surface temperature (bottom) during all nights and smog nights between 7 July and 4 August 2000 (after Sturman *et al.,* 2001).

Fine-tuning of the CAMx4 photochemical model included firstly, reconfiguration, adjustment and time smoothing of the average hourly gridded PM_{10} and $PM_{2.5}$ emissions used for initialising and nudging. Observed particulate matter data collected during CAPS2000 at three observation sites (Coles Place, Polytechnic and Packe Street) were available for the time period from early July up to the middle of August 2000. The observations collected at three ECan sites during winter 2000 provided a very good background for comparison with output from CAMx4 model (Titov, 2004).

Analysis of PM_{10} time series for Coles Place, Polytechnic and Pack Street sites has shown two peaks of particulate pollution in Christchurch. The main night peak (between 8pm-2am) is supposed to be mainly a result of home heating using open-fires and log-burners (domestic

pollution), while the secondary peak during early morning (between 6–9 am) is considered to be the combined result of domestic and vehicular activity. Surface air pollution observations from three sites were used in the CAMx4 experiments to make adjustments to the operation of the photochemical model, including investigating the effect of different numbers of vertical levels, and flexibility of the input emissions.

Winter 2005 was quite warm and the highest concentrations of fine and total aerosol were observed during the first winter 2005 months: May and June. Winter 2006 was much colder than winter 2005 with the highest peaks of aerosol in June-July. The middle part of winter 2006 (June-July) was also chosen for evaluation as the second part of winter 2006 presented a rather different synoptic-microclimate situation than in early winter 2005. Averaged statistics including mean, median and maximum values of total PM concentration ($\mu g\ m^{-3}$) are presented in Table 7.1 for winter 2005 and 2006 research periods.

Table 7.1 PM_{10} ($\mu g\ m^{-3}$) averaged statistics for winter 2005 (1 May to10 June 2005) and winter 2006 (10 June to15 July 2006) obtained for the Coles Place observation site.

Statistics	Mean	Median	Minimum	Maximum	Lower Quartile	Upper Quartile	Standard Deviation	Skewness
PM_{10} - 2005	33.92	18.05	0.50	403.80	10.70	39.50	44.08	3.83
PM_{10} - 2006	57.72	23.05	0.33	491.10	9.38	70.15	79.45	2.21

Table 7.1 shows that the mean, median and maximum peak of PM_{10} concentrations were much higher for winter 2006 study period. Both study periods (winter 2005 and 2006) were the periods that included high values of aerosol mean and peak concentrations, and were considered to reflect severe smog conditions for winter 2005 and winter 2006. Figure 7.4 presents whisker plots of PM_{10} concentrations for the 2005 and 2006 winter research periods, and includes median, lower (25%) and upper (75%) quartiles, and a range inside 90% of the peak concentrations for the total PM. Figure 7.4 reflects higher average values of PM_{10} concentrations for winter 2006 compared with winter 2005 (see Table 7.1). Time intervals 1 May to 10 June 2005 and 10 June to 15 July 2006 are found to be the periods with highest smog concentrations and the most representative ones for inter-season comparison.

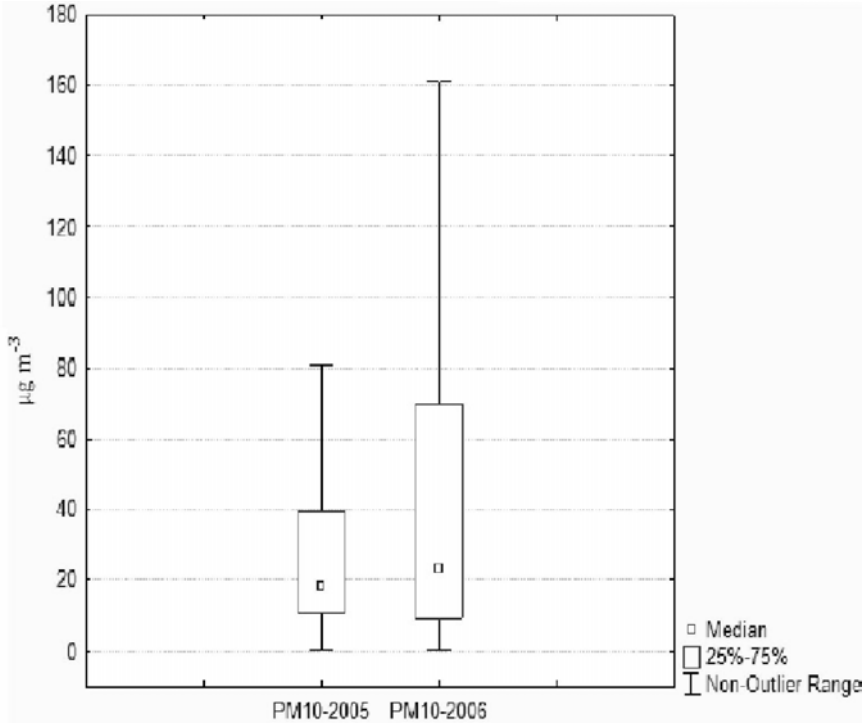

Figure 7.4 Observed PM_{10} average concentrations (µg m^{-3}) for 2005 and 2006 winter research periods (40-day observation period).

Modelled and observed PM – winter 2005

Winter 2005 was characterized by quite cold weather and high values of PM in the first part (several very cold nights in May-June) and a quite mild second part (July-August). August also included several high PM concentration peaks but fine aerosol concentrations were not measured in August. Averaged PM_{10} and $PM_{2.5}$ statistics, including mean, median and maximum values of PM concentrations are presented in Table 7.2 for 7 episodes (May-June 2005 study period, 17 days), obtained from the Coles Place observation site. Maximum values correspond to hourly averaged maximum concentrations.

Table 7.2 PM_{10} and $PM_{2.5}$ (µg m^{-3}) averaged statistics for 7 episodes in winter 2005 (May-June 2005), obtained for the Coles Place observation site.

Statistics	Mean	Median	Minimum	Maximum	Lower Quartile	Upper Quartile	Standard Deviation	Skewness
PM_{10}	44.70	21.15	0.50	388.40	11.05	62.90	54.31	2.65
$PM_{2.5}$	35.37	15.90	0.30	350.80	5.15	50.45	47.96	2.66

The Skewness of the observed ambient aerosol distribution is quite high that proves far from normal distribution (a lot of peak values) of concentration time series with maximum PM values

higher 350 μg m^{-3} for fine and total PM. This result shows a big difference in day-night temperatures leading to active PM dispersion during day-time, and processes of PM accumulation with the secondary aerosol creation during cold night-time. Minimum values of fine and total PM indicate very low background aerosol concentrations. Figure 7.5 presents whisker plots of PM_{10} and $PM_{2.5}$ averaged concentrations (May-June 2005) for Coles Place, including median, lower (25%) and upper (75%) quartiles and a range inside 90% of the peak concentrations for fine and total PM.

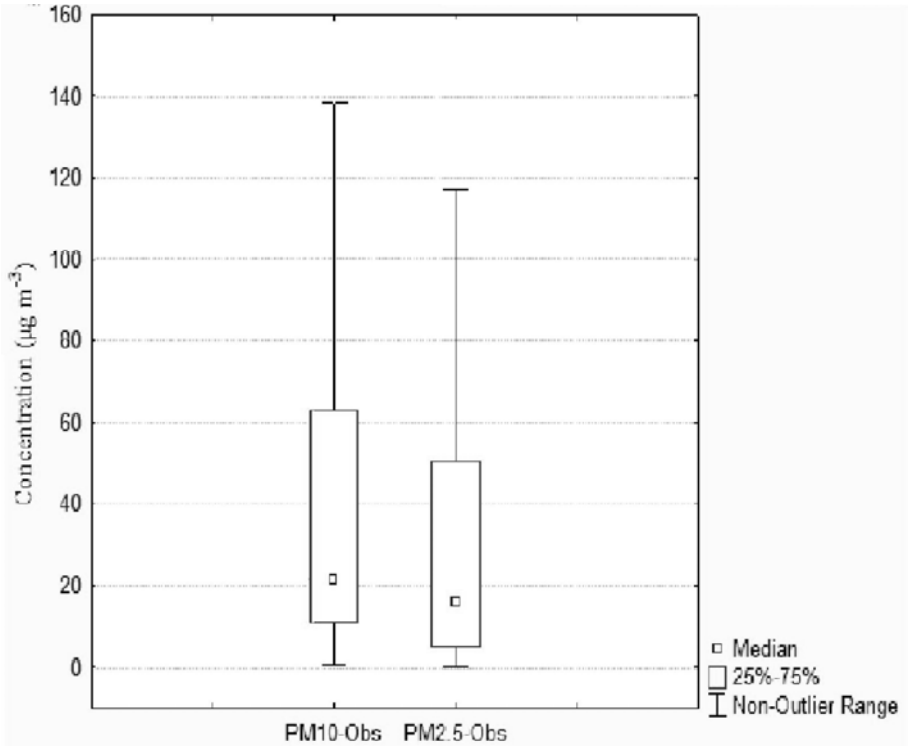

Figure 7.5 Observed PM_{10} and $PM_{2.5}$ average concentrations (μg m^{-3}) for 7 modelled episodes in winter 2005 (May-June 2005), obtained for the Coles Place site.

Averaged modelled PM_{10} and $PM_{2.5}$ concentration statistics including mean, median and maximum values of PM concentrations (μg m^{-3}) is presented in Table 7.3 for 7 episodes (17 days) for the May-June 2005 research period (Coles Place site). Maximum values mean hourly averaged predicted maximum concentrations. The maximum values of fine and total PM are much lower than observations, and the Skewness is also not so high (compared with Table 7.2). Modelled aerosol concentrations are closer to a normal distribution as a result of the deterministic origin of the modelled output compared with more stochastic observed ambient data.

Table 7.3 PM_{10} and $PM_{2.5}$ ($\mu g\ m^{-3}$) averaged statistics for 7 modelled episodes in winter 2005 (17 days), extracted for the Coles Place observation point.

Statistics	Mean	Median	Minimum	Maximum	Lower Quartile	Upper Quartile	Standard Deviation	Skewness
PM_{10}	38.11	14.50	0.20	222.50	1.90	52.60	51.92	1.84
$PM_{2.5}$	34.01	12.10	0.10	208.00	1.60	46.40	47.89	1.92

Figure 7.6 presents whisker plots of PM_{10} and $PM_{2.5}$ concentrations averaged for 7 modelled episodes (May-June 2005) and extracted for the Coles Place point, including median, lower (25%) and upper (75%) quartiles with a range inside 90% of peak concentrations for $PM_{.2.5}$ and PM_{10}.

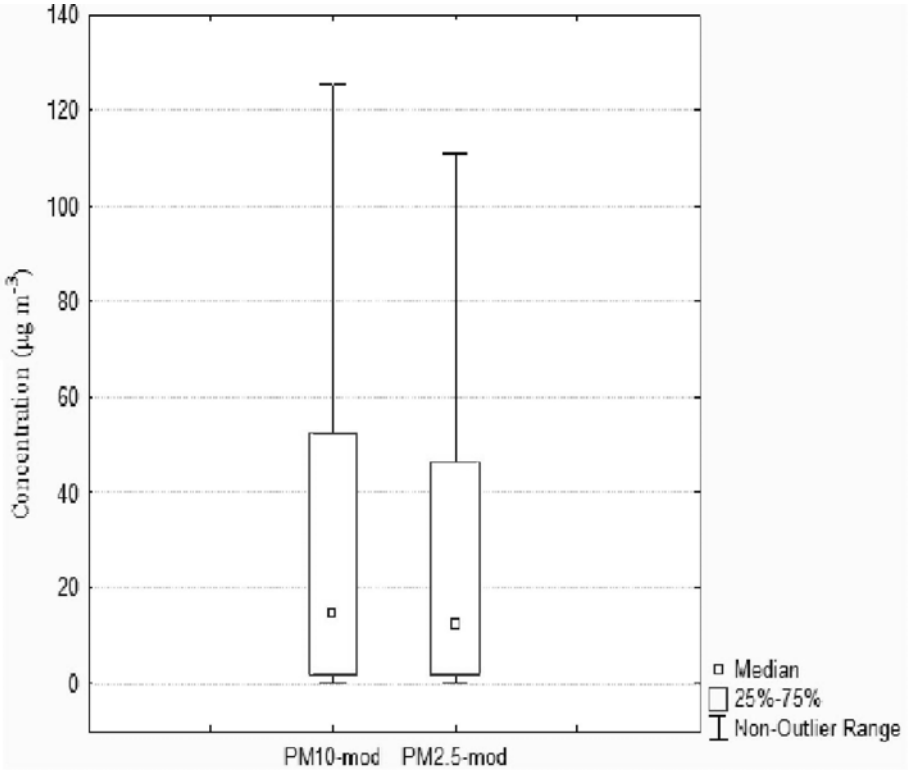

Figure 7.6 Modelled PM_{10} and $PM_{2.5}$ average concentrations ($\mu g\ m^{-3}$) for 7 modelled episodes in winter 2005 (May-June 2005) extracted for the Coles Place point.

Under-prediction of observed PM_{10} and $PM_{2.5}$ concentrations is not high as can be seen from Figures 7.5 and 7.6, and also is evident statistically from Tables 7.2 and 7.3. The difference between observed and modelled mean PM concentrations doesn't exceed 25-35%, which provides a positive assessment of CAMx output postulated by EPA USA. However, it is obvious that the observed maximum hourly values of PM_{10} and $PM_{2.5}$ could not be predicted exactly by the numerical modelling system.

Modelled and observed PM – winter 2006

Winter 2006 was much colder than winter 2005, but is characterized by low PM peak concentrations in the first part (mild meteorological conditions in May), and by very high PM concentrations during the severe second part (June-July). In June-July hourly mean PM_{10} concentrations were up to 500 μg m^{-3}, which was close to record values for the last 10 years. Short days and long nights exacerbated PM night peak concentrations in June-July. Averaged PM_{10} statistics obtained for two observation sites (Coles Place and Woolston) including mean, median and quartile values of PM concentrations, are presented in Table 7.4 for 8 smog episodes (June-July 2006 study period, 19 days). Maximum values correspond to hourly mean maximum concentrations.

Table 7.4 PM_{10} (μg m^{-3}) averaged statistics for 8 episodes in winter 2006 (June-July 2006), obtained for Coles Place and Woolston observation sites.

Statistics	Mean	Median	Minimum	Maximum	Lower Quartile	Upper Quartile	Standard Deviation	Skewness
PM_{10} – Coles Place	84.48	40.00	0.91	491.10	15.07	116.21	95.69	1.44
PM_{10} - Woolston	70.89	41.12	1.23	353.41	17.60	98.53	73.50	1.56

The Skewness of the observed ambient aerosol is much lower than for winter 2005 (Table 7.2), which suggests a close to normal distribution of aerosol time series with maximum concentrations higher than 350 μg m^{-3} for PM_{10} for the Woolston observation site, and nearly 500 μg m^{-3} for the Coles Place site. This fact presumes a decreased (compared to winter 2005) difference in day-night temperatures leading to PM accumulation, re-suspension and dispersion in a shallow near-surface layer during day-time, and active processes of the secondary aerosol creation during very cold nights. Also, low values of the Skewness are a result of high peak concentrations. Figure 7.7 presents whisker plots of PM_{10} mean concentrations for 8 episodes (June-July 2006), obtained from the Coles Place and Woolston sites, including median, lower (25%) and upper (75%) quartiles and a range inside 90% of concentrations for total PM. More severe smog conditions for 8 research episodes in middle winter 2006 compared with the averaged statistics for 2005 modelled episodes is obvious from Tables 7.2 and Table 7.4, and from Figure 7.5 and Figure 7.7. As expected spatial variability of mean statistics (for 2 sites) is much lower than temporal variability for one site, as fine PM (contributing up to 80-85% of PM_{10}) is well mixed on a local spatial scale.

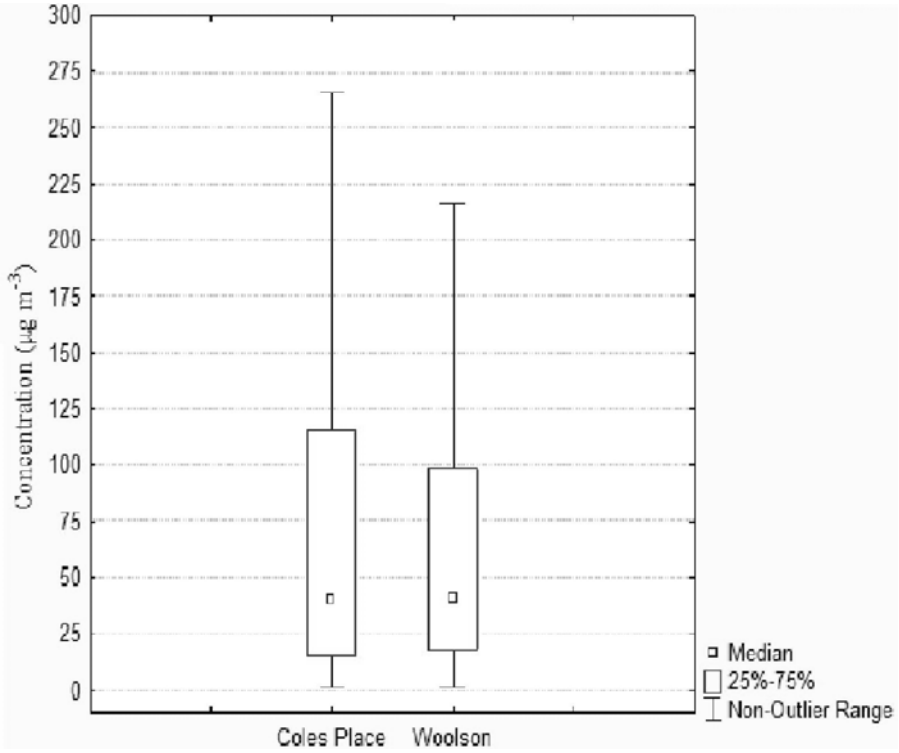

Figure 7.7 Observed PM_{10} mean concentrations (µg m^{-3}) for 8 episodes in winter 2006 (June-July 2006), obtained for Coles Place and Woolston observation sites.

MM5-CAMx4 modelled PM_{10} concentration statistics including mean, median and maximum values of PM concentrations (µg m^{-3}) extracted for Coles Place and Woolston is presented in Table 7.5 for 8 episodes (19 days): June-July 2006 study period. Maximum values present hourly averaged predicted maximum concentrations. The mean and the maximum values of the total PM are definitely much lower than observed ones (Table 7.4) which suggests a stable tendency to underpredict the real PM_{10} peaks. The Skewness is lower (compared with observations – Table 7.4), and modelled aerosol concentrations again are closer to normal distribution.

Table 7.5 Predicted (MM5-CAMx4) PM_{10} (µg m^{-3}) averaged statistics for 8 episodes in winter 2006 (June-July 2006), extracted for the Coles Place and Woolston observation points.

Statistics	Mean	Median	Minimum	Maximum	Lower Quartile	Upper Quartile	Standard Deviation	Skewness
PM_{10} – Coles Place	55.61	43.00	1.60	202.50	23.00	74.00	45.68	1.19
PM_{10} - Woolston	42.29	35.25	1.60	172.00	20.00	65.00	37.79	1.23

A comparison of the Tables 7.3 and 7.5 indicates that the numerical modelling system catches the inter-seasonal fluctuation in mean aerosol concentrations from a quite mild winter in 2005 to a quite severe in winter 2006.

Statistical results are well exhibited in Figure 7.8 for MM5-CAMx4 modelled PM_{10} concentrations (whisker plots), averaged for 8 study episodes (June-July 2006) and extracted for Coles Place and Woolston geographical points. Figure 7.8 includes median, lower (25%) and upper (75%) quartiles, and a range inside 90% of peak concentrations for the total PM.

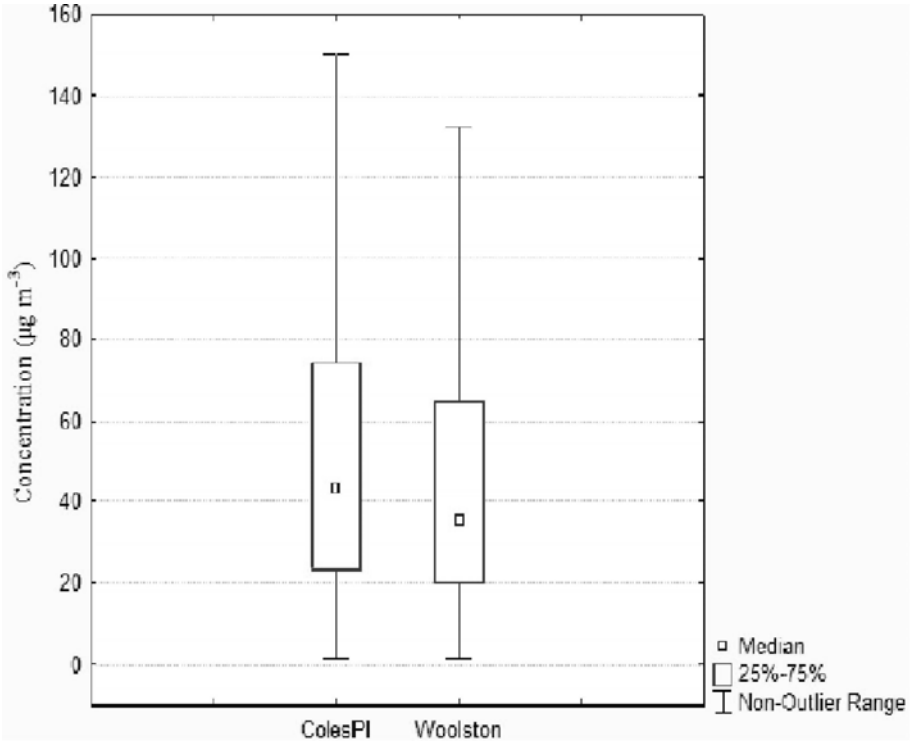

Figure 7.8 Predicted (MM5-CAMx4) PM_{10} mean concentrations (µg m^{-3}) for winter 2006 8 episodes (June-July 2006), extracted for the Coles Place and Woolston observation sites.

All averaged statistical parameters (median, quartiles and peak concentrations) for modelled PM_{10} concentrations (Figure 7.8) are a little bit higher for the Coles Place and lower for the Woolston (reflecting local scale variability). The modelled PM_{10} concentrations are much lower to compare with Coles Place and Woolston ambient data for 8 smog episodes in winter 2006 (Figure 7.7).

7.3 WRF-CAMx numerical system

Use of WRF version 2.1.2 in September-October 2006 (on IBM P575 HPC) provided a possibility to evaluate the WRF-CAMx4 numerical modelling system for 8 winter 2006 smog episodes. Latest

versions of ARW WRF (v2.1.2 and v2.2) are used by the world scientific community for purposes to receive (in nearest future) more accurate meteorological data for running photochemical models. This is evident from the WRF and CAMx4 users' forums, as WRF to CAMx4 interpolation was mentioned several times in discussions. But it is difficult to find a paper in the leading journals devoted to aerosol experiments with application of the WRF-CAMx4 numerical modelling system. Tesche and et al. (2006) compared CMAQ and CAMx4 performance using input meteorology predicted by WRF, but not MM5-CAMx4 and WRF-CAMx4. Such evaluation will be provided in the following chapters.

Application of the WRF-CAMx numerical modelling system

The problem of the WRF-CAMx4 numerical modelling system utilization mostly consists of WRF utilization only, and WRF installation (versions 2.1.2 and 2.2) was done on IBM P575 HPC (high-performance computer) in September 2006–March 2007. But all results 8 research episodes in winter 2006 8 research episodes were obtained with application of ARW WRF version 2.1.2 before year 2007.

Another important step was to install a WRF2CAMx special program (on HPC, for Unix AIX) that allowed use of ARW WRF output (stored in netCDF format) to obtain the near-surface meteorology for CAMx4 (including wind speed and direction, temperature and relative humidity, vertical turbulence and moisture-clouds). WRF2CAMx output meteorological fields with gridded emissions were used as input-nudging fields to evaluate CAMx4.2-CAMx4.3 versions for 8 study episodes in winter 2006. All CAMx4 calculations were done on a Sun workstation ("Tornado") as the CAMx4 model was utilized and exploited on a Sun workstation only. Fast external interface between IBM HPC and the Sun station made the process of file transportation very quick.

PM_{10} reproduction – late winter 2006

Winter 2006 was characterized by low PM peak concentrations in the first part and by very high PM concentrations during June-July with hourly mean PM_{10} concentrations up to 500 $\mu g\ m^{-3}$. Averaged modelled PM_{10} statistics obtained for two observation sites (Coles Place and Woolston) including mean, median and quartile values of PM concentrations is presented in Table 7.6 for 8 smog episodes (June-July 2006 study period, 19 days). Maximum values correspond to hourly

averaged maximum concentrations. This evaluation is done on the base of predicting by WRF-CAMx4 numerical modelling system PM_{10} concentrations for 8 winter 2006 episodes.

Table 7.6 Predicted (WRF-CAMx4) PM_{10} (μg m^{-3}) averaged statistics for 8 episodes in winter 2006 (June-July 2006), extracted for Coles Place and Woolston observation points.

Statistics	Mean	Median	Minimum	Maximum	Lower Quartile	Upper Quartile	Standard Deviation	Skewness
PM_{10} – Coles Place	32.05	20.00	1.00	159.00	8.45	49.25	31.20	1.41
PM_{10} – Woolston	30.10	18.25	1.40	128.00	9.00	44.75	28.22	1.25

Table 7.6 shows that the WRF-CAMx4 numerical modelling system underpredicts the mean and peak PM_{10} concentration up to 50-75% compared with MM5-CAMx4 (Table 7.5), and up to 150-200% to compare with observed data (Table 7.4). The main reason of such serious underprediction lies in input meteorological fields and will be discussed in the next chapters.

Statistical plots for WRF-CAMx4 modelled PM_{10} concentrations (whisker plots) are presented in Figure 7.9 and are averaged for 8 study episodes (June-July 2006), extracted for Coles Place and Woolston points. Figure 7.9 includes median, lower (25%) and upper (75%) quartiles, and non-outlier range inside 90% of peak concentrations for the total PM.

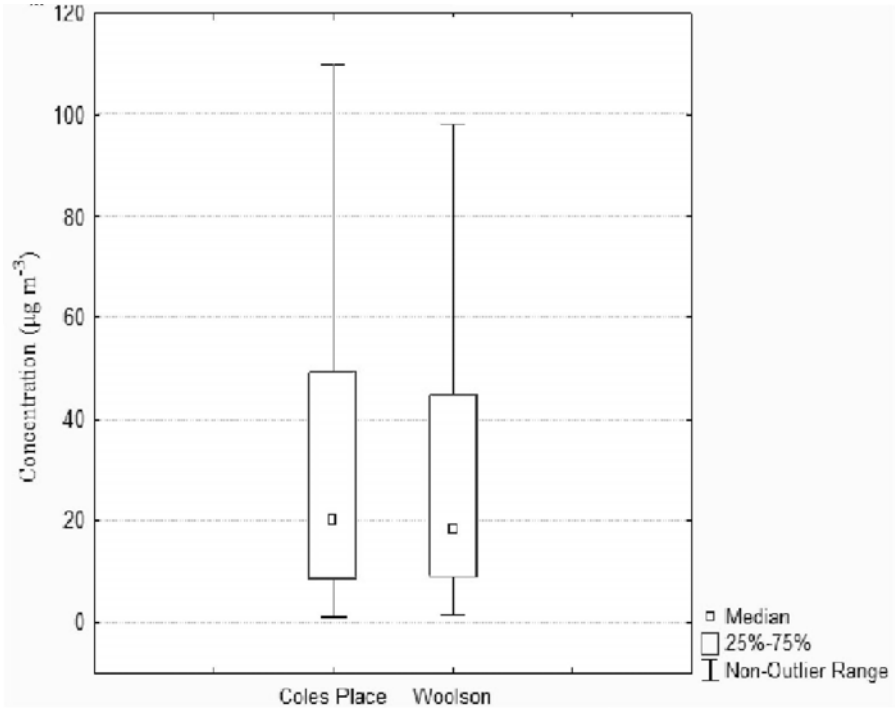

Figure 7.9 Predicted (WRF-CAMx4) PM_{10} mean concentrations (μg m^{-3}) for 8 episodes in winter 2006 (June-July 2006), extracted for the Coles Place and Woolston observation sites.

All averaged statistical parameters (median, quartiles and peak concentrations) for WRF-CAMx4 modelled PM_{10} concentrations (Figure 7.9) are a little bit higher for Coles Place compared with Woolston (spatial variability), but all modelled PM concentrations are lower compared with Coles Place and Woolston ambient data for winter 2006 (Figure 7.7).

7.4 Summary

Prediction of fine and total PM with application of MM5-CAMx4 and WRF-CAMx4 numerical modelling systems shows the tendency to underpredict the mean values of PM, mostly because of underestimation of the peak aerosol concentrations. Hourly averaged time series of the modelled PM concentrations has the tendency to be normally distributed as characteristics of deterministic system; while the observations are quite far from normal or log-normal distribution, and represent a more stochastic system.

Modelled total PM values are more underpredicted for winter 2006 (compared with observations) than for winter 2005, as June-July 2006 show much higher observed PM peak concentrations than May-June 2005. The WRF-CAMx4 numerical system underestimation is 50-75% higher than MM5-CAMx4, but for both numerical modelling systems output concentrations are higher for Coles Place than for Woolston.

PART C: MODELLING RESULTS

The most important part of the modelling results includes description of a new method for defining the split of aerosol emissions components using different chemical scenarios, and demonstrating a method to find an optimal PM chemical content by validating modelled output PM concentrations against the ambient data. A principle evaluation of the method of chemical scenarios was done for winter 2005 (single observation site), and a bias reduction (including inter-seasonal and numerical error decrease) was completed for winter 2006 (two observation sites). As the input near-surface meteorology plays an essential role in modelled aerosol spatial-temporal distribution accuracy, a level of the limited-area meteorological model (MM5) reproduction of the local circulation over complex terrain (in the Christchurch region) was accurately researched.

Chapter 8: MM5 near-surface meteorology - Christchurch

Reproduction of local near-surface meteorology of the complex terrain (in the Christchurch area) is vital for accurate spatial and temporal PM prediction during stagnant synoptic situations. Photochemical model uses initial and nudging (hourly) wind, temperature, humidity, vertical turbulence and clouds' water content fields calculated by MM5, and low quality input-nudging meteorological data could seriously influence modelled PM concentration spatial-temporal distribution, and potentially lead to faulty results to compare with observed PM trends. The importance of the input meteorology for better understanding of the difference between modelled and observed pollution patterns has been described in many works (Otte, 2003; Titov, 2004; Berg and Zhong, 2005; Mao et al., 2006; Smith et al., 2006; Titov et al., 2007; Chen et al., 2007).

In this chapter different types of MM5 derived meteorological plots (including vertical profiles and back-trajectories) will be presented for more precise evaluation of MM5 ability to reproduce boundary layer processes for the city of Christchurch during winter 2005 and 2006 pollution episodes. All winter heavy smog episodes had local emission sources, and were governed by the local air circulation that is be proven with application of HYSPLIT 4 single-particle trajectory model.

8.1 Day-time local scale near-surface air circulation

Seven winter 2005 synoptic episodes were evaluated using MM5 with input data from National Center for Environment Protection (NCEP, USA) recent dataset DS083.2 (1^0x1^0 resolution) for the coarse and 3 nested grids. Four grids were chosen for accurate air circulation modelling over the South Island and Christchurch areas with spatial resolutions of 27, 9, 3 and 1 km. As can be seen from Figure 8.1, the coarse (mother) grid covers nearly all of New Zealand and the 4th (the finest one) covers Christchurch, its suburbs and the Bank Peninsula.

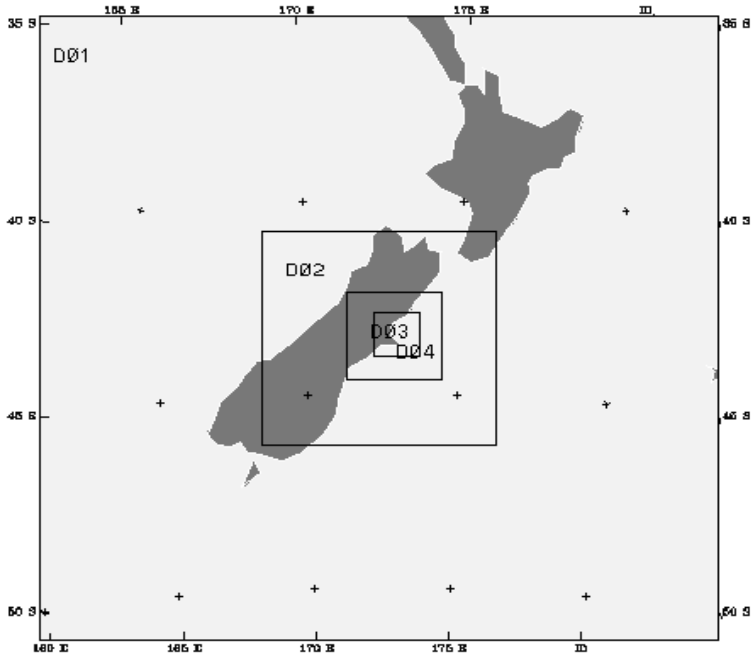

Figure 8.1 Coarse (mother) grid and 3 nested (daughter) MM5 grids (RIP, MM5).

The centre of all 4 grids was pinpointed on the University of Canterbury in Christchurch, with latitude φ = - 43^o.3183 and longitude λ = 172^o.345. The total number of spatial nodes for every grid remains constant throughout the research. The respective values are as follows: grid 1 (27 km resolution) – 65 x 65 nodes, grid 2 (9 km resolution) – 67 x 67 nodes, grid 3 (3 km resolution) – 82 x 82 nodes and grid 4 (1 km resolution) – 121 x 121 nodes. Number of domains was the same for all MM5 runs, and all 4 grids start together (4 domains–4 grids) in all 7 experimental runs. Principal physical parameterisation applied to all 4 grids of MM5 was described in Titov (2004). In the research for winter 2005, two different PBL parameterisation schemes were applied to 7 pollution episodes: five-layer soil model with bucket soil moisture scheme (called 'run 1') and the Pleim-Xiu seven-layer soil model with urban soil moisture scheme (called 'run 2'). Application of

land-surface model (LSM) ensemble is considered to provide less MM5-biassed input meteorology for evaluating CAMx4.

Information regarding orography and landuse distribution was taken from the United States Geological Survey (USGS) global database, and was interpolated over all four grids. Input databases of different spatial resolution were used to represent orography for the different resolution grids, from 2-minute resolution for grid 1 up to 30-second resolution for grids 3-4 (an example of interpolated orography for grid 4 is shown in Figure 8.2). The difference between real orography and the interpolated one is not more than a 25% reduction of mean height in modelled topography, resulting from coarse input terrestrial data and the ways of their interpolation. Local topography was not used in the study as a procedure of local terrain (utilized for MM5 fine domains only) was considered not to be in a good agreement with USGS topography (for coarse grid).

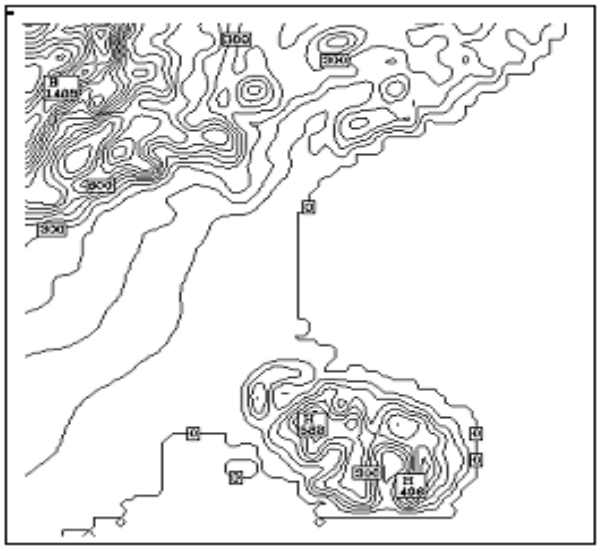

Figure 8.2 Interpolated 30-second global database topography for grid 4.

All 7 chosen episodes were working days (weekend episodes were excluded) to reproduce near-surface air circulation and pollution situations with the highest contribution from domestic, transport and industry groups. Episode 4 (4 May 2005 – 6 May 2005) was selected to analyse in details a possibilities of MM5 to predict main niceties of the local air circulation during day-time and night-time. General statistic for all 7 episodes is given to compare with meteorological observations obtained from 3 sites (Coles Place, Christchurch International Airport and University of Canterbury as Geography building roof).

For all 7 winter 2005 episodes the dominance of the local air circulation over synoptic scale air processes was a result of a weak pressure gradient over the South Island of New Zealand. Figure 8.3 presents geopotential heights for 1000 hPa (Figure 8.3a) and for 850 hPa (Figure 8.3b) obtained from 6-hourly NCEP/NCAR reanalysis data (site http://www.cdc.noaa.gov/Composites/Hour/). Figure 8.3 demonstrates an anticyclonic situation with high pressure and weak pressure gradients over the South Island for 1000 and 850 hPa atmospheric layers. Approximately the same stagnant synoptic situation with dominance of local circulation processes was observed for all 7 winter 2005 episodes.

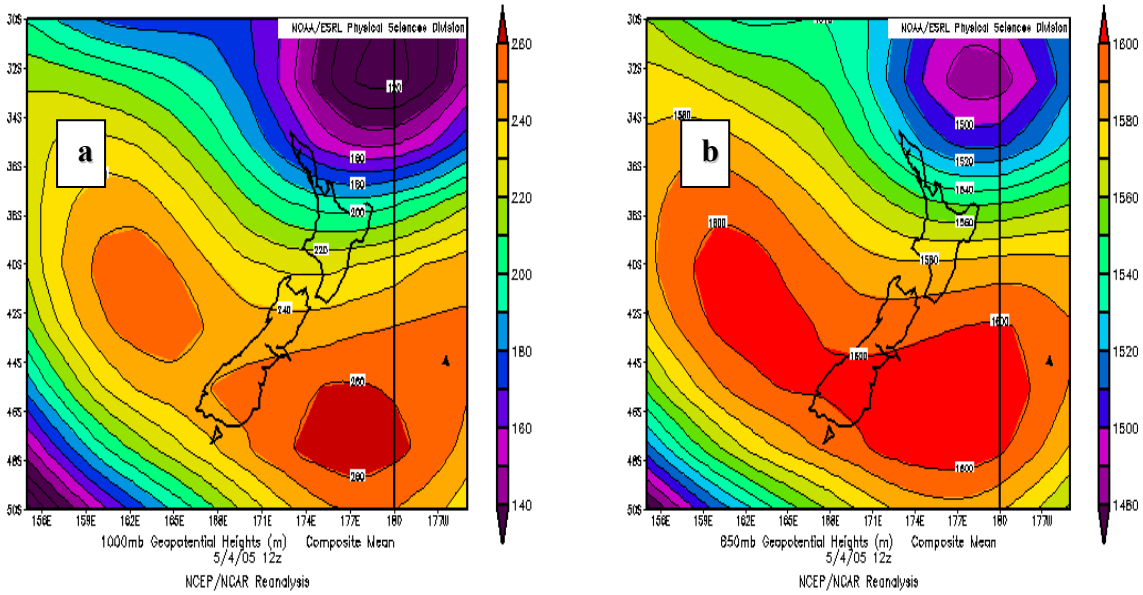

Figure 8.3 Geopotential heights distribution over New Zealand at 12:00 on 5 May 2005 (NZST) from 6-hourly NCEP/NCAR reanalysis for two levels: a) 1000 hPa, and b) 850 hPa.

Figure 8.4 shows backward trajectories with a Christchurch area end point, calculated over 24 hours for levels 500, 1000 and 1500 metres using the on-line HYSPLIT 4 (Draxler and Hess, 1997) Lagrangian model at 0000 NZST on 5 May 2005 (Figure 8.4a) and at 0000 NZST on 6 May 2005 (Figure 8.4b). Figure 8.4 illustrates the weak anticyclonic air circulation for the Christchurch area on 5-6 May 2005 with local scale of the synoptic flow and descending air close to the ground.

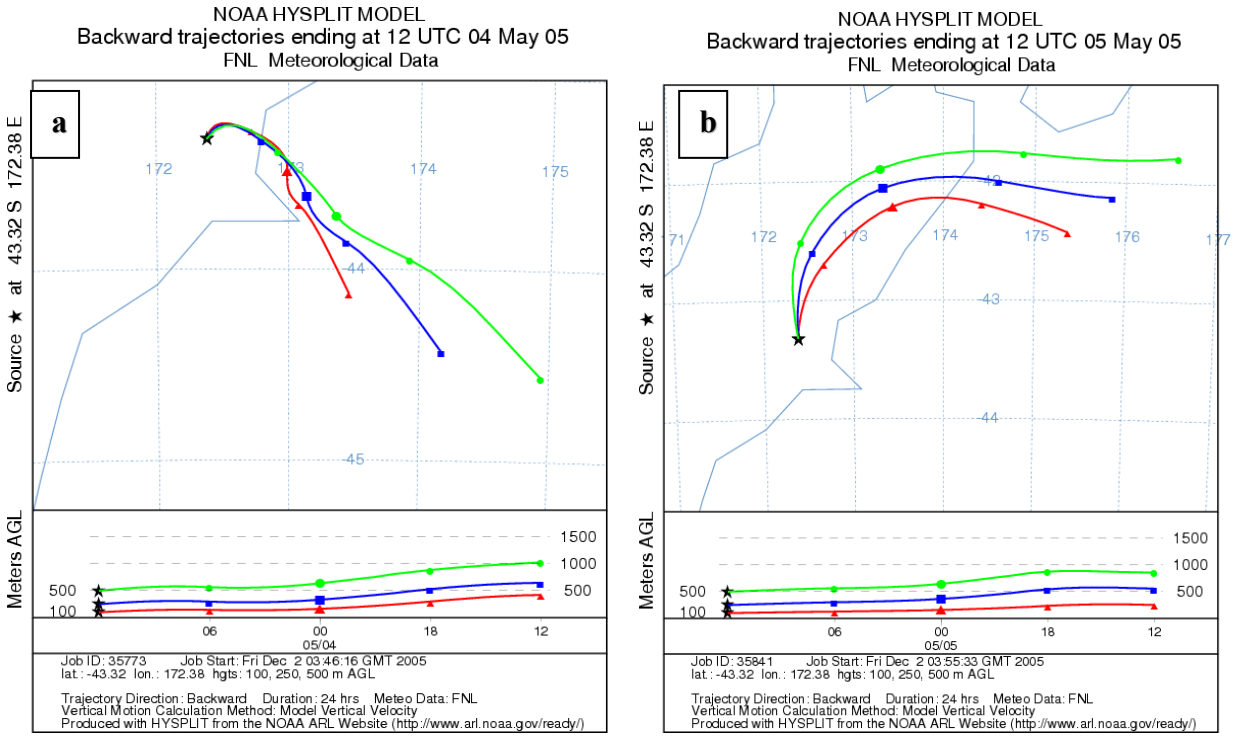

Figure 8.4 24-hour back-trajectories ending in the Christchurch area derived from HYSPLIT 4 for 500, 1000 and 1500 m levels for: a) at 0000 NZST on 5 May 2005; b) at 0000 NZST on 6 May 2005.

The back-trajectory method was applied to episode 4 (winter 2005) to trace the origin of the regional-scale (synoptic-scale) air flow over Christchurch as described in Chapter 9. From Figures 8.3 and 8.4 the synoptic-scale winds (received from NCEP global dataset) in the near-surface layer have west – north-west direction, and the global data with spatial resolution about 100 km don't include any local-scale air processes. The wind fields presented in Figure 8.5 are obtained from the MM5 output for domain 4 (nested grid 3) for σ-level=0.998 (that is approximately 10–12 metres above surface topography) for two times in episode 4: at 1600 NZST on 4 May 2005, showing daytime easterly–northeasterly winds over the Christchurch area (the daytime breeze circulation – Figure 8.5a) and at 1100 NZST on 4 May 2005 with an obvious wind direction change from westerly–southwesterly on easterly-northeasterly winds as a result of a breakdown of the nocturnal breeze and drainage air circulation (Figure 8.5b).

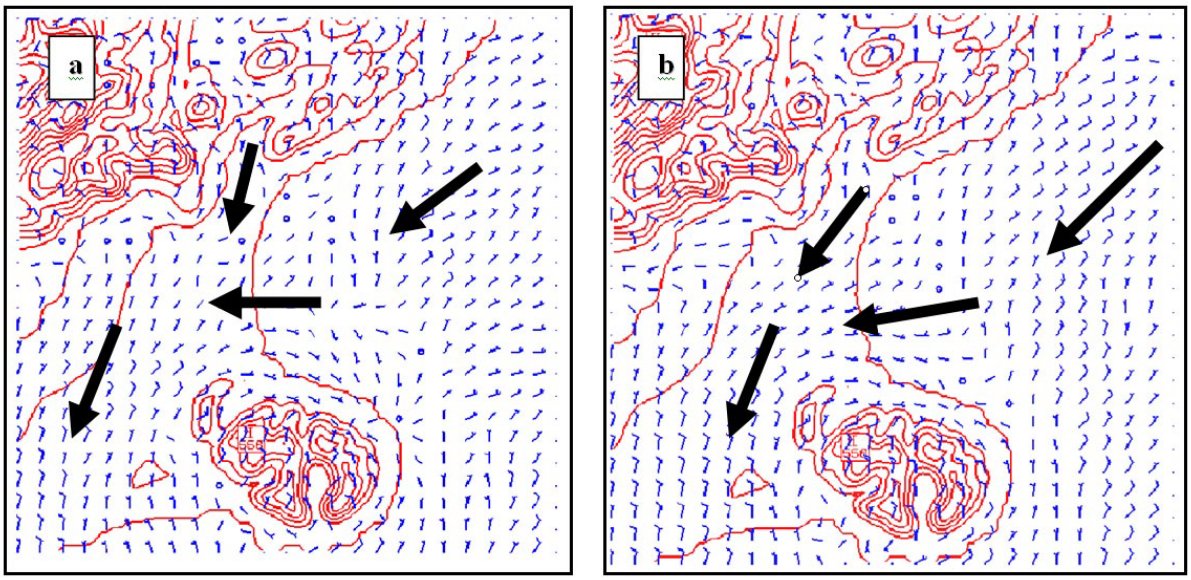

Figure 8.5 Spatial distribution of MM5 modelled near-surface wind for episode 4, grid 4, σ = 0.998 (10-12 metres), bucket LSM scheme: a) at 1600 NZST on 4 May 2005 (15-hour forecast); and b) at 1100 NZST on 4 May 2005 (10-hour forecast).

The ability of MM5 at fine spatial resolution (3-1 km) to reproduce breakdown of the night off-shore breeze circulation and development of the day-time on-shore breeze circulation is evident from Figure 8.5a and 8.5b.

Figure 8.6 shows vertical west-east (Figure 8.6a) and south-north (Figure 8.6b) cross-sections of the near-surface 3-dimensional wind circulation for a layer between 1013-900 hPa plotted for 1600 NZST on 4 May 2005. The results are presented for bucket LSM. Orography is presented by a solid blue line and a part of the Canterbury Plains can be seen in Figure 8.6a, and Port Hills and the Canterbury Plains in Figure 8.6b. Black arrows show wind vectors (m s^{-1}) and grey lines shows vorticity (dPa s^{-1}). Position of cross-sections inside domain 4 is presented in Figure 8.5a using black straight line A (west-east cross-section) and black straight line B (south-north cross-section).

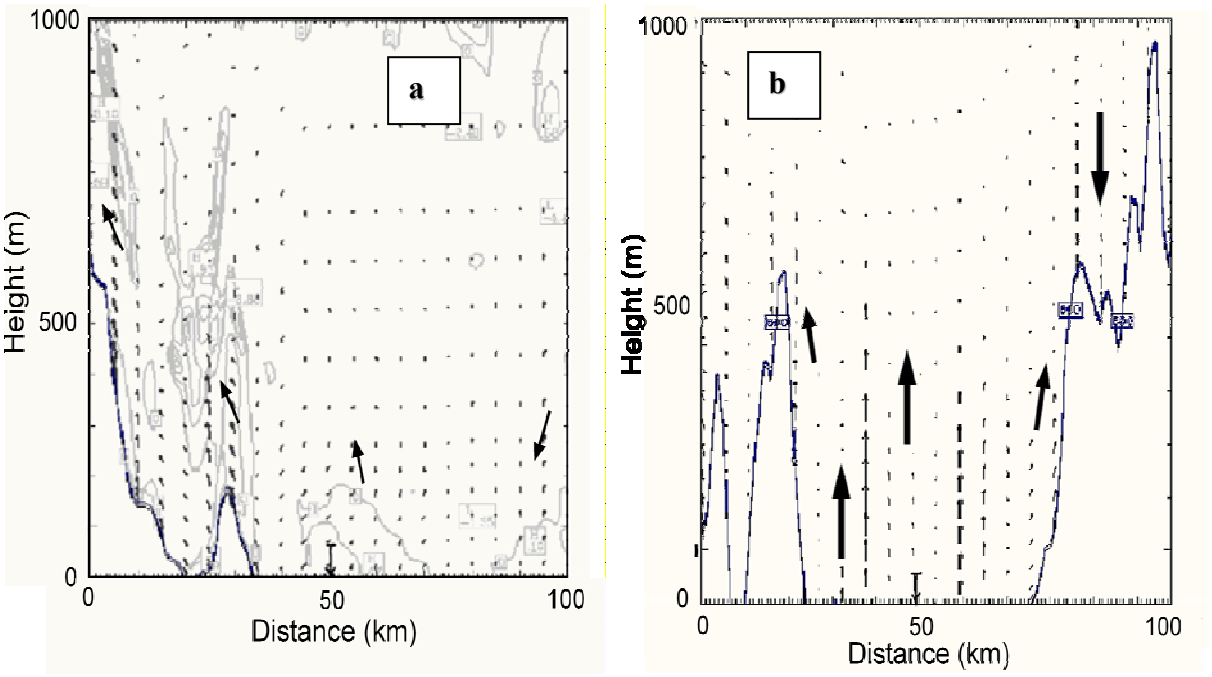

Figure 8.6 Cross-section of MM5 modelled near-surface 3-dimensional wind circulation for episode 4, grid 4, pressure layer 1013-900mb, at 1600 NZST on 4 May 2005 (15-hour forecast), bucket LSM model: a.) West-East cross-section; b) South-North cross-section.

From Figure 8.6 it is apparent that active upward motion of the near-surface air is associated with day-time surface heating. This process especially is active in the south-north cross-section (Figure 8.6b), as there is no water surface for this cross-section compared with Figure 8.6a, where vertical motion is suppressed by descending air motion over the ocean area of the cross-section (eastern part of Figure 8.6a).

Active vertical turbulent processes lead to an increase of the modelled planetary boundary layer (PBL) height during day-time over the Christchurch area. Figure 8.7 shows the spatial distribution of PBL height for MM5 grid 4 averaged over 4 hours (12pm-4pm) for the episode 4 (4 May 2005) using the urban Pleim-Xiu LSM parameterisation in MM5. From Figure 8.7 it is apparent that the Christchurch area (red contoured island) is shifted towards Banks Peninsula in the USGS land-cover global dataset.

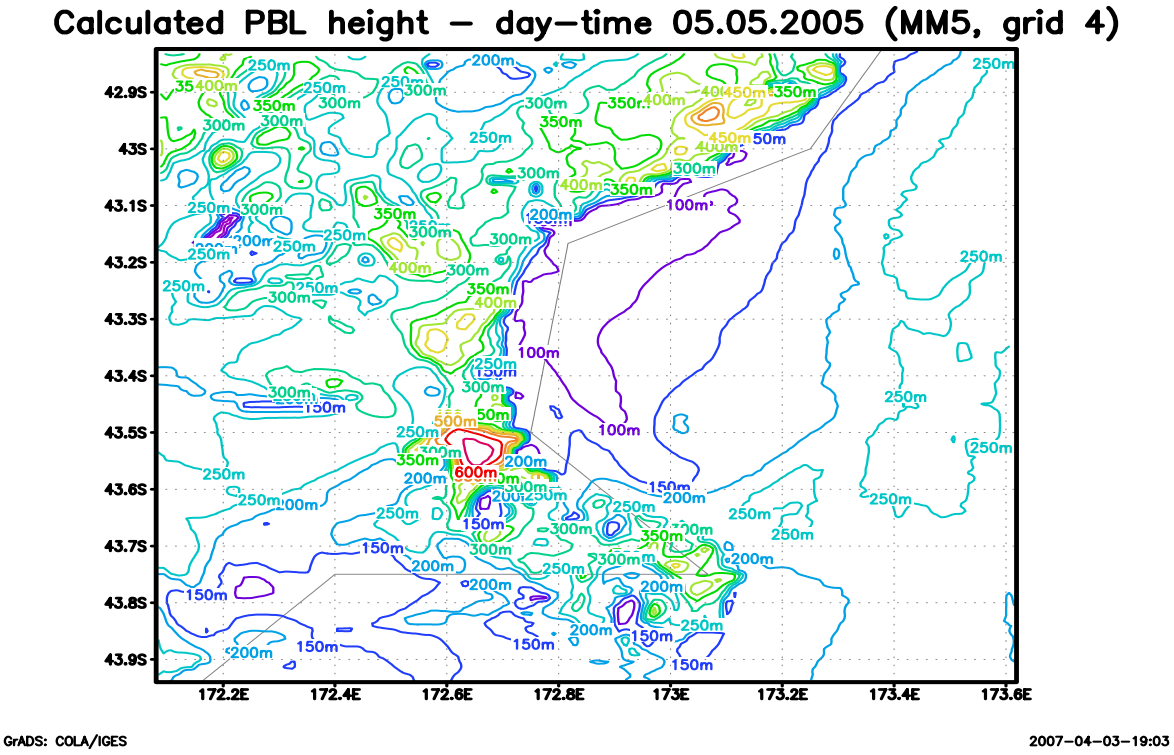

Figure 8.7 Spatial distribution of the modelled PBL height in metres (MM5, grid 4), averaged for 12-4pm NZST (day time) on 4 May 2005 using the Pleim-Xiu urban LSM parameterisation.

The highest values of modelled PBL height of about 500-600 meters are reached over the city of Christchurch shifted to the southern suburbs as a result of the faulty USGS global 30-second landuse data. Over the northern part of Christchurch the average PBL height varies between 450–500 meters (Figure 8.7). These values are lower than ones from observations (about 750-800m) described in Sturman and Kossmann (2004), but Figure 8.7 definitely shows the possibility of MM5 to reproduce the construction of the day-time PBL as a result of local scale heating and vertical turbulence processes. Unfortunately, there is no possibility to compare modelled daytime PBL spatial distribution with a nighttime one as MM5 doesn't calculate PBL for stable atmosphere (negative buoyant) as error in these calculations is very high (Steeneveld et al., 2007).

Figure 8.8 shows vertical profiles of dry-bulb temperature as a function of height derived from MM5 modelled output for Coles Place (Figure 8.8a) and for Christchurch Airport (Figure 8.8b) observation points. The vertical profiles are averaged over 12 pm – 4 pm (5 midday hours) on 4 May 2005 (MM5 domain 4). Diurnal modelled temperature profiles shows higher near-surface temperatures for residential areas of Christchurch (Coles Place - Figures 8.8a) compared with the more rural Christchurch Airport observation point (Figure 8.8b), and confirms the ability of MM5

to reproduce day-time temperature profiles and the breakdown of the night-time temperature inversions for the Christchurch area.

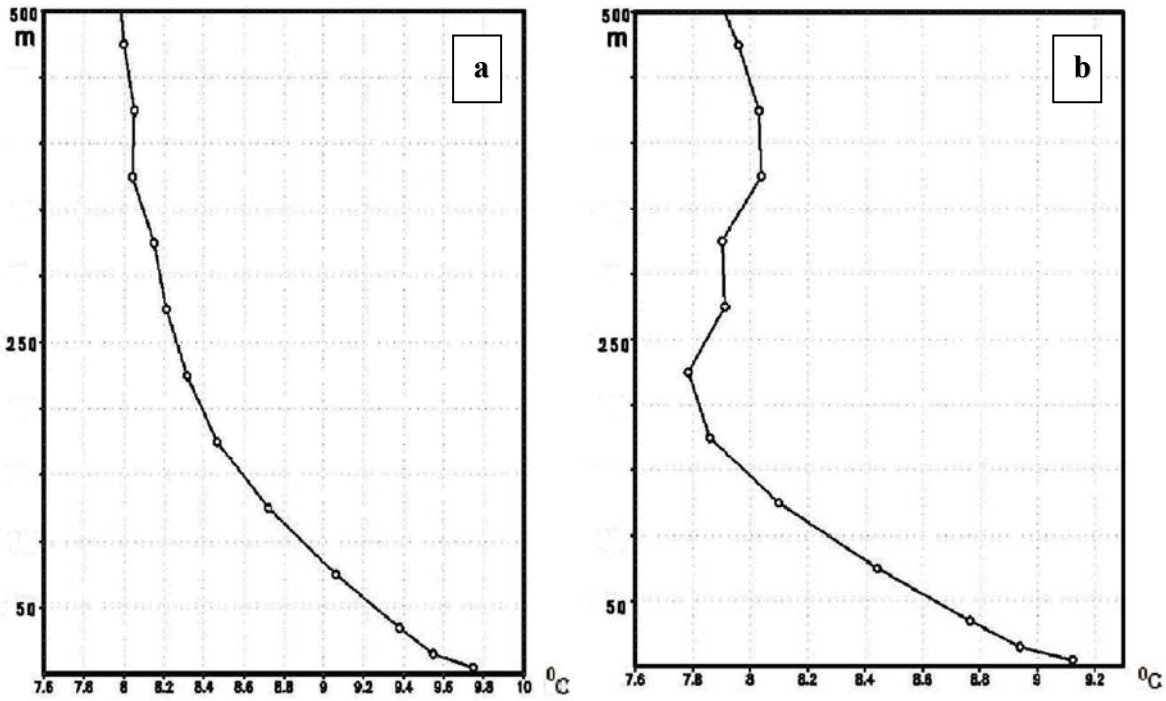

Figure 8.8 Vertical profiles of the modelled dry-bulb temperature for winter 2005 episode 4, grid 4 averaged over 12 pm – 4 pm on 4 May 2005 (bulk LSM model): a) Coles Place observation point; b) Christchurch Airport.

The average for winter 2005 episode 4 statistics calculated for day-evening time (9 am – 7 pm) only for 3 observation sites (Coles Place, Christchurch International Airport and the Geography Department roof) are presented in Table 8.1. While comparing the statistics, slightly better results are obtained for wind components in the case of MM5 LSM2 (urban LSM model) parameterisation. This fact could be important when using the modelled near-surface wind fields in the CAMx4 for more reasonable prediction of aerosol spatial dispersion. On the other hand, more realistic results are obtained for near-surface temperature and relative humidity in bulk LSM (LSM1) case. Temperature and relative humidity are important factors for fine and total PM concentrations as higher relative humidity and lower temperature (see LSM1 in the Table 8.1) lead to a more active creation of secondary PM (secondary organic aerosol and nitrate ammonium). Table 8.1 statistics show approximately equal day-time near-surface atmosphere conditions, resulting from bulk and urban land-surface model parameterisations in MM5.

Table 8.1 Index of Agreement (IOA), Pearson's Correlation Coefficient (PCC), Systematic & Unsystematic Root Mean Square Error (S-RMSE & U-RMSE), and additional statistics of observed and modelled data for 4–6 May 2005 (day-evening time, 3 sites) for episode 4 for two MM5 LSM schemes (bulk – LSM1, Pleim-Xiu – LSM2): near-surface wind, 2 metre temperature and relative humidity.

EPISODE 4	NUMBER OF TIME POINTS	OBSERVED MEAN	MODELLED MEAN	OBSERVED DEVIATION	MODELLED DEVIATION	PCC	OBSERVED MAX	MODELLED MAX	IOA
WIND SPEED ($m\ s^{-1}$)									
LSM1	90	3.55	4.12	1.78	2.15	0.85	8.80	9.7	0.79
LSM2	90	3.55	2.85	1.78	1.86	0.78	8.80	6.6	0.80
AVERAGE	90	**3.55**	**3.48**	**1.78**	**2.01**	**0.82**	**8.80**	**8.1**	**0.80**
U-COMPONENT ($m\ s^{-1}$)									
LSM1	90	2.77	3.23	1.91	2.28	0.86			0.86
LSM2	90	2.77	2.31	1.91	2.15	0.86			0.83
AVERAGE	**90**	**2.77**	**2.77**	**1.91**	**2.22**	**0.86**			**0.85**
V-COMPONENT ($m\ s^{-1}$)									
LSM1	90	1.55	0.85	0.96	0.88	0.35			0.41
LSM2	90	1.55	0.61	0.96	0.68	0.23			0.35
AVERAGE	**90**	**1.55**	**0.73**	**0.96**	**0.78**	**0.28**			**0.38**
TEMPERATURE (^0C) – 2 m									
LSM1	30	11.42	10.67	2.16	3.36	0.85	14.2	15.1	0.88
LSM2	30	11.42	10.31	2.16	3.47	0.76	14.2	13.2	0.71
AVERAGE	**30**	**11.42**	**10.48**	**2.16**	**3.41**	**0.81**	**14.2**	**13.8**	**0.79**
RELATIVE HUMIDITY (%)									
LSM1	90	79.50	81.50	3.55	5.40	0.71	91.6	97.2	0.74
LSM2	90	79.50	81.30	3.55	3.80	0.47	91.6	100.0	0.68
AVERAGE	**90**	**79.50**	**81.40**	**3.55**	**4.60**	**0.59**	**91.6**	**98.8**	**0.71**

8.2 Night-time local scale near-surface air circulation

The ability of MM5 to model rapid day-night changes of near-surface wind direction was evaluated using a 'deep' atmosphere with additional vertical levels in the PBL and upper troposphere–lower stratosphere. This step allowed a realistic replication of mesoscale baroclinity in the real atmosphere corresponding to orographic–thermal effects over Christchurch complex terrain.

Usually the process of near-surface modelled temperature inversion development is associated with a wind speed decrease that is a first sign of local wind direction change. This process will be discussed in the next paragraph with examples for episode 4 (LSM1 and LSM2). Downslope drainage winds will be traced spatially (including modelled back-trajectories) with application of vertical profiles for Coles Place and Christchurch International Airport. Breakdown of a night-time near-surface inversion will be shown with examples of wind direction change and temperature re-distribution for different near-surface levels.

Winter 2005 episode 4 statistics calculated for evening-night time (7 pm – 8 am) only for 3 observation sites (Coles Place, Christchurch International airport and UoC geography roof) are presented in Table 8.2. While comparing the statistics, again better results are received for wind components in the case of MM5 LSM2 (urban LSM model) parameterisation, but LSM2 over-predicts night-time temperature minima and relative humidity compared with MM5 LSM1 and with observations.

Information form the Tables 8.1 and 8.2 (especially about temperature peaks) provides an understanding of quite mild weather conditions for winter 2005 Episode 4 with not a big amplitude of average near-surface meteorology between day-time (Table 8.1) and night-time (Table 8.2) periods.

Table 8.2 Index of Agreement (IOA), Pearson's Correlation Coefficient (PCC), Systematic & Unsystematic Root Mean Square Error (S-RMSE & U-RMSE), and additional statistics of observed and modelled data for 4–6 May 2005 nights (3 sites) for episode 4 for two MM5 LSM schemes (bulk – LSM1, Pleim-Xiu – LSM2): near-surface wind, 2 metre temperature and relative humidity.

EPISODE 4	NUMBER OF TIME POINTS	OBSERVED MEAN	MODELLED MEAN	OBSERVED DEVIATION	MODELLED DEVIATION	PCC	OBSERVED MAX	MODELLED MAX	IOA
WIND SPEED (m s^{-1})									
LSM1	82	2.65	3.15	1.75	1.45	0.87	5.8	7.1	0.90
LSM2	82	2.65	1.55	1.75	1.05	0.78	5.8	4.4	0.88
AVERAGE	**82**	**2.65**	**2.35**	**1.75**	**1.22**	**0.82**	**5.8**	**6.7**	**0.89**
U-COMPONENT (m s^{-1})									
LSM1	82	1.55	2.55	1.84	1.76	0.63			0.88
LSM2	82	1.55	0.85	1.84	1.46	0.66			0.92
AVERAGE	**82**	**1.55**	**1.70**	**1.84**	**1.62**	**0.64**			**0.90**
V-COMPONENT (m s^{-1})									
LSM1	82	1.07	0.75	0.86	1.12	0.42			0.57
LSM2	82	1.07	0.85	0.86	0.82	0.38			0.55
AVERAGE	**82**	**1.07**	**0.80**	**0.86**	**0.97**	**0.40**			**0.56**
TEMPERATURE (^{0}C) – 2 m									
LSM1	21	8.17	7.40	3.35	2.75	0.89	10.7	13.1	0.93
LSM2	21	8.17	6.10	3.35	3.15	0.96	10.7	12.2	0.91
AVERAGE	**21**	**8.17**	**6.75**	**3.35**	**2.95**	**0.93**	**10.7**	**12.7**	**0.92**
RELATIVE HUMIDITY (%)									
LSM1	82	86.75	89.95	9.90	8.86	0.94	97.5	99.0	0.94
LSM2	82	86.75	96.15	9.90	7.24	0.93	97.5	100.0	0.81
AVERAGE	**82**	**86.75**	**93.05**	**9.90**	**8.05**	**0.94**	**97.5**	**99.5**	**0.87**

Near-surface inversion development

The local scale process of night-time near-surface inversion development is a pre-cursor to a potentially high nighttime PM concentrations, and it starts with the decrease of the day-time on-shore wind that is shown in Figure 8.9. The wind fields presented in Figure 8.9 result from MM5 output for domain 4 and σ-level = 0.998 (10–12 metres above surface topography) for two episode 4 time points: at 2000 NZST and at 2100 NZST on 4 May 2005 (LSM2). Figure 8.9 displays the process of break down of the daytime easterly–northeasterly winds over the Christchurch area (Figure 8.9a) with a change to a more chaotic air circulation over the Christchurch area (Figure 8.9b). The process of wind direction reverse is coupled with a decrease of wind speed.

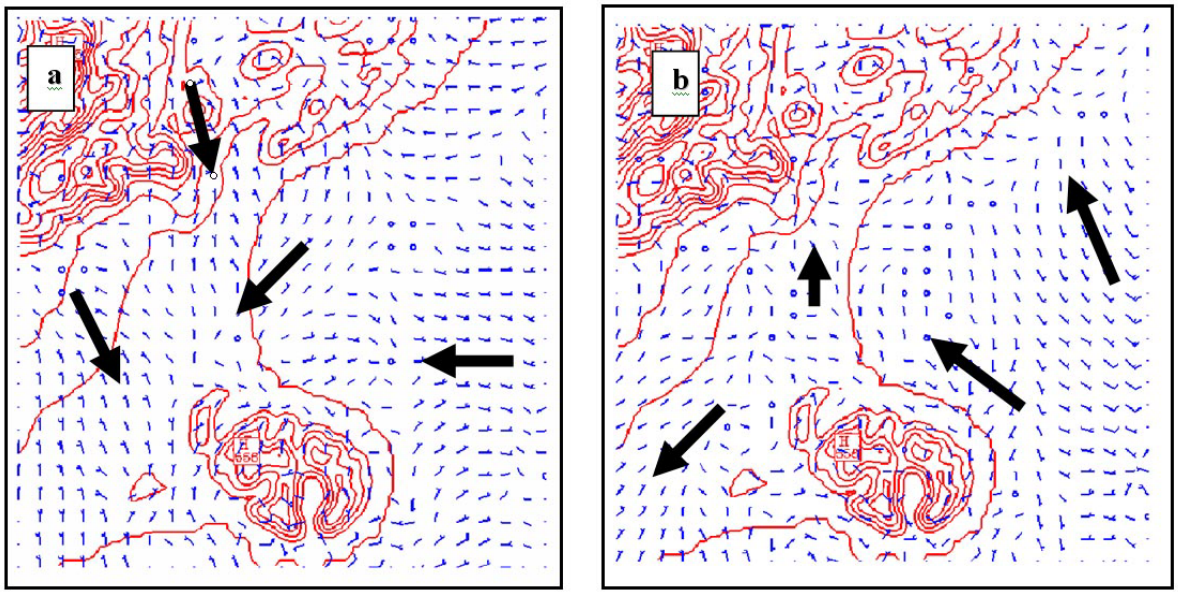

Figure 8.9 Spatial distribution of MM5 modelled near-surface wind for episode 4, grid 4, σ = 0.998 (10-12 metres): a) at 2000 NZST on 4 May 2005 (19-hour forecast); and b) at 2100 NZST on 4 May 2005 (20-hour forecast).

Figure 8.10 shows the vertical south-north cross-sections of the modelled near-surface 3-dimensional wind circulation for a layer between 1013-900 hPa plotted for the two times: at 2000 NZST (Figure 8.10a), and 2100 NZST (Figure 8.10b) on 4 May 2005 (LSM2). The decrease of the upward vertical air circulation over the Christchurch area (Figure 8.10a) from 2000 to 2100 is accompanied by a disappearance of any vertical motion over the mountains (Figure 8.10b).

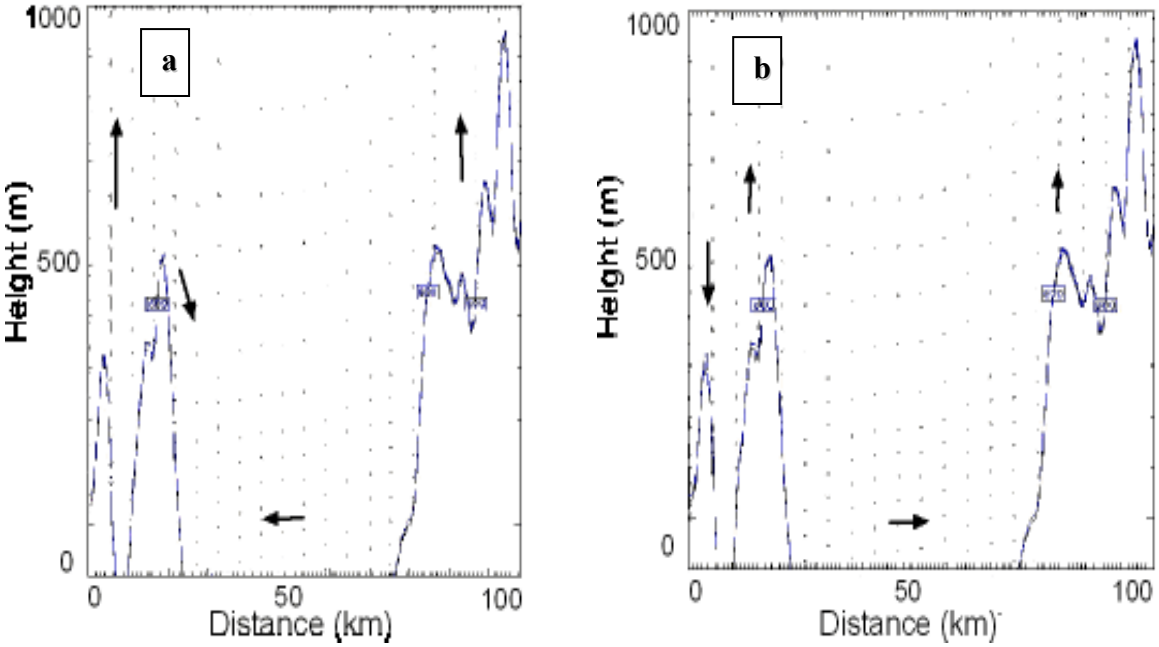

Figure 8.10 South-north cross-section of the modelled near-surface 3-dimensional wind circulation for episode 4 (domain 4) pressure layer 1013-900 hPa: a) at 2000 NZST on 4 May 2005 (19-hour forecast); b) at 2100 NZST on 4 May 2005 (20-hour forecast).

Figure 8.11 shows vertical profiles of dry-bulb temperature as a function of height derived from MM5 domain 4 output for Coles Place (Figure 8.11a) and for Christchurch Airport (Figure 8.11b) observation sites averaged over 8-10 pm period (3 evening hours) on 4 May 2005. The evening modelled temperature profiles show the active process of near-surface temperature inversion development for a residential area of Christchurch (Coles Place - Figures 8.11a), and for a more rural Christchurch Airport location (Figure 8.11b). The inversion for the Christchurch Airport (more rural area) is a little stronger than in the residential area, which is in good agreement with observations (Figure 7.3). The modelled near-surface layer transforms from unstable (day-time - Figure 8.8) to a stable condition (Figure 8.11) creating excellent near-surface meteorological conditions for aerosol accumulation in the lowest 100 m.

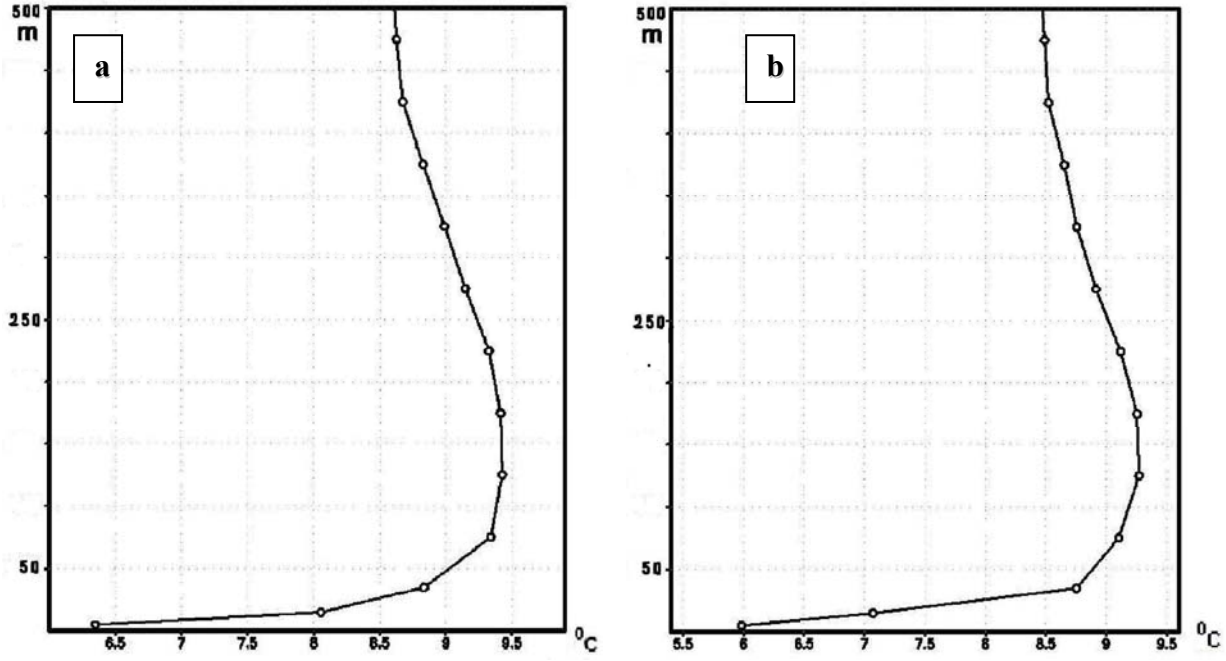

Figure 8.11 Vertical profiles of the modelled dry-bulb temperature for winter 2005 episode 4 (domain 4) averaged over 8-10 pm on 4 May 2005 (LSM2): a) Coles Place; b) Christchurch Airport.

The process of evening modelled inversion development is presented by a decrease of the vertical-horizontal air motion, and an appearance of the temperature inversion in the lowest 100 meters layer.

Night-time inversion and downslope cold air drainage

Nigh-time near-surface local-scale temperature inversions are supported and strengthened by two processes: surface cooling and downslope drainage of the cold air. Both processes decrease the near-surface temperature and increase stability of the near-surface air, ousting warmer air. Figure

8.12 presents the night-time modelled spatial wind distribution (MM5 domain 4) for σ-level=0.998 (10–12 metres AGL) for two times during episode 4: at 0000 NZST and at 0400 NZST on 5 May 2005. Figure 8.12a (midnight on 5 May 2005) displays downslope winds from the Canterbury Plains that bring cold air over Christchurch (as north-westward drainage winds), and a stagnant situation with very weak air movement inside the Christchurch area. Figure 8.12b (4 am on 05 May 2005) displays a further development of the modelled cold air drainage that includes not only the Canterbury Plains downslope winds, but also the Port Hills downslope winds.

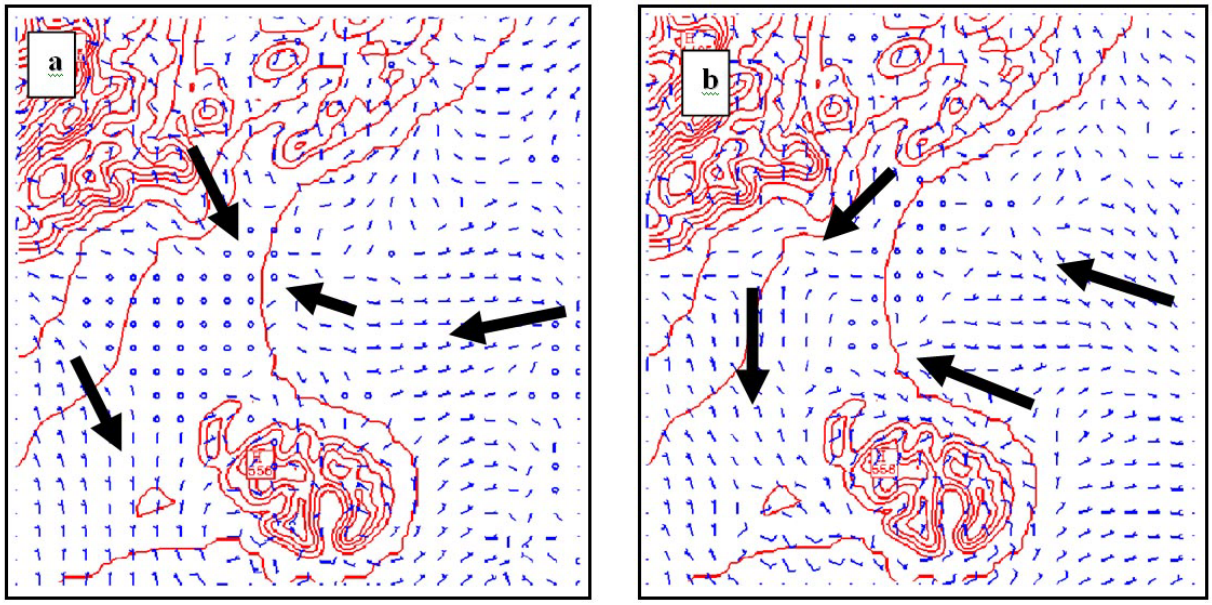

Figure 8.12 Spatial distribution of MM5 modelled near-surface wind for episode 4, grid 4, σ = 0.998 (10-12 metres) and urban LSM at: a) 0000 NZST on 5 May 2005 (24-hour forecast); and b) 0400 NZST on 5 May 2005 (28-hour forecast).

Figure 8.13 shows vertical south-north cross-sections of the modelled near-surface 3-dimensional wind circulation for a layer between 1013-900 hPa plotted for two times at night: at 0000 NZST (Figure 8.13a) and at 0400 NZST (Figure 8.13b) on 5 May 2005. It is remarkable that if modelled vertical circulation only negative for midnight on 5 May 2005 (Figure 8.13a), at 4 am MM5 output shows not only a downward air motion but also upward movement over the south-east part of the Canterbury Plains. This process can be explained only as a compensating boundary air flow in 3-D domain 4 of MM5, as this upward motion was not traced for domain 3 (not shown). One-way interaction was used in all MM5 runs, and daughter grid (domain 4) could not influence on the modelled circulation of the mother grid (domain 3) that made MM5 time integration more stable.

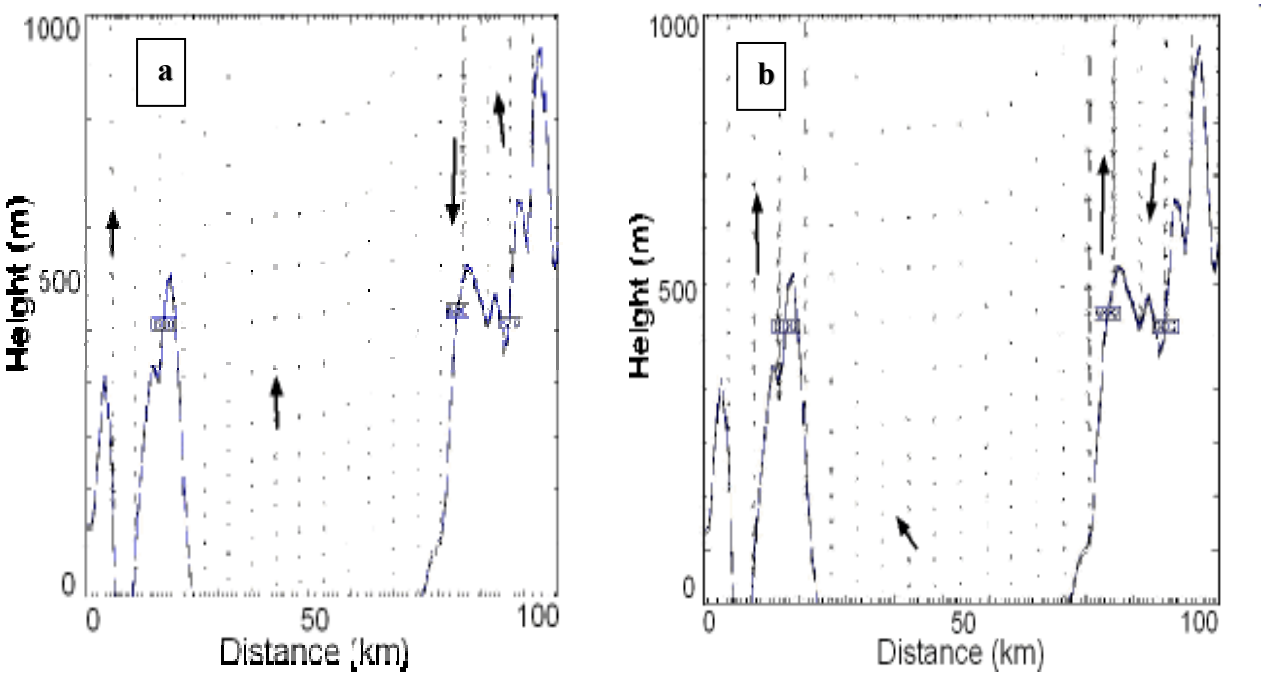

Figure 8.13 South-north cross-section of the modelled near-surface 3-dimensional wind circulation for episode 4, grid 4 pressure layer 1013-900 hPa (urban LSM): a) at 0000 NZST on 5 May 2005 (24-hour forecast); b) at 0400 NZST on 5 May 2005 (27-hour forecast).

The process of radiative and dynamical cooling of near-surface air increases the near-surface temperature inversion. Figure 8.14 shows vertical profiles of dry-bulb temperature as a function of height derived from MM5 domain 4 output for Coles Place (Figure 8.14a) and for Christchurch Airport (Figure 8.14b) averaged over 12 pm - 04 am period (5 night hours) on 5 May 2005. Night modelled temperature profiles shows additional increase of the near-surface temperature inversion as over the residential area of Christchurch (Coles Place - Figures 8.14a), and so for a background rural Airport (Figure 8.14b). The modelled inversion for the Airport modelled point is 1.5^0C stronger than for the city residential area (Coles Place) and is consistent with observations (Figure 7.3). But it should be stressed that during the nighttime values of the air temperature didn't drop to zero or to negative values. Mostly this was a result of a quite warm land surface and quite high day-time air temperatures during May 2005 (as was described earlier).

Comparison of Figure 8.14a and Figure 8.14b demonstrates the difference between temperature profiles in the lowest 25-30 metres between an inner city urban site (Coles Place) and more rural site (Christchurch Airport). A modelled temperature profile over 5 hours during the night for a rural site shows absence of the inversion in the lowest 25-30 metres, which initially looks quite strange. However, from a conceptual model (Figure 4.11) and from observations during CAPS2000 (Figure 7.2) it is well known that cold air drainage from the Canterbury Plains and Port

Hills ousts more warm inner city near-surface air not only vertically, but also in 2 horizontal directions: to the east (the Pacific Ocean) and in a west-southwest direction undercutting cold air.

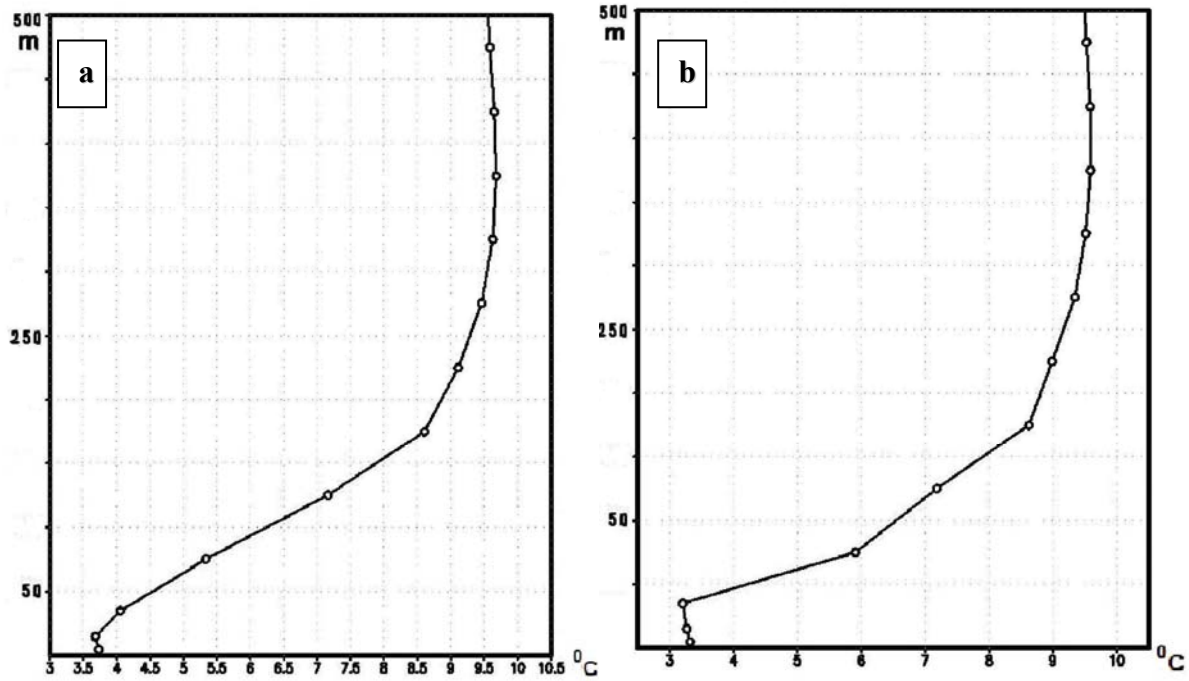

Figure 8.14 Vertical profiles of the modelled dry-bulb temperature for winter 2005 episode 4, grid 4 averaged over 12 pm – 4 am on 5 May 2005: a) Coles Place; b) Christchurch Airport.

It is apparent that the warm inner city air pushed over the Pacific Ocean is advected by nocturnal off-shore breeze over a warmer sea surface, so it is difficult to trace the influence of the inner city air over a warm sea surface. However, for the west-southwest direction (from city centre) a movement of warmer to compare with rural air inner city near-surface air a little mitigate rural temperature inversion in the lowest 10-20 meters (see Figure 8.14b).

Figure 8.15 presents vertical profiles of the modelled dry-bulb temperature (MM5, LSM2) as a function of height for the inner city Polytechnic site (Figure 8.15a) and for Hornby in the southwest suburbs (Figure 8.15b). As for Figure 8.14, observation points are averaged over 12 pm – 4 am period on 5 May 2005. These figure proves a hypothesis about more sharp profile of the modelled near-surface temperature inversion for the inner city point (Polytechnic – Figure 8.15a) and nearly neutral temperature profile in the lowest 25-30 m for an outskirt site (Hornby – Figure 8.15b). The Hornby night temperature vertical profile is the result of warm air advection from the inner areas of the city ‘heat island’.

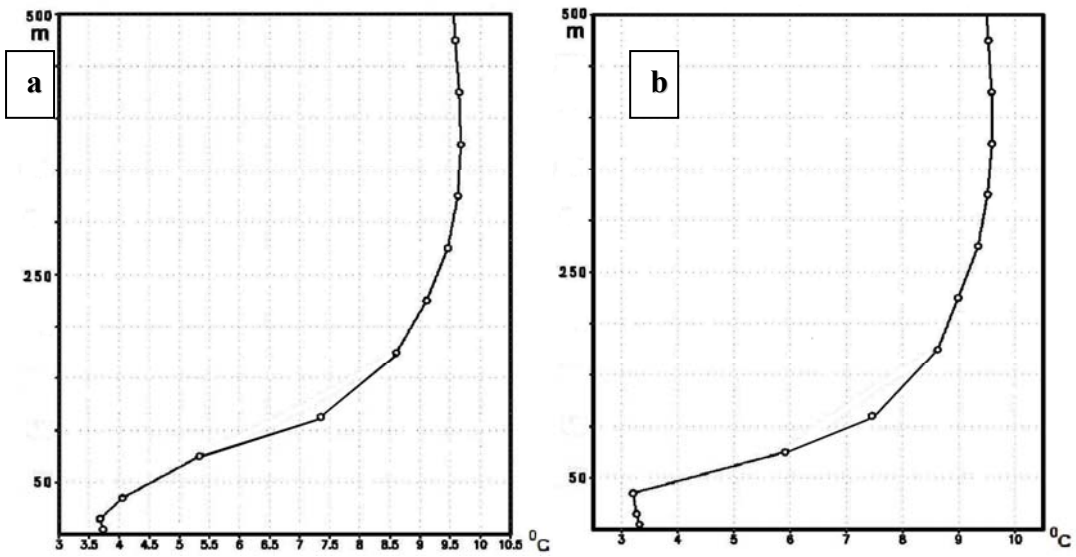

Figure 8.15 Vertical profiles of the modelled dry-bulb temperature for winter 2005 episode 4, grid 4 averaged over 12 pm – 4 am on 5 May 2005 (LSM2): a) Polytechnic, b) Hornby.

To revise more accurately the possibilities of MM5 to reproduce night-time air circulation over the Christchurch area back and forward trajectories were plotted using special visualisation MM5 post-processing software RIP4 (Read-Interpolate-Plot, version 4 – Stoelinga, 1995). Figure 8.16 demonstrates backward (Figure 8.16a) and forward (Figure 8.16b) trajectories of the local near-surface nigh-time airflow for time period 6 am – 12 pm (backward) and 12 pm – 6 am (forward) on 5 May 2005 (episode 4, MM5 LSM2).

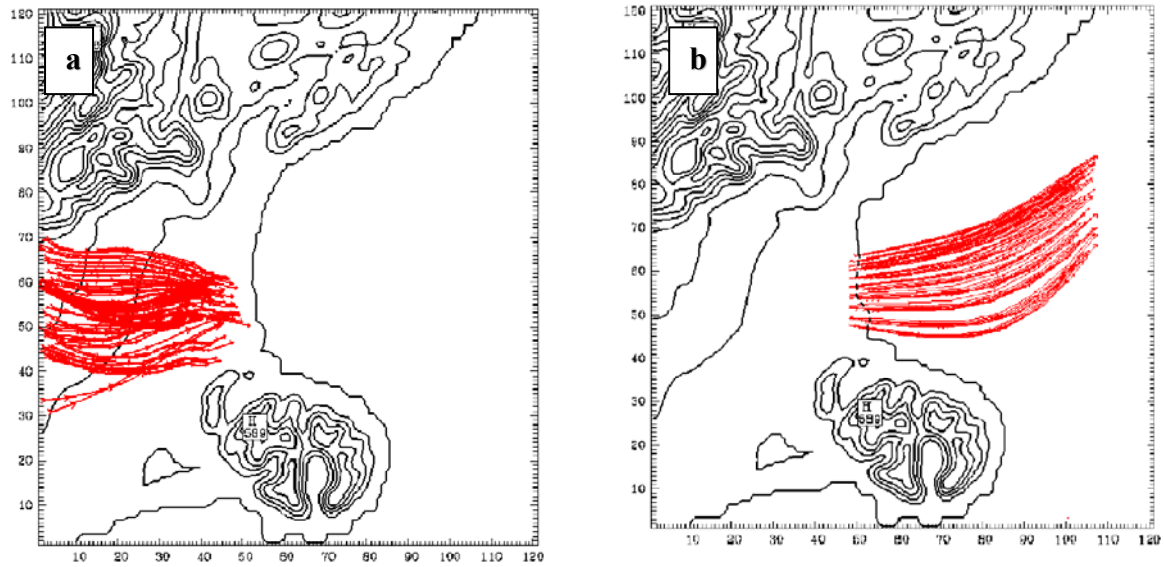

Figure 8.16 Trajectories (MM5, LSM2) of the modelled near-surface air circulation for episode 4, grid 4, σ = 0.998 (10-12 metres): a) backward trajectories - over 6 am – 12 pm period on 5 May 2005; and b) forward trajectories - over 12 pm – 6 am period on 5 May 2005.

Dominance of the downslope flow during night time is evident from Figure 8.16a and the well-developed character of this process is proven by near-surface cold air advection from Christchurch in the south direction and over warmer sea surface. Vertical back- and forward trajectories for a southeast-northwest cross-section are presented in Figure 8.17 for the same backward 6 am – 12 pm (backward trajectories – Figure 8.17a) and forward 12 pm – 6 am (forward trajectories – Figure 8.17b) time intervals.

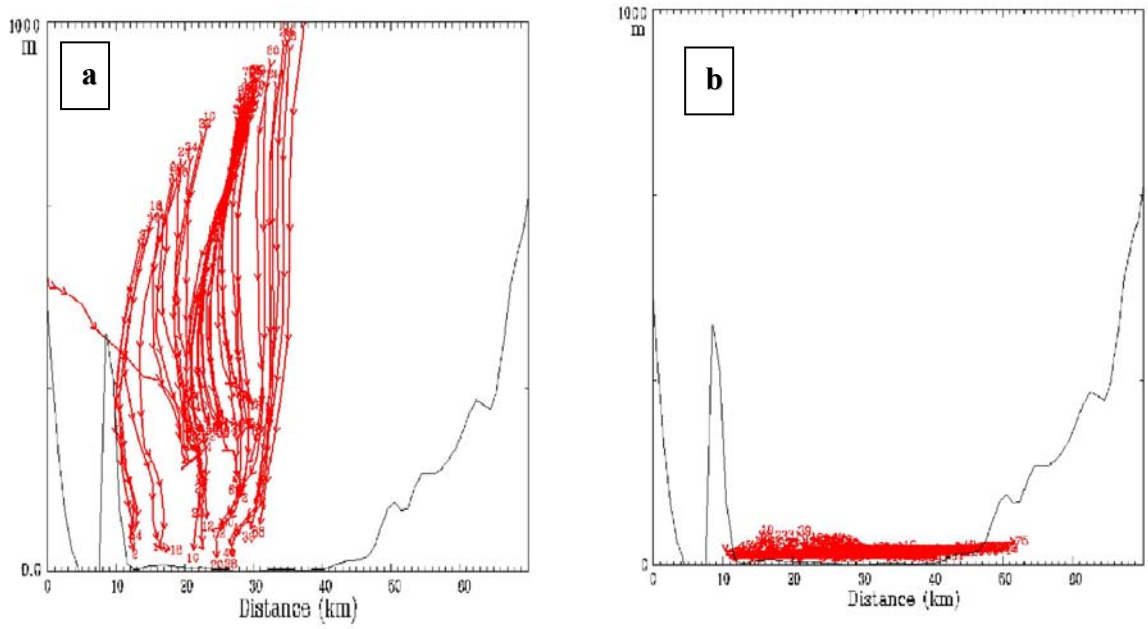

Figure 8.17 Southeast-northwest cross-section trajectories (MM5, LSM2) of the modelled air circulation for episode 4 (MM5, LSM2) pressure layer 1013-900 hPa: a) backward trajectories - over 06 am – 12 pm time period on 5 May 2005; and b) forward trajectories - over 06 am – 12 pm time period NZST on 5 May 2005.

Figure 8.17 shows that modelled 6 am near-surface cold air over the Christchurch area is a result of drainage from surrounding mountain slopes (Figure 8.17a), and modelled midnight near-surface cold air is advected from the Christchurch area only in a very shallow (20-30 meters) layer (MM5, LSM2). This specific process of the cold air circulation leads to pushing of the inner city warmer air in the direction of the southern suburbs and the Pacific Ocean.

Night-time inversion breakdown

The breakdown of the night-time strong temperature inversion is a result of the morning-day active surface heating on the background of anticyclonic clear sky weather. One the most important features of the day-time circulation is a destruction of night-time near-surface off-shore wind circulation and a change of the off-shore winds on the on-shore winds over the Christchurch area. Figure 8.18 exhibits a morning-time modelled wind field (MM5, LSM2) for σ-level=0.998 (10–12

metres AGL) for two times during episode 4: at 0900 NZST and at 1100 NZST on 6 May 2005. Figure 8.18a (early morning on 05 May 2005) shows a disappearance of the downslope winds close to seashore area, and development of the northeasterly near-surface winds over the Christchurch area. Figure 8.18b (late morning on 05 May 2005) displays a further activation of the modelled north-easterly on-shore winds that presumably are also stimulated by the parts of the night drainage winds from the Canterbury Plains and Port Hills apart from the seashore.

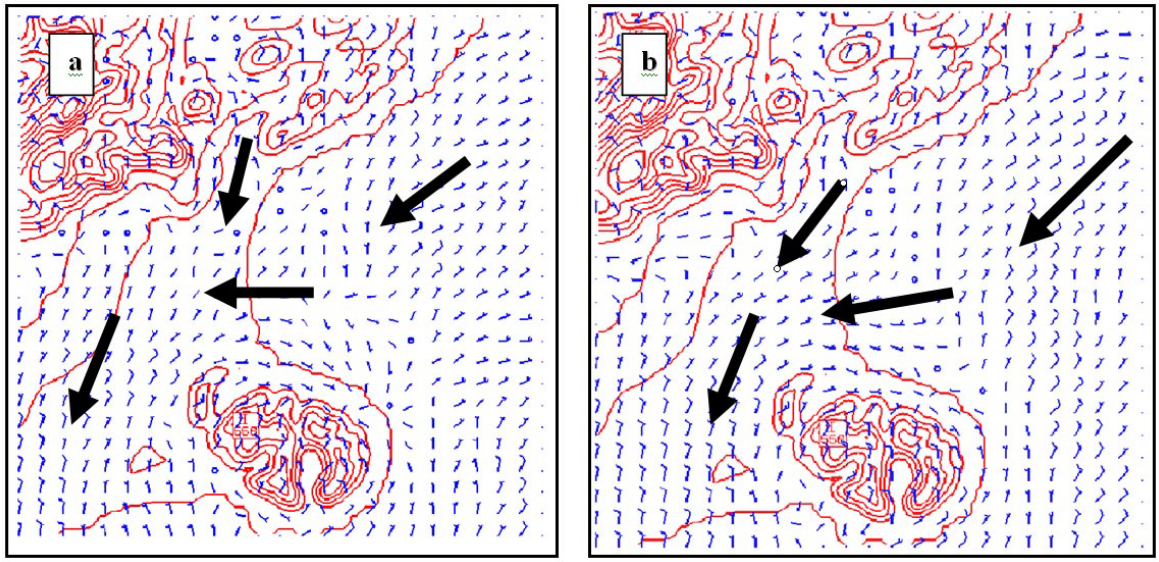

Figure 8.18 Spatial distribution of MM5 modelled near-surface wind for episode 4, grid 4, σ = 0.998 (10-12 metres): a) at 0900 NZST on 5 May 2005 (33-hour forecast); and b) at 1100 NZST on 5 May 2005 (35-hour forecast).

Figure 8.19 shows a vertical south-north cross-section of the modelled near-surface 3-dimensional wind circulation for a layer between 1013-900 hPa plotted for two times: at 0900 NZST (Figure 8.19a) and at 1100 NZST (Figure 8.19b) on 5 May 2005. Figure 8.19a shows a nearly neutral modelled PBL with still descending cold air over the Canterbury Plains and Port Hills slopes at 9am on 5 May 2005. At 11am MM5 (domain 4, LSM2) generates an increase of upward air motion over the Christchurch area and for the Canterbury Plains slope, but still downward movement over the Port Hills apart from Pacific ocean (see Figure 8.18).

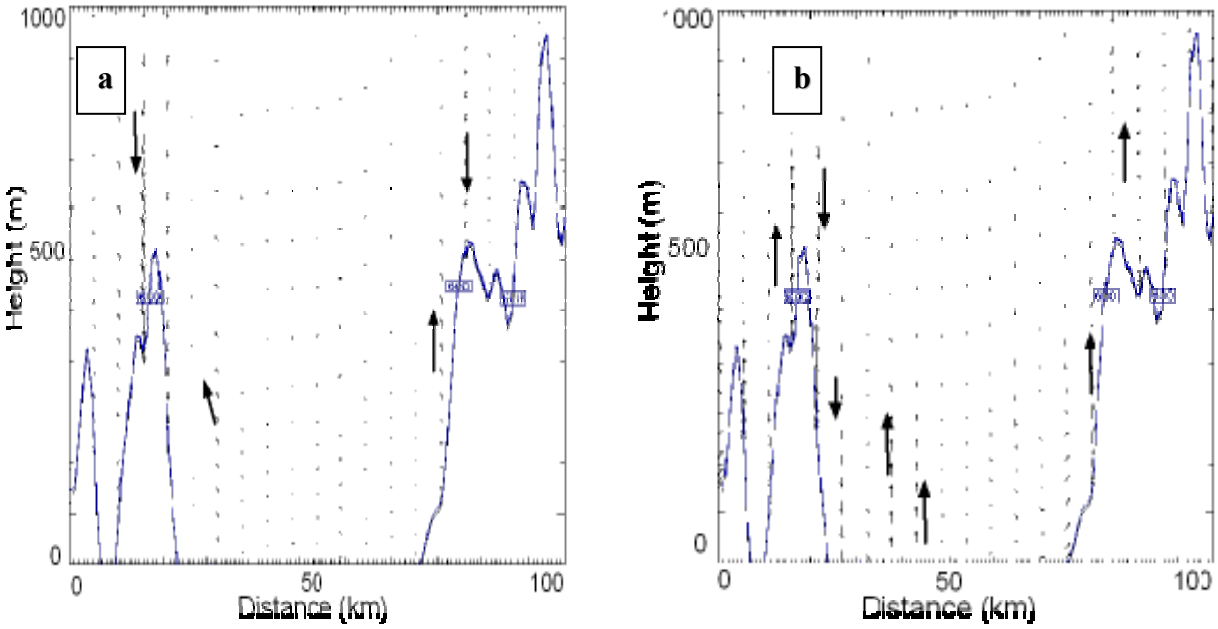

Figure 8.19 South-north cross-section of the modelled near-surface 3-dimensional wind circulation for episode 4 (MM5, LSM2) pressure layer 1013-900 hPa: a) at 0900 NZST on 5 May 2005 (33-hour forecast); b) at 1100 NZST on 5 May 2005 (35-hour forecast).

The process of insolation and surface heating breaks the modelled temperature inversion as is demonstrated in Figure 8.20, which shows vertical profiles of dry-bub temperature as a function of height derived from MM5 domain 4 output for Coles Place (Figure 8.20a) and for Christchurch airport (Figure 8.20b) averaged over the 9 am – 11 am period (4 morning hours) on 5 May 2005.

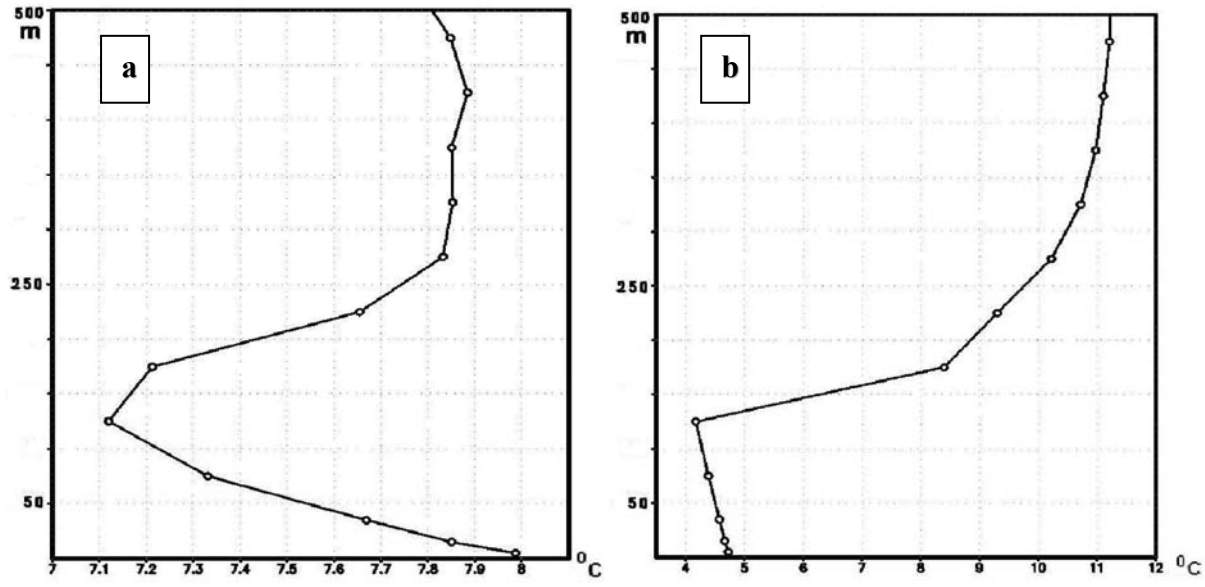

Figure 8.20 Vertical profiles of the modelled dry-bulb temperature for winter 2005 episode 4, grid 4 averaged over 8 am - 11am on 5 May 2005: a) Coles Place; b) Christchurch airport.

Averaged vertical temperature profiles for both sites show unstable conditions for the near-surface layer air, and temperature inversion (stable air layer) over this layer inside PBL (maximum about 450-500 m – Figure 8.7). At the Christchurch Airport 'rural' site the near-surface heating creates only a small positive vertical gradient leaving the atmosphere to be absolutely stable above 150-200 metre (Figure 8.20b), at the inner city Coles Place site the averaged morning vertical temperature profile shows much higher positive buoyancy (Figure 8.20b) being under influence of the urban 'heat island'. There is also an inversion at 150-200 meters, but the near-surface air is absolutely or conditionally unstable through the whole modelled PBL inside the inner Christchurch.

8.3 Local air circulation over complex terrain

Evaluation of MM5 ability of accurately reproduce local air circulation over complex terrain is split into several steps. In this section general statistics including histograms and scatter-plots (for 7 episodes in winter 2005) will be combined with time series of observed and modelled wind, temperature and relative humidity for 3 observation sites (winter 2005 episode 4, MM5 LSM2). All statistics was calculated for episode 4 described in former sections of the chapter.

Winter 2005 episode 4 average statistics calculated for 3 observation sites (Coles Place, Christchurch International Airport, the UoC geography roof) are presented in Table 8.3. While comparing the statistics for two MM5 Land-Surface Models (LSM1 – bulk scheme, LSM2 – urban scheme) approximately the same statistical results were obtained for wind components in the case of LSM1 and LSM2, with weaker winds for LSM2 compared with observations and LSM1. Bulk LSM over-predicts mean and maximum values of the wind, and the urban version of LSM has a tendency to under-predict the wind. LSM2 has a tendency to under-predict mean and day-time peak temperatures compared with observations. On the other hand LSM1 gives mean temperatures closer to observed ones for all 3 sites, but definitely over-predicts maximum temperature values. The mitigation tendencies of the urban LSM can be explained by the 'heat island' parameterisation included in LSM2, while LSM1 reflects the near-surface processes for more rural areas with sharper day-night near-surface temperature extremes as well as with higher wind peaks. The relative humidity reaches 100% (saturation condition) much faster for LSM2 that could lead to a development of the chemical instability in CAMx4 (as discussed previously). For our purposes, the LSM2 scheme is considered to be a bit more preferable for using modelled near-surface meteorology in CAMx4, as for modelled PM calculations PH_2O specie direct participation in PM

building was excluded to prevent development of PH_2O chemical instability during CAMx4 evaluation. On the other hand, an elimination of the aerosol water from total PM mass leads to systematic underprediction of PM concentration. This problem could be avoided while using LSM1, but LSM1 scheme produces more active near-surface wind and lead to more active PM dispersion (Table 8.3).

Table 8.3 Index Of Agreement (IOA), Pearson's Correlation Coefficient (PCC), Systematic & Unsystematic Root Mean Square Error (S-RMSE & U-RMSE), and additional statistics of observed and modelled data for 4–6 May 2005 (3 sites), episode 4 for two MM5 LSM schemes (bulk – LSM1, Pleim-Xiu – LSM2): near-surface wind, 2 metre temperature and relative humidity.

EPISODE 4	NUMBER OF TIME POINTS	OBSERVED MEAN	MODELLED MEAN	OBSERVED DEVIATION	MODELLED DEVIATION	PCC	OBSERVED MAX	MODELLED MAX	IOA
WIND SPEED (m s^{-1})									
LSM1	150	2.78	3.22	1.74	1.65	0.81	8.80	9.70	0.79
LSM2	150	2.78	2.07	1.74	1.45	0.78	8.80	6.55	0.75
AVERAGE	**150**	**2.78**	**2.63**	**1.74**	**1.50**	**0.79**	**8.80**	**8.12**	**0.77**
U-COMPONENT (m s^{-1})									
LSM1	150	2.08	2.65	2.45	2.55	0.79			0.78
LSM2	150	2.08	1.68	2.45	2.35	0.77			0.82
AVERAGE	**150**	**2.08**	**2.16**	**2.45**	**2.45**	**0.78**			**0.80**
V-COMPONENT (m s^{-1})									
LSM1	150	1.54	1.92	1.22	0.95	0.24			0.41
LSM2	150	1.54	1.44	1.22	1.00	0.22			0.52
AVERAGE	**150**	**1.54**	**1.67**	**1.22**	**0.98**	**0.23**			**0.46**
TEMPERATURE (^{0}C) – 2 m									
LSM1	50	9.12	9.03	4.46	3.05	0.82	14.2	15.1	0.87
LSM2	50	9.12	7.44	4.46	3.38	0.86	14.2	13.3	0.85
AVERAGE	**50**	**9.12**	**8.32**	**4.46**	**3.22**	**0.84**	**14.2**	**14.65**	**0.86**
RELATIVE HUMIDITY (%)									
LSM1	150	87.25	85.65	9.62	9.86	0.74	97.5	99.5	0.85
LSM2	150	87.25	93.75	9.62	8.80	0.78	97.5	100.0	0.78
AVERAGE	**150**	**87.25**	**89.70**	**9.62**	**9.23**	**0.76**	**97.5**	**99.8**	**0.82**

In Figure 8.21, modelled near-surface wind speed time series from MM5 for 2 LSM schemes (bulk LSM/run1 – green line, urban LSM/run2 – blue line) are compared with the observed wind (red line) obtained for three observations site: Coles Place (Figure 8.21a), Christchurch Airport (Figure

8.21b) and the UoC Geography roof (Figure 8.21c) over a 48-hour time period on 4-5 May 05 (winter 2005 episode 4). Figure 8.21 displays good agreement between modelled and ambient wind through all 48 hours of the forecast except the case of the UoC geography roof (on 5 May), when the roof observed wind compared with the same level exhibits lower values, as there is a different roughness between the campus building and open-space modelled wind for the same level (about 25 m). In the case of the Christchurch Airport site mast measurements were obtained.

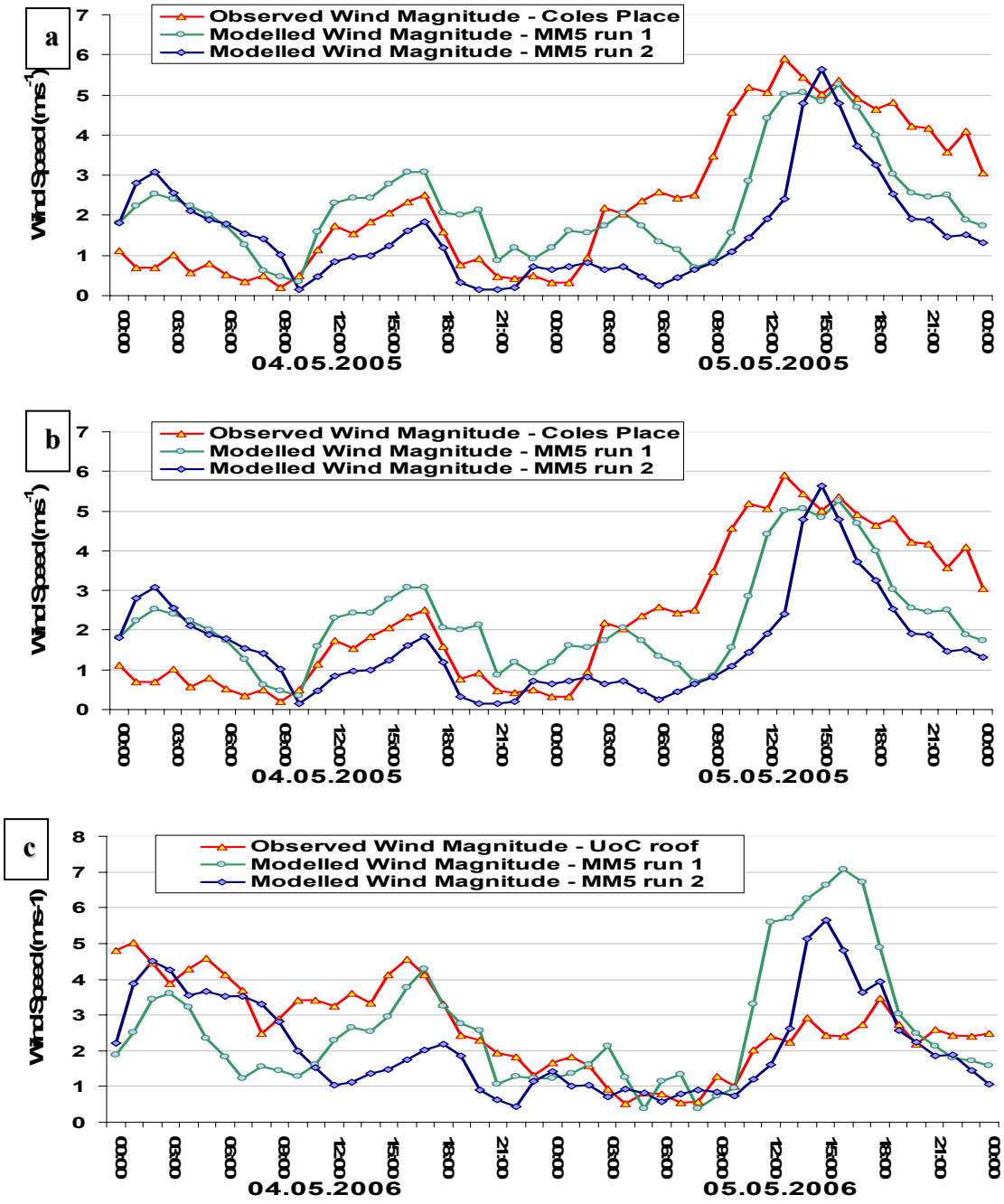

Figure 8.21 Modelled MM5-LSM1 (run1, green line) and MM5-LSM2 (run2, blue line) and observed (red line) near-surface wind speed (m s^{-1}) for episode 4, domain 4, from 00 NZST on 4 May 2005 to 00 NZST on 6 May 2005: a) Coles Place, b) Christchurch Airport, c) UoC Geography department roof.

In Figure 8.22, modelled wind direction time series for 2 LSM schemes (run1–green line, run2–blue line) are compared with the observed wind direction (red line) for Coles Place (Figure 8.22a), Christchurch Airport (Figure 8.22b), the UoC (Figure 8.22c) on 48 hours on 4-5 May 05 (episode 4).

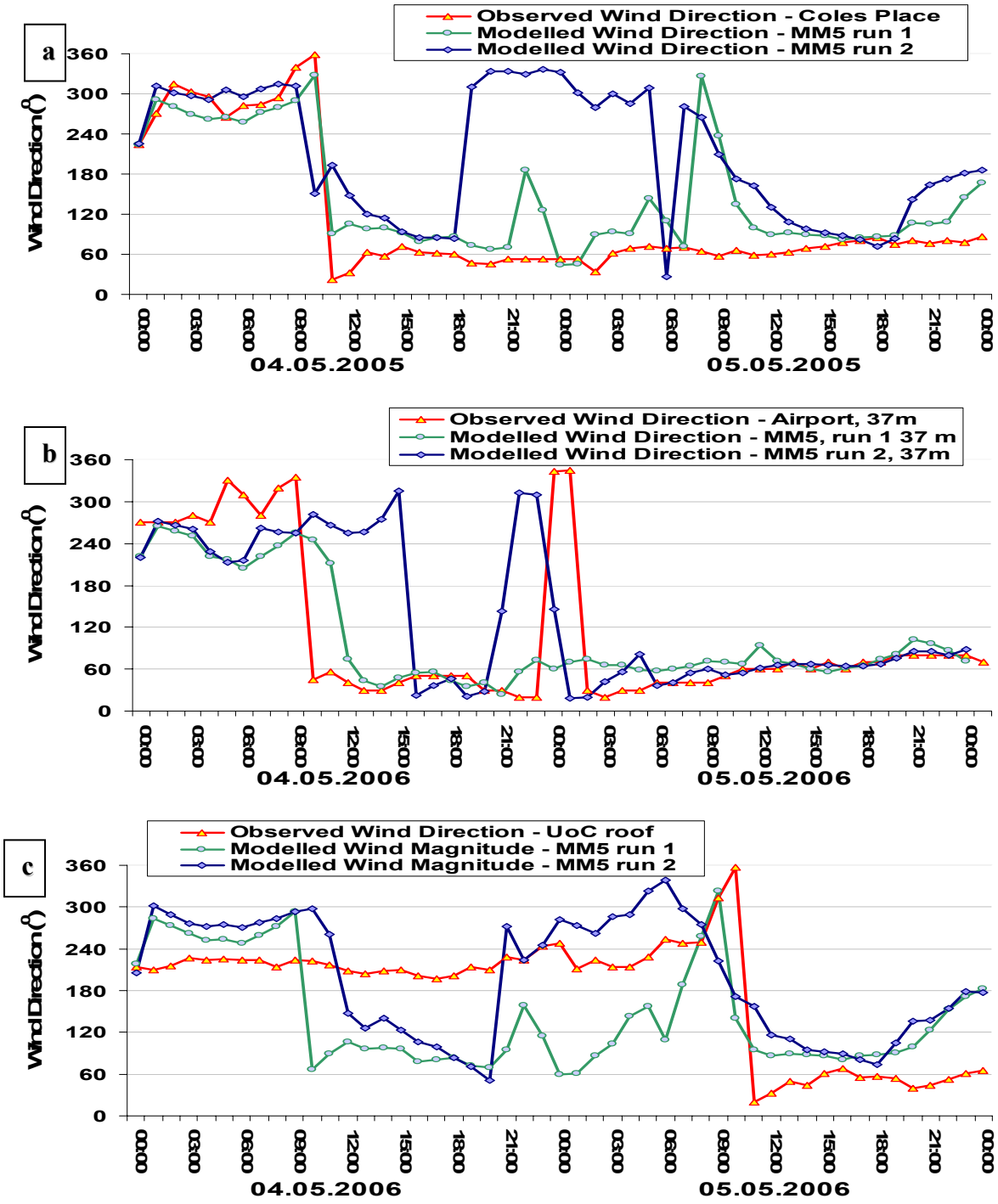

Figure 8.22 Modelled MM5-LSM1 (run1, green line) and MM5-LSM2 (run2, blue line) and observed (red line) near-surface wind direction (^{0}) for episode 4, domain 4, from 0000 NZST on 4 May 2005 to 0000 NZST on 6 May 2005: a) Coles Place, b) Christchurch Airport, c) UoC Geography department roof.

Figure 8.22 displays a good agreement between modelled and ambient wind time trends through all 48 hours and demonstrates a possibility of MM5 (LSM1 only) to catch day-night abrupt wind direction change in different Christchurch observation points. Figure 8.23 presents modelled near-surface temperature for MM5 2 LSM schemes (run1 – green line, run2 – blue line) and the observed temperature (red line) obtained at Coles Place (Figure 8.23a), Airport (Figure 8.23b) and the UoC (Figure 8.23c) over 4^{th}-5^{th} May 5 time period (episode 4). In Figure 8.23, modelled near-surface temperature (rural LSM, run1 – green line, urban LSM, run2 – blue line) is compared with the observed temperature (red line) obtained at Coles Place (Figure 8.23a), Christchurch Airport (Figure 8.23b) and the UoC (Figure 8.23c).

The agreement of all time-series is very high but the best one is found to be for the Airport mast (37 meters above ground level), and the worst for the UoC roof (roof micro-climate). Both LSM schemes underpredict nighttime temperature minimum on 4 June 2005. In Figure 8.24, modelled near-surface relative humidity (RH) for 2 LSM schemes (run1 – green line, run2 – blue line) is compared with the observed relative humidity (red line) obtained at Coles Place (Figure 8.24a), Christchurch Airport (Figure 8.24b), and the UoC Geography department roof (Figure 8.24c) over 48 hours period.

Time trends of the modelled RH principally follow the time trend of the observations for both LSM schemes, but (as was described before) urban LSM parameterisation exhibits over-estimation of the real RH and during night time tends toward saturation (100%).

General statistics consist of the histograms prepared for all winter 2005 7 episodes (3 observation sites), and includes MM5 output time series for bulk Land Surface Model only (used for histograms building). Figure 8.25 compares modelled (Figure 8.25a) and observed (Figure 8.25b) wind speed distribution and shows higher frequency of low wind speed occurrence in observations, and longer right tail (negative skewness) in modelled data that implies more cases with high wind speed.

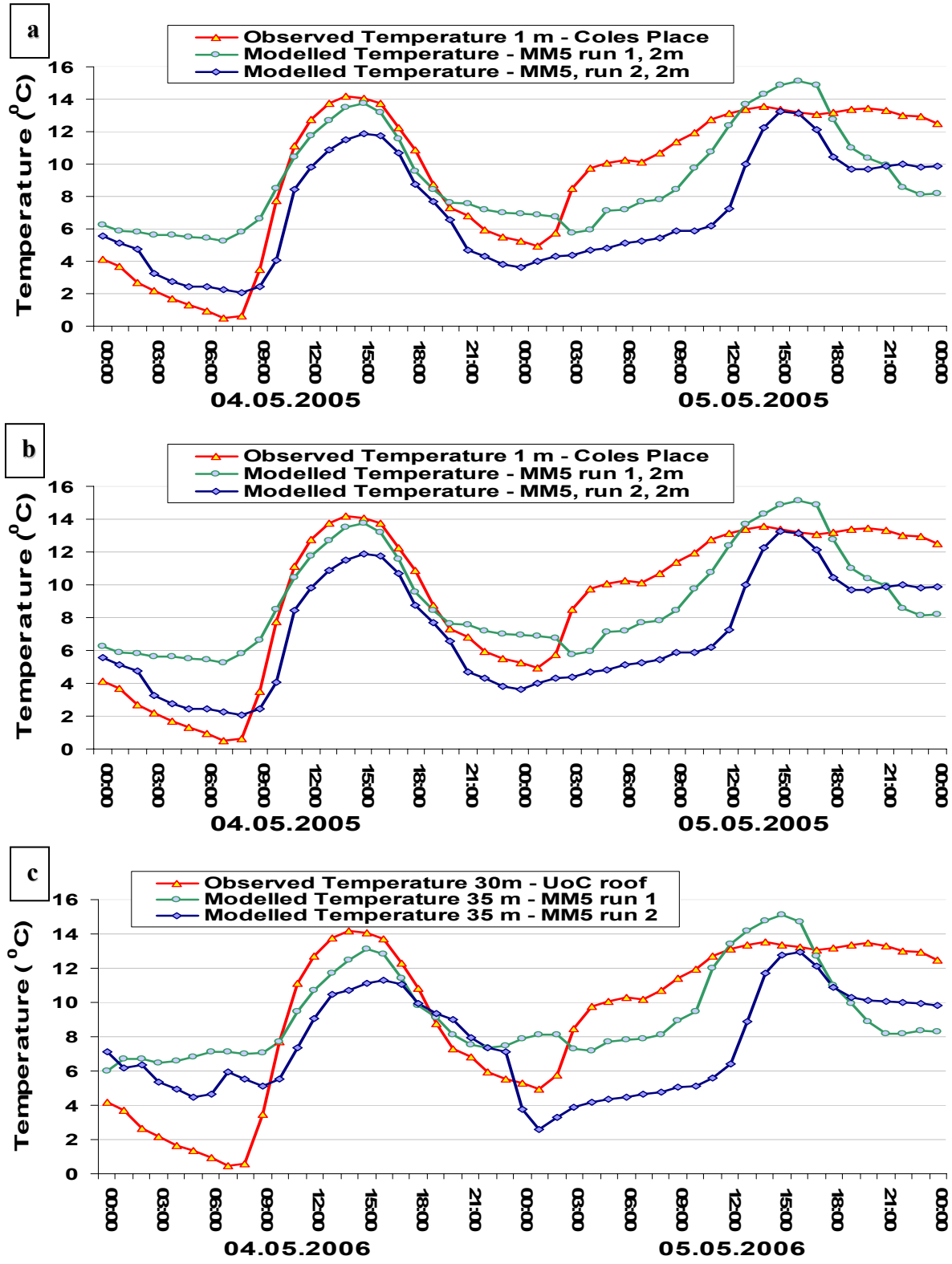

Figure 8.23 Modelled MM5-LSM1 (run1, green line) and MM5-LSM2 (run2, blue line) and observed (red line) near-surface temperature (^{0}C) for episode 4, domain 4, from 0000 NZST on 4 May 2005 to 0000 NZST on 6 May 2005: a) Coles Place, b) Christchurch Airport, c) UoC Geography department roof.

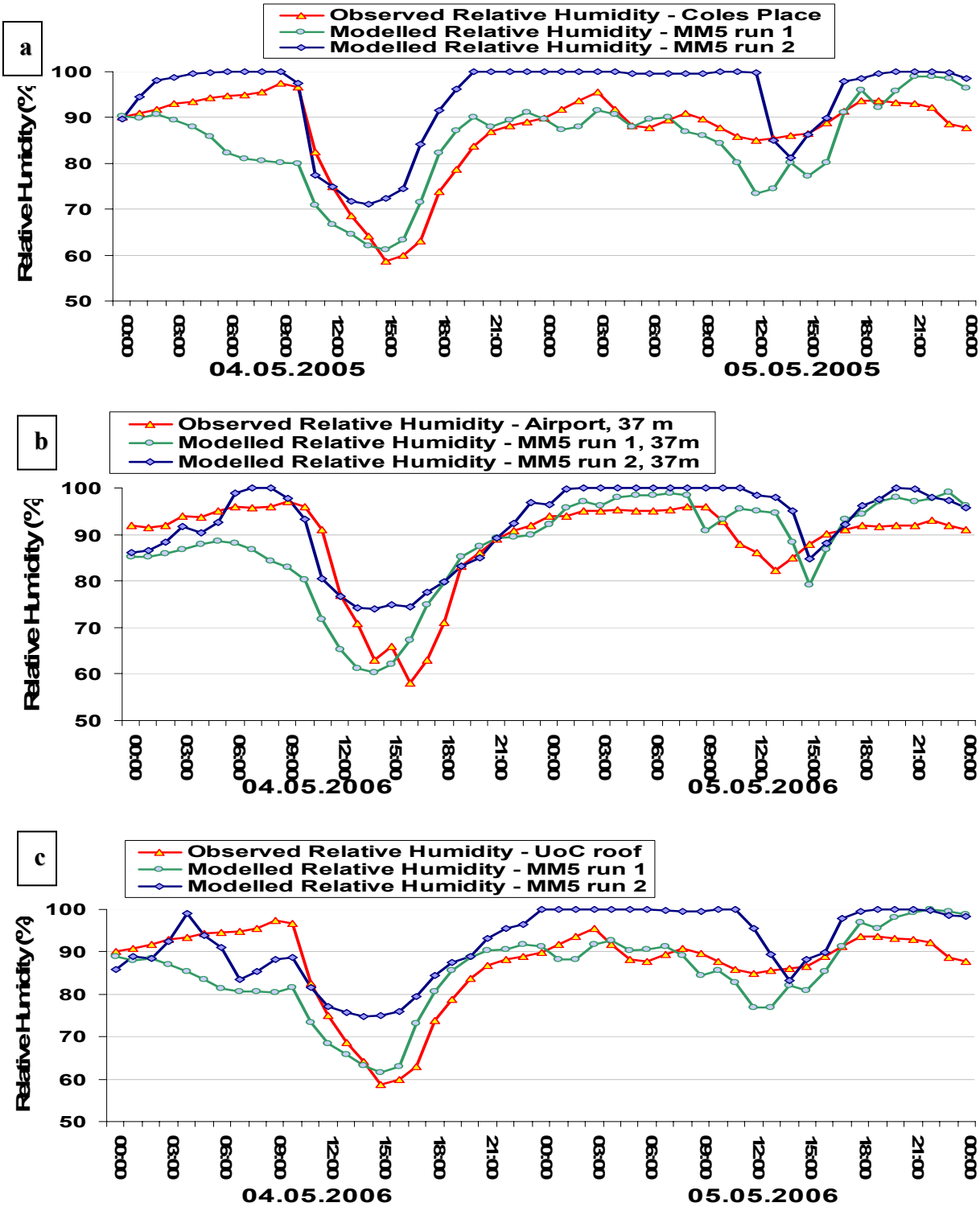

Figure 8.24 Modelled MM5-LSM1 (run1, green line) and MM5-LSM2 (run2, blue line) and observed (red line) near-surface relative humidity (%) for episode 4, domain 4, from 0000 NZST on 4 May 2005 to 0000 NZST on 6 May 2005: a) Coles Place, b) Christchurch Airport, c) UoC Geography department roof.

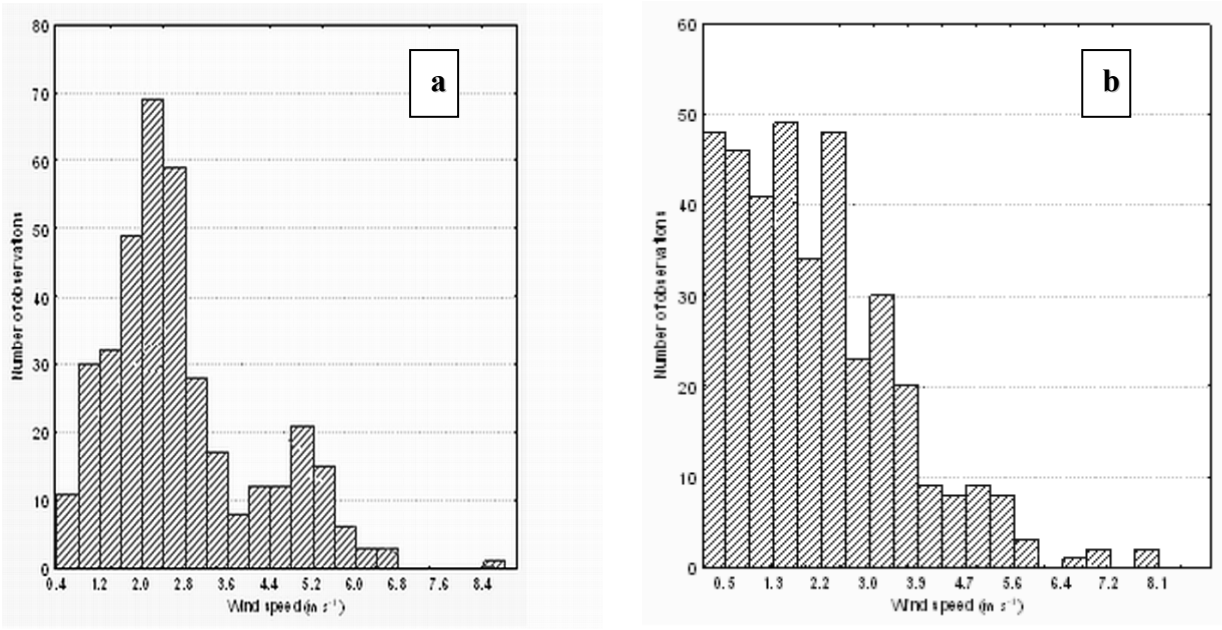

Figure 8.25 Histogram of the modelled wind speed (a) and observed wind speed (b) averaged over 7 winter 2005 pollution episodes for 3 observational sites (MM5 LSM1 only). Red curve represents adjusted normal distribution.

Figure 8.26 compares modelled (Figure 8.26a) and observed (Figure 8.26b) wind direction distribution and shows a good agreement (m s^{-1}) between modelled and observed data with a higher frequency of north-easterly and south-westerly winds (for both observations and so modelled winds) reflecting a dominance of the local air circulation in the near-surface layer.

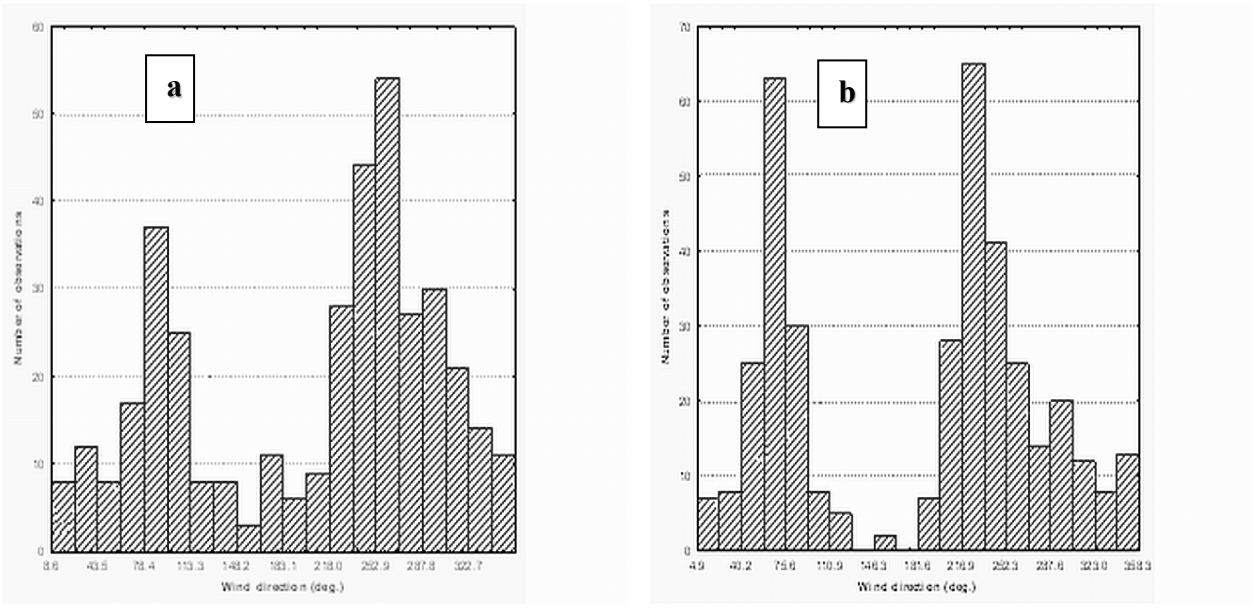

Figure 8.26 Histogram of the modelled wind direction (a) and observed wind direction (b) averaged over 7 winter 2005 pollution episodes for 3 observational sites (MM5 LSM1 only). Red curve represents adjusted normal distribution.

Figure 8.27 compares modelled 1-m (blue) and 10-m (red) temperature (Figure 8.27a) with observed 1-m (back slash) and 10-m (normal slash) temperature (Figure 8.27b). Figure 8.27 displays a satisfactory agreement between modelled and observed temperature (C^0) data. The consistency of the modelled 1-m temperature with the observed 1-m temperature distribution is better than for 10-m temperature, which suggests good representation of the long and short wave radiation balance and diffusion parameterisation for MM5 surface.

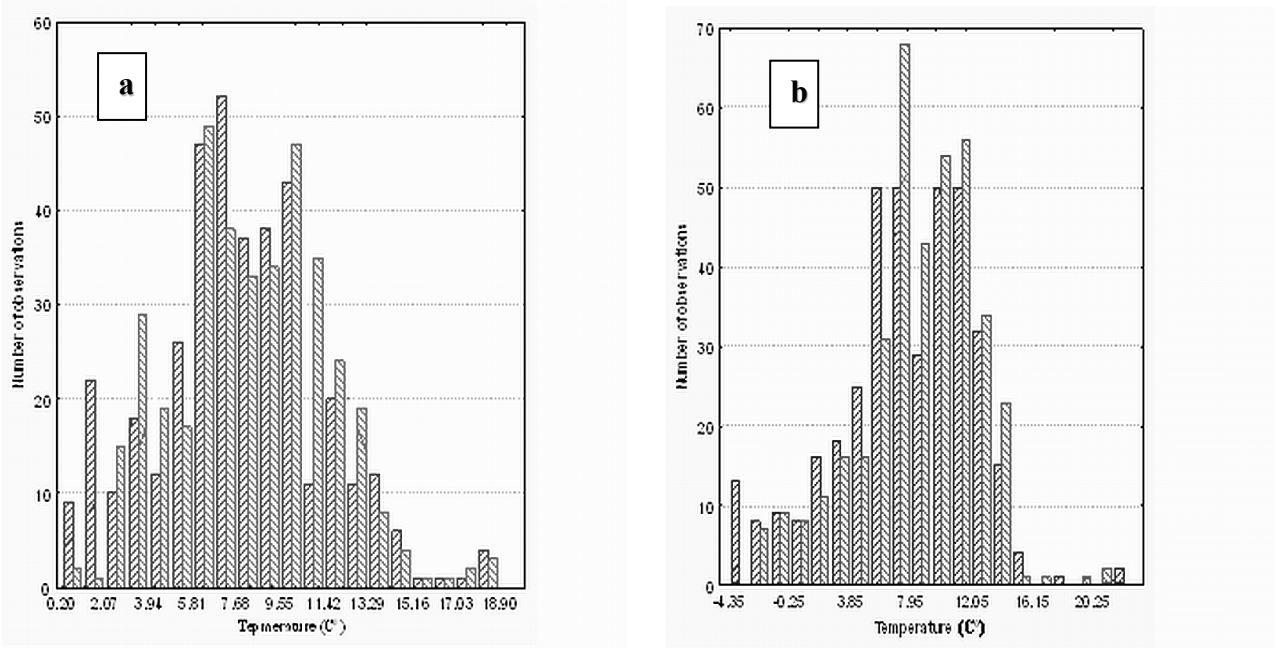

Figure 8.27 Histogram of the modelled 1-metre (blue) and 10-metre (red) temperature (a) and observed 1-metre (blue) and 10-metre (red) temperature (b) averaged over all 7 winter 2005 pollution episodes for 3 observational sites (MM5 LSM1 only). Red curve represents adjusted normal distribution. Red and blue curves correspondingly represent adjusted normal distribution for observed and modelled temperature.

Comparison of Figure 8.27a and Figure 8.27b for 10-m temperature shows some problems in near-surface sensible and latent heat flux parameterisation as the modelled average 10-m temperature has pronounced bi-modal distribution compared with a more close to a uni-modal distribution for observations. Also, modelled 1-m and 10-m temperature distributions have additional peaks at about 18 ^{0}C. The problem of LSM1 over-prediction of the day-time near-surface temperature maximum was described earlier (Table 8.1 and Table 8.3).

Figure 8.28 compares modelled 2-m relative humidity RH (Figure 8.28a) with observed 2-m relative humidity (Figure 8.28b) and exhibits quite reasonable agreement between modelled RH time series and observations. While ambient the RH distribution is uni-modal, the calculated RH

has a bi-modal distribution with the second mode in the range of 55-70% and lower frequencies of high night-time RH, which suggests under-prediction by the LSM1 scheme of the real RH values.

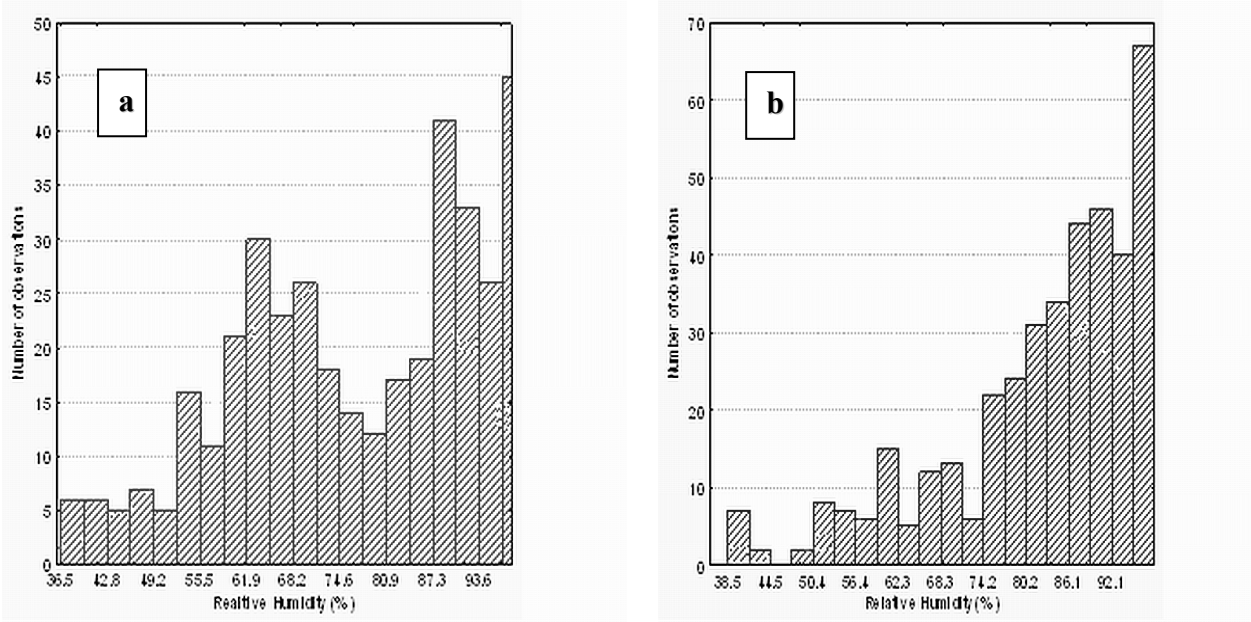

Figure 8.28 Histogram of the modelled 2-meter relative humidity (a) and observed 2-meter relative humidity (b) averaged over all 7 winter 2005 pollution episodes for 3 observational sites (MM5 LSM1 only). Red curve represents adjusted normal distribution.

A secondary peak of modelled RH below 69% (a critical point for the process of secondary inorganic soluble ions production) initially suggests under-prediction of secondary PM (especially nitrate ammonium) during evening - morning time that will be examined in the next 2 Chapters. In general for all 7 winter 2005 episodes it is considered that the near-surface modelled meteorology is adequate for use in CAMx4 for evaluation of the spatial and temporal variations in the aerosol dispersion.

8.4 Summary

A careful evaluation of the reproduction of local-scale air circulation by MM5 for two LSM schemes has shown the ability of the limited-area model to reproduce the main features of the air circulation over the complex terrain of the Christchurch area. Inter-comparison of the bulk and urban land-surface parameterisation schemes did not identify the superiority of one of them against the other one, as both LSM models have their advantages and disadvantages. This conclusion allows both schemes to be used in the process of meteorological data preparation for CAMx4 experiments.

Chapter 9: Scenarios evaluation - winter 2005

Chemical composition of the outdoor total (PM_{10}), fine ($PM_{2.5}$) and coarse (PM_{10}-$PM_{2.5}$) fractions of the aerosol obtained using complex and expensive equipment is an essential part of contemporary studies of the aerosol chemistry in different geographical areas (Ho et al., 2003; Dan et al., 2004; Chow et al., 2005; Duan et al., 2006). Improved understanding of the origin and chemical composition of ambient levels of particulate material (PM) in the air has been gained in big air pollution field experiments (Spronken-Smith et al., 2001; Kossmann, Sturman, 2002; Baertch-Ritter et al., 2003; Arnold et al., 2004; Minvielle et al., 2004), and local pollution studies (Putaud et al., 2004; Molnar et al., 2005; Scott 2005; Senaratne et al., 2005; Glasius et al., 2006), which usually involve detailed investigation of the chemical composition of PM (Senaratne 2003; Scott and Gunatilaka 2004; Sun et al., 2004; Borrego et al., 2005; Senaratne et al., 2005; Wu et al., 2006). Such experiments require highly technical field sampling and laboratory analysis, which are time-consuming and expensive (Fung et al., 2002; Chow et al., 2005). Chemical composition of PM obtained from field studies is usually used to identify the most important sources of natural and anthropogenic PM. The knowledge of the observed PM chemical composition is actively applied in the numerical modelling of air pollution dispersion based on gridded, line or point input emissions (Zannetti 1990; Arnold et al., 2003; Titov et al., 2005; Zawar-Reza et al., 2006). Such models are used to predict spatial-temporal accumulation and re-distribution of aerosols (Borrego et al., 2003; Wang, Shooter, 2005; Wilson, Zawar-Reza, 2006). The uncertainties associated with winter PM chemical composition created a problem of defining the chemical split of the input gridded emissions used in the chemical model CAMx4.2 (ENVIRON, 2005) to study winter pollution in the Christchurch area (Titov et al., 2005). The absence of accurate knowledge of winter PM composition has stimulated a series of experiments with the application of the MM5-CAMx4 numerical modelling system and development of a new method of evaluating several different chemical scenarios. This chapter aims to obtain the chemical composition of modelled fine ($PM_{2.5}$) and total (PM_{10}) aerosol that provides numerically predicted PM concentrations that are closest to the measured ones.

9.1 Co-located $PM_{2.5}$ and PM_{10} observations – Coles Place

Seven episodes for the time period 2 May - 10 June 2005 were evaluated by the MM5-CAMx4.2 numerical modelling system. These episodes were selected from data obtained by the inner city

observation site working routinely. Seven winter 2005 episodes are considered to have the most appropriate meteorological conditions and a diversity of observed $PM_{2.5}$ (PM_{10}) peak values at the Christchurch observation site in Coles Place (marked by a dot in Figure 9.1).

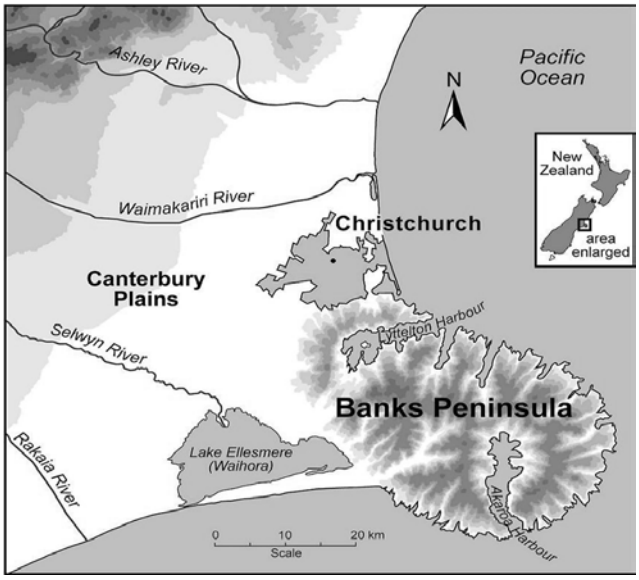

Figure 9.1 Position of Coles Place inner city (residential area) observation site.

As was described in Chapter 4 (section 4.2), both $PM_{2.5}$ and PM_{10} were measured at Coles Place site using two TEOM samplers, fitted with fine and total PM sampling heads (Aberkane, 2004). However, for our researches only winter 2005 May-July fine aerosol observations were available (from ECan). In any way for May-June 2005 time period measurements of the fine and total aerosol done by co-located TEOM samplers were obtained, and in Figure 9.2 are presented hourly averaged values of $PM_{2.5}$ (red line) and PM_{10} (blue line) concentrations ($\mu g\ m^{-3}$) for period 01 May–10 June 2005. This time period included all 7 episodes (marked by black arrows) that were investigated using the MM5-CAMx4 numerical modelling system for different aerosol chemical scenarios.

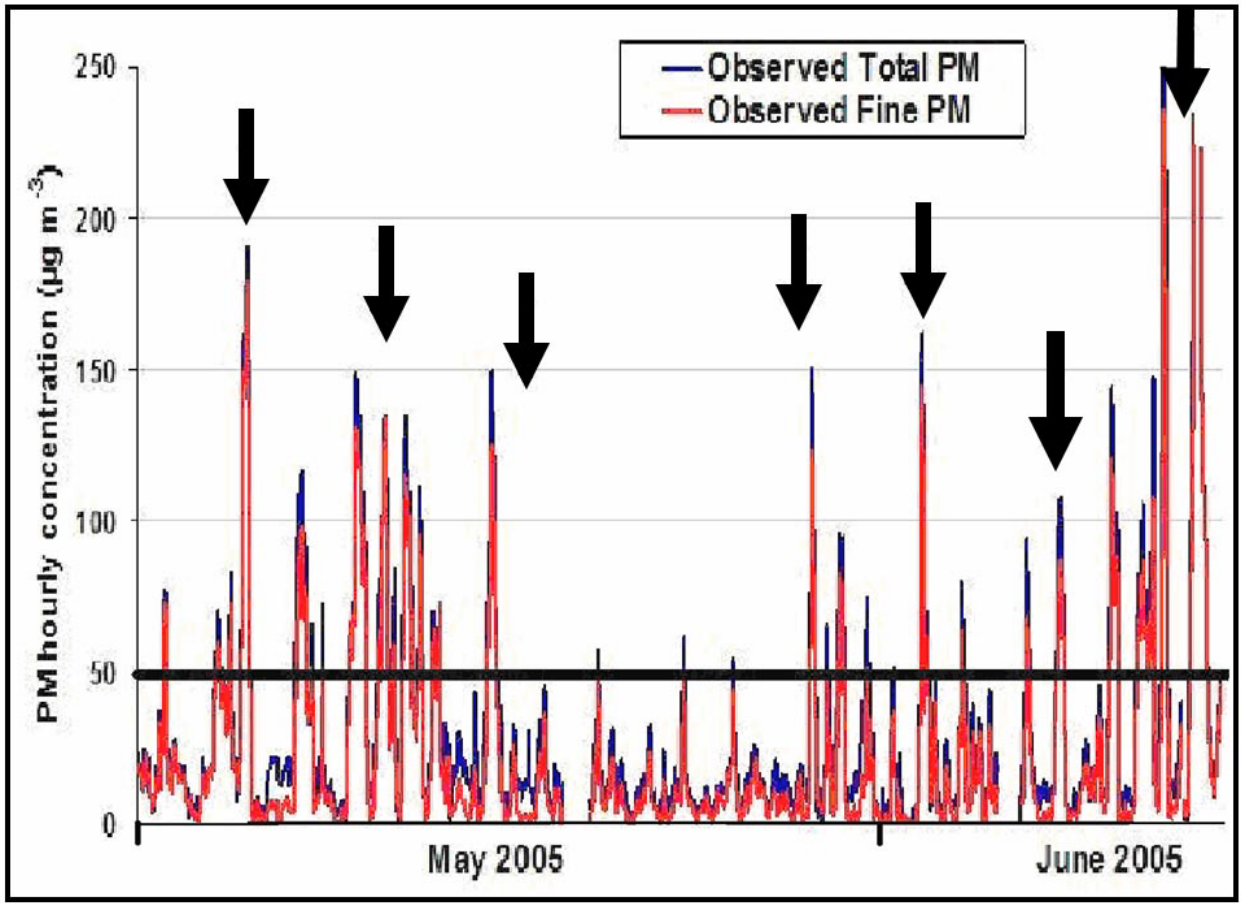

Figure 9.2 Observed hourly averaged $PM_{2.5}$ (red line) and PM_{10} (blue line) concentrations (µg m^{-3}) for the period 1 May – 10 June 2005. The horizontal black line shows WHO 24-hour PM_{10} concentration limit.

It is important to stress that $PM_{2.5}$ measurements were stopped in August 2005 because of faulty results received from the TEOM co-located samplers. For example, $PM_{2.5}$ concentrations in July-August 2005 were higher than PM_{10} concentrations for evening and morning peaks of aerosol pollution. The ambient PM data were corrected with application of Filter Dynamic Measurements System (FDMS, from protocol) on loss of the semi-volatile organic matter (SVOM) in the TEOM's inlet that is heated to 40-50 ^{0}C to remove moisture particles. Still a certain loss of PM_{10} is observed from output fine and total PM time trends (Figure 9.2). Ammonium nitrate semi-volatile matter (SVM, Favez et al., 2007) definitely was lost from PM_{10} total mass (especially for night-morning PM peak concentrations) as FDMS presumably was calibrated on SVOM only. This could be a possible reason of PM_{10} underestimation (to compare with $PM_{2.5}$), especially in the second half of winter 2005. Basic statistics indicates the 3-month (May-July) average aerosol concentrations to be about 34.05 and 40.45 µg m^{-3} for $PM_{2.5}$ and PM_{10} correspondingly, and the 3-month mean ratio between fine and total PM being close to 0.84 ($PM_{2.5}$ /PM_{10} *100 =84%).

9.2 Statistical background of the method

Two co-located routine measurements of fine and total PM using 2 different TEOM samplers for winter 2005 have created two PM data series that were obtained independently of each other by two separate instruments. The optimal way to correlate two sequences independently measured with one variable ($PM_{2.5}$) being a fundamental part of a second variable (PM_{10}) is to use linear regression between total and fine PM (Wilks, 2006). Linear regression and its parameters (the intercept and regression coefficient) could be compared with single moment statistics like Pearson correlation coefficient PCC) and index of agreement (IOA). PCC and IOA are considered to be unstable statistics (Wilks, 2006), as PCC could depend on a single big modelled-observed value that will increase the mean value, and IOA depends on modelled-observed perturbations (expressed in the standard deviation) agreement only and doesn't include directly mean tendency.

Linear regression is more stable in response to single value fluctuations (Wilks, 2006), and describes a statistical relationship between two independently obtained time series (like PM_{10} and $PM_{2.5}$), and is simple to interpret in regarding to physical processes. The stability of linear regression is demonstrated in Figure 9.3 where Figure 9.3a presents linear regression between observed total and fine PM (hourly ambient data) calculated for time period 01 May – 10 June 2005 (40 days of winter 2005). To check the stability of the PM linear regression 2 big values of PM_{10} (and respectively 2 small values of $PM_{2.5}$) were added to the linear regression and the result is plotted in Figure 9.3b. These values can imitate possible observational error, or a possible faulty modelled output as a result of the numerical-chemical instability of the MM5-CAMx4 numerical system. Results were obtained for $PM_{10} > 5$ μg m^{-3} as values of ambient fine aerosol are usually very close to zero when total PM_{10} is lower then 5 μg m^{-3}, or generates negative values of $PM_{2.5}$ are generated as a result of instrumental error. This 5 μg m^{-3} threshold is considered to represent PM_{10} background concentrations being an average minimum of the total aerosol for 24-hour observations. For PM_{10}-$PM_{2.5}$ ambient data linear regression (Figure 9.3a) we have $PM_{2.5} = -4.8287 + 0.9149*PM_{10}$; and for PM linear regression with two error points (Figure 9.3b) we have $PM_{2.5} = -4.2172 + 0.8864*PM_{10}$.

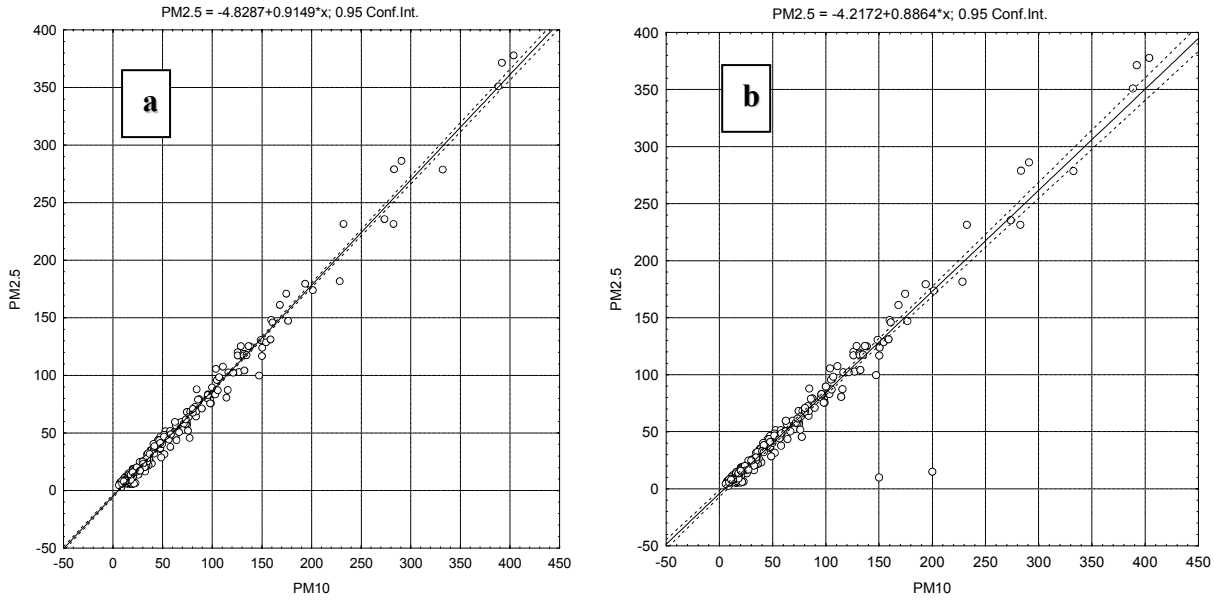

Figure 9.3 Observed hourly linear regression between PM_{10} and $PM_{2.5}$ (μg m^{-3}) for the period 1 May–10 June 2005 for PM_{10} > 5 μg m^{-3}: a) ambient observations; b) observations plus 2 noise points (PM_{10}=150 μg m^{-3} - $PM_{2.5}$=5 μg m^{-3}; PM_{10}=200 μg m^{-3} - $PM_{2.5}$=5 μg m^{-3}).

The difference for correlation coefficient is less than 3% and for intercept is about 10% that speaks about statistical stability of the linear regression and a possibility to produce reliable 2-moment statistics operating potentially unstable numerical chemical processes. Linear correlation method that includes two independently measured ambient variables in one regression equation is a wide-spread one, and can be found in previous work dedicated to ambient air aerosol pollution (Arya, 1999; Lu, 2003; Liu et al., 2004; Querol et al., 2004; Zhang et al., 2006).

9.3 Optimal temporal chemical scenario

As was mentioned before serious discrepancies associated with winter PM chemical composition has created the problem of defining the chemical split of the input gridded emissions used in the chemical model CAMx4 for more accurate studies of the winter aerosol pollution in the Christchurch area. These uncertainties about winter PM composition were overcome in the series of experiments with the application of the MM5-CAMx4 numerical modelling system and 4 $PM_{2.5}$ chemical scenarios evaluated over 7 chosen winter 2005 episodes. The $PM_{2.5}$ chemical scenarios are based on prior winter PM studies for the Christchurch area as well as the ambient aerosol chemical content obtained in other countries with similar winter pollution problems.

High winter PM concentrations in the Christchurch area are basically a result of local scale activity only, and this is apparent from the application of Lagrangian single particle back-trajectory model

HYSPLIT to all the winter 2005 episodes (HYSPLIT 4, Draxler, Hess, 1998). In Figure 9.4 24-hour back-trajectories (for 500, 1000 and 1500 meters start levels) are presented for 4 winter 2005 episodes (episode 4 HYSPLIT 4 trajectories are also presented in Figure 8.4).

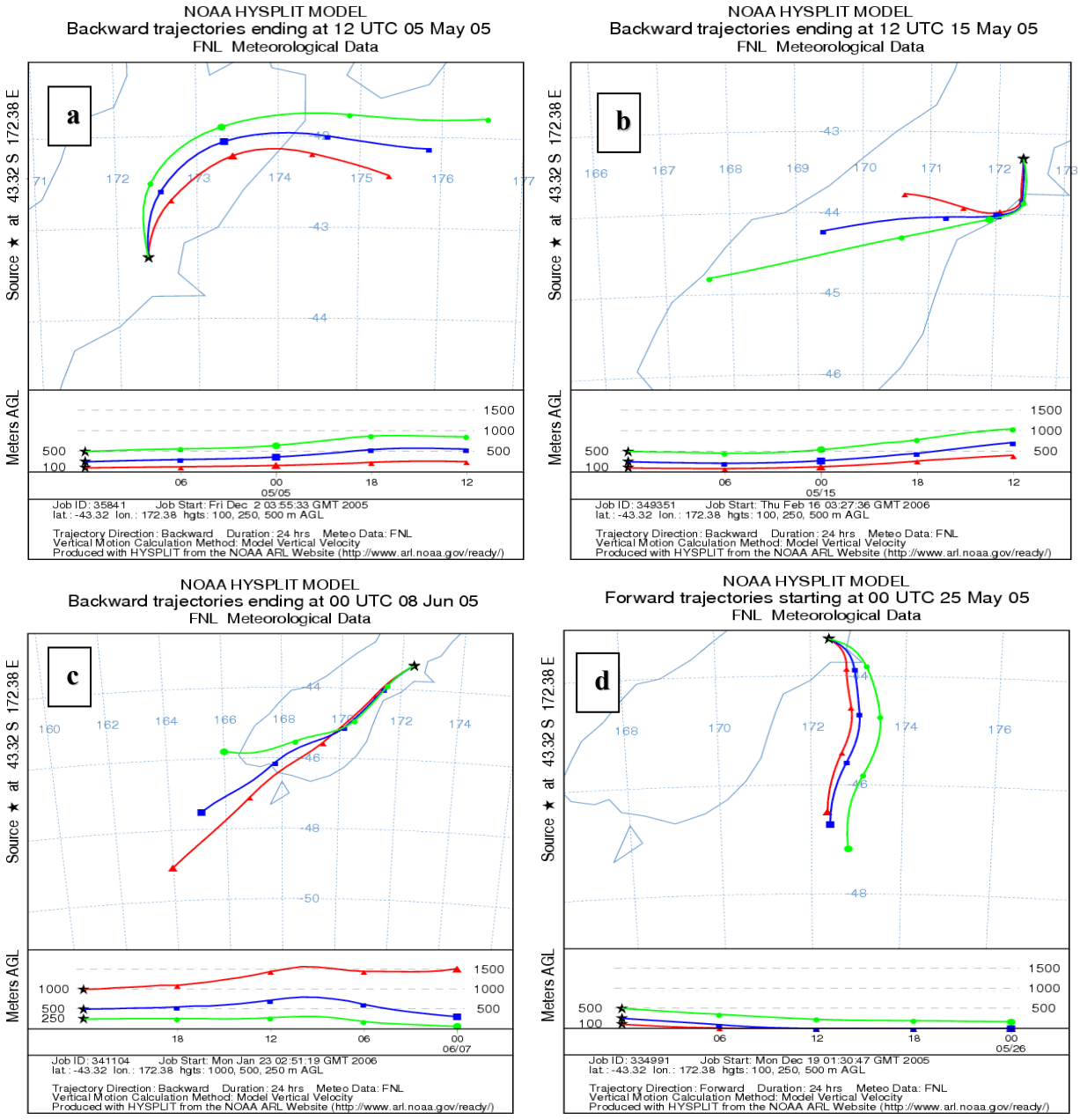

Figure 9.4 24-hour back-trajectories ending in the Christchurch area calculated from HYSPLIT 4 for 500, 1000 and 1500 m levels for: a) at 0000 NZST on 06 May 2005 – episode 4; b) 0000 NZST on 16 May 2005 – episode 2; c) 1200 NZST on 08 June 2005 – episode 3; d) 1200 NZST on 25 May 2005 – episode 5.

Air circulation presents 4 different wind directions for 4 episodes (episode 1 – Figure 9.4a, episode 4 – Figure 9.4b, episode 3 – Figure 9.4c, and episode 5 – Figure 9.4d), but because of anticyclonic synoptic scale circulation the speed of air circulation is low for all 4 episodes. Mostly the near-surface air has passed over the ocean or over cold southern part of the Southern Island where there

is no significant anthropogenic activity (especially during winter time) or serious biological (natural) emission sources.

An example of 72-hour averaged wind roses for episode 4 is presented in Figure 9.5 for observed (Figure 9.5a) and modelled (Figure 9.5b) near-surface (10 m) air circulation over the Coles Place observation site.

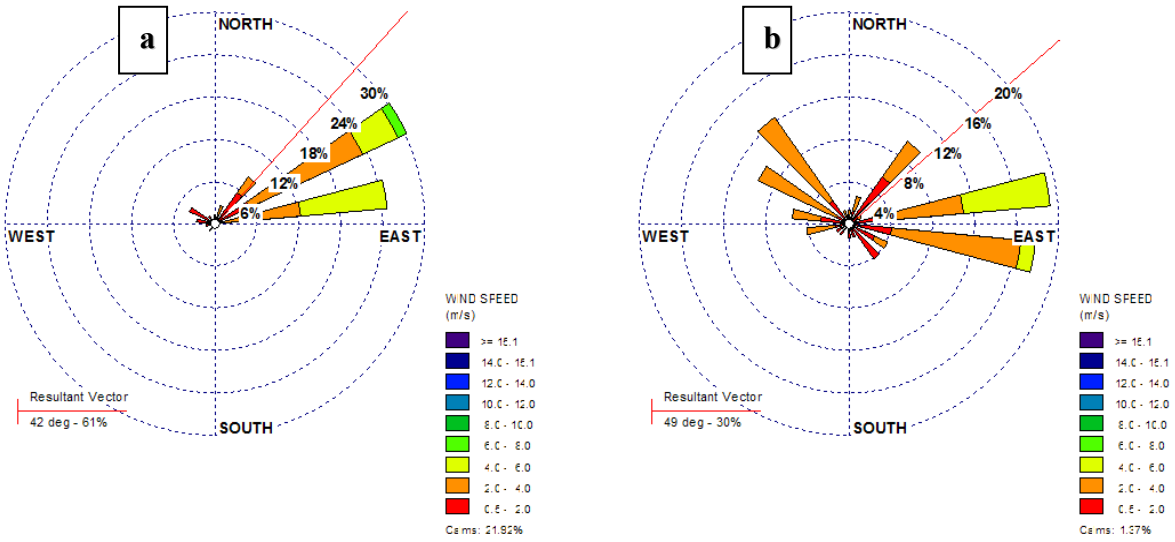

Figure 9.5 Near-surface (10m) wind for Coles Place site averaged over time interval 00 NZST 04 May 2005 – 00 NZST 07 May 2005 for the Coles Place site: a) observations; b) MM5 domain 4 output.

The dominance of the local on-shore winds with low speed is obvious, especially from the observations results. The evidence of the night drainage winds is masked in the inner city observations (at last for the lowest several meters) as a result of the surrounding urban obstacles, but more pronounced in MM5 modelled output without local urban topography (Figure 8.22).

9.3.1 Principal chemical components

The contribution of the basic chemical components to $PM_{2.5}$ for four different chemical scenarios is presented in Table 9.1 (see List of acronyms and abbreviations for all abbreviations). It should be mentioned that the distribution of the chemical components for all 4 scenarios is an approximate one, although each scenario reflects the dominance of the near-surface processes described later. Chemical components of PM_{10} are obtained by re-calculating $PM_{2.5}$ values using a ratio (R_{PM}) between fine and total aerosol ($PM_{2.5}/PM_{10}$) equal to 0.84 (relying on the basic statistics from section 9.1) for all species except EC (R_{PM} = 0.95) and crustal elements (R_{PM} = 0.65). The output time series of $PM_{2.5}$ (PM_{10}) for different scenarios are usually highly correlated for the closest

scenario pairs (e.g. 1-2, 2-3, 3-4), but the Normalized Coefficient of Divergence (NCD, Pinto et al., 2004) has the range 0.20-0.48 for $PM_{2.5}$ (and PM_{10}) between different chemical scenarios for the same pollution episode.

Table 9.1 The contribution of the basic chemical components (in %) to $PM_{2.5}$ - 4 chemical scenarios.

Chemical split (%)	**TC**	**TOC**	**POC**	**SOA**	**EC**	**PSO_4+PNO_3+PNH_4 +PCl+Na+K**	**FCRS + FPRM (CCRS + CPRM)**
Scenario 1 (control study)	92	52	40	12	40	8	0
Scenario 2 (sensitivity scenario 1)	80	60	35	25	20	20	0
Scenario 3 (sensitivity scenario 2)	60	45	25	20	15	30	10
Scenario 4 (sensitivity scenario 3)	40	32	20	12	8	50	10

A 2-level version of CAMx4.2 (as less computer time consuming) was chosen for prediction of the spatial and temporal variation of concentrations of $PM_{2.5}$ (PM_{10}), although results from a 10-level version were used for comparison. The top level in the 2-level model reached a height of 75–80 m, which is close to the top of near-surface nocturnal inversion layer that usually traps about 90% of PM (McKendry et al., 2004). The difference between 2-level and 10-level CAMx4.2 versions is evident for daytime only, when a coefficient of vertical diffusion K_v is higher for the 10-level model, and vertical movement is higher for the 10-level model by definition. More active vertical diffusion leads to more active dilution of fine PM and slightly lower $PM_{2.5}$ concentrations. However, the difference between 2- and 10-level versions is negligible for the main evening and secondary morning PM peaks, when the calculated PBL height for all episodes is lower than 75-80 metres.

Scenario 1 – control

For Scenario 1 (control scenario, Titov et al., 2007) the ratio POC/EC is close to 1 (Scott 2005), emulating the fossil fuel combustion process with a burner efficiency level predominantly higher than 60% as in modern domestic burners, industrial boilers and petrol-diesel engine ignition chambers (Schmid et al., 2001; Fung et al., 2002). Total contribution of primary carbon to $PM_{2.5}$ for Scenario 1 is more than 90% (Table 9.1). Secondary Organic Aerosol groups (SOA1-4) are added to minimize chemical instability of CAMx4.2. SOA is a compulsory species of the aerosol chemistry in CAMx4 and is bound with 4 groups of condensable gases (CG1-4 - ENVIRON, 2005) allowing secondary pollutants to function between gaseous and solid modes depending on the ambient air temperature and relative humidity. However, secondary organic aerosol makes no serious contribution to $PM_{2.5}$ in the control scenario compared with primary carbon. The amount of soluble inorganic ions is minimal and equal to 8%: PSO_4+PNO_3+PNH_4 = 6%, and Na+K = 2%. Mineral dust, primary and crustal elements are not included in Scenario 1 (Table 9.1), which means that for Scenario 1 (control scenario) all 7 winter 2005 episodes are considered to have very low winds in the vicinity.

The purpose of the control scenario is to validate the photochemical model CAMx4.2 when primary carbonaceous species dominate $PM_{2.5}$ input emissions, as the control scenario corresponds to conditions of the chemical stability during CAMx4 evaluation (Yarwood et al., 2004). Such aerosol chemical content is most appropriate for laboratory petrol-diesel engine exhaust studies or for aerosol samples from big roads with heavy traffic (Schmid et al., 2001). The local scale weather for Scenario 1 is characterized as a morning strong near-surface temperature inversion breakdown with low near-surface temperature and downslope drainage winds from the Port Hills and Canterbury Plains. Usually in this case peak PM concentrations are attained in the early morning at 7-8 am, but smog is observable for a short time period because of a rapid erosion of the near-surface temperature inversion.

Input gridded aerosol emissions were split according to Scenario 1 and all 7 winter 2005 episodes were evaluated with application of the MM5-CAMx4.2 numerical modelling system. Statistics for 7 episodes (at Coles Place) including the total number of cases, mean absolute error (MAE), correlation and power (correlation in power 2) coefficients for fine and total PM for bulk and urban LSM schemes are shown in Table 9.2.

Table 9.2 Number of Cases (NC), Mean Absolute Error (MAE), Pearson Correlation Coefficient (PCC) and Power Correlation Coefficient (Power CC), for 7 episodes, Scenario 1, fine and total PM, bulk and urban MM5 Land-Surface Model (LSM).

Modelled PM	NC	MAE	PCC	Power CC
$PM_{2.5}$ – bulk MM5 LSM	408	8.55	0.64	0.41
PM_{10} – bulk MM5 LSM	408	10.34	0.62	0.38
$PM_{2.5}$ – urban MM5 LSM	408	11.00	0.63	0.40
PM_{10} – urban MM5 LSM	408	12.15	0.63	0.39

Figure 9.6 shows predicted PM_{10} and $PM_{2.5}$ concentration time series for episode 4 separately for bulk (per.4–green lines) and urban (per.4_1–blue lines) MM5 LSM obtained for Scenario 1.

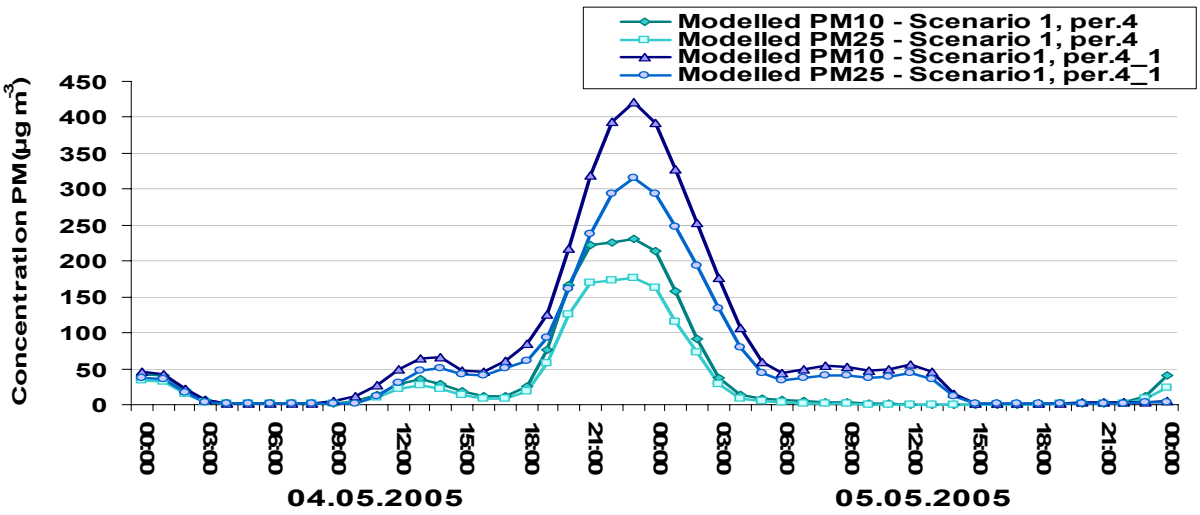

Figure 9.6 Modelled PM_{10} (dark) and $PM_{2.5}$ (light) concentrations (µg m^{-3}) for bulk (green) and urban (blue) LSM schemes, chemical Scenario 1, 00 NZST 04 May – 00 NZST 06 May 2005 (episode 4, 48 hours, Coles Place).

It is important to stress that Scenario 1 is stable through all stages of chemical simulations and has no chemical instability in relation to calculated high relative humidity and low temperature values. This is expected as Scenario 1 (control scenario) consists of 90% of primary aerosol with minimal secondary aerosol partitioning. Scenario 1 is numerically unstable for high concentrations of PM (as shown below).

Scenario 2 – domestic

The major input from residential heating to $PM_{2.5}$ chemical content is expected in Scenario 2 (domestic scenario), or sensitivity Scenario1 (Scott, 2005, Glasius et al., 2006). Scenario 2 approximates the process of fossil fuel combustion with a burner efficiency level lower than 60% (with a modelled ratio of TOC/EC equal to 3, Chow et al., 2005), and includes the active process of SOA formation from condensable gases (CG) during cold nights (Table 9.1). A burning process

with an efficiency level lower than 60% is characteristic of the old-fashion open-fires and log-burners. Such burners dominate in the residential area of Christchurch. The amount of soluble inorganic ions is increased to 20% (after Scott, 2005): PSO_4+PNO_3+PNH_4 = 16%, and Na+K = 4%. As in Scenario 1, mineral dust and crustal elements are not included in Scenario 2 (Table 9.1), so once again for Scenario 2 (domestic scenario) all 7 winter 2005 episodes are considered to have very low near-surface wind speed.

It should be mentioned that even for low near-surface wind (< 2.0 m s^{-1}) dust re-suspension could add up to 10-15% of the $PM_{2.5}$ mass, but in the case of the Christchurch night time aerosol concentration peak (between 10pm-2am) this is unlikely (at least in winter during working days) as transport activity in the city after 8 pm drops almost to zero. The local scale weather conditions for Scenario 2 could be described as a night-time strong near-surface temperature inversion with very low temperatures, clear sky and calm winds. Usually in this case, peak (or sometimes double peak) PM concentration is reached between 10pm and 2 am, and aerosol smog is visually easily observable for 4-5 hours.

Input gridded aerosol emissions were split according to Scenario 2, and all 7 winter 2005 episodes were evaluated with application of the MM5-CAMx4.2 numerical modelling system. Statistics for 7 episodes (at Coles Place) including the total number of cases, mean absolute error (MAE), correlation (r) and power (r^2) coefficients for fine and total PM for bulk and urban LSM schemes is shown in Table 9.3.

Table 9.3 Number of Cases (NC), Mean Absolute Error (MAE), Pearson Correlation Coefficient (PCC) and Power Correlation Coefficient (Power CC), for 7 episodes, Scenario 2, fine and total PM, bulk and urban MM5 Land-Surface Model (LSM).

Modelled PM	NN	MAE	PCC	Power CC
$PM_{2.5}$ – bulk MM5 LSM	408	6.52	0.58	0.35
PM_{10} – bulk MM5 LSM	408	6.05	0.58	0.35
$PM_{2.5}$ – urban MM5 LSM	408	13.25	0.64	0.41
PM_{10} – urban MM5 LSM	408	10.15	0.62	0.38

Figure 9.7 shows predicted PM_{10} and $PM_{2.5}$ concentration time series for episode 4 separately for bulk (per.4–green lines) and urban (per.4_1–blue lines) MM5 LSM obtained for Scenario 2.

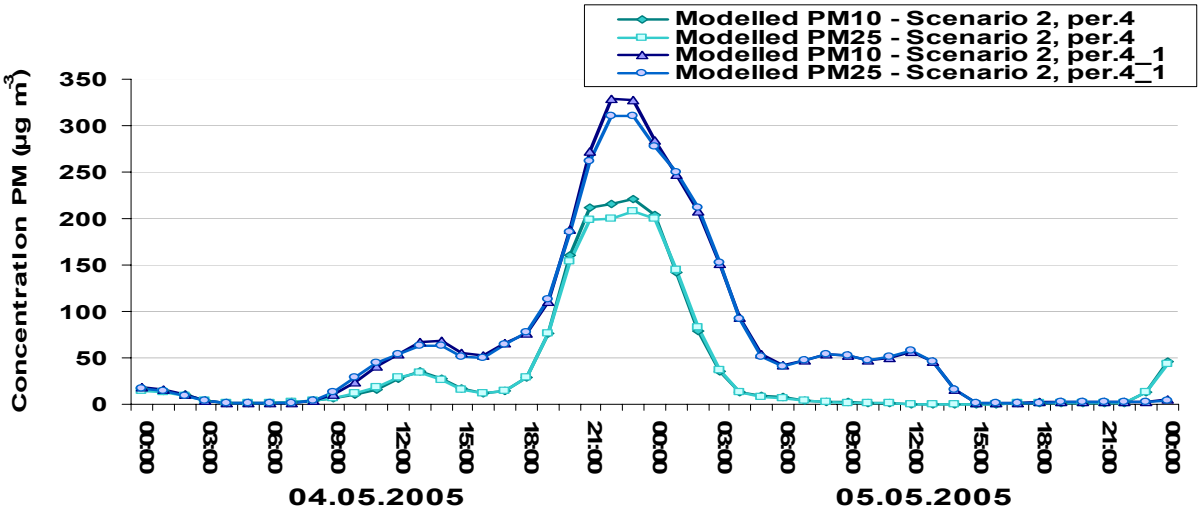

Figure 9.7 Modelled PM_{10} (dark) and $PM_{2.5}$ (light) concentrations (µg m^{-3}) for bulk (green) and urban (blue) LSM schemes, chemical Scenario 2, 00 NZST 04 May – 00 NZST 06 May 2005 (episode 4, 48 hours, Coles Place site).

Scenario 2 is numerically nearly stable one, but fine PM concentrations sometimes can be higher then total PM in after night-time peak as a result of CAMx4 chemical numerical instability. Scenario 2 didn't show any chemical instability to low temperatures and high values of near-surface relative humidity.

Scenario 3 – domestic and transport

Scenario 3 (domestic and transport scenario - sensitivity Scenario 2) is based on the studies of Senaratne for Christchurch (Senaratne et al., 2003), and Hueglin et al. (2005) of winter aerosol pollution in alpine towns of Switzerland. The ratio TOC/EC is equal to 3, as for Scenario 2, but the amount of TC in $PM_{2.5}$ is decreased to 60%. The level of soluble inorganic ions (especially nitrates and sulphates) is increased to 30% (Table 9.1). Night-time conditions of low temperature and high relative humidity lead to the creation of secondary inorganic complexes with 'particulate water' (PH_2O) contributions. Particulate nitrate (PNO_3) contributes 40% of the inorganic ions reflecting active PNO_3 outdoor production in conditions of low ambient air temperatures and high levels of NO_x (Aberkane et al., 2004; Hueglin et al., 2005). PSO_4 (particulate sulphates) and PNH_4 (particulate ammonium) provide the second (after nitrates) highest contribution to the inorganic ions (20% each). Usually PNH_4 actively reacts with nitrates and sulphates creating neutralized salts nitrate and sulphate ammonium. Sodium and potassium together contribute about 20% of the fine aerosol inorganic soluble ions. The role of mineral dust and crustal elements is set at 10% (Table 9.1), reflecting not only sea breeze salt aerosol generation, but mostly crustal elements and road dust particles re-suspension (Senaratne, 2003; Hueglin et al., 2005; Senaratne et al., 2005).

The local weather conditions for Scenario 3 could be described by second-third repetition of the near-surface temperature inversion during night time, low near-surface temperature, and weak but pronounced near-surface westerly winds inherited from the synoptic scale circulation over the city of Christchurch. Usually in this case peak PM concentrations are attained between 10pm and midnight and are less protracted in time than in the case of Scenario 2.

Input gridded aerosol emissions were split according to Scenario 3, and all 7 winter 2005 episodes were evaluated with application of the MM5-CAMx4.2 numerical modelling system. Statistics for 7 episodes (at Coles Place) including the total number of cases, mean absolute error (MAE), correlation and power coefficients for fine and total PM for bulk and urban LSM schemes is shown in Table 9.4.

Table 9.4 Number of Cases (NC), Mean Absolute Error (MAE), Pearson Correlation Coefficient (PCC) and Power Correlation Coefficient (Power CC), for 7 episodes, Scenario 3, fine and total PM, bulk and urban MM5 Land-Surface Model (LSM).

Modelled PM	NN	MAE	PCC	Power CC
$PM_{2.5}$ – bulk MM5 LSM	408	5.42	0.68	0.45
PM_{10} – bulk MM5 LSM	408	8.35	0.67	0.44
$PM_{2.5}$ – urban MM5 LSM	408	8.45	0.72	0.52
PM_{10} – urban MM5 LSM	408	9.63	0.70	0.48

Figure 9.8 shows predicted PM_{10} and $PM_{2.5}$ concentration time series for episode 4 separately for bulk (per.4–green lines) and urban (per.4_1–blue lines) MM5 LSM obtained for Scenario 3.

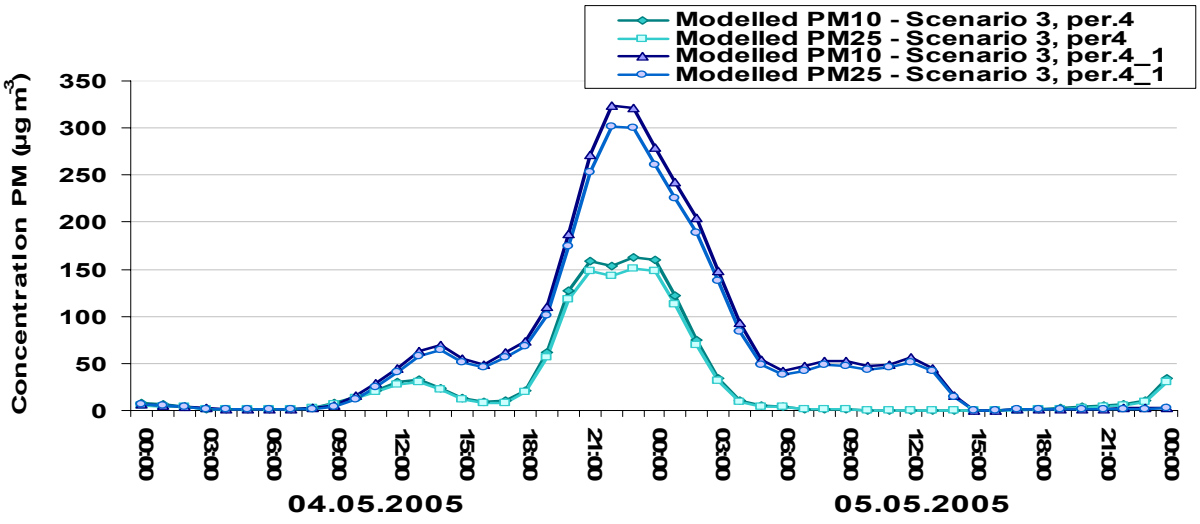

Figure 9.8 Modelled PM_{10} (dark) and $PM_{2.5}$ (light) concentrations (µg m^{-3}) for bulk (green) and urban (blue) LSM schemes, chemical Scenario 3, 00 NZST 04 May – 00 NZST 06 May 2005 (episode 4, 48 hours, Coles Place site).

Scenario 3 is numerically stable without fine PM concentrations exceeding total PM during the night-time peaks, as is the case for Scenario 2. But Scenario 3 has shown (in 1 case – episode 7) conditions that were close to chemical instability resulting from low temperatures and high values of relative humidity. This is considered to be a result of increasing partitioning of the secondary aerosol. Additionally calculated Index of Agreement gave values between 0.81 (PM_{10}) and 0.85 ($PM_{2.5}$).

Scenario 4 – secondary aerosol partitioning

For Scenario 4 (secondary aerosol partitioning scenario - sensitivity Scenario 3), the ratio EC/TOC is the highest and equal to 4, but the value of TC is only 40% of $PM_{2.5}$ (Table 9.1). TOC provides only one third of $PM_{2.5}$ in agreement with the research of Sun et al. (2004) into winter aerosol pollution of big cities like Beijing during winter time. The level of soluble inorganic ions is increased to 50% (Table 9.1), representing active processes of water condensation and creation of PNO_3PNH_4 and $PSO_4(PNH_4)_2$ complexes during evening-night strong near-surface fog situations (Sun et al., 2004; Scott 2005). The contribution of PNO_3 and PSO_4 to $PM_{2.5}$ ion concentration is about 30% each, and the contribution of PNH_4 is equal to 20%. As in Scenario 3 sodium and potassium together contribute about 20% of the fine aerosol inorganic soluble ions. The role of mineral dust and crustal elements continues to be quite important (Table 9.1) because of the influence of sea breeze salt aerosol generation and dust-crustal elements re-suspension. The local weather for Scenario 4 is characterized by a near-surface temperature inversion, moderately low near-surface temperature, and pronounced near-surface on-shore sea breeze inherited from day-time local air circulation over the city. Typically, in this case peak PM concentrations are attained not later than at 9-10 pm and smog tends to disappear after midnight (Titov et al., 2007). Input gridded aerosol emissions were split according to Scenario 4, and 7 winter 2005 episodes were evaluated with application of the MM5-CAMx4.2 numerical modelling system. Statistics for 7 episodes (Coles Place) including number of cases, mean absolute error (MAE), correlation and power coefficients for $PM_{2.5}$ and PM_{10}, bulk and urban LSM is shown in Table 9.5.

Table 9.5 Number of Cases (NC), Mean Absolute Error (MAE), Pearson Correlation Coefficient (PCC) and Power Correlation Coefficient (Power CC), for 7 episodes, Scenario 3, fine and total PM, bulk and urban MM5 Land-Surface Model (LSM).

Modelled PM	NN	MAE	PCC	Power CC
$PM_{2.5}$ – bulk MM5 LSM	408	8.65	0.67	0.45
PM_{10} – bulk MM5 LSM	408	14.50	0.66	0.44
$PM_{2.5}$ – urban MM5 LSM	408	5.15	0.70	0.51
PM_{10} – urban MM5 LSM	408	7.34	0.69	0.48

Figure 9.9 shows predicted PM_{10} and $PM_{2.5}$ concentration time series for episode 4 separately for bulk (per.4–green lines) and urban (per.4_1–blue lines) MM5 LSM obtained for Scenario 4.

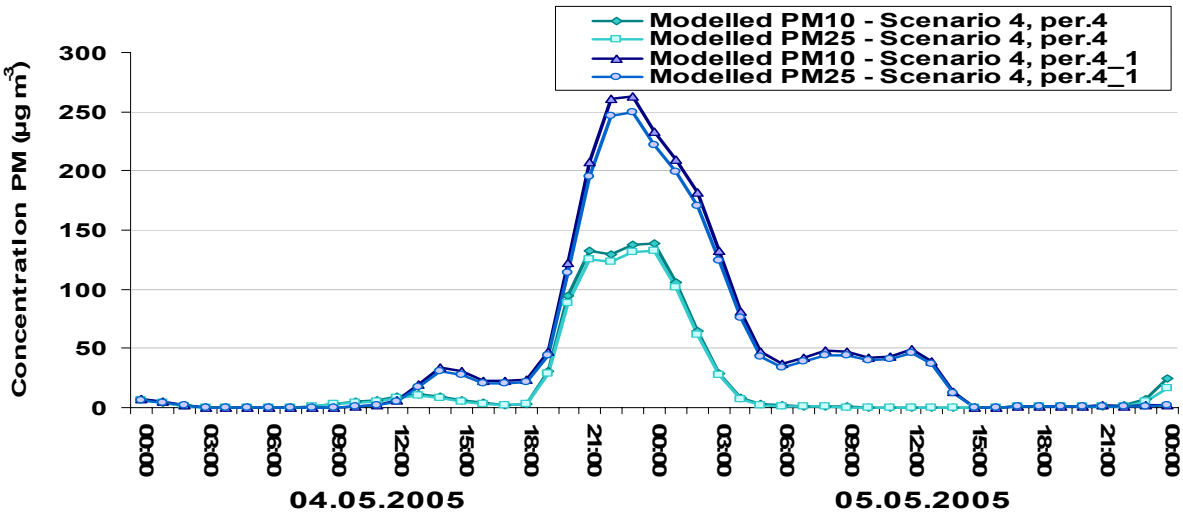

Figure 9.9 Modelled PM_{10} (dark) and $PM_{2.5}$ (light) concentrations (µg m^{-3}) for bulk (green) and urban (blue) LSM schemes, chemical Scenario 4, 00 NZST 04 May – 00 NZST 06 May 2005 (episode 4, 48 hours, Coles Place site).

Scenario 4 is numerically nearly stable, and also has no fine PM concentrations exceeding total PM during the night-time peaks. But Scenario 4 shows (in 2 cases) chemical instability to low temperatures and high values of relative humidity. As Scenario 4 is a secondary aerosol partitioning scenario this instability is a product of dominating partitioning of the secondary aerosol. For comparison of the modelled output for the 4 chemical scenarios Figure 9.10 presents observed PM_{10} and $PM_{2.5}$ concentration time series for episode 4.

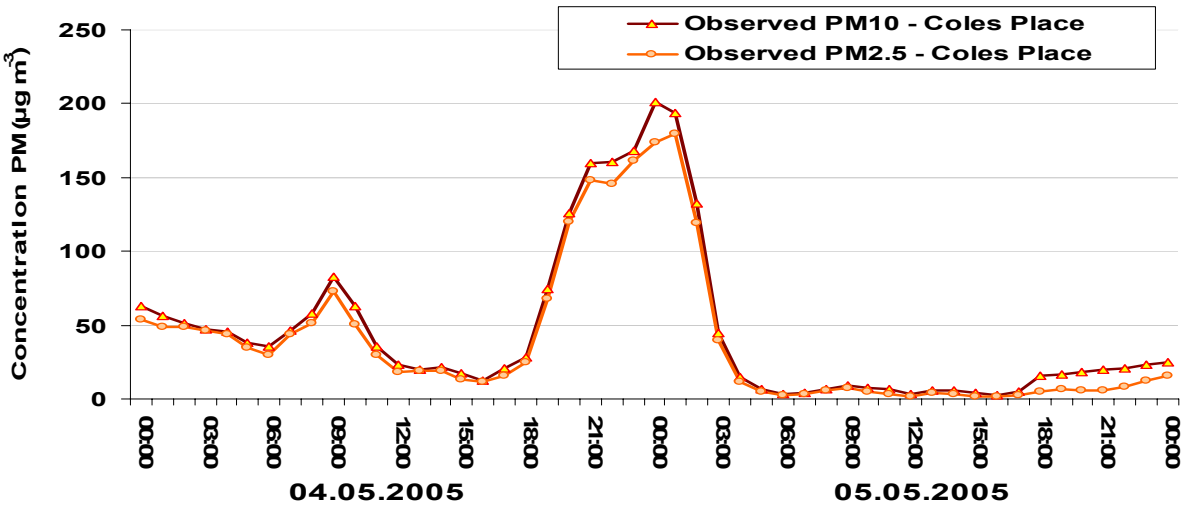

Figure 9.10 Observed PM_{10} (red) and $PM_{2.5}$ (light red) concentrations (µg m^{-3}) 0000 NZST 04 May – 0000 NZST 06 May 2005 (episode 4, 48 hours, Coles Place site).

Modelled time series don't show pronounced morning fine and total PM concentration peaks (to compare with ambient data in Figure 9.10), as CAMx4 needs as minimum 12 hours spin-up time.

9.3.2 Optimal temporal scenario – winter 2005 aerosol pollution study

Evaluation of the 4 aerosol chemical scenarios provides a possibility to compare statistical results to consider a potentially optimal PM chemical content for CAMx4.2, which produces the lowest error and best correlation with observed fine and total PM concentrations. Averaged statistics of the modelled $PM_{2.5}$ (and PM_{10}) concentrations (using 4 chemical scenarios and 2 PBL parameterisation schemes) compared with observations for seven CAMx4.2 runs are presented in Table 9.6. The MM5 Pleum-Xiu PBL scheme includes the urban LSM, and the MM5 Blackadar PBL scheme includes the bulk LSM.

Table 9.6 Pearson correlation coefficient (PCC), and Mean Absolute Error (MAE): CAMx4.2, seven winter 2005 episodes, comparison of modelled and observed values.

Scenario	MM5 PBL scheme	PCC		MAE (μg m^{-3})	
		$PM_{2.5}$	PM_{10}	$PM_{2.5}$	PM_{10}
Scenario 1	Pleum-Xiu	0.63	0.63	11.00	12.15
	Blackadar	0.64	0.62	8.55	10.35
Scenario 2	Pleum-Xiu	0.64	0.62	13.25	10.15
	Blackadar	0.58	0.58	6.52	6.05
Scenario 3	Pleum-Xiu	0.72	0.70	8.45	9.63
	Blackadar	0.70	0.69	5.42	8.35
Scenario 4	Pleum-Xiu	0.70	0.69	5.85	8.84
	Blackadar	0.67	0.66	8.75	14.50

From Table 9.6 the highest values of PCC and lowest values of MAE are obtained for Scenario 3, especially for the Blackadar PBL parameterisation (bulk LSM). MAE for $PM_{2.5}$ is usually lower than for PM_{10} reflecting the more accurate representation of fine aerosol by CAMx and also some problems of representing the coarse $PM_{10-2.5}$ fraction. The origin of this error is probably due to the fact that CAMx4.2 uses only 2 fractions for coarse-fine crustal (CCRS - FCRS) and coarse-fine (CPRM - FPRM) primary aerosol (see List of acronyms and abbreviation). An imprecision of R_{PM} ($PM_{2.5}/PM_{10}$) calculation could also contribute to this discrepancy. From Table 9.6 the advantages of Scenario 3 are very shaky and ambiguous. Linear regression statistics will be used to prove more accurately the advantages of any chemical scenario over the other ones.

Scenarios 1-4 evaluation – 7 winter 2005 episodes

Assessment of scenarios 1-4 use scatterplot diagrams and linear regression equations obtained for every chemical scenario. Scatterplots are plotted and linear regression parameters are calculated for all 7 winter episodes that including about 17 days, or 408 hourly PM concentrations. In Figures 9.12-9.15 modelled results for the MM5 Blackadar PBL scheme (bulk LSM) are presented. Figure

9.11 shows a scatterplot diagram of observed $PM_{2.5}$-PM_{10} and a linear regression obtained for 1 May–10 June 2005 (40 days) for Coles Place inner city observation site.

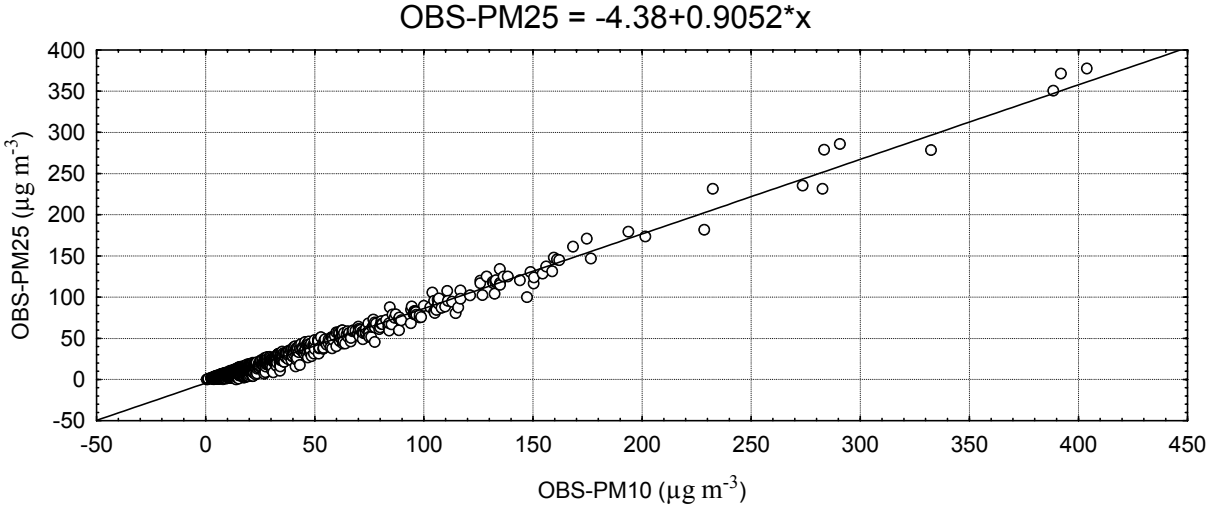

Figure 9.11 Scatterplot diagram and linear regression for observed $PM_{2.5}$-PM_{10} concentrations (µg m^{-3}) obtained for 1 May-10 June 2005 at the Coles Place site.

From Figure 9.11 an excellent agreement is evident between observed $PM_{2.5}$ and PM_{10} concentrations with the linear regression intercept (INT) equal to -4.38 and regression coefficient (RC) equal to 0.9052 (where x-axis is PM_{10} concentrations in the linear regression equation). Figure 9.12 presents the modelled $PM_{2.5}$-PM_{10} scatterplot and linear regression following application of CAMx4.2 and initial and nudging of PM gridded emissions for 7 study episodes for Coles Place. Input-nudging emissions were split into chemical components according to Scenario 1 – control-transport scenario (Table 9.1).

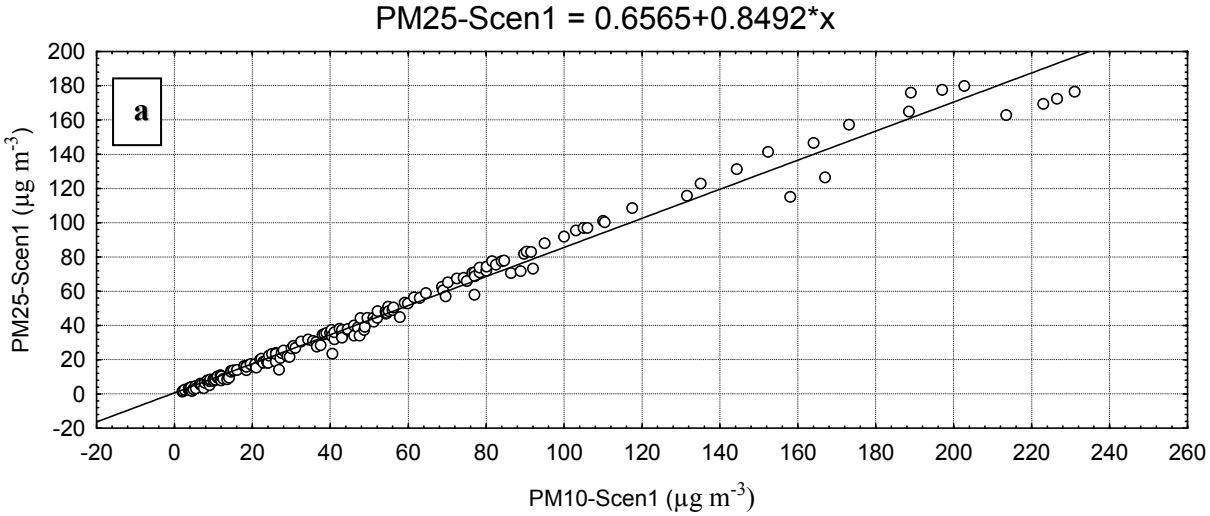

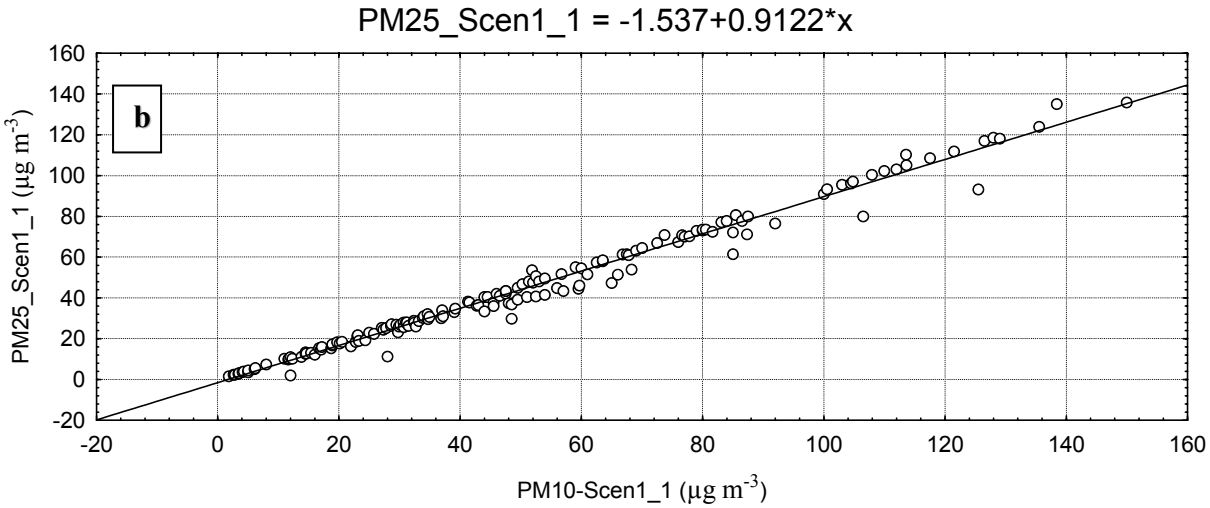

Figure 9.12 Scatterplot diagram and linear regression for modelled $PM_{2.5}$-PM_{10} concentrations (µg m^{-3}) for 7 winter 2005 episodes (Coles Place) and the Scenario 1 chemical split (urban LSM): a) $0 < PM_{10} < 300$ µg m^{-3}; b) $0 < PM_{10} < 150$ µg m^{-3}.

From Figure 9.12a a good agreement is evident between observed $PM_{2.5}$-PM_{10} concentrations, especially for PM_{10} concentrations that are lower than 150 µg m^{-3}. Regression coefficient (RC) is equal to 0.8492, but the linear regression intercept (INT) is positive and equal to 0.6565, which suggests CAMx numerical instability in the case of Scenario 1 high concentrations of the total (and fine) PM. Calculations of $PM_{2.5}$ for total PM concentrations less than 150 µg m^{-3} produces new regression parameters: INT = -1.537 and RC = 0.9122 and a more accurate scatterplot that is demonstrated in Figure 9.12b.

Figure 9.13 presents a modelled $PM_{2.5}$-PM_{10} scatterplot and linear regression following application of CAMx4.2 and initial-nudging PM gridded emissions for 7 study episodes for Coles Place. Input-nudging emissions were split into chemical components according to Scenario 2 – domestic scenario (Table 9.1).

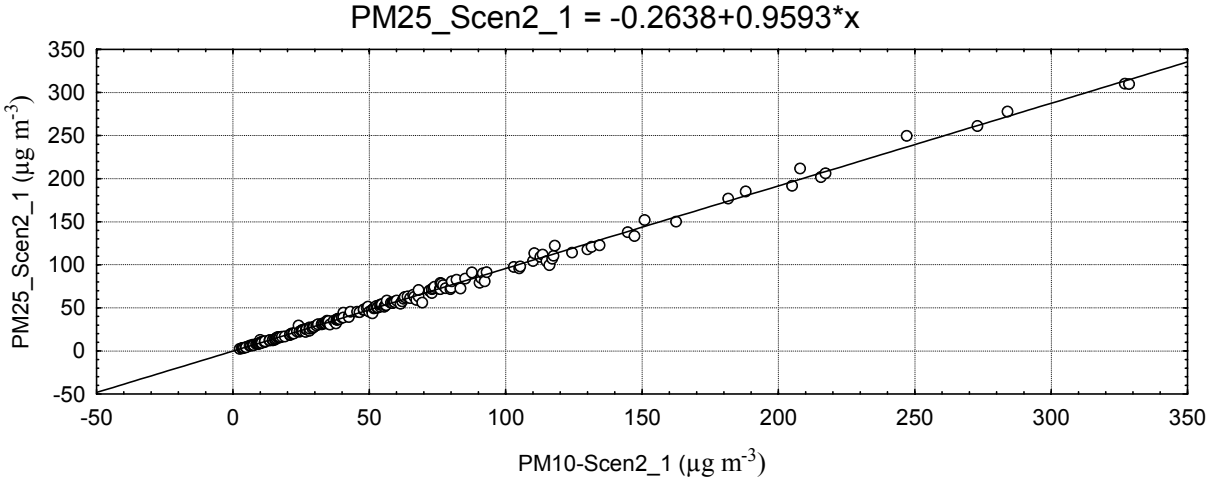

Figure 9.13 Scatterplot diagram and linear regression for modelled $PM_{2.5}$-PM_{10} concentrations (µg m^{-3}) for 7 winter 2005 episodes (Coles Place) and the Scenario 2 chemical split (urban LSM).

Figure 9.13 shows a good agreement between modelled $PM_{2.5}$ and PM_{10} concentrations with linear regression intercept INT = -0.2638 and regression coefficient RC = 0.9593 (where x means PM_{10} in the linear regression equation). Scenario 2 modelled outputs don't show serious numerical instability to big concentrations of total PM. Figure 9.14 presents modelled $PM_{2.5}$-PM_{10} scatterplot and linear regression following application of CAMx4.2 and initial-nudging PM gridded emissions for 7 study episodes for Coles Place. Input-nudging emissions were split into chemical components according to Scenario 3 – mixed domestic - domestic-transport scenario (Table 9.1).

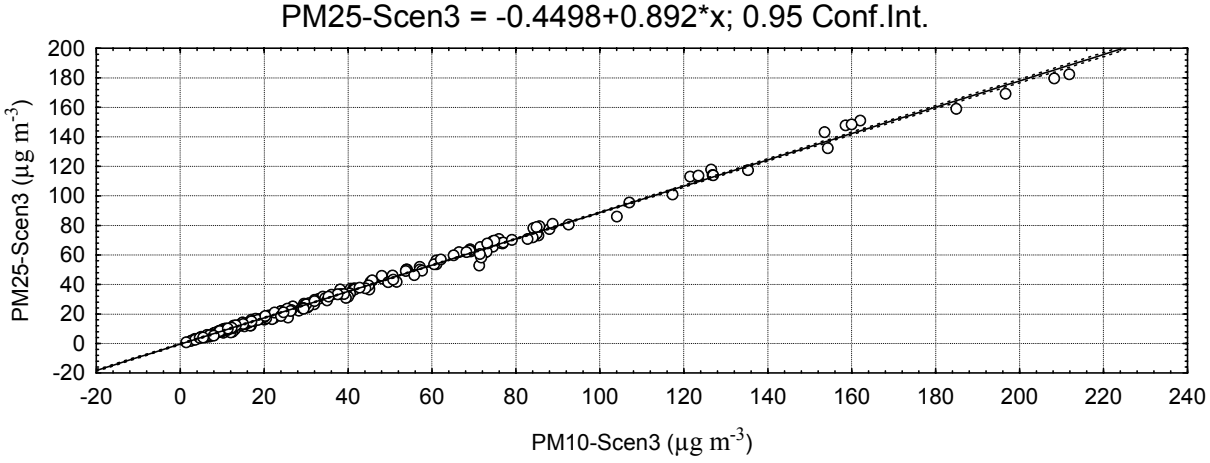

Figure 9.14 Scatterplot diagram and linear regression for modelled $PM_{2.5}$-PM_{10} concentrations (µg m^{-3}) for 7 winter 2005 episodes (Coles Place) and the Scenario 3 chemical split (urban LSM).

Figure 9.14 exhibits a good agreement between modelled $PM_{2.5}$ and PM_{10} concentrations with linear regression intercept INT = -0.4498 and regression coefficient RC = 0.8926 (where the x-axis

presents PM_{10} concentrations in the linear regression equation). Scenario 3 modelled outputs also show no instability at high concentrations of total PM. Figure 9.15 presents modelled $PM_{2.5}$-PM_{10} scatterplot and linear regression following application of CAMx4.2 and initial-nudging PM gridded emissions for 7 study episodes for Coles Place. Input-nudging emissions were split on chemical components according to Scenario 4 – secondary partitioning scenario (Table 9.1).

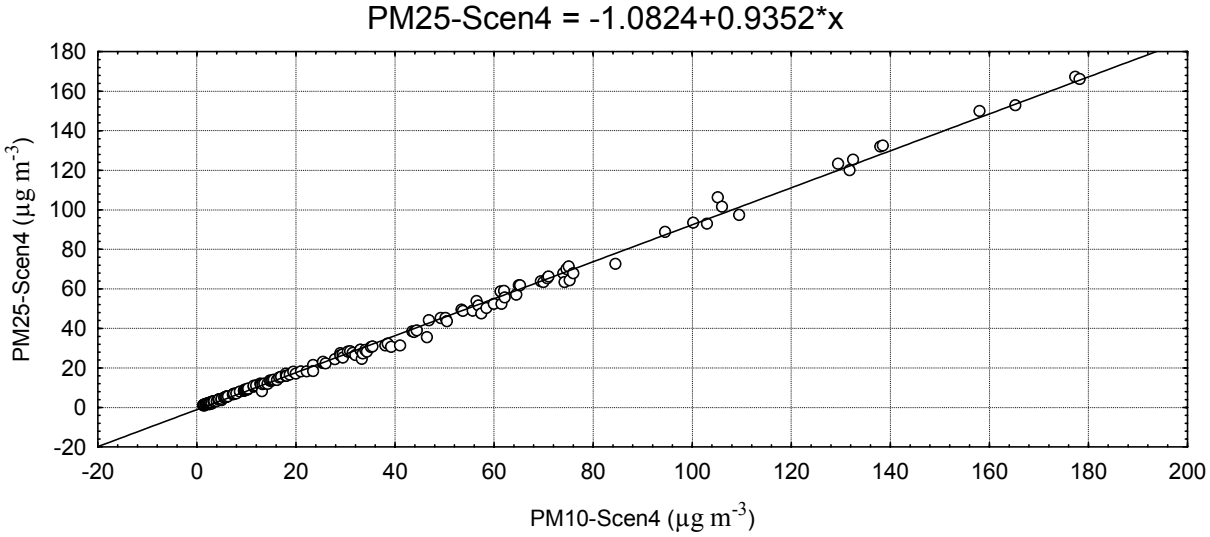

Figure 9.15 Scatterplot diagram and linear regression for modelled $PM_{2.5}$-PM_{10} concentrations (µg m^{-3}) for 7 winter 2005 episodes (Coles Place) and the Scenario 4 chemical split (urban LSM).

Figure 9.15 presents a good agreement between modelled $PM_{2.5}$ and PM_{10} concentrations with linear regression intercept INT = -1.0824 and regression coefficient RC = 0.9352 (x is equal to PM_{10} concentrations in the linear regression equation). Scenario 4 modelled outputs show no instability at high concentrations of total PM.

Scenario 1-3mix as a best fit CAMx chemical scenario

The summary of linear regression parameters (intercept and regression coefficient) derived for observed and modelled $PM_{2.5}$ (PM_{10}) concentrations (Figure 9.11- Figure 9.15) is shown in Table 9.7 for all four chemical scenarios and two MM5 PBL parameterisations. The observed $PM_{2.5}$ and PM_{10} (from one site co-located measurements, Kingham et al., 2005) are used to build a linear regression for ambient $PM_{2.5}$ (from PM_{10}). The observed linear regression ($PM_{2.5}$ from PM_{10}) intercept and regression coefficient (Table 9.7, last line) are compared with the modelled $PM_{2.5}$ (from PM_{10}) intercept and linear regression coefficient for every chemical scenario for 2 PBL schemes. Modelled $PM_{2.5}$ and PM_{10} are calculated separately for all 7 episodes (for every

scenario), and a linear regression for $PM_{2.5}$ (from PM_{10}) is calculated for all episodes for hourly PM concentrations (17 days – 408 hourly values).

Table 9.7 $PM_{2.5}$ (PM_{10}) linear regression intercept (INT) and regression coefficient (RC) for 4 chemical scenarios and observations.

Scenario	MM5 PBL Scheme	Linear regression: Intercept (R>0.98, P<0.01)	Linear regression: Coefficient (R>0.98, P<0.01)
Scenario 1	Pleum-Xiu	$PM_{2.5}$ (PM_{10}): 2.3697 (-1.3455)	$PM_{2.5}$ (PM_{10}): 0.7974 (0.9108)
	Blackadar	$PM_{2.5}$ (PM_{10}): 0.6565 (-1.5370)	$PM_{2.5}$ (PM_{10}): 0.8492 (0.9122)
Scenario 2	Pleum-Xiu	$PM_{2.5}$ (PM_{10}): -0.2642	$PM_{2.5}$ (PM_{10}): 0.9485
	Blackadar	$PM_{2.5}$ (PM_{10}): -0.2638	$PM_{2.5}$ (PM_{10}): 0.9593
Scenario 3	Pleum-Xiu	$PM_{2.5}$ (PM_{10}): -0.6261	$PM_{2.5}$ (PM_{10}): 0.8883
	Blackadar	$PM_{2.5}$ (PM_{10}): -0.4498	$PM_{2.5}$ (PM_{10}): 0.8926
Scenario 4	Pleum-Xiu	$PM_{2.5}$ (PM_{10}): -0.8018	$PM_{2.5}$ (PM_{10}): 0.9441
	Blackadar	$PM_{2.5}$ (PM_{10}): -1.0824	$PM_{2.5}$ (PM_{10}): 0.9352
Observed	**1.05-10.06.05**	$PM_{2.5}$ (PM_{10}): -4.3810	$PM_{2.5}$ (PM_{10}): 0.9052

From Table 9.7 the best fit between modelled and observed (1 May–10 June 2005 time period) $PM_{2.5}$ regression parameters (minimal Intercept difference – **3.755**, and minimal Coefficient difference – **0.0126**) are observed for Scenario 3 for the bulk LSM (Blackadar PBL), and for the urban LSM (Pleum-Xiu PBL). This statement will be proven by graphical methods based on the observed and several versions of the modelled linear regressions.

Figure 9.16 presents plots of the absolute error between modelled and observed regression calculations for $PM_{2.5}$ (modelled minus observed) for all 4 scenarios for the MM5 Blackadar PBL scheme (bulk LSM). It is evident that accumulation of the $PM_{2.5}$ error with linear increasing PM_{10} values is minimal for Scenario 3, although Scenario 1 (not restricted) shows the lowest $PM_{2.5}$ error from linear regression with PM_{10} concentrations in a range 60-80 μg m^{-3}.

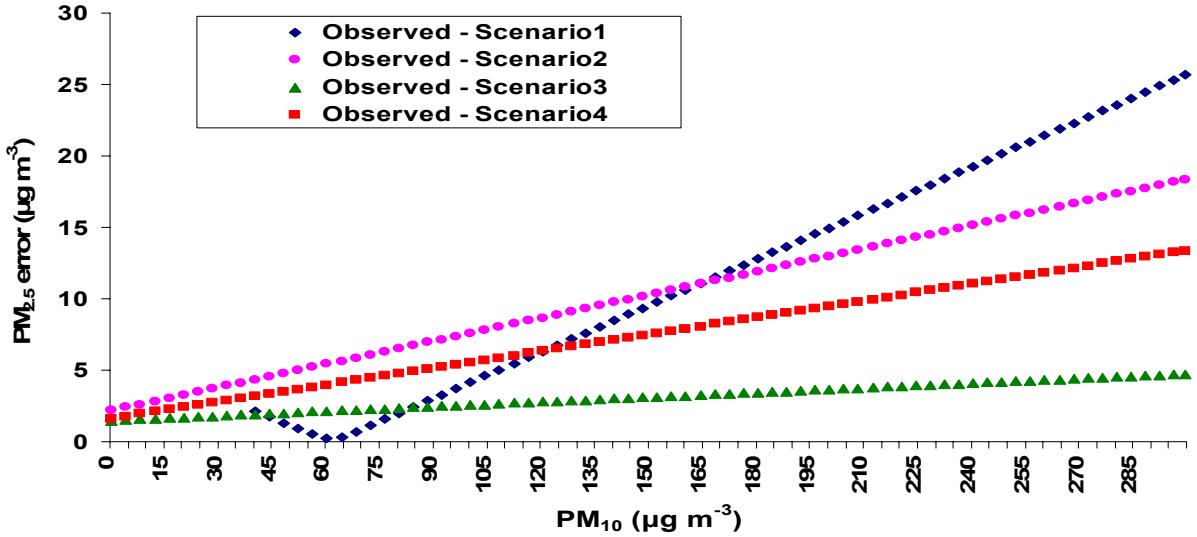

Figure 9.16 Absolute error between observed and modelled $PM_{2.5}$ based on hourly average linear regression for 40-day observations and CAMx output (MM5 Blackadar PBL scheme).

Numerical instability in CAMx4.2 is evident for Scenario1 high PM_{10} values (>150 µg m^{-3}), as the $PM_{2.5}$ regression intercept as positive is shown in Table 9.7 and in Figure 9.12a. A new regression equation derived for Scenario 1 by applying regression analysis to $0 < PM_{10} < 150$ µg m^{-3} only (intercept and regression coefficient in brackets in Table 9.7 and also in Figure 9.12b)), represents the best fit to the observed $PM_{2.5}$ (PM_{10}) regression (Table 9.7). Thus chemical Scenario 1 can be used to split input-nudging PM emissions on the chemical species for simulation of the morning aerosol peaks (over the 6-11am time interval) when PM concentrations usually do not exceed 80–120 µg m^{-3} (Aberkane et al., 2004; Scott 2005).

A new complex scenario (Scenario 1-3mix) as a best fit CAMx chemical scenario is produced from 2 initial chemical scenarios: Scenario 1 (transport control scenario with dominance of the primary PM species) and Scenario 3 (domestic - domestic-transport, sensitivity scenario 2 with nearly balanced primary and secondary partitioning). Scenario 1 and Scenario 3 statistically are proven to be the best fit to observations for midday–night (Scenario 3) and morning-midday (Scenario 1) time intervals (Table 9.7 and Figure 9.15). Scenario 1 is employed to build the day-time part (6am-5pm) of a new complex Scenario 1-3mix, and Scenario 3 is applied to build the night-time part (6pm-5am) of a new complex Scenario 1-3mix.

Evaluation of Scenario 1-3mix against primary scenarios

The new complex Scenario 1-3mix is used to re-calculate all pollution episodes to obtain new values of $PM_{2.5}$ and PM_{10} with presumably minimum error compared to the primary scenarios.

Input gridded aerosol emissions were split according to Scenario 1 for day-time (6am-5pm) and according Scenario 3 for night-time (6pm-5am), and all 7 winter 2005 episodes were re-evaluated with application of the 2-level CAMx4.2 photochemical model. Statistics for 7 episodes (at Coles Place) including modelled-observed average concentration (μg m^{-3}), mean absolute error (MAE), correlation and power coefficients for total and fine PM for bulk and urban LSM schemes is shown in Table 9.8 for Scenario 1-3mix.

Table 9.8 Modelled (Mod.) and Observed (Obs.) Average, Mean Absolute Error (MAE), Pearson Correlation Coefficient (PCC) and Power Correlation Coefficient (Power CC), for 7 episodes, complex Scenario 1-3mix, total and fine PM, bulk and urban MM5 Land-Surface Model (LSM).

Modelled PM	AVERAGE Mod. – Obs.	MAE	PCC	Power CC
PM_{10} – bulk MM5 LSM	37.50 – 54.25	6.15	0.75	0.56
$PM_{2.5}$ – bulk MM5 LSM	34.75 – 43.30	5.92	0.73	0.53
PM_{10} – urban MM5 LSM	35.85 – 54.25	6.85	0.71	0.51
$PM_{2.5}$ – urban MM5 LSM	32.45 – 43.30	6.50	0.71	0.51

Scenario 1-3mix shows the best agreement with observational data but these results are close to scenario 3, and Scenario 3 is the best at representing night peaks of aerosol pollution. Figure 9.17 shows predicted PM_{10} and $PM_{2.5}$ concentration time series for episode 4 only for bulk (per.4–green lines) and urban (per.4_1–blue lines) MM5 LSM obtained for complex Scenario 1-3mix.

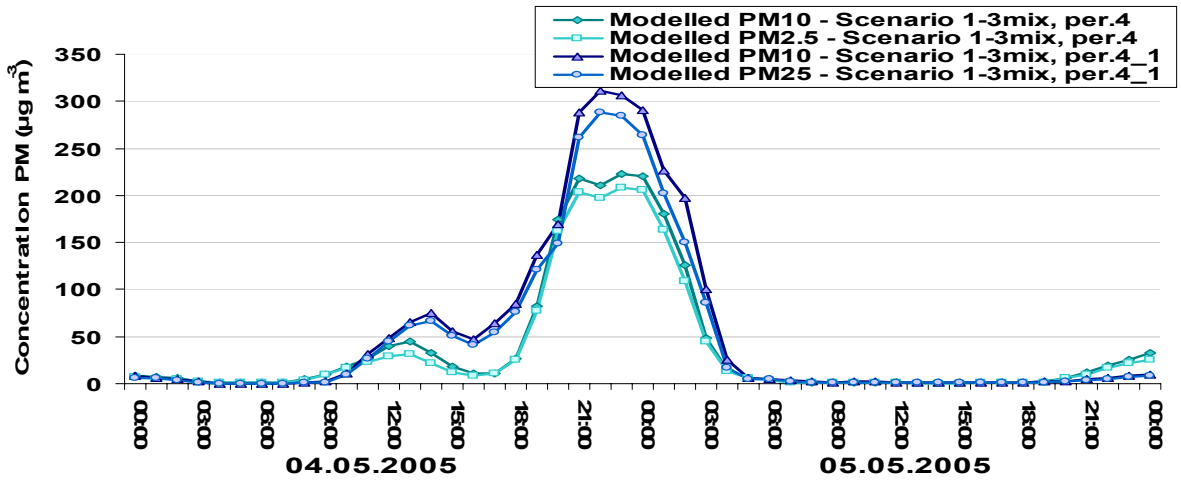

Figure 9.17 Modelled PM_{10} (dark) and $PM_{2.5}$ (light) concentrations (μg m^{-3}) for bulk (green) and urban (blue) LSM schemes, complex Scenario 1-3mix, 00 NZST 4 May – 00 NZST 6 May 2005 (episode 4, 48 hours, Coles Place site).

Scenario 1-3mix is numerically stable without fine PM concentrations exceeding total PM for peak aerosol values. Also Scenario 1-3mix doesn't shows chemical instability at low temperatures and

high values of relative humidity inheriting stable chemical conditions from the day-time Scenario 1 (primary scenario) combined with numerically stable Scenario 3.

Scenario 1-3mix assessment (as for primary scenarios 1-4) uses scatterplot diagrams and linear regression. For Scenario 1-3mix scatterplots are plotted and linear regression parameters are calculated for all 7 winter episodes, including about 17 days or more than 400 hourly PM concentration values. Figure 9.18 presents the modelled $PM_{2.5}$-PM_{10} scatterplot and linear regression following application of CAMx4.2 and initial-nudging PM gridded emissions for 7 study episodes for Coles Place. Input-nudging emissions were split into chemical components according to a new complex Scenario 1-3mix, being a combination of Scenario1 and Scenario 3 (Table 9.1).

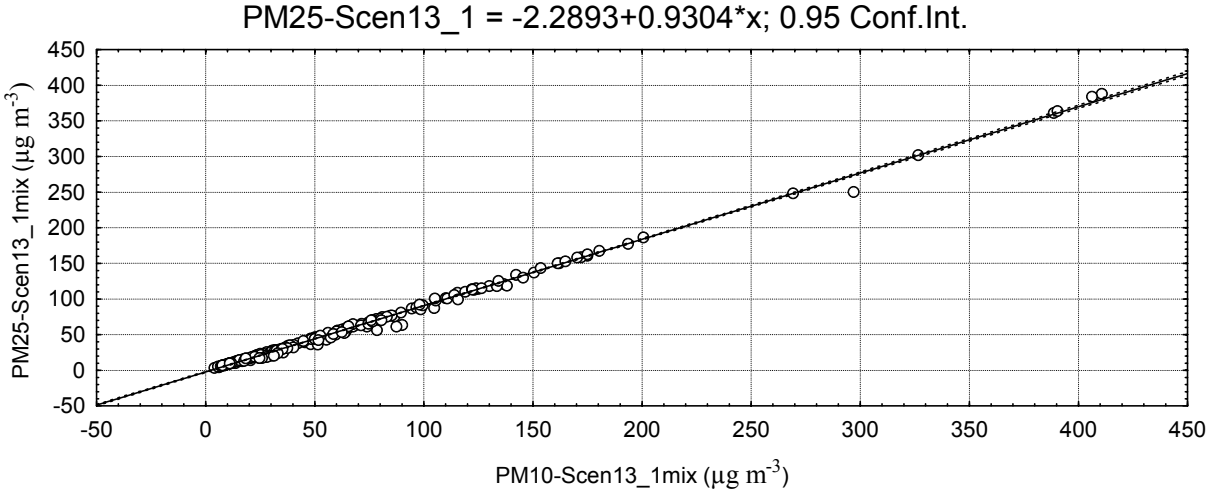

Figure 9.18 Scatterplot diagram and linear regression for modelled $PM_{2.5}$-PM_{10} concentrations (µg m^{-3}) for 7 winter 2005 episodes (Coles Place) and Scenario 1-3mix chemical split (urban LSM).

Figure 9.18 presents excellent agreement between modelled $PM_{2.5}$ and PM_{10} concentrations with the linear regression intercept INT = -2.2893 and regression coefficient RC = 0.9304 (x means PM_{10} in the linear regression equation). Scenario 1-3 mix modelled outputs show no any instability to high concentrations of the total PM, as observed for Scenario 1.

Table 9.9 presents the linear regression intercept (INT) and regression coefficient (RC) for the predicted $PM_{2.5}$ (and PM_{10}) for Scenario 1, Scenario 1-3mix and Scenario 3 (over seven winter 2005 episodes, and for two PBL schemes) compared with linear regression parameters from ambient data. Running the three optimal scenarios for 7 winter 2005 episodes only (17 days), the differences between observed and modelled PM are reduced (compared with Table 9.7). Scenarios

1 and 3 are retained in Table 9.9 to compare with the combined Scenario 1-3mix to illustrate the improvements in the predicted $PM_{2.5}$ (PM_{10}) linear regression parameters with application of Scenario 1-3mix.

Table 9.9 $PM_{2.5}$ (PM_{10}) linear regression intercept and regression coefficient for Scenario 1, Scenario 1-3mix, Scenario 3 (2 MM5 PBL schemes, 7 winter 2005 episodes) and observations.

Scenario	**MM5 PBL scheme**	**Linear regression: Intercept (R>0.98, P<0.01)**	**Linear regression: Coefficient (R>0.98, P<0.01)**
Scenario 1	Pleum-Xiu	$PM_{2.5}$ (PM_{10}): -1.3455	$PM_{2.5}$ (PM_{10}): 0.9108
	Blackadar	$PM_{2.5}$ (PM_{10}): -1.5370	$PM_{2.5}$ (PM_{10}): 0.9122
Scenario 1-3mix	Pleum-Xiu	$PM_{2.5}$ (PM_{10}): -2.2340	$PM_{2.5}$ (PM_{10}): 0.9295
	Blackadar	$PM_{2.5}$ (PM_{10}): -2.2893	$PM_{2.5}$ (PM_{10}): 0.9304
Scenario 3	Pleum-Xiu	$PM_{2.5}$ (PM_{10}): -0.6261	$PM_{2.5}$ (PM_{10}): 0.8883
	Blackadar	$PM_{2.5}$ (PM_{10}): -0.4498	$PM_{2.5}$ (PM_{10}): 0.8926
Observed	7 episodes only	$PM_{2.5}$ (PM_{10}): -4.8287	$PM_{2.5}$ (PM_{10}): 0.9058

From Table 9.9 the best fit with observations corresponds to Scenario 1-3mix while corrected Scenario 1 is in second place. But Scenario 1 degenerates (numerically unstable) for high concentrations of the total-fine PM (>150 μg m^{-3}) and is not appropriate for night PM peaks. To visualize advantages of Scenario 1-3mix Figure 9.19 presents the plots of absolute error for $PM_{2.5}$ (modelled minus observed), derived using the linear regression parameters (Table 9.9) for Scenario 1-3mix and Scenario 3 (Pleum-Xiu and Blackadar PBL schemes).

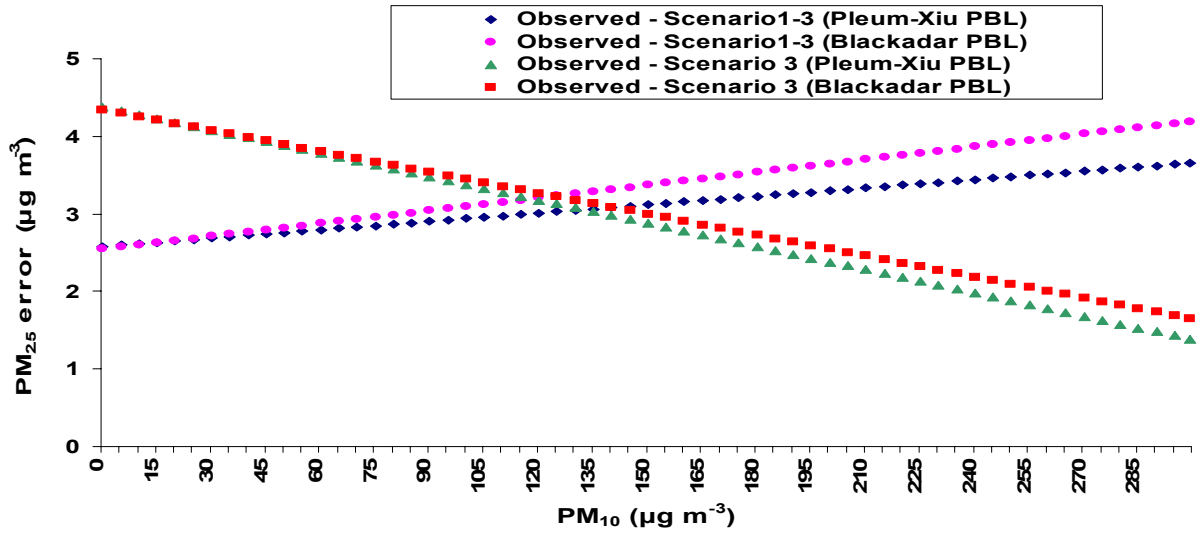

Figure 9.19 Absolute error between observed and modelled $PM_{2.5}$ based on the corrected linear regression: Scenario 1-3mix compared with observations and Scenario 3 (MM5 bulk and urban LSM schemes).

It is remarkable that $PM_{2.5}$ error grows with PM_{10} increase for Scenario 1-3mix, but has lower absolute error values than Scenario 3. For Scenario 1-3mix, the $PM_{2.5}$ linear regression error is lower than for Scenario 3, but only for PM_{10} concentrations not more than 130–140 µg m^{-3}. Above this level, the dominance of Scenario 3 over Scenario 1-3mix for high pollution episodes becomes evident (Figure 9.19). This result can be explained by the influence of Scenario 1 (the day-time part of Scenario 1-3mix) on the night-time PM peak values especially on the second-third calculated (with application of CAMx4) day. As was mentioned before, Scenario 1 does not adequately represent cases with PM_{10} > 150 µg m^{-3}. It should be stressed that a reduction of the mean absolute error between observed and modelled $PM_{2.5}$ for Scenario 1-3mix relative to Scenario 3 is close to 25% for 0 < PM_{10} < 140 µg m^{-3} (Figure 9.19). As the likelihood of the modelled hourly PM_{10} concentrations being higher than 140 µg m^{-3} is only 20% ($P<0.01$, Spearman rank test) for the 1 May-10 June 2005 time period, the predicted $PM_{2.5}$ error decreases in 8 cases out of 10 for the Scenario 1-3mix.

Figure 9.20 shows (as an example from winter 2005 episode 4) the spatial distribution of PM_{10} (Scenario 1-3mix) for midnight (Figure 9.20a) and 6am (Figure 9.20b) on 5 May 2005 over the Christchurch region. Figure 9.20a demonstrates that the peak values of calculated midnight PM_{10} are located near the city centre. Figure 9.20b indicates a split of the PM_{10} single night peak and formation of two diluted morning peaks.

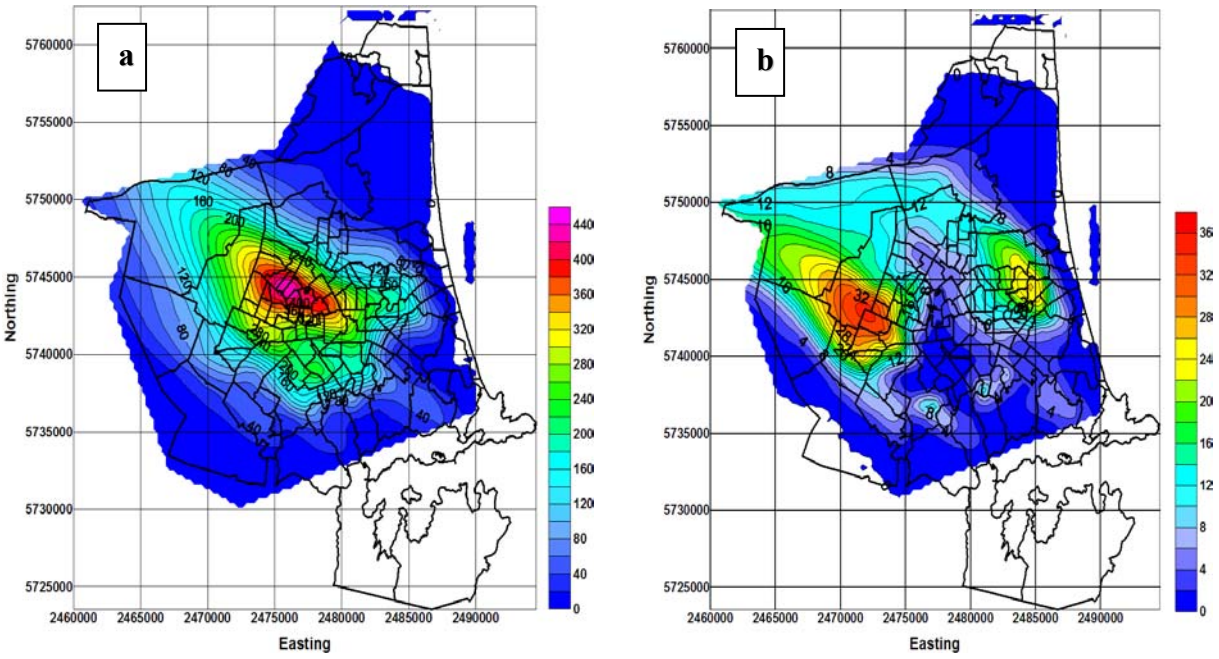

Figure 9.20 Spatial near-surface (8-10 metres) distribution of PM_{10}: a) for midnight – 24-hour forecast (5 May 2005, episode 4, Scenario 1-3mix, Blackadar PBL scheme); b) for 6am – 30-hour forecast (5 May 2005, episode 4, Scenario 1-3mix, Blackadar PBL scheme).

Modelling suggests that two PM_{10} peaks appear either side of the city centre as a result of cold air drainage from the Canterbury Plains (north-west) and from the Port Hills (south-east), resulting in dispersion of aerosol in two different directions. This local scale air flow process was precisely described in Chapter 8.

9.4 Summary

The numerical analysis of 4 primary chemical scenarios demonstrate that the most representative chemical composition of $PM_{2.5}$ is close to Scenario 3, with carbonaceous species about 55-65% of the PM total content, and with a ratio of organic to elemental carbon close to 3 (Hueglin et al., 2005; Senaratne et al., 2005). The contribution of soluble inorganic ions is about 30%, indicating active secondary reactions under low temperature conditions. The contribution of dust and crustal particles to PM emissions is about 10%. The day-time Scenario 1 represents the increased contribution of vehicular (and maybe industrial) emissions, with higher values of primary particles and elemental carbon. Scenario 1-3mix, generated from Scenario 3 and Scenario 1, is proven to be the best for modelling $PM_{2.5}$ (PM_{10}) concentrations in the range 0-140 μg m^{-3} (Figures 9.16 and 9.19) for 7 winter 2005 case episodes.

The method of scenarios is a tool not only to find the optimal chemical split of input gridded PM emissions for CAMx4, but also a complex numerical instrument to find a first approximation of the main chemical components relative contribution in the fine and total PM. Figure 9.21 presents the chemical composition of PM_{10} in inner Christchurch obtained from short-term observations at Coles Place for winter 2004 (Wang et al., 2005).

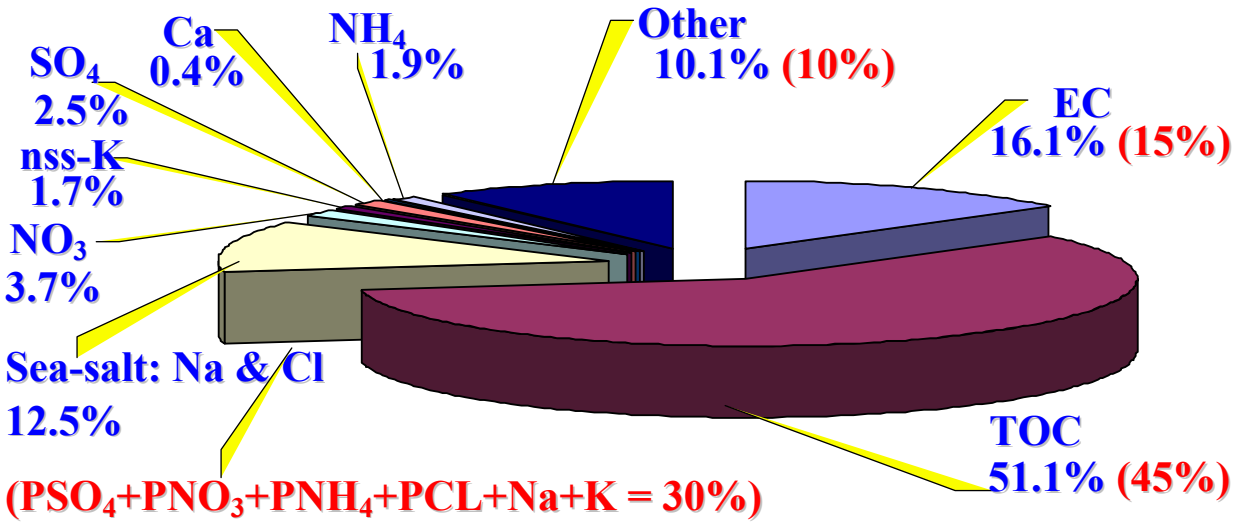

Figure 9.21 PM_{10} chemical composition in Christchurch for a typical 24 hour period in July 2004 based on several days (after Wang et al., 2005).

The chemical composition of the complex Scenario 1-3mix (red font and in brackets), and the observed chemical composition of PM_{10} (blue font) for a Christchurch winter day (July 2004) in Figure 9.20 are very close. This comparison supports the validity of the approach.

Chapter 10: Scenarios bias reduction – winter 2006

To reduce the accumulated systematic bias in the method of chemical scenarios all 5 chemical scenarios (including Scenario 1-3mix) are evaluated for 8 winter 2006 (June–July) heavy smog episodes to eliminate a seasonal bias of the method. As the next phase of research, it is important to reduce systematic error of the method that consists of:

1. Seasonal error - winter 2006 data are used;
2. Meteorological model error – MM5 MPP v3.7.3 and ARW WRF v2.1.2 models are used;
3. Chemical model error - CAMx version 4.3 is applied;
4. Observation site error - PM data from an additional observation site are obtained;
5. Input gridded emissions error - 2002 inventory emissions are employed. 2002 inventory was compiled for inner city and suburbs in total, without providing gridded emissions. So 1999 inventory data were engaged again, and 2002 inventory would be applied in Applications (future scenarios of proposed PM reduction).

For winter 2006 ECan didn't measure fine PM or at least did not provide any information about $PM_{2.5}$. But as compensation total PM observations from another site (Woolston) were available, and this gave an opportunity to check the spatial variability of the method of several scenarios using a spatial-temporal variability of ambient PM data. The observational site (Coles Place) bias is considered to decrease by using an additional observation site (Woolston). MM5 version 3.7.3, WRF v2.1.2, and a new version of CAMx (4.31) are used to decrease modelling bias.

10.1 Winter 2006 high PM_{10} episodes

As was discussed in Chapter 8 winter 2006 was colder and with much higher night–morning peaks of aerosol pollution. Table 7.1 gives PM_{10} ($\mu g\ m^{-3}$) averaged statistics for winter 2005 (1 May-10 June 2005) and winter 2006 (10 June-15 July 2006) obtained for the Coles Place observation site over a 45-day time period PM_{10} concentrations were 1.5-1.7 times higher for winter 2006 compared with winter 2005. June-July 2006 total PM hourly averaged concentrations ($\mu g\ m^{-3}$, TEOM samplers) are presented in Figure 10.1 for Coles Place (blue line) and Woolston (red line). This time period included all 8 episodes (black arrows) that were evaluated using the MM5/WRF-CAMx numerical modelling system for different aerosol chemical scenarios.

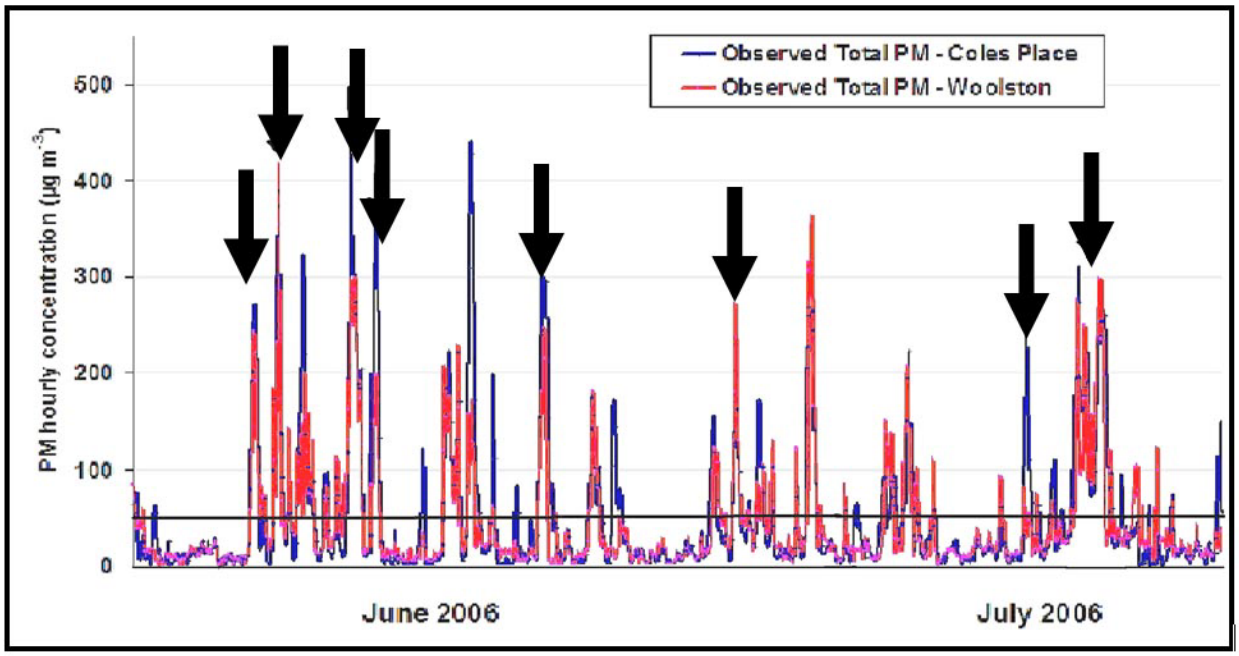

Figure 10.1 Observed hourly averaged PM_{10} concentrations (µg m^{-3}) for 1 June –10 July 2006 for Coles Place (blue line) and Woolston (red line) observational sites. Parallel black line shows WHO 24-hour PM_{10} concentration limit.

For 8 chosen aerosol pollution episodes the highest PM_{10} hourly concentrations were equal to 491.10 and 416.72 µg m^{-3} for Coles Place and Woolston sites respectively. Total PM averaged over the 40-day time period were: Coles Place - 54.1 µg m^{-3}; Woolston – 46.6 µg m^{-3}. It should be noted that Woolston and Burnside observational data have been kindly provided by Watercare (who operated this site for the Ministry for the Environment). The position of the Woolston site being in the residential area of Christchurch is fairly close to the seashore (east from the city centre) and a little bit apart from the inner city so that PM_{10} hourly peak concentrations should be less (compared with Coles Place ambient data) because of more active nocturnal near-surface air circulation. PM_{10} data were routinely measured for Woolston and for Burnside by two methods: application of a TEOM sampler (Woolston) and the BAM (Beta Attenuation Monitoring – Chakrabati et al., 2004) method (Burnside). PM data obtained by the BAM method were not used in the bias reduction research as they are incompatible with TEOM observations for the Coles Place observational site.

Six of eight winter 2006 episodes were working days that allowed simulation of near-surface air circulation and pollution patterns with the highest proportional contribution from domestic, transport and industry groups. Over all 8 winter 2006 episodes the dominance of the local air

circulation over synoptic scale air processes was a result of the weak pressure gradient over the South Island of New Zealand. Figure 10.2 presents geopotential height of the 850 hPa surface obtained from 6-hourly NCEP/NCAR reanalysis data (site http://www.cdc.noaa.gov/Composites/Hour/) for midnight of episode 1 (on 6 June 2006 – Figure 10.2a), episode 3 (on 10 June 2006 – Figure 10.2b), episode 7 (on 17 June 2006 – Figure 10.2c) and episode 5 (on 11 July 2006 – Figure 10.2d). All four figures are saved directly from NOAA site, the appearance of these figures including contour intervals are prepared by NOAA/NCAR on-line special procedure and beyond any corrections. Anticyclonic southwesterly circulation is presented in case of episodes 2 and 3 (Figure 10.2 a, b), cyclonic trough in case of episode 7 (Figure 10.2c) and north-westerly air circulation in case of episode 5 (Figure 10.2 d), with low pressure gradients over the South Island for the boundary layer atmospheric circulation (850 hPa), except Figure 10.2c where more active synoptic scale processes were evident. Approximately the same (as in Figure 10.2 a, b & d) low gradient synoptic situation with dominance of the local circulation processes were observed for the other 4 winter 2006 episodes.

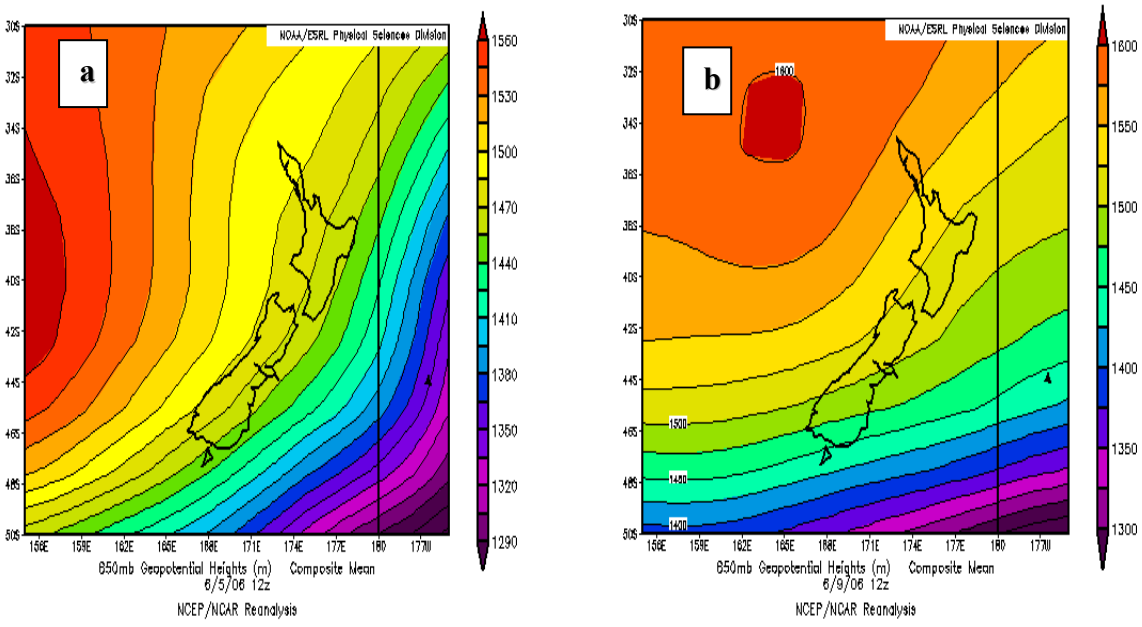

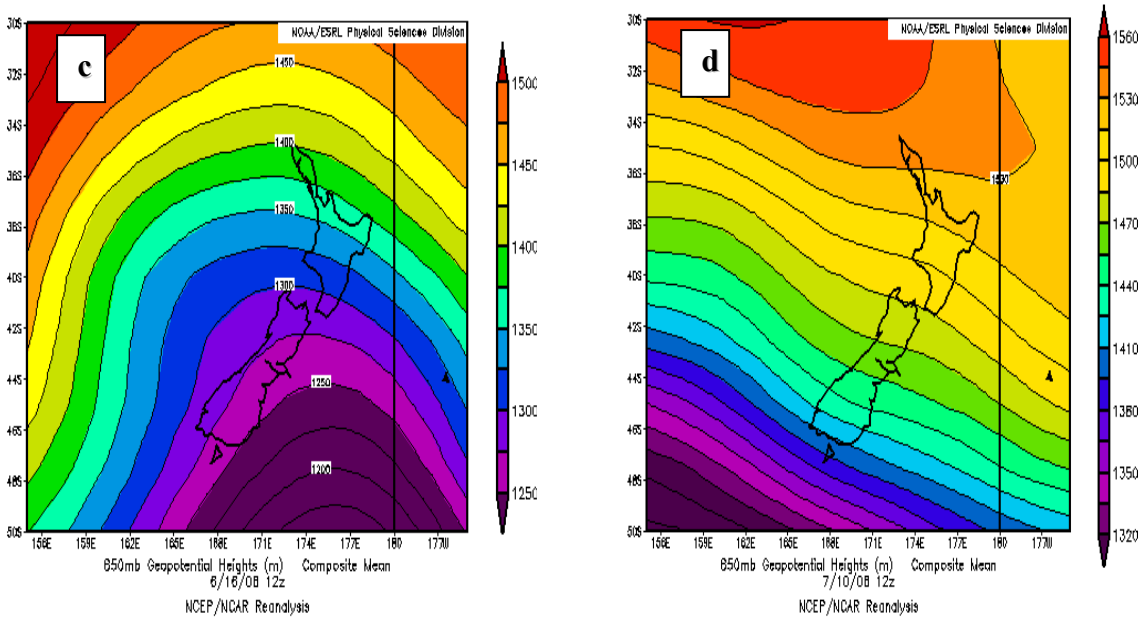

Figure 10.2 Geopotential height distribution over New Zealand at midnight at 850 hPa from 6-hourly NCEP/NCAR reanalysis for 4 winter 2006 episodes: a) episode 1 - 6 June 2006; b) episode 3 - 10 June 2006; c) episode 7 - 17 June 2006; d) episode 5 - 11 July 2006.

Figure 10.3 shows backward trajectories for the Christchurch area end point, calculated over 48 hours for levels 500, 1000 and 1500 metres with application of on-line HYSPLIT 4 Lagrangian model for midnight of episode 1 (0000 NZST 6 June 2006 – Figure 11.2a), episode 3 (0000 NZST 10 June 2006 – Figure 11.2b), episode 7 (0000 NZST 17 June 2006 – Figure 11.2c) and episode 5 (0000 NZST 11 July 2006 – Figure 11.2d). Figure 10.3 and Figure 10.2 make it evident a weak synoptic scale air circulation over the Christchurch area for chosen episodes with the regional scale winds mostly from the sea in the lowest 1500 meters layer. Also Figure 10.3a, Figure 10.3b and Figure 10.3d prove the local origin (or local scale origin) of the total PM emissions as the boundary layer air passes over a clean sea-land surface without any aerosol emission sources (especially during winter time). This fact is important to stress while considering emission sources inside the Christchurch city. The only exclusion could be episode 7, when geopotential field (Figures 10.2c) and 48-hour back-trajectories (Figure 10.3c) show more complex trajectories and stochastic mixing of the PBL air on its way to the Christchurch area over the Southern Island. Such a mixing can potentially increase crustal and primary species investment in a coarse fraction of the total PM.

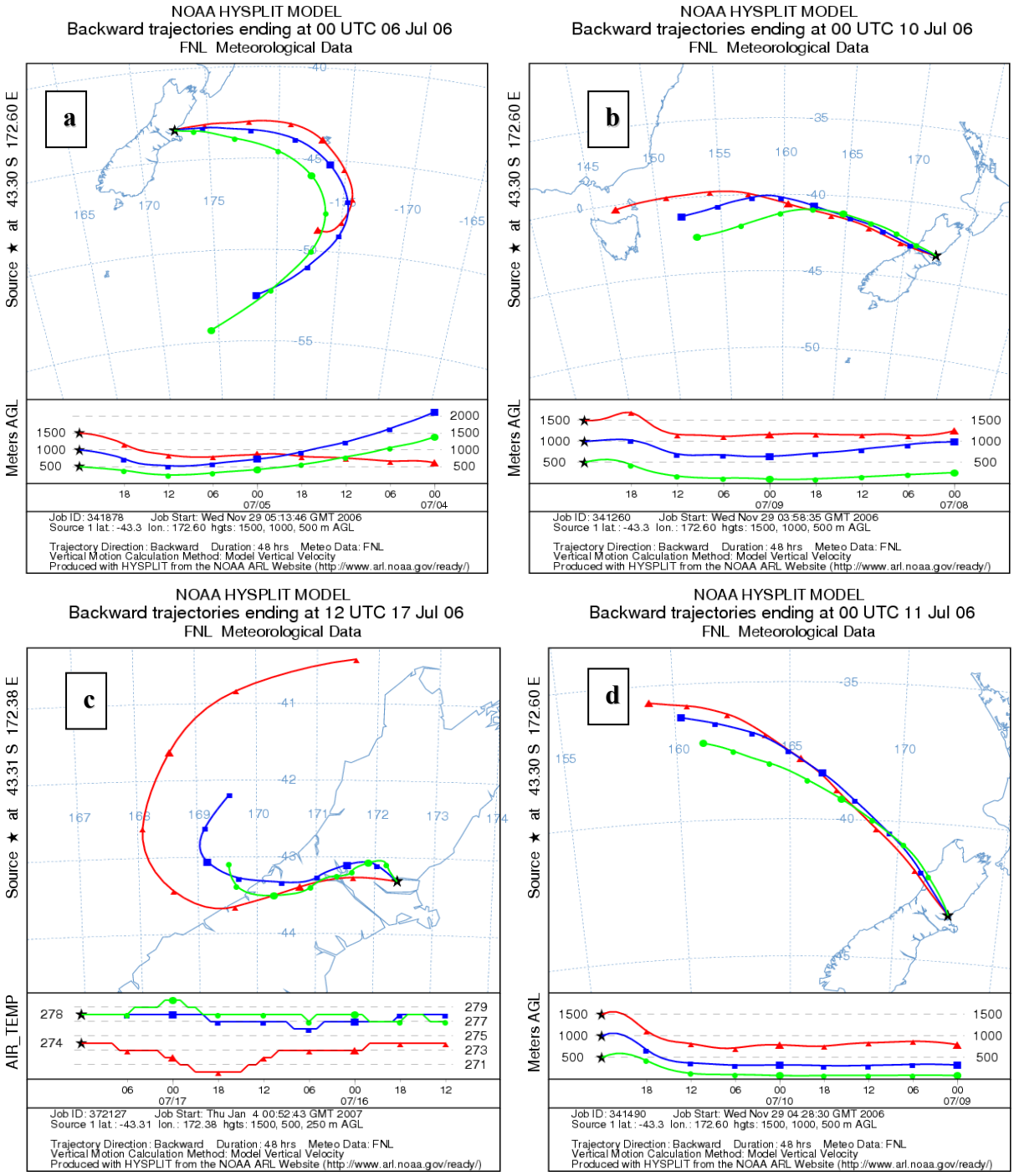

Figure 10.3 48-hour back-trajectories ending in the Christchurch area calculated from HYSPLIT 4 for 500, 1000 and 1500 m levels for 4 winter 2006 episodes: a) episode 1 - 6 June 2006; b) episode 3 - 10 June 2006; c) episode 7 - 17 June 2006; d) episode 5 - 11 July 2006.

10.2 Seasonal, observational and numerical bias reduction

As the main aim of the winter 2006 experiment is a reduction of the chemical scenarios method accumulated systematic bias it is useful to split the total bias into groups. The total bias consists of seasonal bias being a result of using only winter 2005 ambient data, of observational bias being a

result of observations from one site, and of numerical bias being a result of application of numerical modelling system MM5 v3.6.1 – CAMx v4.2. The quality of the input gridded emissions plays a vital role in the accumulated systematic bias (Baertch-Ritter et al., 2003; Brulfert et al., 2006; Miller et al., 2006), but gridded emissions will be evaluated in Chapter 11 with an assessment of the 1999 inventory by assessment of the input gridded emissions separately in the "Domestic", "Transport", and "Industry" groups (and in the "Total" group) using hourly emissions for every group. For observational-numerical bias reduction it is preferable to use the same gridded emissions that were used in the method of scenarios investigation.

To reduce the subjectivity and systematic error of the method all five composed chemical scenarios (4 primary chemical scenarios and complex scenario 1-3mix) are evaluated for 8 winter 2006 (June–July) heavy pollution episodes. Evaluation of the second winter season (2006 against 2005) will allow reduction of the seasonal bias. Observational bias also was presumed to originate from use of co-located measurements from one site resulting in observational systematic error. This error will be decreased as a result of using data from 2 differently located observational sites. MM5 version 3.7.3, WRF v2.1.2, and a new version of CAMx (4.31) allow comparison of two new versions of the numerical modelling system: MM5 MPP v3.7.3-CAMx4.31 and WRF v2.1.2-CAMx4.31. The use of these two additional numerical modelling systems will help to decrease modelling bias. This procedure as a first step allows an inter-comparison of the near-surface meteorology for MM5 MPP and ARW WRF and Coles Place meteorological data (Woolston and Burnside PM_{10} data didn't include any meteorology).

Coles Place and Woolston PM_{10} data validation

PM_{10} concentration data were obtained using TEOM from Coles Place and Woolston sites, and using BAM from Burnside in Christchurch and should be analyzed with application of basic statistics as there was no calibration between these three sites. Table 10.1 shows basic statistics for 45-day time interval (June–July 2006 – see Figure 10.1) including Pearson correlation coefficient (PCC) between aerosol ambient data obtained from Coles Place, Woolston and Burnside sites.

Table 10.1 Basic statistics (including Pearson correlation coefficient – PCC) for winter 2006 45-day period (1 June-15 July 2006) PM_{10} ambient data, extracted from Coles Place, Woolston and Burnside observation sites. Coles Place and Woolston means TEOM (FDMS) observations, and Burnside means thermo BAM observations.

Statistics	Mean	Standard deviation	Min	Max	PCC Coles – Woolston	PCC Coles – Burnside	PCC Woolston – Burnside
PM_{10} – Coles Place	54.06	76.88	0.33	491.10	0.800	0.877	
PM_{10} – Woolston	46.58	59.88	0.72	416.72	0.800		0.698
PM_{10} – Burnside	44.74	59.35	-7.00	371.49		0.877	0.698

First of all, Table 10.1 statistics show much higher temporal variability for one site than spatial variability between three observation sites. This result is described in many works (Hoek et al., 2002; Gehrig and Buchmann, 2003; Duan et al., 2006) and speaks about the same local origin of PM_{10} for both sites inside the same airshed for the city of Christchurch. It is remarkable that PCC for Coles Place - Burnside (BAM) is higher than for Coles Place-Woolston time series obtained by TEOM samplers (0.800). The BAM has been designated as the USA EPA Equivalent Method for 24-h PM_{10} measurements. In this study BAM is considered as the reference for continuous total PM measurements over another continuous monitor – the Tapered Element Oscillating Microbalance with Filter Dynamics Measurement System (TEOM FDMS, Ruppercht & Patashinck Co.Inc). Previous field investigations (Chakrabarti et al., 2004) showed that performance of the BAM was in excellent agreement with total (and fine) PM obtained with application of the filter-based Federal Reference Method. It was not affected by particle composition or meteorological conditions, outperformed TEOMs and nephelometers, and thus seemed to be a suitable candidate for deployment in real-time continuous PM_{10} and $PM_{2.5}$ monitoring. However, the negative minimum PM_{10} concentration and much lower maximum values for Burnside suggest either a faulty BAM sampler, or faulty initial calibration of the instrument. Better PCC for Coles Place – Burnside speaks about the same PM dispersion pattern for 2 points.

Table 10.2 shows basic statistics over a 45-day period (June–July 2006) including Pearson correlation coefficient (PCC) and Index of Agreement (IOA) between PM_{10} ambient data obtained

from Coles Place, Woolston and Burnside sites for the 7pm-7am time interval as 12-hour time period with maximum concentrations of ambient PM.

Table 10.2 Basic statistics (including PCC and IOA) over the winter 2006 45-day period (1 June-15 July 2006) PM_{10} ambient data, extracted from Coles Place, Woolston and Burnside observation sites for the 7pm-7am time interval. Coles Place, Woolston means TEOM observations, Burnside means thermo BAM observations.

Statistics	Mean	Standard deviation	Min	Max	PCC (IOA) Coles – Woolston	PCC (IOA) Coles – Burnside	PCC (IOA) Woolston – Burnside
PM_{10} – Coles Place	135.36	96.39	10.90	491.10	0.671 (0.723)	0.790 (0.815)	
PM_{10} – Woolston	102.10	79.21	5.23	416.72	0.671 (0.723)		0.545 (0.673)
PM_{10} – Burnside	103.78	76.34	3.83	371.49		0.790 (0.815)	0.545 (0.673)

Once again PCC between Coles Place and Burnside (0.790) is higher than between two TEOM time series for Coles Place and Woolston (0.671). This event is quite consistent as peak values contribute most to the Pearson correlation coefficient. Also Coles Place and Burnside are both inland from the city centre, and use to measure PM_{10} concentrations from co-located aerosol dispersion patterns. The negative background values for BAM (Burnside) potentially diminished PM_{10} peak concentrations and supported the decision to use TEOM observation data only (Woolston, Coles Place).

MM5 MPP v3.7.3 and ARW WRF v2.1.2 comparison

To decrease the meteorological model systematic error (bias), the latest versions of MM5 MPP (v3.7.3) and ARW WRF (v. 2.1.2) were employed to simulate all 8 winter 2006 episodes. All episodes were evaluated using input data from the NCEP 83.2 global dataset for the mother and 3 nested grids. Four grids were chosen for accurate air circulation modelling over the South Island and Christchurch areas with spatial resolutions of 27 km, 9 km, 3 km and 1 km. The appropriate description of all parameters was given in Chapter 8 (Section 8.1).

Episodes 2-3 (4 days–96 hours) are used to compare calculated near-surface meteorology from MM5 and WRF with observations obtained from the Coles Place site (there were no meteorological observations at Woolston site). Basic meteorology includes wind speed, wind

direction, relative humidity, and temperature (in ^{0}C) at 1 and 10 metres. Wind rose diagrams and basic statistics for all 8 episodes will be shown, but spatial plots are not used for inter-comparison as WRF output plotting interface is in early phases of development and MM5/WRF visualisation options on the University's high performance computer very restricted.

Winter 2006 episodes 2-3 basic statistics calculated for the Coles Place observation site are presented in Table 10.3. It should be noticed that MM5 MPP was run using the bulk Land-Surface Model (LSM1) as there was no possibility to run sensitive studies for WRF urban LSM. For all 8 episodes WRF was run with default physical-dynamical parameterisation that was quite close to the parameterisation in MM5, as WRF had inherited default physical parameterization from MM5 optimal parameterization. The absence of sensitivity studies using WRF physical and dynamical options presumably decreased the level of accuracy of the WRF output near-surface meteorology.

From Table 10.3 it is evident that WRF tends to over-predict mean, fluctuations and maximum values of the wind speed compared to MM5 (all output results are provided for domain 4 – 1 km spatial resolution). Also, in near-surface layer WRF has a tendency to over-predict mean 1-metre and 10-metre temperature, and under-predict relative humidity compared with MM5 and observations. The calculated WRF near-surface meteorology with the highest IOA for temperature (0.66-0.68) and the lowest values for wind (0.33) and relative humidity (0.25) doesn't offer much hope for reproducing PM_{10} concentration very accurately. Wind speed and wind direction (Table 10.3) were calculated in Excel using an equation to transform U-V calculated values in wind speed-direction. However it is important to note of that low quality near-surface WRF modelled meteorology doesn't change the possibility to engage WRF (as a new limited area meteorological model) to decrease the modelled bias being a result of MM5 usage only.

Table 10.3 Index Of Agreement (IOA), Pearson's Correlation Coefficient (PCC), Systematic & Unsystematic Root Mean Square Error (S- & U-RMSE), and additional statistics of observed and modelled data for 8–12 June 2006 (Coles Place site), episodes 2-3 for MM5 MPP and WRF v2.1.2: near-surface wind, 1+10 metre temperature and relative humidity.

PISODE 4	NUMBER OF TIME POINTS	OBSERVED MEAN	MODELLED MEAN	OBSERVED DEVIATION	MODELLED DEVIATION	PCC	OBSERVED MAX	MODELLED MAX	IOA
WIND SPEED (m s^{-1})									
MM5 MPP	190	1.42	2.12	1.05	0.87	0.67	4.4	6.0	0.71
WRF v2.1.2	190	1.42	3.59	1.05	2.06	0.35	4.4	9.0	0.33
WIND DIRECTION (^{0})									
MM5 MPP	190	181.57	213.28	97.05	82.07	0.76			0.78
WRF v2.1.2	190	181.57	228.36	97.05	86.07	0.37			0.45
TEMPERATURE (^{0}C) – 1 m									
MM5 MPP	190	7.25	8.02	5.86	3.40	0.90	17.9	14.7	0.92
WRF v2.1.2	190	7.25	9.50	5.86	3.03	0.63	17.9	14.4	0.66
TEMPERATURE (^{0}C) – 10 m									
MM5 MPP	190	8.78	9.21	4.80	3.27	0.89	17.3	16.5	0.90
WRF v2.1.2	190	8.78	10.33	4.80	2.37	0.65	17.3	14.5	0.68
RELATIVE HUMIDITY (%)									
MM5 MPP	190	73.91	71.06	18.67	11.56	0.73	98.8	90.0	0.71
WRF v2.1.2	190	73.91	61.95	18.67	12.10	0.13	98.8	93.0	0.25

In Figure 10.4 modelled near-surface 2-metre wind speed (Figure 10.4a) and direction (Figure 10.4b) time series from MM5 (green line) and WRF (blue line) outputs are compared with the observed wind (red line) obtained for the Coles Place site (96-hour time period 8-12 June 2006). Figure 10.4 displays a good agreement between MM5 MPP modelled and ambient wind through for 3-day forecast except on 10 June, when modelled wind speed was too strong (Figure 10.4a) and MM5 failed to reproduce the observed wind direction rapid changes (Figure 10.4b). WRF wind magnitude is characterized by abrupt increases of wind speed during day-time (Figure 10.4a), but quite adequate reproduction of wind direction change (Figure 104b) that suggests that about WRF may be able to reproduce the local scale air circulation regime.

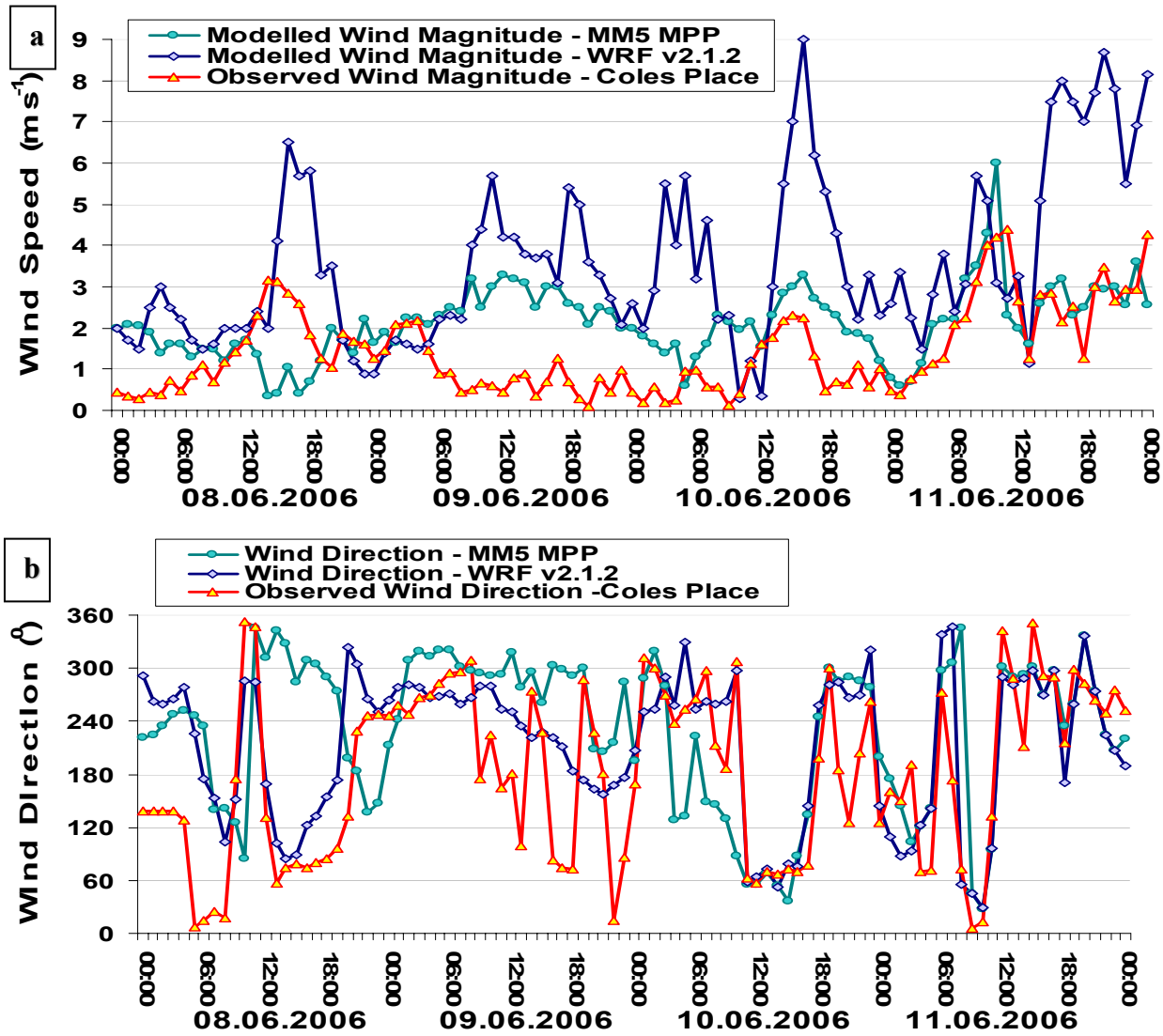

Figure 10.4 Modelled MM5 MPP (green line) and WRF v2.1.2 (blue line) and observed (red line) near-surface wind for episodes 2-3, domain 4, from 00 NZST on 8 June 2006 to 00 NZST on 12 June 2006 (Coles Place site): a) wind speed; b) wind direction.

Figure 10.5 shows wind roses plotted for time period 6-14 June 2006 (episodes 1-3) using MM5 modelled wind data (Figure 10.5a) and WRF modelled data (Figure 10.5b) for level 10-12 meters above ground level (AGL). WRF mean wind speed is much higher than MM5 wind speed but the directions of the predicted local scale circulation are very close for two models (see Figure 10.4b).

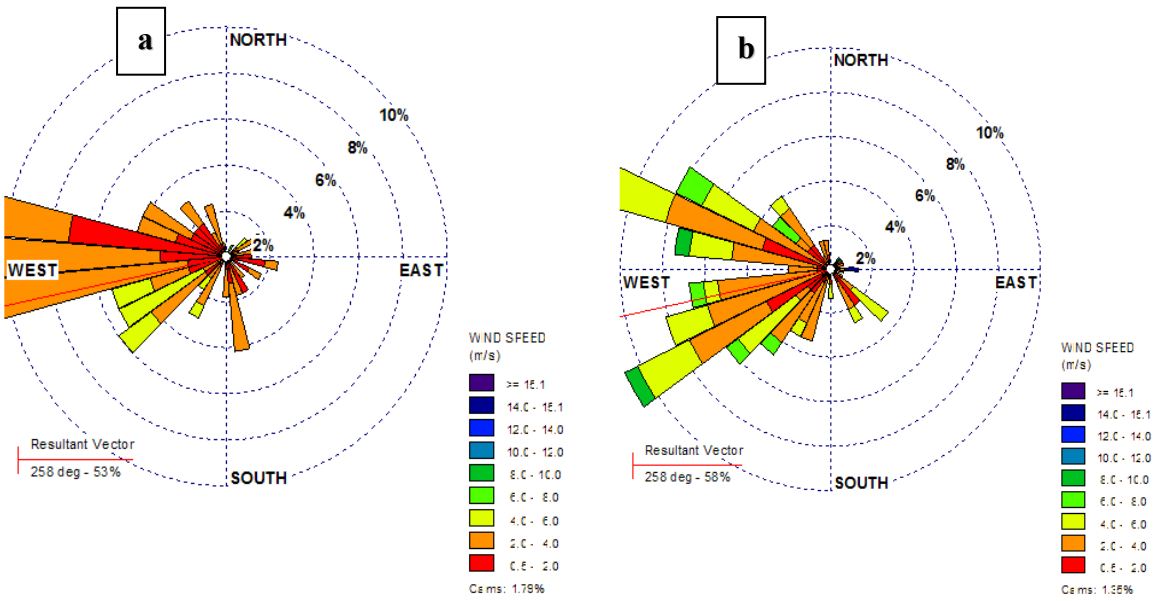

Figure 10.5 Modelled wind roses averaged for the period 6-14 June 2006 (episodes 1-3) for 10-12 m AGL, at Coles Place: a) MM5 MPP, domain 4; b) WRF v2.1.2, domain 4.

The wind fields presented in Figure 10.6 are from MM5 and WRF runs for domain 4 σ-level=0.998 (10–12 metres AGL) for 18 NZST on 10 June 2006. An on-shore breeze is evident over Christchurch for MM5 (Figure 10.6a) and strong westerly winds are evident for the WRF run (Figure 10.6b).

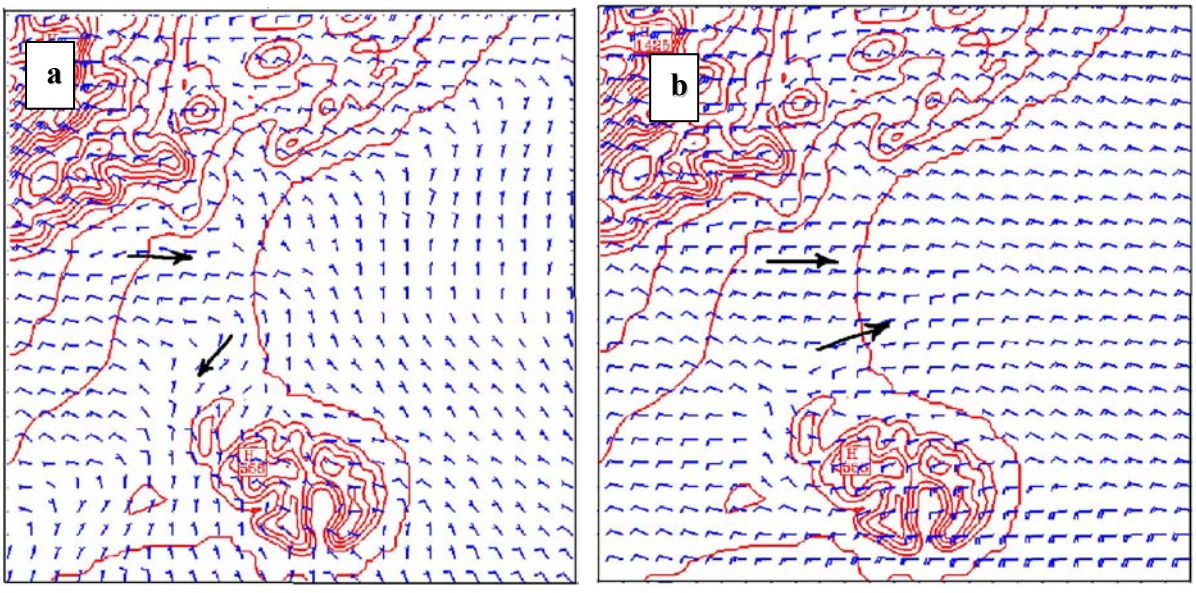

Figure 10.6 Spatial distribution of modelled near-surface wind for episode 3 (winter 2006), σ = 0.998 (10-12 metres), 1800 NZST on 10 June 2006 (137-hour forecast): a) MM5 MPP v3.7.3 domain 4; b) ARW WRF v2.1.2 domain 4.

The ability of MM5 and inability of WRF to reproduce real near-surface air circulation for 18 NZST 10 June 2006 time point (see Figure 10.4) is evident for the spatial wind distribution over

the Christchurch area. The day-time on-shore breeze is well developed in MM5, but is substituted by synoptic-scale westerly circulation in the case of WRF.

Figure 10.7 presents modelled 1 metre temperature (Figure 10.7a) and 10 metre temperature (Figure 10.7b) obtained from MM5 output (green line) and WRF (blue line) output, compared with the observed 1 metre and10 metre temperature (red line) obtained for the Coles Place site (96-hour time period 8-12 June 2006). Figure 10.7 shows the ability of the MM5 and WRF models to reproduce a general day-night trend of the near-surface temperature, showing much better agreement between MM5 and observations than between WRF and observations. For WRF one can see night time increase of modelled temperature for both 1 metre (Figure 10.7a), and 10 metre temperature (Figure 10.7b). This night heat influx could be explained by too strong night winds (see Figure 10.4a) that destroy the near-surface inversion and bring warm air downward to the near-surface cold layer. Definitely, MM5 MPP demonstrates better results, but also under-predicts the temperature extreme values, especially for night-time, weakening the modelled (compared with observed) near-surface temperature inversion.

Figure 10.8 presents modelled 2-metre relative humidity (RH) calculated using MM5 (green line) and WRF (blue line) compared with the observed 2-metre relative humidity (red line) obtained for Coles Place (96-hour time period 8-12 June 2006). MM5 shows good skills in reproduction of the observed RH (Figure 10.8) and managed to catch 4 of 5 night-time RH peaks and only over-predicted the last night's relative humidity. Changeable RH time trend on 11 June 2006 is a result of activation of the synoptic-scale air circulation over the Christchurch area (see Figure 10.4 and 10.7). WRF model has failed to reproduce the observed RH time-trend on the first 2 days showing a negative correlation (Figure 10.8) with observations. WRF modelled RH tendency improved after 2 days of the model evaluation, which suggests that a 24- 48-hour spin up period is required for WRF runs.

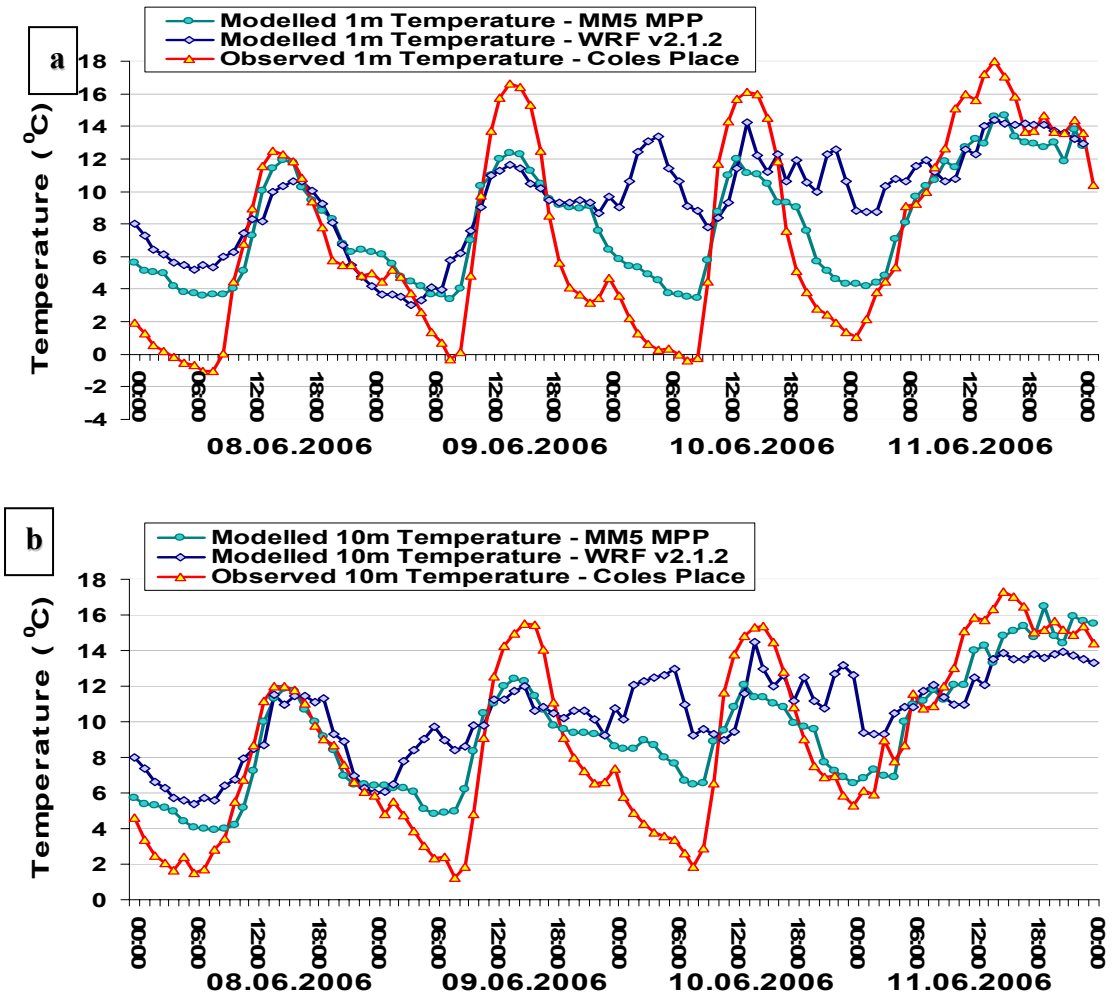

Figure 10.7 Modelled MM5 MPP (green line) and WRF v2.1.2 (blue line) and observed (red line) near-surface temperature (^{0}C) for episodes 2-3, domain 4, for time period 00 NZST 8 June 2006 - 00 NZST 12 June 2006 (at Coles Place): a) 1-metre temperature; b) 10-metre temperature.

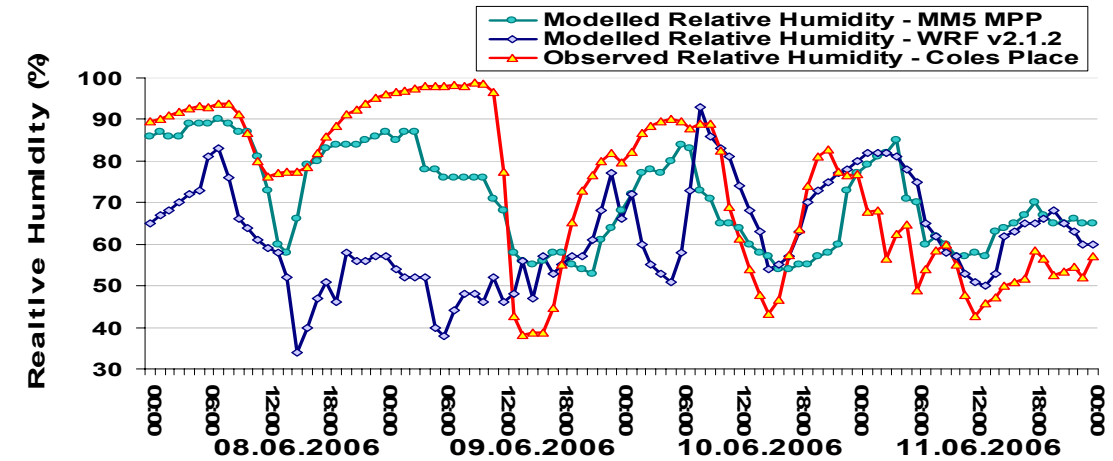

Figure 10.8 Modelled MM5 MPP (green line) and WRF v2.1.2 (blue line), and observed (red line) 2-meter relative humidity (%) for episodes 2-3, domain 4, for time period 00 NZST 08 June 2006 - 00 NZST 12 June 2006 (Coles Place).

The ability of WRF v2.1.2 to reproduce accurately near-surface winter-time local-scale circulation over complex terrain of the Christchurch area is very limited compared with MM5 MPP. High modelled wind speeds will lead to dispersion of the emitted aerosol and to an abrupt decrease of the night-time primary and morning secondary PM concentration peaks. Over-estimated night temperature and under-estimated relative humidity will suppress the process of secondary organic and ionic aerosol species production during night time. According to these results, WRF modelled near-surface meteorology will be used only for complex 1-3mix chemical scenario inter-seasonal evaluation only, and not will be used to assess the ability of the numerical modelling system (meteorological model – photochemical model) to reproduce observed PM_{10} temporal-spatial trends (8 winter 2006 smog episodes).

CAMx4.31-CAMx4.4 aerosol chemistry and input emissions

CAMx versions 4.31-4.4 provided the following additional capabilities and features over previous versions described in Chapters 6-7.

- PM chemistry and Particle Source Apportionment Technology (PSAT) have been added to the PiG sub-model. As part of this change, PiG now includes dry and wet deposition. Also, two PiG algorithms have been fully unified, and Greatly Reduced Execution and Simplified Dynamics GREASD) PiG continues to treat only early inorganic chemical reactions in large NO_x plumes;
- Model speed has been increased by revising the time step calculation approach. The maximum allowable time step has been increased for the Bott advection algorithm because it has demonstrated numerical stability for CFL (Courant–Friedreich–Levy) criteria near 1;
- CAMx4 can now optionally write concentration fields to HDF5 (high density format) files following the conventions of the Regional Atmospheric Modeling System (RAMS). Both core model and probing tool fields can be written in HDF, for both computational and PiG sampling grids. Use of HDF requires that HDF5 libraries have been installed and built on the machine that is running the CAMx Makefile;
- The output average, deposition, and surface fields for each grid (computational and PiG sampling) are now separately output to individual files in the standard format, which is consistent with the formats of the CAMx input emissions, input initial conditions, and master grid output format;
- The SAPRC chemical mechanism has been enhanced to include three additional optional species: Ethanol (ETOH), Methyl Tertiary Butyl Ether (MTBE), and Methylbutenol (MBUT),

and gas-phase reactions involving these species. The SAPRC99 chemistry parameters file now uses molecular units for reaction rate parameters;

- The Integrated Processes Rate (IPR) component of PA has been updated to include aerosol chemistry and PM species (ENVIRON, 2006).

The changes and improvements are not considered to be very important, but for re-evaluation of winter 2006 5 chemical scenarios the Piecewise Parabolic Method (PPM) advection solver (instead of Bott) and Implicate-Explicate Hybrid (IEH) chemistry solver (instead of fast chemistry CMC solver) were used (CAMx versions 4.31 and 4.40) to vary the solver mechanisms regarding to the former ones employed in the previous versions of CAMx (ENVIRON, 2004; ENVIRON, 2006). Input gridded emissions (for groups "Domestic", "Transport", "Industry" and "Total") used in the winter 2006 experiment were the same ones exploited for the winter 2005 study. Absence of spatial emissions in the 2002 inventory (the Christchurch area was split into three areas only – see Figure 4.5) made it difficult to prepare new gridded emissions for total PM. However, in Chapter 11 linear and non-linear evaluation of gridded emissions for all 4 groups that was undertaken to assess validity of the inventory 1999 gridded aerosol emissions.

10.3 Evaluation of Scenario 1-3mix against Scenarios 1-4

For inter-seasonal evaluation of the method of chemical scenarios all 4 basic scenarios and the complex chemical scenario 1-3mix (described in Chapter 9) were studied for eight heavy smog episodes in June-July 2006. To exclude the influence of the input modelled near-surface meteorology on an assessment of the best fit chemical scenario two limited-area meteorological models (MM5 MPP v3.7.3 and ARW WRF v2.1.2) were employed. To decrease a single photochemical model chemical-numerical parameterization influence on a quality of the modelled ambient PM concentrations spatial-temporal distribution a new version of CAMx4 model was run. For all 8 winter episodes only CAMx version 4.4 was used, as CAMx version 4.31 in control runs made no difference in the output results to compare with CAMx4.2. All together 80 runs of the MM5-CAMx4 and the WRF-CAMx4 numerical modelling systems were done to assess the method of scenarios, and to decrease the seasonal and numerical bias of the method.

Numerical-statistical assessment

For an assessment of the 5 chemical scenarios for winter 2006 only MM5 MPP-CAMx4 results are discussed as the WRF v2.1.2 output near-surface meteorology showed a poor agreement with observations (see Section 10.2). However, data obtained from numerical modelling system WRF-CAMx4 will be used in general statistical evaluation.

For every chemical scenario (including complex Scenario 1-3mix) scatterplots are plotted and linear regression parameters are calculated for all 8 winter episodes including about 19 days or about 500 hourly PM_{10} concentration values. Scatterplots were calculated for modelled PM_{10} against observed PM_{10} for two observation sites: Coles Place and Woolston. Values of total PM concentrations less than 5 μg m^{-3} were excluded from the time series as unreliable and corresponding to zero fine PM (see Table 9.7). Values with concentrations higher than 200 μg m^{-3} were also excluded to avoid numerical instability, which was described in Chapter 9 (especially for scenarios 1 and 2). Figure 10.9 presents modelled-observed PM_{10} scatterplots and linear regression calculated following application of CAMx4.4 and initial-nudging PM gridded emissions for 8 study episodes for Coles Place (Figure 10.9a) and Woolston (Figure 10.9b) ambient sites. Input-nudging emissions were split into chemical species according to Scenario 1 (see Table 9.1).

From Figure 10.9 it is evident that agreement between modelled and observed PM_{10} concentrations (correlation coefficient about 0.7-0.74) is not bad, especially for Coles Place. The regression coefficient (RC) is equal to 0.831 for Coles Place (Figure 10.9a) and 1.0624 for Woolston, but the linear regression intercept (INT) is positive and quite big, especially for Woolston. Figure 10.9 clearly shows underprediction of the ambient PM_{10} concentrations by the MM5 MPP-CAMx4.4 numerical system. This negative numerical bias, first of all is, a result of a much colder winter 2006 episodes with very high night-morning peaks of outdoor total PM.

Figure 10.10 presents modelled-observed PM_{10} scatterplot and linear regression calculated with application MM5-CAMx4.4 for 8 study episodes for Coles Place (Figure 10.10a) and Woolston (Figure 10.10b) observational sites. In this case, input-nudging emissions were split into chemical species according to Scenario 2 (see Table 9.1).

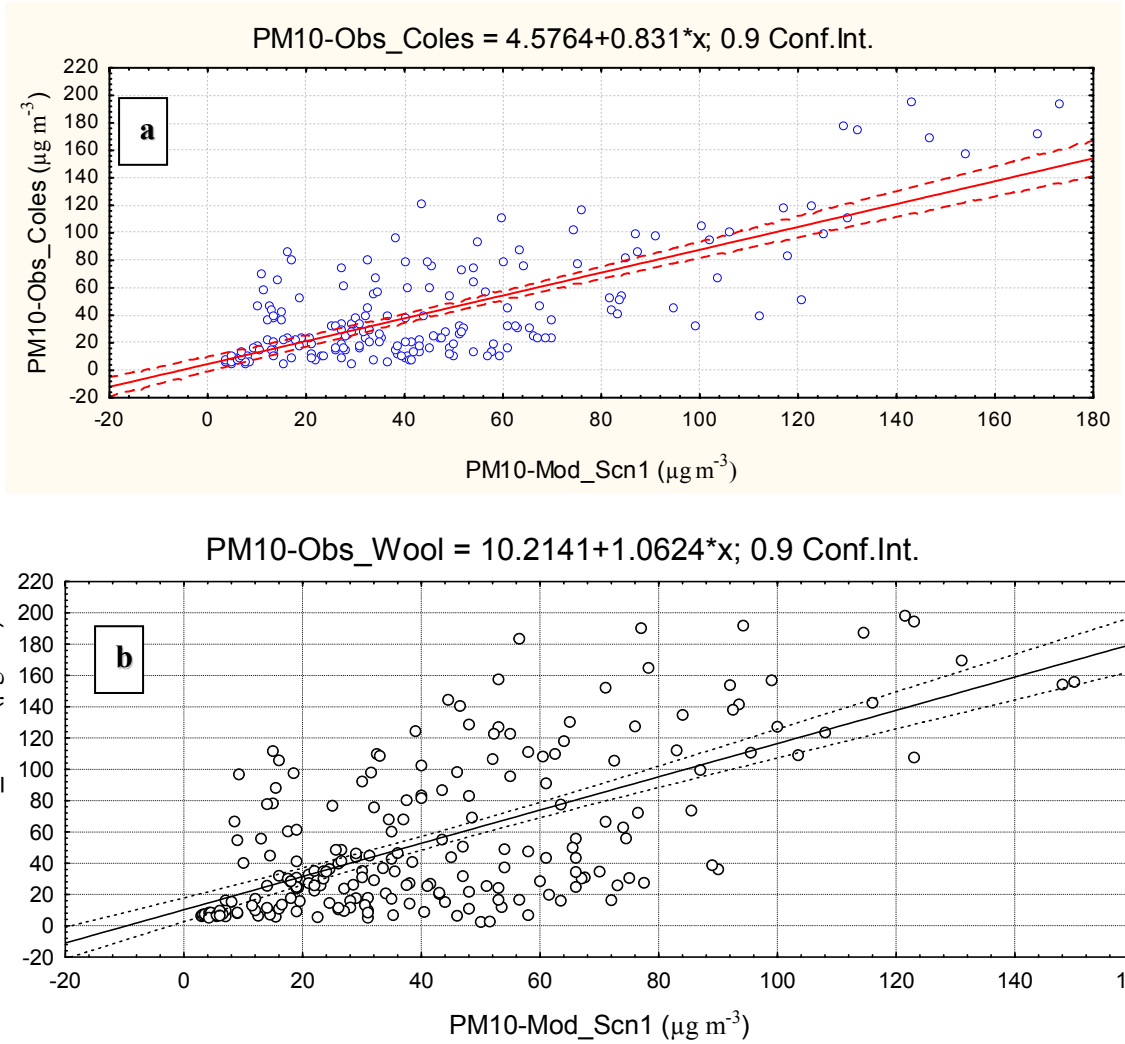

Figure 10.9 Scatterplot diagram and linear regression for modelled-observed PM_{10} concentrations (µg m^{-3}) for 8 winter 2006 episodes and Scenario 1 chemical split: a) Coles Place site; b) Woolston site.

Figure 10.10 demonstrates a quite low agreement between modelled and observed PM_{10} concentrations (correlation coefficient about 0.5-0.55), especially for Woolston. RC is equal to 0.5619 for Coles Place (Figure 10.10a) and 0.8099 for Woolston (Figure 10.10b), and INT is positive and large especially for Woolston. Figure 10.10 indicates considerable underprediction of ambient PM_{10} concentrations by MM5 MPP-CAMx4 in case of Scenario 2.

Figure 10.11 shows modelled-observed PM_{10} scatterplot and linear regression for 8 study episodes for Coles Place (Figure 10.11a) and Woolston (Figure 10.11b) observational sites. In this case, input-nudging emissions were split into chemical species according to Scenario 3 (see Table 9.1).

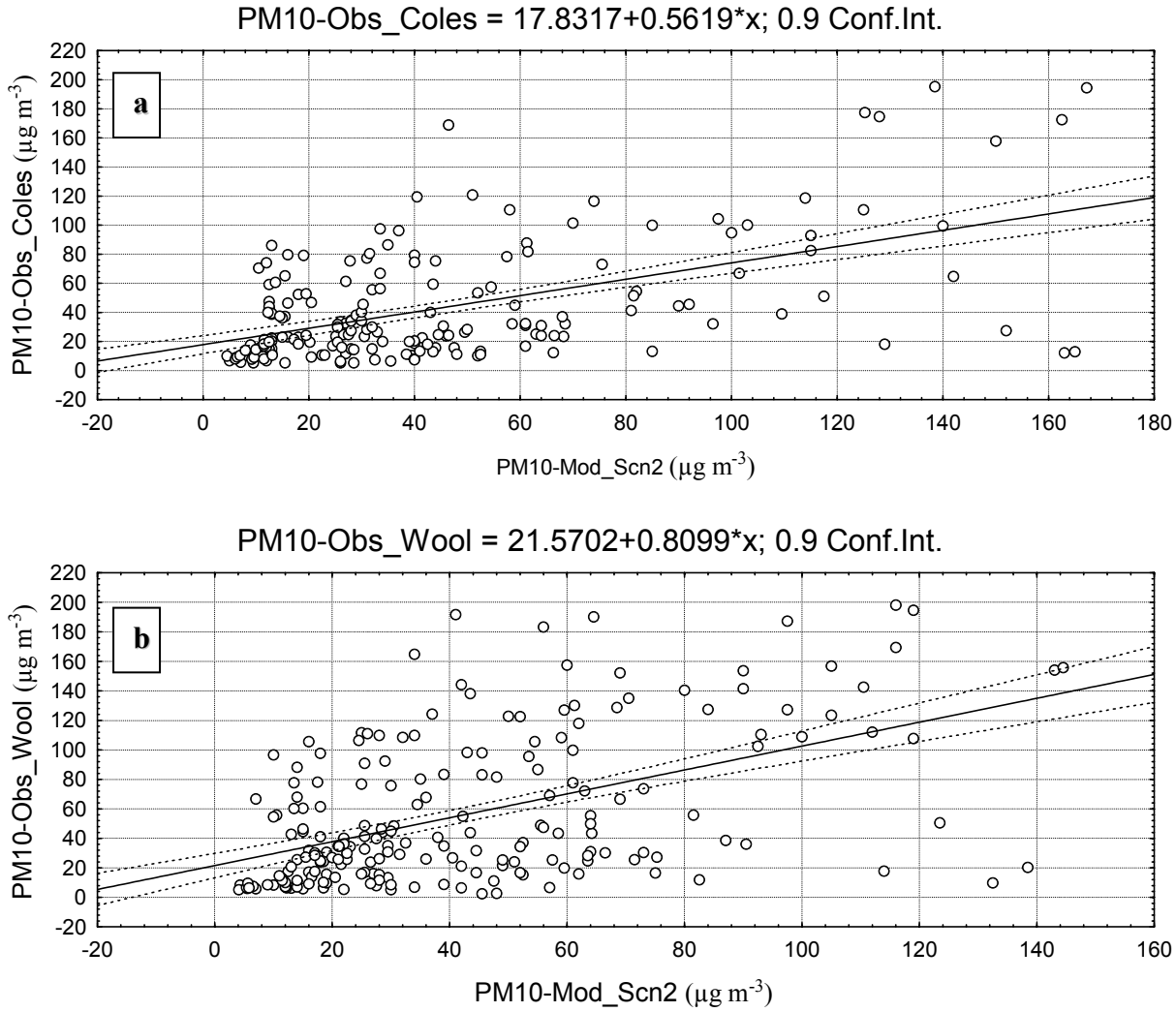

Figure 10.10 Scatterplot diagram and linear regression for modelled-observed PM_{10} concentrations (µg m^{-3}) for 8 winter 2006 episodes and Scenario 2 chemical species: a) Coles Place site; b) Woolston site.

Figure 10.11 demonstrates a quite good agreement between modelled and observed PM_{10} concentrations (correlation coefficient about 0.68-0.73), especially for Coles Place. RC is equal to 0.8735 for Coles Place (Figure 10.11a) and 1.0585 for Woolston (Figure 10.11b), INT is positive and smaller than in case of Scenario 2, especially for Woolston (12.14 against 21.57). From Figure 10.11 the underprediction of the ambient PM_{10} concentrations by MM5 MPP-CAMx4 is lower compared with Scenario 1, and particularly with Scenario 2. Slightly better results for the Coles Place site are explained by one site bias that is inherit in the method used only one site for the winter 2005 method of scenarios development.

Figure 10.12 shows a modelled-observed PM_{10} scatterplot and linear regression for winter 2006 episodes for Coles Place (Figure 10.12a) and Woolston (Figure 10.12b) observation sites. Input-nudging emissions were split into chemical species according to Scenario 4 (see Table 9.1).

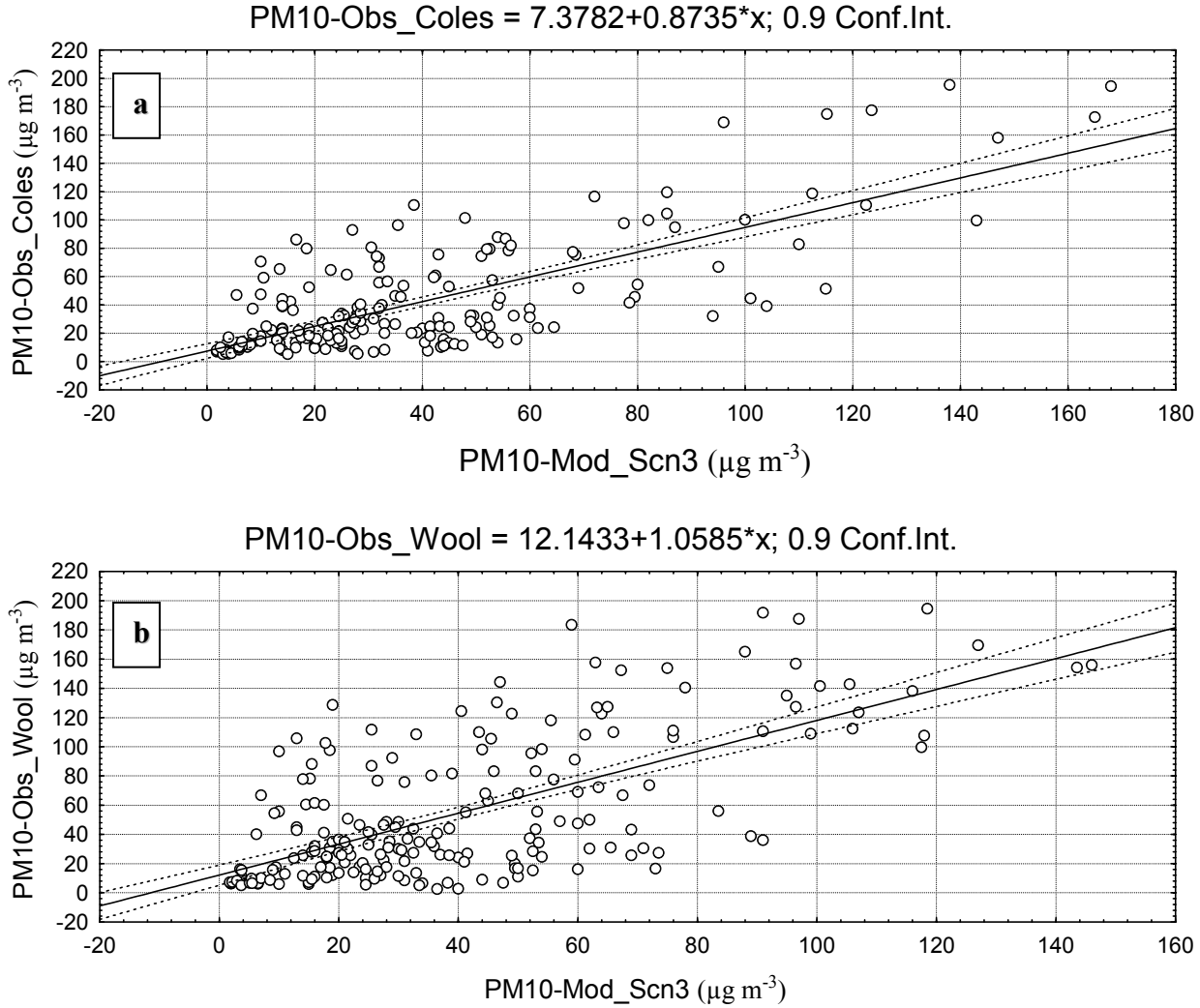

Figure 10.11 Scatterplot diagram and linear regression for modelled-observed PM_{10} concentrations (µg m^{-3}) for 8 winter 2006 episodes and Scenario 3 input emissions chemical split: a) Coles Place site; b) Woolston site.

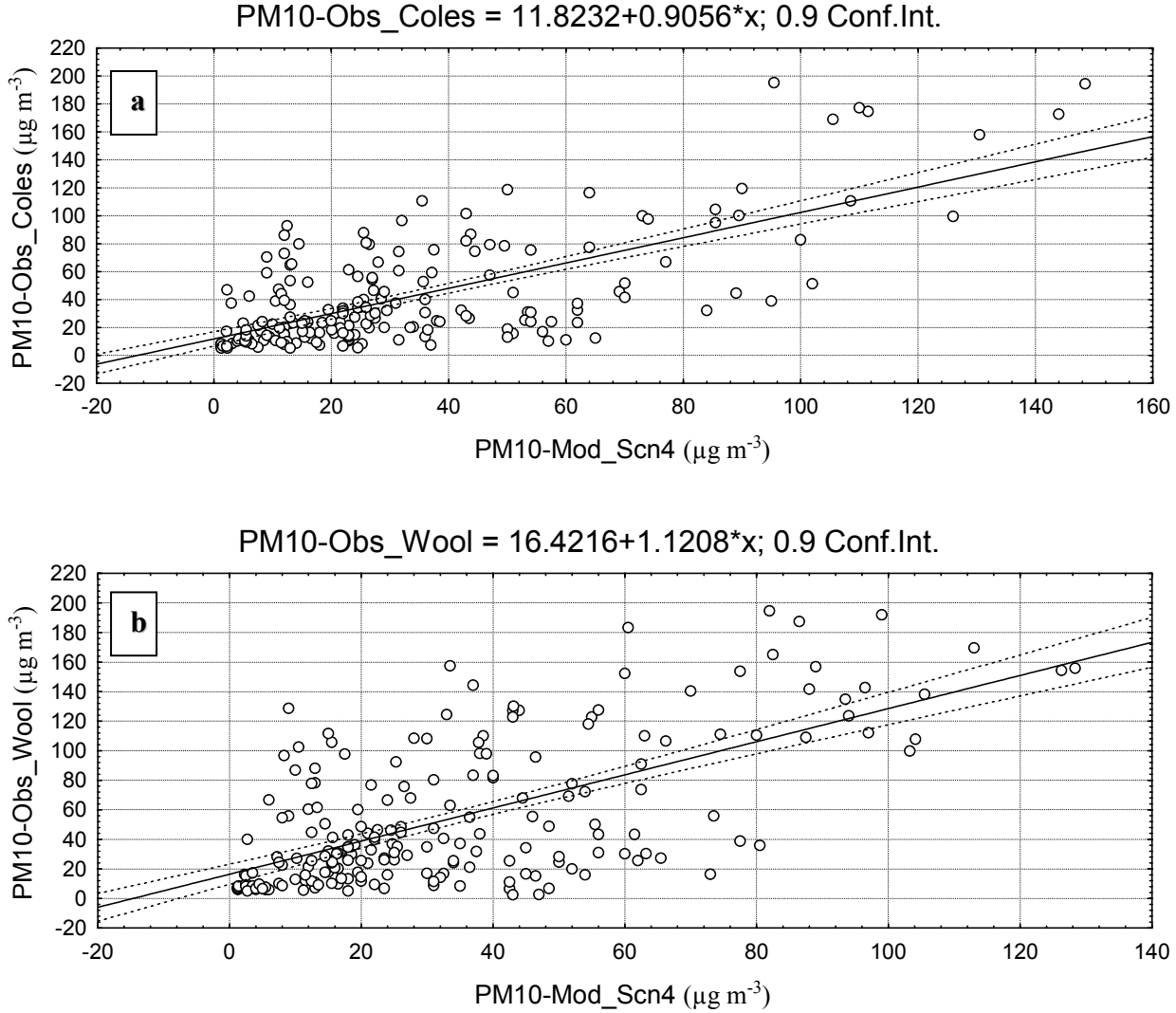

Figure 10.12 Scatterplot diagram and linear regression for modelled-observed PM_{10} concentrations (μg m^{-3}) for 8 winter 2006 episodes and Scenario 4 input emissions chemical split: a) Coles Place site; b) Woolston site.

Figure 10.12 demonstrates a reasonable agreement between modelled-observed PM_{10} concentrations (correlation coefficient about 0.64-0.68), but once again is better for Coles Place. RC is equal to 0.9056 for Coles Place (Figure 10.12a) and 1.1208 for Woolston (Figure 10.12b). Once again INT is positive and quite big: 11.82 for Coles Place and 16.42 for Woolston. Figure 10.12 shows underprediction of the ambient PM_{10} concentrations by MM5 MPP-CAMx4.

Figure 10.13 shows modelled-observed PM_{10} scatterplots and linear regression for winter 2006 episodes for Coles Place (Figure 10.13a) and Woolston (Figure 10.13b) observation sites obtained using the chemical species split according to complex Scenario 1-3mix (composed from scenario 1 and 3).

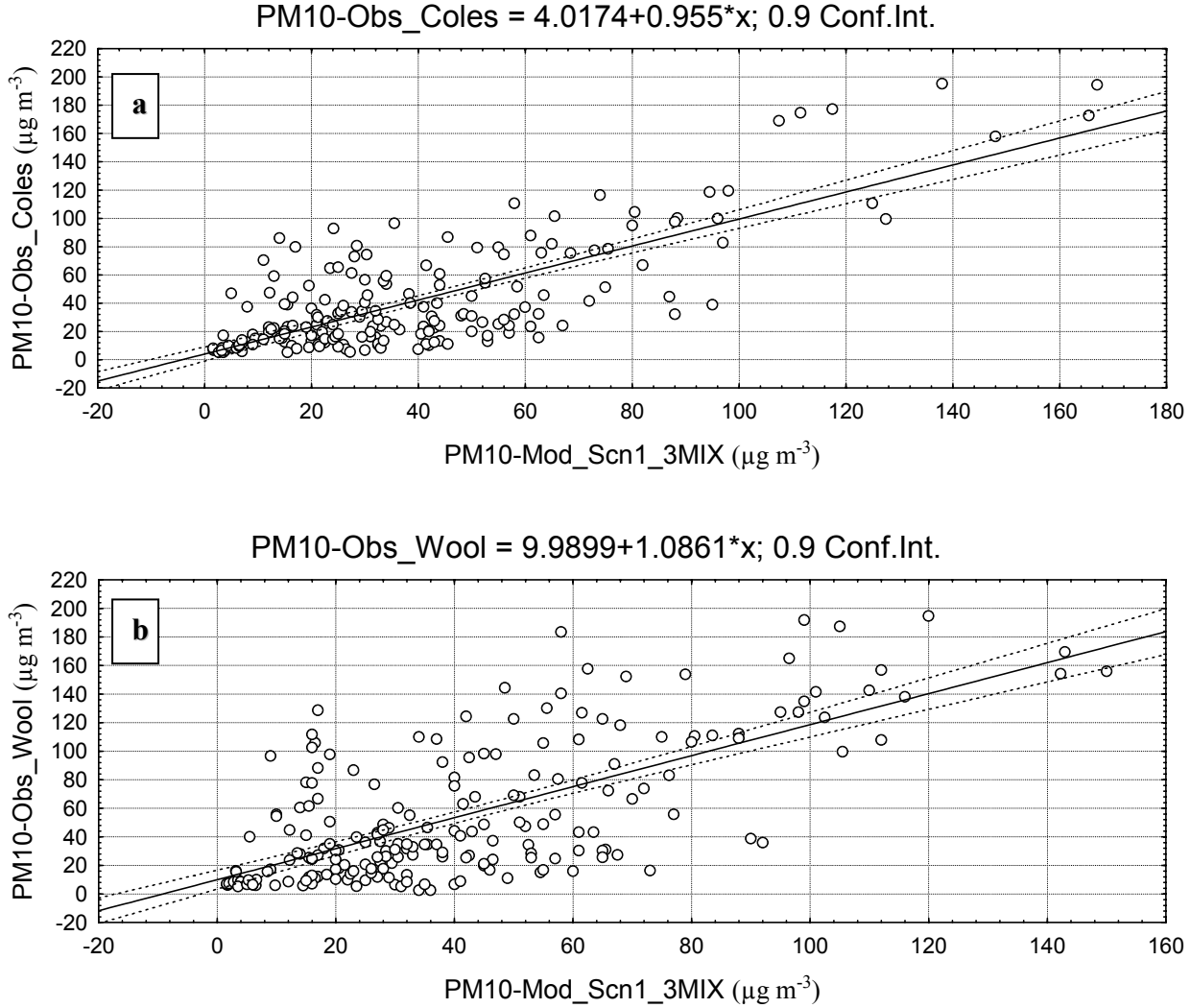

Figure 10.13 Scatterplot diagram and linear regression for modelled-observed PM_{10} concentrations (μg m^{-3}) for 8 winter 2006 episodes and Scenario 1-3mix input emissions chemical split: a) Coles Place site; b) Woolston site.

Figure 10.13 demonstrates the best agreement between modelled and observed PM_{10} concentrations (correlation coefficient about 0.70-0.76), especially for Coles Place. RC is equal to 0.955 for Coles Place (Figure 10.13a) and 1.0861 for Woolston (Figure 10.13b). INT is positive but quite small: 4.01 for Coles Place and 9.99 for Woolston. Figure 10.13 exhibits decrease of real aerosol concentration underprediction by MM5 MPP-CAMx4 compared with the other chemical scenarios (particularly compared with Scenario 2 and 4). The better results for Coles Place site can be explained by the tuning of the optimal chemical scenario based on the inner city Coles Place site. This bias is inherit in the method of using one site for winter 2005 studies, and this systematic error is overcome with the ambient data from an additional site.

The summary of the linear regression parameters (intercept and regression coefficient) derived for predicted and observed from modelled PM_{10} concentrations (Figure 10.9- Figure 10.13) is shown in Table 10.4 for all five chemical scenarios and two observational sites.

Table 10.4 Observed (modelled) PM_{10} linear regression intercept (INT), regression coefficient (RC) and Pearson Correlation Coefficient (PCC) for 5 chemical scenarios: winter 2006 8 smog episodes, MM5 v3.7.3-CAMx4.4.

Scenario	Observation Site	Linear regression: Intercept (R>0.98, P<0.01)	Linear regression: Coefficient (R>0.98, P<0.01)	PCC Observed – Modelled
Scenario 1	Coles Place	PM_{10}: 4.5764	PM_{10}: 0.8310	0.734
	Woolston	PM_{10}: 10.2141	PM_{10}: 1.0624	0.655
Scenario 2	Coles Place	PM_{10}: 17.8317	PM_{10}: 0.5619	0.545
	Woolston	PM_{10}: 21.5702	PM_{10}: 0.8099	0.511
Scenario 3	Coles Place	PM_{10}: 7.3782	PM_{10}: 0.8735	0.731
	Woolston	PM_{10}: 12.1433	PM_{10}: 1.0585	0.667
Scenario 4	Coles Place	PM_{10}: 11.8232	PM_{10}: 0.9056	0.694
	Woolston	PM_{10}: 16.4216	PM_{10}: 1.1208	0.641
Scenario 1-3mix	Coles Place	PM_{10}: 4.0174	PM_{10}: 0.9550	0.766
	Woolston	PM_{10}: 9.9899	PM_{10}: 1.0861	0.691

From Table 10.4 the best fit between modelled and observed (1 June–15 July 2006 time period) PM_{10} regression parameters was obtained for the complex Scenario 1-3mix for both Coles Place and Woolston observation sites.

Correlation statistics including Pearson Correlation Coefficient (PCC) and Index of Agreement (IOA) for winter 2005-2006 for all 5 chemical scenarios are presented in Table 10.5. The highest PCC and highest IOA belong to scenario 1-3 mix for both the first part of winter 2005 and the middle part of winter 2006.

Table 10.5 Pearson correlation coefficient (PCC) and Index of Agreement (IOA) for simulated (MM5-CAMx4) winter 2005 (first part) and winter 2006 (middle part) episodes: PM_{10} modelled data for all 5 scenarios was extracted for Coles Place and Woolston observation points.

PM_{10} Scenario	**MM5 – CAMx application:**	**Coles Place site**		**Woolston site**	
		PCC	**IoA**	**PCC**	**IoA**
Scenario 1	winter 2005	0.748	0.831	--	--
	winter 2006	0.703	0.820	0.765	0.806
Scenario 2	winter 2005	0.742	0.768	--	--
	winter 2006	0.715	0.702	0.638	0.675
Scenario 3	winter 2005	0.813	0.871	--	--
	winter 2006	0.725	0.766	0.798	0.784
Scenario 4	winter 2005	0.805	0.806	--	--
	winter 2006	0.732	0.778	0.802	0.782
Scenario 1-3 mix	**winter 2005**	**0.828**	**0.860**	**--**	**--**
	winter 2006	**0.778**	**0.840**	**0.817**	**0.811**

The statistics from Tables 10.5 help to illustrate the superiority of the complex Scenario 1-3mix over the initial Scenarios 1-4 for winter 2005, and similarly for winter 2006 after reduction of the systematic error including numerical, seasonal, and spatial bias.

Spatial variability and the best fit scenario

To finalize the winter 2006 research Table 10.6 is presented to compare basic statistics for the modelled data (including mean, standard deviation, minimum and maximum concentrations, Index of Agreement, and Pearson correlation coefficient) obtained for the MM5-CAMx4 and the WRF-CAMx4 numerical systems with ambient data from the Coles Place and Woolston observation sites for the complex Scenario 1-3mix. Calculations were done for all 8 winter episodes (19 days or about 500 hourly PM_{10} concentration values).

Table 10.6, first of all, shows the advantage of MM5 (over WRF) modelled near-surface meteorology for reproducing PM_{10} dispersion for winter 2006 heavy pollution episodes. Inter-comparison of the Tables 10.2 (observed PM_{10}) and 10.5 (modelled PM_{10}) indicates a clear tendency to underpredict observed total aerosol (negative bias) for average (64.85 against 135.36), and maximum peaks (280.25 against 491.10) for both the Coles Place, and for Woolston sites. But this underprediction could not be considered to be long trend representative one, as from "Weather highlights of 2006" (Meteorological Society of New Zealand, 2007) it is reckoned that June 2006

was the coldest June since winter 1972. So, additional winter seasons are needed to stabilize prediction bias for fine and/or total PM.

Table 10.6 Averaged model statistics (MM5-CAMx and WRF-CAMx) for 8 episodes (1 June-15 July) in winter 2006: PM_{10} modelled concentrations ($\mu g\ m^{-3}$) extracted for Coles Place and Woolston observation sites (chemical Scenario 1-3mix).

Statistics	Mean	Standard deviation	Min	Max	PCC (IOA) Coles Place – Woolston (modelled)	PCC (IOA) Coles Place – Coles Place (Mod.–Obs.)	PCC (IOA) Woolston – Woolston (Mod.-Obs.)
MM5 MPP v3.7.3 – CAMx v4.41							
PM_{10} – Coles Place	64.85	51.75	1.6	280.3	0.952 (0.981)	0.735 (0.795)	
PM_{10} – Woolston	60.75	42.55	1.6	224.5	0.952 (0.981)		0.665 (0.775)
WRF ARW v2.1.2 – CAMx v4.41							
PM_{10} – Coles Place	47.75	44.50	0.55	153.4	0.974 (0.986)	0.565 (0.532)	
PM_{10} – Woolston	38.65	37.25	0.45	144.5	0.974 (0.986)		0.505 (0.544)

The complex Scenario 1-3mix, as an optimal chemical split of CAMx4 input gridded emissions, was constructed and validated for two winter seasons to reduce systematic error in the method of scenarios. It is remarkable that PM_{10} spatial correlation between observation sites is lower than the modelled PM_{10} spatial correlation (maximum 0.792 from Table 10.2 against 0.974 from Table 10.6). So the winter 2006 experiments raise a question about the possible spatial variability of the best fit chemical scenario, as from Table 10.6 it is evident that the modelled correlation between two different sites is too high. Initially, complex Scenario 1-3mix was created as a temporal complex scenario only, and consisted of day-time chemical scenario 1 and night-time chemical scenario 3. This was a result of the aerosol data accessed from one observation site only. A possibility to create a complex chemical scenario (that varies with both space and time the contribution of Scenarios 1 and 3 at every spatial point) is considered to be a constructive additional potential of the method of scenarios, and also encourages installation of additional observational sites. This problem will be discussed in regards to optimisation of observation site locations in Chapter 13.

10.4 Summary

A method of several chemical scenarios was used to establish the chemical composition of the calculated $PM_{2.5}$-PM_{10} concentration that is the best fit with the measured $PM_{2.5}$-PM_{10} concentration. The Mesoscale Model (MM5) and the Eulerian air pollution model (CAMx4) were used to evaluate dispersion of $PM_{2.5}$ (PM_{10}) over a 48-72 hour time period for Christchurch, May–June (winter) 2005. To reduce the method's accumulated systematic bias all 5 chemical scenarios (including scenario 1-3mix) are evaluated for eight winter 2006 (June–July) heavy smog episodes to eliminate seasonal bias of the method. The observation site (Coles Place) bias is decreased by using an additional observation site (Woolston). MM5 MPP version 3.7.3, WRF v2.1.2, and a new version of CAMx (4.4) are used to decrease deterministic system bias.

Correlation statistics for winter 2005-2006 for all 5 chemical scenarios (presented in Table 10.5) shows that the highest PCC and IOA are associated with Scenario 1-3mix for the first part of winter 2005 and the second part of winter 2006. Figure 10.14 presents fractional bias-FB (Smith et al., 2006) of the modelled PM_{10} compared with observed PM_{10} (Coles Place observation site) for winter 2005 (blue line) and winter 2006 (green line) high air pollution episodes.

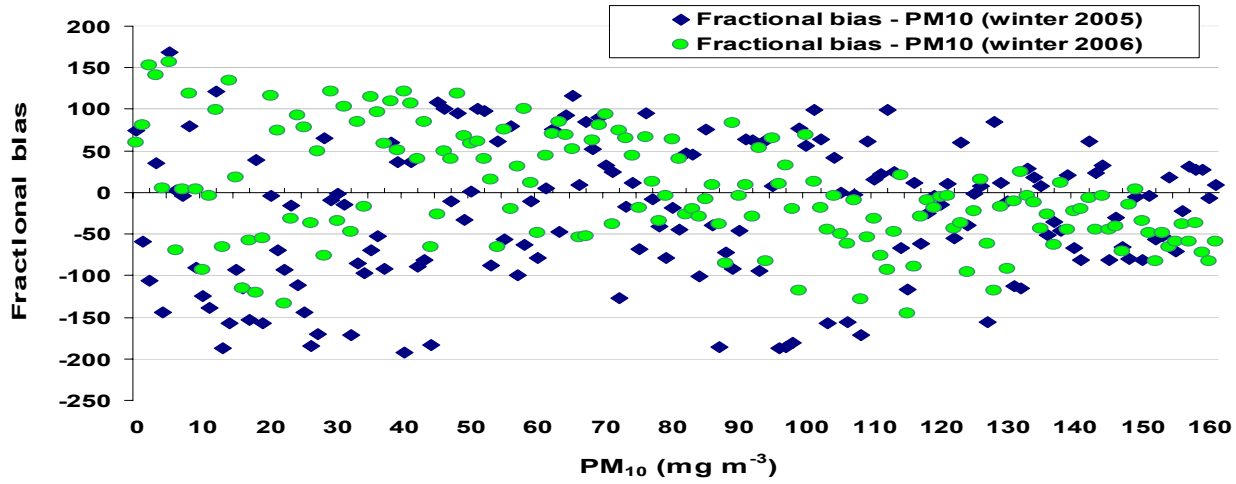

Figure 10.14 Fractional bias (FB) of the modelled PM_{10} compared with observed PM_{10} for 7 winter 2005 (blue dots) and 8 winter 2006 (green dots) heavy smog episodes (Coles Place).

MM5-CAMx4 numerical modelling system demonstrates better skills in prediction high PM_{10} concentrations as the range of FB gets narrower and tends toward zero as PM_{10} concentrations increase. FB for winter 2006 has a negative skewness for big values of aerosol that exhibits underprediction of PM_{10} peak concentrations for very cold nights in June-July 2006.

PART D: APPLICATIONS

Chapter 11: Assessment of human exposure to PM

Assessment of human exposure to PM will be considered using the numerical modelling system MM5 v3.7.3 MPP – CAMx4.4 for chemical Scenario 1-3mix, and on the basis of gridded emissions from "Domestic", "Transport", "Industry", and "Total" groups obtained from the inventory 1999.

11.1 Inventory 1999 evaluation for Scenario 1-3mix

Application and validation of the best fit chemical Scenario 1-3mix provides big possibilities in using basic species of the Scenario 1-3mix chemical composition to vary percentages for each individual component. This ability to change the ratio of species in PM allows future research on proposed reduction of aerosol concentrations, as a result of the proposed decrease of aerosol emissions. In all applications MM5 modelled near-surface meteorology (bulk LSM) for 7 smog episodes in winter 2005 will be used as a background, as synoptic-local scale meteorological conditions from May-June 2005 are considered to be much closer to long-term average winter ambient air conditions (and to conditions of winter 2000 – CAPS2000 experiment) than the severe conditions of June-July 2006. Also, it is easier to work with numerically reproduced PM spatial and temporal distributions for the proposed chemical Scenario 1-3mix reduction options, when the systematic error (compared with observed ambient PM) is low, and there is no serious bias of the modelled PM data (see Figure 10.14) that could distort the results.

Evaluation of the 1999 inventory is very important as the emission data obtained for all four pollution groups must be reliable to be applied to proposed PM reduction scenarios. To verify the 1999 inventory two methods of 50% reduction of fine ($PM_{2.5}$) and total (PM_{10}) emissions from domestic and vehicular sources are applied: non-linear reduction and linear reduction. Group "Industry" will be used in these experiments without any changes from the 2002 inventory (Scott, 2005) industrial aerosol emissions level, which is presumed to be constant from 1999 (1027201 g day^{-1} over the central Christchurch area) to 2006 (1026432 g day^{-1})

11.1.1 Non-linear approach

A 50% non-linear reduction of fine ($PM_{2.5}$) and total (PM_{10}) emissions from domestic and vehicular sources could be achieved by a 50% decrease for selected individual chemical

components (in Scenario 1-3mix) that are considered to contribute up to 85-90% of the aerosol pollution during night ("Domestic" scenario) and day ("Transport" scenario) time periods, producing an overall reduction a little less than 50% (only particulate sulphate considered to be an essential specie of local industry). It should be stressed that a non-linear reduction in the groups "Domestic" (7pm-6am) or "Transport" (7am-6pm) is a reduction for a 12-hour time interval only. In the case of the combined reduction in "Domestic+Transport" group, the 50% decrease is produced for all 24 hours of a day.

Non-linear 50% reduction of the "Domestic-Transport" emissions involves 50% level of decrease of each of the carbonaceous species and inorganic soluble ions (except particulate sulphate PSO_4) in Scenario 1-3mix for day-time (7am-6pm – "Transport" group) and night-time (7pm-6am – "Domestic" group). It is logical to consider first 50% emissions reduction that in the "Transport" group is applied to Scenario 1 only (day-time scenario of the complex Scenario 1-3mix):
PEC (50%) = PEC /2;
POA (50%) = POA /2;
SOA1–4 (50%) = (SOA1–4) /2;
PSO_4 (50%) = PSO_4 – no change;
PNO_3 (50%) = PNO_3 /2;
PNH_4 (50%) = PNH_4 /2;
CCRS, FCRS - Scenario 1 doesn't include these species;
PCL, NA – Scenario 1 doesn't include these species (see List of acronyms and Abbreviations).

Sulphates are considered to be mostly pollutants emitted by the industry sector and are not reduced. It is important to keep in mind that in CAMx4.4 the number of aerosol species is restricted to 13 (including particulate water) chemical components, and it is very difficult to relate SOA1-4 to one emission source during day-time. Fortunately secondary organic aerosols play a secondary role in construction of Scenario 1. Table 11.1 shows basic statistics (modelled-observed average, mean absolute error and correlation coefficient) for modelled PM_{10} and $PM_{2.5}$ in the "Total" group (100%), and in the "Total" group with a 50% non-linear transport emissions reduction evaluated against ambient observations (Coles Place site).

Table 11.1 Average (modelled – observed), Mean Absolute Error (MAE), Pearson Correlation Coefficient (PCC) and Power Correlation Coefficient (Power CC – Pearson in power 2), 7 episodes average, complex Scenario 1-3mix, total and fine PM (μg m^{-3}): 50% non-linear transport emissions reduction.

Modelled PM	AVERAGE Mod. – Obs.	MAE	PCC	Power CC
PM_{10} - 100%	37.50 – 54.25	6.15	0.75	0.56
$PM_{2.5}$ – 100%	34.75 – 42.30	5.92	0.73	0.53
PM_{10} – 50% (transport)	33.55 – 54.25	15.15	0.75	0.56
$PM_{2.5}$ – 50% (transport)	29.05 – 42.30	14.85	0.76	0.57

Table 11.1 exhibits a small decrease of average PM concentration and a little better agreement of the reduced PM time series with observations for the reduced PM time series. A 50% emissions reduction in the "Domestic" group is applied to Scenario 3 only (night-time scenario of the complex Scenario 1-3mix):

PEC (50%) = PEC *0.75 (half of night PEC is considered to be inherited from day transport);

POA (50%) = POA /2;

SOA1–4 (50%) = (SOA1–4) /2;

PSO_4 (50%f) = PSO_4 – no change;

PNO_3 (50%) = PNO_3 /2;

PNH_4 (50%) = PNH_4 /2;

CCRS, FCRS, PCL, NA – no change (see List of acronyms and Abbreviations).

Once again, sulphates are considered to be an essential pollutant of the industry sector and are not reduced. Crustal elements and dust particles are considered to have only natural origin and are kept without change; particulate chloride and sodium are also considered to have a natural source (sea spray). Secondary Organic Aerosols are considered to originate principally from the "Domestic" emission group, as average transport-industrial activity is lower during night-time to compare with day-time. But still the night-time period (7pm-6am) includes a part of afternoon rush-time. Table 11.2 presents modelled and observed averages, mean absolute error and correlation coefficient for modelled PM_{10} and $PM_{2.5}$ in the "Total" group (100%), and in the "Total" group with 50% non-linear domestic emissions reduction evaluated against ambient observations (Coles Place site).

Table 11.2 Average (modelled - observed), Mean Absolute Error (MAE), Pearson Correlation Coefficient (PCC) and Power Correlation Coefficient (Power CC), 7 episodes average, complex Scenario 1-3mix, total and fine PM (μg m^{-3}): 50% non-linear domestic emissions reduction.

Modelled PM	AVERAGE Mod. – Obs.	MAE	PCC	Power CC
PM_{10} - 100%	37.50 – 54.25	6.15	0.75	0.56
$PM_{2.5}$ – 100%	34.75 – 42.30	5.92	0.73	0.53
PM_{10} – 50% (domestic)	28.15 – 54.25	21.35	0.71	0.51
$PM_{2.5}$ – 50% (domestic)	22.85 – 42.30	17.65	0.70	0.49

For a non-linear domestic emissions reduction Table 11.2 shows a significant decrease of the average PM concentrations, and a better agreement of the initial PM time series with observations compared with the non-linear reduced PM time series. Combined "Transport" + "Domestic" group 50% emissions reduction is applied to Scenario 1 only for day-time (7am-6pm) and to Scenario 3 only for night-time (7pm-6am). The percentage variation for each individual chemical component for each scenario is as described before. In Table 11.3 are exhibited modelled-observed average, mean absolute error and correlation coefficient for modelled PM_{10} and $PM_{2.5}$ in the "Total" group (100%), and in the "Total" group with 50% non-linear domestic-transport emissions reduction (50% domestic & transport) evaluated against ambient observations (Coles Place site).

Table 11.3 Average (modelled-observed), Mean Absolute Error (MAE), Pearson Correlation Coefficient (PCC) and Power Correlation Coefficient (Power CC), 7 episodes average, complex Scenario 1-3mix, total and fine PM (μg m^{-3}): 50% non-linear domestic and transport emissions reduction.

Modelled PM	AVERAGE Mod. – Obs.	MAE	PCC	Power CC
PM_{10} - 100%	37.50 – 54.25	6.15	0.75	0.56
$PM_{2.5}$ – 100%	34.75 – 42.30	5.92	0.73	0.53
PM_{10} – 50% (domestic & transport)	23.05 – 54.25	24.75	0.71	0.51
$PM_{2.5}$ – 50% (domestic & transport)	19.15 – 42.30	19.25	0.69	0.48

Table 11.3 shows a significant decrease of the average total and fine PM modelled concentration, although this time a better agreement with observations is found for the modelled PM time series without non-linear reduction. From Table 11.3 it is evident that non-linear 50% reduction in 2 emission groups decreased average values for modelled PM_{10} by 39% and for $PM_{2.5}$ by 45% from the initial modelled aerosol concentrations. Most part of the modelled aerosol decrease is a result of the 50% reduction in "Domestic" group (see Tables 11.1 and 11.2).

11.1.2 Linear approach

A 50% linear reduction in emissions of fine ($PM_{2.5}$) and total (PM_{10}) aerosol from domestic and vehicular sources can be achieved by dividing the domestic and/or transport emissions obtained from the Christchurch 1999 inventory of Environment Canterbury (Scott and Gunatilaka, 2004) by a factor of two. As linear reduction in the groups "Domestic' or/and "Transport" means a linear reduction in the "Total" group the linear reduction procedure involves arithmetic manipulations of 2-dimensional arrays of gridded PM emissions. Linear reduction of PM emissions in any group means a reduction for all 24 hours of a winter day as any group emissions are split into 4 time intervals only and these intervals (6am-10am, 10am-4pm, 4pm-10pm, and 10pm-6am) don't coincide with day-time (7am-6pm – Scenario 1) and night-time (7pm-6am – Scenario 3) periods of the non-linear reduction scheme. Consequent decrease of PM emission values at every grid point for the gridded emissions used for CAMx4.4 initialisation and hourly nudging is applied.

A 50% reduction is based on the predicted change in total aerosol emissions between year 1999 (inventory year) and year 2005 (year of winter meteorology) suggested by ECan (Scott and Gunatilaka, 2004; Scott, 2005) for the inner area of the city of Christchurch (area about 17,680 ha). Table 11.4 shows group emissions for years 1999 and 2005 calculated in grams $area^{-1}$ day^{-1}. The decrease of emissions is different for "Domestic" and "Transport" groups but was made equal to 50% (close to "Total" group reduction) in both groups; as it is impossible to properly separate domestic emissions from transport ones in a non-linear reduction method.

Table 11.4 PM_{10} emissions in groups "Domestic", "Transport", "Industry" and "Total": 1999 and 2005 for the inner area of Christchurch city (after ECan forecast). Emissions are given in grams $area^{-1}$ day^{-1} (where area= 17,680 ha).

GROUP	1999	2005	2005/1999
Domestic			
Emissions	8340845.0	4124524.7	0.494
Motor Vehicles	1115365.0	782348.9	0.701
Industrial	1027021.0	1006763.9	0.980
Total	**10483231.0**	**5913637.5**	**0.564**

A process of a linear 50% reduction of the vehicular emissions includes two times decrease of PM_{10} and $PM_{2.5}$ emissions in "Transport" group, and subsequent adding of the "Domestic", "Transport"/2 and "Industry" emissions to prepare fine and total PM emissions for the "Total"

group. A 50% reduction of the transport emissions is applied to all 24 hourly values of the day. Table 11.5 presents modelled-observed average, MAE and correlation coefficient for modelled PM_{10} and $PM_{2.5}$ in "Total" group (100%), and in "Total" group with 50% linear transport emissions reduction (50% linear-transport) evaluated against Coles Place observations.

Table 11.5 Average (modelled-observed), Mean Absolute Error (MAE), Pearson Correlation Coefficient (PCC) and Power Correlation Coefficient (PCC*PCC), 7 episodes average, complex Scenario 1-3mix, total and fine PM ($\mu g\ m^{-3}$): 50% linear transport emissions reduction.

Modelled PM	AVERAGE Mod. – Obs.	MAE	PCC	Power CC
PM_{10} – 100%	37.50 – 54.25	6.15	0.75	0.56
$PM_{2.5}$ – 100%	34.75 – 42.30	5.92	0.73	0.53
PM_{10} – 50% linear-transport	32.25 – 54.25	12.85	0.75	0.56
$PM_{2.5}$ – 50% linear-transport	28.40 – 42.30	11.90	0.75	0.56

Table 11.5 displays a small decrease of modelled average PM concentration that is a little bigger for the linear reduction compared with the non-linear reduction (Table 11.1), and nearly the same correlation with observations for non-reduced and reduced PM time series.

A linear 50% reduction of the "Domestic" PM emissions involves a 50% decrease of PM_{10} and $PM_{2.5}$ emissions in the "Domestic" group and subsequent compilation of all 3 groups to create the "Total" group. A 50% reduction of the residential emissions is applied to all 24 hourly values of the day. Table 11.6 presents modelled-observed average, mean absolute error and correlation coefficient for modelled PM_{10} and $PM_{2.5}$ in the "Total" group (100%), and in the "Total" group with a 50% linear domestic emissions reduction (50% linear-domestic) compared with ambient data from Coles Place.

Table 11.6 Average (modelled-observed), Mean Absolute Error (MAE), Pearson Correlation Coefficient (PCC) and Power Correlation Coefficient (PCC*PCC), 7 episodes average, complex Scenario 1-3mix, total and fine PM ($\mu g\ m^{-3}$): 50% linear domestic emissions reduction.

Modelled PM	AVERAGE Mod. – Obs.	MAE	PCC	Power CC
PM_{10} – 100%	37.50 – 54.25	6.15	0.75	0.56
$PM_{2.5}$ – 100%	34.75 – 42.30	5.92	0.73	0.53
PM_{10} – 50% linear-domestic	25.85 – 54.25	21.10	0.68	0.48
$PM_{2.5}$ – 50% linear-domestic	20.30 – 42.30	15.45	0.70	0.49

Table 11.6 shows a significant decrease of average PM concentrations, with an average linear decrease for total and fine PM being bigger than in the case of non-linear 50% reduction (see Table 11.2). Correlation between reduced modelled aerosol concentrations and observed ones are lower compared with the initially modelled PM time series.

A linear 50% reduction of the "Domestic+Transport" PM emissions involves a decrease of PM_{10} and $PM_{2.5}$ emissions in the "Domestic" and "Transport" groups and subsequent compilation of 3 emission groups to create the "Total" group. A 50% reduction of the emissions is applied to all 24 hourly values of the day. Table 11.7 presents modelled-observed average, mean absolute error and correlation coefficient for modelled PM_{10} and $PM_{2.5}$ in the "Total" group (100%), and in the "Total" group with a 50% linear domestic-transport emissions reduction (50% linear domest-trans) compared with ambient data from Coles Place.

Table 11.7 Average (modelled - observed), Mean Absolute Error (MAE), Pearson Correlation Coefficient (PCC) and Power Correlation Coefficient (Power CC), 7 episodes average, complex Scenario 1-3mix, total and fine PM ($\mu g\ m^{-3}$): 50% linear domestic-transport emissions reduction.

Modelled PM	AVERAGE Mod. – Obs.	MAE	PCC	Power CC
PM_{10} – 100%	37.50 – 54.25	6.15	0.75	0.56
$PM_{2.5}$ – 100%	34.75 – 42.30	5.92	0.73	0.53
PM_{10} – 50% linear domest-trans	21.40 – 54.25	21.80	0.66	0.45
$PM_{2.5}$ – 50% linear domest-trans	17.95 – 42.30	16.75	0.67	0.46

Table 11.7 shows a significant decrease of the average total and fine PM concentration, and this time a better agreement with observations is shown for the initially modelled PM time series without linear emissions reduction. From Table 11.7 it is apparent that a linear 50% reduction in 2 emission groups decreases average values for modelled PM_{10} by 43% and $PM_{2.5}$ by 48% compared with initial modelled aerosol concentrations, which is very close to the PM decrease resulting from non-linear-reduction (see Table 10.3). Most of the modelled aerosol decrease is a result of the 50% reduction in the "Domestic" group.

11.1.3 Convergence in emission groups and 1999 inventory

Inter-comparison of the linear and non-linear approaches supports the quality of the 1999 emissions inventory for all emission groups if it is shown that modelled total $PM_{2.5}$ and PM_{10} concentrations for linear and non-linear reduction methods belong to one general population (null hypothesis). The null hypothesis is considered separately for 50% non-linear and linear emissions

reduction into “Transport”, “Domestic” and ”Domestic+Transport” groups and for all 7 winter 2005 episodes. Table 11.8 presents the ratio between reduced and initial concentrations, correlation and Spearman rank test (level of reliability) for linear and non-linear reduced fine and total PM concentrations in the groups “Domestic”, “Transport” and ”Domestic+Transport”.

Table 11.8 Reduced from initial PM concentrations (μg m^{-3}), Pearson correlation and Spearman rank test: linear and non-linear reduced modelled PM in groups “Domestic”, “Transport” and “Domestic+Transport” (7 winter 2005 episodes)

GROUP	DOMESTIC		TRANSP		DOMESTIC+TRANSP	
50% reduction In GROUP	Linear	Non-linear	Linear	Non-linear	Linear	Non- linear
PM_{10} (50%) / PM_{10}	0.49 – 0.59	0.52 – 0.63	0.78 – 0.90	0.78 – 0.88	0.45 – 0.53	0.46 – 0.57
Pearson Correlation R (PM_{10}^{lin} - $PM_{10}^{non-lin}$)	0.84 – 0.94	0.84 – 0.94	0.89 – 0.96	0.89 – 0.96	0.89 – 0.97	0.89 – 0.97
Spearman rank test P (level of reliability)	< 0.05	< 0.05	< 0.01	< 0.05	< 0.01	< 0.01
$PM_{2.5}$ (50%) / $PM_{2.5}$	0.51 – 0.61	0.56 – 0.68	0.80 – 0.94	0.80 – 0.92	0.46 – 0.55	0.47 – 0.58
Pearson Correlation R ($PM_{2.5}^{lin}$ - $PM_{2.5}^{non-lin}$)	0.78 – 0.94	0.78 – 0.94	0.88 – 0.97	0.88 – 0.97	0.90 – 0.99	0.90 – 0.99
Spearman rank test P (level of reliability)	< 0.05	< 0.05	< 0.01	< 0.01	< 0.02	< 0.02

It is very important to scrutinize carefully Table 11.8 to trace the 3-step (for 3 groups) convergence process of two differently produced sub-populations (linear and non-linear) to one general population. In the case of the 50% reduction of the “Domestic” input emissions, the ratios of reduced to original predicted PM concentrations lie between 0.49–0.59 for the linear and 0.52–0.63 for the non-linear schemes (only PM peak values are considered). For all winter episodes, time sequences of the PM values resulting from the linear and non-linear reductions belong to the same population ($P<0.05$, Spearman test). The Pearson Correlation Coefficient (PCC) between the PM values derived from linear and non-linear reduction schemes lies between 0.75–0.94. The difference between linear and non-linear reduction schemes is mainly a result of the reduction of night-time emissions only in the non-linear scheme for the “Domestic” group.

In the case of the 50% reduction of the “Transport” input emissions, the ratios of reduced to original predicted PM concentrations lie between 0.70–0.88 for the linear and 0.72–0.90 for the non-linear schemes, as the “Transport” group’s contribution to total PM is lower compared with

the “Domestic” group. Time sequences of linear and non-linear PM belong to the same population ($P<0.01$, Spearman test) for all modelled winter episodes, while PCC lies between 0.85–0.95. Once again, the difference between linear and non-linear reduction schemes is mostly a result of the day-time 50% reduction only in the non-linear scheme.

In the case of the 50% reduction of the “Domestic + Transport” input emissions, the ratios of reduced to original predicted PM concentrations lie between 0.45–0.54 for the linear and 0.46–0.56 for the non-linear schemes. Reduction in the “Domestic + Transport” group emissions was applied to the entire day (24 hours) in both the linear and non-linear schemes. Time sequences of linear and non-linear reduced PM values definitely belong to the same population ($P<0.02$, Spearman test) for all modelled episodes, with the PCC between 0.89–0.96. So there is an obvious decrease in the difference between the two reduction schemes.

The results of the linear and non-linear reduction approaches prove the hypothesis that the two sequences belong to one general population, and support the quality of the 1999 emissions inventory for the “Domestic”, “Transport” and “Total” groups (and explicitly for the “Transport” group). The linear and non-linear outcomes also support the rationale of using chemical Scenario 1-3mix, and provide the option of using linearly reduced gridded emissions in the non-linear photochemical model with a certainty of avoiding additional systematic errors as a result of reduction scheme simplification. Also, these results allow the start of a new series of experiments to evaluate probable winter PM scenarios (up to the year 2013) using a linear scheme applied to “Total”, “Domestic”, “Transport” and “Industry” emission groups instead of working with non-linear approach where it is sometimes very difficult to separate emission origin.

11.2 Validation of PM decrease in the “Domestic” group

Validation of dispersion of fine and total PM concentrations from the “Domestic” group will be given for a 50% linear against non-linear reduction of the aerosol emissions of domestic (residential) origin. Evaluation of the MM5-CAMx4.4 (Scenario 1-3mix) numerical modelling system for “Domestic” aerosol emissions will be done to assess of the residential source contribution to total ambient aerosol. All results in this and next 4 sections are calculated for all 7 winter 2005 episodes with high- medium night-morning aerosol pollution episodes (see Figure 9.2).

Figure 11.1 presents the spatial distribution of modelled total $PM_{2.5}$ at midnight 5 May 2005 (episode 4, winter 2005 meteorology) calculated for Scenario 1-3mix (Figure 11.1a) and for 6am 5 May 2005 (Figure 11.1b). Predicted spatial distribution of fine PM in the early morning of 5 May 2005 is given to illustrate the peak concentration level that is obvious from Figure 11.1a. The results in Figure 11.2 are comparable with the modelled PM_{10} distribution in Figure 9.20. The colour scale is different in Figures 11.1a and 11.1b to stress the peak PM concentrations spatial localisation as for night main peak (Figure 11.1a), and so for early morning secondary peak (Figure 11.1b).

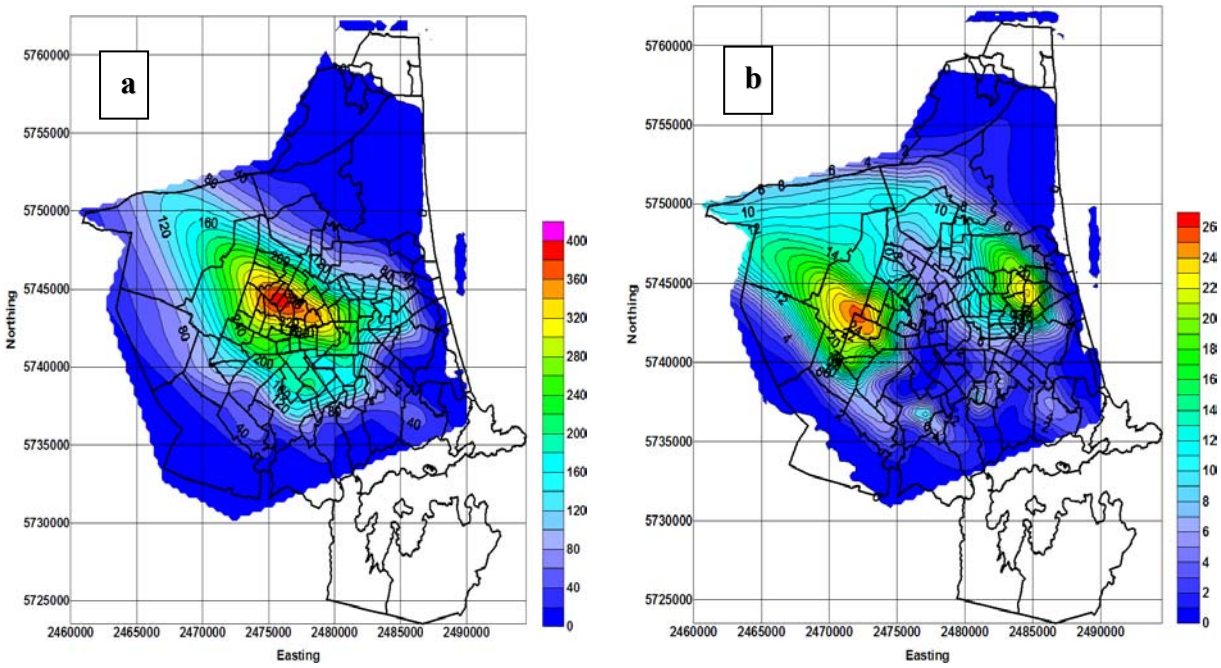

Figure 11.1 Spatial near-surface (8-10 metres) distribution of modelled $PM_{2.5}$ for episode 4 (winter 2005), and Scenario 1-3mix: a) midnight 5 May 2005; b) 6 am 5 May 2005.

Figure 11.2 presents the spatial distribution of modelled total $PM_{2.5}$ at midnight 5 May 2005 (episode 4, winter 2005 meteorology) obtained as a result of a linear 50% night-time reduction of the input domestic emissions (Figure 11.2a), and as a result of a non-linear 50% night-time emissions reduction (Figure 11.2b).

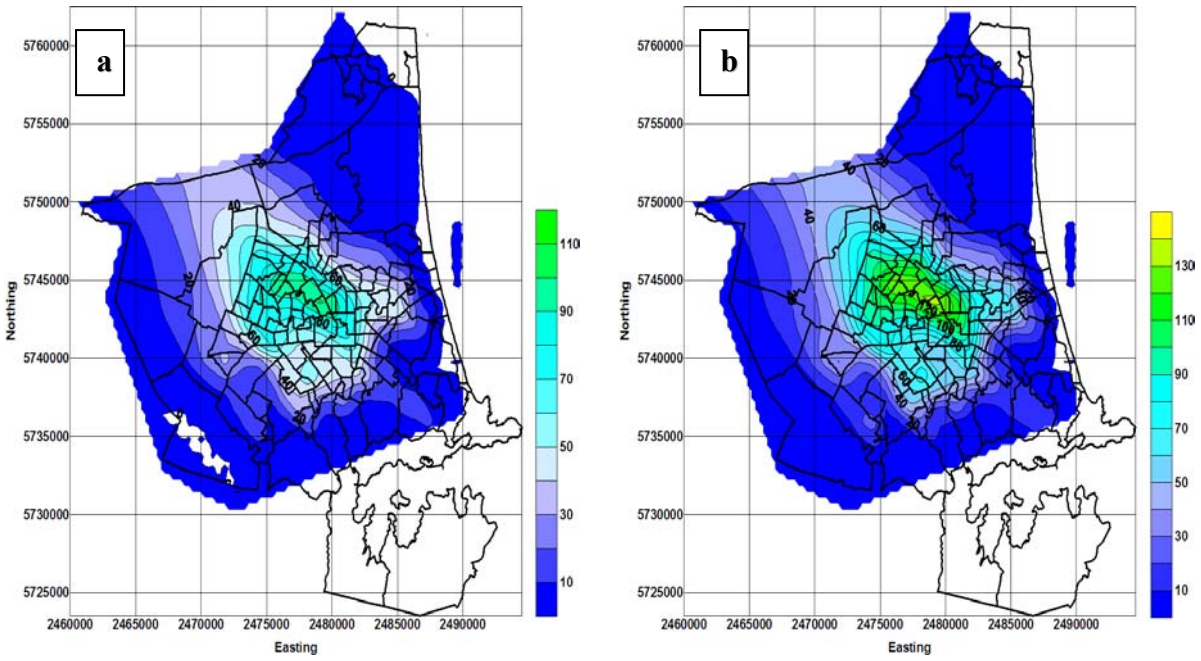

Figure 11.2 Spatial near-surface (8-10 metres) distribution of $PM_{2.5}$ at midnight 5 May 2005, episode 4, and Scenario 1-3mix: a) for "Total" group with 50% linear reduced domestic contribution; b) for "Total" group with 50% non-linear reduced domestic contribution.

Comparison of Figures 11.1 and 11.2 coloured scales shows that there is a nearly 3 times decrease of the peak PM concentrations (at midnight) in the case of the 50% non-linear reduction in domestic daily emissions (Figures 11.1a and 11.2a), and more than 3 times decrease in the case of the 50% linear reduction in domestic daily emissions (Figures 11.1a and Figure 11.2b). To understand an importance of "Domestic" emission group in total PM concentrations building are considered methods "emission out" (total emissions without domestic source) and "emission in" (domestic emissions only).

Table 11.9 presents modelled-observed average, mean absolute error and correlation coefficient of modelled PM_{10} and $PM_{2.5}$ for "Total" group, and for the "Total" group minus the "Domestic" group compared with ambient data from Coles Place site (winter 2005 meteorology).

Table 11.9 Average (modelled - observed), Mean Absolute Error (MAE), Pearson Correlation Coefficient (PCC) and Power Correlation Coefficient (Power CC – PCC*PCC), 7 episodes average, complex Scenario 1-3mix, total and fine PM (μg m^{-3}): "Total" without "Domestic" emission group.

Modelled PM	AVERAGE Mod. – Obs.	MAE	PCC	Power CC
PM_{10} - 100%	39.50 – 54.25	14.25	0.75	0.56
$PM_{2.5}$ – 100%	37.75 – 42.30	11.75	0.73	0.53
PM_{10} – 100% domestic	7.75 – 54.25	42.85	0.12	0.01
$PM_{2.5}$ – 100% domestic	6.50 – 42.30	35.25	0.15	0.02

Table 11.9 shows a significant decrease of average PM concentration (about 80-82%) as a result of linear remove of the "Domestic" group and a sharp increase of MAE between observations and reduced fine and total PM concentrations. Correlation of the reduced modelled aerosol concentrations with ambient data (7 winter 2005 episodes) tends to zero, which suggests the principal role of the domestic aerosol emissions in the winter PM "Total" group concentrations. Table 11.10 presents modelled-observed average, MAE and correlation coefficient for modelled PM_{10} - $PM_{2.5}$ for "Domestic" group emissions only compared with ambient data from the Coles Place site (winter 2005 meteorology).

Table 11.10 Average (modelled-observed), Mean Absolute Error (MAE), Pearson Correlation Coefficient (PCC) and Power Correlation Coefficient (Power CC – PCC*PCC), 7 episodes average, complex Scenario 1-3mix, total and fine PM (μg m^{-3}): "Domestic" input emissions.

Modelled PM	AVERAGE	MAE	PCC	Power CC
PM_{10} - total	39.50 – 54.25	14.25	0.75	0.56
$PM_{2.5}$ – total	37.75 – 42.30	11.75	0.73	0.53
PM_{10} - domestic	36.45 – 54.25	15.50	0.59	0.34
$PM_{2.5}$ – domestic	35.55 – 42.30	14.75	0.62	0.38

Table 11.10 shows a significant contribution (nearly 88-90%) to average modelled total PM_{10} and $PM_{2.5}$ concentrations from the "Domestic" group, plus the same magnitude MAE for total and domestic PM_{10} and $PM_{2.5}$ modelled concentrations. Correlation of the domestic modelled aerosol concentrations with ambient data (7 winter 2005 episodes) is slightly lower than total modelled PM, which suggests a significant role of the domestic aerosol emissions for average PM composition as it has been stipulated in the 1999 inventory.

11.3 Validation of PM decrease in the "Transport" group

Figure 11.3 presents the spatial distribution of modelled $PM_{2.5}$ at midnight 5 May 2005 (episode 4, winter 2005) obtained as a result of a linear 50% daily reduction of input transport emissions (Figure 11.3a), and as a result of non-linear 50% day-time emissions reduction (Figure 11.3b).

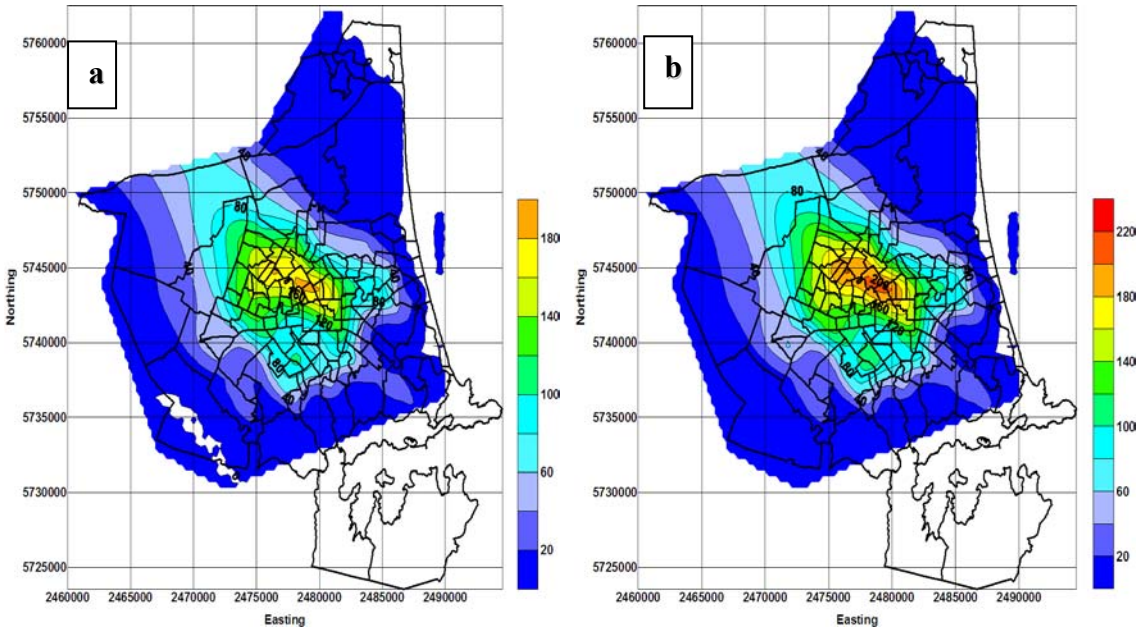

Figure 11.3 Spatial near-surface (8-10 metres) distribution of $PM_{2.5}$ at midnight 5 May 2005, episode 4, and Scenario 1-3mix: a) for the "Total" group with 50% linear reduced transport emissions; b) for the "Total" group with 50% non-linear reduced transport emissions.

Comparison of Figures 11.1 and 11.3 shows that there is nearly a 50% decrease of peak PM concentrations (at midnight) in the case of the 50% non-linear reduction in vehicular day-time emissions (Figure 11.3b), and there is more than 50% in the case of the 50% linear reduction in vehicular daily emissions (Figure 11.3a). This decrease is obtained in the "Transport" group 50% reduction only, when transport contributes about 12-13% of emissions (see Table 11.4). Table 11.11 presents modelled-observed average, mean absolute error and correlation coefficient of modelled PM_{10} - $PM_{2.5}$ for the "Total" group, and for the "Total" group minus the "Transport" group (100% linear vehicular emissions reduction) compared with ambient data from Coles Place (winter 2005 meteorology).

Table 11.11 Average (modelled - observed), Mean Absolute Error (MAE), Pearson Correlation Coefficient (PCC) and Power Correlation Coefficient (Power CC – PCC*PCC), 7 episodes average, complex Scenario 1-3mix, total and fine PM (μg m^{-3}): "Total" without "Transport" emission group.

Modelled PM	AVERAGE Mod. – Obs.	MAE	PCC	Power CC
PM_{10} – 100%	39.50 – 54.25	14.25	0.75	0.56
$PM_{2.5}$ – 100%	37.75 – 42.30	11.75	0.73	0.53
PM_{10} – 100% transport	28.65 – 54.25	15.25	0.71	0.50
$PM_{2.5}$ – 100% transport	27.15 – 42.30	12.75	0.73	0.53

Table 11.11 shows some decrease of average PM concentrations (about 27-28%) as a result of linear remove of the "Transport" group emissions, and a very close MAE for initial and reduced fine and total PM concentrations. Correlation of the reduced modelled aerosol concentrations with ambient data (7 winter 2005 episodes) is high, which suggests a secondary role of the transport PM emissions in the winter PM "Total" group building.

Table 11.12 presents modelled-observed average, MAE and correlation coefficient for modelled PM_{10} - $PM_{2.5}$ for "Transport" group emissions only compared with ambient data from Coles Place site (winter 2005 meteorology).

Table 11.12 Average (modelled - observed), Mean Absolute Error (MAE), Pearson Correlation Coefficient (PCC) and Power Correlation Coefficient (Power CC), 7 episodes average, complex Scenario 1-3mix, total and fine PM (μg m^{-3}): "Transport" input emissions.

Modelled PM	AVERAGE Mod. – Obs.	MAE	PCC	Power CC
PM_{10} - total	39.50 – 54.25	14.25	0.75	0.56
$PM_{2.5}$ – total	37.75 – 42.30	11.75	0.73	0.53
PM_{10} – transport	5.10 – 54.25	43.15	0.02	<< 0.01
$PM_{2.5}$ – transport	4.75 – 42.30	36.50	0.02	<< 0.01

Table 11.12 shows a quite low contribution (about 12%) to average modelled total PM_{10} and $PM_{2.5}$ concentrations from the "Transport" group, but a very high magnitude of MAE for the transport PM_{10} and $PM_{2.5}$ modelled concentrations. There is no correlation between the transport modelled aerosol concentrations and ambient aerosol (7 winter 2005 episodes), which indicates a secondary role of the transport aerosol emissions in average and peak aerosol production. But it should be noted that these results are received on the base of input emissions obtained during the 1999 inventory, and depends on the reliability of the domestic and transport models (used to develop the inventory).

11.4 Validation of PM decrease in the "Industry" group

The non-linear 50% reduction in aerosol emissions suggested for the "Industry" group is applied to Scenario 1 (day time) and Scenario 3 (night time) of Scenario 1-3mix (in "Total" group). Only particulate sulphate is reduced on 50% as an essential tracer of industrial emissions, and primary elemental carbon is reduced on 25% originated mostly from transport emissions but in a lower degree from industrial emissions.

PEC (50%) = PEC *0.75;

POA (50%) = POA (no change);

SOA1–4 (50%) = SOA1–4 (no change);

PSO_4 (50%) = PSO_4*0.50;

PNO_3 (50%) = PNO_3 (no change);

PNH_4 (50%) = PNH_4 (no change);

CCRS, FCRS, PCL, NA - no change.

Sulphates are considered to be an essential pollutant of the industry sector and are reduced on a half. Crustal elements and dust particles are considered to have only natural origin and are kept without change; particulate chloride and sodium are also considered to have natural source. Figure 11.4 presents the spatial distribution of modelled total $PM_{2.5}$ at midnight 5 May 2005 (episode 4, winter 2005 meteorology) obtained as a result of a linear 50% daily reduction of the input industry emissions (Figure 11.4a), and as a result of non-linear 50% daily missions reduction (Figure 11.4b).

Comparison of the Figures 11.1a and 11.4 shows that there is more than twice decrease of the peak PM concentrations (at midnight) in the case of the 50% non-linear reduction in the industry daily emissions (Figure 11.4b), and 2.5 times decrease in case of the 50% linear reduction in the industry daily emissions (Figure 11.4a). This decrease is obtained for the 50% "Industry" group reduction only; when industrial PM is believed to provide about 16-17% of total particulate matter emissions for year 2005 (see Table 11.4). Table 11.13 presents modelled-observed average, mean absolute error and correlation coefficient of modelled PM_{10} - $PM_{2.5}$ for "Total" group, and for "Total" group with "Industry" group out (100% linear domestic emissions reduction) compared with ambient data from Coles Place site (winter 2005 meteorology).

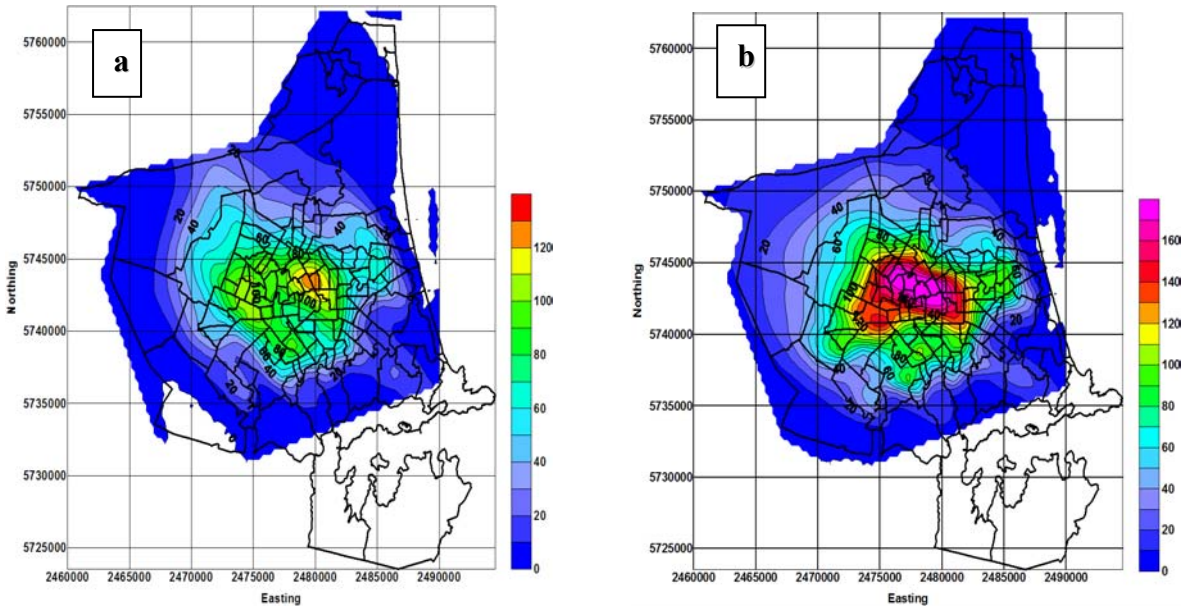

Figure 11.4 Spatial near-surface (8-10 metres) distribution of $PM_{2.5}$ at midnight 5 May 2005, episode 4, and Scenario 1-3mix: a) for the "Total" group with 50% linear reduced industrial emissions; b) for the "Total" group with 50% non-linear reduced industrial emissions.

Table 11.13 Average (modelled - observed), Mean Absolute Error (MAE), Pearson Correlation Coefficient (PCC) and Power Correlation Coefficient (Power CC – PCC*PCC), 7 episodes average, complex Scenario 1-3mix, total and fine PM (μg m^{-3}): "Total" without "Industry" emission group.

Modelled PM	AVERAGE Mod. – Obs.	MAE	PCC	Power CC
PM_{10} – 100%	39.50 – 54.25	14.25	0.75	0.56
$PM_{2.5}$ – 100%	37.75 – 42.30	11.75	0.73	0.53
PM_{10} – 100% industry	29.85 – 54.25	15.85	0.69	0.48
$PM_{2.5}$ – 100% industry	28.45 – 42.30	13.55	0.70	0.49

Table 11.13 shows some decrease of average PM concentration (about 25%, which is not far from transport emissions for years 2005-2006 emissions) as a result of linear removal of the "Industry" group, and similar MAE for not reduced and reduced fine and total PM concentrations as well. Correlation of the reduced modelled aerosol concentrations with ambient PM (7 winter 2005 episodes) is high, which suggests a secondary role of the industrial PM emissions in the winter PM "Total" group building. Table 11.14 presents modelled-observed average, MAE and correlation coefficient for modelled PM_{10} - $PM_{2.5}$ for the "Industry" group emissions only compared with ambient data from Coles Place site (winter 2005 meteorology).

Table 11.14 Average (modelled-observed), Mean Absolute Error (MAE), Pearson Correlation Coefficient (PCC) and Power Correlation Coefficient (Power CC), 7 episodes average, complex Scenario 1-3mix, total and fine PM (μg m^{-3}): "Industry" input emission group.

Modelled PM	AVERAGE Mod. – Obs.	MAE	PCC	Power CC
PM_{10} – total	39.50 – 54.25	14.25	0.75	0.56
$PM_{2.5}$ – total	37.75 – 42.30	11.75	0.73	0.53
PM_{10} – industry	4.65 – 54.25	45.00	-0.16	<< 0.01
$PM_{2.5}$ – industry	3.95 – 42.30	39.25	-0.18	<< 0.01

Table 11.14 shows a low contribution (about 10-11%) to average modelled total PM_{10} and $PM_{2.5}$ concentrations from the "Industry" group, and a high magnitude of MAE for the industrial PM_{10} and $PM_{2.5}$ modelled concentrations compared with ambient observations. There is a weak negative correlation between the industrial modelled aerosol concentrations and observed total and fine PM (7 winter 2005 episodes) that indicates a secondary role of the industrial aerosol emissions in average and peak PM concentrations.

It should be stressed that the "emission out" and "emission in" numerical results for separate emission groups described in this section cannot be considered as a linear response, and definitely cannot be directly compared with modelled PM spatial and temporal concentrations from the "Total" emission group. All results were obtained as a result of applying linear varying of the input gridded emissions to an absolutely non-linear numerical modelling system, and should be interpreted very carefully in case of the "group emission out of total" and "group emission only" procedure usage. However, proposed modelled decreases of peak aerosol concentrations exhibited in Figures 11.2-11.4 are very interesting particularly compared with the modelled results in Figure 11.1a. Also it is important to remember that modelled fine PM (averaged over 17 days of winter 2005 7 smog episodes) invests about 95% of total PM against 78% of $PM_{2.5}$ in ambient PM_{10}. This can be explained by $PM_{2.5}/PM_{10}$ ratio in the 1999 inventory gridded emissions, by influence of day-time transport scenario (Scenario 1-3mix) without crustal elements, and by poorly treated coarse part of PM in CAMx4.4.

11.5 Validation in the "Total" group

The "Total" group is not very useful to evaluate using linear (or non-linear) reductions as total PM emissions consist of three principal (domestic, transport and industry) local sources that have already been examined. However, it is interesting to investigate the ratio between different

chemical components of the total PM concentrations. It is important to know the proportion of carbon, ionic and other species of the Scenario 1-3mix in modelled aerosol concentrations (emission chemical species ratios were studied in some details in Chapter 9). Seven winter 2005 meteorological events are used for this part of the study that should show a direction of numerical drift (modelling error accumulation) in the photochemical model CAMx4.4 and the total numerical modelling system MM5-CAMx4 (modelled aerosol time dispersion against initial emissions under certain meteorological conditions).

Table 11.15 presents modelled species compared with modelled (total) PM averages, a percentage for every species (or species group), correlation and power (correlation in power 2) coefficients for modelled total PM_{10} and $PM_{2.5}$ concentrations (winter 2005 meteorology – 7 episodes). Input gridded emissions were obtained with application of the complex Scenario 1-3mix (for abbreviations see "List of acronyms and abbreviation').

Table 11.15 Predicted average (species-total), species fraction, Pearson Correlation Coefficient (PCC) and Power Correlation Coefficient (Power CC), 7 episodes average, complex Scenario 1-3mix, total and fine PM ($\mu g\ m^{-3}$): "Total" input emission group, year 2005.

Species – total PM	AVERAGE ($\mu g\ m^{-3}$)	FRACTION (%)	PCC	Power CC
TOC_{10} - PM_{10}	20.65 – 39.50	54.10	0.77	0.59
$TOC_{2.5}$ - $PM_{2.5}$	18.55 – 37.75	53.30	0.80	0.64
POC_{10} - PM_{10}	11.80 – 39.50	31.50	0.71	0.51
$POC_{2.5}$ - $PM_{2.5}$	11.40 – 37.75	32.90	0.73	0.53
SOA_{10} - PM_{10}	8.20 – 39.50	23.90	0.77	0.59
$SOA_{2.5}$ - $PM_{2.5}$	7.45 – 37.75	22.50	0.78	0.61
EC_{10} - PM_{10}	6.60 – 39.50	17.40	0.60	0.36
$EC_{2.5}$ - $PM_{2.5}$	6.40 – 37.75	18.20	0.70	0.49
$IONs_{10}$ - PM_{10}	10.35 – 39.50	27.00	0.78	0.41
$IONs_{2.5}$ - $PM_{2.5}$	10.35 – 37.75	27.80	0.80	0.64
$(PNO_3)_{10}$ - PM_{10}	6.45 – 39.50	16.90	0.78	0.61
$(PNO_3)_{2.5}$ - $PM_{2.5}$	3.90 – 37.75	9.50	0.71	0.50
$(PSO_4)_{10}$ - PM_{10}	4.30 – 39.50	6.20	0.73	0.53
$(PSO_4)_{2.5}$ - $PM_{2.5}$	5.00 – 37.75	13.50	0.79	0.63
$(PNH_4)_{10}$ - PM_{10}	1.60 – 39.50	4.30	0.78	0.61
$(PNH_4)_{2.5}$ - $PM_{2.5}$	1.65 – 37.75	4.80	0.80	0.64

It should be noted that there is a small difference of PM concentrations obtained directly from the CAMx4.4 output to compare with PM concentrations, which are calculated by summing POC, PEC, SOA and ions species from CAMx4.4 output. Usually the POC+SOA+EC+ions (crustal elements cannot be included - scenario 1, or can be included - scenario 1-3mix) sum is a little

higher that can be explained by imprecise post-processing software used to calculate PM concentrations from the species. In any way, comparison of the average concentrations (Table 11.15) with the input emissions split (Table 9.1 and Figure 9.21) suggests a slight positive drift (increase) of the organic carbon partitioning (53-54%), a stable percentage of elemental carbon (17-18%), and low negative drift (decrease) of inorganic ions (27-28%). CAMx4.4 uses to drift to a more stable regime with bigger number of primary chemical reactions. As was discussed in Chapter 4, CAMx4 shows more stable results to carbon primary-secondary species and not such good skills (leading to chemical instability and poorer prediction level) in case of inorganic secondary species dominance (such as in Scenario 4). Nearly all basic species (except EC) have a very good PCC (and Power CC) with total PM concentrations, which is not a surprise, bearing in mind the hourly nudging gridded emissions with a dominance of primary carbon species. Also from Table 11.15 it is apparent that particulate sulfate concentrations are much higher for fine PM, and particulate nitrate concentrations are higher for total PM. Analysis of the average correlations between different principal components of the complex Scenario 1-3mix used to evaluate all 7 winter 2005 episodes (including particulate water – PH_2O) has shown (in addition to the Table 11.15) a high correlation between all CAMx4.4 basic chemical species (PCC = 0.88–0.99) except particulate water, where a negative correlation with all other components was observed (is not shown).

11.6 Influence of decreased gaseous precursors on PM

Gaseous precursors play a very important role in secondary organic aerosol formation (condensable gases –> nucleation -> Aitken mode of SOA), and in formation of the secondary inorganic aerosol (NO_x in PNO_3 and PNH_4, SO_2 in PSO_4). But in this research, application of the numerical modelling system first of all identified a tendency for the numerical modelling system to provide a better treatment of the primary carbons. The quality level of the input gaseous emissions (described in Titov, 2004) leaves a big question about precision of the input gridded gaseous emissions and their influence on PM concentrations building.

To investigate the relationship between observed/modelled gaseous precursors and observed/modelled fine PM winter 2005 7 episodes were studied using scatterplot diagrams to find a correlation tendency between CO, NO_x, SO_2 and $PM_{2.5}$. Figure 11.5 shows an observed CO-$PM_{2.5}$ scatterplot and linear regression (Figure 11.5a), and modelled CO-$PM_{2.5}$ scatterplot and

linear regression (Figure 11.5b) for winter 2005 seven episodes for Coles Place. Input-nudging modelled gridded emissions were split on chemical species according to Scenario 1-3mix.

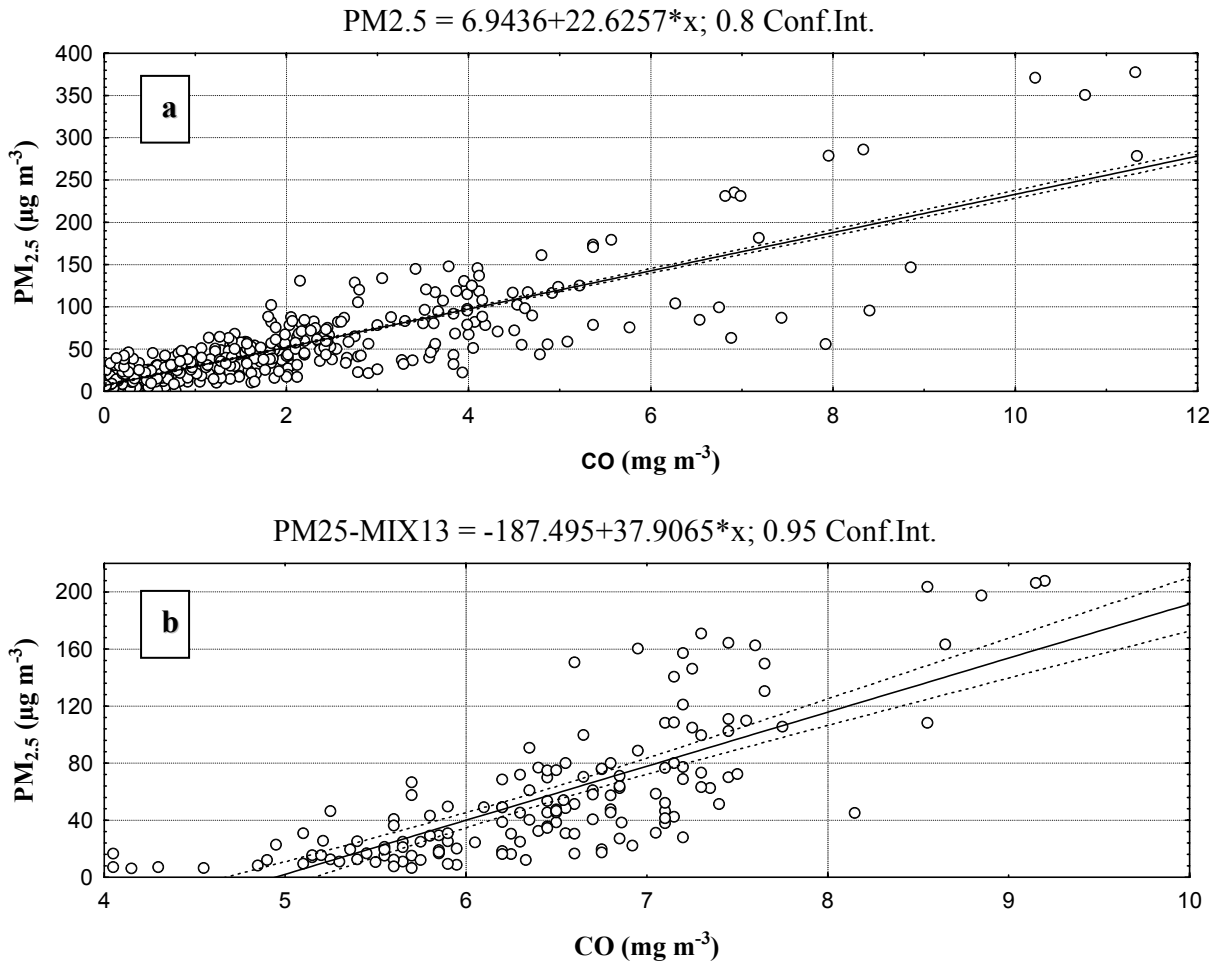

Figure 11.5 Scatterplot diagram and linear regression for CO-$PM_{2.5}$ concentrations (mg m^{-3} and µg m^{-3} respectively) for 7 winter 2005 episodes: a) ambient data from Coles Place; b) modelled data for Coles Place (chemical Scenario 1-3mix).

In both cases, there is a high positive correlation between carbon monoxide and fine PM that is close to 0.80 for observations and to 0.77 for modelled output. But for CAMx4.4 predicted output the amount of CO-particulate carbon chemical transformation is much lower. From Figure 11.5b it is apparent that there is an excess of modelled CO concentrations when fine PM is nearly equal to zero, which is not the case for observations (Figure 11.5a) where the CO-$PM_{2.5}$ ratio is much better balanced.

Figure 11.6 illustrates the observed SO_2-$PM_{2.5}$ scatterplot and linear regression (Figure 11.6a), and modelled SO_2-$PM_{2.5}$ scatterplot and linear regression (Figure 11.6b) for seven episodes in winter

2005 for Coles Place. Input-nudging emissions for the photochemical model were split into chemical species according to Scenario 1-3mix.

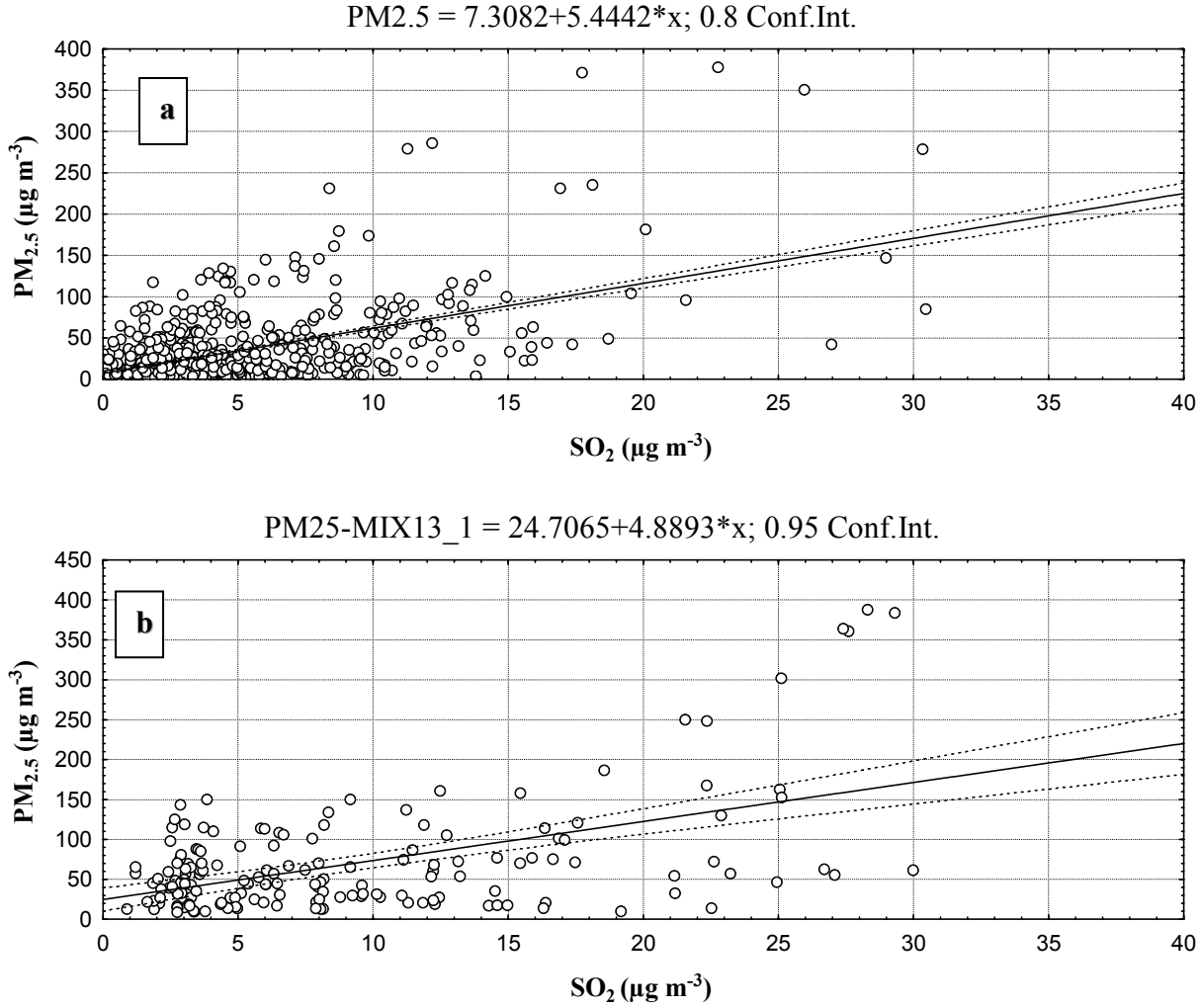

Figure 11.6 Scatterplot diagram and linear regression for SO_2-$PM_{2.5}$ concentrations (µg m^{-3}) for 7 winter 2005 episodes: a) ambient data from Coles Place; b) modelled data for Coles Place (chemical Scenario 1-3mix).

For observed and modelled SO_2-$PM_{2.5}$ scatterplots the correlation is positive but much lower (than between CO and fine PM), being about 0.57 for observations and about 0.53 for modelled data. In case of the simulated concentrations, the rate of SO_2-PSO_4 conversion does play quite an important role in secondary aerosol formation (see Table 11.15). The modelled sulphur concentrations for fine PM obtained from observations (Figure 11.6a) and received from calculations (Figure 11.6b) are close to each other.

In Figure 11.7 are presented the NO_x-$PM_{2.5}$ scatterplots and linear regression obtained from observations (Figure 11.7a), and from the MM5-CAMx4.4 numerical modelling system output

(Figure 11.7b) for winter 2005 studies (Coles Place site). Once again gridded emissions for CAMx4.4 were split into chemical species according to Scenario 1-3mix.

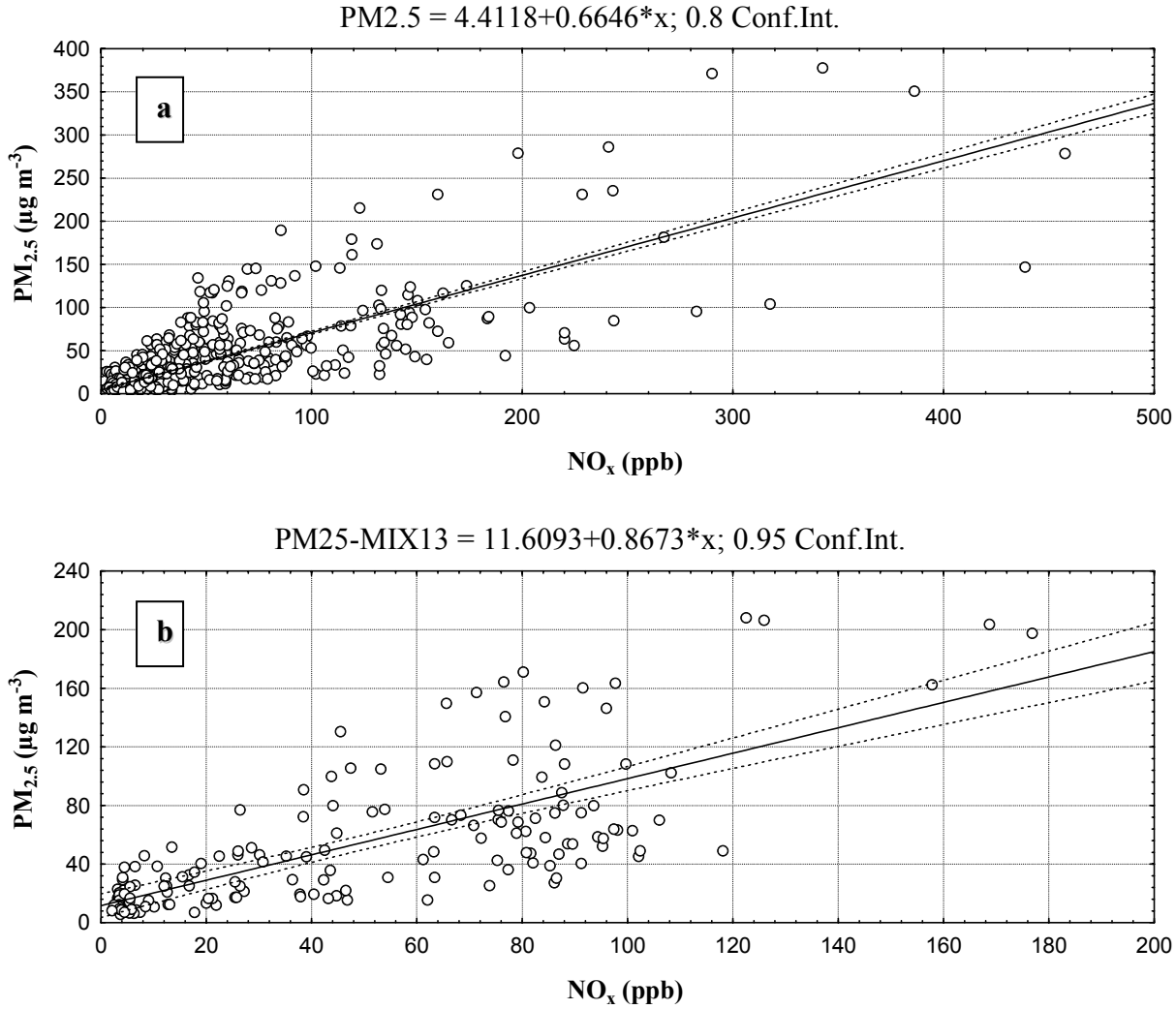

Figure 11.7 Scatterplot diagram and linear regression for XO_x-$PM_{2.5}$ concentrations (µg m^{-3}) for 7 winter 2005 episodes: a) ambient data from Coles Place; b) modelled data for Coles Place (chemical Scenario 1-3mix).

For observed and modelled scatterplots NO_x-$PM_{2.5}$ correlation is positive and quite high (as expected) being nearly 0.80 for observations and about 0.73 for modelled data. In the case of the simulated nitrate concentrations, the predicted NO_x concentrations (Figure 11.7b) are nearly half of the observed nitrate levels (Figure 11.7a) with under-estimation of PNO_3 and PNH_4. This artificial process is especially well pronounced during night time, when gaseous-particulate two-way transformation of nitrate is very active. The negative bias of the modelled NO_x values is well known and is described in Gaydos et al. (2007). As particulate nitrate plays an important role in night-morning fine-total aerosol peak development (see Table 11.15) about 22-25% (PNO_3 and PNH_4) of total PM concentration, the underprediction of NO_x (especially in total PM calculations)

is considered to be one of the most important reasons of failure to predict aerosol peak concentrations (Gaydos et al., 2007).

Observed dependence of NO_x on near-surface temperature is demonstrated in Figure 11.8 for the period 1 May – 10 June 2005 (Coles Place).

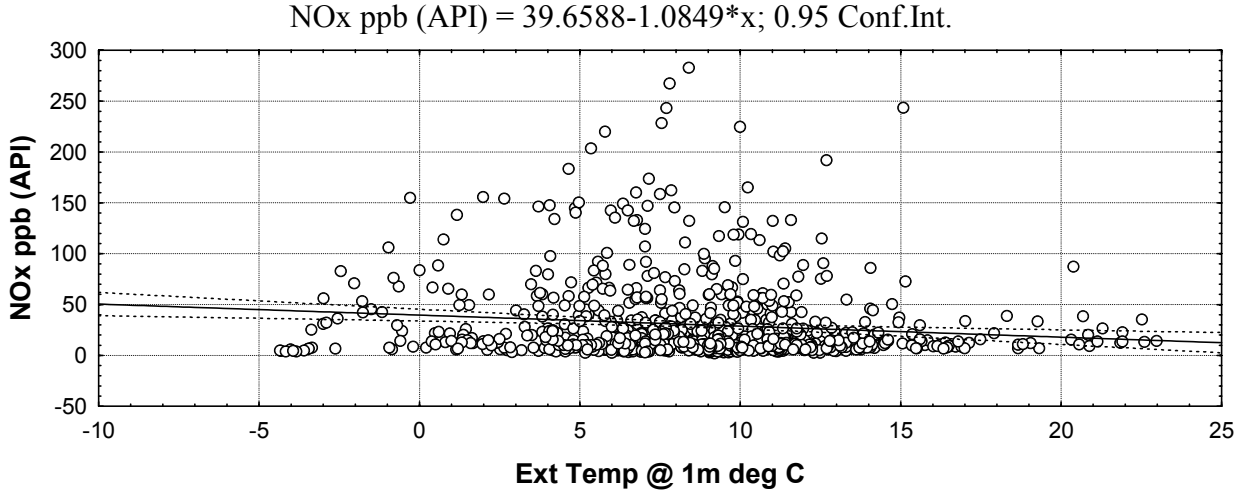

Figure 11.8 Scatterplot diagram and linear regression for external 1 m temperature (^{0}C) and NO_x concentrations (ppm) for 40 winter 2005 days (ambient data from Coles Place site).

Maximum gaseous nitrate is observed for temperatures between 5 and 15^0 C, while below 5^0 C NO_x is actively transformed to particulate nitrate and this process is definitely under-predicted by CAMx4.4 for winter 2005 case studies. For high day-time near-surface temperatures (> 15 ^{0}C) the process of NO_x titration is observed (Figure 11.8).

Table 11.16 presents modelled-observed average, mean absolute error and correlation coefficient of modelled PM_{10} and $PM_{2.5}$ for the "Total" group, and for the "Total" group with 3 times decreased gases in Scenario 1-3mix (on 75%), compared with ambient data from Coles Place (winter 2005 meteorology).

Table 11.16 Average (modelled - observed), Mean Absolute Error (MAE), Pearson Correlation Coefficient (PCC) and Power Coefficient (Power CC), 4 episodes average, complex Scenario 1-3mix, total and fine PM (μg m^{-3}): "Total gases*0.25" emission group.

Modelled PM	AVERAGE Mod. – Obs.	MAE	PCC	Power CC
PM_{10} – 100%	39.50 – 54.25	14.25	0.75	0.56
$PM_{2.5}$ – 100%	37.75 – 42.30	11.75	0.73	0.53
PM_{10} – 3/4 gases	37.95 – 54.25	15.40	0.72	0.52
$PM_{2.5}$ – 3/4 gases	36.05 – 42.30	13.00	0.75	0.56

Table 11.16 shows a small decrease of average PM concentration (about 10% - less than a half of the transport or industry emissions being removed) as a result of a linear 3 fold decrease of gaseous species in input gridded emissions, and a comparable MAE for not reduced and reduced fine and total PM concentrations as well. Correlation of the reduced modelled aerosol concentrations with ambient PM (7 winter 2005 episodes) is high suggesting about a minor role of the numerical gaseous component in modelled PM concentrations calculation for the "Total" group.

11.7 Summary

Evaluation of the 1999 inventory with application of linear and non-linear approaches has shown the validity of the linear emissions reduction method (for different groups) and confirmed the good quality of the 1999 inventory for PM domestic, transport, and total (and presumably industrial) emissions. Application of the input gridded emissions linear reduction procedure in groups has allowed assessment of the level of importance of every emission group in development of fine and total PM. Winter 2005 near-surface meteorology is used in all experiments as it is close to average winter day meteorology for the Christchurch area.

Chapter 12: Assessment of PM management strategies

Numerical modelling systems MM5-CAMx and WRF-CAMx have great potential to be applied in different areas of New Zealand for use in decision making and for evaluation of the proposed pollution abatement strategies, following the recent establishment and implementation of the National Environmental (Air Quality) Standards (Ministry for Environment, 2003). The numerical dispersion modelling system MM5 MPP v3.7.3–CAMx4.4 is used for gaining deeper understanding of observed spatial and temporal variations in air quality, as the basic tool to assess air quality in locations without observations under a range of different chemical and environmental scenarios. In Chapter 12, MM5–CAMx4.4 numerical modelling system is employed to evaluate ECan's environmental scenarios for ambient aerosol pollution abatement strategies (Scott, 2005). Extensive use of the numerical modelling systems MM5-CAMx4 and WRF-CAMx4 (in future) will be able to help to validate progress in achieving the new air quality standards.

12.1 Possible total PM decrease for the period 2005-2013

Evaluation of the possible decrease of aerosol will be discussed separately for PM_{10} and $PM_{2.5}$ with application of winter 2005 calculated meteorology and the Scenario 1-3mix split of the input-nudging aerosol emissions. The proposed change of a winter day's PM_{10} emissions in the groups "Domestic", "Transport" and "Industry" (in grams area^{-1} day^{-1}, area of the inner Christchurch = 17,680 ha – see Figure 4.5) is presented in Table 12.1 and includes the emissions for the 2005-2013 year strategic time period (Ministry for Environment, 2003). Table 12.1 also includes emissions for the 1999 year inventory as the year of initial emissions in this research.

Table 12.1 Change in a winter day PM_{10} emissions for "Domestic", "Transport" and "Industry" groups (grams area^{-1} day^{-1}, inner Christchurch area = 17,680 ha) for 2005-2013 years

Group / Year	1999	2005	2006	2007	2008
Domestic	8340845	4124525	2973757	2431735	1834468
Transport	1115365	782349	730140	677931	625722
Industry	1027021	1006764	1026432	1046100	1065768
Total	10483231	5913637	4730329	4155765	3525958
Group / Year	2009	2010	2011	2012	2013
Domestic	1612973	1457518	1302064	1149162	998435
Transport	573513	521303	469094	445215	421335
Industry	1085436	1105104	1124772	1144440	1164108
Total	3271921	3083925	2895930	2738816	2583878

Data in groups from Table 12.1 are used to change PM_{10} emissions (with reference to 1999 values) at every point of the gridded emissions array for all 3 groups (using linear decrease, or increase in case of "Industry" group), and to compile gridded emissions in the "Total" group as the sum of domestic, transport and industrial emissions. Also, time distribution of the emissions load was changed at every spatial point of the group's gridded emissions. Table 12.2 demonstrates a temporal scenario (2002 inventory) that provides a winter day emissions percent distribution in the "Domestic", Transport" and "Industry" groups (after ECan).

Table 12.2 Hourly emissions distribution in "Domestic", "Transport" and "Industry" groups in percents (after ECan, Scott, 2005).

Hour ending	Domestic	Transport	Industry
1	3.5%	0.61%	2.0%
2	3.5%	0.50%	2.0%
3	3.5%	0.80%	2.0%
4	3.5%	1.29%	2.0%
5	3.7%	1.62%	2.0%
6	3.6%	1.93%	2.0%
7	4.6%	4.22%	8.0%
8	3.9%	6.86%	8.0%
9	4.0%	6.17%	8.0%
10	3.9%	5.69%	8.0%
11	3.5%	5.68%	6.0%
12	3.0%	6.11%	6.0%
13	2.7%	6.34%	6.0%
14	2.2%	6.27%	6.0%
15	2.2%	6.47%	6.0%
16	2.3%	6.82%	6.0%
17	3.8%	7.22%	3.0%
18	7.4%	6.79%	3.0%
19	8.4%	5.73%	3.0%
20	8.0%	4.08%	3.0%
21	6.8%	2.91%	3.0%
22	4.9%	2.54%	3.0%
23	3.5%	1.98%	2.0%
24	3.5%	1.37%	2.0%
SUM of %	100.00%	100.00%	100.00%
Day: 7am – 6pm	31.37%	74.64%	70.53%
Night: 7pm – 6am	68.63%	25.36%	29.47%

Table 12.2 shows peak of total aerosol emissions falling in day-time in groups "Transport" (74.64%) and "Industry" (70.53%) and at night-time in group "Domestic" (68.63%). As domestic

emissions are shown to play the most important role in PM peak concentrations, this temporal distribution (with the additional increase of transport emissions during afternoon rush hours) pre-defines a dominance of the night-time aerosol peak for the local scale air circulation (for 7 episodes from winter 2005). Four time periods used in former calculations were replaced by the hourly changing emissions in every grid point in all three emission groups. This was done by applying the ratio data from Tables 12.1 and 12.2 to every point value of the group's gridded emissions obtained from 1999 inventory.

Possible decrease of total PM (averaged for 7 winter 2005 episodes) is calculated for 2005-2013 years, but is presented for years 2005 (about 50% total emissions decrease), 2007 (60% decrease), 2010 (70 % decrease) and for 2013 (3 fold decrease compared with 1999). Figure 12.1 presents the spatial distribution of modelled total PM_{10} concentrations at midnight on 5 May 2005 (episode 4, winter 2005 meteorology) obtained for the 2005 proposed reduction (of 50% - Table 12.1) of the input total emissions (Figure 12.1a) compared with total PM concentrations calculated for the initial 1999 PM_{10} emissions (Figure 12.1b). Bulk MM5 LSM and complex Scenario 1-3mix are used in the MM5 v3.7.3-CAMx4.4 numerical system.

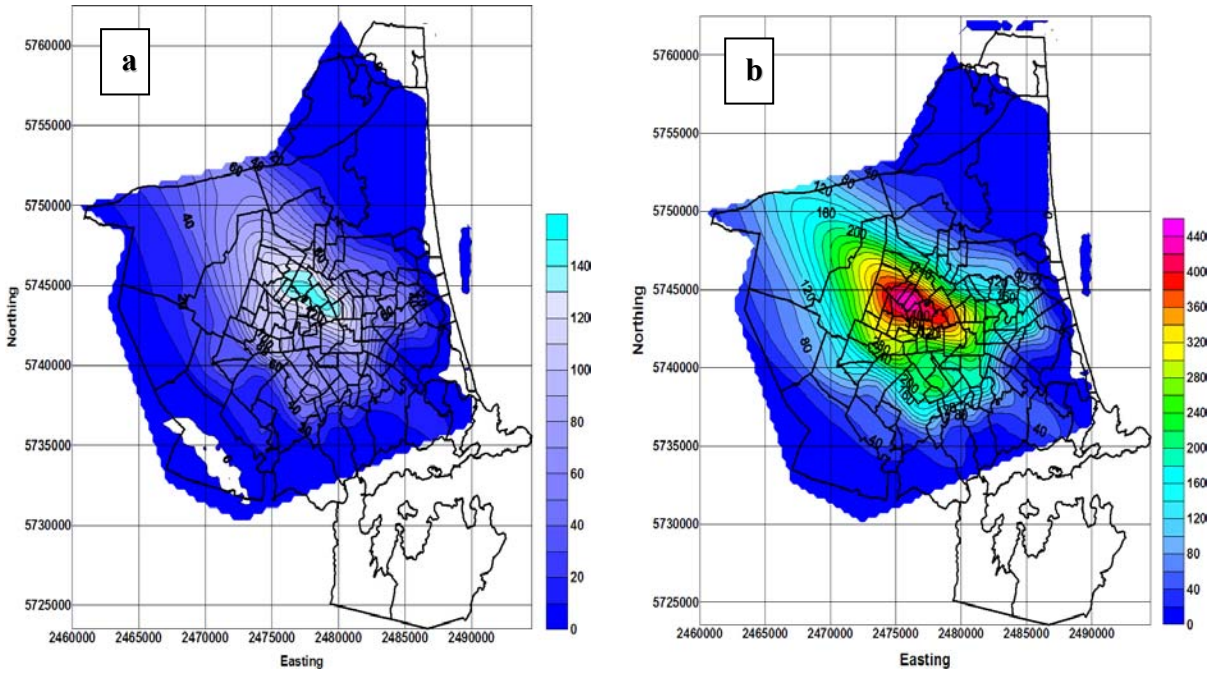

Figure 12.1 Spatial near-surface (8-10 metres) distribution of PM_{10} concentrations (μg m^{-3}) at midnight 5 May 2005, episode 4, and Scenario 1-3mix: a) for the winter 2005 proposed 45% reduction of the total emissions; b) for the initial 1999 "Total" group emissions.

Comparison of Figures 12.1a and 12.1b shows that there should be 2.5 times decrease of the peak PM_{10} concentrations (at midnight) compared with use of the 1999 input emissions. Table 12.3 presents modelled-observed average, mean absolute error and correlation coefficient of modelled PM_{10} in the "Total" group for 1999 and 2005 emissions (linear emissions reduction) compared with ambient data from Coles Place (7 winter 2005 meteorological episodes).

Table 12.3 Average (modelled - observed), Mean Absolute Error (MAE), Pearson Correlation Coefficient (PCC) and Power Correlation Coefficient (Power CC – PCC*PCC), 7 episodes average, complex Scenario 1-3mix, total PM (μg m^{-3}): "Total" 1999 and "Total" 2005 emissions.

Modelled PM	AVERAGE Mod. – Obs.	MAE	PCC	Power CC
PM_{10} - 1999 total	39.50 – 54.25	14.25	0.75	0.56
PM_{10} – 2005 total	31.75 – 54.25	16.15	0.71	0.51

Table 12.3 shows a decrease of the modelled average PM_{10} concentrations (for proposed year 2005 reduced emissions) on 20% only to compare with year 1999 modelled PM_{10} concentration (31.75 versus 39.50 μg m^{-3}), and 41% lower modelled concentrations to compare with year 2005 ambient PM_{10} concentrations (31.75 versus 54.25 μg m^{-3} - Coles Place). Correlation of the reduced modelled aerosol values (7 winter 2005 episodes) is very close to PCC of the 1999 modelled concentrations (0.71 via 0.75 – Table 12.3), which suggests the same time distribution of PM_{10} emissions for the winter 2005 proposed emissions scenario (see Table 12.2). The modelled PM_{10} average concentration reduction is lower than aerosol emissions reduction from Table 12.1 (20% versus 45%), and the proposed level of PM concentrations has not been reached for winter 2005.

Figure 12.2 presents the spatial the distribution of modelled total PM_{10} concentrations at midnight on 5 May 2005 (episode 4, winter 2005 meteorology) obtained for the 2007 proposed reduction (of 60% - Table 12.1) of the input total emissions (Figure 12.2a) compared with total PM concentrations calculated for the initial 1999 PM emissions (Figure 12.2b). Bulk MM5 LSM and complex Scenario 1-3mix are used in the MM5 v3.7.3-CAMx4.4 evaluation.

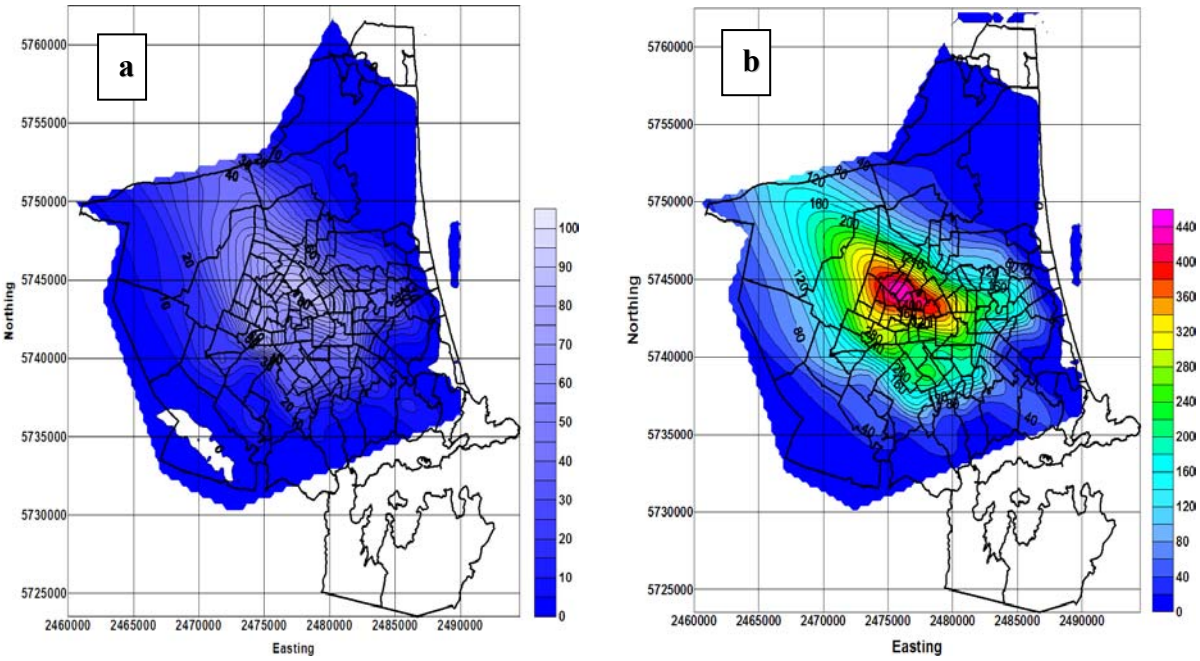

Figure 12.2 Spatial near-surface (8-10 metres) distribution of PM_{10} concentrations (μg m^{-3}) at midnight 5 May 2005, episode 4, and Scenario 1-3mix: a) for the winter 2007 proposed 60% reduction of the total emissions; b) for the initial 1999 "Total" group emissions.

Figures 12.2a and 12.2b demonstrate that there should be nearly 4 fold decrease of the peak PM_{10} concentrations (at midnight) compared with use of 1999 input emissions. Table 12.4 presents modelled-observed average, mean absolute error and correlation coefficient of modelled PM_{10} in the "Total" group for 1999 and 2007 emissions (linear emissions decrease) compared with ambient data from Coles Place (7 winter 2005 episodes).

Table 12.4 Average (modelled - observed), Mean Absolute Error (MAE), Pearson Correlation Coefficient (PCC) and Power Correlation Coefficient (Power CC), 7 episodes average, complex Scenario 1-3mix, total PM (μg m^{-3}): "Total" 1999 and "Total" 2007 emissions.

Modelled PM	AVERAGE Mod. – Obs.	MAE	PCC	Power CC
PM_{10} - 1999 total	39.50 – 54.25	14.25	0.75	0.56
PM_{10} – 2007 total	20.70 – 54.25	27.10	0.61	0.37

Table 12.4 illustrates a decrease of the modelled average PM_{10} concentrations (for proposed year 2007 reduced emissions) of 48% compared with year 1999 modelled PM_{10} concentrations (20.70 versus 39.50 μg m^{-3}), and a 62% lower modelled concentrations compared with year 2005 ambient PM_{10} concentration (54.25 μg m^{-3} - Coles Place). Correlation of the reduced modelled aerosol values (7 winter 2005 episodes) is lower than 1999 modelled aerosol PCC (0.61 versus 0.75 – Table 12.4), which suggests elimination of PM_{10} peaks and a time shift of PM_{10} concentrations for

the proposed 2007 emissions scenario. The modelled PM_{10} average concentration reduction is lower compared with the proposed year 2007 emissions reduction from the Table 12.1 (48% versus 60%) as a result of MM5-CAMx4 modelling system replication to the modelled PM_{10} non-linear time-space dispersion.

Figure 12.3 presents the spatial distribution of modelled total PM_{10} concentrations at midnight on 5 May 2005 (episode 4, winter 2005 meteorology) obtained for the 2010 proposed reduction (of 70% - Table 12.1) of the input total emissions (Figure 12.3a) compared with total PM concentrations calculated for the initial 1999 PM emissions (Figure 12.3b). Bulk MM5 LSM and complex Scenario 1-3mix are used in the MM5 v3.7.3-CAMx4.4 evaluation.

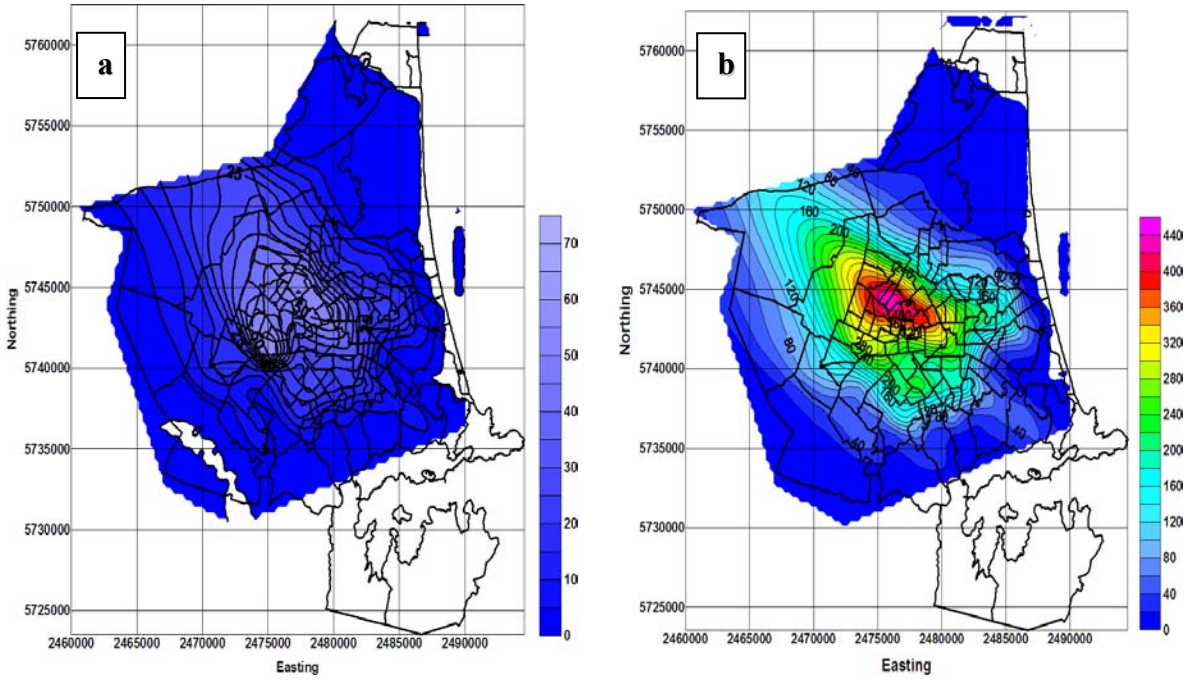

Figure 12.3 Spatial near-surface (8-10 metres) distribution of PM_{10} concentrations (μg m^{-3}) at midnight 5 May 2005, episode 4, and Scenario 1-3mix: a) for the winter 2010 proposed 70% reduction of total emissions; b) for the initial 1999 "Total" group emissions.

Figures 12.3a and 12.3b reveal that there should be more than a 5 fold decrease of the peak PM_{10} concentrations (at midnight, episode 4) compared with originally used 1999 input emissions. Table 12.5 presents modelled-observed average, mean absolute error and correlation coefficient of modelled PM_{10} in "Total" group for 1999 and 2010 emissions (linear emissions decrease) compared with ambient data from Coles Place (7 winter 2005 episodes).

Table 12.5 Average (modelled-observed), Mean Absolute Error (MAE), Pearson Correlation Coefficient (PCC) and Power Correlation Coefficient (Power CC), 7 episodes average, complex Scenario 1-3mix, total PM (μg m^{-3}): "Total" 1999 and "Total" 2010 emissions.

Modelled PM	AVERAGE Mod. – Obs.	MAE	PCC	Power CC
PM_{10} - 1999 total	39.50 – 54.25	14.25	0.75	0.56
PM_{10} – 2010 total	14.25 – 54.25	33.75	0.51	0.26

Table 12.5 shows a decrease of the modelled average PM_{10} concentrations (for the proposed year 2010 total emissions reduction) of 64% compared with year 1999 modelled PM_{10} concentration (14.25 versus 39.50 μg m^{-3}), and a 74% lower year 2010 modelled concentrations to compare with observed ambient PM concentration (14.25 versus 54.25 μg m^{-3} - Coles Place site). Correlation of the reduced modelled aerosol values (7 winter 2005 episodes) continues to decrease compared with 1999 modelled aerosol PCC (0.51 via 0.75 – Table 12.4), which suggests elimination of PM_{10} peaks and possible time shift of PM_{10} peak concentrations for the 2010 proposed reduction scenario. The modelled PM_{10} average concentration reduction is lower compared with proposed for year 2010 (Tables 12.1) emissions reduction (64% versus 70%) as a result of modelled PM non-linear time-space dispersion.

Figure 12.4 presents the spatial distribution of modelled total PM_{10} concentrations at midnight on 5 May 2005 (episode 4, winter 2005 meteorology) obtained for year 2013 proposed reduction (of 80% - Table 12.1) of the input total emissions (Figure 12.4a) compared with PM_{10} concentrations calculated for the initial 1999 PM emissions (Figure 12.4b). Bulk LSM and complex Scenario 1-3mix are used in the MM5-CAMx4 numerical modelling system.

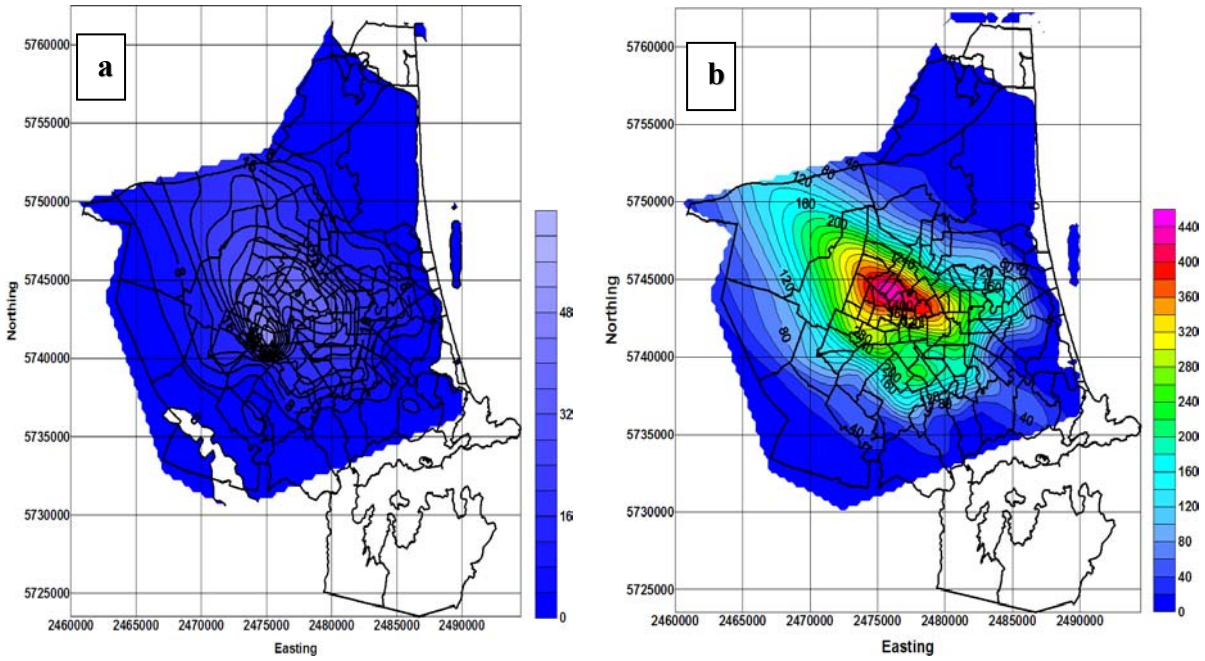

Figure 12.4 Spatial near-surface (8-10 metres) distribution of PM_{10} concentrations (μg m^{-3}) at midnight 5 May 2005, episode 4, and Scenario 1-3mix: a) for the winter 2013 proposed 75% reduction of the total emissions; b) for the initial 1999 "Total" group emissions.

Figures 12.4a and 12.4b reveal that there should be nearly a 6 times decrease of the peak PM_{10} concentrations (at midnight, episode 4) compared with year 1999 input emissions. Table 12.6 presents modelled-observed average, mean absolute error and correlation coefficient of modelled PM_{10} in the "Total" group for year 1999 and year 2013 emissions (linear emissions decrease) compared with ambient data from Coles Place (7 winter 2005 episodes).

Table 12.6 Average (modelled-observed), Mean Absolute Error (MAE), Pearson Correlation Coefficient (PCC) and Power Correlation Coefficient (Power CC), 7 episodes average, complex Scenario 1-3mix, total PM (μg m^{-3}): "Total" 1999 and "Total" 2013 emissions.

Modelled PM	AVERAGE Mod. – Obs.	MAE	PCC	Power CC
PM_{10} - 1999 total	39.50 – 54.25	14.25	0.75	0.56
PM_{10} – 2013 total	12.05 – 54.25	41.25	0.48	0.23

Table 12.6 illustrates a further decrease of the modelled average PM_{10} concentrations (for proposed year 2013 aerosol emissions reduction) of nearly 70% to compare with year 1999 modelled PM_{10} concentrations, and a 78% lower year 2013 modelled concentrations versus year 2005 observed ambient PM_{10} (54.25 μg m^{-3} - Coles Place). Correlation of the reduced modelled aerosol values (7 winter 2005 episodes) is weak compared with 1999 modelled aerosol PCC (0.48 versus 0.75 – Table 12.6) showing a decrease of PM_{10} peaks and a potential time shift of PM_{10} peaks for year 2013 emission scenario. Once again year 2013 modelled PM_{10} average

concentration reduction is lower than proposed year 2013 emissions reduction from the Table 12.1 (70% against 75%) as a result of MM5-CAMx4 reproduction of the total PM non-linear time-space dispersion.

As year 2013 is considered to be the final year of the "Clean Air over New Zealand" project (Ministry for Environment, 2003) it is worth providing one more visual image of the spatial PM_{10} distribution (compared with 1999 inventory emissions) for winter 2005 episode 7. Figure 12.5 presents the spatial distribution of modelled total PM_{10} concentrations at midnight on 14 May 2005 obtained for year 2013 proposed 75% reduction of the input total emissions (Figure 12.5a) compared with PM_{10} concentrations calculated for initial year 1999 PM emissions (Figure 12.5b).

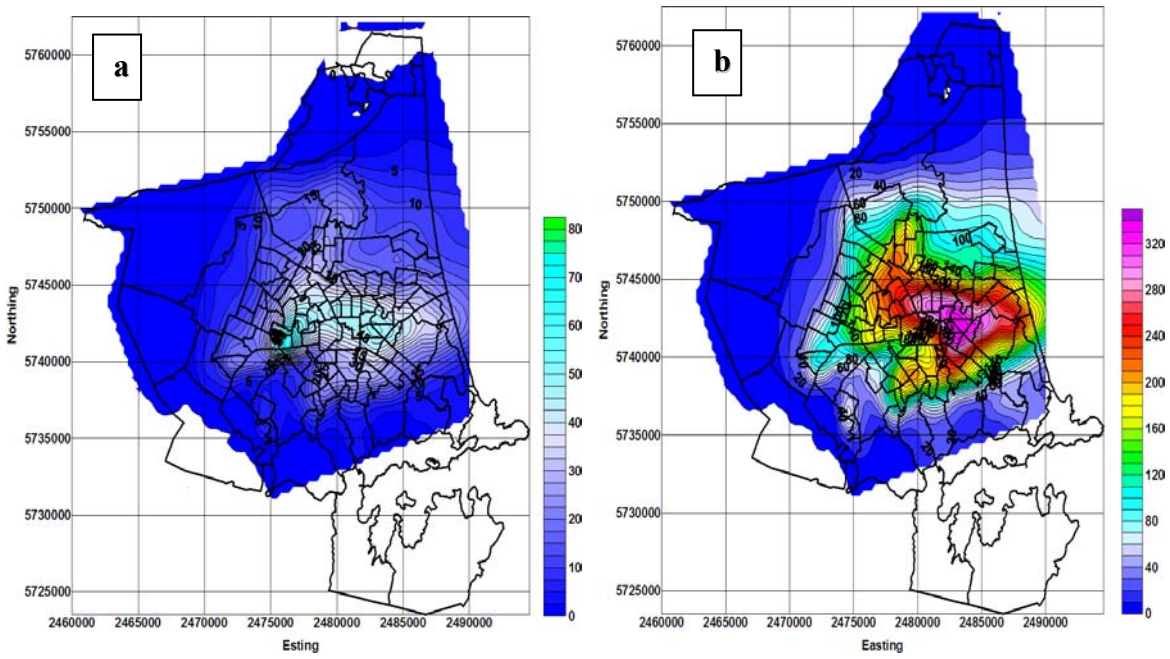

Figure 12.5 Spatial near-surface (8-10 metres) distribution of PM_{10} concentrations (µg m^{-3}) at midnight 14 May 2005, episode 7 and Scenario 1-3mix: a) for the winter 2013 proposed 75% reduction of the total emissions; b) for the initial 1999 "Total" group emissions.

Figure 12.5 shows a projected decrease of predicted PM_{10} of about 4.5 fold (winter 2013) compared with winter 1999 total aerosol concentrations, and shows the variability of the reduction level depending on the actual meteorological conditions (in this study – meteorological conditions of the winter 2005 case studies). The modelled years 2005-2013 proposed reductions of a winter day's PM_{10} concentrations are valid only for the inner Christchurch (about 17,680 ha –see Figure 4.5).

12.2 Possible fine PM decrease for the period 2005-2013

In Section 12.1 it was explained that the data from Table 12.1 are used to calculate PM_{10} emissions in every point of the gridded emissions array for all 3 groups and to compile gridded emissions for group "Total" as a sum of the domestic, transport and industrial emissions 2-dimensional arrays. Also time distribution of the emissions load was changed at every spatial point. Fine PM emissions were obtained with application of a coefficient R_{PM}, where R_{PM} (see Section 9.3.1) is a ratio between fine and total aerosol ($PM_{2.5}/PM_{10}$) equal to 0.84 for all species except EC (R_{PM} = 0.95) and crustal elements (R_{PM} = 0.65).

Figure 12.6 presents the spatial distribution of modelled total $PM_{2.5}$ concentrations at midnight on 5 May 2005 (episode 4, winter 2005 meteorology) obtained for year 2005 proposed reduction (of 45% for PM_{10} - Table 12.1) of the input total emissions (Figure 12.6a) compared with fine PM concentrations calculated for the initial 1999 $PM_{2.5}$ emissions (Figure 12.6b). Bulk MM5 LSM and complex Scenario 1-3mix are used in the MM5 v3.7.3-CAMx4.4 evaluation.

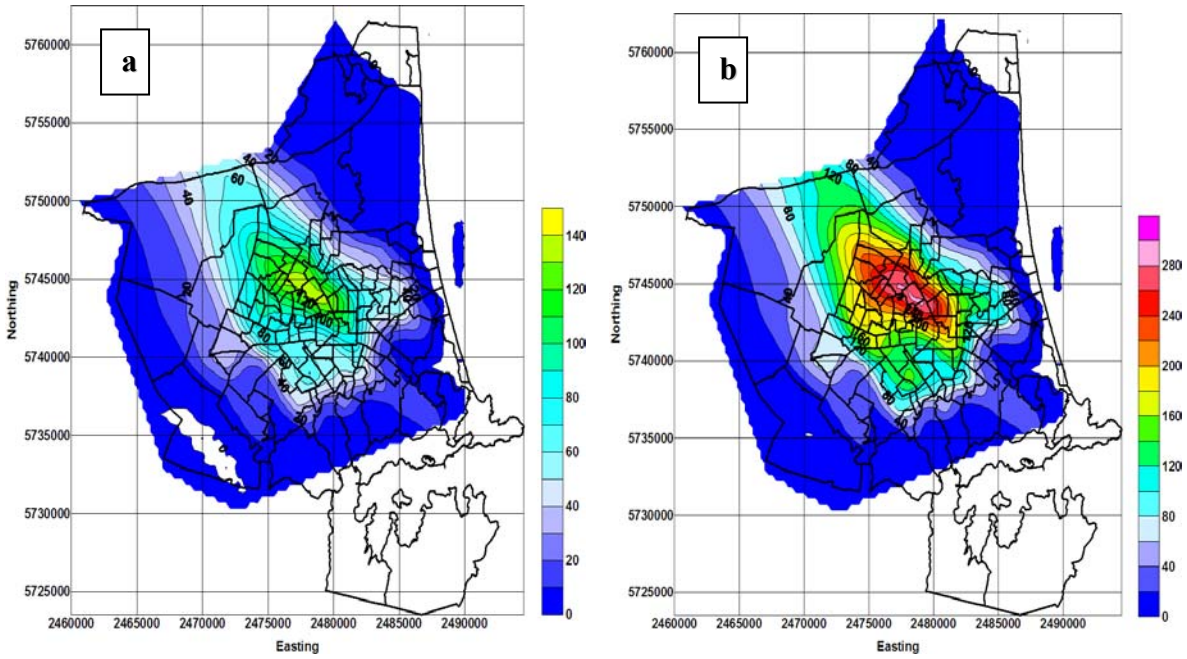

Figure 12.6 Spatial near-surface (8-10 metres) distribution of $PM_{2.5}$ concentrations (μg m^{-3}) at midnight 5 May 2005, episode 4, and Scenario 1-3mix: a) for the winter 2005 proposed 45% reduction of total emissions; b) for the initial 1999 "Total" group emissions.

Comparison of the Figures 12.6a and 12.6b shows that there should be a 2.5 fold decrease of the peak $PM_{2.5}$ concentrations (at midnight) compared with year 1999 gridded emissions usage. Table 12.7 presents modelled-observed average, mean absolute error and correlation coefficient of modelled $PM_{2.5}$ in the "Total" group for 1999 and 2005 emissions (after linear emissions

reduction) compared with ambient data from Coles Place site (7 winter 2005 meteorological episodes).

Table 12.7 Average (modelled-observed), Mean Absolute Error (MAE), Pearson Correlation Coefficient (PCC) and Power Correlation Coefficient (Power CC – PCC*PCC), 7 episodes average, complex Scenario 1-3mix, fine PM (μg m^{-3}): "Total" 1999 and "Total" 2005 emissions.

Modelled PM	AVERAGE Mod. – Obs.	MAE	PCC	Power CC
$PM_{2.5}$ - 1999 total	37.75 – 42.30	11.75	0.73	0.53
$PM_{2.5}$ – 2005 total	29.25 – 42.30	12.65	0.68	0.42

Table 12.7 shows a decrease of the modelled average $PM_{2.5}$ concentrations (for the proposed year 2005 total emissions) on 23% (20% for PM_{10}) to compare with year 1999 modelled $PM_{2.5}$ concentrations, and 31% lower year 2005 modelled fine PM concentrations compared with ambient fine PM for winter 2005 (42.30 μg m^{-3} - Coles Place). Correlation of the reduced modelled aerosol values (7 winter 2005 episodes) is close to PCC of the 1999 modelled concentrations (0.68 via 0.73 – Table 12.7) that proves the same time distribution of $PM_{2.5}$ emissions for winter 2005 proposed emissions scenario (see Table 12.2).

Figure 12.7 presents the spatial distribution of modelled total $PM_{2.5}$ concentrations at midnight on 5 May 2005 (episode 4, winter 2005 meteorology) obtained for year 2007 proposed reduction (of 60% for PM_{10} - Table 12.1) of the input gridded emissions (Figure 12.7a) compared with fine PM concentrations calculated for the initial year 1999 PM emissions (Figure 12.7b). Bulk MM5 LSM and complex Scenario 1-3mix are used in the MM5 v3.7.3-CAMx4.4 evaluation.

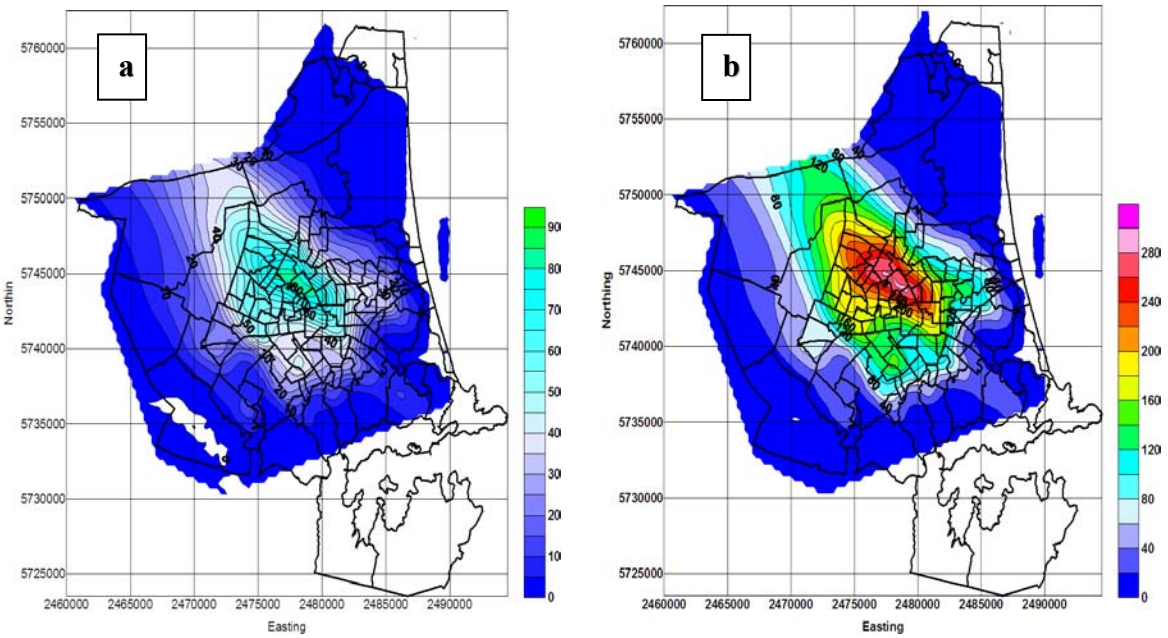

Figure 12.7 Spatial near-surface (8-10 metres) distribution of $PM_{2.5}$ concentrations (μg m^{-3}) at midnight 5 May 2005, episode 4, and Scenario 1-3mix: a) for the winter 2007 proposed 60% reduction of total emissions; b) for the initial 1999 "Total" group emissions.

Figures 12.7a and 12.7b demonstrate that there should be about a 3 times decrease of the peak $PM_{2.5}$ concentrations (at midnight) for year 2007 compared with use of year 1999 input emissions for episode 4. Table 12.8 presents modelled-observed average, mean absolute error and correlation coefficient of modelled $PM_{2.5}$ in the "Total" group for year 1999 and year 2007 emissions (linear emissions decrease) compared with ambient data from Coles Place site (7 winter 2005 episodes).

Table 12.8 Average (modelled-observed), Mean Absolute Error (MAE), Pearson Correlation Coefficient (PCC) and Power Correlation Coefficient (Power CC), 7 episodes average, complex Scenario 1-3mix, total PM (μg m^{-3}): "Total" 1999 and "Total" 2007 emissions.

Modelled PM	AVERAGE Mod. – Obs.	MAE	PCC	Power CC
$PM_{2.5}$ - 1999 total	37.75 – 42.30	11.75	0.73	0.53
$PM_{2.5}$ – 2007 total	18.55 – 42.30	19.65	0.63	0.40

Table 12.8 illustrates a decrease of the modelled average $PM_{2.5}$ concentrations (for the proposed year 2007 reduction of total emissions) on a 51% (versus 48% for PM_{10}) compared with year 1999 modelled $PM_{2.5}$ concentrations, and 57% (62% - PM_{10}) lower year 2007 modelled concentrations compared with the year 2005 observed $PM_{2.5}$ (42.30 μg m^{-3} - Coles Place site). Correlation of the reduced modelled aerosol values (7 winter 2005 episodes) is lower than year 1999 modelled aerosol PCC (0.63 versus 0.73 – Table 12.8), which suggests elimination of $PM_{2.5}$ peaks and a time shift of aerosol concentrations for year 2007 proposed emissions scenario. The modelled $PM_{2.5}$

concentration average reduction in 2007 has a big drop compared with the moderate modelled aerosol concentrations decrease for the year 2005 (the same can be said about PM_{10}).

Figure 12.8 presents the spatial distribution of modelled $PM_{2.5}$ concentrations at midnight on 5 May 2005 (episode 4, winter 2005 meteorology) obtained for the year 2010 proposed reduction (of 70% for PM_{10} - Table 12.1) of the input total emissions (Figure 12.8a) compared with total PM concentrations calculated for the initial year 1999 PM emissions (Figure 12.8b). Bulk MM5 LSM and complex Scenario 1-3mix are used in the MM5 v3.7.3-CAMx4.4 evaluation.

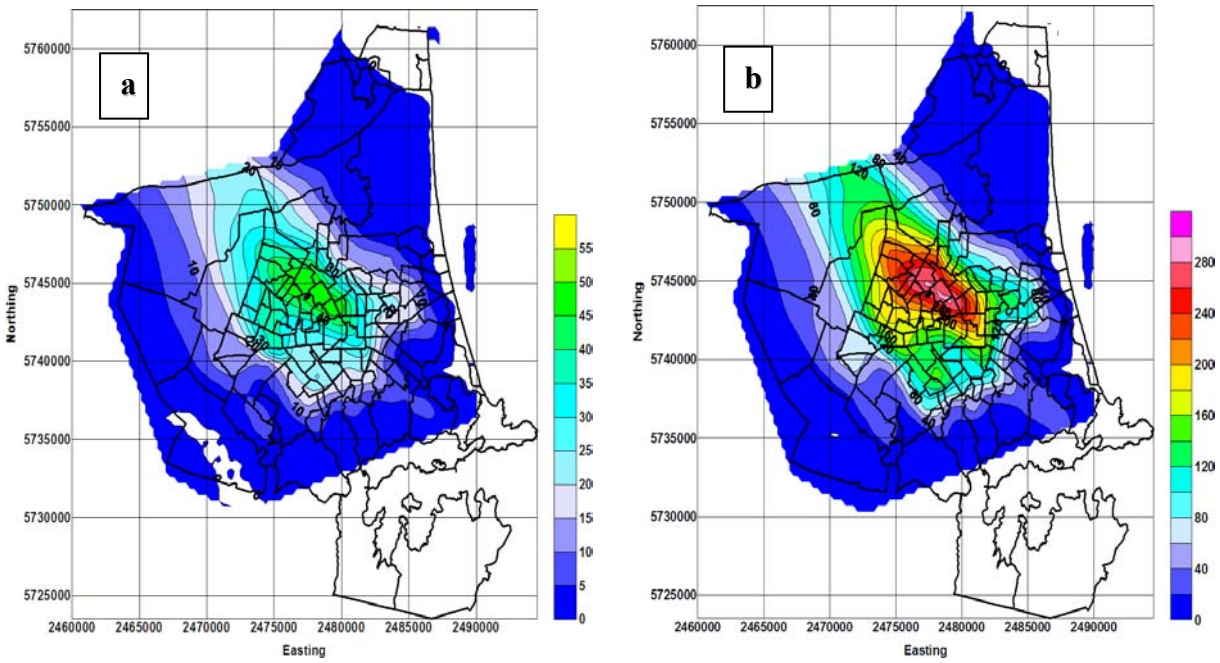

Figure 12.8 Spatial near-surface (8-10 metres) distribution of $PM_{2.5}$ concentrations (μg m^{-3}) at midnight 5 May 2005, episode 4, and Scenario 1-3mix: a) for the winter 2010 proposed 70% reduction of total emissions; b) for the initial 1999 "Total" group emissions.

Figures 12.8a and 12.8b reveal that there should be about a 5.5 fold decrease of the peak $PM_{2.5}$ concentrations (at midnight, episode 4) compared with year 1999 modelled $PM_{2.5}$ concentrations. Table 12.9 presents modelled-observed average, mean absolute error and correlation coefficient of modelled $PM_{2.5}$ in the "Total" group for year 1999 and year 2010 emissions (linear emissions decrease) compared with ambient data from Coles Place (7 winter 2005 episodes).

Table 12.9 Average (modelled-observed), Mean Absolute Error (MAE), Pearson Correlation Coefficient (PCC) and Power Correlation Coefficient (Power CC – PCC*PCC), 7 episodes average, complex Scenario 1-3mix, fine PM (μg m^{-3}): "Total" 1999 and "Total" 2010 emissions.

Modelled PM	AVERAGE Mod. – Obs.	MAE	PCC	Power CC
$PM_{2.5}$ - 1999 total	37.75 – 42.30	11.75	0.73	0.53
$PM_{2.5}$ – 2010 total	13.05 – 42.30	29.05	0.60	0.36

Table 12.9 shows a further decrease of the modelled $PM_{2.5}$ concentrations (for the proposed year 2010 reduction of the total emissions) of 65% (64% - total PM) compared with the year 1999 modelled $PM_{2.5}$ concentrations, and 70% (74% - total PM) lower the year 2010 modelled concentrations against observed year 2005 ambient fine PM (42.30 μg m^{-3} - Coles Place site). Correlation of the reduced modelled aerosol values (7 winter 2005 episodes) continues to decrease compared with 1999 modelled aerosol PCC (0.60 versus 0.73 – Table 12.9), which suggests elimination of $PM_{2.5}$ peaks and a possible time shift of $PM_{2.5}$ peak concentrations for the year 2010 proposed reduction scenario.

Figure 12.9 presents the spatial distribution of modelled total $PM_{2.5}$ concentrations at midnight on 5 May 2005 (episode 4, winter 2005 meteorology) obtained for the year 2013 proposed reduction (of 75% for PM_{10} - Table 12.1) of the input emissions (Figure 12.9a) compared with $PM_{2.5}$ concentrations calculated for the initial year 1999 PM emissions (Figure 12.9b).

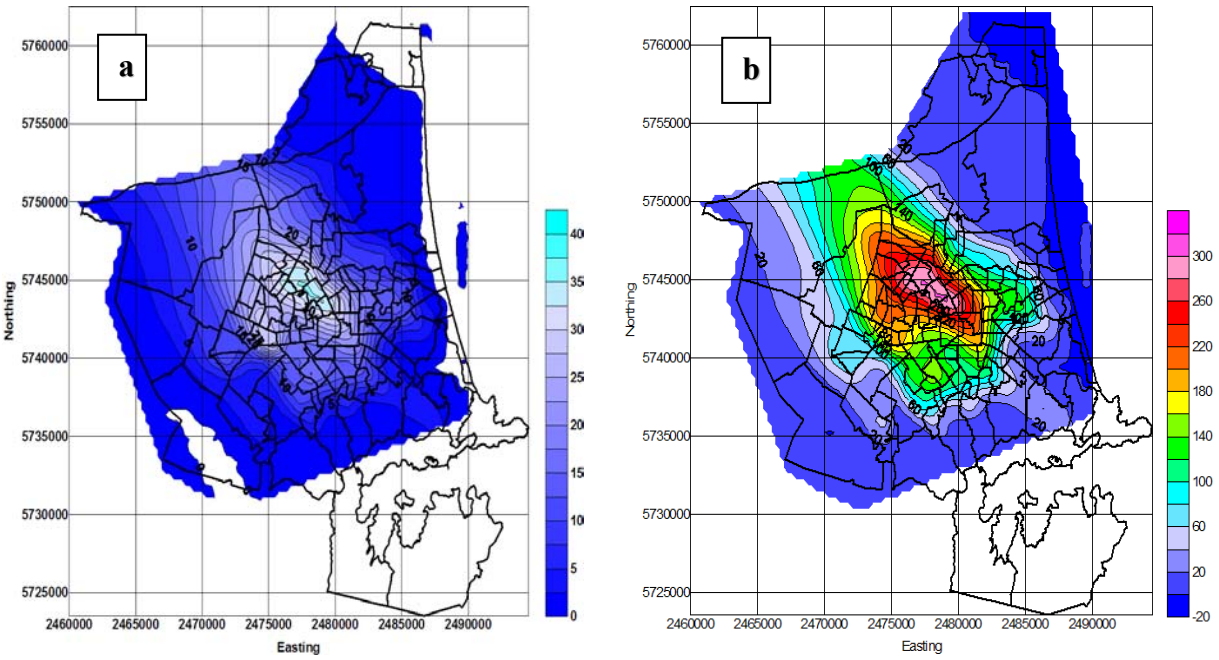

Figure 12.9 Spatial near-surface (8-10 metres) distribution of $PM_{2.5}$ concentrations (μg m^{-3}) at midnight 5 May 2005, episode 4, and Scenario 1-3mix: a) for the winter 2013 proposed 75% reduction of the fine emissions; b) for the initial 1999 "Total" group emissions.

Figures 12.9a and 12.9b reveal that there should be more than a 7 fold decrease of the $PM_{2.5}$ peak concentrations (at midnight, episode 4) for the year 2013 compared with the year 1999 fine PM modelled concentrations. Table 12.10 presents modelled-observed average, mean absolute error and correlation coefficient of modelled $PM_{2.5}$ in the "Total" group for 1999 and 2013 emissions (linear emissions decrease) compared with ambient data from Coles Place (7 winter 2005 episodes).

Table 12.10 Average (modelled-observed), Mean Absolute Error (MAE), Pearson Correlation Coefficient (PCC) and Power Correlation Coefficient (Power CC – PCC*PCC), 7 episodes average, complex Scenario 1-3mix, fine PM (μg m^{-3}): "Total" 1999 and "Total" 2013 emissions.

Modelled PM	AVERAGE Obs. – Mod.	MAE	PCC	Power CC
$PM_{2.5}$ - 1999 total	37.75 – 42.30	11.75	0.73	0.53
$PM_{2.5}$ – 2013 total	8.70 – 42.30	34.15	0.55	0.30

Table 12.10 illustrates a further decrease of the modelled average $PM_{2.5}$ concentrations (for the year 2013 aerosol emissions proposed reduction) on 77% (70% for PM_{10}) to compare with 1999 emissions modelled $PM_{2.5}$, and a 80% (78% for PM_{10}) lower year 2013 modelled concentrations compared with year 2005 observed ambient $PM_{2.5}$ concentrations (42.30 μg m^{-3} - Coles Place site). Correlation of the reduced modelled aerosol values (7 winter 2005 episodes) is weak compared with 1999 modelled aerosol PCC (0.55 versus 0.73 – Table 12.10) but bigger than for decreased PM_{10} peaks for the year 2013 emission scenario. Fine modelled PM is revealed to decrease faster than total PM as $PM_{2.5}$ contains nearly all the chemical species that are treated well by CAMx4.4 chemical mechanism. Also, a certain fraction of PM_{10} consists of natural aerosol particles (like crustal-primary elements and natural dust) that are proposed not to decrease seriously in the years 2005-2013 emission scenarios.

One more example of the modelled $PM_{2.5}$ distribution for winter 2005 episode 7 is shown in Figure 12.10. $PM_{2.5}$ concentrations at midnight on 14 May 2005 are obtained for the year 2013 proposed 75% (PM_{10}) reduction of the input gridded emissions (Figure 12.10a) compared with $PM_{2.5}$ concentrations calculated for 1999 PM emissions (Figure 12.10b).

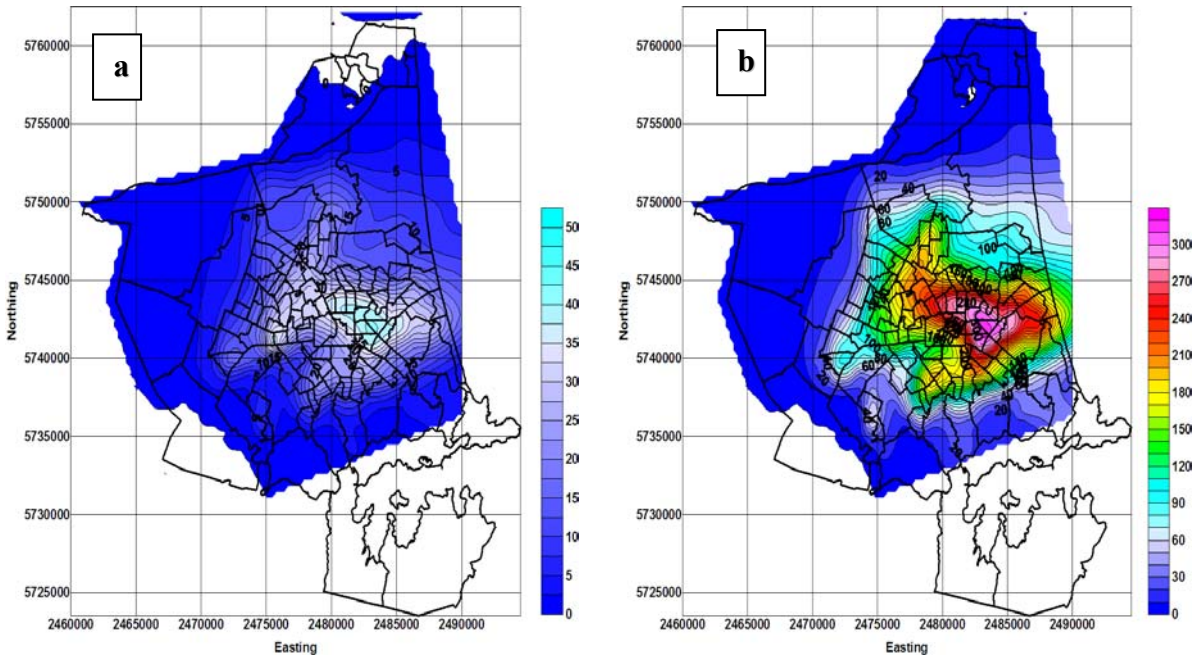

Figure 12.10 Spatial near-surfaces (8-10 metres) distribution of $PM_{2.5}$ concentrations (µg m^{-3}) at midnight 14 May 2005, episode 7 and Scenario 1-3mix: a) the winter 2013 reduced emissions; b) the 1999 "Total" group emissions.

Figure 12.10 shows the proposed decrease of predicted $PM_{2.5}$ concentration peak about 6 times (winter 2013) compared with winter 1999 fine aerosol concentrations, which confirms the variability of the degree of PM concentration reduction for different episodes depending on the meteorological conditions.

12.3 Influence of groups on a proposed future PM scenario

From ECan's proposed future total aerosol reduction scenario (2005-2013 time period) consists of the negative/positive tendency of PM_{10} in groups (calculated in grams per inner part of the city daily). The proposed ratio decrease/increase for a winter day's PM_{10} emissions in the groups "Domestic", "Transport" and "Industry" (grams $area^{-1}$ day^{-1}, area of the inner Christchurch = 17,680 ha – see Figure 4.5) is presented in Table 12.11 and includes the changes in emissions for the 2005-2013 year time period (Ministry for Environment. 2003). Table 12.11 also includes the emissions ratio for the 1999 inventory as equal to one in all groups.

Table 12.11 Ratio for a winter day PM_{10} emissions in "Domestic", "Transport" and "Industry" groups (grams $area^{-1}$ day^{-1}, inner Christchurch area = 17,680 ha) for 2005-2013 years emissions in relation to year 1999 winter day equal to 1.0.

Group / Year	1999	2005	2006	2007	2008
Domestic	1.000	0.494	0.357	0.292	0.220
Transport	1.000	0.701	0.655	0.608	0.561
Industry	1.000	0.980	0.999	1.019	1.038
Total	1.000	0.564	0.451	0.396	0.336
Group / Year	**2009**	**2010**	**2011**	**2012**	**2013**
Domestic	0.193	0.175	0.156	0.138	0.120
Transport	0.514	0.467	0.421	0.399	0.378
Industry	1.057	1.076	1.095	1.114	1.133
Total	0.312	0.294	0.276	0.261	0.2465

From Table 12.11 it could be inferred that up to year 2007 emissions from the domestic group will reduce by more than 3 times and to 2013 will be just 12% of the initial 1999 emissions. Also, a very fast decrease is suggested in the "Transport" group: a 40% reduction to year 2007, and more than 60% by year 2013. A small increase is evident in the "Industry" group that presumably is a result of industrial sector growth in the Christchurch city. In any way such a reduction in the "Domestic" (especially) and "Transport" groups are unrealistic: the total number of old-style open-fires and log-burners has no steep tendency to decrease, and the total car fleet has a tendency to increase with gradual substitution of the old engine cars with new ones, and a tendency for diesel cars (Sport UV) ratio to increase. The reasons for these processes are quite simple and apparent: the energy prices keep increasing and householders just don't have enough money to heat their dwellings using electricity, and second-hand cars and diesel cars are very popular, being much cheaper under conditions of constantly increasing petrol prices. But it is productive to analyse the Table 12.11 ratios in different groups for the key years 2005, 2007, 2010 and 2013 to provide a better understanding of the basic sources of modelled PM_{10} concentrations reduction obtained from the MM5-CAMx4 modelled data and discussed in Sections 12.1–12.2. Basic results are converted to ratios (%) and don't include absolute values, which to a certain degree could mask time tendency. Table 12.12 presents modelled-observed average, mean absolute error, correlation coefficient and ratio for 2005/1999 of modelled PM_{10} and $PM_{2.5}$ in the "Total" group for 1999 and 2005 emissions for 7 winter 2005 meteorological episodes (for Coles Place).

Table 12.12 Average (modelled-observed), Mean Absolute Error (MAE), Pearson Correlation Coefficient (PCC), 2005/1999 concentrations ratio for 7 episodes, complex Scenario 1-3mix, total-fine PM (μg m^{-3}): "Total" 1999 and "Total" 2005 emissions.

Modelled PM	AVERAGE Mod. – Obs.	MAE	PCC	2005/1999 (%)
PM_{10} – 2005 total	31.75 – 39.50	16.15	0.71	80.3
$PM_{2.5}$ – 2005 total	29.25 – 37.75	12.65	0.68	77.5

From Table 12.12 it is apparent that there was no serious decrease of either total (80%) or fine (77.5%) modelled average aerosol concentrations in spite of the proposed (modelled) 50% reduction in "Domestic" emissions and, as a result of residential sector dominance, a nearly 46% reduction in the group "Total" for year 2005. Table 12.13 presents modelled-observed average, mean absolute error, correlation coefficient and ratio for 2007/1999 of modelled PM_{10} and $PM_{2.5}$ in the "Total" group for 1999 and 2007 emissions for 7 winter 2005 meteorological episodes (for Coles Place).

Table 12.13 Average (modelled-observed), Mean Absolute Error (MAE), Pearson Correlation Coefficient (PCC), 2007/1999 concentrations ratio for 7 episodes average, complex Scenario 1-3mix, total-fine PM (μg m^{-3}): "Total" 1999 and "Total" 2007 emissions.

Modelled PM	AVERAGE Mod. – Obs.	MAE	PCC	2007/1999 (%)
PM_{10} – 2007 total	20.70 – 39.50	27.10	0.61	52.4
$PM_{2.5}$ – 2007 total	18.55 – 37.75	19.65	0.63	49.1

Table 12.13 shows that there is a significant decrease for both total (48%) and fine (51%) modelled average aerosol concentrations in response to the proposed (modelled) 70% reduction in "Domestic" emissions and, as a result of residential sector dominance, a nearly 60% reduction in the group "Total". The Tables 12.12-12.13 results help to assume that there should be a 3 fold decrease of residential aerosol emissions and nearly a half reduction of vehicular emissions to decrease by 50% average concentrations of total and fine PM (Table 12.13). This is true for average aerosol concentrations only (long-term PM exposure) as in the case of a short-term exposure (night-morning PM concentration peaks for any smog episode) a 50% decrease in group "Transport" or "Industry" sometimes is enough to lessen PM peak in 2 fold (Figure 11.4 and 11.5). Table 12.14 presents modelled-observed average, mean absolute error, correlation coefficient and ratio for 2010/1999 of modelled PM_{10} and $PM_{2.5}$ in "Total" group for 1999 and 2010 emissions for 7 winter 2005 meteorological episodes (for Coles Place).

Table 12.14 Average (modelled-observed), Mean Absolute Error (MAE), Pearson Correlation Coefficient (PCC), 2010/1999 concentrations ratio for 7 episodes average, complex Scenario 1-3mix, total-fine PM (μg m^{-3}): "Total" 1999 and "Total" 2010 emissions.

Modelled PM	AVERAGE Mod. – Obs.	MAE	PCC	2010/1999 (%)
PM_{10} – 2010 total	14.25 – 39.50	33.75	0.51	36.1
$PM_{2.5}$ – 2010 total	13.05 – 37.75	29.05	0.60	34.5

Table 12.14 demonstrates one more significant decrease for total (64%) and for fine (65.5%) modelled average aerosol concentrations in response to a proposed (modelled) 82% reduction in "Domestic" emissions and, as an effect of residential sector dominance, a nearly 70% reduction in the group "Total". Table 12.15 demonstrates modelled-observed average, mean absolute error, correlation coefficient and ratio for 2013/1999 of modelled PM_{10} and$PM_{2.5}$ in the "Total" group for 1999 and 2013 emissions for 7 winter 2013 meteorological episodes (for Coles Place).

Table 12.15 Average (modelled-observed), Mean Absolute Error (MAE), Pearson Correlation Coefficient (PCC), 2013/1999 concentrations ratio for 7 episodes average, complex Scenario 1-3mix, total-fine PM (μg m^{-3}): "Total" 1999 and "Total" 2007 emissions.

Modelled PM	AVERAGE Mod. – Obs.	MAE	PCC	2013/1999 (%)
PM_{10} – 2013 total	12.05 – 54.25	41.25	0.48	22.2
$PM_{2.5}$ – 2013 total	8.70 – 42.30	34.15	0.55	20.5

Table 12.15 shows a third significant decrease for total (78%) and fine (79.5%) modelled average aerosol concentrations as a result of the proposed (modelled) 85% reduction in "Domestic" emissions and, as an outcome of residential sector dominance, a 75% reduction in the group "Total". It is important to stress that it is a first time when the proposed level of PM emissions reduction (Table 12.11) is less than the level of the modelled average PM concentrations decrease (for the year 2013 only) regarding to observed concentration.

From the Tables 12.12-12.15 it is clear that 3 fold decrease of the initial (year 1999) residential aerosol emissions and nearly a 50% reduction of vehicular emissions is required to halve average PM concentrations (Table 12.13). However, after this modelled average PM concentrations rapidly decrease from 2007 until 2013. The decrease of the average aerosol concentrations gains a stable trend for total and fine PM, definitely improving winter-time long-term ambient air conditions.

It is also important to discuss the straight and curved line paths (SLiPs & CLiPs) PM_{10} concentration abatement strategy introduced by the Ministry for the Environment (Fisher et al., 2005) to develop targets and predict the compliance of aerosol pollution reduction strategies for the 2005-2013 time period. In the SLiPs and CLiPS discussion document (Fisher et al., 2005) in the Section 1.2 it is stated:

"Straight line paths (SLiPs) are defined in the AQNES amendments under Regulation 17 subclause (5) as *"... a straight line that –*

a. starts on the y-axis of a graph at a point representing, as at the relevant date, the extent to which the concentration of PM_{10} in the airshed breaches its ambient air quality standard; and

b. ends on the x-axis of the graph at a point representing, as at 1 September 2013, the ambient air quality standard for PM_{10} in the airshed."

The *relevant date* means –

a. *in the case of an airshed that is the region of a regional council, 1 September 2005:*

b. *in the case of an airshed that is part of the region of a regional council, the date of the notice in the Gazette that specifies the part to be a separate airshed*.

Curved line paths (CLiPs) are defined in the AQNES amendments under Regulation 17 subclause (5) as *"... a curved line that –*

a. starts on the y-axis of a graph at a point representing, as at 1 September 2005 or the date that the plan is publicly notified (whichever is the later), the concentration of PM_{10} in the airshed; and

b. ends on the x-axis of the graph at a point representing, as at 1 September 2013, the ambient air quality standard for PM_{10} in the airshed."

A CLiP can **only** be used when considering resource consents if the CLiP has been outlined in the regional plan **and** if there are rules ensuring that resource consents are declined for applications that are likely to cause, at any time, the concentration of PM10 in the airshed to be above the CLiP (see Regulation 17B of the AQNES for further details)." (SLiPs and CLiPs discussion document; Fisher et al., 2005).

From the document extract it is apparent that there are no serious reasons to apply CLiP strategy and the rest of this section of the document is dedicated to the SLiP methodology only. But from first 3 Sections of Chapter 12 it is absolutely obvious that the SLiP instrument is an unreal one for aerosol concentration reduction, as well as for gaseous pollution. Both (aerosol and gaseous) pollutants have very complex and extremely non-linear spatial and temporal dispersion patterns that as shown in this chapter.

"The SLiP and **an example of a CLiP** are illustrated in Figure 12.11.

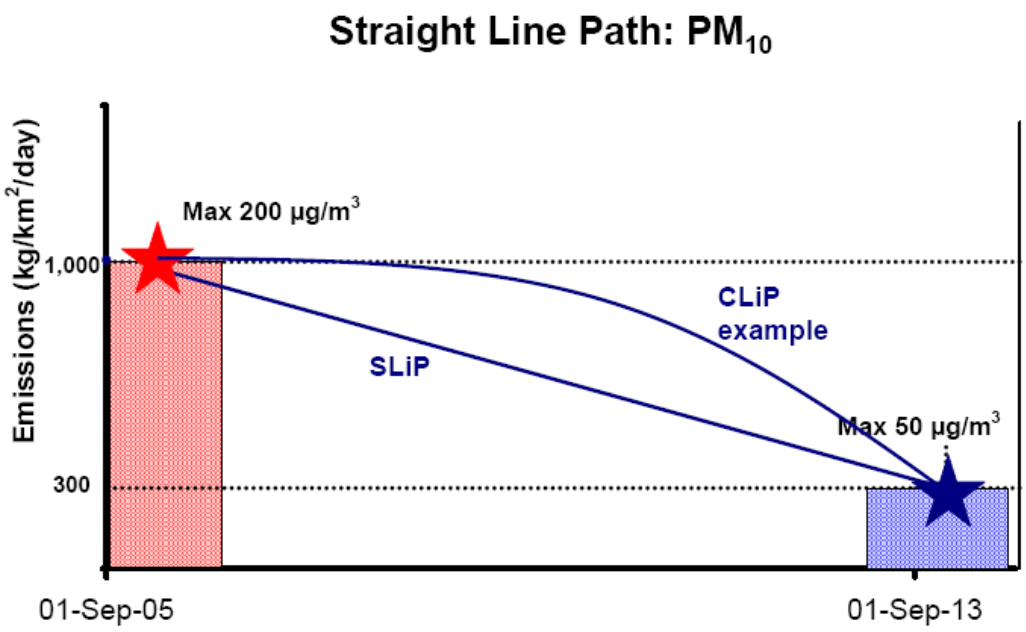

Figure 12.11 Straight line path, and curved line path example (from Fisher et al., 2005).

The authors of the key strategy document discuss the use of the SLiP method using linear statistical methods, including the box model (Fisher et al., 2005). However, 4-D dynamical variations of ambient air pollution (and air pollution 4-D numerical modelling) represent a non-linear n-dimensional system (where n tends to infinity) and would never comply with straight reduction lines. From Tables 12.2-12.5 and their description it is clear that numerically modelled PM proposed decreases (2005-2013 time period) follow the CLiP graphic only, with the PM reduction gradient increasing between 2007-2009. It is import to understand that application of SLiP strategy (as a template) in abatement strategies could mask the real tendency and would potentially lead to wrong actions.

12.4 Re-distribution of PM species for the period 2005-2013

The proportion of carbon, ionic and other species of the Scenario 1-3mix in developing aerosol concentrations building for the proposed reduced emissions is studied for the years 2007 and 2013. Seven winter 2005 meteorological situations are used in this study. The direction of the chemical-numerical drift of the photochemical model CAMx4.4 will be obtained for the key years 2007 (Table 12.13) and 2010 (Table 12.14). The results for year 2005 (as a fundamental year of the study) were presented in the Table 11.14. The results of the year 2013 are very close to the average concentration values of year 2010.

Table 12.16 presents modelled species mean concentration versus modelled average PM concentration, the fraction for every species (or species group), correlation (r) and power (r*r) coefficients for modelled average PM_{10} and $PM_{2.5}$ concentrations (winter 2005 meteorology – 7 episodes) for the proposed year 2007 emissions with application of the complex Scenario 1-3mix (for abbreviations see "List of acronyms and abbreviation').

Table 12.16 Predicted average (species versus total), species fraction, Pearson Correlation Coefficient (PCC) and Power Correlation Coefficient (Power CC), 7 episodes average, complex Scenario 1-3mix, total and fine PM (μg m^{-3}): "Total" input emission group, proposed year 2007.

Specie – total PM	AVERAGE (μg m^{-3})	FRACTION (%)	PCC	Power CC
TOC_{10} - PM_{10}	26.20 – 39.50	47.50	0.77	0.59
$TOC_{2.5}$ - $PM_{2.5}$	22.65 – 37.75	52.40	0.80	0.64
POC_{10} - PM_{10}	9.10 – 39.50	28.30	0.54	0.29
$POC_{2.5}$ - $PM_{2.5}$	8.40 – 37.75	31.60	0.57	0.33
SOA_{10} - PM_{10}	7.40 – 39.50	20.30	0.68	0.46
$SOA_{2.5}$ - $PM_{2.5}$	5.75 – 37.75	21.10	0.67	0.45
EC_{10} - PM_{10}	6.30 – 39.50	18.10	0.64	0.41
$EC_{2.5}$ - $PM_{2.5}$	6.15 – 37.75	21.30	0.68	0.46
$IONs_{10}$ - PM_{10}	7.45 – 39.50	23.40	0.74	0.55
$IONs_{2.5}$ - $PM_{2.5}$	6.70 – 37.75	24.70	0.77	0.59
$(PNO_3)_{10}$ - PM_{10}	5.15 – 39.50	15.10	0.75	0.56
$(PNO_3)_{2.5}$ - $PM_{2.5}$	2.20 – 37.75	12.20	0.75	0.56
$(PSO_4)_{10}$ - PM_{10}	2.40 – 39.50	4.20	0.74	0.55
$(PSO_4)_{2.5}$ - $PM_{2.5}$	3.80 – 37.75	6.80	0.77	0.59
$(PNH_4)_{10}$ - PM_{10}	1.30 – 39.50	3.70	0.72	0.52
$(PNH_4)_{2.5}$ - $PM_{2.5}$	1.25 – 37.75	4.30	0.74	0.55

Comparison of the average concentrations ratios (Table 12.16) for the year 2007 proposed emissions scenario with input emissions split (Table 9.1 and Figure 9.21) shows a CAMx4.4 a negative drift (decrease) of organic carbon (48-52% versus 53-54% from Table 11.14, year 2005), a positive drift (increase) of elemental carbon (18-21%), and negative drift (decrease) of inorganic soluble ions presence (23-25%). With total PM concentrations decrease, the role of primary components (and primary chemical reactions) becomes more important in CAMx4.4. Concentration ratio of the primary and crustal species has a positive tendency.

Table 12.17 presents modelled species mean concentration versus modelled average PM concentration, a percentage for every species (or species group), correlation and power coefficients for modelled average PM_{10} and $PM_{2.5}$ concentrations (winter 2005 meteorology study episodes) for

the proposed year 2010 emissions (input emissions split with application of the complex Scenario 1-3mix).

Table 12.17 Predicted average (species versus total), species fraction, Pearson Correlation Coefficient (PCC) and Power Correlation Coefficient (Power CC), 7 episodes average, complex Scenario 1-3mix, total and fine PM (μg m^{-3}): "Total" input emission group, proposed year 2010.

Specie – total PM	AVERAGE (μg m^{-3})	FRACTION (%)	PCC	Power CC
TOC_{10} - PM_{10}	13.20 – 39.50	48.80	0.76	0.58
$TOC_{2.5}$ - $PM_{2.5}$	11.65 – 37.75	51.20	0.78	0.61
POC_{10} - PM_{10}	7.30 – 39.50	27.50	0.54	0.29
$POC_{2.5}$ - $PM_{2.5}$	5.40 – 37.75	32.60	0.56	0.32
SOA_{10} - PM_{10}	6.00 – 39.50	21.40	0.67	0.45
$SOA_{2.5}$ - $PM_{2.5}$	4.65 – 37.75	20.00	0.67	0.45
EC_{10} - PM_{10}	4.30 – 39.50	18.90	0.62	0.38
$EC_{2.5}$ - $PM_{2.5}$	3.75 – 37.75	22.15	0.66	0.44
$IONs_{10}$ - PM_{10}	5.20 – 39.50	21.20	0.72	0.52
$IONs_{2.5}$ - $PM_{2.5}$	4.60 – 37.75	22.80	0.75	0.56
$(PNO_3)_{10}$ - PM_{10}	3.85 – 39.50	13.20	0.73	0.53
$(PNO_3)_{2.5}$ - $PM_{2.5}$	1.95 – 37.75	10.20	0.75	0.56
$(PSO_4)_{10}$ - PM_{10}	1.95 – 39.50	4.40	0.72	0.52
$(PSO_4)_{2.5}$ - $PM_{2.5}$	3.05 – 37.75	7.80	0.75	0.56
$(PNH_4)_{10}$ - PM_{10}	1.00 – 39.50	3.50	0.73	0.53
$(PNH_4)_{2.5}$ - $PM_{2.5}$	0.85 – 37.75	3.70	0.74	0.54

Comparison of the average concentration ratios (Table 12.17) for the year 2010 proposed emissions scenario with input emissions split (Table 9.1) exhibits a CAMx4.4 small negative organic carbon drift (49-51% versus 53-54% from Table 11.14) for the year 2005; and no any drift (49-51% versus 48-52% from Table 12.16) for the year 2007; a stable percentage of chemically inert elemental carbon (19-22%), and once again a negative drift of inorganic soluble ions (21-23%). As PM concentration decrease, the role of primary components (primary reactions) has become dominant in CAMx4.4 (for Carbon Bond 4 chemical mechanism). Concentration ratio of the primary and crustal elements uses to increase.

12.4 Summary

Assessment of a possible fine-total PM reduction for the time period 2005-2013, undertaken based on seven winter 2005 meteorological episodes, was run with application of the MM5-CAMx4.4 numerical modelling system according to the proposed PM reduction scenarios developed by ECan (Scott, 2005). From modelling output with application of the complex chemical Scenario 1-3mix and re-calculated hourly gridded emissions in groups "Domestic", "Transport", "Industry" it is

apparent (for group “Total”) that it is enough to reduce vehicular emissions by 50% to decrease aerosol hourly concentrations 2 or more fold (short-term pollution exposure). However, for long-term PM exposure decrease more radical abatement strategies should be applied. The winter aerosol abatement strategies would potentially lead to a considerable decrease of fine-total PM average concentrations (3-4 fold), but demand several fold reductions of “Domestic” and “Transport” emissions.

It was stressed that PM reduction scenarios developed for the 2005-2013 time period could not be properly realized because of objective reasons (petrol and electricity prices grow much faster than average family income), but in the nearest future (5-10 years) contribution to $PM_{2.5}$–PM_{10} daily concentrations would be more evenly re-distributed between the groups “Domestic”, “Transport” and “Industry” with the dominance of carbonaceous species in PM content.

Chapter 13: Optimisation of the location of observation sites using a numerical approach

Two winter seasons were evaluated using the MM5-CAMx4 numerical modelling system with one validation site for winter 2005, and two validation sites for winter 2006. It is clear that the greater the number of the observation sites - the better the results for PM spatial and temporal dispersion studies. However, the high cost of installing additional permanent sites provides an incentive use a numerical modelling system to develop a new scheme for optimal observation site location. Under current circumstances, an 'additional' site strategy will be developed to identify the optimal location of the next observation site when there is one (winter 2005) or 2 (winter 2006) already operating sites. At the end of this chapter, the efficiency of CAPS2000 ambient aerosol observation site locations will be evaluated on the basis of the winter 2005 4 heavy smog episodes, which present different PM dispersion patterns.

13.1 Winter 2005 aerosol pollution: single site approach

All seven episodes from early winter 2005 were selected based on time series from the single Coles Place site, which is said to reflect well the aerosol pollution in residential areas located inner Christchurch (English Park, St. Albans district). Four winter 2005 episodes (4, 5, 6 and 7) are used to assess the reliability of single observation site and to find an optimal location for a second site. The four winter 2005 episodes present different patterns of night-morning PM dispersion. In the study, only night and morning peak time concentrations (short-term exposure of high PM_{10} concentrations) are considered, as the level of the off-peak long-term exposure (including daily, weekly or monthly average aerosol) concentration variations have much lower amplitude than PM concentration fluctuations during smog peak hours. The peak approach is developed based on the unpaired prediction accuracy (UPA) statistical measure (US EPA, 1991), which compares the difference between the highest observed value and the highest predicted value found over some time period. However, in this case a new application of the UPA statistics will be outlined to find the location for a new optimal observation site ('existing + one new' strategy).

Four winter 2005 smog episodes show different spatial and temporal scenario between PM_{10} accumulation and dispersion (at the local scale of the inner city) during night-morning time over the city of Christchurch. Total PM is predominantly used as the total aerosol (PM_{10}) was measured during winter 2005 (single site approach) and during winter 2006 (2 sites approach). Figure 13.1 presents the spatial distribution of modelled PM_{10} concentrations at 12 pm (midnight) and at 6 am

on 5 May 2005 (episode 4, winter 2005) obtained for 1999 input PM gridded emissions (Scenario 1-3mix chemical split). Scenario 1-3mix is used in the MM5-CAMx4 evaluation as the best chemical scenario for simulation of night-early morning (10 pm-8 am) total PM peak concentrations.

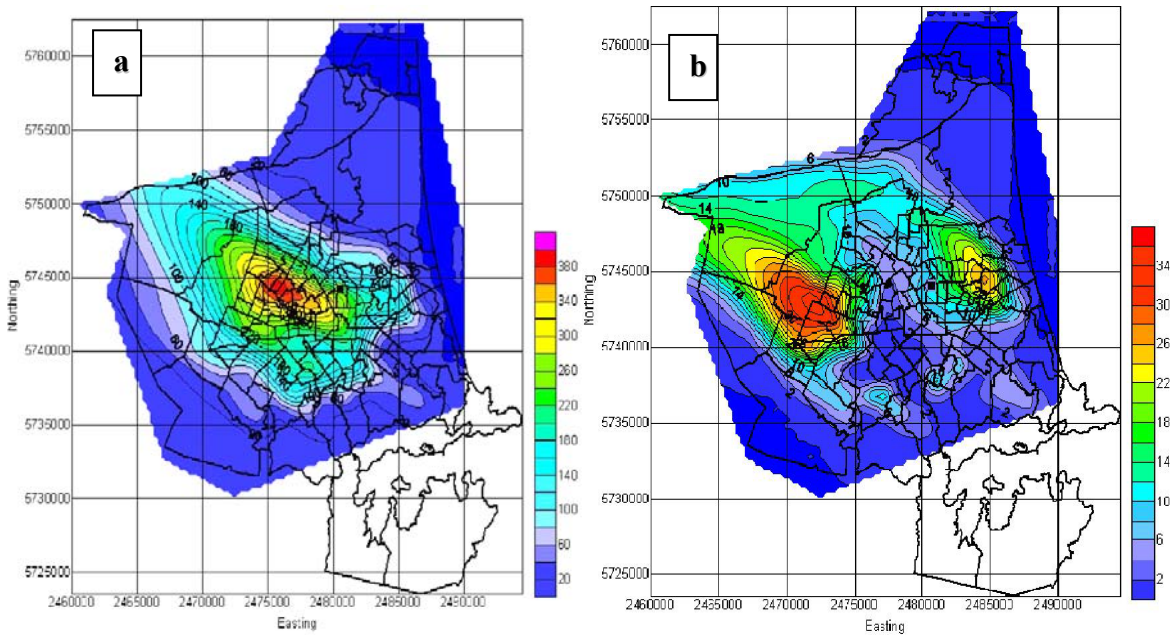

Figure 13.1 Spatial near-surface (8-10 metres) distribution of PM_{10} concentrations (μg m^{-3}) for episode 4 (winter 2005) and Scenario 1-3mix split of the 1999 "Total" gridded emissions: a) 12 pm (midnight) 5th of May 2005 – 24 hours forecast, b) 6 am 5th of May 2005 – 30 hours forecast.

Figure 13.1 shows the modelled spatial distribution of total PM for nigh-time peak maximum observed concentrations (12 pm – Figure 13.1a) and morning-time peak maximum observed concentrations (6 am – Figure 13.1b). It is important to stress that the exact PM_{10} peak concentration time differs for different episodes (based on Coles Place ambient observations), but the following figures will show only the hours with maximum aerosol concentrations. Coles Place observation site is marked by a black rectangular dot in Figure 13.1, and is located quite close (a little to the north-east) to modelled highest PM_{10} concentrations during the night (Figure 13.1a) and in a saddle between two modelled morning peaks (Figure 13.1b).

Figure 13.2 presents the spatial distribution of modelled PM_{10} concentrations at 10 pm on 26th of May 2005 and at 8 am on 26th May 2005 (episode 5, winter 2005) received for 1999 input total emissions (Scenario 1-3mix chemical split). Scenario 1-3mix is used for CAMx evaluation as a best chemical scenario for night-morning total aerosol reproduction.

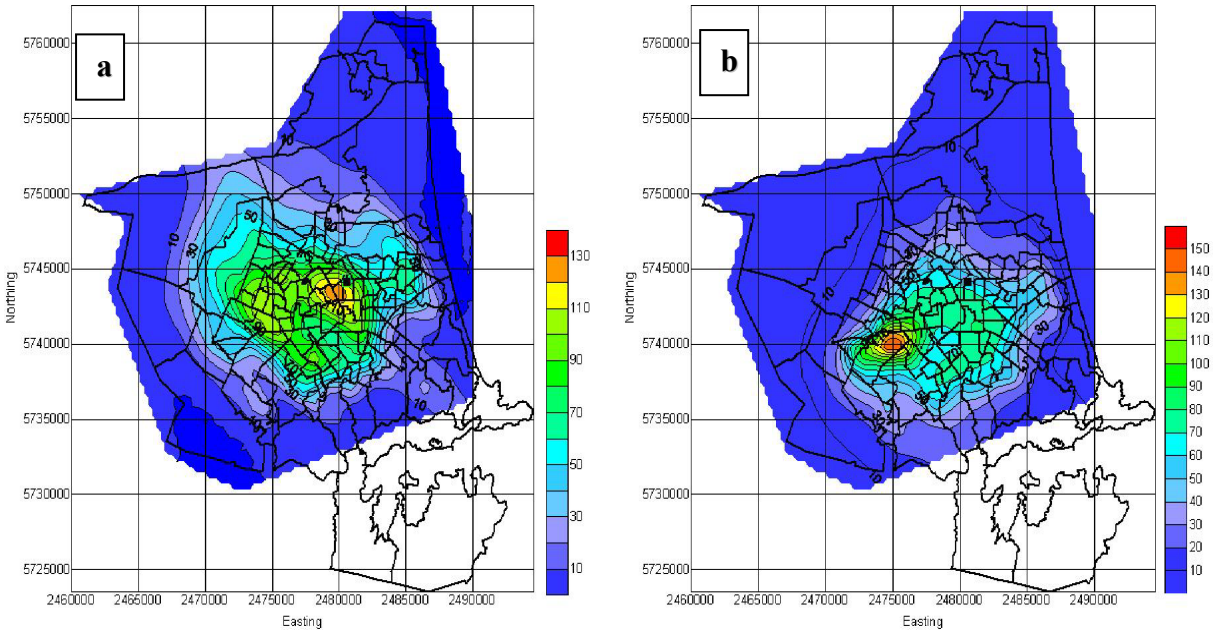

Figure 13.2 Spatial near-surface (8-10 metres) distribution of PM_{10} concentrations (µg m^{-3}) for episode 5 (winter 2005) and Scenario 1-3mix split of the 1999 "Total" gridded emissions: a) 10 pm 26th of May 2005 – 46 hours forecast, b) 8 am 26th of May 2005 – 32 hours forecast.

Figure 13.2 displays the predicted PM_{10} spatial distribution for the night-time maximum observed concentrations (10 pm – Figure 13.2a) and the morning-time maximum observed concentrations (8 am – Figure 13.2b). Coles Place observation site is marked by a black rectangular dot and located just near (a little north-east) the modelled highest PM_{10} concentrations during the night (Figure 13.2a) and some distance north-east of the modelled morning peak (Figure 13.2b).

Figure 13.3 shows spatial distribution of modelled PM_{10} concentrations at 10 pm on 4th of June 2005 and at 6 am on 4th of June 2005 (episode 6, winter 2005) calculated for 1999 input total emissions with Scenario 1-3mix gridded emissions chemical split. Once again scenario 1-3mix is used for photochemical evaluation as the best chemical scenario for spatial reproduction of the night-morning aerosol peak concentrations.

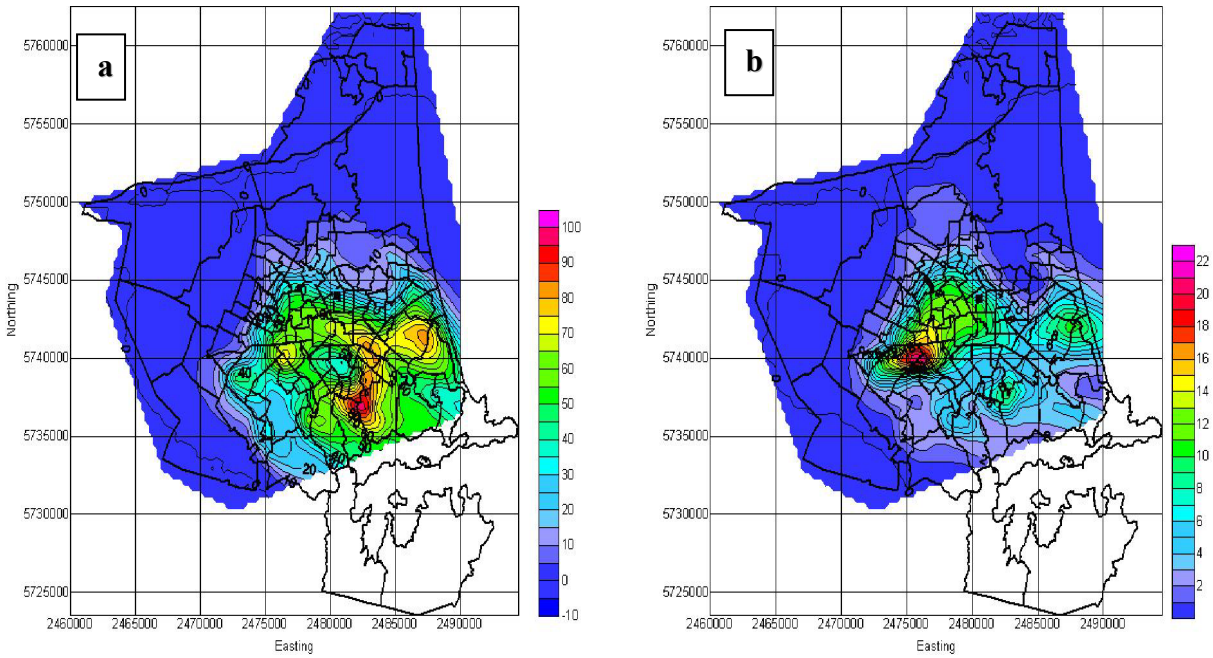

Figure 13.3 Spatial near-surface (8-10 metres) distribution of PM_{10} concentrations (μg m^{-3}) for episode 6 (winter 2005) and Scenario 1-3mix split of the 1999 "Total" input gridded emissions: a) 10 pm 4th of June 2005 – 46 hours forecast, b) 6 am 4th of June 2005 – 30 hours forecast.

Figure 13.3 displays the predicted PM_{10} spatial distribution for night-time maximum observed concentrations (10pm – Figure 13.3a) and morning-time maximum observed concentrations (6 am – Figure 13.3b). Coles Place observation site (black rectangular dot) is situated well north from the modelled highest PM_{10} concentrations during the night (Figure 13.3a) and some distance (to the north-east) from the modelled morning peak (Figure 13.3b).

Figure 13.4 presents the spatial distribution of modelled PM_{10} concentrations at 12 pm (midnight) on 14th of May 2005 and at 8 am on 14th of May 2005 (episode 7, winter 2005) calculated for the 1999 input total emissions (with application of the Scenario 1-3mix chemical split).

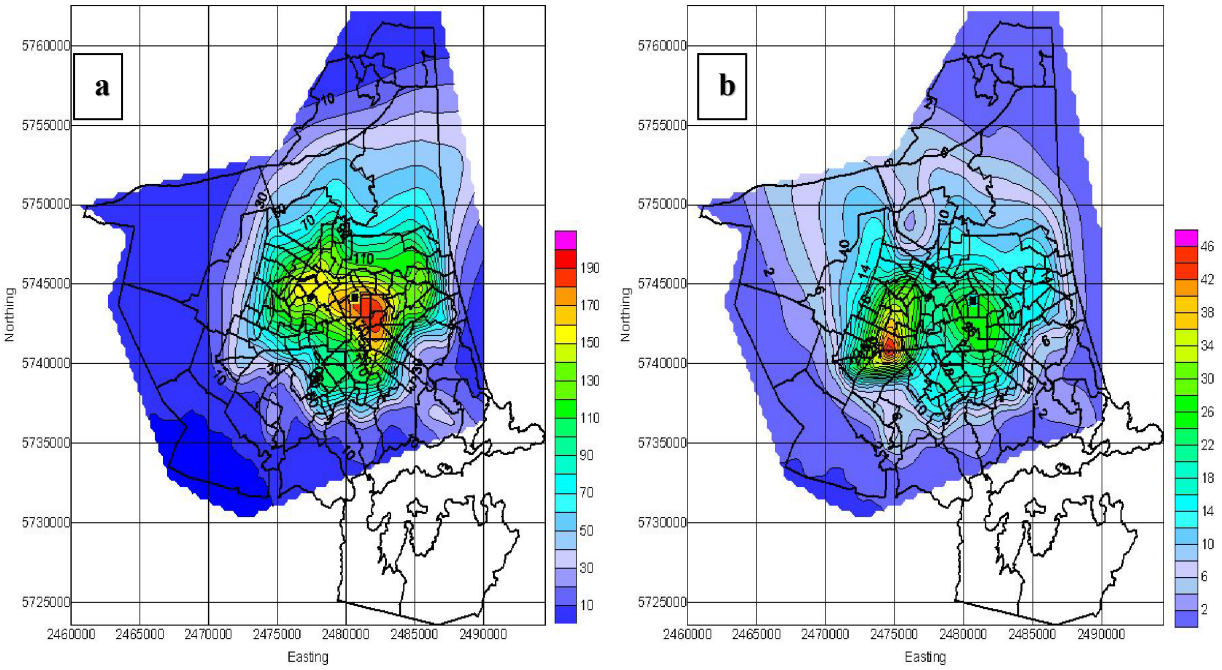

Figure 13.4 Spatial near-surface (8-10 metres) distribution of PM_{10} concentrations (µg m^{-3}) for episode 7 (winter 2005) and Scenario 1-3mix split of the 1999 "Total" input gridded emissions: a) 12 pm (midnight) 14th of May 2005 – 24 hours forecast, b) 8 am 14th of May 2005 – 32 hours forecast.

Figure 13.4 displays the predicted PM_{10} spatial distribution for the night-time peak maximum observed concentrations (12 pm – Figure 13.4a) and morning-time peak maximum observed concentrations (8 am – Figure 13.4b). Coles Place observation site (black rectangular dot) is a bit north from the modelled highest PM_{10} concentrations during the night (Figure 13.4a) and a north–northeast of the modelled main morning peak being in the centre of the second morning peak (Figure 13.4b).

To evaluate the efficiency of the observation site for all 4 above episodes (spatial patterns) the ratio of the modelled PM concentration for Coles Place point to the PM_{10} absolute maximum for the inner Christchurch area was calculated separately for night and morning peaks based on Figures 13.1-13.4. From observations the mean PM_{10} concentrations averaged over 40 days (1 May–10 June 2005) for the 10 pm-2 am time interval (night peak) and for the 5 am-9 am (morning peak) time interval are equal to 50.7 µg m^{-3} (for night peak) and 27.3 µg m^{-3} (for morning peak) respectively. These data allow calculation of a weight coefficient for the night peak (weightN = 0.65) and for the morning peak (weightM = 0.35) to develop a night-morning joint efficiency coefficient. Table 13.1 presents evaluation of the Coles Place observation site based on ratios and weights for the 4 modelled night/morning episodes (see Figures 13.1-13.4).

Table 13.1 Night-morning weights and ratios for modelled total PM_{10} at the Coles Place site related to the maximum modelled PM_{10} concentration: 4 winter 2005 episodes, night (weightN) and morning (weightM) peaks.

weight	Episode	Episode 4	Episode 5	Episode 6	Episode 7
weightN – 0.65	Ratio (night)	0.65	0.80	0.30	0.92
weightM – 0.35	Ratio (morning)	0.30	0.40	0.45	0.50

The efficiency of the Coles Place observation site is calculated from Table 13.1 by summing up of night/morning ratio multiplied by the night/morning weight (Σ(Ratio*weight)) respectively. For Coles Place the modelled efficiency is equal to 2.313. As the maximum modelled efficiency theoretically could be 4.000 (from Table 13.1 if all Ratios are equal to 1.00) so the efficiency of Coles Place = 57.8% based on the night/morning PM_{10} peak concentrations for 4 different modelled heavy smog patterns. The method of site efficiency calculation will be applied in the next 2 sections to calculate the efficiency of existing and potential observation sites. In conclusion it is worth noting that from Figures 13.1-13.4 it is obvious that the next proposed optimal site should be installed somewhere south-east of the city centre as the Coles Place site is situated north-west to north of PM_{10} spatial maxima.

13.2 Winter 2006 aerosol pollution: 2 sites approach

During winter 2006, 2 observation sites were running routinely: Coles Place and Woolston. Four winter 2005 episodes (4, 5, 6 and 7) once again are used to characterize the location of the second observation site in Woolston, and the site efficiency technique is applied to calculate the efficiency of the Woolston site for numerically predicted aerosol spatial distribution. Modelled PM_{10} is used as the only aerosol measured during winter 2006 (at the two sites). The Woolston site position is assumed to coincide with the location of a proposed additional observation site (Section 13.1). This work contributes to the successful management of the observational network locations in the Christchurch inner city.

Figure 13.5 presents the spatial distribution of modelled PM_{10} concentrations at 12 pm (midnight) and at 6 am on 5 May 2005 (episode 4, winter 2005) obtained for the 1999 input total emissions (Scenario 1-3mix chemical split). Complex Scenario 1-3mix is used in the MM5-CAMx4.4 evaluation as the best chemical scenario for night-morning total aerosol peak simulation.

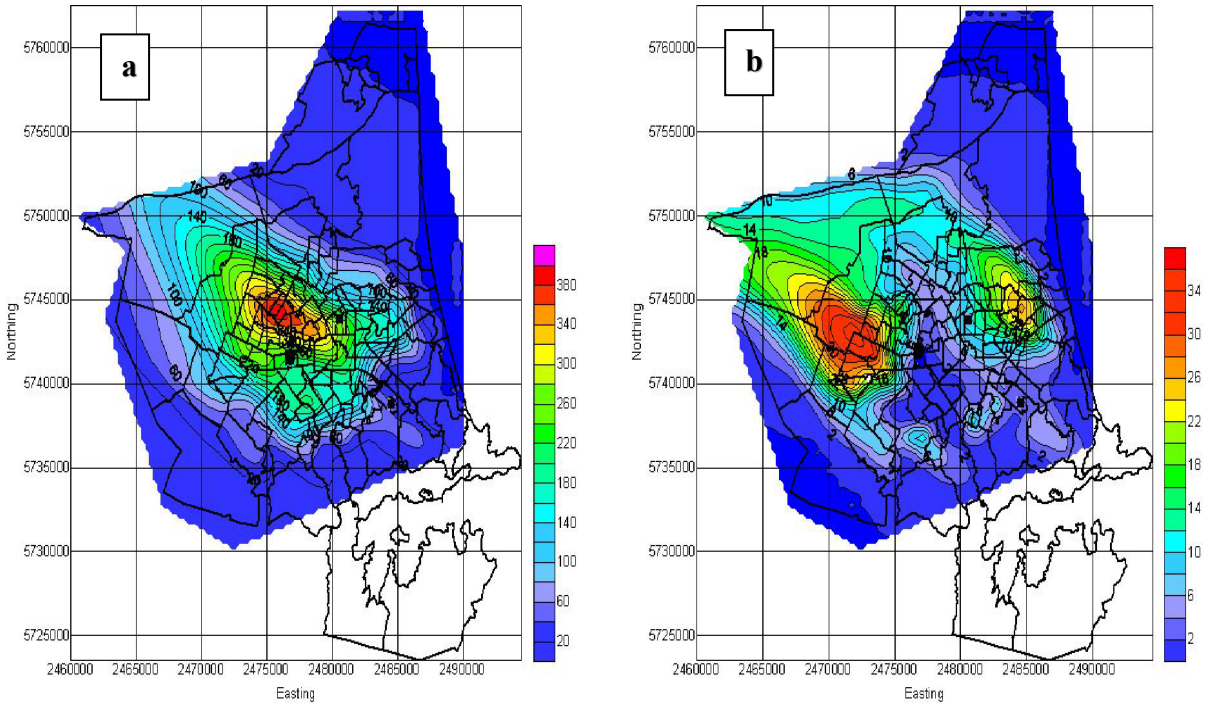

Figure 13.5 Spatial near-surface (8-10 metres) distribution of PM_{10} concentrations (µg m^{-3}) for episode 4 (winter 2005) and Scenario 1-3mix split of the 1999 "Total" gridded emissions: a) 12 pm (midnight) 5th of May 2005 – 24 hours forecast, b) 6 am 5th of May 2005 – 30 hours forecast.

Woolston observation site is marked by a second black rectangular dot located south-east of the modelled highest PM_{10} concentrations during night peak (Figure 13.5a) and south and south-east of the modelled morning peaks (Figure 13.5b). A black round dot south-west of the city centre denotes a proposed position (Riccarton) of an additional third observation site. In such a way 3 sites will be able to surround the night PM_{10} peak location in inner Christchurch. The proposed site is located south from maximum PM_{10} at night (Figure 13.5a) and nearly between two depleted centres of the PM morning peak (Figure 13.5b).

Figure 13.6 presents the spatial distribution of modelled PM_{10} concentrations at 10 pm on 26th of May 2005 and at 8 am on 26th May 2005 (episode 5, winter 2005) obtained for the 1999 input total emissions (Scenario 1-3mix chemical split). Complex Scenario 1-3mix is used for CAMx evaluation the best chemical scenario for night-morning total aerosol peak values reproduction. Figure 13.6 includes 3 observation sites: 2 existing ones (Coles Place and Woolston) marked by a rectangular dot and a proposed one (Riccarton) marked by a black round dot.

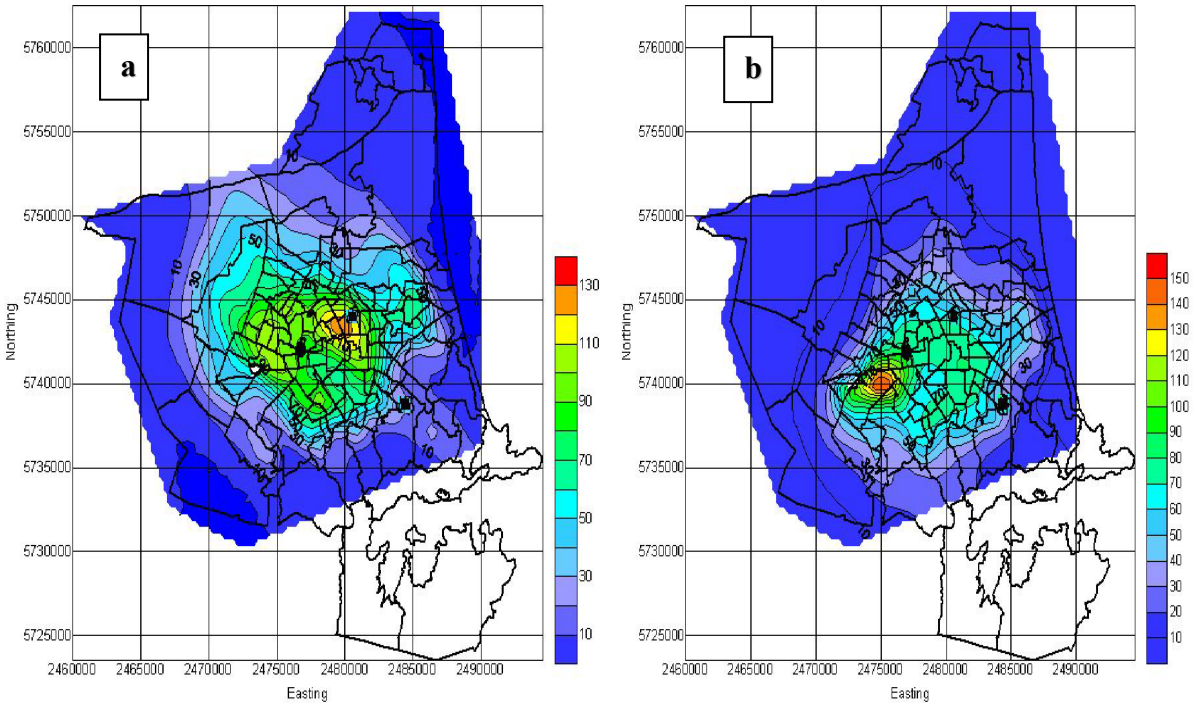

Figure 13.6 Spatial near-surface (8-10 metres) distribution of PM_{10} concentrations (µg m^{-3}) for episode 5 (winter 2005) and Scenario 1-3mix split of the 1999 "Total" gridded emissions: a) 10 pm 26th of May 2005 – 46 hours forecast, b) 8 am 26th of May 2005 – 32 hours forecast.

Woolston observation site is marked by a black rectangular dot situated south-east from the modelled highest PM_{10} concentrations during the night peak (Figure 13.6a) and east of the modelled morning peak (Figure 13.6b). The proposed Riccarton site is located south-west from maximum concentrations at night (Figure 13.6a) and a little north of the centre of the PM morning peak (Figure 13.6b).

Figure 13.7 shows the spatial distribution of modelled PM_{10} concentrations at 10 pm on 4th of June 2005 and at 6 am on 4th of June 2005 (episode 6, winter 2005) calculated for 1999 input total emissions (Scenario 1-3mix chemical split). Figure 13.7 pinpoints all 3 observation sites: 2 existing ones (Coles Place and Woolston) marked by rectangular dots and a proposed one (Riccarton) marked as a black round dot.

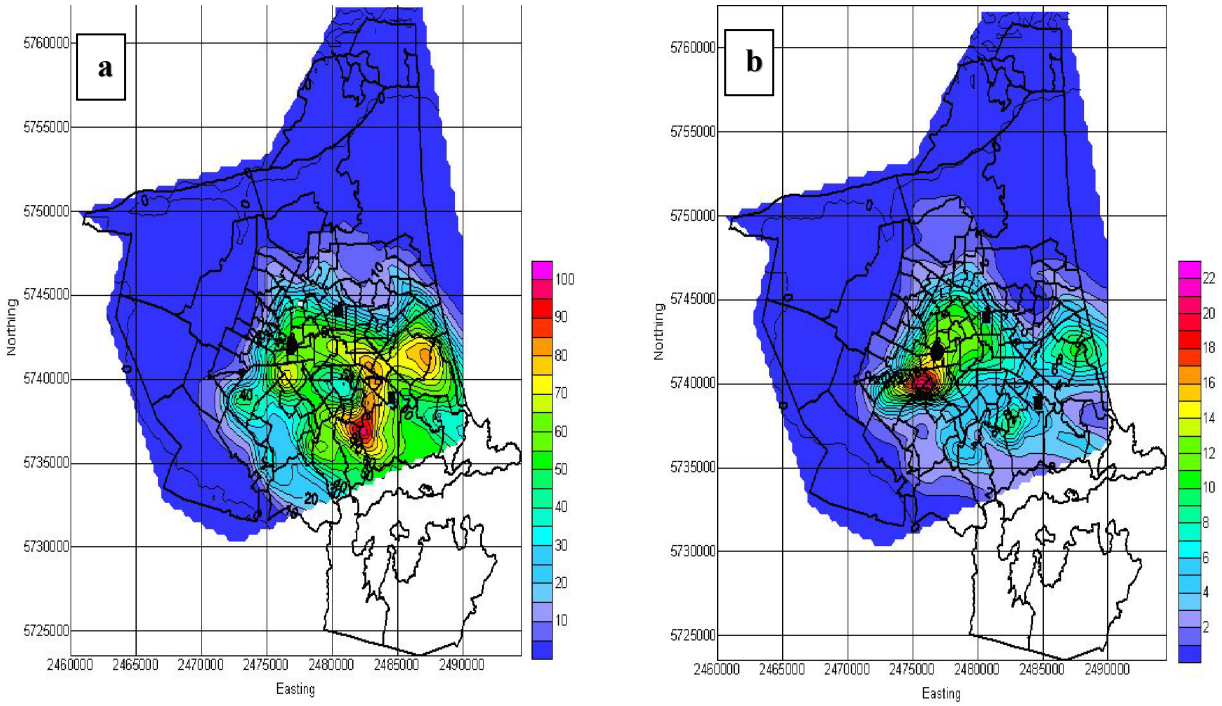

Figure 13.7 Spatial near-surface (8-10 metres) distribution of PM_{10} concentrations (µg m^{-3}) for episode 6 (winter 2005) and Scenario 1-3mix split of the 1999 "Total" input gridded emissions: a) 10 pm 4th of June 2005 – 46 hours forecast, b) 6 am 4th of June 2005 – 30 hours forecast.

The Woolston site (black rectangular dot) is situated south-east from the centre of the modelled PM_{10} night peak concentrations (Figure 13.7a) and east from the main morning peak (Figure 13.7b). The proposed Riccarton site is located west from maximum PM_{10} at night (Figure 13.7a) and very close (a little northward) to the centre of the morning main peak (Figure 13.7b).

Figure 13.8 presents the spatial distribution of modelled PM_{10} concentrations at 12 pm (midnight) on 14th of May 2005 and at 8 am on 14th of May 2005 (episode 7, winter 2005).

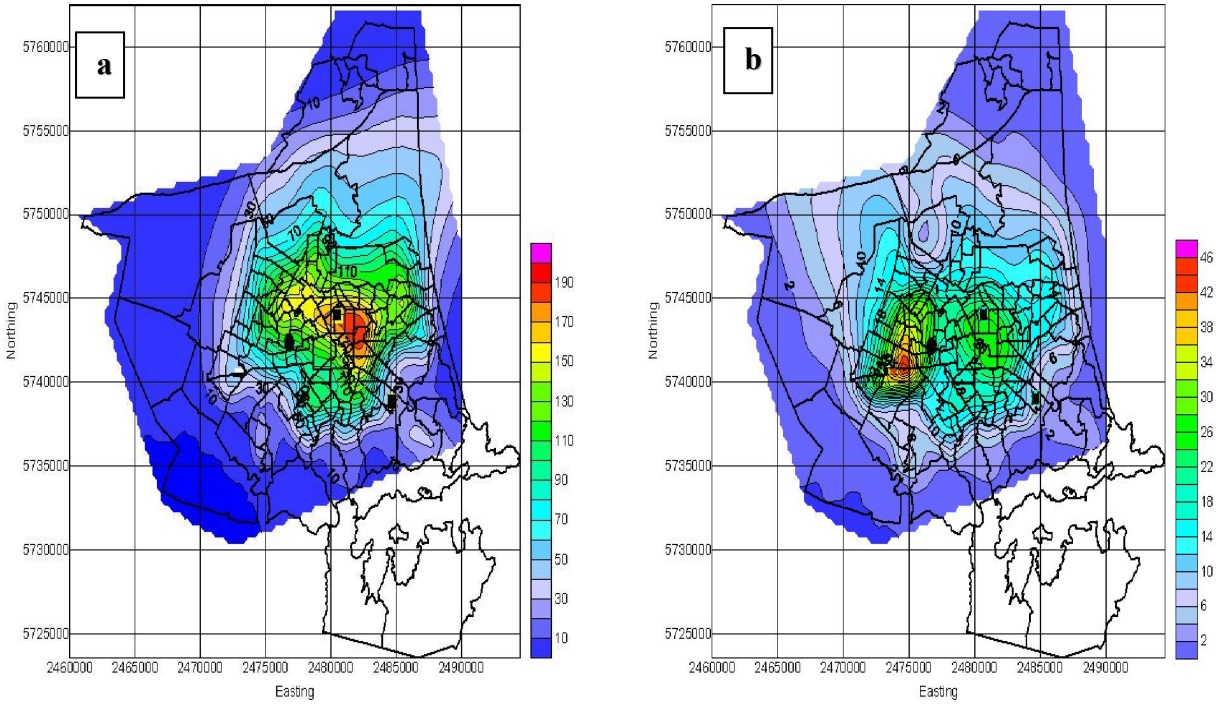

Figure 13.8 Spatial near-surface (8-10 metres) distribution of PM_{10} concentrations (µg m^{-3}) for episode 7 (winter 2005) and Scenario 1-3mix split of the 1999 "Total" input gridded emissions: a) 12 pm (midnight) 14th of May 2005 – 24 hours forecast, b) 8 am 14th of May 2005 – 32 hours forecast.

The Woolston observation site (black rectangular dot) lies south-east and not very close to the modelled highest PM_{10} concentrations during the night (Figure 13.8a) and far east from the modelled 2 morning peaks (Figure 13.8b). The proposed Riccarton site is located westward of the maximum PM_{10} at night (Figure 13.8a) and nearly in the center of the most pronounced peak in the morning (Figure 13.8b).

Numerical efficiency is calculated to evaluate the effectiveness of the Woolston observation site and the proposed Riccarton site. Table 13.2 presents evaluation of the Woolston site using calculated ratios and weights for 4 modelled night/morning episodes (Figures 13.5-13.8).

Table 13.2 Night-morning weights and ratios for modelled total PM_{10} at the Woolston site relative to the maximum modelled PM_{10} concentration: 4 winter 2005 episodes, night (weightN) and morning (weightM) peaks.

weight	Episode	Episode 4	Episode 5	Episode 6	Episode 7
weightN – 0.65	Ratio (night)	0.32	0.30	0.35	0.45
weightM – 0.35	Ratio (morning)	0.20	0.40	0.35	0.30

For the Table 13.2 modelled absolute efficiency of the Woolston site is equal to 1.365. Given the maximum modelled efficiency that is equal to 4.000, and the efficiency of Woolston site = 34.1% based on the night/morning PM_{10} peak concentrations for 4 modelled smog episodes. The

Woolston efficiency is considerably lower than for the official ECan observation site at Coles Place. Table 13.3 is used to evaluate the efficiency of the proposed Riccarton observation site presenting calculated ratios and weights for 4 modelled night/morning episodes (Figures 13.5-13.8).

Table 13.3 Night-morning weights and ratios for modelled total PM_{10} at the Riccarton site relative to the maximum modelled PM_{10} concentration: 4 winter 2005 episodes, night (weightN) and morning (weightM) peaks.

weight	Episode	Episode 4	Episode 5	Episode 6	Episode 7
weightN – 0.65	Ratio (night)	0.75	0.78	0.63	0.63
weightM – 0.35	Ratio (morning)	0.35	0.65	0.68	0.70

For the proposed Riccarton proposed site the modelled efficiency is equal to 2.648. Using the maximum modelled efficiency of 4.000 the efficiency of the recommended site at Riccarton is equal to 66.2% based on the night/morning PM_{10} peak concentrations for 4 modelled smog episodes. The proposed Riccarton site efficiency is higher than Coles Place or Woolston.

In principal, it is reasonable to stipulate an appropriate level of efficiency to be not less than 50-55% (regarding the Coles Place score) and the only exception from this rule will be the efficiency of a background site, which should tend to 0. It is difficult to find the top real level of efficiency as the theoretical top (max = 4.000) will never be attained for stochastic processes such as PM spatial-temporal accumulation-dispersion. The efficiency scores for CAPS2000 ambient aerosol observation sites (including background site score) will be calculated in the next Section.

13.3 Efficient optimization – CAPS2000

The hourly averaged spatial efficiency distribution was calculated for four selected night-morning winter 2005 peak aerosol pollution episodes representing 4 different local patterns of $PM_{2.5}$ and PM_{10} night-morning dispersion. All calculations were done using the MM5-CAMx4.4 numerical modelling system and additional software was written to obtain hourly averaged efficiency. Peak hours were chosen depending on peak ambient PM concentrations (for the Coles Place observation site) for night and morning of each episode. In Figure 13.9 the spatial efficiency distribution is presented for fine aerosol (4-episode average) for night pollution peaks only (Figure 13.9a) and for early morning secondary pollution peaks only (Figure 13.9b).

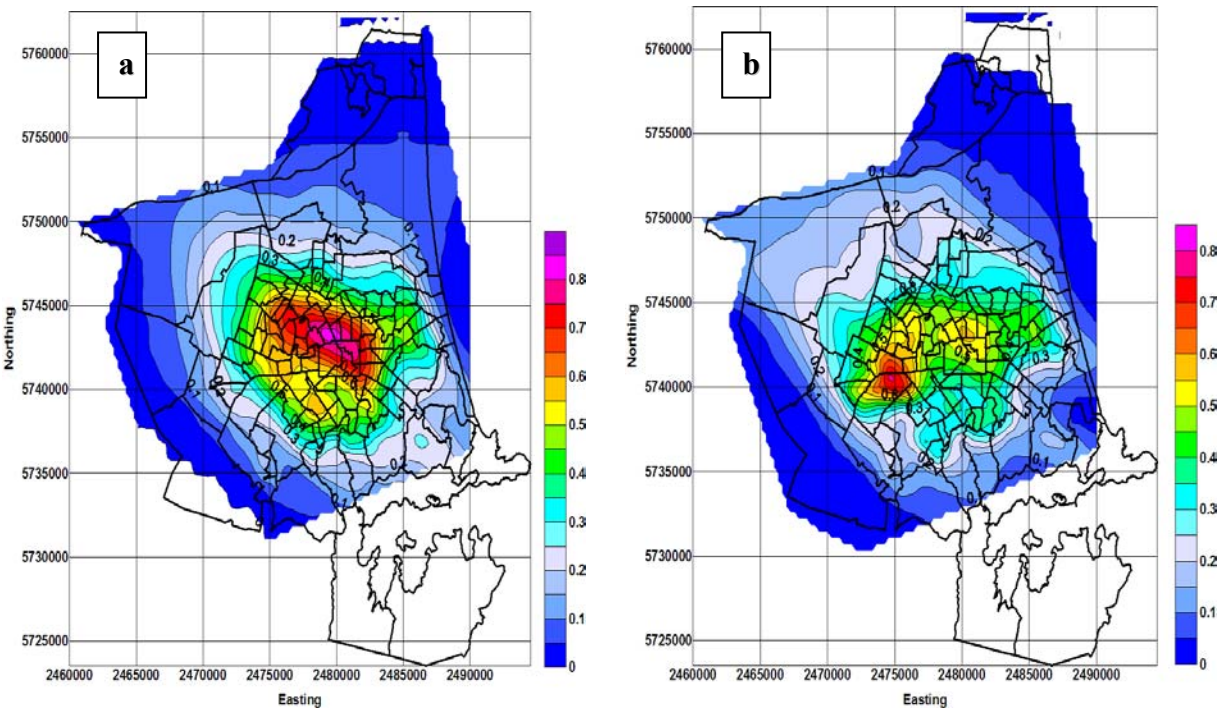

Figure 13.9 Spatial near-surface (8-10 metres) distribution of $PM_{2.5}$ peak efficiency ($EF_{2.5}$) for 4 episodes (winter 2005) and Scenario 1-3mix split of the 1999 "Total" input gridded emissions: a) night $PM_{2.5}$ peak efficiency - $EF_{2.5}$(night), b) morning $PM_{2.5}$ peak efficiency - $EF_{2.5}$(morning).

Night-time $EF_{2.5}$(night) has a compact spatial distribution with a single peak about 0.85 not far from the inner city center (Figure 13.9a). Opposite to a single night peak, the morning-time $EF_{2.5}$ (morning) has 2 maxima with a main peak (about 0.75) over Riccarton-Hornby districts and a secondary peak (about 0.60) to the east (closer to the Pacific Ocean).

Figure 13.10 shows combined night-morning spatial $EF_{2.5}$(night-morning) distribution for fine aerosol (4-episode average) that was calculated using the night PM peaks weight (weightN=0.65) and the early morning PM peaks weight (weightM=0.35) described in Section13.1.

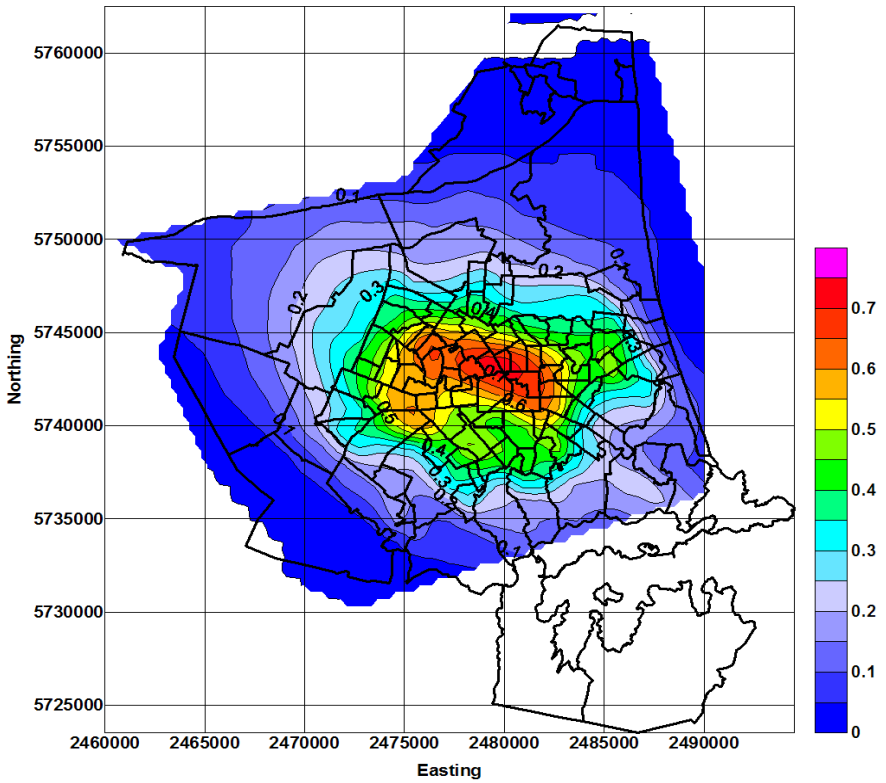

Figure 13.10 Spatial near-surface (8-10 metres) distribution of $PM_{2.5}$ night-morning peak efficiency ($EF_{2.5}$(night-morning)) for 4 episodes (winter 2005) and Scenario 1-3mix split of the 1999 "Total" input gridded emissions.

From Figure 13.10 it is apparent (and consistent) that fine aerosol night-morning peak efficiency ($EF_{2.5}$(night-morning)) has a major peak (about 0.75) that is located very close to the night efficiency peak (see Figure 13.9a,) and an additional secondary peak over the Riccarton-Hornby area (about 0.60), mostly built up by morning efficiency $EF_{2.5}$(morning) maximum values (see Figure 13.9b).

In Figure 13.11 shows the spatial EF distribution for total aerosol (4-episode average) for night pollution peaks only (Figure 13.11a) and for early morning secondary pollution peaks only (Figure 13.11b).

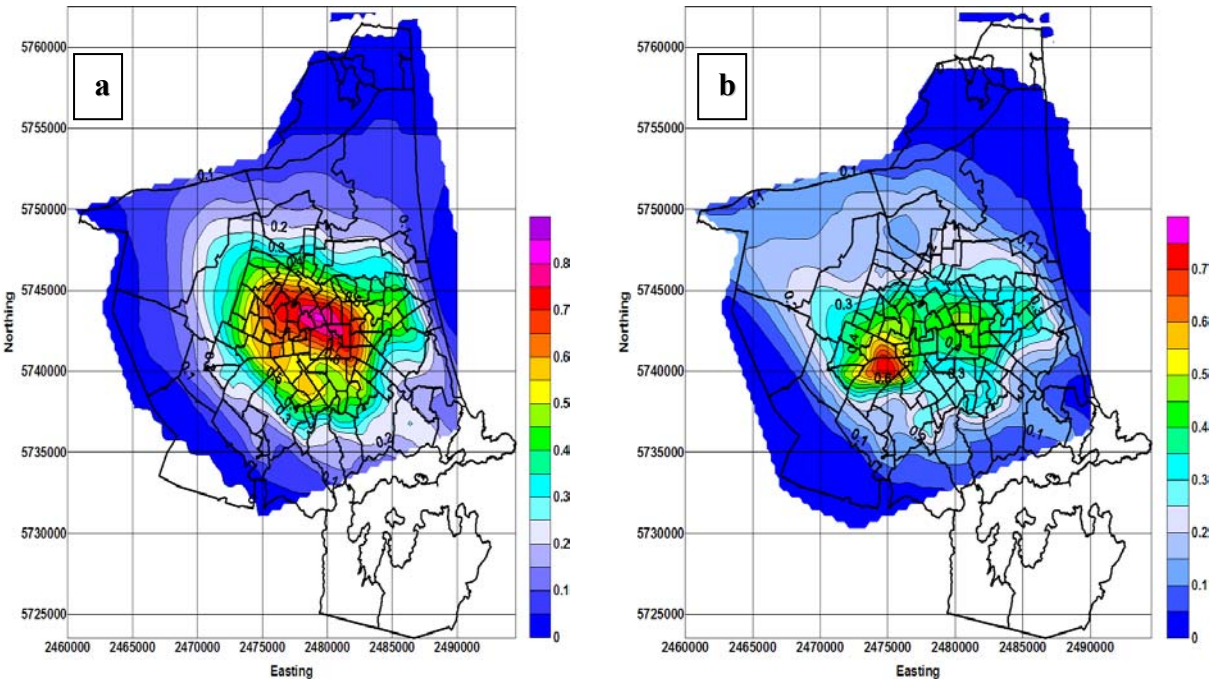

Figure 13.11 Spatial near-surface (8-10 metres) distribution of PM_{10} peak efficiency (EF_{10}) for 4 episodes (winter 2005) and Scenario 1-3mix split of the 1999 "Total" input gridded emissions: a) night PM_{10} peak efficiency - EF_{10}(night), b) morning PM_{10} peak efficiency - EF_{10}(morning).

Once again night-time EF_{10}(night) has a more compact spatial distribution with a single peak about 0.85 not far from the inner city centre (Figure 13.11a). However, the double peak of the morning-time EF_{10}(morning) has changed compared with the fine PM efficiency spatial distribution. A dominant peak (about 0.70) occurs over the Riccarton-Hornby districts, with a much weaker secondary peak (about 0.45) to the east (Pacific Ocean direction). This difference between fine and total EF morning peaks (Figure 13.9b and 13.11b) suggests about higher coarse PM concentrations over the Riccarton-Hornby area associated with a higher morning transport-industry contribution in these districts (industrial area with busy traffic including heavy diesel transport) compared with Woolston-Brighton districts (residential areas).

Figure 13.12 illustrates a combined night-morning spatial EF_{10}(night-morning) distribution for total aerosol (4-episode average) that was calculated using the night PM peaks weight (weightN=0.65) and the early morning PM peaks weight (weightM=0.35).

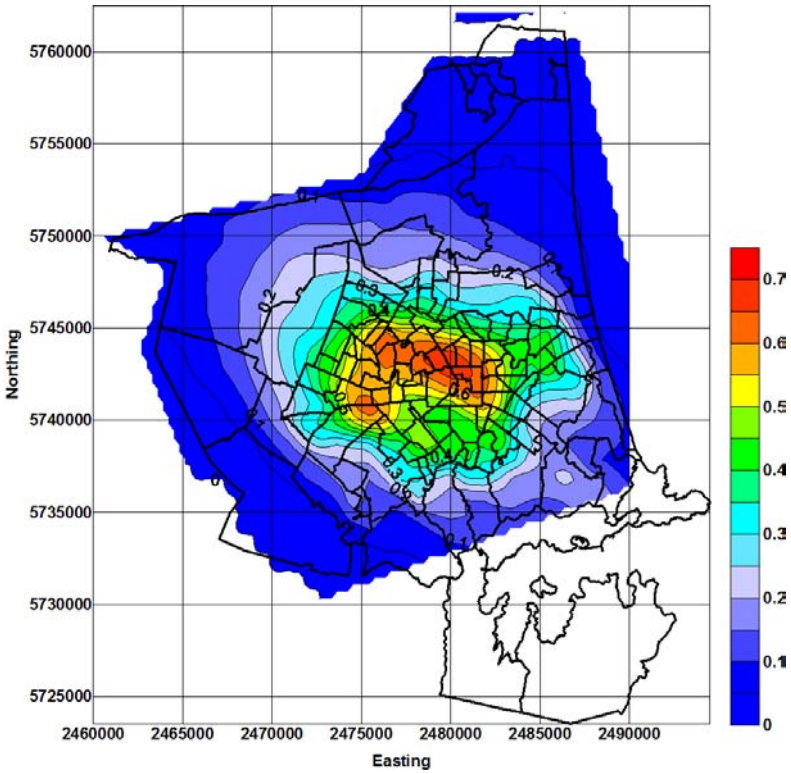

Figure 13.12 Spatial near-surface (8-10 metres) distribution of PM_{10} night-morning peak efficiency (EF_{10}(night-morning)) for 4 episodes (winter 2005) and Scenario 1-3mix split of the 1999 "Total" input gridded emissions.

Figure 13.12 demonstrates that total aerosol night-morning peak efficiency (EF_{10}(night-morning)) has a major peak (about 0.70) located very close to the night efficiency peak (see Figure 13.11a,) but with an additional secondary peak over the Riccarton-Hornby area (about 0.60) associated with the morning efficiency EF_{10}(morning) peak values (see Figure 13.11b). The secondary peak for PM_{10} is more evident (Figure 13.12) to compare with EF secondary peak for $PM_{2.5}$ (Figure 13.10).

During winter 2000 CAPS200, 6 PM measurement sites were located inside the Christchurch area (Figure 13.13). In Figure 13.13, ambient PM measuring sites are marked in yellow and numbered. A background observation site is picked up in North Brighton and is marked "B". There were no any ambient PM measurements at the North Brighton background site during CAPS2000 and a virtual background site (marked 'B' in the figure) was pinpointed to calculate background site efficiency to compare with peak efficiency.

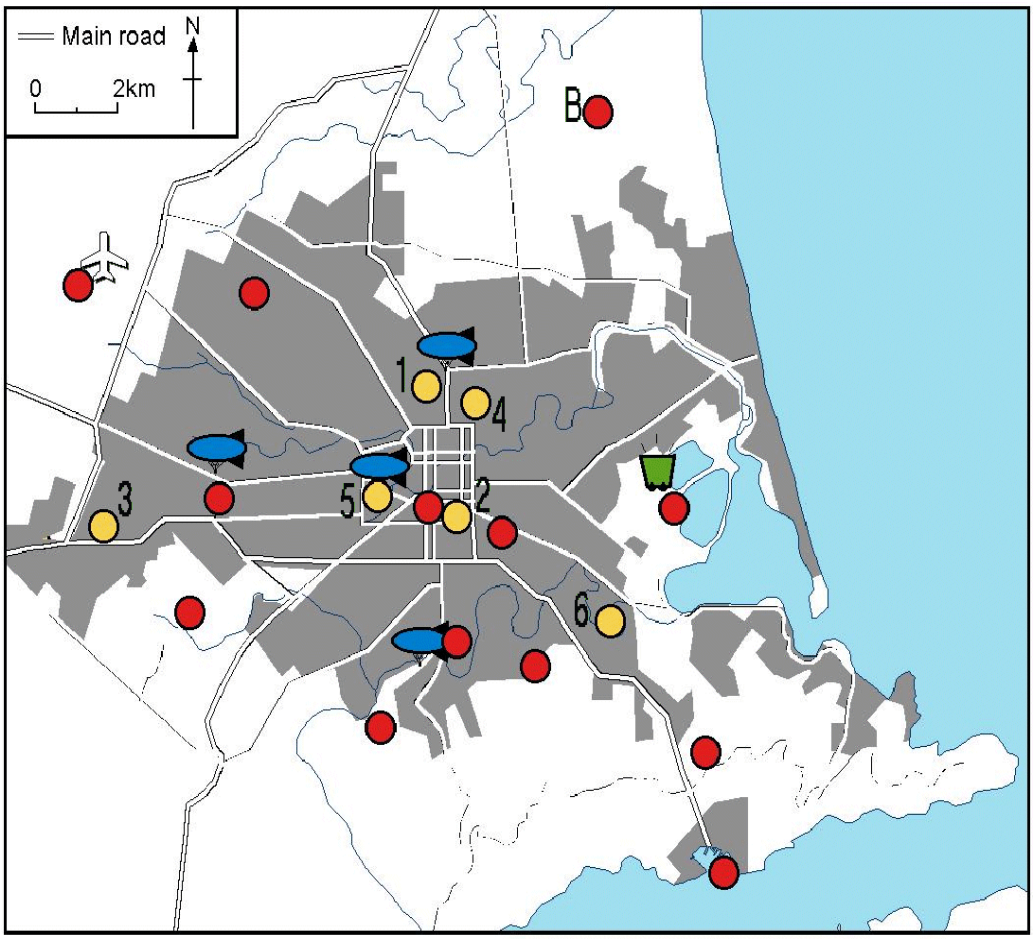

Figure 13.13 Network of observation sites inside the Christchurch area during the winter period of CAPS2000 (after Sturman *et al.,* 2001).

A full list of place names and coordinates, with a list of meteorological measurements and time intervals, is provided in Table 13.4. The number against every site name coincides with the number in Figure 13.13.

Table 13.4 List of PM measurement sites in Christchurch during CAPS200, where: T - Temperature, RH–Relative Humidity, U–zonal wind component, V–meridional wind component, DIR–wind direction, P–pressure, AP–air pollutant.

Site name	Latitude	Longitude	Time frame	Measurements
1 Coles Place	-43.305	172.382	Hourly	RH, T, U, V, DIR, **AP**
2 Polytechnic	-43.323	172.388	Hourly	RH, T, U, V, DIR, **AP**
3 Hornby	-43.326	172.311	Hourly	RH, T, U, V, DIR, **AP**
4 Packe Street	-43.311	172.385	I0 minutes	RH, T, U, V, DIR, **AP**
5 Hagley Park	-43.317	172.369	Hourly	RH, T, U, V, DIR, **AP**
6 Woolston-CAPS	-43.304	172.437	Hourly	RH, T, U, V, DIR, **AP**

Table 13.4 lists the routine PM_{10} hourly concentration measurements (except Polytechnic site – amibient$PM_{2.5}$ was measured at this site) for 5 sites, and 10-minute PM_{10} time series for Pack

Street at last during the winter period of CAPS2000. Figure 13.14 presents spatial EF distribution for PM_{10} (4-episode average) separately for night pollution peaks (Figure 13.14a) and for early morning secondary pollution peaks (Figure 13.14b) with the network of observation sites indicated and numbered in Figure 13.13. Observation sites include all aerosol measuring sites from Table 13.4 and a background site (noted "B") located in North Brighton.

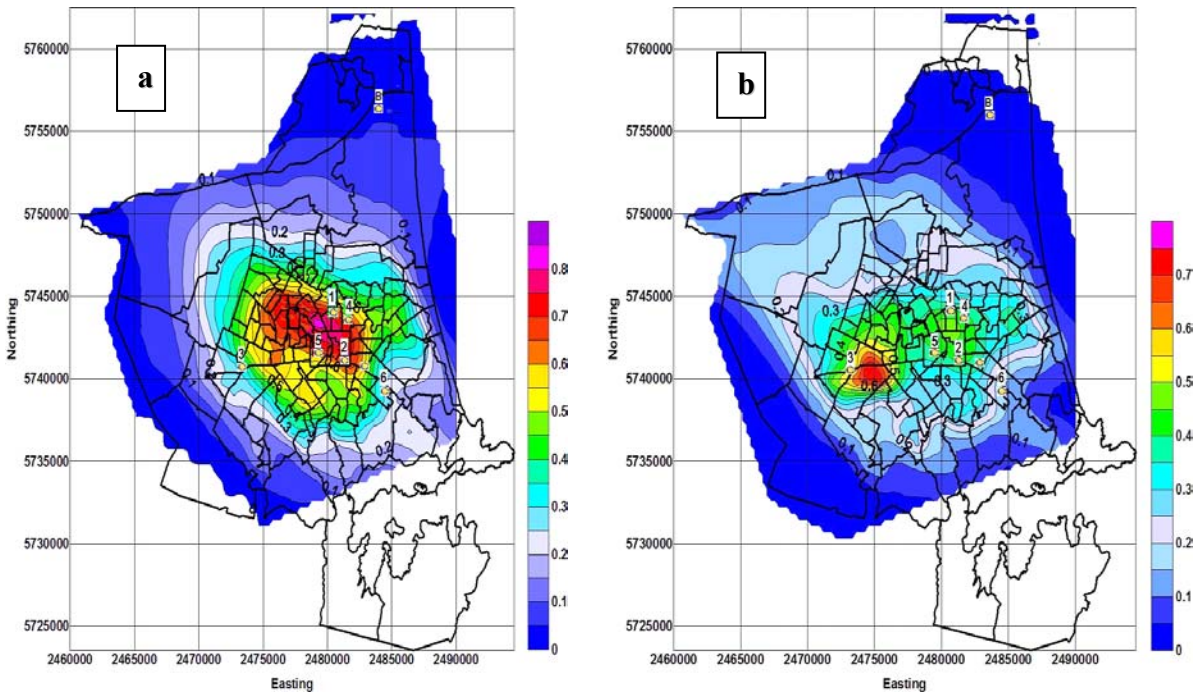

Figure 13.14 Spatial near-surface (8-10 metres) distribution of PM_{10} peak efficiency (EF_{10}) for 4 episodes (winter 2005) and Scenario 1-3mix split of the 1999 "Total" input gridded emissions and 6 observation sites : a) night PM_{10} peak efficiency - EF_{10}(night), b) morning PM_{10} peak efficiency - EF_{10}(morning).

The efficiency (EF_{10}) of CAPS200 sites (Table 13.4) was calculated on the basis of numerical data used to plot Figure 13.14 for all sites except Polytechnic where fine PM efficiency ($EF_{2.5}$) was calculated. Coles Place efficiency was calculated in Section 13.1. An efficiency of Hornby site (site 3 in Figure 13.13 and 13.14) is close to the efficiency calculated for the proposed Riccarton and with correction (according to Figure 13.14 a-b) reckoned to be a little lower – 2.405 (EF(Hornby) = 60.1%). The efficiency of the Pack Street site (the former ECan basic observation site marked 4 in Figure 13.13 and 13.14) is a little lower than for Coles Place – 2.276: EF(Pack) = 56.9%. An efficiency of the Woolston-CAPS (marked 6 in Figure 13.13 and 13.14) is equal to the Woolston observation site (from winter 2006): 1.365 (EF(Woolston-CAPS) = 34.1%).

Table 13.5 is used to evaluate the efficiency of the Hagley Park observation site (site 5 in Figure 13.13 and 13.14) and presents calculated ratios and weights for 4 modelled night/morning episodes (Figures 13.5-13.8).

Table 13.5 Night-morning weights and ratios for modelled total PM_{10} at the Hagley Park site relative to the maximum modelled PM_{10} concentration: 4 winter 2005 episodes, night (weightN) and morning (weightM) peaks.

weight	Episode	Episode 4	Episode 5	Episode 6	Episode 7
weightN – 0.65	Ratio (night)	0.68	0.86	0.68	0.68
weightM – 0.35	Ratio (morning)	0.30	0.53	0.55	0.52

For the Hagley Park site (CAPS2000) the modelled efficiency (EF(Hagley)) is equal to 2.550. Once again using the maximum modelled EF of 4.000 an efficiency of the CAPS2000 site EF(Hagley) is equal to 63.8% for the night/morning PM_{10} peak concentrations (4 modelled smog episodes). Hagley Park site efficiency is therefore considered to be highest for CAPS2000 to capture PM_{10} peak concentrations, and second after proposed Riccarton site efficiency.

Table 13.6 is used to evaluate the efficiency of the Polytechnic observation site (site 2 in Figure 13.13) and presents calculated ratios and weights for 4 modelled night/morning episodes using $PM_{2.5}$ night/morning spatial distribution (not shown). The same night and morning weights were used in the calculations. The calculated from 4 episodes efficiency is compared with more rough calculations of Polytechnic site efficiency obtained from Figure 13.9 (EF(Polytechnic) = 60%). $PM_{2.5}$ was measured at the Polytechnic site during CAPS2000 so that a calculated efficiency based on the spatial distribution of fine PM peaks was used instead of the total PM EF distribution for all 4 chosen winter 2005 patterns.

Table 13.6 Night-morning weights and ratios for modelled fine PM at the Polytechnic site relative to the maximum modelled $PM_{2.5}$ concentration: 4 winter 2005 episodes, night (weightN) and morning (weightM) peaks.

Weight	Episode	Episode 4	Episode 5	Episode 6	Episode 7
weightN – 0.65	Ratio (night)	0.58	0.77	0.84	0.78
weightM – 0.35	Ratio (morning)	0.30	0.67	0.45	0.61

For Polytechnic site (CAPS2000) the modelled EF(Polytechnic) is equal to 2.676. If the maximum modelled EF is 4.0, then the efficiency of the CAPS2000 site EF(Polytechnic) is equal to 66.9% (night/morning $PM_{2.5}$ peak concentrations for 4 modelled smog episodes). Four episodes efficiency is higher compared to first assumption calculation done using data in Figure 13.9 (66.9% versus 60%). So an increase of the number of studied episodes could correct the efficiency values

obtained in this Chapter. The Polytechnic site efficiency is the highest one and Polytechnic site is the best fit observation point for night PM peak study (at least for fine PM), as the Polytechnic has the highest night score. The proposed Riccarton and used during CAPS2000 Hornby sites have the highest morning PM peak efficiency score. As the Polytechnic and Riccarton sites are quite apart from each other and correspond to the different PM dispersion patterns (Tables 13.3 and Table 13.6) the efficiency about 60-65% appears to be the best for night-morning peak PM_{10} measurements. These results are in good agreement with efficiency peak results obtained from Figure 13.10 (for fine PM) and Figure 13.12 (for total PM). Table 13.7 compares the routine PM measurement sites with calculated modelled efficiency for CAPS2000 winter campaign.

Table 13.7 List of PM the measurement sites in Christchurch plus efficiency of each site (EF) during the winter period of CAPS200.

Site name	Latitude	Longitude	Time frame	PM – Efficiency (EF)
1 Coles Place	-43.305	172.382	Hourly	**PM_{10} – 57.8%**
2 Polytechnic	-43.323	172.388	Hourly	**$PM_{2.5}$ – 66.9%**
3 Hornby	-43.326	172.311	Hourly	**PM_{10} – 60.1%**
4 Packe Street	-43.311	172.385	I0 minutes	**PM_{10} – 56.9%**
5 Hagley Park	-43.317	172.369	Hourly	**PM_{10} – 63.8 %**
6 Woolston-CAPS	-43.302	172.435	Hourly	**PM_{10} – 34.1 %**

From Table 13.7, it is obvious that Coles Place site position is not too bad, but the efficiency is only 4th one between 6 sites (at least for PM peak measurements) and is below the good site efficiency of 60-65%. All 6 observation sites in the Table 13.5 have one common feature that only high concentrations of local aerosol during heavy smog night-morning time were used for the sites.

An observation point in North Brighton (red point marked “B” - Figure 13.13 and 13.14) is used to calculate background site efficiency. Table 13.8 shows the efficiency of the North Brighton site and presents calculated ratios and weights for 4 modelled night/morning episodes.

Table 13.8 Night-morning weights and ratios for modelled total PM_{10} at North Brighton virtual site relative to the maximum modelled PM_{10} concentration: 4 winter 2005 episodes, night (weightN) and morning (weightM) peaks.

weight	Episode	Episode 4	Episode 5	Episode 6	Episode 7
weightN – 0.65	Ratio (night)	0.00	0.05	0.00	0.25
weightM – 0.35	Ratio (morning)	0.05	0.05	0.10	0.15

From Table 13.8 for North Brighton background site the modelled EF(North) is equal to 0.283. As the maximum modelled EF is 4.0 so the efficiency of the site EF(North) is equal to 7.1%

(night/morning PM_{10} peak concentrations for 4 modelled smog episodes). It is important to stress that calculation of background site efficiency was done for input gridded PM emissions prepared for inner Christchurch only, and no other information about regional scale background aerosol was included. The ratio between high pollution site (Polytechnic) and a background site (North Brighton) is about 9.5 to 1 (11% for the background site), which is close to the ratio for a background site described in many studies (Putard et al., 2004; van Dingenen et al., 2004; Ecudero et al., 2007; Salvador et al., 2007). Also, background site efficiency EF(North)) is close to the ratio of the minimum observed values of PM_{10} (4.37 μg m^{-3} – intercept in Table 9.7) to the ambient average PM_{10} of 50.7 μg m^{-3} for May-June 2005 (Section 13.1).

13.4 Summary

A numerical approach to the observation sites optimal positioning is an important part of fine-total PM spatial and temporal dispersion modelling using the MM5 (WRF)–CAMx4 numerical system. As installation of a new routine measurement sites costs big money it is important carefully to locate the position of proposed new observation sites. In Chapter 13 four heavy pollution episodes in winter 2005 (which include different aerosol spatial patterns) were used, and a technique 'existing + one new' was developed to predict the approximate position of additional sites based on winter 2005 and winter 2006 PM measurements. Evaluation of the efficiency for existing and proposed sites calculated for night-morning peak time periods using 4 episodes of PM_{10} and $PM_{2.5}$ spatial distribution (night and morning peak concentration time points) demonstrated that the efficiency of the Coles Place observation site (ECan) is quite high (> 55%), while proposed Riccarton and CAPS2000 Polytechnic and Hagley Park sites have higher efficiency in capturing PM peak concentrations. The maximum calculated efficiency inside the inner part of the city is found from evaluation of CAP2000 site position and is considered to be 60-65%, while background site efficiency is calculated to be about 7%.

Chapter 14: Summary and conclusions

The following outcomes were successfully achieved by this study:

- Detailed analysis of MM5 modelled near-surface air circulation indicated the ability of MM5 to reproduce local-scale air circulation over the complex terrain of the Christchurch area. At this stage of the WRF system development its ability to reproduce local near-surface circulation for low wind speed is considered to be much lower. The processes controlling the pattern of ground level concentrations of PM over the Christchurch region during winter time are complex, but the MM5-CAMx4 system showed reasonable skill in reproducing the temporal evolution of spatial dispersion of PM10 & PM2.5;
- The MM5-CAMx4 modelling results show that the most representative chemical composition of particulate material in Christchurch is close to the scenario having carbonaceous species about 65-70% of aerosol content (Scenario 1-3mix), and with a ratio of organic to elemental carbon close to 3. The method of chemical scenarios was developed to find the optimal chemical split of input aerosol gridded emissions to obtain (from MM5-CAMx4 numerical modelling system) numerical PM concentrations with minimum error compared to observed fine-total aerosol concentrations for winter 2005 heavy pollution episodes;
- Stability of the method of chemical scenarios was tested using different seasons observations and different numerical systems, and a bias reduction of the method was undertaken based on winter 2005-2006 PM heavy pollution episodes;
- Numerical assessment of the total PM contribution in the groups "Domestic", "Transport" and "Industry" was completed for different proposed emissions reduction scenarios using linear and non-linear methods to reduce CAMx4 input gridded emissions. Evaluation of MM5-CAMx4.2 using a complex chemical split and linear reduction of hourly gridded emissions (in 'Domestic' and 'Transport' groups) indicated that a 50% decrease of transport emissions (only) would lead to 2-2.5 fold decrease of peak PM **hourly** concentrations (for short-term exposure);
- Numerical assessment of proposed $PM_{2.5}$ and PM_{10} abatement strategies for the 2005-2013 time periods was completed using linear aerosol emissions reductions in the groups "Domestic" and "Transport" for the winter 2005 meteorology. Examination of options to decrease (during winter time) long-term PM exposure using the MM5-CAMx4 system indicated that proposed aerosol abatement strategies potentially lead to a considerable reduction (3-4 times) of fine-total PM **daily** concentrations, but require a several fold reduction of domestic and transport emissions;

- The effect of the proposed total PM abatement strategy for Christchurch was assessed through to the year 2013 and shown to follow a curved line (**CLiP**) reduction;
- A new numerical method was developed to define an optimal location of observation sites using the MM5-CAMx4 numerical system. A spatial index of site efficiency to catch heavy aerosol pollution episodes (during winter time) has been created for several (four) different local scale near-surface air circulation patterns over the Christchurch area.

This chapter summarises the key findings in relation to the study objectives, and outlines the justification to use the MM5 (potentially WRF) – CAMx4 numerical modelling system in long-term aerosol air quality programmes, especially for areas with complex orography and a small number of observation sites.

14.1 Key findings

14.1.1 Ability of MM5 and WRF to reproduce a local air circulation

Winter near-surface air circulation over the Christchurch area for heavy smog episodes is characterized as a very complex local-scale system (under stagnant synoptic scale air conditions) and includes the processes of night-time (day-time) near-surface temperature inversion development (break up), a day-time (night-time) on-shore (off-shore) sea breeze, and downslope drainage of cold air from the Canterbury Plains and Port Hills over the urban heat island of the city (night time).

Analysis of the ability of MM5 to reproduce this complex local air circulation was split into day-time and night-time air circulation analysis, and was completed for a fine MM5 grid (domain 4 with 1 km spatial resolution) that covered the whole Christchurch area and included all features of the local topography-landuse.

It was shown that the limited area mesoscale model (MM5) managed to reproduce the processes of evening-night near-surface temperature inversion development and morning - day-time modelled temperature inversion destruction. Also, the important role of cold air downslope drainage in the temperature inversion development was demonstrated, as well as the essential role of the drainage winds in dispersion of near-surface heavily polluted air (50-70 meters layer) in 2 directions (to the seashore and to the south). The modelled cold air drainage increased dispersion over the city during night-time heavy smog episodes. The modelled night-time off-shore land breeze was also

reckoned to improve near-surface ventilation, but restoration of the day-time on-shore sea breeze returned aloft part of the night-time polluted air removed from the Christchurch area during the night-early morning period. This re-circulated polluted air increased day-time PM near-surface concentrations and was dispersed in south-west direction.

Statistical analysis of the near-surface modelled meteorology for 7 heavy smog winter 2005 episodes (compared with observations from 3 sites) demonstrated the good skill of MM5 to reproduce the local circulation, and the much lower WRF skill over the complex local orography. The WRF model (domain 4) failed to reproduce observed wind time-series and tended to over-predict wind speed. This wind speed 24-hour over-prediction was crucial for aerosol dispersion during CAMx4 photochemical model evaluation.

14.1.2 Method of scenarios as a tool to finding optimal PM content

The application of 4 basic chemical scenarios with CAMx4 demonstrated that the most representative chemical composition of $PM_{2.5}$ was close to Scenario 3, with carbonaceous species about 55-65% of the PM total content, and with a ratio of organic to elemental carbon close to 3 (Hueglin et al., 2005). The contribution of soluble inorganic ions (secondary and primary) was close to 30%. This fact indicated active secondary aerosol production (from condensable gases) in the photochemical model under low temperature and high relative humidity conditions. The contribution of dust and crustal particles to PM emissions was considered to be about 10%. The uncertainty of the method (13 aerosol species only are included in the CAMx4 aerosol chemistry mechanism CB4) was considered to be not more than15-20% (Scott, 2005) and was distributed more or less evenly between all main chemical groups. It was impossible to calculate more accurately the percentage contribution of unknown species contribution in fine-total particulate matter. This unknown and undescribed aerosol caused an increase of Mean Absolute Error (MAE) between modelled and ambient aerosol concentrations.

The day-time Scenario 1 was considered to present the increased contribution of vehicular-industrial emissions, with high values of primary particles and elemental carbon. The basic night-time Scenario 3 was shown to represent "Domestic" emissions chemical split (biomass burning in residential districts) with active secondary aerosol formation during very cold nights. Scenario 1-3mix, generated from Scenario 3 and Scenario 1, was shown to be the best for modelling $PM_{2.5}$ (PM_{10}) concentrations in the range 0-140 $\mu g\ m^{-3}$ for all winter 2005 heavy smog episodes.

The method of scenarios was shown to be a quite skilful numerical tool for finding the optimal chemical split of input gridded PM emissions for CAMx4, and controlling the proportional contribution of the main chemical components to the local fine and total PM. It should be stressed that the chemical composition of the complex Scenario 1-3mix and the observed chemical composition of PM_{10} (Wang et al., 2005) for a Christchurch winter day (July 2004) was found to be very close supporting the validity of the method of scenarios.

14.1.3 Stability-bias of the method of scenarios

The method of chemical scenarios was developed and applied to winter 2005 smog episodes to find the aerosol input gridded emissions chemical split to calculate $PM_{2.5}$-PM_{10} concentrations that had best agreement with ambient $PM_{2.5}$-PM_{10}. MM5 and CAMx4 were used to evaluate $PM_{2.5}$ (PM_{10}) time trends over a 48-72 hour time periods over the area of Christchurch, and to find ratios between principal chemical species of the modelled aerosol composition.

To reduce the method's accumulated systematic bias all 5 chemical scenarios (4 basic scenarios and a new complex scenario) were evaluated for seven winter 2006 (June–July) heavy smog episodes to eliminate a seasonal bias and to decrease a numerical and observational bias of the method. The observational bias was reduced by using an additional observation site in Woolston. The numerical bias was decreased with application of the latest MM5 MPP version 3.7.3 and WRF v2.1.2. Also, a more recent version of CAMx (CAMx4.2) was used to decrease bias of the deterministic system.

Correlation statistics for winter 2005-2006 for all 5 chemical scenarios showed that highest PCC and IOA for the complex Scenario 1-3mix occurred in the first part of winter 2005, and the second part of winter 2006. For both winter seasons (2005 and 2006) the numerical modelling system demonstrated better skills in prediction of high $PM_{2.5}$-PM_{10} concentrations as a range of fractional bias (FB) became less and tending to zero as fine-total PM concentrations increase. It was found that FB for winter 2006 was negative skewed for high PM concentrations, which meant an underprediction of $PM_{2.5}$-PM_{10} peak concentrations for very cold nights of June-July 2006.

14.1.4 Numerical assessment of different group's exposure to total PM

Evaluation of the aerosol part of the 1999 inventory using linear and non-linear emissions reduction in the groups "Domestic", "Transport" and "Industry" definitely proved the validity of

the linear emissions reduction method for different groups. An inter-comparison of the modelled PM concentrations for liner and non-linear 50% emissions reduction (in groups separately, and for 2 groups together) numerically indicated the good quality of the 1999 inventory for the "Domestic", "Transport", "Industry" and "Total" groups.

Application of the input emissions linear reduction procedure to groups was done using an "out of total" method (when emissions of certain groups were removed from the total emissions) and an "in method" (when emissions of certain groups only were used instead of the total emissions). This approach allowed assessment of the importance of every emission group in fine and total PM development. Winter 2005 near-surface meteorology was used in all experiments, as winter 2005 meteorology was considered to be close to the average winter meteorology for the Christchurch area.

14.1.5 Numerical assessment of the proposed PM abatement strategy

Evaluation of the proposed (developed by ECan, Scott, 2005) fine-total PM reduction strategy for the time period 2005-2013 was undertaken on the base of 7 winter 2005 meteorological episodes, and was run using the MM5 MPP-CAMx4.4 numerical modelling system. From modelling results for the complex chemical scenario 1-3mix and for the re-built hourly gridded emissions in the groups "Domestic", "Transport", "Industry" it was clearly demonstrated that a 50% decrease of input transport emissions was enough to diminish aerosol hourly peak concentrations by 2-2.5 fold. This reduction in PM peak concentrations was determined to be an essential part of the short-term pollution exposure abatement strategy.

It was calculated that for long-term PM exposure abatement a more dramatic emissions decrease should be applied. The winter aerosol abatement strategy was shown to lead to a considerable decrease of fine-total PM average concentrations (3-4 times), but it demands a several fold reduction in the "Domestic" and "Transport" group emissions.

With application of future PM emissions scenarios it was numerically demonstrated that the PM reduction strategy developed for the 2005-2013 time period could only follow a Curve Line Path (CLIP) abatement plan. Ambient air pollution is a 4-D process and considered to be a non-linear stochastic system, which can not respond linearly (follow the proposed Straight Line Path abatement plan - SLIP). The abatement strategy developed by ECan could not be properly realized

because of objective reasons (inflating prices on energy versus average family income), but in the near future (5-10 years) contribution to $PM_{2.5}$–PM_{10} daily concentrations would be more evenly distributed between emission groups "Domestic", "Transport" and "Industry", with dominance of carbonaceous species, and with a total PM concentrations (short-term and long-term) decrease.

14.2 Numerical optimization of observation sites location

Location of new observation sites is a very actual problem for any field studies and especially for long-term routine measurements of ambient aerosol-gaseous pollution. A new numerical approach to the optimal location of observation sites was developed as a very important and flexible numerical tool of PM spatial and temporal dispersion modelling using the MM5 –CAMx4 numerical system.

As installation of new routine observation sites costs big money it is important to locate carefully the position for proposed new observation sites. Winter 2005 four heavy pollution episodes (which include different aerosol spatial dispersion patterns in response to winter 2005 near-surface meteorology) were used, and initially a technique 'existing + one new' was developed to predict the approximate position of a second site when there is an existing one (winter 2005), and to predict a third site location for situation when there are two existing sites (winter 2006) on the basis of winter 2005 meteorology only.

Evaluation of the efficiency (EF(site)) for existing and proposed sites calculated for night-morning peak time periods using 4 episodes of PM_{10} and $PM_{2.5}$ spatial distribution (night and morning peak concentration time points) demonstrated that the efficiency of Coles Place observation site (ECan) in relation to heavy smog episodes was quite good (>55%) for 4 different spatial PM night-morning peak patterns. Consequent evaluation of the existing Woolston and proposed Riccarton sites demonstrated much higher efficiency to capture PM peak concentrations at Riccarton. A maximum calculated efficiency for the inner city was found from the calculated EF(site) spatial values (for PM peak concentration hours only) compared with CAP2000 site positions. It was proven that heavy pollution site efficiency of more than 60-65% was a high efficiency, while for a background site EF(background site) efficiency was calculated to be about 7% (1:9.5 ratio to maximum PM values) for local aerosol input emissions.

As a definition of efficiency can be assigned to any spatial and temporal maximum-minimum variable or gradient it has been numerically proven (on the basis of PM peak concentration efficiency) that the efficiency method (EF) could be applied to a great diversity of air pollution research that includes new filed measurements of any air pollutant associated with installation of a new observation site/sites. Number of cases (patterns) can be considerably increased (to increase an accuracy of the method), but also should be restricted by a minimum additional change of an efficiency per any additional case (pattern).

14.3 Limitations

There are number of limitations to this research, including:

- Inaccurate reproduction of the near-surface wind field. This is not surprising given the very light winds involved in high air pollution events.
- Lack of precision of the input data, especially the spatial and temporal variation of air pollution emissions.
- The inability of the chemical model to satisfactorily reproduce the secondary reactions between different chemical components, which make up aerosols.

14.4 Suggestions for future work

The most important suggestion for future work concerns the potential improvement of the input PM and gaseous (especially aerosol precursors) emissions quality. Reliability of the modelled aerosol temporal and spatial dispersion crucially depends on the quality of input gridded emissions. This stipulation demands the regular generation of new more precise databases of the gases-aerosol emissions in groups “Domestic”, “Transport” and “Industry”, and logically leads to a new emission inventory for the Christchurch area. It is especially important to re-calculate gaseous emissions of the 1999 inventory as it is apparent (from this work) that secondary aerosol partitioning is very important in determining modelled total PM peak concentrations.

A new routine observation site was installed at Riccarton Mall by ECan in 2007. This very important step could help to obtain additional spatial information about ambient PM time trends and will promote the evaluation of MM5/WRF-CAMx4 numerical modelling system against observations, especially for winter time.

Assimilation of new ambient pollution information via input gridded gaseous-aerosol gridded emissions will help to explore the MM5/WRF-CAMx4 numerical modelling system to obtain a more accurate numerical reproduction of spatial fine and total particulate matter distribution over the city of Christchurch for winter smog episodes. Potentially the MM5/WRF-CAMx4 numerical modelling system can be used in quasi-operational mode to provide spatial and temporal forecast for different inner city districts, but this possibility is very difficult to realize because of a number of obstacles including financial issues.

The research has demonstrated the outstanding ability of the MM5-CAMx4 numerical modelling system to address a large diversity of problems concerning evaluation of winter time PM distribution, including application of MM5-CAMx4 as a reliable numerical tool to assess efficiency of air pollution abatement strategies. However, some form of testing of the contribution to uncertainty should be included in future research; this could include comparison of different types of model.

References

Abdalmogith, S.S., Harrison, R.M. 2005. The use of trajectory cluster analysis to examine the long-range transport of secondary inorganic aerosol in the UK, *Atmospheric Environment*, **39**: 6686–6695.

Aberkane, T., Harvey, M., Webb, M. 2004. Annual air quality monitoring report 2003. Report No. U04/58, *Environment Canterbury*, Christchurch, New Zealand, 51p.

Ackermann, I.J., Hass, H., Memmesheimer, M.E.A., Binkowski, F.S., Shankar, U. 1998. Modal aerosol dynamics model for Europe: development and first applications, *Atmospheric Meteorology*, **36**: 2981–2999.

Adhikari, A., Reponen, T., Grinshpun, S.A., Martuzevicius, D., LeMasters G. 2006. Correlation of ambient inhalable bioaerosols with particulate matter and ozone: A two-year study, *Environmental Pollution*, **140**: 16–28.

Allwine, K.J., Dabberot, W.F., Simmons, L.L. 1998. Peel review of the CALMET/CALPUFF modelling system, *EPA contract N 68-D-98-092*, N 1-03 report.

American Interpretation Dictionary. 2006.

Anderson, R.R., Martello, D.V., Lucas, L.J., Davidson, C.I., Modley, W.K., Eatough, D.J. 2006. Apportionment of ambient primary and secondary pollutants during a 2001 summer study in Pittsburgh using U.S. environmental protection agency UNMIX. *Journal of the Air & Waste Management Association*. **56** (9): 1301-1319.

Ansari, A., Pandis, S.N. 1999. An Analysis of Four Models Predicting The Partitioning of Semi-volatile Inorganic Aerosol Components. *Aerosol Science and Technology*, **31**: 129-153

Arakawa, A., Schubert, W.H. 1974. Interaction of a cumulus cloud ensemble with the large scale environment, Part I. *Journal of the Atmospheric Sciences*, **31**: 674-701.

Arnold, J.R., Dennis, R.L., Tonnesen, G.S. 2003. Diagnostic evaluation of numerical air quality models with specialized ambient observations: testing the Community Multiscale Air Quality modelling system (CMAQ) at selected SOS 95 ground sites, *Atmospheric Environment*, **37** (9–10): 1185–1198.

Arnold, S.J., ApSimon, H., Barlow, J., Belcher, S., Bell, M., Boddy, J.W., Britter, R., Cheng, H., Clark R, Colvile R N, Dimitroulopoulou S, Dorbe A, Greally B, Kaur S, Knights A, Lawton T, Makepeace A, Martin D, Neophytou M, Neville S, Nieuwenhuijsen M, Nickless G, Price C, Robin A, Shallcross D, Simmonds P, Smalley R J, Tate J, Tomlin A S, Wang H, Walsh P. 2004. Introduction to the DAPPLE air pollution project. *Science of the Total Environment*, **332**: 139 – 153.

Arya, S.P. 1988. *Introduction to Micrometeorology*, Academic Press, New York, 307p.

Arya, S.P. 1999. *Air pollution meteorology and dispersion*. Oxford University Press, New York, 310p.

Bae, M.-S., Demerjian, K.L., Schwab, J.J. 2006. Seasonal estimation of organic mass to organic carbon in $PM_{2.5}$ at rural and urban locations in New York state. *Atmospheric Environment*, **40**: 7467-7479.

Baertch-Ritter, N., Prevot, A.H., Dommen, J., Andreani-Aksoyoglu, S., Keller, J. 2003. Model study with UAM-V in the Milan area (I) during PIPAPO: simulations with changed emissions compared to ground and airborne measurements. *Atmospheric Environment*, **37**: 4133 – 4147.

Barna, M.G., Gimson, N.R. 2002. Dispersion modelling of a wintertime particulate pollution episode in Christchurch, New Zealand. *Atmospheric Environment*, **36**, 3531-3544.

Barna, M.G., Gebhart, A., Schichtel, B.A., Malm, W.C. 2006a. Modelling regional sulphate during the BRAVO study: Part 1. Base emissions simulation and performance evaluation. *Atmospheric environment*, **40:** 2436–2448.

Barna M.G., Schichtel B.A., Gebhart K.A., Malm W.C. 2006b. Modelling regional sulphate during the BRAVO study: Part 2. Emission sensitivity simulations and source apportionment. *Atmospheric Environment*, **40**: 2423–2435.

Baron, P.A., Willeke, K. 2001. Aerosol fundamentals. In *Aerosol measurements – Principles, techniques, and applications, 2nd edition*, ed. P.A. Baron and K. Willeke, John Wiley and Sons, New York, 45–60.

Becker, S. 2002. Involvement of microbial components and toll-like receptors 2 and 4 in cytokine responses to air pollution particles. *American journal of respiratory cell and molecular biology*, **27**: 611–618.

Beniston, M., Stephenson, D.B. 2004. Extreme climatic events and their evolution under changing climatic conditions. *Global and Planetary Change*, **44** (1): 1–9.

Berg L.K., Zhong S. 2005. Sensitivity of MM5-simulated boundary layer characteristics to turbulence parameterizations. *Journal of Applied Meteorology*, **44**: 1467–1483.

Bergin, M.S., Russell, A.G., Milford, J.B. 1998. Effects of chemical mechanism uncertainties on the reactivity quantification of volatile organic compounds using a three-dimensional air quality model. *Environmental Science and Technology*, **32**: 694–703.

Bessagnet, B., Hodzic, A., Vautard, R., Beekmann, R., Cheinet, S., Honore, C., Liousse, C., Rouil, L. 2004. Aerosol modelling with CHIMERE: preliminary evaluation at the continental scale. *Atmospheric Environment*, **38**: 2803–2817.

Beyea, J., Hatch, M., 1999. Geographic exposure modelling: a valuable extension of geographic information systems for use in environmental epidemiology. *Environmental Health Perspectives*, **107**: 694–703.

Blackadar, A. K. 1979. High resolution models of the planetary boundary layer. *Advances in Environmental Science and Engineering*, edit by J.R. Pfaffin and E.N. Ziegler, Gordon and Breach, Newark, N.J., 50–85.

Borrego, C., Martins, H., Lopes, M. 2005. Portuguese industry and the EU trade emissions directive: development and analysis of CO_2 emission scenarios. *Environmental Science & Policy*, **8**: 75 – 84.

Bott, A. 1989. A positive definite advection scheme obtained by non-linear renormalization of the advective fluxes. *Monthly Weather Review*, **117**: 1006–1015.

Boucouvala, D., Bornstein, R., Wilkinson, J., Miller, D. 2003. MM5 simulations of a SCOS97 – NARSTO ozone episode. *Atmospheric Environment*, **37** (2): 95–117.

Brimblecombe, P. 1996. *Air composition and chemistry*, 2nd edition. Cambridge University Press, Cambridge, UK, 253p.

Brown, M.J., Locatelli, J.D., Stoelinga, M.T., Hobbs, P.V. 1999. Numerical modelling of precipitation cores on cold fronts. *Journal of the Atmospheric Sciences*, **56**: 1175-1196.

Brulfert, G., Chemel, C., Chaxel, E., Chollet, J.-P., Jouve, B., Villard, H. 2006, Assessment of 2010 air quality in two Alpine valleys from modelling: weather type and emission scenarios. *Atmospheric Environment*, **40**: 7893-7907.

Buizza, R., Houtekamer, P.L., Toth, Z., Pellerin, G., Wei, M., Zhu Y. 2005. A comparison of the ECMWF, MSC, and NCEP global ensemble prediction systems. *Monthly Weather Review*, **133**: 1076–1096.

Burnett, R.T. 2000. Association between particulate- and gas-phase components of urban air pollution and daily mortality in eight Canadian cities. *Inhalation toxicology,* **12**: 15–39.

Byun, D.W., Ching K.S. 1999. Science algorithms of the EPA Model-3 CMAQ modeling system. Washington, DC, U.S. *Environmental Protection Agency, Office of Research and Development*.

Cachier, H. 1998. Carbonaceous combuction aerosols. In *Atmospheric Particles*, ed. R.M. Harrison and R.E. van Grieken, IUPAC series on analytical and physical chemistry of environmental systems. Volume 5, John Wiley and Sons, New York, 348-395.

Canterbury Regional Council 1998a. *Christchurch inventory of total emissions*. Revised edition June 1998 including aircraft emissions, Technical Report N. R97/7.

Carter, W.P.L. 1996. Condensed Atmospheric Photooxidation Mechanisms for Isoprene. *Atmospheric Environment,* **30**: 4275-4290.

Chan, Y.C., Simpson, R.W., Mctainsh, G.H., Vowles, P.D., Cohen, D.D., Bailey, G.M. 1999. Source apportionment of visibility degradation problems in Brisbane (Australia) Using the Multiple Linear Regression Techniques. *Atmospheric Environment*, **33**: 3237-3250.

Chakrabarti, B., Fine, P.M., Delfino, R., Sioutas, C. 2004. Performance evaluation of the active-flow personal DataRAM PM2.5 mass monitor (Thermo Anderson pDR-1200) designed for continuous personal exposure measurements. *Atmospheric Environment*, **38**: 3329-3340.

Chang, J.S., Brost, R.A., Isaksen, I.S.A., Madronich, S., Middleton, P., Stockwell, W.R., Walcek, C.J. 1987. A three-dimensional Eulerian Acid Deposition model (EURAD): physical concepts and formulation. *Journal of Geophysical Research*, **92** (14): 681–700.

Chang, S.-Y., Lee, C.-T., Chou, C.C.-K., Liu, S.-C., Wen, T.-X. 2007. The continuous field measurements of soluble aerosol compositions at the Taipei aerosol supersite, Taiwan. *Atmospheric Environment*, **41**: 1936-1949.

Charron, A., Harrison, R.M., Moorcroft, S., Booker, J. 2004. Quantitative interpretation of divergence between PM_{10} and $PM_{2.5}$ mass measurement by TEOM and gravimetric (Partisol) instruments. *Atmospheric Environment*, **38**: 415–423.

Chen, J.-L., Lee, C.-T., Chang, S.-Y., Chou, C.C.K. 2001. The elemental contents and fractional dimensions of $PM_{2.5}$ in Taipei City. *Aerosol and Air Quality Research*, **1** (1): 9-20.

Chen, D.S., Cheng, S.Y., Liu, L., Chen, T., Guo, X.R. 2007. An integrated MM5-CMAQ modelling approach for assessing trans-boundary PM_{10} contribution to the host city of 2008 Olympic summer games – Beijing, China. *Atmospheric Environment,* **41**: 1237-1250.

Cheng T., Liu Y., Lu D., Xu Y., Li H., 2006, Aerosol properties and radiative forcing in Hunshan Lake desert, northern China. *Atmospheric Environment*, vol. 40, pp. 2169 – 79.

Chow, J.C., Watson, J.G., 1998. Guideline *on speciated particulate monitoring – Draft 3*. Prepared for the Office of Air Quality Planning and Standards, United States Environmental Protection Agency (EPA).

Chow, J.C., Watson, J.G., Edgerton, S.E., Vega, E., Ortiz, E. 2002. Spatial differences in outdoor PM_{10} mass and aerosol composition in Mexico city. *Journal of the Air & Waste Management Association*, **52** (4): 423 – 434.

Chow, C-K., Huang, S-H., Chen, T-K., Lin, C-Y., Wang, L-C. 2005. Size-segregated characteristic of atmospheric aerosol in Taipei during Asian outflow episodes. *Atmospheric Research*, **75**: 89–109.

Claes, M., Gysels, K., van Grieken, R.E., Harrison, R. 1998. Inorganic composition of atmospheric aerosol. In *Atmospheric particles*, ed. R.M. Harrison and R.E. van Grieken, John Wiley and Sons, Chichester, 95–146.

Coats, C.J., Tryanov, Jr.A., McHenry, J.N., Xiu, A., Gibbs-Lario, A., Peters-Lidard, C.D. 1999. An extension of the EDSS/Model-3 I/O API for coupling concurrent environmental models, with applications to air quality and hydrology. Paper J10.6, *Preprint volume: 14th Conference on Hydrology, American Meteorology Society, Dallas, Texas*.

Colella, P., Woodward, P.R. 1984. The Piecewise Parabolic Method (PPM) for gas-dynamical simulations. *Journal of Computational Physics*, **54**: 174–201.

Colvile, R.N., Gamez-Perales, J.E., Nieuwenhuijsen, M.J. 2003. Use of dispersion modelling to assess road-user exposure to $PM_{2.5}$ and its source appointment. *Atmospheric Environment,* **37** (20): 2773–2782.

Cox, R.M, Sontowski, J., Fry, R.N.Jr., Dougherty, C.M., Smith, T.J. 1998. Wind and diffusion for complex terrain. *Journal of Applied Meteorology*, **37**: 996–1006.

Cuvelier, C., Thunis, P., Vauntard, R., Amann, M. 2007. CityDelta: a model intercomparison study to explore the impact of emission reductions in European cities in 2010. *Atmospheric Environment*, **41**: 189-207.

Cyrys, J., Dietrich, G., Kreyling, W., Tuch, T., Heinrich, J. 2001. PM2.5 measurements in ambient aerosol: comparison between Harvard impactor (HI) and the tapered element oscillating microbalance (TEOM) system. *Science of the Total Environment*, **278**: 191–197.

Dailey, P.S., Keller, J.L. 2002. Modelling of extreme wind events using MM5: approach and verification, *MM5 Workshops*, *Division 3*, **www.mmm.ucar.edu/mm5/workshop/workshop-program-2002.html**.

Dan, M, Zhuang, G, Li X, Tao, H, Zhuang, Y. 2004. The characteristics of carbonaceous species and their sources in $PM_{2.5}$ in Beijing. *Atmospheric Environment*, **38**: 3443 – 3452.

Dassios, K., Pandis, S.N. 1999. The mass accommodation coefficient of ammonium nitrate. *Atmospheric Environment*, **33**: 2993-3003.

Davis, J.M., Eder, B.K., Nychka, D., Yang, Q. 1998. Modeling the effects of meteorology on ozone in Houston using cluster analysis and generalized additive models. *Atmospheric Environment*, **32**: 2505–2520.

Davy, P., Markwitz, Z., Trompetter, W.J. 2002. Elemental analysis and source appointment of ambient particulate matter in the Wellington Region of New Zealand. *Proceedings of the 16th International Clean Air and Environment Conference*, Clean Air Society of Australia and New Zealand, Christchurch, New Zealand, 19-22 August.

de Haan, P., Rotach, M.W., Werfeli, M. 1998. Extension of an operational short-range dispersion model for applications in an urban environment. *International Journal of Vehicle Design*, **20**: 105–114.

Dockery, D.W., Pope, C.A., III, Xu, X., Spengler, J.D., Ware, J.H., Fay, M.E., Ferris, B.G., Speizer, F.A. 1993. An Association between air pollution and mortality in six U.S. cities. *The New England Journal of Medicine*, **329**: 1753-1759.

Dore, A.J., Mousavi-Baygi, M., Smith, R.I., Hall, J., Fowler, D., Choularton, T.W. 2006. A model of annual orographic precipitation and acid deposition and its application to Snowdonia. *Atmospheric Environment*, **40**: 3316–3326.

Draxler, R.R. and Hess, G.D. 1997. Description of HYSPLIT-4modelling system, NOAA Technical Memorandum ERL ARL-224, *Air Research Laboratory, Silver Spring, Maryland*, December 1997.

Draxler, R.R., Hess, G.D. 1998. An overview of the Hysplit-4 modelling system for trajectories, dispersion and deposition. *Austrian Meteorological Magazine*, **47**: 295–308.

Duan, F.K., He, K.B., Ma, Y.L., Yang, F.M., Yu, X.C., Cadle, S.H., Chan, T., Mulawa, P.A. 2006. Concentration and chemical characteristics of $PM_{2.5}$ in Beijing, China: 2001–2002. *Science of the Total Environment*, **355**: 264–275.

Dudhia, J. 1993. A non-hydrostatic version of the Penn State/NCAR mesoscale model: Validation tests and simulation of an Atlantic cyclone and cold front. *Monthly Weather Review*, **121**: 1493-1513.

Dudhia, J., Bresch, J.F. 2000. A global version of MM5. *Tenth Annual PSU/CAR Mesoscale Model User's Workshop*, Boulder CO, June 2000: 23–26.

Dudhia, J., Grell, G.A., Guo, Y., Manning, K., Wang, W., Chiszar, J. 2000b. *PSU/NCAR mesoscale modelling system tutorial class notes and user's guide: MM5 modelling system Version 3*. Mesoscale and Microscale Meteorology Division, NCAR, Boulder, Colorado, USA.

Dudhia, J. 2005. MM5: current status and plans, *MM5 Workshops*, *Division 1*, **www.mmm.ucar.edu/mm5/workshop/workshop-program-2005.html**.

Ecudero, M., Querol, X., Avila, A., Cuevas, E. 2007. Origin of the exceedences of the European daily PM limit value in regional background areas of Spain. *Atmospheric Environment*, **41**: 730-744.

Environet Ltd. 2003. *Amenity effects of PM_{10} and TSP concentrations in New Zealand*. Prepared for the Ministry for Environment, 17p.

ENVIRON. 2003. Development of an Advanced Photochemical Model for Particulate Matter: PM CAMx." ENVIRON International Corporation, Novato, CA. Prepared for Coordinating Research Council, Inc. Project A-30 (available at www.crcao.com).

ENVIRON Int. Corp. 2005. CAMx comprehensive air quality model with extensions, version 4.2, User's guide, 236p.

ENVIRON Int. Corp. 2006. CAMx comprehensive air quality model with extensions, version 4.40, User's guide, 261p.

Fahey, K.M., Pandis, S.N., 2001. Optimizing model performance: variable size reduction in cloud chemistry modeling. *Atmospheric Environment*, **35**: 4471-4478.

Favez, O., Cachier, H., Sciare, J., le Moullec, Y. 2007. Characterization and contribution to $PM_{2.5}$ of semi-volatile aerosols in Paris (France). *Atmospheric Environment*, **41**: 7969-7976.

Fine, J., Vuilleumier, L., Reynolds, S., Roth, P., Brown, N. 2003. Evaluating uncertainties in regional photochemical air quality modeling. *Annual Review of Environmental Resources*, **28**: 59–106.

Foster, E. 1998a. *An investigation into the measurement of PM_{10} in Christchurch*. Report U98/69, Environment Canterbury, Christchurch, 24p.

Forster, E. 1998b. Reductions *in suspended particulate concentrations in Christchurch*. Report R98(1), Environment Canterbury, Christchurch, 51p.

Ford-Robertson, J., Robertson, K., Maclaren, P., 1999. Modelling the effect of land-use practices on greenhouse gas emissions and sinks in New Zealand. *Environmental Science & Policy*, **2**: 135–144.

Fisher, G., Thompson, A., Kuschel, G. 1998. *A study of the sources of haze and smoke found in Christchurch during winter: Final report*. NIWA report AK97138, prepared for the Canterbury Regional Council, Auckland, 80p.

Fisher, G., Kuschel, G., Mahon, K. 2005. *Straight and Curved Line Pathes (SliPs & CliPs): developing the targets and predicting the compliance, Discussion, methodology and example: a report to regional councils*. SliP and CliPs Discussion Document, NIWA report, 27p.

Fung K, Chow J, Watson J. 2002. Evaluation of OC/EC specification by thermal manganese dioxide oxidation and the IMPROVE method. *Journal of the Air & Waste Management Association*, **52**: 1333 – 1341.

Gangoiti, G., Albizuri, A., Alonso, L., Navazo, M., Matabuena, M., Valdenebro, V., García, J.A. and Millán, M.M. 2006. Sub-continental transport mechanisms and pathways during two ozone episodes in northern Spain. *Atmospheric Chemistry and Physics*., **6**: 1469-1484.

Gaydos, T.M., Pinder, R., Koo, B., Fahey, K.M., Yarwood, G., Pandis, S.N. 2007. Development and application of a three-dimensional aerosol chemical transport model, PMCAMx. *Atmospheric Environment*, **41**: 2594-2611.

Gebhart, K.A., Malm, W.C., Ashbaugh, L.L. 2005. Spatial, temporal and interspecies patterns in fine particulate matter in Texas. *Journal of the Air & Waste Management Association*, **55**: 1636 – 1648.

Gehrig, R., Buchmann, B. 2003. Characterising seasonal variations and spatial distribution of ambient PM10 and PM2.5 concentrations based on long-term Swiss monitoring data. *Atmospheric Environment*, **37:** 2571–2580.

Gery, M.W., G.Z. Whitten, J.P. Killus, and M.C. Dodge. 1989. A Photochemical Kinetics Mechanism for Urban and Regional Scale Computer Modelling. *Journal of Geophysics Researches*, **94**: 925-956.

Gimson, N.R. 1998. *The wintertime meteorology of Christchurch and its effects on air pollution dispersion*. Report No. U98/58, Environment Canterbury, Christchurch, 39p.

Gimson, N.R., Fisher, G.W. 1997. *The relationship between emissions to air and measured ambient air concentrations of contaminants in Christchurch*. Report U97(67), Environment Canterbury, Christchurch, 11p.

Giugliano, M., Lonati, G., Butelli, P., Romele, L., Tardivo, R., Grosso, M. 2005. Fine particulate ($PM_{2.5}$ – PM_1) at urban sites with different traffic exposure. *Atmospheric Environment*, **39**: 2421–2431.

Glasius, M., Ketzel, M., Wahlin, P., Jensen, B., Monster, J., Berkowicz, R., Palmgren, F. 2006. Impact of wood combuction on particle levels in a residential area in Denmark. *Atmospheric Environment*, **40**: 7115–7124.

Gobbi, G.P., Barnaba, F., Ammannato, L. 2007. Estimating the impact of Saharan dust on the year 2001 PM_{10} record of Rome, Italy. *Atmospheric Environmental*, **41**: 261–275.

Godfrey, J. 2002. A method for better wind fields for air quality applications in complex atmospheric environments at fine scales. Proceedings of the *16th International Clean Air and Environment Conference*, Christchurch, New Zealand, pp. 246-252.

Goldfrey, J.J., Clackson, T.S. 1998. Air quality modelling in a stable polar environment – Ross Island, Antarctica. *Atmospheric Environment*, **32**: 2899–2911.

Gotschi, T., Hazenkamp, M.E., Bono, R., Burney, P., Forsberg, B., Jarvis, D., Maldonado, J., Norback, D., Stern, W.B. 2005. Elemental composition and reflectance of ambient fine particles at 21 European locations. *Atmospheric Environment*, **39**: 5947-5958.

Grell, G.A., Dudhia, J. and Stauffer D. 1994, A description of the Fifth-Generation Penn State/NCAR Mesoscale Model (MM5). *NCAR Tech Note NCAR/TN-398+STR*, 138 pp.

Hamill T. 2003. *Introduction to numerical weather prediction and ensemble weather forecasting*, Climate Diagnostics Center, NOAA-CIRES, PowerPoint Presentation, Boulder, Colorado, USA.

Hanna, S. R. 2001. Evaluation of the ADMS, AERMOD, and ISC3 dispersion models with the OPTEX, Duke Forest, Kincaid, Indianapolis and Lovett field data sets. *International Journal of Environment and Pollution*, **16**: 301-314

Hales, S., Salmond, C., Town, G.I., Kjellstrom, T., Woodward, A. 1999. Daily mortality in relation to weather and air pollution in Christchurch. *New Zealand, Australian and New Zealand Journal of Public Heath*, **24**(1).

Hansen, D.A., Edgerton, E.S., Hartsell, B.E., Jansen, J.J., Kandasamy, N., Hidy, G.M., Blanchard, C.L. 2003. The Southeastern Aerosol Research and Characterization study: Part 1 – overview. *Journal of the Air & Waste Management Association*, **53**: 1460-1471.

Health aspects of air pollution with particulate matter, ozone and nitrogen dioxide. *Report on a WHO Working Group*, Bonn, Germany, 13-15 January 2003.

Hernandez, J.F., Cremades, L., Baldasano, J.M. 1997. Simulation of tracer dispersion from elevated and surface releases in complex terrain. *Atmospheric Environment*, **31**: 2337–2348.

Ho, K., Lee, S., Chan, C., Yu, J. C., Chow, J. C. 2003. Characterization of chemical species in $PM_{2.5}$ and PM_{10} aerosol in Hong Kong. *Atmospheric Environment*, **37**: 31–33.

Hobbs, P.V. 2000. *Introduction to atmospheric chemistry*. University of Washington, Cambridge University Press, 262 p.

Hoek, G., Meliefste, K., Cyrys, J., Lewne, M., Bellander, T., Brauer, M., Fisher, P., Gehring, U., Heinrich, J., van Vliet, P., Brunekreef, B. 2002. Spatial variability of fine particle concentrations in three Europian areas. *Atmospheric Environment*, **36:** 4077–4088.

Hogrefe, C., Sistia, G., Zalewsky, E., Hao, W., Ku, J.-Y. 2003. An assessment of the emissions inventory processing systems EMS-2001 and SMOKE in grid-based air quality models. *Journal of the Air & Waste Management Association*, **53**: 1121–1129.

Holland, W.W., Bennet, A.E., Cameron, I.R., Florey, C.V. et al. 1979. Health effects of particulate pollution: reappraising the evidence. *American Journal of Epidemiology*, **110**: 527-659.

Holton, J.R. 1992. *Dynamic meteorology*, New York, Academic Press, 456p.

Houthuijs, D., Breugelmans, O., Hoek G. 2001. PM_{10} and $PM_{2.5}$ concentrations in Central and Eastern Europe: results from the Cesar study. *Atmospheric Environment*, **35**: 2757–2771.

Hsu, Y.K., Holsen, T.M., Hopke, P.K. 2003. Comparison of hybrid receptor models to locate PCB sources in Chicago. *Atmospheric Environment*, **37**: 545–562.

Hueglin, C., Gehrig, R., Baltensperger, U., Gysel, M., Monn, C., Vonmont H. 2005. Chemical characterisation of $PM_{2.5,}$ PM_{10} and coarse particles at urban, near-city and rural sites in Switzerland. *Atmospheric Environment*, **39**: 637–651.

Hurley, P. 2002. *The Air Pollution Model (TAPM) Version 2. Part 1: Technical Description*, CSIRO, Australia, 49 p.

Hurley, P., Manins, P., Lee, S., Boyle, R., Leung, Y., Dewundege, P. 2003, Year-long, high-resolution, urban airshed modelling: verification of TAPM predictions of smog and particles in Melbourne, Australia. *Atmospheric Environment*, **37** (14): 1899–1910.

Hwang, I.-J., Hopke, P.K. 2007. Estimation of source appointment and potential source locations of $PM_{2.5}$ at a west coastal IMPROVE site. *Atmospheric Environment*, **41**: 506–518.

IPCC. 2001. Climate change 2001: the science of climate change. Technical summary of the working group I report. *World Meteorological Organization*, Genf.

Jaecker-Voirol, A., Mirabel, P. 1989. Hetero-molecular nucleation in the sulphuric acid water System. *Atmospheric Environment*, **23**: 2053-2057.

Jaecker-Voirol, A., Lipphardt, M., Martin, B., Quandalle, P., Salles, J., Carissimo, B., Dupont, E., Mussongenon, L., Riboud, P.M., Aumont, B., Bergametti, G., Bey, I. And Toupance, G. 1998. A 3D regional scale photo-chemical air quality model application to a 3 day summertime episode over Paris, *Revue de l'Institut Francais du Petrole*, **53**: 225–237.

Jazcilevich, A.D., Garcia, A.R., Ruiz-Suarez, L.G., Cruz-Nunez, X., Delgado, J.C., Tellez, C., Chias L.B. **2003**. An air quality modelling study comparing two possible sites for the new

international airport for Mexico city. *Journal of the Air & Waste Management Association*, **53**: 366–378.

Jirak I.L., Cotton W. R., 2006. Effect of air pollution on precipitation along the Front Range of the Rocky Mountains, *Journal of Applied Meteorology and Climatology*, **45**(1): 236–244.

Kain, J.S., Fritsch, J.M. 1993. Convective parameterization for mesoscale models: The Kain-Fritsch scheme, The Representation of cumulus in numerical models, Meteorological Monographs. *American Meteorological Society*, **46**: 165–177.

Kawamoto, K., Hayasaka, T., Nakajima, T., Street,s D., Woo, J.-H. 2004. Examining the aerosol indirect effect over China using an SO_2 emission inventory. *Atmospheric Research*, **72**: 353–363.

Kingam, S., Durand, M., Aberkane, T., Harrison, J., Wilson, J.G., Epton, M. 2005, Winter comparison of TEOM, MiniVol and DustTrak PM_{10} monitors in a wood-smoke environment. *Atmospheric Environment*, **40**: 338–347.

Klaussmann, A.M., deFoy, B., Godfrey, J., Scire, J. 2001. MM5 simulation over New Zealand – Application to the America's Cup races. *MM5 Workshops*, *Division 4*, **www.mmm.ucar.edu/mm5/workshop/workshop-program-2001.html**.

Koracin, D., Isakov, V., Frye, J. 1998. A Lagrangian particle dispersion model (LAP) applied to transport and dispersion of chemical tracers in complex terrain. Presented at the Tenth Joint Conference on the *Applications of Air Pollution teorology*, Phoenix, AZ, 11–16 January 1998. Paper 5B.5, pp. 227–230.

Koracin, D., Isakov, V., Podnar, D., Frye, J. 1999. Application of a Lagrangian random particle dispersion model to the short-term impact of mobile emissions. *Proceedings of the Transport and Air Pollution conference*, Graz, Austria, 31 May–2 June 1999.

Koracin, D., Frye, J., Isakov, V. 2000. A method of evaluating atmospheric models using tracer measurements. *Journal of Applied Meteorology*, **39**: 201–221.

Kossmann, M., Sturman, A. P. 2002. Analysis of surface wind fields in Christchurch and Canterbury (NZ) during winter smog nights – results from the CAPS2000. 16th International clean air and environmental *Conference of the Clean Air Society of Australia and New Zealand,* Christchurch, New Zealand 18 – 22 August 2002, 452–458.

Kossmann, M., Sturman, A. 2004. The surface wind field during winter smog nights in Christchurch and coastal Canterbury, New Zealand. *International Journal of Climatology*, **24**: 93-108.

Kotroni, V., Kallos, G., Lagouvardos, K., Varinou, M., Walko, M. 1999. Numerical simulations of the meteorological and dispersion conditions during an air pollution episode over Athens, Greece. *Journal of Applied Meteorology*, **38**: 432–447.

Kotroni, V., Lagouvardos, K. 2002. MM5 fine scale simulations for the support of Athens 2004 Olympic Games: evaluation of the first year of operational activities. *MM5 Workshops*, *Division 3*, **www.mmm.ucar.edu/mm5/workshop/workshop-program-2003.html**.

Krichak, S.O., Tsidulko, M., Pinhas, A. 2002. A study of an INDOEX period with aerosol transport to the eastern Mediterranean area. *Journal of Geophysical Research*, **107** (D18): 18/1–18/9.

Krishnamurti, T.N., Ingles, K., Cocke, S., Kitade, T., Pasch, R. 1984. Details of low latitude medium range numerical weather prediction using a global spectral model. *Journal of the Meteorological Society of Japan*, **62**: 613-649.

Kunz M., Kottmeier C. 2006a. Orographic enhancement of precipitation over low mountain ranges. Part I: Model formulation and idealized simulations. *Journal of Applied Meteorology and Climatology*. **45** (8): 1025–1040.

Kunz M., Kottmeier, C. 2006b. Orographic enhancement of precipitation over low mountain ranges. Part II: Simulations of heavy precipitation events over Southwest Germany. *Journal of Applied Meteorology and Climatology*. **45** (8): 1041-1055.

Kuo, L. 1974. Further studies of the parameterisation of the influence of cumulus convection on large-scale flow. *Journal of the Atmospheric Sciences*, **31**: 1232-1240.

Lee, C.T., Chou, C.C.K. 1994. Application of fractal geometry in quantitative characterization of aerosol morphology. *Particle and Particle Systems Characterization*, **11**: 436-441.

Lee C.-G., Yuan, C.-S., Chang, J.-C., Yuan, C. 2006, Effects of aerosol species on atmospheric visibility in Kaohsiung city, Taiwan. *Journal of the Air & Waste Management Association*, **55**: 1031-1041.

Lee, K.H., Kim, J.E., Kim, Y.J., Kim, J., von Hoyningen-Huene, W. 2005. Impact of the smoke aerosol from Russian forest fires on the atmospheric environment over Korea during May 2003. *Atmospheric Environment*, **39**: 85 – 99.

Levin, L. 2006. The global mercury emissions inventory. *The magazine for environmental managers*, N. 12: 20–25.

Lewis, C.W., Norris, G.A., Conner, T.L., Henry, R.G. 2003. Source appointment of Phoenix $PM_{2.5}$ aerosol with the Unmix receptor model. *Journal of the Air & Waste Management Association*, **53**: 325–338.

Lippmann, M. et. al. 200. *Association of particulate matter components with daily mortality and morbidity in urban populations*. HEI Health Effects Institute, Cambridge Massachusetts, **95**: 1–86.

Liu, W., Hopke, P.K., VanCuren, R.A. 2003a. Origins of fine aerosol mass in the western United States using positive matrix factorization. *Journal of Geophysical Research*, **108 (D23)**: 4716.

Liu, W., Hopke, P.K., Han, Y.J., Yi, S.M., Holsen, T.M., Cybart, S., Kozlowski, K., Milligan, M. 2003b. Application of receptor modelling to atmospheric constituents at Potsdam and Stockton, NY. *Atmospheric Environment*, **37**: 4997–5007.

Liu Y., Chen R., Shen X., Mao X. 2004. Wintertime indoor air levels of PM_{10}, $PM_{2.5}$ and PM_1 at public places and their contributions to TSP. *Environment International*, **30**: 189–197.

Lohman, K., Pai, P., Seigneur, C., Mitchell, D., Heim, K., Wandland, K., Levin, L. 2000. A probabilistic analyses of regional mercury impacts on wildlife. *Human and Ecological Risk Assessment*, **6** (1): 103–130.

Loibl, W., Orthofer, R. 2001. From national emission totals to regional ambient air quality information for Austria. *Advances in Environmental Research*, **5**: 395–404.

Low-Nam, S., Davis, C. 2002. Development of a Tropical Cyclone bougussing scheme for the MM5 system. *MM5 Workshops*, *Division 6*, **www.mmm.ucar.edu/mm5/workshop/workshop-program-2002.html.**

Lu H.-C. 2003, Comparison of statistical characteristic of air pollutants in Taiwan by frequency distribution. *Journal of the Air & Waste Management Association*, **53**: 608–616

Malm, W.C., Pitchford, M.L. 1997. Comparison of calculated sulphate scattering efficiencies as estimated from size-resolved particle measurements at three national locations. *Atmospheric Environment*, **31**: 1315-1325.

Malm, W.C., Schichtel, B.A., Pitchford. M.L., Ashbaugh, L.L., Elder R.A. 2004. Spatial and monthly trends in speciated fine particulate concentrations in the United States. *Journal of Geophysical Research*, **109**: DOI 10.1029/203JD003739.

Manabe S. (ed.) 1985. Issues in atmospheric and oceanic modelling, part A, Climate dynamics. *Advances in Geophysics*, **28**, Academic Press: New York, 591 p.

Manabe, S., Hahn, D.G., 1981. Simulation of atmospheric variability. *Monthly Weather Review*, **109**: 2260-2286.

Mao, Q., Gautney, L.L., Cook, T.M., Jacobs, M.E., Smith, S.N., Kelsoe, J.J., 2006. Numerical experiments on MM5-CMAQ sensitivity to various PBL schemes. *Atmospheric Environment*, **40**: 3092–3110.

Marenco, F., P. Bonasoni, F. Calzolari, M. Ceriani, M. Chiari, P. Cristofanelli, A. D'Alessandro, P. Fermo, F. Lucarelli, F. Mazzei, S. Nava, A. Piazzalunga, P. Prati, G. Valli, Vecchi R. 2006. Characterization of atmospheric aerosols at Monte Cimone, Italy, during summer 2004: Source apportionment and transport mechanisms. *Journal of Geophysical Researches*, **111:** D24202, doi:10.1029/2006JD007145.

Martuzevicius, D., Grinshpun, S., Reponen, T., Gorny, R.L., Shukla, R., Lockey, J., Hu, S., McDonald, R., Biswas, P., Kliucininkas, L., LeMasters, G. 2004. Spatial and temporal variation of $PM_{2.5}$ concentration and composition throughout an urban area with high freeway density – the Greater Cincinnati study. *Atmospheric Environment*, 38: 1091–11105.

McDonnel, W.F. et al. 2000. Relationships of mortality with the fine and coarse fractions of long-term ambient PM_{10} concentrations in non-smokers. *Journal of exposure analysis and environmental epidemiology,* **10**: 427–436.

McGowan, H.A., Sturman, A.P. 1993. Synoptic and local effects on the climate of the Waimate area, South Canterbury. *Weather and Climate*, **13**: 22–33.

McGruffie K. and Henderson-Sellers A. 2001. Forty years of numerical climate modelling. *International Journal of Climatology*, **21**: 1067–1109.

McKendry, I.G. 1983. Spatial and temporal aspects of the surface wind regime on the Canterbury Plains, New Zealand. *Journal of Climatology*, **3**: 155–166.

McKendry, I.G., Sturman, A.P., Owens, I.F. 1986. A study of interacting multi-scale wind systems, Canterbury Plains, New Zealand. *Meteorology and Atmospheric Physics*, **35**: 242-252.

McKendry, I.G., Sturman, E.P., Owens, I.F. 1987. The Canterbury Plains northeasterly. *Weather and Climate*, **7**: 61–74.

Meng, Z., Seinfeld, J.H. 1996. Time scales to achieve atmospheric gas aerosol equilibrium for volatile species. *Atmospheric Environment*, **30**: 2889-2900.

Meteorological Society of New Zealand: *Weather Highlights of 2006*, **http://www.scoop.co.nz/stories/SC0612/S00067.**

Meyer, M.B., Patashnick, H., Ambs, J.L., Rupprecht, E. 2000. Development of a sample equilibration system for the TEOM continuous PM monitor. *Journal of the Air & Waste Management Association*, **50**: 1345–1349.

Michelson, S.A., Bao, J.-W., McKeen, S.A., White, A., Grell, G.A. 2002. An evaluation of real-time forecasts from a weather-chemistry forecasting model using observations from the Texas AQS 2000 field experiment. *MM5 Workshops*, *Division 4*, **www.mmm.ucar.edu/mm5/workshop/workshop-program-2003.html**.

Mihajlidi-Zelic, A., Desek-Timotic, I., Relic, D., Popovic, A., Derodevic, D. 2006. Contribution of marine and continental aerosols to the content of major ions in the precipitation of the central Mediterranean. *Science of the Total Environment*, **370**: 441–451.

Mikael, L.A., Brady, T.J., Hay, J.E. 1999. *Chemical characterisation of Christchurch aerosol*. School of Marine Sciences and Environment, University of Auckland, Auckland.

Miller, C.A., Hidy, G., Hales, J., Kolb, C.R., Werner, A.S., Haneke, B., Parrish, D., Frey, H.C., Rojas-Bracho, L., Deslauriers, M., Pennell, B., Mobley, J.D. 2006. Air emission inventories in North America: a critical assessment. *Journal of the Air & Waste Management Association*, **56** (8): 1115–1129.

Ministry for Environment 2004. *Good practice for Atmospheric Dispersion Modelling*, June 2004, Reference ME522, Wellington.

Ministry for the Environment 2003. *Regulatory impact and compliance cost statement: National Environmental standards for Air Quality*. Wellington.

Minvielle, F., Cautenet, G., Lasserre, F., Foret, G., Cautenet, S., Lacon, J.F., Andreae, M.O., Mayol, R., Chazette, P., Roca, R. 2004. Modelling the transport of aerosol during INDOEX 1999 and comparison with experimental data. Part 1: carbonaceous aerosol distribution. *Atmospheric Environment*, **38**: 1811 – 1822.

Miranda A.I., Borrego, C. 1996. A prognostic meteorological model applied to the study of a forest fire. *International Journal of Wildland Fire*, **6**: 157–163.

Mobley, J.F., Cadle, S.H. 2003. Innovative methods for emission inventory development and evaluation: workshop summary. *Journal of the Air & Waste Management Association*, **53**: 1422–1439.

Molnar, P, Gustafson, P, Johannesson, S, Boman, J, Barregard, L, Sallsten, G. 2005. Domestic wood burning and $PM_{2.5}$ trace elements: personal exposure, indoor and outdoor levels. *Atmospheric Environment*, **39**: 2643–2653.

Moody, T. 1983. Air pollution in Canterbury: into the '80s or back to the '30s? In *Canterbury at the crossroad: Issues for the eighties* (Bedford R.D. & Sturman A.P., eds.), 138–166.

Morris, R.E., Yarwood, G, Emery, C., Pandis, S., Lurmann, F. 2003. Implementation of State-of-Science PM modules into PMCAMx photochemical grid model. Presented at the *96th Annual Conference and Exhibition of the AWMA*, San Diego, California (June 2003).

Moussiopoulos, N., Douros, I. 2005. Efficient calculation of urban scale air pollutant dispersion and transformation using the OFIS model within the framework of CityDelta. *International Journal of Environment and Pollution*, **24**: 64–74.

Nenes, A, Pilinis, C, Pandis. S N. 1999. Continued development and testing of a new thermodynamic aerosol module for urban and regional air quality models. *Atmospheric Environment*, **33**: 1553-1560.

Nenrkorn, T., Hoffman, R.N. 2006. Creating pseudo-forecast ensembles statistically using a characterization of displacements: a pilot study. *Journal of Applied Meteorology*, **45** (11): 1542–1556.

Nielsen-Gammon, J.W. 2003. The Houston heat pump: modulation of a land-sea breeze by an urban heat island. *Thirteen PSU/NCAR MM user's workshop*, 5p.

Odman, M., Russell, A. 1991. Multiscale modeling of pollutant transport with chemistry. *Journal of Geophysical Research*, **96**: 7363–7370.

Odman, M.T., Wilkinson, J.G., MacNair, L.A., Russell, A.G., Ingram, C.L. and Houyoux, M.R. 1996, *Horizontal advection solver uncertainty in the Urban Airshed Model*, Prepared for California Air Resources Board and California EPA, April.

Oke, T.R. 1978. *Boundary layer climates*, Methuen: London.

Ostro, B.D., Eskeland, G.S., Canchez, J.M., Feyzioglu, T. 1999. Air pollution and daily mortality in the Coachella Valley, California: A study of PM10 dominated by coarse particles. *Environmental research,* **81**: 231–238.

Otte, T.L., Locser, A. 2001. Implementation of an urban canopy parameterization for fine-scale simulations, *MM5 Workshops*, *Division 5*, **www.mmm.ucar.edu/mm5/workshop/workshop-program-2001.html**.

Otte T.L. 2003. Using MM5v3 with ETA analysis for air-quality modelling at the EPA. *Thirteen PSU/NCAR MM user's workshop*, 4 pp.

Otte, T.L., Pouliot, G., Pleim, J.E., Yaung, O. 2005. Linking the ETA model with the Community Multiscale Air Quality (CMAQ) modelling system to build a national air quality forecasting system. *Weather and Forecasting*, **20** (3): 367–385.

Oanh N.T. and Zhang B. 2003, Photochemical smog modelling for assessment of potential impacts of different management strategies on air quality of the Bangkok metropolitan region, Thailand. *Journal of the Air & Waste Management Association*, **53**: 1321–1338.

Parrish, D.D. 2006. Critical evaluation of US on-road vehicle emission inventories. *Atmospheric Environment*, **40**: 2288–2300.

Pasken, R., Pietrowicz, J.A. 2005. Using dispersion and mesoscale meteorological models to forecast pollen concentrations. *Atmospheric Environment*, **39**: 7689–7701.

Pedlosky, J. 1979. *Geophysical Fluid Dynamics*, vol. I-II, Springer-Verlag, Berlin and New York.

Peters-Lidard, C.D., McHenry, J.N. and Coats, C.J. 2002. Design and evaluation of the coupled MM5/TOPLATS modeling system for Texas air quality accidence episode. *MM5 Workshops*, *Division 4*, **www.mmm.ucar.edu/mm5/workshop/workshop-papers_ws02.html**

Pielke, R.A. 1984. *Mesoscale meteorological modelling*, Academic Press, New York, 267 pp.

Pielke, R.A., Cotton, W.R., Walko, R.L., Tremback, C.J., Lyons, W.A., Grasso, L.D., Nicholls, M.E., Morgan, M.D., Wesley, D.A., Lee, T.J., Coperald, J.H. 1992. A comprehensive meteorological modelling system – RAMS. *Meteorology and Atmospheric Science*, **49**: 69–91.

Pietrowicz, J. 2002. Testing of mesoscale meteorological models as a tool to forecast pollen concentration. *MM5 Workshops*, *Division 6*, **www.mmm.ucar.edu/mm5/workshop/workshop-papers_ws02.html**.

Pilinis, C., Seinfeld, J.H. 1987. Continued development of a general equilibrium model for inorganic multi-component atmospheric aerosols. *Atmospheric Environment*, **21**: 2453-2462.

Pilinis, C., Seinfeld, J.H., Grosjean, D. 1989. Water content of atmospheric aerosol. *Atmospheric Environment*, **23**: 1601–1606.

Pilinis, C., Capaldo, K.P., Nenes, A., Pandis, S.N. 2000. MADM - A new multi-component aerosol dynamics model. *Aerosol Science Technology*, **32** (5): 482-502.

Pope, C.A., III, Thun, M.J., Namboodiri, M.M., Dockery, D.W., Evans, J.S., Speizer, F.E., Heath, J.C.W. 1995. Particulate Air Pollution as a Predictor of Mortality in a Prospective Study of U.S. Adults. *American Journal of Respiratory and Critical Care Medicine*, **151**: 669-674.

Pope, C.A., III, Burnett, R.T., Thun, M.J., CAlle, E.E. 2002. Lung cancer, cardiopulmonary mortality, and long-term exposure to fine particulate air pollution. *Journal of the American medical association*, **287**: 1132–1141.

Pope, C.A., III, Dockery, D.W. 2006. Health effects of fine particulate air pollution: lines and connect. *Journal of the Air & Waste Management Association*, **56**: 709-742.

Price, M., Bulpitt, S., Meyer, M.B. 2003. A comparison of PM10 monitors at a kerbside site in the northeast of England. *Atmospheric Environment*, **37**: 4425–4434.

Puri, K., Dietachmayer, G., Mills, G., Davidson, N., Bowen, R., Logan, L. 1998. The BMRC limited area prediction systems, LAPS. ***Australian Meteorological Magazine***, **47**.

Putaud J-P, Raes F, Van Dingenen R, Bruggemann E, Facchini M-C, Decesari S, Fuzzi S, Gehrig R, Huglin C, Laj P, Lorbeer G, Maenhaut W, Mihalopoulos N, Muller K, Querol X, Rodriguez S, Schneider J, Spindler G, ten Brink H, Torseth K, Wiedensohler A. 2004. A European aerosol phenomenology – 2: chemical characteristics of particulate matter at kerbside, urban, rural and background sites in Europe. *Atmospheric Environment*, **38**: 2579 – 2595.

Querol X., Alastuey A., Viana M.M., Rodriguez S., Artinano B., Salvador P., Garcia de Santos S., Fernandez Patiers R., Ruiz C.R., de la Rosa J., de la Campa A.S., Menendez M., Gil J.I. 2004. Specification and origin of PM10 and PM2.5 in Spain. *Aerosol Science*, **35**: 1151–1172.

Smith S.C., Yin D., Roth H., Jiang W. 2006. The impact of GEM and MM5 modelled meteorological conditions on CMAQ air quality modelling results in Eastern Canada and the Northeastern United States. *Journal of Applied Meteorology*, **45** (11): 1525–1541

Reisner, J., Rasmussen, M.R. and Bruintjes, R.T. 1998. Explicit forecasting of supercooled liquid water in winter storms using the MM5 mesoscale model. *Quarterly Journal of the Royal Meteorological Society*, **124**: 1071-1107.

Roosli, M., Kunzli, N., Braun-Fahrlander, C., Egger, M. 2005. Years of life lost attributed to air pollution in Switzerland: Dynamic exposure-response model. *International Journal of Epidemiology* **34:** 1029-1035.

Rupprecht & Patashnick Co., I. 1993. Low Temperature Operation of the TEOMs Series 1400 PM–10 Monitor. Rupprecht & Patashnick Co., Inc. Technical note 4.

Russell, L. M., Pandis, S.N., Seinfeld, J.H. 1994. Aerosol production and growth in the marine boundary layer. *Journal of Geophysical Research*, **99**: 20,989-21,003.

Russel, A. 1997. Regional photochemical air quality modelling – model formulations, history, and state of the science. *Annual Review of Energy and the Environment*, **22**: 537–588.

Ryan, A.P. 1987. *The climate and weather of Canterbury (including Aorangi)*. New Zealand Meteorological Service, Miscellaneous Publication, **115** (17), 66p.

Ryan, R. 2002. Specification profiles and assignment files located on EMCH, *Memorandum*, EPA, U.S.A.

Salvador, P., Artinano, B., Querol, X., Alastuey, A., Costoya, M. 2007. Characterization of local and external contribution of atmospheric particulate matter at a background coastal site. *Atmospheric Environment*, **41**: 1–17.

Sarrat, C., Lemonsu, A., Masson, V., Guedalia D., 2006. Impact of urban heat island on regional atmospheric pollution. Atmospheric Environment, 40: 1743–1758.

Schaap, M. et al. 2004. Anthropogenic black carbon and fine aerosol distribution over Europe. *Journal of Geophysical Research* 109, D18207.

Schmid, H, Laskus, L, Abraham, H J, Baltensperger, U, Lavanchy, V, Bizjak, M, Bubra, P, Cachier, H, Crow, D, Chow, J, Gnauk, T, Even, A, ten Brink, H, Giesen, K, Hitzenberger, R, Hueglin, C, Maenhaut, W, Pio, C, Carvalho, A, Putaud, J, Toom-Sauntry, D, Puxbaum, H. 2001. Results of the "carbon conference" international aerosol carbon round robin test stage I. *Atmospheric Environment*, **35**: 2111 – 2121.

Scott, A., Gunatilaka, M. 2004. 2002 Christchurch inventory of emissions to air, Report N. R04/03, ISBN 1-86937-518-1, *Environmental Canterbury*, 55p.

Scott, A.J. 2002. Chemical characterisation of wintertime fine particles in Christchurch, New Zealand. *Proceedings of the 16th International Clean Air and Environment Conference*, Clean Air Society of Australia and New Zealand, Christchurch, New Zealand, 19-22 August.

Scott A.J., 2005. *Source appointment and chemical characterisation of airborne fine particulate matter in Christchurch*, New Zealand, A Thesis Submitted for the Degree of Doctor of Philosophy, University of Canterbury, July 2005.

Scott, A.J., Gunatilaka M. 2004. *2002 Christchurch inventory of emissions to air*, Report N. R04/03, ISBN 1-86937-518-1, Environmental Canterbury.

Seinfeld J.H., Pandis, S.N. 1998. *Atmospheric chemistry and physics – from air pollution to climate change*. John Wiley and Sons Inc., New York, 1326 p.

Senaratne, I. 2003. Chemical characterisation of airborne particulate matter in New Zealand cities, Ph.D. Thesis, The University of Auckland, New Zealand.

Senaratne, I., Shooter, D. 2004. Elemental composition in source identification of brown haze in Auckland, New Zealand. *Atmospheric Environment*, **38**: 3049–3059.

Senaratne. I, Kelliher, F.M., Triggs, C. 2005. Source appointment of airborne particles during winter in contrasting, coastal cities. *Aerosol and Air Quality*, **5**: 51–67.

Simpson, D., Fagerli, H., Jonson, J.E., Tsyro, S., Wind, P. 2003. Transboundary acidification, eutrophication and ground level ozone in Europe, Part 1. *Unified EMEP model description*. EMEP Report 1/2003.

Sista, G., Civerolo, K., Hao, W. 2002. An evaluation of the UAM-V predicted concentrations of carbon monoxide and reactive nitrogen compounds over the Eastern United States during summer 1995. *Journal of the Air & Waste Management Association*, **52**: 1324–1332.

Shy, C.M. 1979. Epidemiologic evidence and the United States air quality standards. *American Journal of Epidemiology*, **110**: 661-671.

Smith, S.C., Jiang W., Yin, D., Roth, H., Giroux, E. 2006. Evaluation of CMAQ O_3 and $PM_{2.5}$ performance using Pacific 2001 measurement data. *Atmospheric Environment*, **40**: 2735–2749.

Smagorinsky, J. 1983. The beginnings of numerical weather prediction and general circulation modelling: early recollections. *Advances in Geophysics*, **25**: 3-37.

Smallcomb, C. 2002. Using an operational MM5 in the Fire Weather Forecast process for West Texas and Southeastern New Mexico, *Division 5*, **www.mmm.ucar.edu/mm5/workshop/workshop-papers_ws02.html**.

Smith, S.C., Jiang, W., Yin, D., Roth, H., Giroux E. 2006. Evaluation of CMAQ O_3 and $PM_{2.5}$ performance using Pacific 2001 measurement data. *Atmospheric Environment*, **40**: 2735–2749.

Someshwar, D., Dudhia, J., Baker, D. and Moncreiff, M. 2002. A heavy rainfall episode over the west coast of India using analysis nudging in MM5, *Division 2*, **www.mmm.ucar.edu/mm5/workshop/workshop-papers_ws02.html**.

Sloane, C.S., Watson, J.G., Chow J.C., Pritchett, L.C., Richards, L.W. 1991. Sized-segregated fine particle measurements by chemical species and their impact on visibility impairment in Denver. *Atmospheric Environment*, **25A**: 1013-1024.

Someshwar, D., Dudhia, J., Baker, D., Moncreiff, M. 2002. A heavy rainfall episode over the west coast of India using analysis nudging in MM5. *Division 2*, **www.mmm.ucar.edu/mm5/workshop/workshop-papers_ws02.html**.

Sorteberg, A., Berge, E., Eastwood, S. 2001. Results from high-resolution operational meteorological forecasts in complex terrain during wintertime inversions. *Division 6*, **www.mmm.ucar.edu/mm5/workshop/workshop-papers_ws01.html**.

Soukup, J.M. 2000. Soluble components of Utah Valley particulate pollution alter alveolar macrophage function in vivo and in vitro. *Inhalation Toxicology,* **12**: 401–414.

Soukup, J.M., Becker, S. 2001. Human alveolar macrophage responses to air pollution are associated with insoluble components of course material, including particulate endotoxin. *Toxicology and applied pharmacology,* **171**: 20–26.

Souto, J.A., Perez-Munuzuri, V., de Castro, M., Souto, M.J., Casares, J.J., Lucas, T. 1998. Forecasting and diagnostic analysis of plume transport around a power plant. *Journal of Applied Meteorology*, **37**: 1068–1083.

Spronken-Smith, R.A., Sturman, A.P., Wilton, E. 2001. The air pollution problem in Christchurch, New Zealand. *Clean Air and Environmental Quality*, **36**: 23–28.

Spronken-Smith, R.A., Sturman, A.P., Kossman, M., Zawar-Reza, P. 2002. An overview of the Christchurch Air Pollution Study (CAPS) 2000, *16th International clean air and environmental Conference of the Clean Air Society of Australia and New Zealand*, *Christchurch, New Zealand 18 – 22 August 2002*, 758–763.

Spronken-Smith, R.A., Kossmann, M., Zawar-Reza, P. 2004. Where does all the energy go? *Energy partitioning in suburban Christchurch under stable wintertime conditions. Theoretical and applied climatology*. [accepted; selected by the International Association for Urban Climate (IAUC) for inclusion in a special issue].

Steenburg, W.J., Onton, D.J., Siffert, A.J., Cheng, L., Haymore, B. 2001. MM5 based modelling and model output statistics for the 2002 Olympic winter games. Division 6, **www.mmm.ucar.edu/mm5/workshop/workshop-papers_ws01.html**.

Steeneveld, G.J., van de Wiel, B.J.H., Holtslag A.A.M. 2007, Diagnostic equations for the stable boundary layer height: evaluation and dimensional analysis. *Journal of Applied Meteorology and Climatology*, **46**(2): 212-225.

Stein, A.E., Lamb, D., Draxler, R.R. 2000. Incorporation of detailed chemistry into a three-dimensional Lagrangian – Eulerian hybrid model: application to regional tropospheric ozone. *Atmospheric Environment*, **34**: 4361–4372.

Stern, R., Yamartino, R., Graff, A. 2003. Dispersion modelling within the European community's air quality directives: long term modelling of O3, PM10 and NO2. In: *Proceedings of the 26th ITM Conference on Air Pollution Modelling and its Application*, May 26–30, 2003, Istanbul, Turkey.

Stohl, A., Wotawa, G. 1994. FLEXTRA - Version 1.0. Modelldokumentation, Internal report. Institute of Meteorology and Physis, Univ. of Vienna. 47 p.

Stohl, A., Wotawa, G. 1995. A method for computing single trajectories representing boundary layer transport. *Atmospheric Environment,* **29:** 3235-3239.

Strader, R., Lurmann, F.W., Pandis, S.N. 1999. Valuation of secondary organic aerosol formation in winter. *Atmospheric Environment*, **33**: 4849-4864.

Streets, D.G., Bond, T.C., Carmichael, G.R., Fernandes, S.D., Fu, Q., He, D., Klimont, Z., Nelson, S.M., Tsai, N.Y., Wang, M.Q., Woo, J.-H., Yarber, K.F. 2003. An inventory of gaseous and primary aerosol emissions in Asia in the year 2000. *Journal of Geophysical Research*, **108**: 8809-8825.

Streets, D.G., Zhang, Q., Wang, L., He, K., Hao, J., Wu, Y., Tang, Y., Carmichael, G.R. 2006. Revisiting China's CO emissions after the Transport and Chemical Evolution over the

Pacific (TRACE-P) mission: Synthesis of inventories, atmospheric modelling, and observations. *Journal of Geophysical Research*, **111**: D14306.

Streets, D.V., Fu, J.S., Jang, C.J. 2007. Air quality during the 2008 Beijing Olympic games. *Atmospheric Environment*, **41**: 480-492.

Sturman, A.P. 2000. Progress in Physical Geography (progress report). *Applied Climatology***, 24**: 129–139.

Sturman, A.P., Tyson, P.D. 1981. Sea breezes along the Canterbury coast in the vicinity of Christchurch, New Zealand. *Journal of Climatology*, **1**: 203–219.

Sturman, A.P., Zawar-Reza, P. 2001. *Application of back-trajectory techniques to the delimitation of a Clean Air Zone for the Christchurch airshed*. Technical Report, U01/3, Environment Canterbury, Christchurch, 23p.

Sturman, A.P., Kossmann, M., Spronken-Smith, R.A., Zawar-Reza, P. 2001. The Christchurch Air Pollution Study (CAPS) 2000 – An overview and preliminary results. Proceedings of the *Third Urban Air Quality Symposium: Measurement, Modelling and Management*, Loutraki, 68–72.

Sturman, A.P., Zawar-Reza, P. 2002. Application of back-trajectory techniques to delimitation of urban clean air zones. *Atmospheric Environment*, **36**: 3339–3350.

Sturman, A.P., Tapper, N.J. 2002, *The weather and climate of Australia and New Zealand*. Oxford University Press, Melbourne, 476 p.

Sun, P., Allen, D.T., McDonald-Buller, E.C., Chang, S., Kimura, Y., Mullins, C.B., Yarwood, G., Neece, J.D. 2000. Development of chlorine mechanism for use in the carbon bond IV chemistry model. *Journal of Geophysical Researches*, **108** (D4): 41-45.

Sun, Y., Wang, Y., Han, L., Guo, J., Zhang, W., Wang, Z., Hao, Z. 2004. The air-borne particulate pollution in Beijing: concentration, composition, distribution and sources. *Atmospheric Environment*, **38**: 5991-6004.

Tao, W.K., Simpson, J. 1993. Goddard Cumulus Ensemble Model. Part I: Model description. *Terrestrial, Atmospheric and Oceanic Sciences,* **4**: 19-54.

Temime, Br., 2005. Atmospheric aerosol: physical properties, chemical composition, health and environmental effect. *Department of Chemistry, University College Cork (UCC*).

Tesche, T.W., Morris, R., Tonnesen, G., McNally, D., Boylan, J., Brewer P. 2006. CMAQ/CAMx annual 2002 performance evaluation over the eastern US. *Atmospheric Environment*, **40**: 4906–4919.

Thunis, P., Rouil, L., Cuveiler, C., Stern, R., Kerschbaumer, A., Bessagnet, B., Schaap, M., Builtjes, P., Tarrason, L., Douros, J., Moussiopoulos, N., Pirovano, G., Bedogni, M. 2007. Analysis of model responses to emission-reduction scenarios within the CtiyDelta project. *Atmospheric Environment*, **41**: 208–220.

Tie, X., Madronich, S., Li, G., Ying, Z., Zhang, R., Garcia, A.R., Lee-Taylor, J., Liu, Y. 2007. Characterizations of chemical oxidants in Mexico City: a regional chemical dynamical model (WRF-Chem) study. *Atmospheric Environment*, **41**: 1989-2208.

Titov M. 2004. *Application of an atmospheric mesoscale modelling system to analysis of air pollution dispersion in the Christchurch area*. Unpublished Masters Thesis in Environmental Science, University of Canterbury, Christchurch, New Zealand.

Titov M., Sturman, A. 2005. Numerical prediction of spatial variability of suspended particulates during winter air pollution episode over Christchurch. *26th Annual Conference of Meteorological Society of New Zealand*, Wellington, New Zealand, 23 November 2005.

Titov M., Sturman A.P., Zawar-Reza P., 2006. A comparison of observed $PM_{2.5} - PM_{10}$ ratio with values modelled for Christchurch, New Zealand using MM5-CAMx numerical system: different chemical scenarios and associated air quality. *Air & Waste Management Association 99th Annual Conference*, New Orleans, 20 to 25 June 2006.

Titov, M., Sturman, A.P., Zawar-Reza, P. 2007. Application of MM5 and CAMx4 to local scale dispersion of particulate matter for the city of Christchurch, New Zealand. *Atmospheric Environment*, **41** (2): 327–338.

Tsai, Y.I., Cheng, M.T. 1999. Visibility and aerosol chemical compositions near the coastal area in central Taiwan. *The Science of the Total Environment*, **231**: 37-51.

Turkiewicz, K., Magliano, K., Najita, T. 2006. Comparison of two winter air quality episodes during the California regional particulate air quality study, 2006. *Journal of the Air & Waste Management Association*, **56**: 467–473.

U.K. Ministry of Health. *Mortality and mobility during the London for of December 1952. Reports on Public Health and Medical Subjects No. 95*. Ministry of Health: London, United Kingdom, 1954.

Unites States Environmental Protection Agency. 1999. *Visibility monitoring guidance*. EPA-454/R-99-University of California. 1995. *IMPROVE data guide*. 13p.

UNITED STATES EPA. *Air Quality Criteria for Particulate Matter (Third External Review Draft)* EPA, 600/P-99/002aB, *http://cfpub.epa.gov/ncea/cfm/partmatt.cfm?ActType=default*. (2002).

Us EPA. 1991. *Guideline for regulatory application of the urban airshed model. US EPA Report No. EPA-450/4-91-013*. Office of Air and Radiation, Office of Air Quality Planning and Standards, Technical Support Division, Research Triangle Park, North Carolina, US.

Van den Assam, S. 1997. *Dispersion of air pollution in the Christchurch area*. Ph.D. Thesis, University of Canterbury, Department of Geography, Christchurch, New Zealand.

van Dingenen R., Raes F., Putaud J.-P., Baltenspreger U., Charron A., Facchini M.-C., Decesari S., Fuzzi S., Gehrig R., Hansson H.-C., Harrison R.M., Huglin C., Jones A.M., Laj P., Lorbeer G., Maenhaut W., Palmgren F., Querol X., Rodriguez S., Schneider J., ten Brink H., Tunved P., Torseth K., Wehner B., Weingartner E., Wiedensohler A., Wahlin P. 2004. A

European aerosol phenomenology – 1: physical characteristics of particulate matter at kerbside, urban, rural and background sites in Europe. *Atmospheric Environment*, **38**: 2561–2577.

Wang, H., Shooter, D. 2002. Coarse-fine and day-night differences of water-soluble ions in atmospheric aerosols collected in Christchurch and Auckland, New Zealand. *Atmospheric Environment*, **36**: 3519–3529.

Wang, H., Kawamura, K., Shooter, D. 2005. Carbonaceous and ionic components in wintertime atmospheric aerosol from two New Zealand Cities: implications for solid fuel combuction. *Atmospheric Environment*, **39**: 5865–5875.

Watson, J.G. 2002. Visibility: Science and Regulation. *Journal of the Air & Waste Management Association*, **52**: 628-713.

Wesely, M.L. 1989. Parameterization of Surface Resistances to Gaseous Dry Deposition in Regional-Scale Numerical Models. *Atmospheric Environment*, **23**: 1293-1304.

Wexler, A. S., Seinfeld, J.H. 1990. The distribution of ammonium salts among a size and composition dispersed aerosol. *Atmospheric Environment*, **24A**: 1231-1246.

WHO *Air Quality Guidelines for Europe,* Second edition. Copenhagen, WHO Regional Office for Europe, 2000 (WHO Regional Publications, European Series, No 91).

Wilkinson, L. 1959. *The air pollution problem in the Christchurch area*. Unpublished PhD Thesis, Environmental Science, Department of Geography, University of Canterbury, 175p.

Wilson T.A.J. Spronken-Smith R.A. 2002. An inexpensive and effective measure of atmospheric visibility. *Proceedings of the 16th International "Clean Air and Environment Conference" of the Clean Air Society of Australia and New Zealand*, 19-22 August 2002, Christchurch, New Zealand on CD ROM.

Wilson, J.G., Zawar-Reza, P. 2006. Intraurban-scale dispersion modelling of particulate matter concentrations: application for exposure estimates in cohort studies. *Atmospheric Environment*, **40**: 1053–1063.

Wilton, E., 1999. *Update: The health effects of suspended particulate*. Report No. U99 (51), Environment Canterbury, Christchurch, 21p.

Wilton, E. 2001. *Christchurch inventory of air emissions*. Report No. R01/28, Environment Canterbury, Christchurch, 59p.

Wilton, E. 2003. *Air quality in Christchurch – an assessment of factors contributing to visibility degradation.* PhD thesis in Environmental Science, University of Canterbury, 193p.

WikiPedia en.wikipedia.org/wiki/**Testbed**

Wotawa, G., Stohl, A., Neininger, B. 1998. The urban plume of Vienna: comparison between aircraft measurements and photochemical model results. *Atmospheric Environment*, **32**: 2479–2489.

WRF ARW version 2 modelling system user's guide, *Mesoscale & Microscale Meteorology Division*, National Center for Atmospheric Research, January 2007.

Wu, Y-S., Fang, G-C., Chen, J-C., Lin, C-P., Huang, S-H., Rau, J-Y., Lin, J-G. 2006. Ambient air particulate dry deposition, concentration and metallic elements at Taichung harbour near Taiwan strait. *Atmospheric Research*, **79**: 52–66.

Yarwood, G., Morris, R.E., Yocke, M.A., Hogo, H., Chico, H. 1996. Development of a methodology for Source Appointment of Ozone concentration estimates from a photochemical grid model. *Presented at the 89th AWMA annual meeting*, *Nashville TN, June 23–28*.

Yarwood, G., Morris, R., Wilson, G. 2004. Particulate matter source appointment technology (PSAT) in the CAMx photochemical model. *NATO International Technical Meeting*, Banff, Canada, October 2004.

Yarwood, G., Rao, S. 2005. Updates to the Carbon Bond chemical mechanism: CB05. *Final Report RT-04-00675*, ENVIRON International Corporation, 246p.

Zannetti, P. Air Pollution Modelling: Theories, Computational and Available Software. *Computational Mechanics Publications*, New York, 1990, 245 pp.

Zawar-Reza, P., Sturman, A., Hurley, P. 2005a. Prognostic urban-scale air pollution modelling in Australia and New Zealand – A review. *Clean Air and Environmental Quality*, **39** (2): 41 – 45.

Zawar-Reza, P., Titov, M., Sturman, A.P. 2005b. Dispersion modelling of PM10 for Christchurch, New Zealand: an intercomparison of performance between Mesoscale Model (MM5) and The Air Pollution Model (TAPM). *Proceedings of the 17th International Clean Air and Environment Conference*, Hobart, Australia, 3-6 May 2005.

Zawar-Reza, P., Kingham, S., Pearce, J. 2006. Evaluation of a year-long dispersion modelling of PM_{10} using the mesoscale model TAPM for Christchurch, New Zealand. *Science of the Total Environment*, **349**: 249–259.

Zhang Q., Zhao C., Tie X., Wei Q., Huang M., Li G., Ying Z., Li C. 2006. Characterizations of aerosols over the Beijing region: a case study of aircraft measurements. *Atmospheric Environment*, **40**: 4513–4527.

Zhou, L., Hopke, P.K., Liu, W. 2004. Comparison of two trajectory based models for locating particle sources for two rural New York sites. *Atmospheric Environment*, **38**: 1955–1963.